Synthetic Studies Toward Aziridinomitosenes and 9-Oxo-pyrrolo[1,2-a]indole Mitosanes Related to the Mitomycin and FR Heterocycles

by

Susan D. Wiedner

A dissertation submitted in partial fulfillment
of the requirements for the degree of
Doctor of Philosophy
(Chemistry)
in The University of Michigan
2009

Doctoral Committee:

Professor Edwin Vedejs, Chair
Professor David Sherman
Associate Professor Anna Mapp
Associate Professor John Wolfe

To my grandfather, Francis Jerome Trick

Acknowledgements

I would first like to thank my advisor, Professor Edwin Vedejs, for advising me over the last six years. His drive for understanding chemical problems and discovering new chemistry imparted on me a desire to understand, analyze, and circumvent multiple synthetic difficulties which I encountered during my graduate work. Without his guidance and example, I would not have been successful. Furthermore, I would like to thank him for the opportunity to discover my "talents" during this incredibly challenging and rewarding research experience.

I also want to thank past and present Vedejs group members. A special thanks goes to Tim, Trisha, and Drew for helping me transition into the lab during my first and second year. Thank you Jeremy and Musong for your previous work on the FK317 project. Thanks John, Aleks, Li, Dan and Eoghan for many discussions about chemistry. I especially want to thank Bob and Val for their insightful suggestions regarding my project, for reading and editing my thesis, and for their friendship.

Most importantly, I would like to thank my family. My husband Eric has been by my side for most of my graduate career and I could not have gotten through this challenging process without his support and love. And finally, my parents, grandparents, siblings, and extended family have all been supportive of me during my graduate studies, and a special thanks goes to them for understanding that during graduate school my time has not always been my own.

Table of Contents

List of Figures

Figures: Chapter 1

Figures: Chapter 2

Figures: Chapter 3

List of Tables

Tables: Chapter 2

Tables: Chapter 3

List of Schemes

Schemes: Chapter 1

Schemes: Chapter 2

Schemes: Chapter 3

List of Appendices

Abstract

The aminobenzoquinone mitomycins and the dihydrobenzoxazine FR compounds are potent antitumor antibiotics. Despite structural differences, the compounds are reductively activated to analogous reactive metabolites known as leucoaziridinomitosenes. Leucoaziridinomitosenes contain two electrophilic sites at the C(1) and C(10) positions which are selectively attacked by two guanosines on complementary strands of DNA, thereby resulting in cross-link formation and cell death. Much has been learned about the complex mechanism of action of these compounds, but a better understanding of their mechanisms of action and biological origins is required in order to produce more potent and less cytotoxic synthetic analogs.

The leucoaziridinomitosene derived from the semisynthetic derivative FK317 was targeted for total syntheses. The tetracyclic core of the target was accessed via intramolecular Michael addition of a chiral lithioaziridine into a vinylogous amide. Temporary protection of a stabilizing formyl group, reduction of an enoate, and subsequent transformation of the resulting alcohol provides the free C(10) carbamate. The C(10) carbamate of the intact leucoaziridinomitosene proved to be extremely labile as it was lost under acidic, basic, and neutral conditions which were explored to remove the final aziridine protecting group. Surprisingly, in contrast to the mitomycin leucoaziridinomitosenes, C(10) heterolysis of the FR leucoaziridinomitosenes was more facile than C(1) heterolysis. Nonetheless, a fully functionalized leucoaziridinomitosene derivative of FK317 was obtained.

In order to probe the related biosynthetic pathways of mitomcyin C and FR900482, a mitosane derivative that could be a common precursor of both structural families was targeted for synthesis. Multiple strategies for tetracycle construction focused on addition of a

lithioaziridine into an appropriate electrophile. The successful strategy employed a palladium catalyzed coupling of a 3,6-diazabicyclo[3.1.0]hexan-2-one to a functionalized aryl triflate, followed by diastereoselective cyclization to the desired stereoisomer of the tetracycle via carbanion addition into an appended lactam. The top face of the tetracycle is blocked by the large aziridine protecting group, which should facilitate diastereoselective reductive cleavage of a C(9) leaving group from the bottom face of the tetracycle to form the required C(9) stereochemistry. These studies culminated in the successful synthesis of a fully functionalized 9-oxo-pyrrolo[1,2a]indole mitosane derivative of the mitomycins and FR compounds.

Chapter 1.

The Antitumor Antibiotic Mitomycins and FR Compounds

The Anticancer Antibiotic Mitomycin Family

The mitomycins are a well known family of natural products first discovered in the 1950s which exhibit antitumor and antibiotic activity. Mitomycin A and B (Figure 1-1, **1**,**2**) were isolated in 1956 by Hata and coworkers from the fermentation broth of *Streptomyces caespituous*.[1] Two years later, Wakaki and coworkers isolated mitomycin C (**3**) from the fermentation broth of the same organism (Figure 1-1).[2] The methylated analog of **3** named poriformycin (**4**) was isolated from *Streptomyces verticillatus*.[3] These four natural products represent the first known examples of the mitomycin family.

The structure of the mitomycins is quite unique among anticancer antibiotics. Structure elucidation studies of **1** using chemical degradation, UV spectroscopy,[4] and X-ray crystallography[5] showed the presence of an aziridine ring fused to a pyrrolo[1,2a]indole and aminobenzoquinone. Since **1** could be converted into **3** upon treatment with methanolic ammonia,[4a] structures **2-4** were assigned by analogy. The unique scaffold of **1-4** was later confirmed by Kishi's total syntheses,[6] and the absolute stereochemistry was revised in 1983 using X-ray dispersion techniques.[7] These compounds were the first examples of aziridine containing natural products, and currently there are over 1000 synthetic analogs.[8]

The structurally unique fused aziridine pyrrolo[1,2-a]indole aminobenzoquinone core leads to a highly complex mechanism of action responsible for cellular toxicity. In order to

understand the relationship between structure, antitumor activity and mechanism of action, the mitomycins have been the subject of intense study over the past half century.[9]

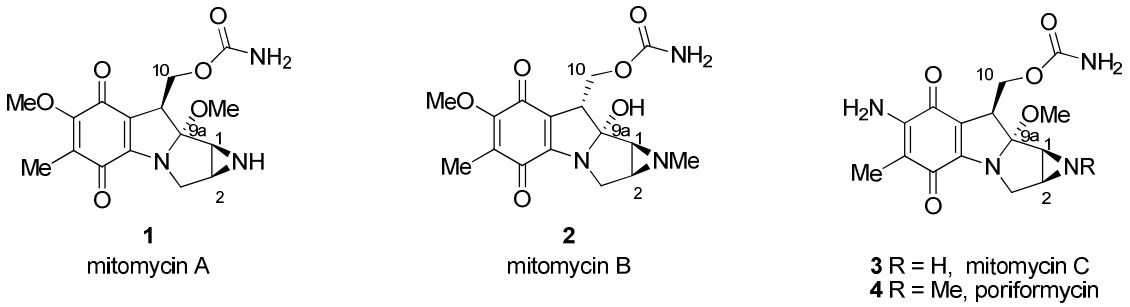

1 mitomycin A

2 mitomycin B

3 R = H, mitomycin C
4 R = Me, poriformycin

Figure 1-1. Mitomycins A, B, C and Poriformycin

During initial bioactivity studies it was found that both **1** and **3** had good antitumor activity *in vivo* with dose ranges between 8-1000 µg/kg.[1,2] However, the LD_{50} values for **1** and **3** in mice were found to be 2.0 mg/kg and 5.0 mg/kg respectively; therefore, **3** is considered the "safer" cytotoxic agent. Ultimately, **3** became the best mitomycin candidate for clinical trials.[10] It was found that hypoxic cancer cells (low O_2 tension and a reducing environment) are particularly sensitive to **3** at low doses,[11] while non-hypoxic cancer cells and non-cancerous cells also become sensitive to **3** at higher dose levels.[12] Since these initial activity studies, the effective dose ranges and dosing schedule for **3** have been optimized, and mitomycin C has been shown to be clinically effective in treatment against a number of cancers.[13] However, even at therapeutic doses **3** can cause bone marrow suppression and gastrointestinal damage. Consequently, it is generally used as a last resort against cancers that do not respond well to more conventional treatments such as radiation. Therefore, Mitomycin C, marketed by BMS as Mutamycin®, has been a chemotherapeutic agent for the past forty years and is still used to treat breast, non-small cell lung, and head and neck cancers when used in combination therapy.[14]

An ultimate goal of the study of the mitomycins is the generation of synthetic analogs that have better selectivity for cancerous cells over non-cancerous cells but without the severe toxic side effects.[9b,9c,11] Achieving this goal is unlikely without a thorough understanding of the mechanism of action of these structurally unique heterocycles. A multitude of mechanistic and

metabolite characterization studies show that the mechanism of action is quite complex. Four main metabolites of **3** have been isolated upon exposure of DNA to **3** in cell cultures, and under various conditions *in vitro*. The main metabolites isolated are the bis-alkylated DNA lesion **5**,[15] the monoalkylated DNA lesions **6**[16] and **7**,[17] and a reduced species 2,7-diaminoaziridinomitosene **8**[18] (Scheme 1-1). The formation of each metabolite is indicative of a different form of activation of the mitomycin. Therefore, the mechanism of activation leading to and the formation of each species will be discussed separately below.

Scheme 1-1. Main DNA adducts of **3**

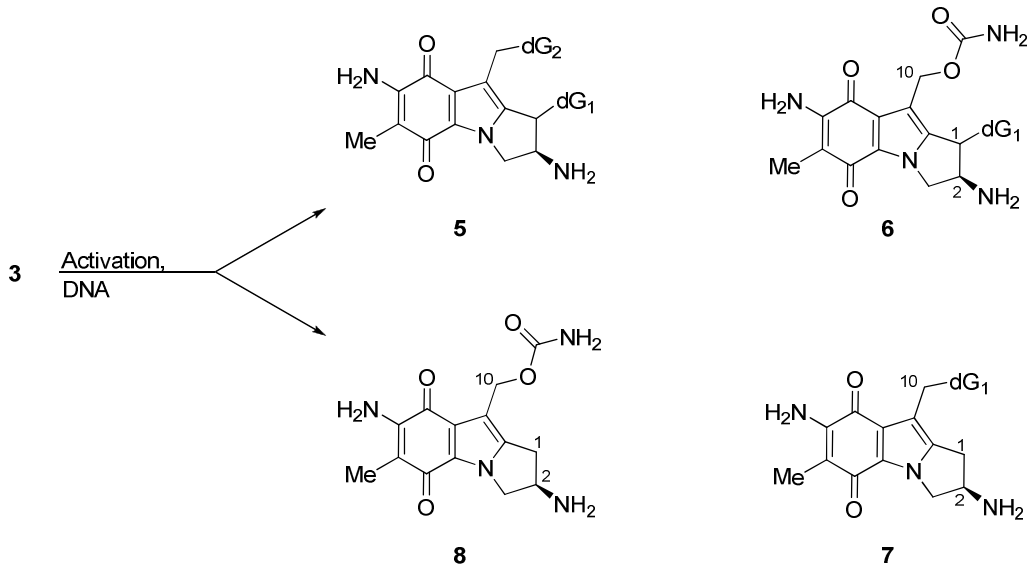

Events Leading to DNA Cross-linking by Mitomycin C

Mitomycin C is a highly active anticancer and antibacterial agent due to its ability to form interstrand DNA cross-links. Although the reduction of the aminobenzoquinone of the mitomycins can lead to the generation of destructive super oxide radicals, hydrogen peroxide, and hydroxy radicals which cause single strand breakage,[19-21] the cytotoxic event leading to cellular death is actually the formation of interstrand DNA cross-links.[22] Interstrand cross-links impede the replication fork and thereby halt replication of the DNA, ultimately resulting in cell death.[23] These cross-links result in thermally stable double stranded DNA that "spontaneously" reanneals under denaturing conditions. However, mitomycin C does not react with purified DNA until it

has been activated with a reducing enzyme or chemical reductants via a 2 electron reduction or two 1 electron reductions.[22-25] Once the mitomycin is reduced, a mechanistic cascade initially proposed by Iyer and Szybalski is started that ultimately leads to a metabolite capable of cross-linking DNA (Scheme 1-2).[24] Initial 2 electron reduction of **3** leads to the hydroquinone leucomitomycin **9**. Loss of the angular methoxy group followed by tautomerization to the indole forms the leucoaziridinomitosene **10** (so named due to loss of the methanol from C(9) and C(9a)).[4a,24,26] In metabolite **10, t**he two latent electrophilic sites of **3**, the aziridine and C(10) carbamate,[26] are activated for heterolysis.

It has been shown that the C(1) position is the first reactive site[27] and derivatives without the aziridine present do not retain the described DNA alkylating activity.[28] Ring opening of the aziridine ring is facilitated by release of ring strain and stabilization of the resulting "benzylic" carbocation at C(1) in the quinone methide **11**.[26] Once the alkylation at C(1) of **11** occurs, the C(10) carbamate is displaced in an S_N1 manner by the indole nitrogen lone pair.[29,30] The second alkylation event can then occur at C(10). Cross-linking of DNA occurs when an appropriately positioned deoxynucleoside of one DNA strand alkylates at C(1) followed by attack at C(10) by a deoxynucleoside on the complementary strand. Thus, the two electrophilic sites at C(1) and C(10) of **3** are essential for cross-linking activity.

The proposed active metabolite **10** was found to be extremely reactive and unstable.[24] Due to the transient nature of the bis-alkylating metabolite, it cannot be isolated or characterized. However, various mechanistic investigations and characterization of the isolated DNA-**3** adducts provide evidence that supports the proposed mechanism of action. In efforts to elucidate the properties and structure of this bis-alkylating agent, the reactivity of reduced **3** in the presence of exogenous nucelophiles was investigated. Hornemann and coworkers found that reduction of **3** with $Na_2S_2O_4$ in the presence of potassium ethylxanthate provided the bis-alkylated products **15b, 16b** and monoalkylated products **15a** and **16a** (Scheme 1-3).[31] The monoadduct was favored with fewer equivalents of the reducing agent, and it could be converted to the bis-adduct upon

retreatment with $Na_2S_2O_4$. This was the first chemical evidence that the reduced mitomycin could alkylate at both the C(1) and C(10) positions. Furthermore, the adducts were isolated in approximately a 1:1 *cis*:*trans* ratio suggesting that ring opening of the aziridine is an acid catalyzed S_N1 process.

Bean and Kohn found that ethyl monothiocarbonate was also an effective nucleophile for C(1) and C(10) attack (Scheme 1-3, **15c**, **15d**, **16c**, **16d**).[32] They could favor monoadduct formation to give **15c** and **16c** by lowering the temperature. Again, the isolation of both *cis* and *trans* isomers supports S_N1 ring opening of the aziridine. Although these studies showed that C(1) and C(10) acted as electrophilic sites under reductive activation, the isolation and characterization of a cross-linked DNA adduct by Tomasz in the 1980s finally confirmed the mechanistic proposal made twenty years earlier.[15a]

Scheme 1-2. Reductive activation and alkylation of **3** by guanine nucleosides (dG)

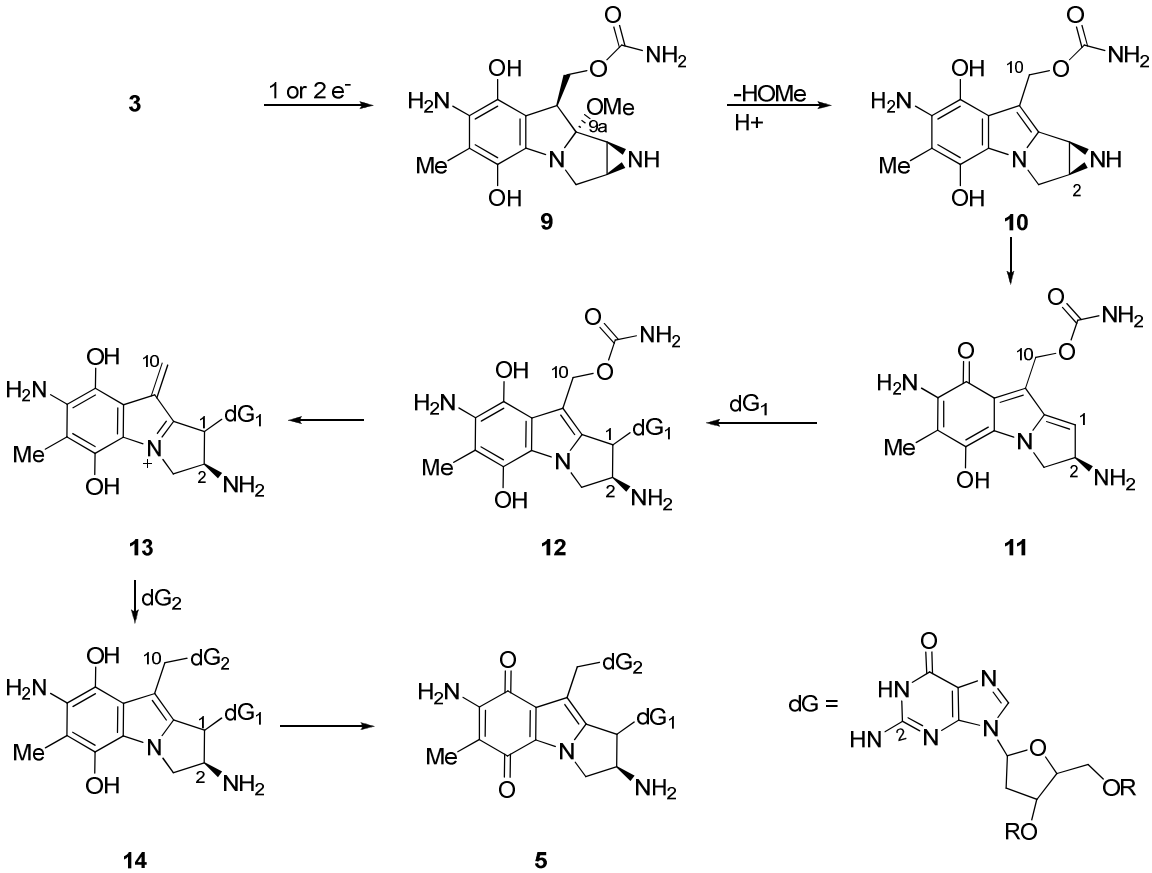

Scheme 1-3. Mono- and Bis-alkylation of reduced **3** with exogenous nucleophiles

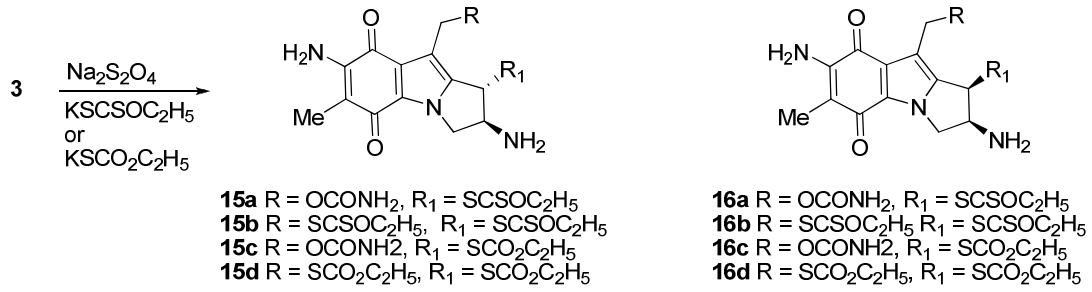

The cross-linked DNA lesion **17a** was obtained upon reduction of **3** with $Na_2S_2O_4$ in the presence of *Micrococcus luteus* DNA.[15a] Analysis of the peracetylated lesion **17b** by ^{1}H NMR spectroscopy, UV spectroscopy and FTIR showed that C(1) and C(10) had been attacked by the exo amino (N2) moiety of two deoxyguanosines (Figure 1-2). Notably, Iyer and Szybalski reported in earlier studies that DNA with a higher percentage of CG base pairs had a greater occurrence of cross-link formation.[24] Furthermore, three independent studies confirmed that cross-link formation is specific for the 5′CG3′ sequence.[33-35] Using computer constructed molecular models and examination of the van der Waals contacts Tomasz and coworkers observed a snug fit of the tetracyclic core of **3** into the minor groove of DNA resulting in only minor perturbation of the backbone.[15a] Surprisingly, Tomasz and coworkers found that reductively activated **3** can form intrastrand cross-links at the 5′GpG3′ sequence *in vitro*; however, there is a preference for interstrand cross-link formation (Figure 1-2).[15b] Thus, the long awaited isolation of the bis-alkylated DNA lesion of mitomycin C gave direct chemical proof of cross-link formation as proposed by Iyers and Szybalski.

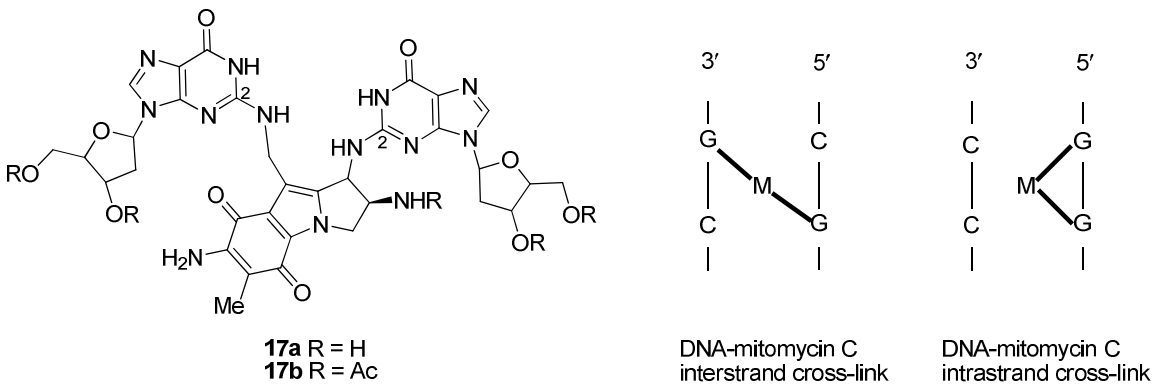

Figure 1-2. DNA lesion of **3**, and schematic of interstand and intrastrand cross-linking.

Isolation of the DNA lesion cross-link confirms that reductively activated mitomycin C is a bis-alkylating agent at C(1) and C(10) capable of cross-linking complementary strands of DNA. However, the oxidation state of the bis-alkylating agent formed in the activation cascade of **3** has been the subject of much debate. Iyer, Szybalski, and others proposed that upon 2 electron reduction the nitrogen lone pair of the leucomitomycin facilitates expulsion of the angular methoxy group via iminium ion formation to start the activation process.[22-26,36] However, ^{1}H NMR studies by Danishefsky showed that the leucomitomycin **19** formed upon hydrogenation of mitomycin **18** in pyridine does not spontaneously expel methanol to form the leucoaziridinomitosene **20** (Scheme 1-4).[25,37] Furthermore, subsequent oxidation of **19** by air affords the parent mitomycin **18** without noticeable degradation.[37] When the 1 electron reducing agent ascorbic acid was used for reduction of **18**, the quinone **23** which had lost methanol was isolated upon air oxidation.[38] Initial formation of the semiquinone radical anion **21**, followed by loss of methanol and rearrangement would provide the semiquinone radical **22**. Finally, oxidation of **22** affords the observed product **23**.[38] This mechanism for expulsion of the angular methoxy group at the quinone anion radical oxidation state was supported by Kohn's observations that loss of methanol occurred upon 1 electron reduction of **3** in polar protic solvents under anaerobic conditions.[39]

Scheme 1-4. One electron reduction to initiate the activation cascade of *N*-methylmitomycin A

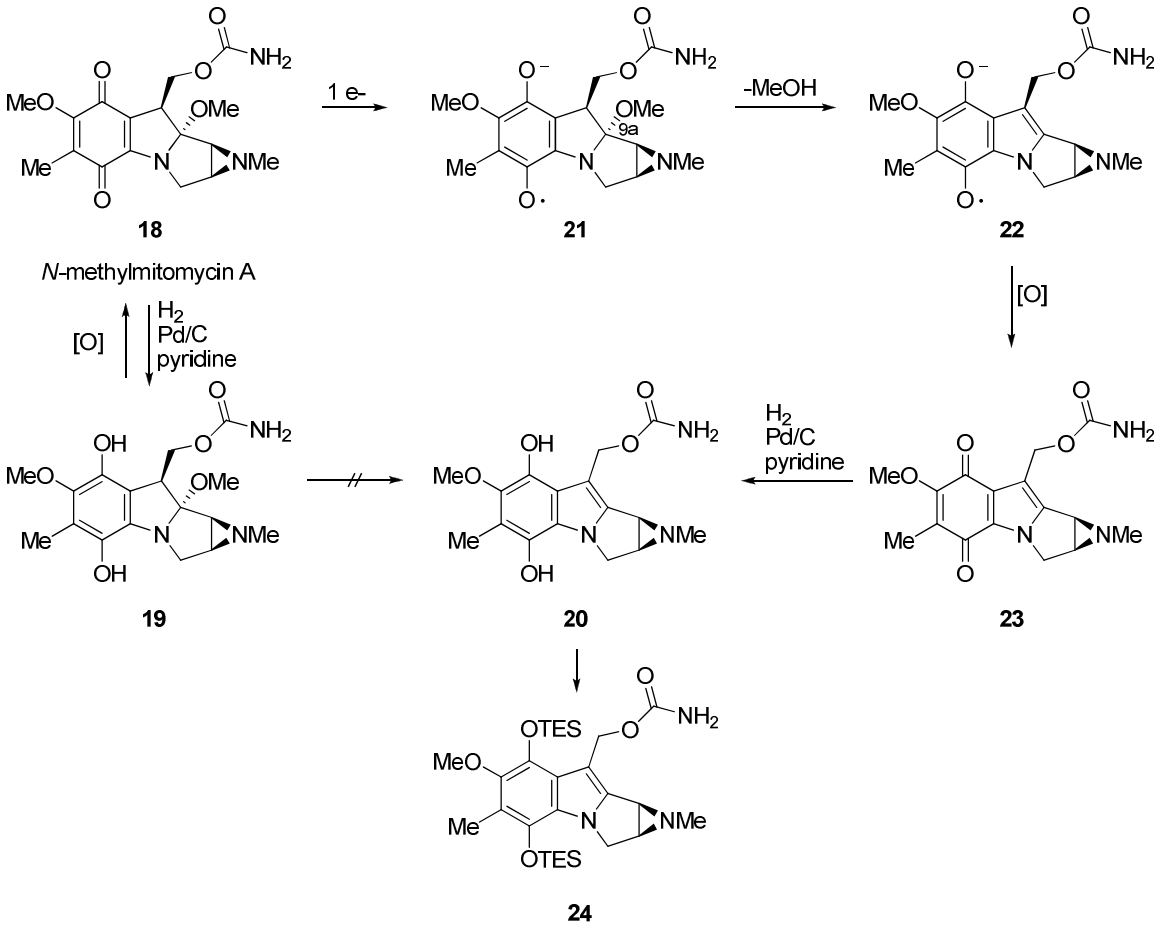

During the ^{1}H NMR spectroscopy studies of the reductive activation of the mitomycins, Danishefsky and coworkers observed the elusive leucoaziridinomitosene **20**.[40] Reduction of the aziridinomitosene **23** under hydrogenation conditions in pyridine provided the unstable **20**. Fortunately, **20** could be trapped as the isolable bis-triethyl silyl ether **24**. Notably, the successful generation of the putative bis-alkylating agent **20** allowed further mechanistic studies on the activation of the mitomcyins.

Since the semiquinone **21** was implicated in the expulsion of the C(9a) angular methoxy and therefore the start of the activation cascade, studies have tried to elucidate the possible role of the semiquinone in the alkylation events. Danishefsky found that the leucoaziridinomitosene **20** was not an efficient bis-alkylating agent when treated with potassium ethyl xanthate under

aqueous pyridine conditions. However, reduction of **23** using catalytic $Na_2S_2O_4$ did result in high yields of the alkylated products in aqueous pyridine.[40] Crothers et. al. found that two electron reduction of **18** in the presence of DNA, followed by 1 electron oxidation with $FeCl_3$ under anaerobic aqueous conditions provided a species that was a more efficient cross-linking agent than **20**.[41] Importantly, the possibility that the hydroquinone is also a bis-alkylating agent was not ruled out. However, controlled electrochemical reduction to either the semiquinone or the hydroquinone of **3** in dimethylformamide (DMF) showed that the semiquinone was more stable than the hydroquinone[25] consistent with Danishefsky's observation of the instability of **20**. Thus, evidence has been provided that the leucoaziridinomitosenes at the hydroquinone oxidation state are too unstable and too inefficient as an electrophile to be the main bis-alkylating agent responsible for DNA cross-link formation.[41]

Although the hypothesis that the bis-alkylating agent is at the semiquinone oxidation state (**22**) is quite intriguing, it has not been unambiguously confirmed. Other analytical methods used during the reductive activation of the mitomycins do not substantiate claims of semiquinone radical formation during ring opening of the aziridine; however, they do not discount the formation of semiquinones such as **21** or **22** *in vivo*.[42] Another puzzling observation by Hoey showed that dismutation of the semiquinone to the hydroquinone occurs before ring opening of the aziridine under aqueous buffer conditions.[43] These inconsistencies may be due to the use of organic media instead of physiological conditions during Danishefsky's and others work. As a result of the various observations, the debate about which oxidation state of the activated **3** is responsible for cross-linking is still ongoing.

Monoalkylation of DNA by Mitomcyin C

Many efforts were made to confirm the bis-alkylating nature of the reduced mitomycins as described above; however, cross-link formation is only one example of how mitomycins can cause DNA damage. Early studies with radioactively labeled **3** showed a greater amount of interaction of the drug with DNA than would be accounted for by the rare cross-link formation

proposed by Iyer and Szybalski.[44] In fact, monoalkylation of DNA is actually 10-20 times more prevalent than the lethal DNA cross-link.[44] Additionally, monoalkylated adducts block DNA polymerases from synthesizing DNA, and therefore, the monoadducts have moderate cytotoxicity.[45]

Reductively activated **3** is monoalkylated selectively by the exo amino (N2) group of a deoxyguanosine nucleotide at the 5′CG3′ sequence (Figure 1-3, **6**).[46] The high selectivity for this sequence is due to hydrogen bond formation between the C(10) O of **3** and a 3′ deoxyguanosine in the 5′CG3′ sequence, which directs the C(1) electrophilic site into the correct proximity for attack by a 5′ deoxyguanosine on the complementary strand.[34,47] The adjacent 3′ nucleotides downstream of the sequence also have a moderate to slight influence on monoalkylation selectivity of 5′CGN3′ sequences (C>T>G>A[47] or G>T, C>A[48]) although the exact selectivity has not been agreed upon. It is proposed that the high selectivity of the monoadduct for deoxyguanosine bases downstream of deoxycytosine bases is necessary for the sequence specificity of cross-link formation (Figure 1-3).[47]

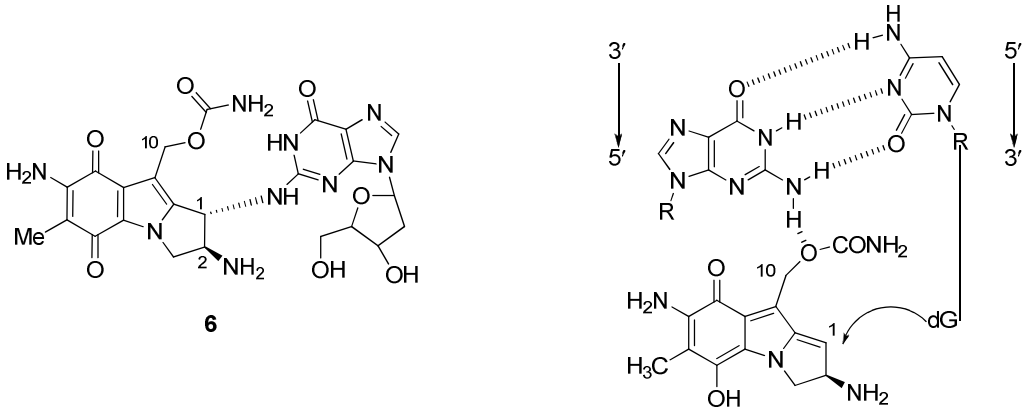

Figure 1-3. Monoalkylated adduct **6** and schematic of precomplexing hydrogen bonding

Since cross-link versus monoadduct formation is one of the factors determining the extent of toxicity of the mitomycins, an understanding of the factors that influence the formation of either DNA adduct is essential. Tomasz and coworkers observed the product distribution of the DNA adducts of **3** under various reduction conditions (Scheme 1-5).[27] It was found that product

distribution is dependent on the reduction kinetics, the presence of O_2, and pH.[49] Tomasz and others observed that the monoalkylation pathway proceeds under autocatalytic conditions.[50] Thus, in the presence of catalytic amounts of reductant, the bis-alkylating hydroquinone (or semiquinone) **10** is oxidized by excess **3** to form the leucomitomycin **9**, which loses methanol to reform **10**, and the aziridinomitosene **25**. Aziridinomitosene **25** is activated for alkylation at C(1), but not C(10). Attack at C(1) by N2 of the deoxyguanosine forms the monoadduct **6**. However, in the presence of larger amounts of reducing agent and at low pH, the formation of **6** was essentially shut down. It is known that cross-link formation is favored at acidic pH.[17b,35,51] Therefore, under acidic conditions excess reducing agent or enzyme allows the buildup of the bis-alkylating agent **10** which can then follow the bifunctional pathway to provide **14** and **26**. Importantly, the bis-alkylation pathway is shut down and the monofunctional pathway is promoted by bubbling O_2 through the system, implicating reoxidation of the monoadduct **12** before elimination of the C(10) carbamate occurs.[27] Additionally, the monoadduct **25** can be reactivated as a cross-linking agent with $Na_2S_2O_4$ to form the cross-link adduct **14**,[27] although this reactivation probably doesn't occur *in vivo* due to steric issues.

Scheme 1-5. Mono-alkylation vs. Bis-alkylation pathways

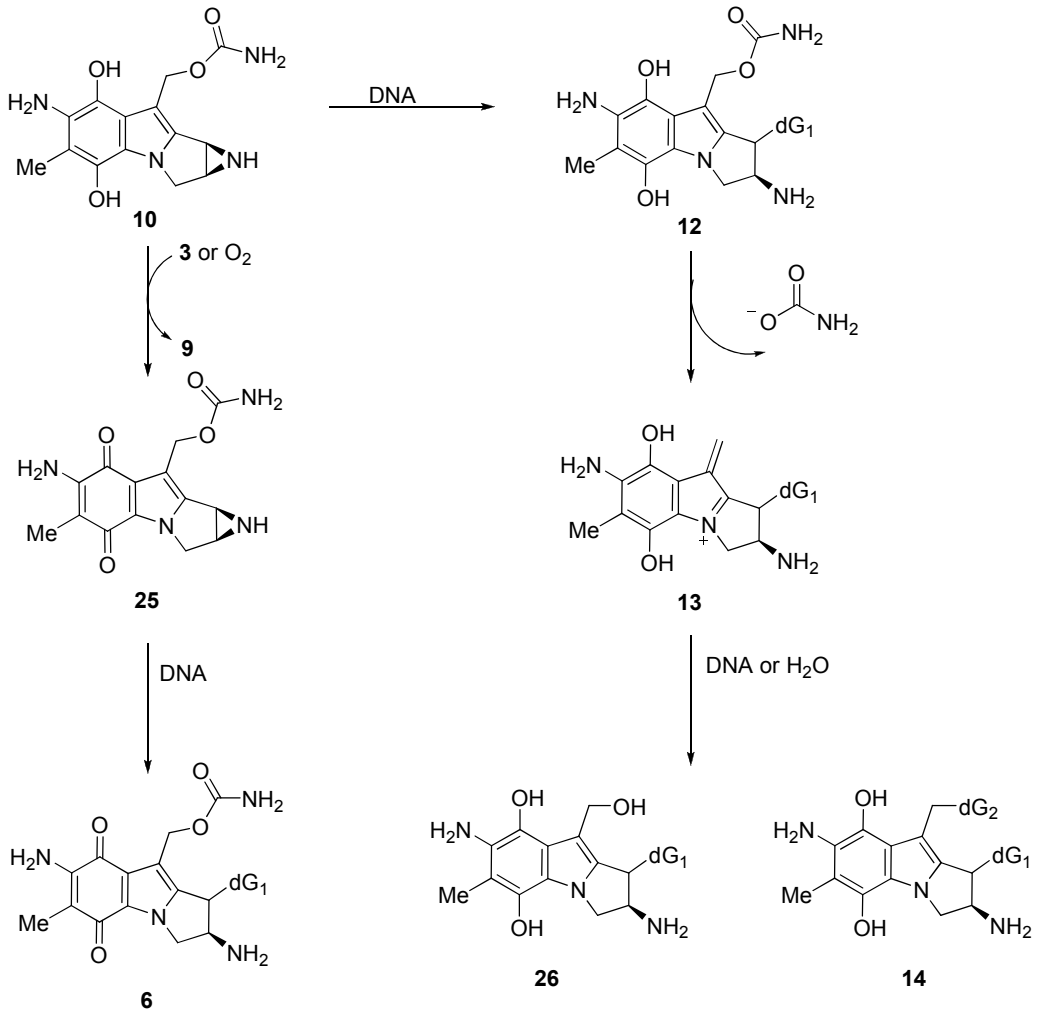

Aziridinomitosenes such as **25** were first isolated by Patrick and coworkers as degradation products of the parent mitomycins.[36] Consistent with the mechanistic outline presented above, they were found to have similar reactivity patterns to the parent mitomycins under reductive conditions. In contrast to the parent mitomycins however, they are more susceptible to C(1) solvolysis with a half life of only 3 min at pH 7.0 (Scheme 1-6: **27a**,**27b**).[52] Furthermore, **25** can monoalkylate DNA *in vitro* without reductive activation (**27c**).[53] However, the C(10) carbamate of **25** is not activated for alkylation as shown by the formation of **27d** upon treatment of **25** with aniline at high pH.[54] Therefore, monofunctionalization of aziridinomitosene **25** at C(1) is favored at high pH in the presence of a strong nucelophile.

Scheme 1-6. C(1) alkylation of aziridinomitosene **25**

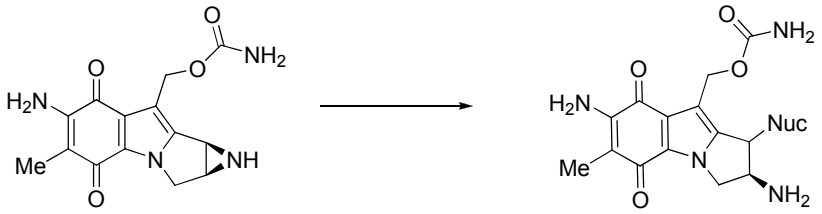

Activation of the C(10) carbamate of the mitomycins and aziridinomitosenes is required for formation of DNA cross-links. Evidence suggests that the activation at C(10) occurs by an S_N1 mechanism via the stable hydroquinone iminium ion **13** (Scheme 1-5).[29] Displacement of the C(10) carbamate is favored at the hydroquinone stage due to the increased electron density of the hydroquinone and mitosene nitrogen. On the other hand, consistent with the mechanism for monoalkylation described above, displacement of the carbamate of the quinone via an S_N1 mechanism would be inhibited due to the presence of the strong electron withdrawing quinone. The S_N1 mechanism of alkylation at C(10) is supported by the observation that the 10-decarbamoyl analog of **3** cannot form DNA cross-links upon reductive action[27] thereby implying that a good leaving group at C(10) such as carbamate is necessary.

Formation of 2,7-Diaminomitosene and its DNA adduct

The third major metabolite of DNA alkylation with **3** is the ring opened product 2,7-diaminomitosene (2,7-DAM) (**8**) and its monofunctional DNA adduct **7** (Scheme 1-7).[17,18,55] Exclusive formation of **8** is observed at low pH (5.5) in the absence of nucelophiles via an electrophilic substitution process.[54] Under acidic conditions, the quinone methide **11** is capable of trapping a proton at C(1) due to the electron density of the C(5) phenol. This tautomerization restores the quinone functionality, thereby affording **8**. However, in the presence of strong nucleophiles such as aniline or DNA, the quinone methide is trapped at C(1) and then the trapped metabolite is funneled to cross-link or monoalkylation pathways.[49] The propensity for trapping of

11 by nucelophiles suggests that formation of 2,7-DAM occurs if **11** is not close enough to DNA for cross-link formation.[54]

Scheme 1-7. Formation of the 2,7-DAM **8** and the DNA monoadduct **7**.

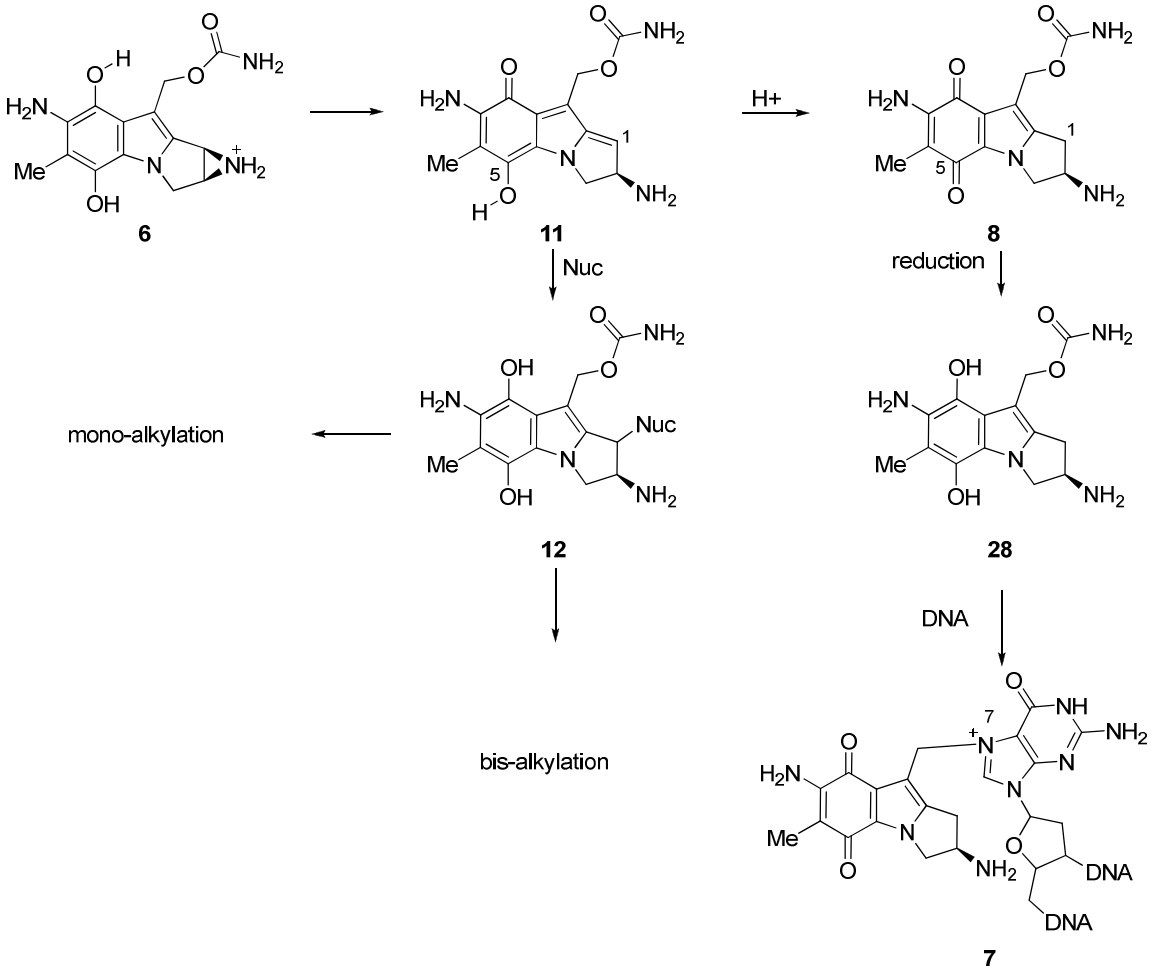

Formation of 2,7-diaminomitosene and subsequent alkylation at C(10) to form **7** was found to be the major pathway of reductive metabolism of the mitomycins.[55,56] The adduct **7** was first observed by Prakash et. al..[17b] They noted that the new adduct was thermally labile, and in stark contrast to the other DNA adducts, lesion **7** was formed by alkylation of the less reactive C(10) moiety by the N7-amine of deoxyguanosine (Scheme 1-7, **7**) in the major groove of the double helix.[17b] The monoadduct **7** is obtained by treating **3** or **8** and DNA *in vitro* with the two electron reducing enzyme DT-diaphorase at pH levels below 7. As described above, this observation suggests that **8** is a metabolite of **3**, which upon further reduction is reactive at C(10)

for monoalkylation. Significantly, it was found that the C(10) carbamate of the reduced 2,7-DAM is displaced by the strongly nucleophilic N7 residue in an S_N2 process instead of a S_N1 process.[17a] Furthermore, formation of **8** was promoted at low **3**:DNA ratios in *in vitro* model studies. DNA adduct **7** is responsible for much of the damage induced by **3**; however, it is less cytotoxic towards cells under hypoxic and aerobic conditions than the analogous adducts of mitomycin C.[56] Consequently, formation of the 2,7-DAM monoadduct **7** is considered a detoxification metabolic pathway of the mitomycins.[54]

Summary of Mitomycin C Activation

Based on the studies of Tomasz, Kohn, Danishefsky and others, the different activation pathways for the mitomcyins can be summarized (Scheme 1-8).[49] Mitomcyin C is reductively activated to the leucomitmycin (or semiquinone) **9** via a one or two electron process. Loss of methanol then provides leucoaiziridinomitosene **10**. At this stage the pathways can diverge depending on the conditions. Under catalytic reduction conditions and high pH, **10** will reduce **3** and be converted into the aziridinomitosene **25**. Activation of the C(1) electrophilic site and subsequent ring opening and alkylation lead to the monoalkylation adducts. When **3** is fully reduced and under acidic conditions, the leucoaziridinomitosene is activated for ring opening. Charge delocalization leads to a longer lifetime of the ring opened quinone methide **11**, which can attack an acidic proton at C(1). A second reduction to **28** then activates the C(10) position for alkylation by the N7 of dexoyguanosines. In the third pathway, the C(1) position is alkylated by the nucleophilic N2 of a deoxyguanosine forming **12**, followed by activation of the C(10) carbamate and displacement to lead to cross-link **5**. This summary of the three mechanistic pathways of **3** is a testimony to the complexity of the activation cascade of the mitomycins *in vivo* and *in vitro*. The ultimate goal of understanding the mechanism of action of **3** is to obtain the ability to fine tune the specificity and reactivity of DNA alkylating agents in order to design more efficient drugs for anticancer use.[9]

Scheme 1-8. Summary of three activation pathways of mitomycin C.

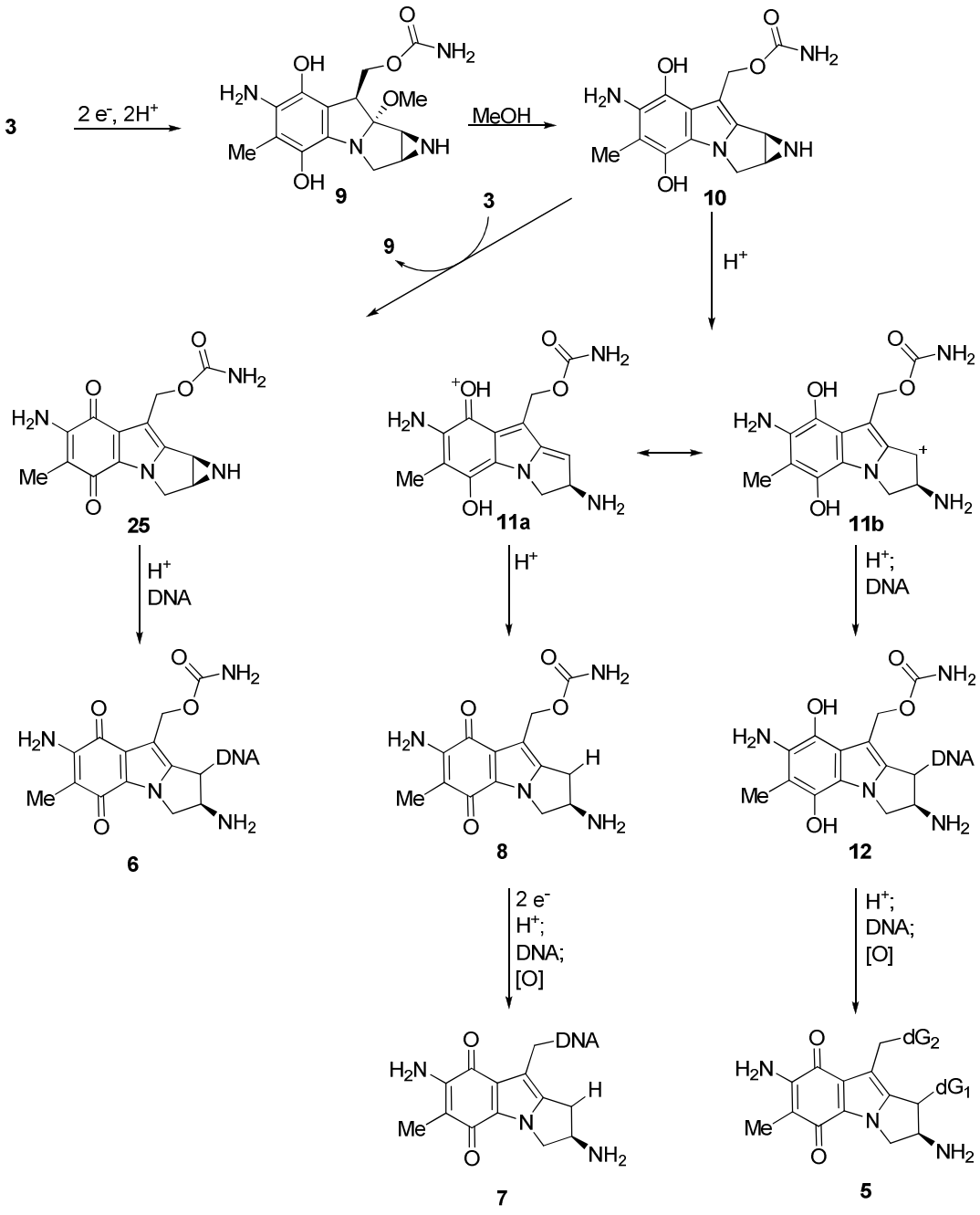

The Antitumor Antibiotic FR Family of Compounds

In the mid 1980's a new class of compounds was isolated from the fermentation broths of *Streptomyces sandaensis* by scientists at the Fujisawa Pharmaceutical Company during an endeavor to find efficient antitumor antibiotics. The natural product FR900482 **29** was isolated

as a mixture of isomers that equilibrate when separated.[57] Based on chemical derivation, ^{1}H NMR studies, and X-ray crystallography the structure was shown to contain a unique hydroxylamine hemi-aminal imbedded in a dihydrobenzoxazine core.[58] Furthermore, **29** shares the unique aziridine and carbamate functionality with the mitomycins, but does not possess the bioactive quinone moiety. A dihydro congener of **29** denoted FR66979 (**30**) was also isolated from *S. sandaensis*.[59] In initial activity studies, **29** was found to have similar or better activity than the clinically used mitomycin C against some cancer cell lines, without the severe thrombocylopenic and myelosuppressive side effects associated with mitomcyin C.[57c,57d] Studies also showed that **29** was active against mitomycin C resistant P388.[57c] Structural similarities of **29** and **30** to **3** led to the hypothesis that these novel antitumor antibiotics also form interstrand DNA cross-links. Furthermore, it was found that FR900482 inhibits the synthesis of DNA and RNA presumably through cross-link formation, but does not induce DNA single strand breakage like mitomycin C.[60] Due to the equal or better activity and generally weaker side effects, the FR compounds were considered viable alternatives to the widely used antitumor antibiotic **3**.[57d]

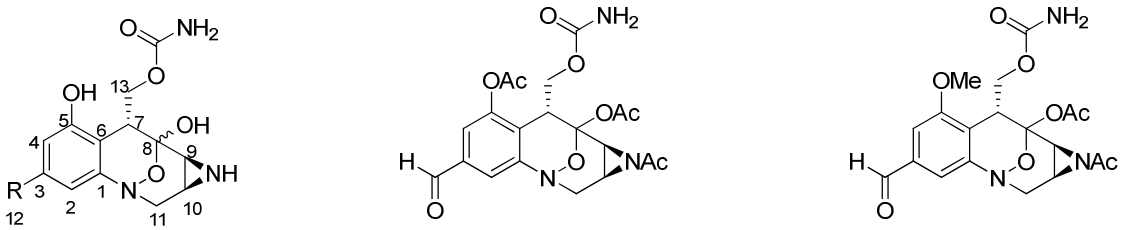

Figure 1-4. The FR antitumor antibiotics

In an effort to increase the efficacy of these antitumor antibiotics, synthetic analogs of FR900482 were synthesized and tested. The triacetylated semi-synthetic derivative FK973 (**31**) was the most promising candidate.[61] It was found to have better or equal activity and to be more stable than **29**, and to have better or equal activity with a larger dose range than mitomycin C *in vitro*.[62] Comparison studies between **3** and **31** showed that both caused dose dependent inhibition of cancerous cells; however, unlike **3** which had full potency immediately upon addition of

cancerous cells, **31** required an induction period for efficient activity.[63] Furthermore, it was found that **31** did not have activity against isolated nuclei.[63] These combined results suggest that FK973 requires activation in the cytoplasm of the cell before it can alkylate DNA. Since **31** was the most promising candidate, it was advance to phase 1 clinical studies; unfortunately, FK973 was dropped from clinical studies when it was found to induce the severe side effect of vascular leak syndrome (VLS).[64]

An understanding of the mode of action of the FR compounds is essential to designing analogs that do not cause severe side effects but still retain high levels of activity. The structural similarities of **29-31** to **3** led to the hypothesis that the FR compounds cross-link DNA via an aziridinomitosene analogous to that which is formed in the mitomcyin series (Scheme 1-9). Fukuyama and Goto proposed that the aziridinomitosene is unmasked by 2 electron reduction of the N-O bond to form the benzazocinone **33**, followed by subsequent condensation (**34**), dehydration (**35**), and aromatization (**36**).[65] Heterolytic cleavage of the hydroxylamine hemi-aminal induced by nucleophilic attack at C(2) has also been proposed,[66] although it has not been widely accepted. Isolation of the dihydroindole **39** upon reductive activation of **30** *in vitro* supports the intermediacy of the hemi-aminal **34** and iminium ion **35** en route to the activated structure.[67] In contrast to the mitomycins the presence of iron salts is required for efficient activation of the FR compounds *in vitro*; the strong reductant $Na_2S_2O_4$ does not efficiently activate the FR compounds in the absence of iron salts.[67] Finally, the isolation and characterization of the peracetylated DNA lesion of **40** obtained after treatment of DNA with **30** substantiates the proposal that the FR compounds undergo bioreductive activation to aziridinomitosene analogs (Figure 1-5).[68]

Scheme 1-9. Bioreductive activation cascade for FR-66979 **30**

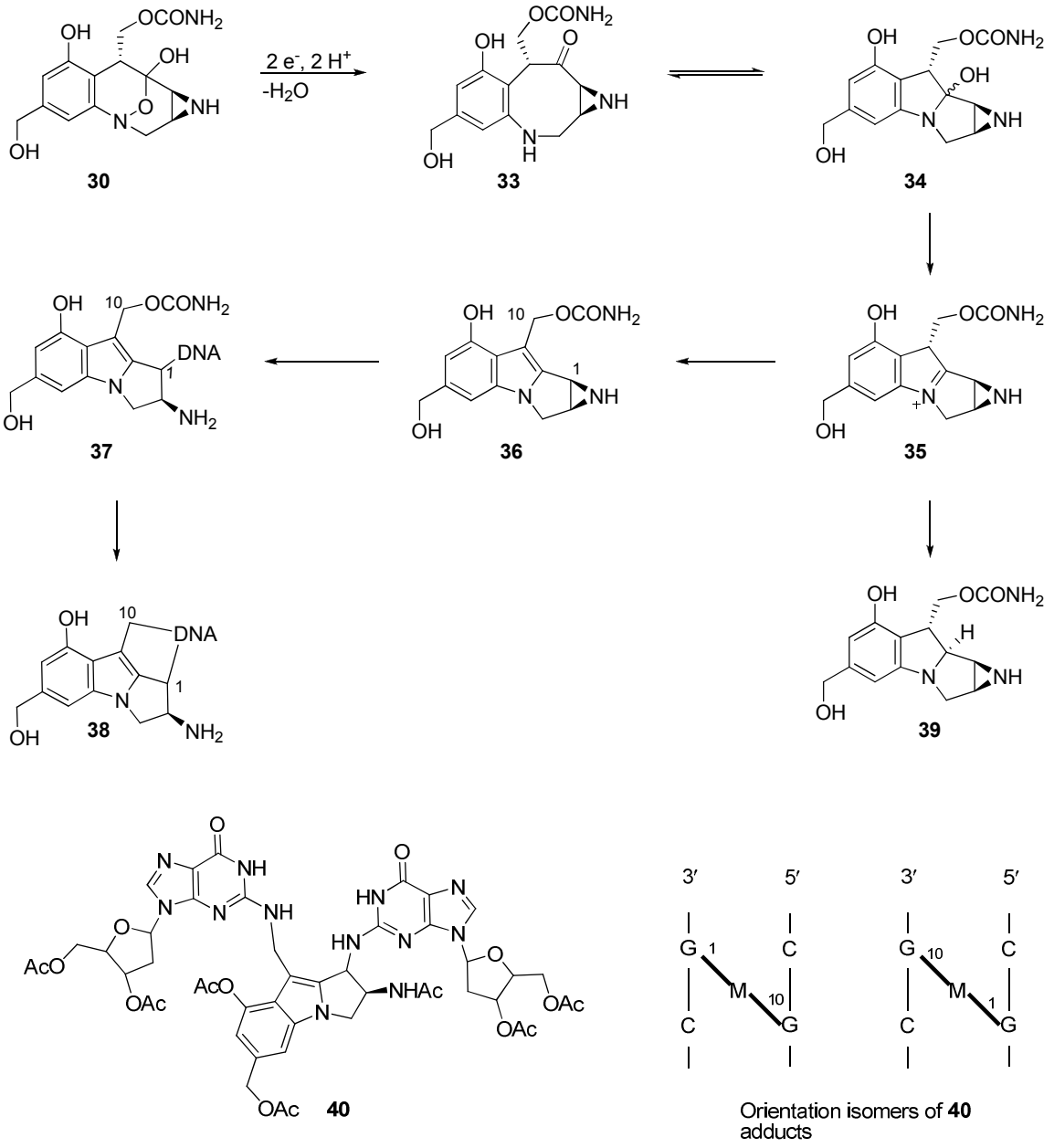

Figure 1-5. Isolated peracetylated DNA lesion of **30** and schematic of orientation isomers

The lesion **40** shows a high degree of similarity to the DNA lesion formed by mitomycin C (Figure 1-5). The C(1) position and C(10) position are covalently linked to the N2 amine of the deoxyguanosine residues, and the dihydrobenzoxazine has been reduced to an indole or mitosene (mitomycin nomenclature and numbering). As expected based on the mitomycin analogy, the FR compounds are specific for the 5′CG3′ sequence as shown by inhibition of cross link formation

when a deoxyguanosine is replaced by a deoxyinosine.[69] Furthermore, cross-links are formed in the minor groove, and the distance between the two amine moieties on the guanosines matches the distance between C(1) and C(10).[70] Williams and Rajski found that two cross-link orientation isomers with dramatically different electrophorectic mobilites are also possible (Figure 5).[70] Isolation of the cross-linked lesions proves that DNA-alkylation is, at least in part, responsible for the complex biological profile of these interesting heterocycles.

As with the mitomycins the FR compounds are also capable of monoalkylating DNA. The selectivity for monoalkylation at the 5′CG3′ site is 5-fold less than the selectivity of the analogous mitomycin C adduct.[71] This decrease in selectivity is indicative of an absence of the precomplexing hydrogen bond necessary for the observed selectivity of the mitomycins. However, Williams proposes that some selectivity is still present due to a precomplexing hydrogen bond between the phenol at C(8) and the N3 group of guanosine on the non-bonding strand (Figure 1-6).[70] On the other hand, Hopkins attributes the decrease in selectivity of monoalkylation to a more reactive quinone methide **41** formed upon ring opening of the aziridine. Hopkins proposes the electrophilicity of quinone methide **11** is attenuated by the presence of the electron donating phenol, while the lack of the analogous electron density in quinone methide **41** increases the electrophilicity of the intermediate and therefore reduces its selectivity.[71] Interestingly, mass spectrometry analysis of the monoadducts obtained by Hopkins via thiol mediated reduction of **30** showed thiol incorporation consistent with alkylation at C(10).[71] Further studies on this intriguing result suggest that monoalkylation by the FR compounds is not on the cross-linking pathway. Furthermore, the decreased selectivity of monoadduct formation and displacement of the C(10) carbamate of the monoadduct may be factors contributing to the different activity and cytotoxicity of the FR compounds.

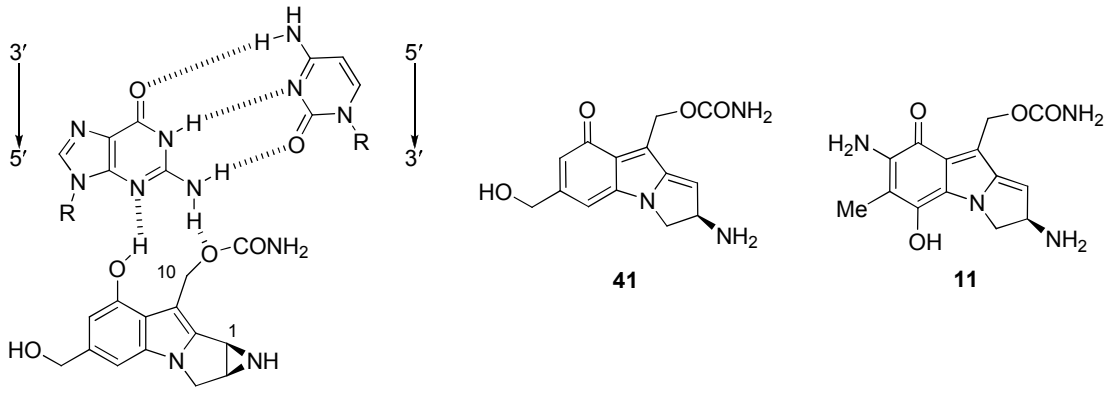

Figure 1-6. Hydrogen bonding facilitating monoalkylation and quinone methides **41** and **11**

The Promising Semi-synthetic Candidate FK317

After **31** was dropped from phase 1 clinical trials, a new semi-synthetic analog of **29** was advanced. The semi-synthetic analog FK317 **32** is a di-acetylated intermediate which has a methoxy group at the C(8) position instead of a phenol (Figure 1-4).[72] Reduction of **32** to the presumed aziridinomitosene analog is required in order for it to cross-link DNA. The 2 electron reducing enzyme DT-diaphorase present at high levels in some cancer cell lines has been implicated as the enzyme responsible for reduction.[72] As with **31**, FK317 has equivalent or better activity than FR900482 and mitomycin C *in vivo*, and FK317 has activity against multidrug resistant cell lines *in vitro*.[72] Initial studies found that FK317 is deacetylated in the cytoplasm of the cell before it is bioreductively activated.[72c] The deacetylation is a key factor in FK317 activity against multidrug resistant cells because the membrane bound efflux p-glycoprotein present in cancer cells cannot interact with the metabolite to remove the drug from the cell.[72b]

In contrast to FR compounds **29** and **31**, FK317 did not lead to VLS in a rat model.[73] The mode of cell death induced by **29** and **32** has been implicated as a factor leading to VLS. The parent **29** induces necrotic cell death at all concentration levels, and necrotic cell death is marked by swelling of the cytoplasm and eventual rupture of the cell membrane.[74] Ultimately, cell membrane rupture of multiple cells and/or tissues undergoing necrotic cell death leads to inflammation responses. However, FK317 induces necrotic cell death at low doses but apoptotic

cell death at high doses.[74] In apoptotic cell death, the cytoplasm shrinks and the apoptotic bodies that bleb off are engulfed by phagocytes, which prevents inflammation.[75] Furthermore, research shows that FR900482 enhances the expression of the Bcl-2 protein which inhibits apoptotic cell death.[74] This switch in mode of cell death is especially intriguing since the proposed active structure of **29** and **31** only differ at one carbon (C(8)).

After multiple studies, various inconsistencies between the mechanism of action of FK317 and the other FR congeners, and the mechanism of action of the mitomycins have become apparent. First, FK317 is selective for the 5′CG3′ site, but it cannot undergo precomplexation via hydrogen bonding between the C(8) methoxy (mitomycin numbering) and a guanosine nucleotide which was proposed for **29** and **30** and which is essential for mitomcyin C.[76] The C(8) methoxy group cannot donate a hydrogen bond to the N3 position of a guanosine in order to properly align the compound for alkylation at C(1). However, based on the selectivity and reactivity of FK317, the methoxy group is sufficiently electron rich to activate the C(1) bond for alkylation (Scheme 1-10). Secondly, recent studies on fully synthetic analogs of the FR compounds that contain a C(10) hydroxymethyl group show that the C(10) carbamate is not essential for efficient cross-link formation.[77] Furthermore, recent observations show that monoalkylation followed by DNA-protein cross-linking in nucleosomal DNA is more prevalent than interstrand cross-linking.[78] All of these observations suggest that the activation and mechanism of action of the FR compounds are more complex than originally proposed.

Scheme 1-10. Activation of FK317 **32**

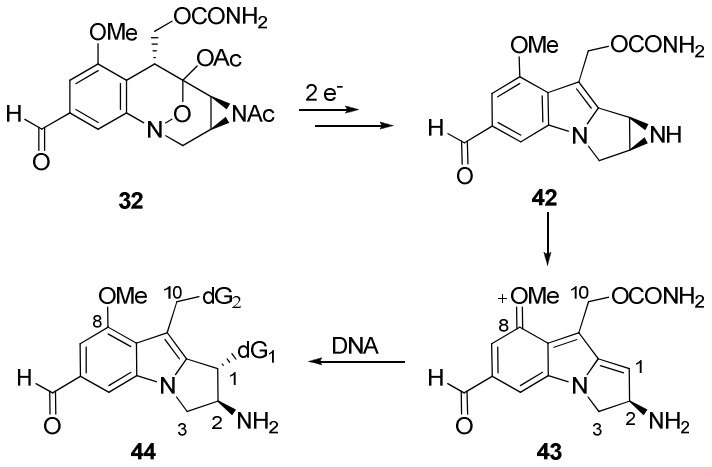

Asymmetric Syntheses of Aziridinomitosenes Derived from the FR compounds

Multiple strategies have been used for the synthesis of the aziridinomitosene tetracyclic core. Five previously described enantioselective approaches to the tetracyclic core of the aziridinomitosenes will be discussed below. The syntheses presented below fall into one of two categories: formation of the aziridine at a late stage, or installation of the intact aziridine early in the synthesis. It is worth noting that the majority of the examples discussed access the aziridinomitosene core without the proper oxidation state at C(10) (mitomycin numbering), and in only two examples is the deprotected aziridinomitosene obtained. This reflects the difficulties of handling the fully functionalized aziridinomitosenes and is a testimony to the inherent instability of these functionally dense tetracycles.

Sulikowski and coworkers showcased metal carbene chemistry to form the mitosene core (Scheme 1-11).[79] They began with conversion of the known chiral pyrrolidine **45**[80] to the deprotected pyrrolidine **46**. Palladium catalyzed amination with 2-bromoiodobenzene **47** provided the *N*-arylated pyrrolidine **48**.[81] Coupling of the aryl bromide with silylketene acetal **49** provided aryl acetate **50**. Acetate **50** was then converted in 9 steps to the diazoacetate precursor carbamate **51**. Carbamate **51** was smoothly converted to the diazoester **52** in good yield. After examining three sets of reaction conditions, it was found that treating **52** with copper (I) triflate in

the presence of ligand **53** provided good conversion to the mitosenes **54** and **55** (9:1) after oxidation with chloranil. The major regioisomer resulted from carbine insertion via path a, and the minor was formed via path b. The desired isomer **54** was then converted to the tosyl-protected aziridinomitosene **56** in 3 steps and good yield. Although this was an intriguing way to obtain the mitosene core, many steps were required to install the *cis* carbamate with the correct absolute stereochemistry necessary for diazo transfer on **52**.

Scheme 1-11. Sulikowski's synthesis of the aziridinomitosene **56**

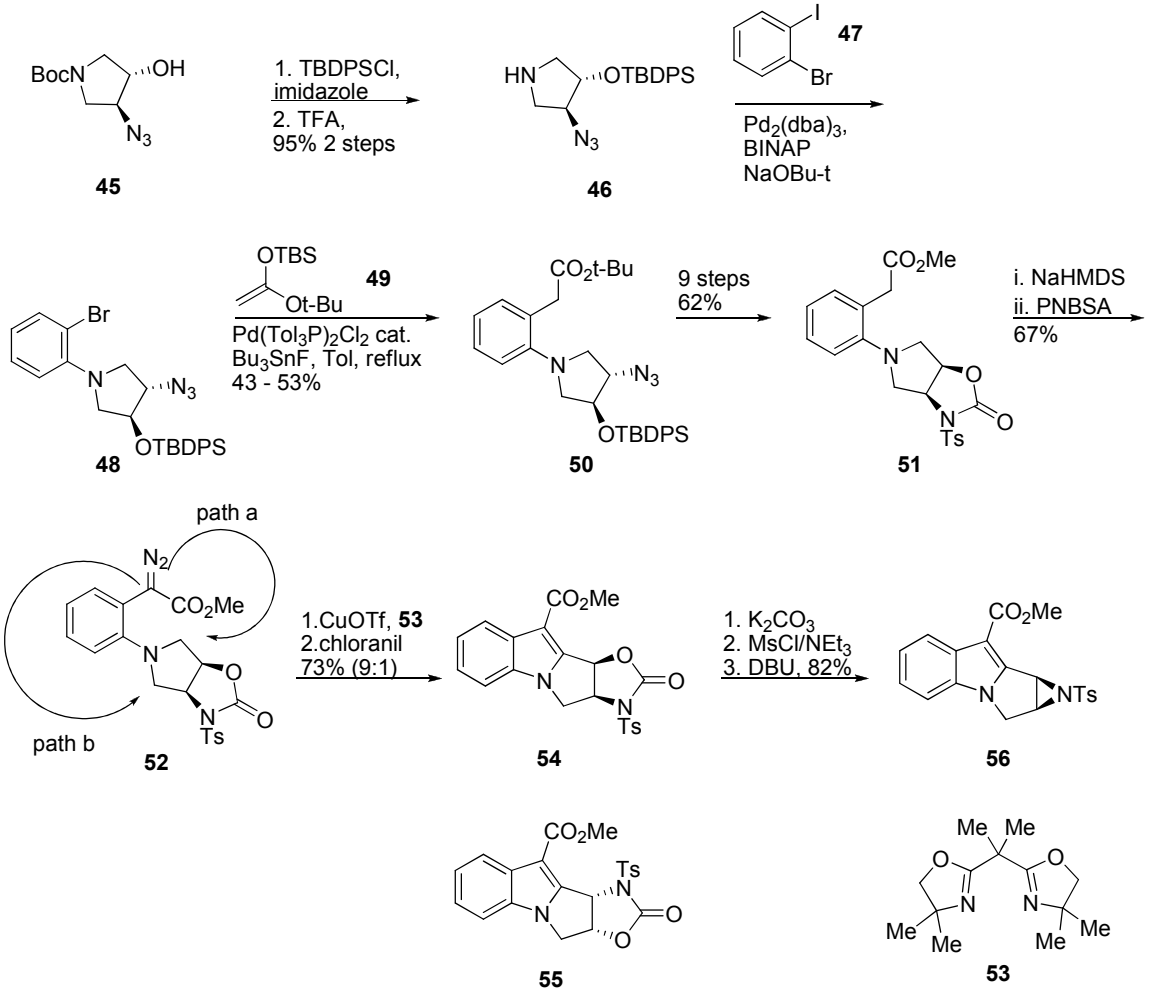

A second approach by Michael and coworkers targets the mitosene by Heck arylation chemistry.[82] Their synthesis began with the known chiral (–)-2,3-*O*-isopropylidene-D-erythronolactone **57**.[83] Lactone **57** was converted to *N*-aryl lactam **58** in good yield over three

steps. Conversion of the amide into the thioamide **59** was followed by conversion into the vinylogous amide **60** using an atypical Reformatsky reaction. Intramolecular Heck arylation, originally developed by Rappaport for the synthesis of aziridinomitosenes derived from the mitomycins[84] using $Pd(OAc)_2$ in the presence of triphenylphosphine and a complex mixture of solvent, base and additive, provided the mitosene **61** in excellent yield. The acetal **61** was converted to the azido alcohol **62** over three steps, and then converted into an azido mesylate and reduced in the presence of trimethyl phosphite to provide the phosphoramidate **63**. Notably, reduction of the mesylate under standard Staudinger conditions afforded an unprotected aziridinomitosene **64** described by the authors as unstable.

Scheme 1-12. Michael's Heck arylation to form tetracycle **63**

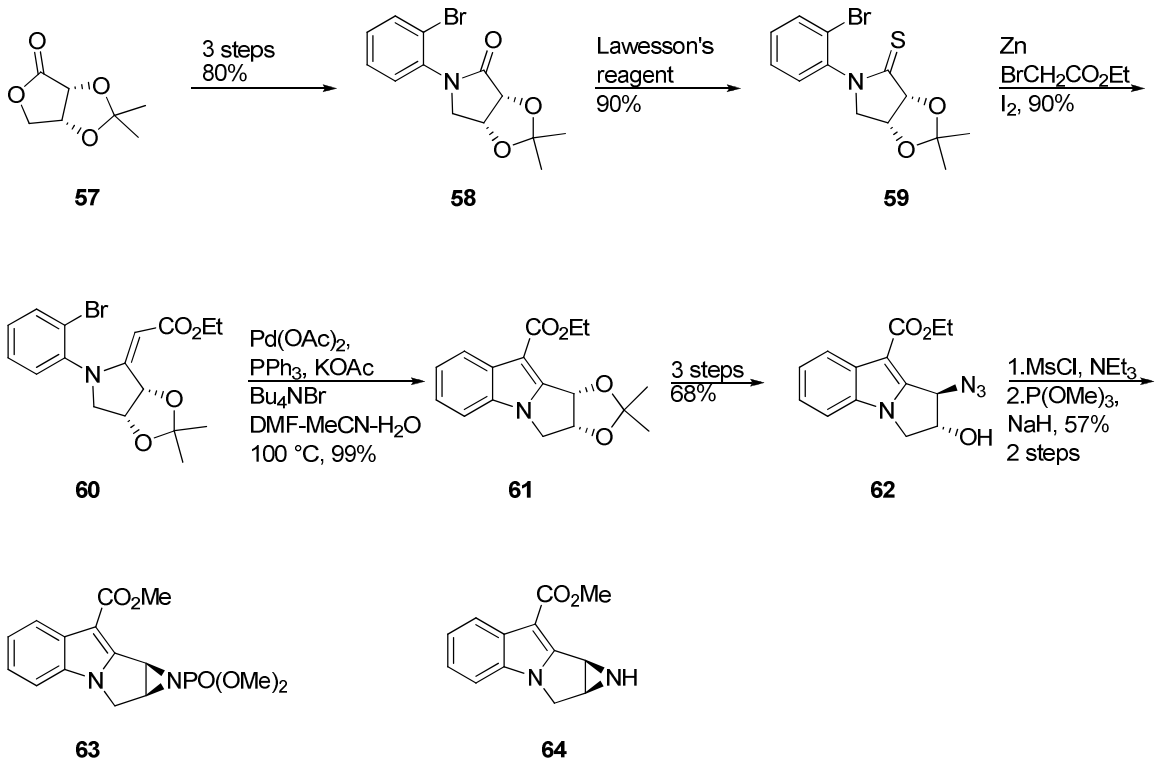

The asymmetric synthesis of the aziridinomitosene core via peptide catalyzed azide conjugate addition was reported by Miller in 2004.[85] Starting with commercially available alcohol **65**, Miller synthesized diene **66** in 6 steps (Scheme 1-13). Ring closing metathesis using

ruthenium alkylidene complex **67**,[86] and subsequent deprotection and oxidation of the allylic alcohol provided enone **68**. Tertiary-amine base catalyzed azidation of enone **68** with trimethylsilyl azide and a peptide catalyst provided the conjugate addition product **69** in good yield and modest enantioselectivity (88% yield, 35% ee). Conversion of the ketone to the mitosene **70** proceeded in moderate yield over four steps. Bromination to an azido-bromide followed by reductive ring closing was unsuccessful as the unprotected aziridinomitosene **71** proved to be unstable. However, nitration of the C(6) position followed by bromination and reductive ring closing provided the desired unprotected aziridinomitosene **72** in modest yield.

Scheme 1-13. Miller's asymmetric synthesis of unprotected aziridinomitosene **72**

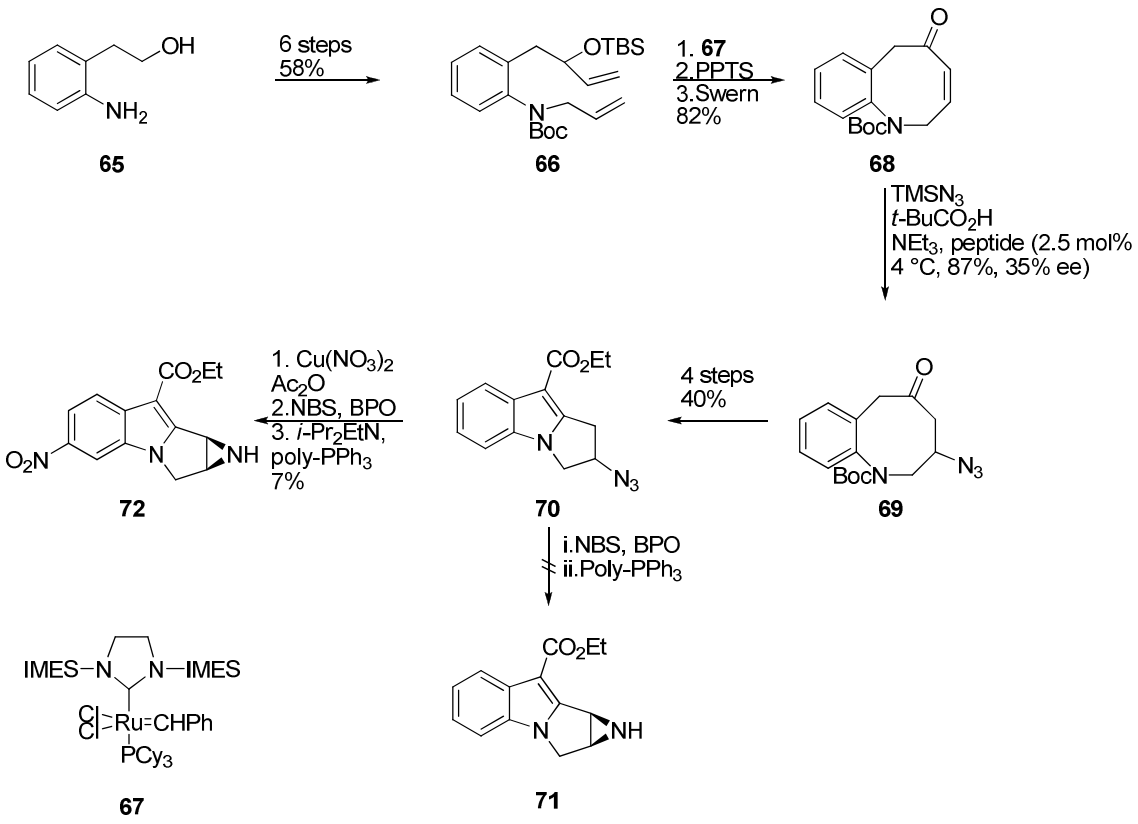

Ziegler and coworkers targeted an aziridinomitosene by the convergent coupling of an indole and aziridine subunit (Scheme 1-14).[87] The triflate aziridine **76** was synthesized in 6 steps from chiral epoxide **73**.[88] The glycidate **73** was protected as a silyl ether, ring opened with NaN_3, and the resulting azido alcohol was cyclized under reduction conditions with PPh_3 to provide **74**

in 57% yield over the three steps as a separable mixture of *trans:cis* isomers (12:1). The *trans* isomer of **74** was protected with di-*tert*-butyl dicarbonate to provide the protected aziridine **75**. Removal of the silyl ether with TBAF followed by conversion of the alcohol to the triflate provided the electrophilic aziridine **76**. The *in situ* generated **76** was then treated with the 3-cyanoindole **77** under basic conditions to provide the coupled product **78** in good yield (72%). The methyl carboxylate was saponified with LiOH and converted to the thiohydroxamic acid anhydride **79**. Ziegler and coworkers envisioned a stereoselective radical cyclization via a chiral aziridinyl radical addition into the indole core. In the event, photolysis of **79** with a 500 W tungsten halogen lamp provided a complex mixture of products including the dimer **80**. Disproportionation of **80** under photolysis conditions with a medium pressure Hanovia Hg lamp provided the desired indole **81** in 22% yield. Although the yields were poor and the dimer formation was the major pathway, this strategy allows stereoselective formation of an aziridinomitosene. However, removal of the protecting group at the aziridine nitrogen and conversion of the nitrile into the correct C(10) oxygen were not discussed.

Scheme 1-14. Ziegler's convergent synthesis of aziridinomitosene **81**.

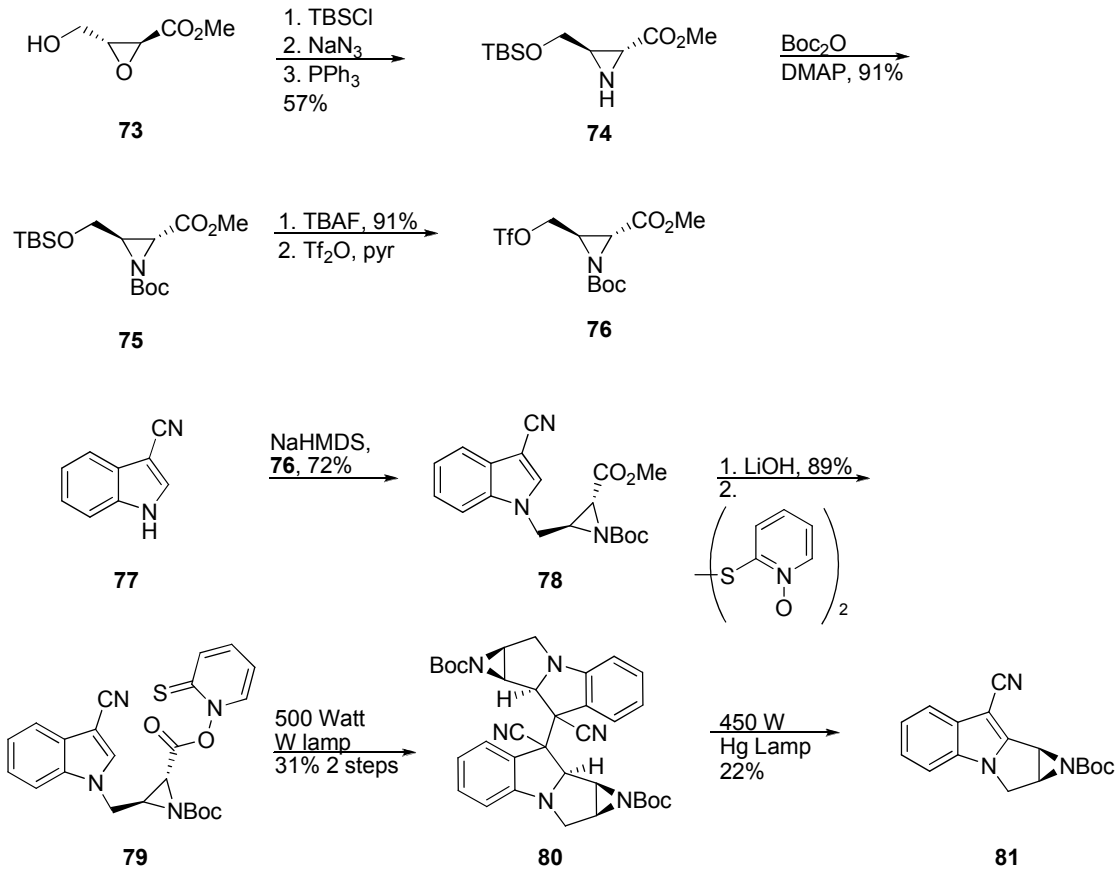

A second approach to aziridinomitosenes utilizing a chiral aziridine was developed by Vedejs and Little.[89] Beginning with the *N*-trityl L-serine methyl ester **82**, the chiral aziridine **83** was obtained in 35% yield over 7 steps.[90] Excess indole-3-carboxylic acid ethyl ester **84** was alkylated with nosylate **83** under basic conditions to provide the cyclized precursor **85**. Competitive deprotonation at C(2) (indole numbering) during attempted tin-lithium exchange inhibited efficient formation of the tetracycle. Therefore, the C(2) position was blocked with deuterium. Facile tin-lithium exchange with excess MeLi, cyclization to the tetracycle, and trapping of the enolate provided tetracycle **87** which re-aromatized upon workup to provide the aziridinomitosene **88**. The aziridinomitosene was found to be relatively stable under acid catalyzed reductive detritylation conditions thereby providing the *N*-H aziridinomitosene **89** in moderate yield.[91] In contrast to the system reported by Miller and Michael, this intermediate was

relatively stable. Alkylation of the aziridine nitrogen with methyl iodide installed the methyl group of **90**, and subsequent reduction of the enoate with excess $LiAlH_4$ afforded the hydroxymethyl group of aziridinomitosene **91**. Notably, the synthesis of **91** differs from the previous examples in that the C(9) and C(10) carbons are at the correct oxidation state of the aziridinomitosenes derived from the FR compounds.

Scheme 1-15. Vedejs and Little's asymmetric synthesis of the deprotected aziridinomitosene **91**

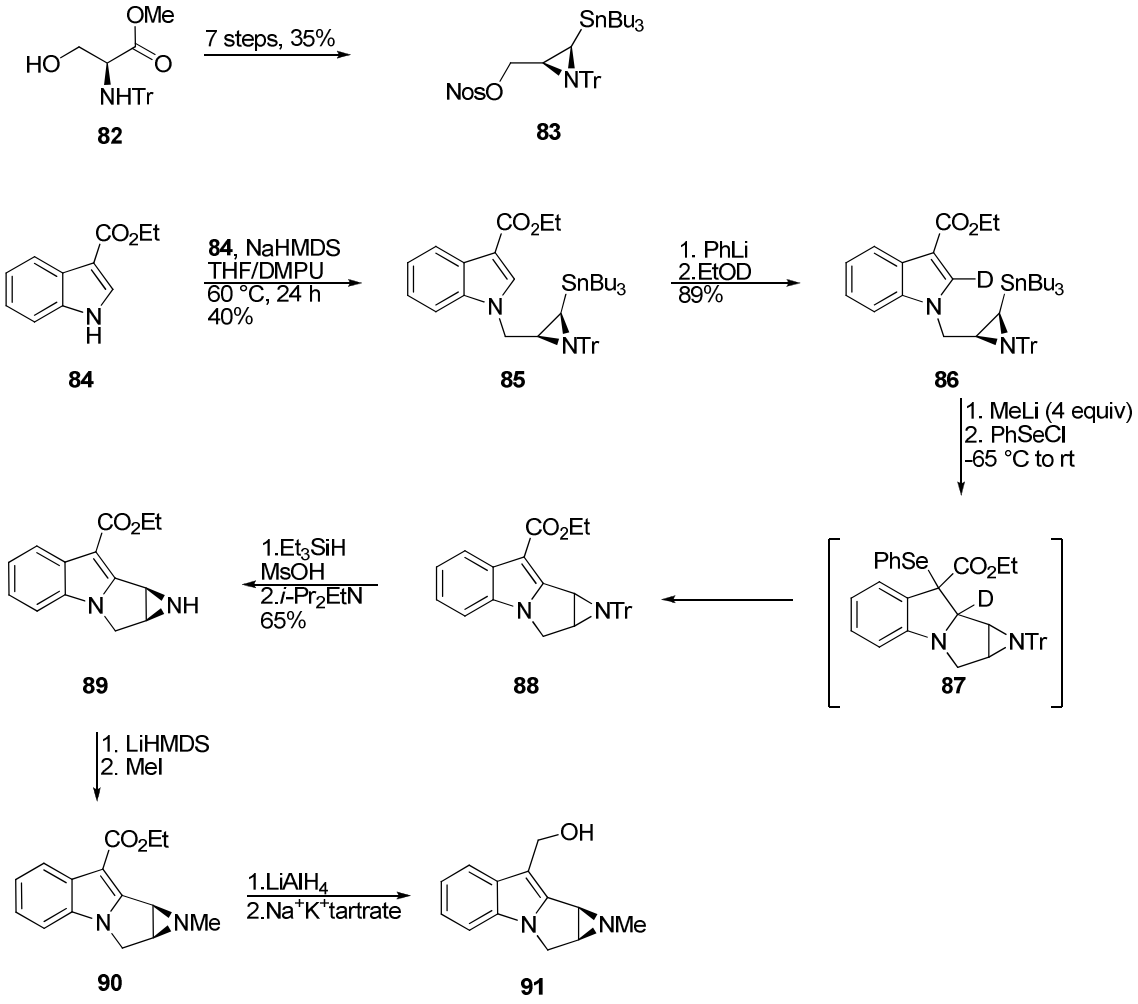

Summary

Since the initial discovery of the mitomycins over 50 years ago, and more recently the FR compounds, considerable effort has been devoted to the study of these compounds. Not only were they the first examples of aziridine containing natural products, but the high levels of

cytotoxicity are a direct result of the unique structure of each family. Extensive investigation of the mechanism of action has resulted in a better understanding of how these "prodrugs" exert their anticancer activity upon activation. However, elucidation of the role of various metabolites in the mechanism of action is warranted. The ultimate goal of such a study is the generation of less toxic anticancer drugs that can be activated under specific conditions to selectively attack cancerous cells over non-cancerous cells.

The putative aziridinomitosenes corresponding to the FR compounds have been targeted for total synthesis. However, the synthesis of the fully functionalized aziridinomitosene derived from FK317 (or the other FR compounds) has not been reported. The main hurdle to overcome in a successful synthesis of these functionally dense compounds with the correct oxidation state at C(9) and the unprotected aziridine is the instability of the fully functionalized system. The system is inherently reactive due to the high electron density of the core and the "benzylic" sites at C(1) and C(10). Most strategies circumvent this problem by installing the acid labile aziridine at a late stage. However, this often requires a large number of steps to install the aziridine with the correct stereochemistry.

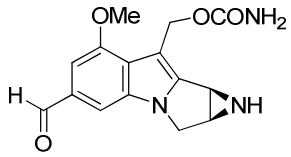

42

Figure 1-7. Target aziridinomitosene derived from FK317.

Ziegler et. al. and Vedejs and Little show that installation of the sensitive aziridine early in the synthesis is possible.[87,89] Furthermore, Little provides an example of an activated aziridinomitosene with a potentially labile hydroxymethyl group at C(10). Therefore, we have targeted the fully functionalized aziridinomitosene **42** derived from FK317 via a strategy analogous to that of Little.[92] However, new strategies will be required to install the potentially labile requisite functionality at C(10) and C(1). The synthesis of a fully functionalized advanced

aziridinomitosene will be described in Chapter 2. A successful synthesis of the putative active intermediate in the activation cascade of FK317 could lead to opportunities to explore the mechanism of these important anticancer antibiotics.

Chapter 1 Bibliography

1. Hata, T.; Sano, Y.; Sugawara, R.; Matsumae, A.; Kanamori, K.; Shima, T.; Hoshi, T. Mitomycin, A New Antibiotic from *Streptomyces. I. J. Antib. Ser. A.* **1956**, *49*, 141.

2. Wakaki, S.; Marumo, H.; Tomioka, K.; Shimizu, G.; Kato, E.; Kamada, H.; Kudo, S.; Fujimoto, Y. Isolation of New Fractions of Antitumor Mitomycins. *Antib*. & *Chem.* **1958**, *8*, 228.

3. Lefemine, D. V.; Dann, M.; Barbatschi, F.; Hausmann, W. K.; Zbinovsky, V.; Monnikendam, P.; Adam, J.; Bohonos, N. Isolation and characterization of mitomycin and other antibiotics by *Streptomyces verticillatus. J. Am. Chem. Soc.* **1962**, *84*, 3184.

4. (a) Webb, J. S.; Cosulich, D. B.; Mowat, J. H.; Patrick, J. B.; Broschard, R. W.; Meyer, W. E.; Williams, R. P.; Wolf, C. F.; Fulmor, W.; Pidacks, C.; Lancaster, J. The Structures of Mitomycins A, B, and C and Porformycin-Part I. *J. Am. Chem. Soc.* **1962**, *84*, 3185. (b) Webb, J. S.; Cosulich, D. B.; Mowat, J. H.; Patrick, J. B.; Broschard, R. W.; Meyer, W. E.; Williams, R. P.; Wolf, C. F.; Fulmor, W.; Pidacks, C.; Lancaster, J. The Structures of Mitomycins A, B, and C and Porformycin-Part II. *J. Am. Chem. Soc.* **1962**, *84*, 3187.

5.Tulinsky, A. The Structure of Mitomycin A. *J. Am. Chem. Soc.* **1962**, *84*, 3188.

6. (a) Nakatsubo, R.; Fukuyama, T.; Cocuzza, A. J.; Kishi, Y. Synthetic Studies Toward Mitomycins. 2. Total Syntheis of *dl*-Porfiromycin. *J. Am. Chem. Soc.* **1977**, *99*, 8115. (b) Fukuymama, T.; Nakatsubo, F.; Cocuzza, A. J.; Kishi, Y. Synthetic Studies Toward Mitomycins. III. Total Syntesis of Mitomycins A and C. *Tetrahedron Lett.* **1977**, 4295. (c) Kishi, Y. The Total Synthesis of Mitomycins. *J. Nat. Prod.* **1979**, *42*, 549.

7. Shirahata, K.; Hirayama, N. Revised Absolute Configuration of Mitomycin C. *J. Am. Chem. Soc.* **1983**, *105*, 7199.

8. (a) Arai, H.; Kanda, Y.; Ashizawa, T.; Morimoto, M.; , Gomi, K.; Kono, M.; Kasai, M. Synthesis and Antitumor Activity of Novel Mitomycin Derivatives Containing Functional Groups at the C-6-Methyl Position. *J. Med. Chem.* **1994**, *37*, 1794. (b) Bradner, W. T.; Remers, W. A.; Vyas, D. M. *Anticancer Res.* **1989**, *9*, 1095.

9. (a)Wolkenber, S. E.; Boger, D. L. Mechanisms of in Situ Activation for DNA-Targeting Antitumor Agents. *Chem. Rev.* **2002**, *102*, 2477. (b) Rajski, S. R.; Williams, R. M. DNA Cross-linking Agents as Antitumor Drugs. *Chem. Rev.* **1998**, *98*, 2723. (c) Tomasz, M.; Palom, Y. The Mitomcyin Bioreductive Antitumor Agents: Cross-linking and Alkylation of DNA as the Molecular Basis of Their Activity. *Pharmacol. Ther.* **1997**, *76*, 73. (d) Tomasz, M. Mitomycin C: Small, Fast, and Deadly (but Very Selective). *Chem. Biol.* **1995**, *2*, 575. (e) Kasai, M.; Kono, M. Studies on the Chemistry of Mitomycins. *Synlett.* **1992**, 778.

10. Frank, W.; Osterberg, A. E. Mitomycin C (NSC-26980)-An Evaluation of the Japanese Reports. *Can. Chemother. Rep.* 1960, *9*, 114.

11. Kennedy, K. A.; Teicher, B. A.; Rockwell, S.; Sartorelli, A. C. The Hypoxic Tumor Cell: A Target for Selective Cancer Chemotherapy. *Biochem. Pharmacol.* **1980**, *29*, 1.

12. Kennedy, K. A.; Rockwell, S.; Sartorelli, A. C. Preferential Activation of Mitomycin C to Cytotoxic Metabolites by Hypoxic Tumor Cells. *Cancer Res.* **1980**, *40*, 2356.

13. Crooke, S. T.; Bradner, W. T. Mitomycin C: a Review. *Cancer. Treat. Rev.* **1976**, *3*, 121.

14. Bradner, W. T. Mitomycin C: a Clinical Update. *Cancer Treat. Rev.* **2001**, *27*, 35.

15. (a)Tomasz, M.; Lipman, R.; Chowdary, D.; Pawlek, J.; Verdine, G. L.; Nakanishi, K. Isolation and Structure of a Covalent Cross-Link Adduct Between Mitomycin C and DNA. *Science* **1987**, *235*, 1204. (b) Bizanek, R.; McGuinness, B. F.; Nakanishi, K.; Tomasz, M. Isolation and Structure of an Intrastrand Cross-Link Adduct of Mitomycin-C and DNA. *Biochemistry* **1992**, *31*, 3084. (c) Bizanek, R.; Chowdary, D.; Arai, H.; Kasai, M.; Hughes, C. S.; Sartorelli, A. C.; Rockwell, S.; Tomasz, M. Adducts of Mitomycin –C and DNA in EMT6 Mouse Mammary-Tumor Cells-Effects of Hypoxia and Dicumarol on Adduct Patterns. *Cancer Res.* **1993**, *53*, 5127.

16. Tomasz, M.; Chowdary, D.; Lipman, R.; Shimotakahara, S.; Veiro, D.; Walker, V.; Verdine, G. L. Reaction of DNA with Chemically or Enzymatically Activated Mitomycin C: Isolation and Structure of the Major Covalent Adduct. *Proc. Natl. Acad. Sci. U.S.A.* **1986**, *83*, 6702.

17.(a) Kumar, G. S.; Musser, S. M.; Cummings, J.; Tomasz, M. 2,7-Diaminomitosene, a Monofunctional Mitomycin C Derivative, Alkylates DNA in the Major Groove. Structure and Base-Sequence Specificity of the DNA Adduct and Mechanism of the Alkylation. *J. Am. Chem. Soc.* **1996**, *118*, 9209. (b) Prakash, A. S.; Beall, H.; Ross, D.; Gibson, N. W. Sequence Selective Alkylation and Cross-linking Induced by Mitomycin C upon Activation by DT-Diaphorase. *Biochemistry* **1993**, *32*, 5518.

18. Chirrey, L.; Cummings, J.; Halbert, G. W.; Smyth, J. F. Conversion of Mitomycin C to 2,7-Diaminomitosene and 10-Decarbamoyl 2,7-Diaminomitosene in Tumor Tissue *in Vivo*. *Cancer Chemother. Pharmacol.* 1995, *35*, 318.

19. Pristos, C. R.; Sartorelli, A. C. "Generation of Reactive Oxygen Radicals Through Bioactivation of Mitomycin Antibiotics." *Cancer Res.* **1986**, *46*, 3528.

20. Lown, J. W. "Newer approaches to the Study of the Mechanisms of Action of Antitumor Antibiotics." *Acc. Chem. Res.* **1982**, *15*, 381.

21. (a) Bachur, N. R.; Gordon, S. L.; Gee, M. V. "A General Mechanism for Microsomal Activation of Quinone Anticancer Agents to Free Radicals." *Cancer Res.* **1978**, *38*, 1745. (b) Bachur, N. R.; Gordon, S. L.; Gee, M. V.; Kon, H. "NADPH Cytochrome P-450 Reductase Activation of Quinone Anticancer Agents to Free Radicals." *Proc. Natl. Acad. Sci. U.S.A.* **1979**, *76*, 954.

22. Szybalski, W.; Iyer, V. N. "Crosslinking of DNA by Enzymatically or Chemically Activated Mitomycins and Porfiormycins, Bifunctionally "Alkylating" Antibiotics." *Federation Proc.* **1964**, *23*, 946.

23. Iyer, V. N.; Szybalski, W. "A Molecular Mechanism of Mitomycin Action: Linking of Complementary DNA Strands." *Proc. Natl. Acad. Sci. U.S.A.* **1963**, *50*, 355.

24. Iyer, V. N.; Szybalski, W. "Mitomycins and Porfiromycin: Chemical Mechanism of Activation and Cross-linking of DNA." *Science* **1964**, *145*, 55.

25. Andrews, P. A.; Pan, S.; Bachur, N. R. “Electrochemical Reductive Activation of Mitomycin C.” *J. Am. Chem. Soc*. **1986**, *108*, 4158.

26. Moore, H. W. “Bioactivation as a Model for Drug Design Bioreductive Alkylation.” *Science* **1977**, *197*, 527.

27. Tomasz, M.; Chawla, A. K.; Lipman, R. “Mechanism of Monofunctional and Bifunctional Alkylation of DNA by Mitomycin C.” *Biochemistry*, **1988**, *27*, 3182.

28. Garrett, E. R. “The Physical Chemical Characterization of the Products, Equilibria, and Kinetics of the Complex Transformations of the Anitbiotic Porfiromycin.” *J. Med. Chem.* **1963**, *6*, 488.

29. Zein, N.; Kohn, H. “Electrophilic and Nucleophilic Character of the Carbon 10 Methylene Group in Miosenes Revealed.” *J. Am. Chem. Soc.* **1986**, *108*, 296.

30. Culvenor, C. C. J.; Dann, A. T.; Dick, A. T. “Alkylation as the Mechanism by Which the Hepatotoxic Pyrrolizidine Alkaloids Act on Cell Nuclei.” *Nature* **1962**, *195*, 570.

31. (a) Hornemann, U.; Iguchi, K.; Keller, P. J.; Vu, H. M.; Kozlowski, J. F.; Kohn, H. “Reactions of Mitomycin C with Potassium Ethyl Xanthate in Neutral Aqueous Solution.” *J. Org. Chem.* **1983**, *48*, 5026. (b) Hornemann, U.; Keller, P. J.; Kozlowski, J. F. “Formation of 1-ethylxanthyl-2,7-diaminomitosene and 1,10-diethyxanthyl-2,7-diaminodecarbamoylmitosene in Aqueous Solution Upon Reduction-Reoxidation of Mitomycin C in the Presence of Potassium Ethylxanthate.” *J. Am. Chem. Soc.* **1979**, *101*, 7121.

32. Bean, M.; Kohn, H. “Studies on the Reaction of Mitomycin C with Potassium ethyl monothiocarbonate Under Reductive Conditions.” *J. Org. Chem.* **1983**, *48*, 5033.

33. Millard, J. T.; Weidner, M. F.; Raucher, S.; Hopkins, P. B. “Determination of the DNA Cross-Linking Sequence Specificity of Reductively Activated Mitomycin C at Single-Nucleotide Resoltuion: Deoxyguanosine Residues at CpG Are Cross-Linked Preferentially.” *J. Am. Chem. Soc.* **1990**, *112*, 3637.

34. Borowy-Borowski, H.; Lipman, R.; Tomasz, M. “Recognition between Mitomycin C and Specfici DNA Sequences for Cross-Link Formation.” *Biochemistry* **1990**, *29*, 2999.

35. Teng, S. P.; Woodson, S. A.; Crothers, D. M. “DNA Sequence Specificity of Mitomycin Cross-linking.” *Biochemistry* **1989**, *28*, 3901.

36. Patrick, J. B.; Williams, R. P.; Meyer, W. E.; Fulmor, W.; Cosulich, D. B.; Broschard, R. W.; Webb, J. S. “Aziridinomitosenes: A New Class of Antibiotics Related to Mitomycins.” *J. Am. Chem. Soc.* **1964**, *84*, 1889.

37. Danishefsky, S.; Ciufolini, M. “Leucomitomycins.” *J. Am. Chem. Soc.* **1984**, *106*, 6424.

38. Danishefsky, S. J.; Egbertson, M. “On the Characterization of Intermediates in the Mitomycin Activation Cascade: A Practical Synthesis of an Aziridinomitosene.” *J. Am. Chem. Soc.* **1986**, *108*, 4648.

39. Kohn, H.; Zein, N.; Lin, X. Q.; Ding, J. –Q.; Kadish, K. M. “Mechanistic Studies on the Mode of Reaction of Mitomycin C under Catalytic and Electrochemical Reductive Conditions.” *J. Am. Chem. Soc.* **1987**, *109*, 1833.

40. Egbertson, M.; Danishefsky, S. J. “Modeling of the Electrophilic Activation of Mitomycins: Chemical Evidence for the Intermediacy of a Mitosene Semiquinone as the Active Electrophile.” *J. Am. Chem. Soc.* **1987**, *109*, 2204.

41.Cera, C.; Egbertson, M.; Teng, S. P.; Crothers, D. M.; Danishefsky, S. J. “DNA Cross-Linking by Intermediates in the Mitomycin Activation Cascade.” *Biochemsitry*, **1989**, *28*, 5665.

42. Rao, G. M.; Begleiter, A.; Lown, J. W.; Plambeck, J. A. “Electrochemical Studies of Antitumor Antibiotics. II. Polarographic and Cycli Voltammetric Studies of Mitomycin C.” *J. Electrochem. Soc.* **1977**, *124*, 199.

43. Hoey, B. M.; Butler, J.; Swallow, A. J. “Reductive Activation of Mitomycin C.” *Biochemistry* **1988**, *27*, 2608.

44.Weissbach, A.; Lisio, A. “Alkylation of Nucleic Acids by Mitomcyin C and Porfiromycin.” *Biochemistry*, **1965**, *4*, 196.

45. Basu, A. K.; Hanrahan, C. J.; Malia, S. A.; Kumar, S.; Bizanek, R.; Tomasz, M. “Effect of Site-Specifically Located Mitomycin C-DNA Monoadducts in Vitro DNA Synthesis by DNA Polymerases.” *Biochemistry* **1993**, *32*, 4708.

46. Tomasz, M.; Lipman, R. “Reassignment of the Guanine-Binding Mode of Reduced Mitomycin C.” *Biochemistry* **1986**, *25*, 4337.

47. Kumar, S.; Lipman, R.; Tomasz, M. “Recognition of Specific DNA Sequences by Mitomycin C for Alkylation.” *Biochemistry* **1992**, *31*, 1399.

48. Li, V. S.; Kohn, H. “Studies on the Bonding Specificity for Mitomycin C-DNA Monoalkylation Processes.” *J. Am. Chem. Soc.* **1991**, *113*, 275.

49. Suresh Kumar, G.; Lipman, R.; Cummings, J.; Tomasz, M. “Mitomycin-DNA Adducts Generated by DT-Diaphorase. Revised Mechanism of the Enzymatic Reductive Activation of Mitomycin C.” *Biochemistry* **1997**, *36*, 14128.

50. Peterson, D. M.; Fisher, J. “Autocatalytic Quinone Methide Formation from Mitomycin C.” *Biochemistry* **1986**, *25*, 4077.

51. Siegel, D.; Beall, H.; Senekowitsch, C.; Kasai, M.; Arai, H.; Gibson, N. W.; Ross, D. “Bioreductive Activation of Mitomycin C by DT-Diaphorase.” *Biochemistry* **1992**, *31*, 7879.

52. Han, I.; Kohn, H. “7-Aminoaziridinomitosenes: Synthesis, Structure, and Chemistry.” *J. Org. Chem.* **1991**, *56*, 4648.

53. Li, V. S.; Choi, D.; Tang, M.; Kohn, H. “Concerning *in Vitro* Mitomycin-DNA Alkylation.” *J. Am. Chem. Soc.* **1996**, *118*, 3765.

54. Schiltz, P.; Kohn, H. “Studies on the Reactivity of Reductively Activated Mitomycin C.” *J. Am. Chem. Soc.* **1993**, *115*, 10510.

55. Tomasz, M.; Lipman, R. “Reductive Metabolism and Alkylating Activity of Mitomycin C Induced by Rat Liver Microsomes.” *Biochemistry* **1981**, *20*, 5056.

56. Palom, Y.; Belcourt, M. F.; Suresh Kumar, G.; Arai, H.; Kasai, M.; Sartorelli, A. C.; Rockwell, S.; Tomasz, M. “Formation of a Major DNA Adduct of the Mitomycin Metabolite 2,7-Diaminomitosene in EMT6 Mouse Mammary Tumor Cells Treated with Mitomycin C.” *Oncol. Res.***1998**, *10*, 509.

57. (a)Iwami, M.; Kyoto, S.; Terano, H.; Kohsaka, M. Aoki, H.; Imanaka, H. “A New Tumor Antibiotic, FR900482. Taxonomic Studies on the producing strain. A New Species of Streptomyces.” *J. Antibiot*. **1987**, *40*, 589. (b) Kiyoto, S.; Shibata, T.; Yamashita, M.; Komori, T.; Okuhata, M.; Terano, H.; Kohsaka, M.; Aoki, H.; Imanka, H. “A New Antitumor Antibiotic, FR900482. Production, Isolation, Characterization, and Biological Activity.” *J. Antibiot.* **1987**, *40*, 594. (c) Shimomura, K.; Hirai, O.; Mizota, T.; Matsumoto, S.; Shibayama, F.; Kikuchi, H. A “New Antitumor Antibiotic, FR900482. Antitumor activity in transplantable experimental tumors.” *J. Antibiot.* **1987**, *40*, 600. (d) Hirai, O; Shimomura, K.; Mizota, T.; Matsumoto, S.; Mori, J.; Kikuchi, H. “A New Antitumor Antibiotic, FR900482. Hematological Toxicity in Mice.” *J. Antibiot.* **1987**, *40*, 607.

58. Uchida, I.; Takase, S.; Kayakiri, H.; Kiyoto, S.; Hashimoto, M. “Structure of FR900482, a Novel Antitumor Antibiotic from a *Streptomyces*.” *J. Am. Chem. Soc.* **1987**, *109*, 4108.

59. Terano, H, Takase, S.; Hosoda, J.; Kohsaka, M. “A New Antitumor Antibiotic, FR-66979.” *J. Antibiot.* **1989**, *42*, 145.

60. Masuda, K.; Nakamura, T.; Shimomura, K. “A New Antitumor Antibiotic, FR-900482: V. Interstrand DNA-DNA Cross-Links in L1210 Cells.” *J. Antibiot.* **1988**, *41*, 1497.

61. (a) Moriuchi, S.; Shimizu, K.; Yamada, M.; Mabuchi, E.; Tamura, K.; Park, K. C.; Hayakawa, T. “Cytotoxic Effects of a New Antitumor Antibiotic, FK973, in Malignant Glioma.” *Anticancer Res.* **1991**, *11*, 2079. (b) Jun-zheng, W.; Adachi, I.; Wananabe, T. “Cytotoxic Activity of FK973 Against Human Oral and Breast Cancer Cells.” *Chen. Med. J. (Beijing, China, Engl. Ed.)* **1991**, *104*, 834. (c) Horiuchi, N.; Nakagawa, K.; Sasaki, Y.; Minato, K.; Fujiwara, Y.; Nezu, K.; Ohe, Y.; Saijo, N. “

62. (a) Hirai, O.; Miyamae, Y.; Hattori, Y.; Takashima, M.; Miyamoto, A.; Zaizen, K.; Mine, Y. “Microbial Mutagenicity and in vitro chromosome aberration induction by FK973, a new antitumor agent.” *Mutat. Res.* **1994**, *324*, 43. (b) Shimomura, K.; Manda, T.; Mukumoto, S.; Masuda, K.; Nakamura, T.; Mizota, T.; Matsumoto, S.; Nishigaki, F.; Oku, T.; Mori, J.; Shibayama, F. *Cancer Res.* **1988**, *48*, 1166. (c) Masuda, K., Nakamura, T.; Mizota, T.; Mori, J.; Shimomura, K. “Interstrand DNA-DNA and DNA-protein Cross-Links by a New Anti-tumor Antibiotic, FK973, in L1210 Cells.” *Cancer Res.* **1988**, *48*, 5172. (d) Horiuchi, N.; Nakagawa, K.; Sasaki, Y.; Minato, K.; Fujiwara, Y.; Nezu, K.; Ohe, Y.; Saijo, N. “In Vitro Antitumor Activity of Mitomycin C Derivative (RM-49) and New Anticancer Antibiotics (FK973) Against Lung Cancer Cell Lines Determined by Tetrazolium Dye (MTT) Assay.” *Cancer Chemother. Pharmacol.* **1988**, *22*, 246.

63. (a) Nakamura, T.; Masuda, K.; Matsumoto, S.; Oku, T.; Manda, T.; Mori, J.; Shimomura, K. “Effect of FK973, a New Antitumor Antibiotic, on the Cell Cycle of L1210 Cells In Vitro” *Japan. J. Pharmacol.* **1989**, *49*, 317. (b) Masuda, K.; Suzuki, A.; Nakamura, T.; Takagaki, S.;

Noda, K.; Shimomura, K.; Noguchi, H.; Shibayama, F. “A New Antitumor Antibiotic, FK973: Its Metabolism in the Blood and the Antitumor Effects of Its Metabolites on Experimental Models.” *Japan. J. Pharmacol*. **1989**, *51*, 219.

64. Pazdur, R.; Ho, D. H.; Daugherty, K.; Bradner, W. T.; Krakoff, I. H.; Raber, M. N. “Phase I trial of FK973: Description of a Delayed Vascular Leak Syndrome.” *Investigational New Drugs* **1991**, *9*, 377.

65.Fukuyama, T.; Goto, S. “Synthetic Approaches Toward FR-900482. I. Stereoselective Synthesis of a Pentacyclic Model Compound.” *Tetrahedron Lett.* **1989**, *30*, 6491.

66. McClure, K. F.; Danishefsky, S. J. “Cycloaddition Reactions of Aromatic Nitroso Compounds with Oxygenated Dienes. An Approach to the Synthesis of the FR-900482 Family of Antibiotics.” *J. Org. Chem.* **1991**, *56*, 850.

67. (a) Paz, M. M.; Hopkins, P. B. “DNA-DNA Interstrand Cross-Linking by FR66979: Intermediates in the Activation Cascade.” *J. Am. Chem. Soc.* **1997**, *119*, 5999. (b) Huang, H.; Rajski, S. R.; Williams, R. M.; Hopkins, P. B. “FR66979 Requires Reductive Activation to Cross-Link DNA Efficiently.” *Tetrahedron Lett.* **1994**, *35*, 9669. (c) Williams, R. M.; Rajski, S. R. “DNA Cross-Linking Studies on FR900482: Observations on the Mode of Activation.” *Tetrahedron Lett.* **1992**, *33*, 2929.

68. Huang, H.; Pratum, T. K.; Hopkins, P. B. “Covalent Structure of the DNA-DNA Interstrand Cross-Link Formed by Reductively Activated FR66979 in Synthetic DNA Duplexes.” *J. Am. Chem. Soc.* **1994**, *116*, 2703.

69. (a) Woo, J.; Sigurdsson, S. T.; Hopkins, P. B. “DNA Interstrand Cross-Linking by Reductively Activated FR900482 and FR66979.” *J. Am. Chem. Soc.* **1993**, *115*, 1199. (b) Williams, R. M.; Rajski, S. R. “Determination of DNA Cross-Linking Sequence Specificity of FR66979: Observations on the Mode of Action of the FR900482 Class of Anti-tumor Compounds.” *Tetrahedron Lett.* **1993**, *34*, 7023.

70. Williams, R. M.; Rajski, S. R.; Rollins, S. B. “FR900482, a Close Cousin of Mitomycin C that Exploits Mitosene-Based DNA Cross-Linking.” *Chem. Biol.***1997**, *4*, 127.

71. Paz, M. M.; Sigurdsson, S. T.; Hopkins, P. B. “Monoalkylation of DNA by Reductively Activated FR66979.” *Bioorg. Med. Chem.* **2000**, *8*, 173.

72. (a) Naoe, Y.; Inami, M.; Kawamura, I.; Nishigaki, F.; Tsujimoto, S.; Matsumoto, S.; Manda, T.; Shimomura, K. “Cytotoxic Mechanisms of FK317, a new Class of Bioreductive Agent with Antitumor Activity.” *Jpn. J. Cancer Res.* **1998**, *89*, 666. (b) Naoe, Y.; Inami, M.; Takagaki, S.; Matsumoto, S.; Kawamura, I.; Nishigaki, F.; Tsujimoto, S.; Manda, T.; Shimomura, K. “Different Effects of DK317 on Multidrug-resistant Tumor *in vivo* and *in vitro*.” *Jpn J. Cancer Res.* **1998**, *89*, 1047. (c) Naoe, Y.; Inami, M.; Matsumoto, S.; Takagaki, S.; Fujiwara, T.; Yamazaki, S.; Kawamura, I.; Nishigaki, F.; Tsujimoto, S.; Manda, T.; Shimomura, K. “FK317, a Novel Substituted Dihydrobenzoxazine, Exhibits Potent Antitumor Activity against Human Tumor Xenografts in Nude Mice.” *Jpn. J. Cancer Res.* **1998**, *89*, 1306.

73. Naoe, Y.; Inami, M.; Matsumoto, S.; Nishigaki, F.; Tsujimoto, S.; Kawamura, I.; Miyayasu, K.; Manda, T.; Shimomura, K. “FK317: a Novel Subsituted Dihydrobenzaoxazine with Potent

Antitumor Activity which does not Induce Vascular Leak Syndrom." *Cancer Chemother. Pharmacol.* **1998**, *42*, 31.

74. Beckerbauer, L.; Tepe, J. J.; Eastman, r. A.; Mixter, P. r.; Williams, R. M.; Reeves, R. "Differential Effects of FR900482 and FK317 on Apoptosis, *IL-2* Gene Expression, and Induction of Vascular Leak Syndrom." *Chem. Biol.* **2002**, *9*, 427.

75. Strasser, A.; O'Conner, L.; Dixit, v. M. "Apoptosis signaling." *Annu. Rev. Biochem.* **2000**, *69*, 217.

76. Williams, R. M.; Ducept, P. "Interstrand Cross-Linking of DNA by FK317 and Its Deacetylated Metabolites FR70496 and FR157471." *Biochemistry* **2003**, *42*, 14696.

77. Judd, T. C.; Williams, R. M. "Synthesis and DNA Cross-Linking of a Phototriggered FR900482 Mitosene Progenitor." *Org. Lett.* **2002**, *4*, 3711.

78. (a) Subramanian, V.; Ducept, P.; Williams, R. M.; Luger, K. "Effects of Photochemically Activated Alkylating Agents of the FR900482 Family on Chromatin." *Chem. Biol.* **2007**, *14*, 553. (b) Beckerbuaer, L.; Tepe, J. J.; Cullison, J.; Reeves, R.; Williams, R. M. "FR900482 Class of Anti-Tumor Drugs Cross-Links Oncoprotein HMG I/Y to DNA *in vivo*." *Chem. Biol.* **2000**, *7*, 805.

79. Lee, S.; Lee, W-M.; Sulikowski, G. A. "An Enantioselective 1,2-Aziridinomitosene Synthesis via a Chemoselective Carbon–Hydrogen Insertion Reaction of a Metal Carbene." *J. Org. Chem.* **1999**, *64*, 4224.

80. Martines, L. E.; Nugent, W. A.; Jacobsen, E. N. "Highly Efficient and Enantioselective Synthesis of Carbocyclic Nucleoside Analogs Using Selective Early Transition Metal Catalysts." *J. Org. Chem.* **1996**, *61*, 7963.

81. (a) Wolfe, J. P.; **Waga, S.; Marcous, J. R.**; Buchwald, S. L. "Rational Development of Practical Catalysts for Aromatic Carbon-Nitrogen Bond Formation." *Acc. Chem. Res.* **1998**, *31*, 805. (b) Hartwig, J. R. "Carbon-Heteroatom Bond-Forming Reductive Eliminations of Amines, Ethers, and Sulfides." *Acc. Chem. Res.* **1998**, *31*, 852. (c) Wolfe, J. P.; Buchwald, S. L. "Room Temperature Catalytic Amination of Aryl Iodides." *J. Org. Chem.* **1997**, *62*, 6066. (d) Hartwig, J. F. "Palladium-Catalyzed Amination of Aryl Halides: mechanism and Rational Catalyst Design." *Synlett* **1997**, 329. (e) Wolfe, J. P.; Wagaw, S.; Buchwald, S. L. "An Improved Catalyst System for Aromatic Carbon-Nitrogen Bond Formation: the Possible Involvement of Bis(Phosphine) Palladium Complexes as Key Intermediates." *J. Am. Chem. Soc.* **1996**, *118*, 7215.

82. Michael, J. P.; de Koning, C. B.; Petersen, R. L.; Stanbury, T. V. "Asymmetric Synthesis of a Tetracyclic Model for the Aziridinomitosenes." *Tetrahedron Lett.* **2001**, *42*, 7513.

83. Cohen, N.; Banner, B. L.; Laurenzano, A. J.; Carozza, L. "2,3-*O*-Isopropylidine-D-erythronolactone." *Org. Syn.* **1985**, *63*, 127.

84. (a) Jones, R. J.; Rapoport, H. "Enantiospecific Synthesis of an Aziridinobenzazocinone, an Advanced Intermediate Containing the Core Nucleus of FR900482 and FK973. (b) Luly, J. R.; Rapoport, H. "Routes to Mitomycins. An Improved Synthesis of 7-Methoxymitosene Using Palladium Catalysis." *J. Org. Chem.* **1984**, *49*, 1671.

85. Tsuboike, K.; Guerin, D. J.; Mennen, S. M.; Miller, S. J. “Synthesis of Aziridinomitosenes through Base-Catalyzed Conjugate Addition.” *Tetrahedron* **2004**, *60*, 7367.

86. Trnka, T. M.; Morgan, J. P.; Sanford, M. S.; Wilhelm, T. E.; Scholl, M.; Choi, T. L.; Ding, S.; Day, M. W.; Grubbs, R. H. “Synthesis and Activity of Futhenium Alkylidene Complexes Coordinated with Phosphine and *N*-Heterocyclic Carbene Ligands.” *J. Am. Chem. Soc.* **2003**, *125*, 2546.

87. Ziegler, F. E.; Belema, M. “Cyclization of Chiral Carbon-Centered Aziridinyl Radicals: A New Route to Azirino[2′,3′:3,4]pyrrolo[1,2-a]indoles.” *J. Org. Chem.* **1994**, *59*, 7962.

88. Dunigan, J.; Weigel, L. O. “Synthesis of Alkyl (*2S,3R*)-4-Hydroxy-2,3-epoxybutyrates from Sodium Erythorbate.” *J. Org. Chem.* **1991**, *56*, 6225.

89. (a) Vedejs, E.; Little, J. “Aziridinomitosenes by Anionic Cyclization: Deuterium as a Removable Blocking Group.” *J. Am. Chem. Soc.* **2002**, *124*, 748. (b) Vedejs, E.; Little, J. “Synthesis of the Aziridinomitosene Skeleton by Intramolecular Michael Addition of α-Lithioaziridines: an Aromatic Route Featuring Deuterium as a Removable Blocking Group.” *J. Org. Chem.* **2004**, *69*, 1794.

90. Vedejs, E.; Little, J.; Seaney, L. M. “Synthesis of the Aziridinomitosene Skeleton by Intramolecular Michael Addition: α-Lithioaziridines and Nonaromatic Substrates.” *J. Org. Chem.* **2004**, *69*, 1788.

91. Vedejs, E.; Klapars, A.; Warner, D. L.; Weiss, A. H. Reductive deprotection of N-tritylaziridines. *J. Org. Chem.* **2001**, *66*, 7542.

92. Kim, M.; Vedejs, E. “A Synthetic Approach Toward the Proposed Tetracyclic Aziridinomitosene Derived from FK317.” *J. Org. Chem.* **2004**, *69*, 7262.

Chapter 2.

Synthesis of a Fully Functionalized Aziridinomitosene

Introduction

The FR family of oxygen-bridged hydroxyl hemi-aminal dihydrobenzoxazines **1**-**4** are anticancer prodrugs related to the mitomycin family (Figure 2-1).[1,2,3,4] Similar to mitomycin C **6**,[5] the FR compounds are reductively converted to an active form which is responsible for DNA cross-linking at the 5′CG 3′ sequence.[6] This family was found to have better activity and less toxicity than the mitomycins.[4,7,8] Fukuyama proposed that N-O bond cleavage to a benzazocinone core followed by loss of water produces an aziridinomitosene **5** (Figure 2-1),[9] similar to the aziridinomitosenes derived from the mitomycins.[5] It is generally accepted that the aziridinomitosene is the active form of the FR family, although the compounds have never been isolated or synthesized. The characterization of a FR66979 (**2**) DNA lesion shows DNA alkylation at the C(1) and C(10) position of an aziridinomitosene core, which supports the proposed active structure.[10] These aziridinomitosenes are synthetically challenging functionally dense heterocycles due to the presence of the acid labile aziridine and carbamate. Our research group is interested in the total synthesis of these compounds while discovering chemistry that can be performed on the sensitive environment of the fully functionalized heterocycle.

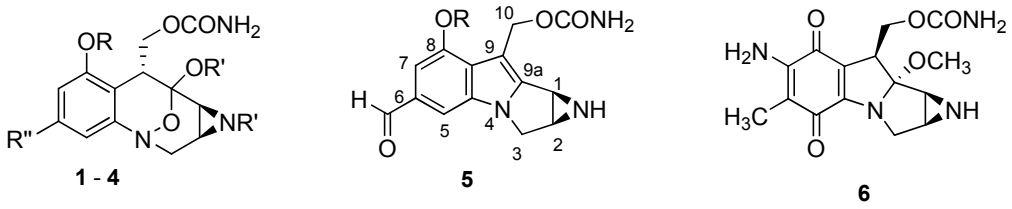

1 FR900482 R= H, R'= H, R''= CHO
2 FR66979 R= H, R'= H, R''= CH_2OH
3 FR973 R= Ac, R'=Ac, R''=CHO
4 FK317 R= Me,R'= Ac, R''=CHO

Figure 2-1. The FR compounds, aziridinomitosene **5**, and Mitomycin C.

Prior reports from our laboratory describe the synthetic strategy towards the aziridinomitosene **7** derived from FK317 **4** (Scheme 2-1).[11-13] The dihydrobenzoxazine **4** is an active diacetylated derivative of **1** which has better activity and fewer side effects such as vascular leak syndrome.[14] The key intermediate in the synthetic strategy towards **7** was the tetracycle **8**.[13] The risk of heterolysis at C(1) due to the acid sensitive aziridine is lowered by the electron withdrawing aldehyde at C(6), which reduces electron density in the indole core allowing for late stage manipulation. Aziridinomitosene **8** was accessed by 1,4-addition of a lithioaziridine, derived from **9** via tin-lithium exchange, into the appended enoate.[11] Indole **9** was accessed by alkylation of the functionalized indole **10**[15] with a known aziridinol **11**, derived from chiral (L)-serine methyl ester hydrochloride.[12] In the previous report, late stage installation of the carbamate at C(10) on **7** was accomplished, but the removal of the trityl protecting group was not successful in the presence of the acid labile carbamate.[13] We now report our continued efforts towards **7**, which have focused on earlier removal of the trityl protecting group at the stage of key intermediate **8**. These studies have culminated in the synthesis of an advanced aziridinomitosene featuring many transformations on acid sensitive aziridine containing heterocycles.

Scheme 2-1. Retrosynthetic analysis of the aziridinomitosene **7** derived from FK317.

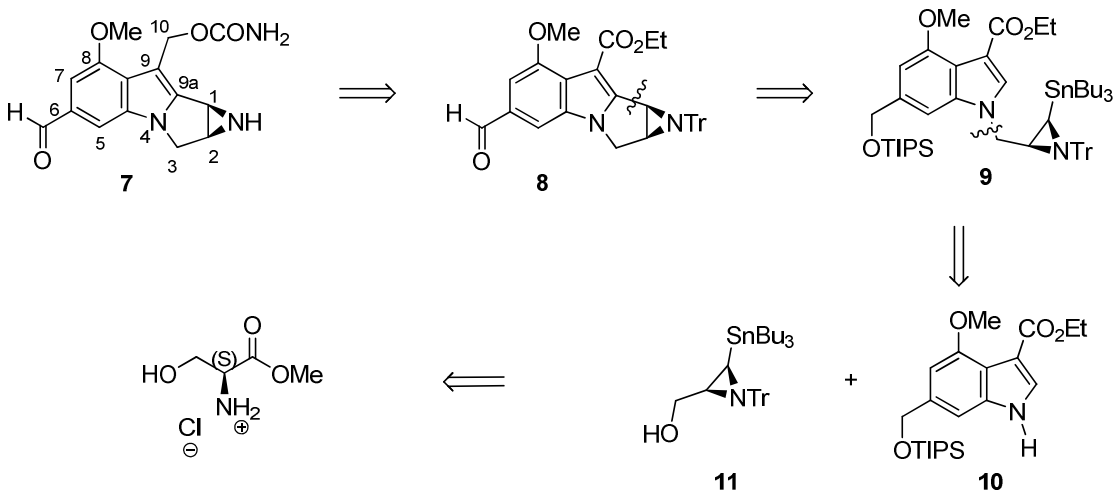

The Synthesis of a fully functionalized Aziridinomitosene

In the course of the studies summarized in Scheme 2-1, it became apparent that alkylation of **10** with an electrophile derived from **11** is difficult (Scheme 2-2).[11-13] The reaction requires heating an excess of the deprotonated **10** with **12** for 3-4 days in order to give acceptable conversion to product **9a**. The low reactivity reflects steric hindrance near the leaving group resulting from the bulky N-trityl and tributylstannane substituents.[12] For example, alkylation of **10** with known mesylate **12** gave only a moderate yield (54%) of **9a** after 4 d of heating at 60 °C (Table 1, entry 1). The unexpected desilylated **9b** was also obtained from this reaction (17%), contributing to the low yield of **9a**. Because of poor reactivity, long reaction time, and byproduct formation, new conditions were examined in order to increase efficiency.

Scheme 2-2. Alkylation of **10** with aziridines **12** and **13**.

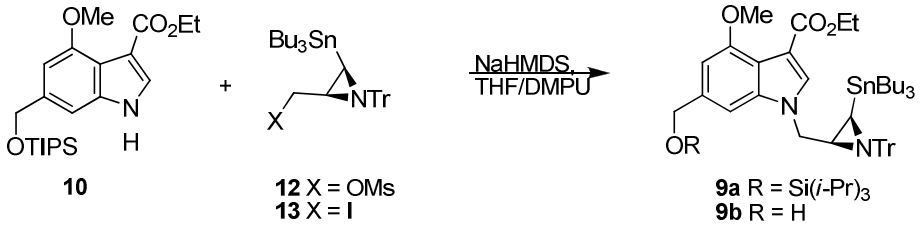

10

12 X = OMs
13 X = I

9a R = Si(*i*-Pr)$_3$
9b R = H

In an attempt to improve the alkylation of **10**, the reaction variables were reinvestigated. Thus, the mesylate was replaced by an iodide leaving group (**13**), obtained in excellent yield using Mistunobu conditions (Eq 1).[16] Treating **13** with 3 equivalents of NaHMDS, 3 equiv of **10**, and heating in a 2:1 mixture of THF and DMPU for 20 h gave **9a** in improved 62% yield, along with trace amounts of **9b** and unreacted starting **13** (^{1}H NMR assay, Table 2-1, entry 2). Longer reaction times resulted in increased formation of **9b** and decomposition of **13**. However, when the reaction was quenched after 3 h of heating at 60 °C, 72% of **9a** was isolated and no **9b** was apparent by ^{1}H NMR assay of the crude reaction mixture (Table 2-1, entry 3). Therefore, the optimized conditions to alkylate **10** used 3 equiv of **10** and 3 equiv of NaHMDS in a 2:1 mixture of THF: DMPU (60 °C for 3 - 4 h). These improvements allowed more efficient utilization of the valuable aziridine subunit and provided sufficient material to explore construction of the tetracycle of **7**.

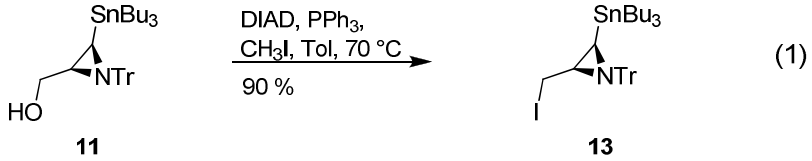

11 **13** (1)

Table 2-1. Preparation of **9a** from **10** [a]

entry	aziridine	NaHMDS	time	**9a**[b]	**9b**[b]
1	**12**	3.3	4 d	54%	17%
2	**13**	3	20 h	62%	trace
3	**13**	3	3 h	72%	--

[a]Conditions: 3 equiv of **9** treated with 3 equiv of NaHMDS at -78 °C. Aziridine was added, and the reaction was warmed to rt while concentrating under N_2. The reaction was then warmed to 60 °C.
[b]Isolated yield.

Once **9a** was in hand, tetracycle formation was targeted by intramolecular 1,4-addition of a lithioaziridine into the appended enoate (Scheme 2-3).[13] Direct tin-lithium exchange on **9a** is not viable due to the acidity of the C(2) proton (indole numbering).[11-13] The resulting C(2) metallation (**14**) impedes the 1,4-addition of the lithioaziridine into the enoate. To avoid this

problem, a deuterium blocking group was deliberately installed at C(2) by selective deprotonation with the bulky mesityllithium in the presence of TMEDA; subsequent quenching with EtOD provided deuterated indole **15a** in 91% yield with excellent (>95%) deuterium incorporation. No mesityllithium addition into the indole was detected. Due to a large kinetic isotope effect,[11,12] **15a** undergoes tin-lithium exchange without significant C(2) lithiation when treated with excess MeLi. Trapping the enolate **16** with phenylselenyl chloride followed by aqueous workup, results in spontaneous elimination and rearomatization to the indole core producing the desired **18**.

The isolation and purification of tetracycle **18** proved to be difficult. The tin-lithium exchange on **15a** gave good conversion to cyclized product, but a small amount of **17** due to incomplete elimination was always present. This byproduct could not be removed by Et_3N deactivated silica gel chromatography and attempted purification of the mixture led to increased decomposition of the desired **18**. Treating the mixture with H_2O_2[17] or heating to 65 °C in $CHCl_3$ for 1 h to induce elimination decreased the amount of **17**, but decomposition of **18** was also observed. Therefore, the inseparable mixture was taken forward. Treatment of **18** and **17** with TBAF afforded a mixture of primary alcohols. Based on the difficulties encountered in the purification of **18**, non-polar selenium residues were removed by quick filtration through a silica gel plug. Oxidation of the alcohol mixture with TPAP/NMO then gave good conversion to a mixture of aldehydes;[13] however, aldehyde **8** decomposed during crystallization attempts and streaked on silica gel. The selenium adduct was finally removed by dissolving the crude residue from oxidation in acetone, and adding hexanes to precipitate **8** in 35% yield over the 3 steps from **15a**. Once isolated, **8** could be stored at low temperature. The sensitivity to purification of **18** and its derivatives is a result of the electron density of the indole core which increases the potential for heterolysis at C(1). Fortunately, this sensitivity is manageable with the relatively robust **8** which was isolated and purified.

Scheme 2-3. Tetracycle formation.

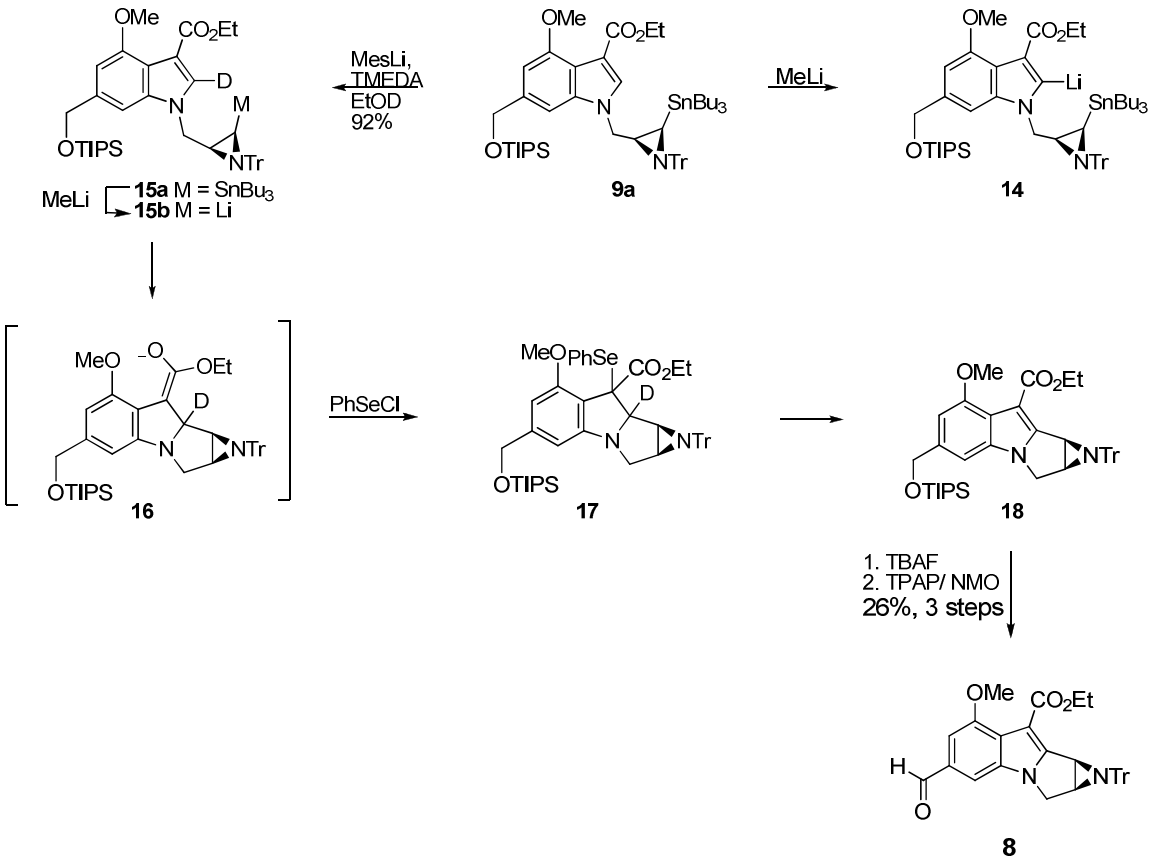

Due to its improved stability, tetracycle **8** is the best candidate for removal of the trityl protecting group. Using acidic reductive detritylation conditions,[18] deprotection provided *N*-H aziridinomitosene **19** in moderate to good yield (Scheme 2-4) as a mixture of nitrogen invertomers.[19] Two pairs of broad aziridine methine protons appeared between δ = 3 and 4 ppm by ^{1}H NMR assay, and a coupling constant of 4.9 Hz was extracted for one of the invertomers by homonuclear decoupling and D_2O exchange experiments. This coupling is small for a *cis* aziridine, but it is consistent with aziridinomitosenes synthesized previously.[12,15,20] The structure of **19** was confirmed by treating the material with trityl chloride and Hünig's base to regenerate **8**. Compound **19** is more susceptible to ring opening than **8** due to removal of the bulky trityl group, but once isolated **19** can be stored at low temperature for long periods of time. As proposed,

deprotection of **8** was the safest choice because the aldehyde and enoate destabilize the "benzylic" carbocation resulting from heterolysis of the C(1) –N bond; thereby allowing removal of the trityl group.

Scheme 2-4. Removal of the trityl protecting group from **8**.

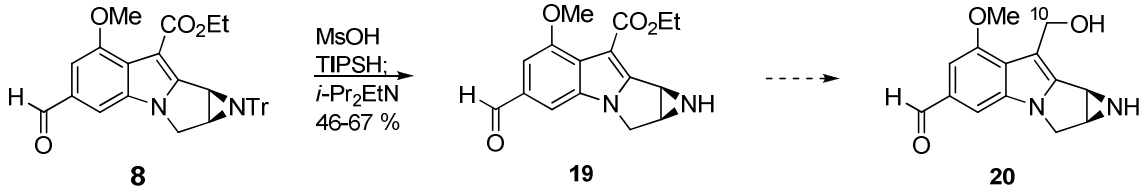

The key aziridinomitosene **19** is partially stabilized by both the enoate and aldehyde substituents, but installation of the requisite carbamate at C(10) required temporary protection of the aldehyde to allow selective reduction of the enoate. The primary alcohol at C(10) of the tetracycles is highly labile under acidic conditions if the formyl group at C(6) is not present; therefore, an aldehyde protecting group is required that survives reduction and that can be removed under basic conditions. The base labile pyrrole carbinol developed by Evans[21] and Dixon[22] was investigated for this purpose. Installation and removal of the pyrrole carbinol was evaluated on *m*-anisaldehyde **21** as a simple model system (Scheme 2-5). Aldehyde **21** was treated with excess C_4H_4NLi, generated from pyrrole and *n*-BuLi at -78 °C,[22] and the tetrahedral intermediate **22** was trapped using hexafluoroisopropyl alcohol (HFIP)[23] as a weakly acidic proton source to afford **23** in 96% yield. Treating a solution of **23** with pH 9 or 10 buffer gave good conversion back to **21**. These studies showed that the pyrrole carbinol was easy to install and remove under basic conditions. However, to further reduce the risk of C(10) heterolysis for eventual use in the "real" system, other conditions to remove the pyrrole carbinol that do not require an aqueous workup were investigated.

Scheme 2-5. Pyrrole carbinol installation on *m*-Anisaldehyde **21**.

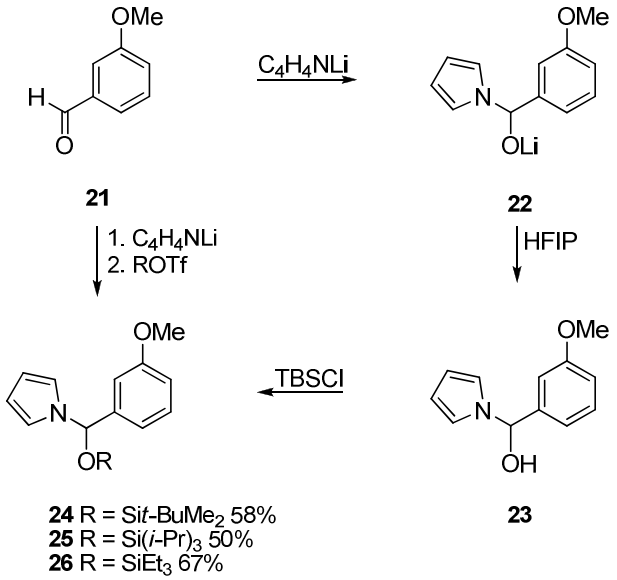

It is known that pyrrole carbinols protected as silyl ethers are converted directly to aldehydes when treated with fluoride sources.[21] As expected from the precedents, the silylated pyrrole carbinol **24** (from **23** and TBSCl/imidazole, 58%)[21] was easily cleaved with TBAF to provide aldehyde **21**. A more direct route to the silylated pyrrole carbinols was trapping the tetrahedral intermediate **22** with a silyl triflate (Scheme 2-5). Thus, treatment of **21** with 2 equiv of C_4H_4NLi, followed by 2 equiv of triisopropylsilyl triflate (TIPSOTf) provided **25** in moderate 50% yield. Quenching the tetrahedral intermediate of **21** with the less bulky triethylsilyl triflate (TESOTf) also provided the silyl ether **26**, but in higher yield (67%). The successful generation of the silylated pyrrole carbinols **24**, **25,** and **26** provided an alternative to an aqueous workup for unmasking the desired aldehyde. Since work on generating and masking pyrrole carbinols had been successful, the conversion of **19** to **20** commenced.

In the fully substituted system, conversion to alcohol **20** was the initial goal. Not surprisingly, installation of the pyrrole carbinol on tetracycle **19** proved to be more difficult than with the model. Using the previously optimized conditions for the conversion to the unprotected pyrrole carbinol, mixtures of **19** and **27** favoring **19** were always recovered. It was found that

adding one equiv of NaH to **19** prior to excess C_4H_4NLi provided **27** in improved 63% yield (Scheme 2-6). Pyrrole carbinol **27** could be purified and was reasonably stable if stored in the freezer. The stage was now set for the challenging reduction of the enoate of **27** with $LiAlH_4$. Isolation of the primary alcohol **28** with the pyrrole carbinol intact at C(6) would increase the risk of C(10)-O cleavage due to the absence of a stabilizing π acceptor; therefore, unmasking the aldehyde before isolation would be ideal. With this in mind, **27** was treated with excess $LiAlH_4$ at 0 °C[12] and the reaction was quenched with HPLC grade ethyl acetate, thereby making a risky aqueous workup unnecessary.[24] The ethoxide generated upon reduction of the ethyl acetate facilitated the removal of the pyrrole carbinol in one pot. The material recovered was difficult to assay due to poor solubility, but two interesting characteristics could be observed: a proton downfield at δ = 9.9 ppm in the ^1H NMR spectrum (CD_3OD), and a broad IR stretch at 3450 cm^{-1}. This information suggests successful reduction at C(10) and subsequent unmasking at C(6), but the C(10) methylene and aziridine protons could not be observed. Based on this limited information, the material was tentatively assigned as the desired alcohol **20**, but the product could not be isolated or further characterized due to high polarity and insolubility. Therefore, installation of the C(10) carbamate at the stage of **20** was not pursued, and the strategy for the synthesis of **7** was revised.

Scheme 2-6. Installation of pyrrole carbinol and enoate reduction.

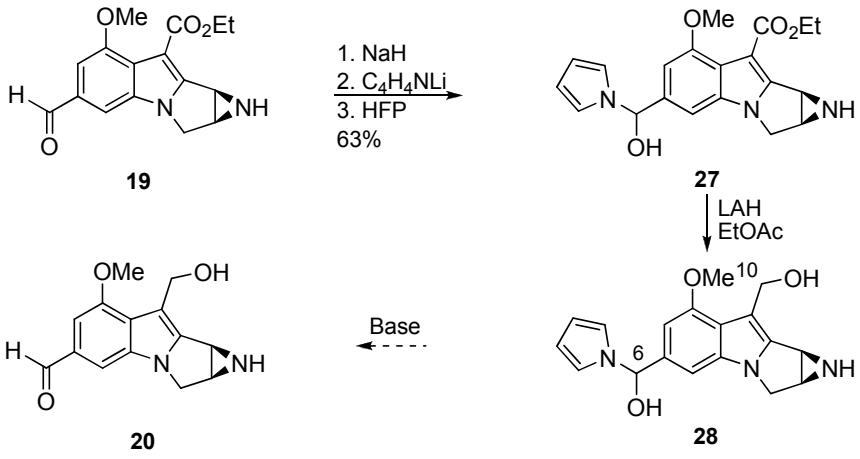

To improve purification and handling of **20**, protection of the aziridine nitrogen with a large silyl group was evaluated.[25] The *t*-butyldiphenylsilyl (TBDPS) protecting group was installed on **19** using 1 equiv of freshly prepared TBDPS triflate (TBDPSOTf)[26] and Hünig's base to provide **29** in moderate to good yield (Scheme 2-7; Table 2-2, entry 1). On the other hand, excess TBDPSOTf resulted in significant decomposition of the tetracycle, most likely from electrophilic activation of the aziridine nitrogen. In order to circumvent the acid sensitivity of **29,** a basic buffer solution (pH 10) was used during workup after the TBDPS protecting group installation. Protection of the aziridine nitrogen with TIPSOTf and Hünig's base resulted in poor yields of the desired aziridinomitosene (data not shown). The TIPS protected aziridinomitosene proved unstable to purification and storage at low temperatures. Because of the greater stability of the TBDPS protected aziridinomitosene **29**, it was taken forward in the synthesis.

Masking the aldehyde **29** as a pyrrole carbinol proved difficult, as the optimized conditions developed for preparation of **27** led to mixtures of **19**, **29** and **30**. Fortunately, replacing the aqueous workup with a HFIP/ether quench led to the recovery of pyrrole carbinol **30** in good yield (Scheme 2-7; Table 2-2, entry 2). As with **27**, the pyrrole carbinol moiety was only moderately stable: pyrrole carbinol **30** could be purified using deactivated preparatory plate chromatography, but even storage at -20 °C could not prevent unmasking of the aldehyde over time. Due to this instability, protection of the pyrrole carbinol as a silyl ether was attempted by trapping the tetrahedral intermediate from **29** with a silyl triflate. However, attempts to silylate the carbinol oxygen using the optimized conditions resulted in cleavage of the N-Si bond. Because of the stability problems with **30**, it was decided to reduce the enoate of **30** immediately after purification. The reduction of the enoate of **30** was expected to be quite challenging; therefore, careful consideration of the reduction and workup conditions was required.

Scheme 2-7. Synthesis of fully functionalized aziridinomitosene **36**.

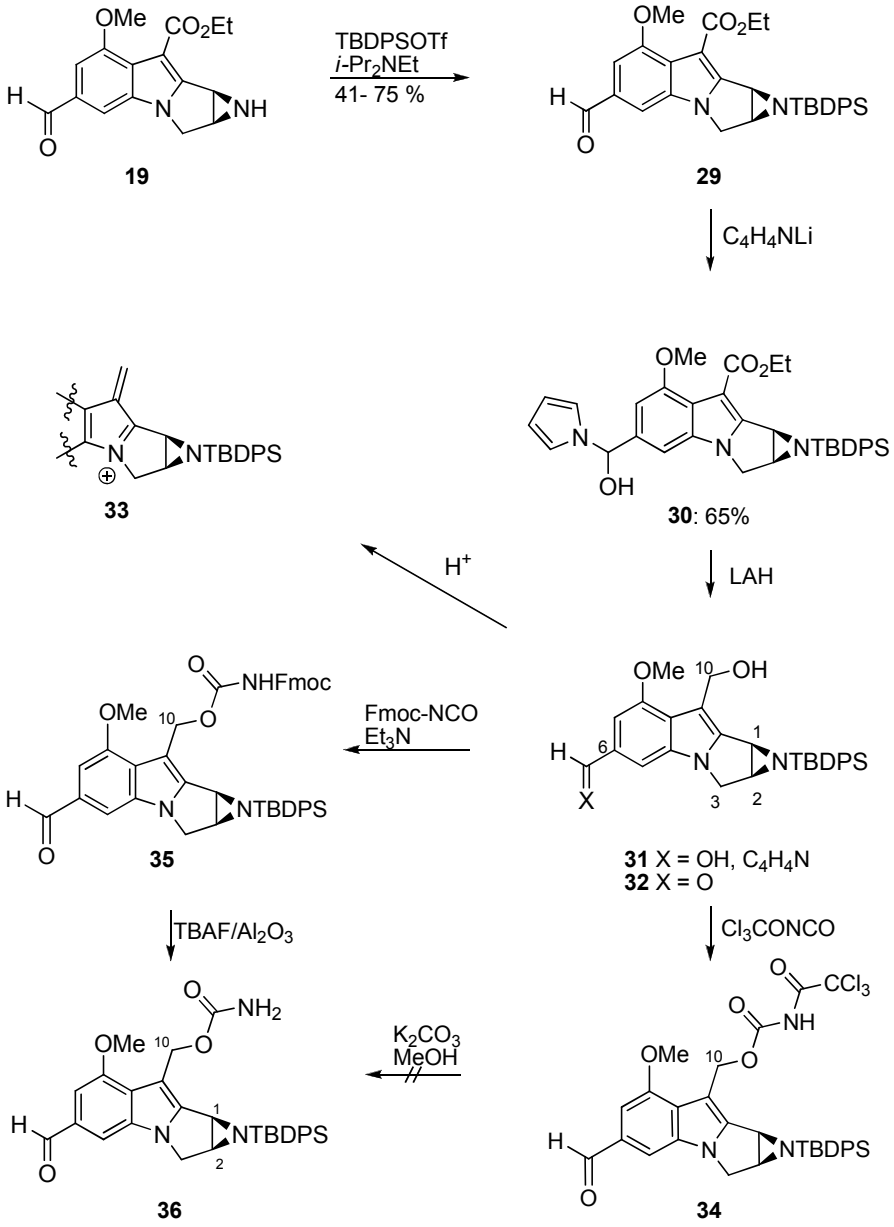

Table 2-2. Characteristic ^{1}H NMR Signals of **29** – **36**[a]

Entry	Tetracycle	C(1)	C(2)	C(3)	C(10)
1	**29**	3.62 d	3.38 t	4.27 d 4.07 dd	NA
2	**30**	3.57 d	3.31 t	4.17 d 3.95 dd	NA
3	**31**	3.22 d	3.28 t	--[b]	4.93 dd 4.73 dd
4	**32**	3.29 d	3.6 dd	4.21 d 4.03 dd	4.95 dd 4.76 dd
5	**34**	3.53 d	--[b]	--[b]	5.66 d 5.56 d
6	**35**	3.36 d	3.29 t	--[b]	5.65 d 5.20 d
7	**36**	3.41 d	3.36 dd	4.22 d 4.02 dd	5.49 d 5.45 d

[a]Chemical shifts given in ppm. [b]Signals obscured.

The planned reduction of **30** to **31** was especially intimidating. Without the C(6) formyl group to reduce electron density of the indole core, the indole nitrogen lone pair can easily displace the C(10) hydroxyl group of **31** via acid catalyzed activation to form iminium ion **33** (Scheme 2-7).[27] Furthermore, the ever present risk of acid-induced C(1)-N heterolysis of the aziridine ring increases as electron donation from the indole increases,[28] a risk that also becomes larger without the C(6) formyl group. It was suspected that even an aqueous workup of the reduction from **30** may be acidic enough to catalyze the undesired heterolytic events from alcohol **31**. Whereas **31** would be especially sensitive, the aldehyde **32** derived from the removal of the pyrrole carbinol of **31** should be less prone to activation at C(1) and C(10) because the π accepting C(6) formyl group is restored. Therefore, if **31** could be converted to **32** during the workup of the $LiAlH_4$ reduction, the material should be isolable. With these considerations in mind, freshly purified **30** was treated with 5 mol equiv of $LiAlH_4$ at 0 °C and quenched with ethyl acetate. Two major products were detected (ca. 1:1 ratio), one of which was stable enough to isolate and was assigned as aldehyde **32.** Aldehyde **32** showed an ABX pair of signals (δ = 4.95 ppm and δ = 4.76 ppm) coupled to a doublet of doublets (δ = 2.88 ppm), which were assigned as the C(10) methylene protons and the hydroxyl proton respectively (Table 2-2, entry 4). The

distinctive C(1) and C(2) aziridine protons were present; however, the C(1) doublet moved upfield from δ = 3.62 ppm (**29**) to δ = 3.29 ppm (**32**), thereby confirming an oxidation state change at C(10) (Table 2-2, entries 1 and 4). Like enoate **30**, aldehyde **32** survived quick chromatography, but was found to decompose during storage in frozen benzene. The other product from reduction was too sensitive to isolate, but it was tentatively assigned as **31** due to the similarity of the upfield ^{1}H NMR signals to those of **32** (Table 2-2, entry 3), plus signals consistent with the presence of the pyrrole moiety. It was reasoned that the pyrrole carbinol of **31** might be cleaved under the basic conditions required for carbamate installation in the next step, thereby avoiding the problematic chromatography. Therefore, the mixture of **31** and **32** was taken on immediately from the ethyl acetate quench procedure.

The inherent risk of C(10) heterolysis of alcohols **31** and **32** made it necessary to approach installation of the carbamate cautiously by using mild carbamoylating reagents and conditions (Scheme 2-7). In a previous report from our laboratory, installation of the carbamate functionality on related aziridinomitosenes using the highly reactive trichloroacetyl isocyanate produced the desired C(10) carbamates.[29,30] Accordingly, reaction of **32** with 1 equiv of trichloroacetyl isocyanate at -78 °C for 1 h followed by stirring at rt for 1 h gave a product corresponding to **34** by ^{1}H NMR assay of the crude reaction mixture (Table 2-2, entry 5). However, attempted cleavage of the trichloroacetyl group from the presumed **34** with K_2CO_3 in MeOH[29] resulted in disappearance of the characteristic AB doublets of C(10) but produced no signals corresponding to the free carbamate. Therefore, an alternative method for carbamate installation using the milder Fmoc-NCO reagent was investigated (Scheme 2-7).[15,31] The mixture of **31** and **32** was treated with freshly prepared Fmoc-NCO and Et_3N to provide the Fmoc protected carbamate **35**. The C(10) methylene proton signals shifted downfield facilitating structure determination (Table 2-2, entries 4 and 6). Treatment of protected carbamate **35** with excess TBAF on alumina provided the free carbamate **36** as a white solid after filtration and solvent removal.[32,33] Attempts to remove the Fmoc protecting group from **35** with previously

optimized conditions of Et_3N in CH_3CN resulted in significant decomposition.[29] Surprisingly, after removal of the Fmoc with TBAF, the ^1H NMR spectrum showed the characteristic TBDPS signals as well as the characteristic sharp doublet of C(1) and "triplet" of C(2) indicative of an intact, N-silylated aziridine (Table 2-2, entry 7).

Deprotection Attempts on Fully Functionalized 36

Due to the unexpected stability of the TBDPS group on **36**, various conditions were screened for the final deprotection of the aziridine nitrogen. Treatment of **36** with the inorganic fluoride sources CsF and KHF_2 in THF showed unreacted **36** by TLC, while use of Et_3N-HF and TAS-F resulted in decomposition.[34] Surprisingly, when enoate **29** was dissolved in CD_3OD and monitored by ^1H NMR spectroscopy over 20 h the N-H aziridine **19** was regenerated and a new TBDPS signal appeared at δ = 0.99 ppm, as expected from attack of nucleophilic deuterated methanol at the silyl group. Therefore, it was hypothesized that these conditions would be mild enough to deprotect **36**. Aziridinomitosene **36** was dissolved in CD_3OD, and the sample was monitored by ^1H NMR spectroscopy. Despite seeing the TBDPS signal at δ = 0.99 ppm after 45 min, the key C(1) and C(2) signals of the deprotected aziridine **7** were not observed. After 2 d the ^1H NMR spectrum showed a mixture of aziridine ring opened products formed via acid catalysis. This NMR study further demonstrates the facile activation and high reactivity of the aziridinomitosene as well as the need for exceptionally mild conditions for TBDPS removal.

It was hypothesized that the detrimental ring opening of the aziridine in deuterated methanol during silyl group cleavage might be inhibited by buffering the solvent with a carbonate base. Therefore, carbamate **36** and Cs_2CO_3 were dissolved in deuterated methanol, and the reaction was monitored by ^1H NMR spectroscopy. Instead of the expected silyl group cleavage, the spectrum showed that tetracycle **36** had undergone surprising structural changes. Multiple new peaks appeared while the peaks corresponding to **36** decreased in intensity. A 1:1 ratio of new products was observed after 17 h, but after 6 d only one of these products was present. Upon isolation, the ^1H NMR spectrum of the new product showed that the characteristic pyrrole C(3)

and aziridine C(1) and C(2) protons had moved upfield compared to carbamate **36** (Table 2-3, entries 1 and 3), establishing that the protons are more shielded than in any other tetracycle in the series. Even more surprising was that the C(10) AB methylene protons were missing, but two vinylic protons at δ = 5.55 and 6.23 ppm were present. The nominal mass (ESMS; *m/z* = 514 amu) corresponded to loss of the carbamate and incorporation of OCD_3. Based on the above data and comparison with the natural product mitomycin K (**37**),[35] the structure of the isolated unknown was tentatively assigned as the exocyclic olefin **38** (Figure 2-2)**.** Structure determination was based on the characteristic chemical shifts of **37** (Table 2-3, entry 2). Further confirmation of the structure by ^{13}C NMR was not feasible due to the small quantity of **38** isolated.

In order to confirm the structure of **38** and to better understand the rearrangement, the *N*-Tr aziridinomitosene **39**[12] (Figure 2-2) was exposed to the same conditions that had been used with **36**. Carbamate **39** and Cs_2CO_3 were dissolved in deuterated methanol and the reaction was monitored by ^1H NMR spectroscopy. Analogous structural changes appeared in the ^1H NMR spectrum as observed starting with **36**, and two major products were observed in a 1:1 ratio after 3 d. One of the products correlated well with **37** and also with **38** in terms of ^1H NMR chemical shifts (Table 2-3, entry 4). Furthermore, the presence of two alkenyl carbons (δ = 140.2 and δ = 114.4 ppm) and a quaternary hemi-aminal carbon (δ = 106.1 ppm) could be confirmed by ^{13}C NMR spectroscopy; therefore, the structure was assigned as **40** and the structure of **38** was confirmed by analogy. The second product was isolated, and the mass ion observed by ESMS correlated to loss of the C(10) carbamate and incorporation of OCD_3 (M + Na, *m/z* = 540 amu). Inspection of the ^1H NMR spectrum showed a pair of AB doublets at δ = 4.89 and 4.73 ppm, which is characteristic of the presence of an electron donating heteroatom at C(10) (i.e. alcohol **31**, Table 2-3, entry 5). Comparison of the ^1H NMR spectra of the unknown product to the methyl ether **41** (generated from **44** and MeOH by Kim, Eq 2) showed an exact match, except for the signals resulting from the methyl group on the C(10) oxygen (Table 2-3 entry 6)**.** The initially

"unknown" product was therefore assigned as **42**, a substance that differs from **41** only by the presence of a CD_3 in place of a CH_3 (Table 2-3, entries 6 and 7). By analogy, the transient compound observed upon reaction of **36** with $CsCO_3$ in deuterated methanol was assigned as **43** (Table 2-3, entry 8). Although the nucleophilic substitution on these functionally dense heterocycles was quite intriguing from a mode of activation perspective, the susceptibility of the C(10) carbamate of **36** to nucleophilic attack further limits the strategies available for successful removal of the TBDPS group in the sensitive environment.

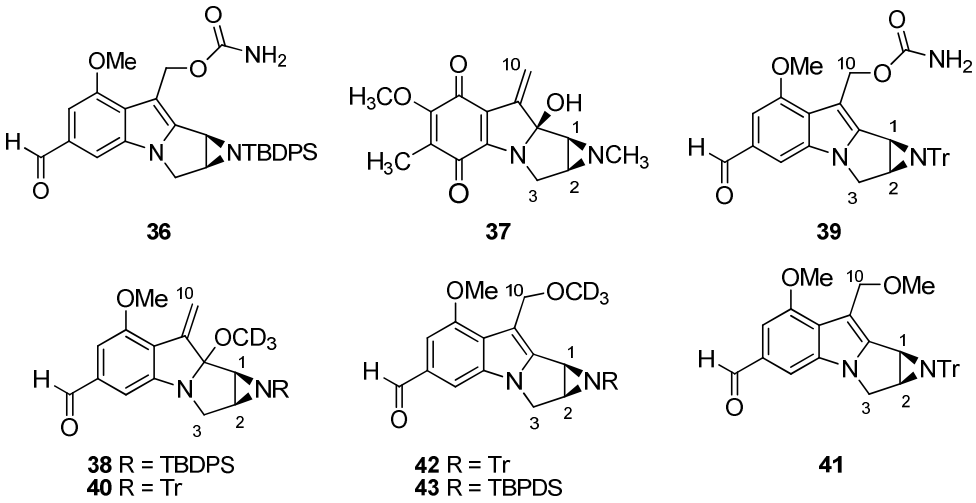

Figure 2-2. Selected aziridinomitosenes.

Table 2-3. Characteristic ^{1}H NMR signals of key tetracycles[a]

Entry	Tetracycle	C(1)	C(2)	C(3)	C(10)
1	**36**	3.41 d	3.36 dd	4.22 d	5.49 d
				4.02 d	5.45 d
2	**37**	2.27 s	2.27 s	3.98 d	6.13 s
				3.45 d	5.53 s
3	**38**	2.66 d	2.43 dd	3.55 d	6.29 s
				3.34 dd	5.55 s
4	**40**	2.28 d	2.13 dd	3.80 d	6.40 s
				3.40 dd	5.47 s
5	**32**	3.29 d	3.6 dd	4.21 d	4.95 dd
				4.03 dd	4.76 dd
6	**41**	3.04 d	3.01 dd	4.44 d	4.90 d
				4.10 dd	4.73 d
7	**42**	3.04 d	3.01 dd	4.44 d	4.90 d
				4.10 dd	4.72 d
8	**43**[b]	3.41 d	3.53 dd	-	4.87 d
					4.73 d

[a]Chemical shifts given in ppm. [b] ^{1}H NMR spectrum in CD_3OD.

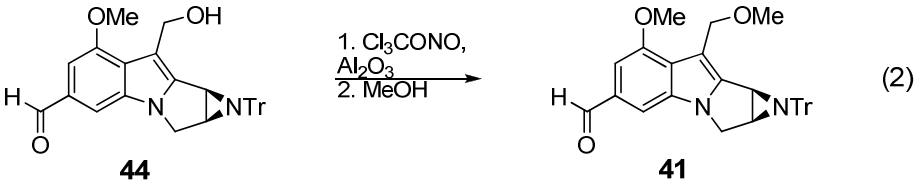

44 **41** (2)

The sensitivity of **36** to nucleophilic, basic, and acidic conditions made the aziridine deprotection extremely difficult. Based on the difficulties associated with removal of the TBDPS group from **36**, it was deemed necessary to test deprotection conditions on a model aziridine **45** in order to more fully explore possible strategies (Eq 3). Although fluoride sources were unsuccessful on previous attempts to deprotect **36**, fluoride anion was considered the best starting point for the model study due to its high affinity for silicon. Treating **45** with 1 equiv of the widely used TBAF in DMF provided N-H aziridine[36] **46** in 56 % yield after 3 h (Table 2-4, entry 1). However, the impurities and residual water[37] which are inevitably present in TBAF were causes for concern because of the sensitivity of **36** to acid and to hydroylsis. Therefore, the non-hygroscopic crystalline tetrabutylammonium difluorotriphenylsilicate (TBAT)[38] was evaluated. Surprisingly, treating aziridine **45** with TBAT in deuterated DMF returned only starting material by ^{1}H NMR assay after 3 d (Table 2-4, entry 2). It was hypothesized that activation of the N-Si bond of **45** by the impurities of TBAF was responsible for the formation of **46**, and that the analogous activation by an additive might allow cleavage of the TBDPS group by TBAT. The non-nucleophilic hydrogen bond donor trifluoroethanol (TFE)[23] was considered for this purpose.

The fluorinated alcohol was expected to activate the N-Si bond because of its high hydrogen bond donor and ionizing power.[23] The more polarized N-Si bond, resulting from the hydrogen bond between the aziridine nitrogen and TFE, should be more susceptible to nucleophilic attack by the fluoride anion. Therefore, **45** was treated with 1 equiv of TFE and 1 equiv of TBAT in deuterated DMF at rt. Formation of **46** was indeed observed by ^{1}H NMR spectroscopy after 1 d (Table 2-4, entry 3), confirming the need for activation of the N-Si bond. Under these activation conditions, the inorganic CsF proved to be a viable alternative to TBAT.

Treatment of **46** with 1 equiv of CsF and 1 equiv of TFE in deuterated DMF provided **46** after only 20 h (Table 2-4, entry 4). Switching the solvent from deuterated DMF to acetonitrile provided **46** in 41% yield, **45** in 11%, and silylated TFE ($TBDPSOCH_2CF_3$) (Table 2-4, entry 5). Furthermore, when **44** was treated with 1 equiv of CsF in TFE as the solvent, aziridine **46** was isolated in 61% yield after 2 d (Table 2-4, entry 6). Because the $TBDPSOCH_2CF_3$ was an unexpected byproduct, **45** was subjected to TFE without an added fluoride source to ascertain whether a fluoride anion was needed for the deprotection. After 2 d, only 14% desilylated **46** was seen by ^{1}H NMR assay as well as a *t*-butyl group corresponding to $TBPDSOCH_2CF_3$ (Table 2-4, entry 7), thereby suggesting that the fluoride anion is crucial for facilitating the TBDPS removal. From the above observations, it is possible that the TFE was both activating and cleaving the N-Si bond, and that the fluoride anion facilitated the reaction by acting as a base.

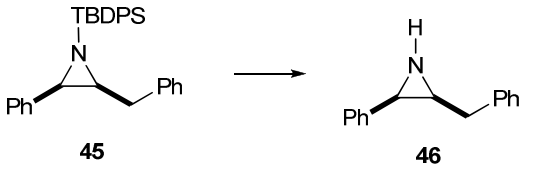

(3)

Table 2-4. Deprotection of Aziridine **45**

Entry	Nucleophile	Additive	Solvent	Time	Conversion[a]
1	TBAF (1)	None	DMF	3 h	56[b]
2	TBAT[c]	None	DMF-d_7	3 d	0
3	TBAT (1)	TFE (1)	DMF-d_7	1 d	75
4	CsF(1)	TFE (1)	DMF-d_7	20 h	93
5	CsF(1)	TFE (5)	CH_3CN	3 d	41[b]
6	CsF (1)	None	TFE	2 d	61[b]
7	None	TFE (1)	DMF-d_7	2 d	14

[a] % conversion by ^{1}H NMR assay. [b]Isolated yield. [c] Excess reagent used. TBAT = tetrabutylammonium trifluorodiphenylsilicate. TFE = trifluoroethanol.

Although mild conditions had been found to remove the TBDPS group from aziridine **45**, it was with trepidation that the conditions were applied to the deprotection of penultimate aziridinomitosene **36**. The ability of TFE to polarize the N-Si bond through hydrogen bonding

would also activate the C(1)-N bond for heterolysis, thereby leading to ring opening of the aziridine. Despite the risk of heterolysis, **36** was treated with 1 equiv of CsF in TFE and THF (8:1) (Scheme 2-8). No apparent reaction was detected after 2 h by TLC, so an excess of CsF was added. After 1 d of stirring, the solvent volume was reduced, and the residue was analyzed by ^{1}H NMR spectroscopy. Not surprisingly, the attempted deprotection had resulted in heterolysis of the C(1)- N bond and the formation of two ring opened products. Once isolated, both products showed a C(1) doublet downfield near δ = 4.6 ppm, which is coupled to a multiplet upfield near δ = 3.9 ppm**.** The presence of a doublet downfield correlates well with what others have seen upon solvolysis at C(1), namely, that the proton at C(1) moves downfield when adjacent to a heteroatom.[39] Also, the C(10) methylene protons of both compounds had moved upfield near δ = 5 ppm, suggesting that the carbamate had also been lost and that a heteroatom had been incorporated (Table 2-3, entries 6 and 7). Analysis of both products by mass spectrometry showed a mass ion corresponding to incorporation of 2 equiv of TFE (ESMS, M + Na, *m/z* = 701 amu). Based on the above data, the products were tentatively assigned as diastereomers of the ring opened mitosene **47**. Structure identification was confirmed by two triplets in the ^{19}F NMR spectrum of both compounds, and by homonuclear and heteronuclear (^{19}F) decoupling experiments. A possible mechanism for formation of **47** could be displacement of the C(10) carbamate, followed by trapping with 1 equiv of TFE, then heterolysis at C(1) and trapping of the benzylic cation with another equiv of TFE. Although the incorporation of 2 equiv of the non-nucleophilic TFE was unexpected, most surprising was the presence of the TBDPS protecting group on the nitrogen despite prolonged stirring with excess CsF. Once again, the aziridinomitosene **36** had proven to be extremely sensitive to C(1)-N bond activation, and heterolysis at both C(1) and C(10) could not be avoided.

Scheme 2-8. Formation of mitosene **47** during final deprotection.

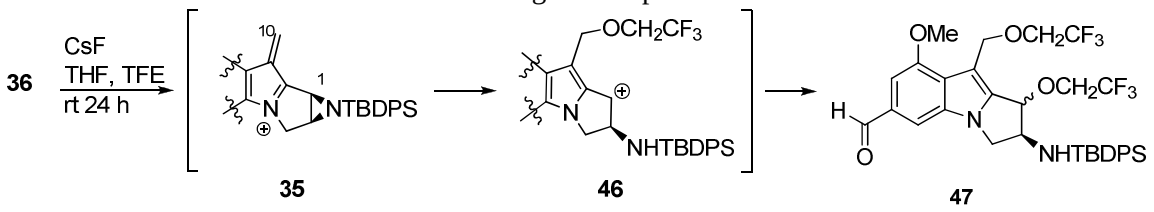

Discussion

From the outset of the synthesis, the aziridine and carbamate moieties were expected to be challenging to install and manipulate due to their acid sensitivity. The risk of acid catalyzed heterolysis of **36** was expected based on the C(1)-N and C(10)-carbamate bond cleavage of fully reduced mitomycin C under acidic conditions. The observed ring opening of the aziridine, C(1)-N heterolysis, of **36** corresponded well with the mitomycin C analogy, but the cleavage of the C(10) carbamate under basic and nucleophilic, as well as acidic conditions, was unexpected. In prior literature, it is generally proposed that the C(10) carbamate of mitomycin C is less reactive than the C(1) aziridine, and that in the cross-linking mechanism for fully reduced mitomycin C, alkylation occurs at C(1) before C(10).[40] Furthermore, under certain conditions, monoalkylation of DNA by mitomycin C is known, where alkylation occurs at C(1) but not at C(10).[41]

Kohn showed that mitomycin C derived aziridinomitosene **49** is an intermediate in one activation pathway of mitomycin C.[42] Under neutral conditions, **49** was able to monoalkylate DNA.[42] Also, in the presence of exogenous nucleophiles, **49** was attacked at C(1) and not C(10), producing a mixture of *cis* and *trans* diastereomers (Scheme 2-9).[39d] The lower reactivity at C(10) of **49** could be due to the conjugation of the pyrrole-N to the electron withdrawing quinone carbonyls, but a smilar conjugation effect would apply at C(1).[28b] The aziridinomitosene **36** also has an electron withdrawing formyl group at C(6) which should reduce the electron density of the indole core, but observations show that the indole N is still capable of facilitating the cleavage of the carbamate at C(10).

Scheme 2-9. Solvoylsis of aziridinomitosene **49**.

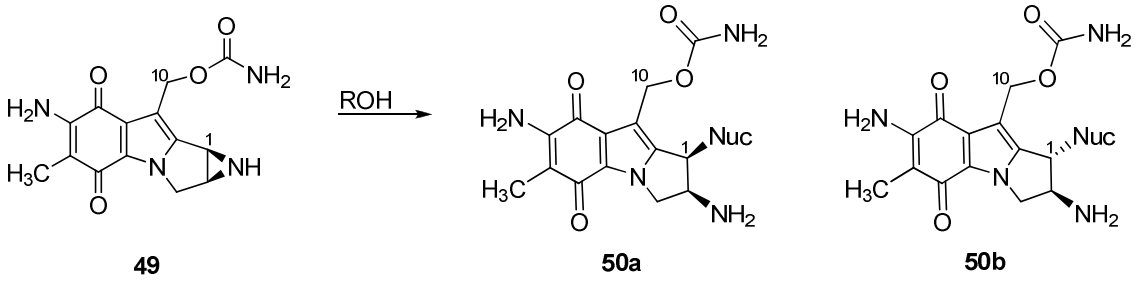

49 **50a** **50b**

Scheme 2-10. Deprotection studies on aziridinomitosene **51**.

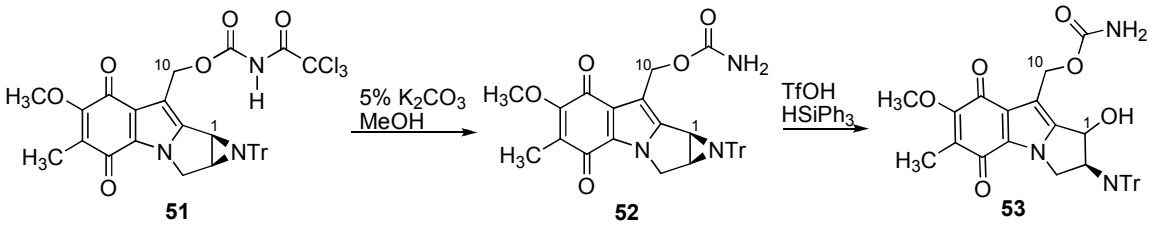

51 **52** **53**

A direct comparison of the reactivity of the C(10) carbamate can be made between the FK317 aziridinomitosene derivative **36** and an aziridinomitosene A derivative **51**. In the attempted synthesis of aziridinomitosene A (Scheme 2-10), the carbamate at C(10) did not have the reactivity that was observed in **36**. The C(10) carbamate survived treatment with basic (K_2CO_3, MeOH), as well as acidic (TfOH, TESH) conditions.[29] As expected based on Kohn's work, the C(1)-N bond of **51** was found to be more susceptible to activation and hydrolysis under acidic conditions than the C(10) carbamate bond, and under basic conditions, the carbamate was not displaced by methoxide anion. In contrast, when **36** was treated with Cs_2CO_3 and CD_3OD, the methoxide ion was incorporated at C(10), and when **39** was treated with methanesulfonic acid and triisopropyl silane, a hydride was incorporated at C(10) (Scheme 2-11). The difference in reactivity at C(10) of **36, 39** and **51** supports the hypothesis that the quinone of **51** reduces the electron density of the tetracycle more efficiently than the C(6) formyl group of aziridinomitosene **36** and **39.**

Scheme 2-11. Summary of the reactivity of the C(10) carbamate of **36** and **39**.

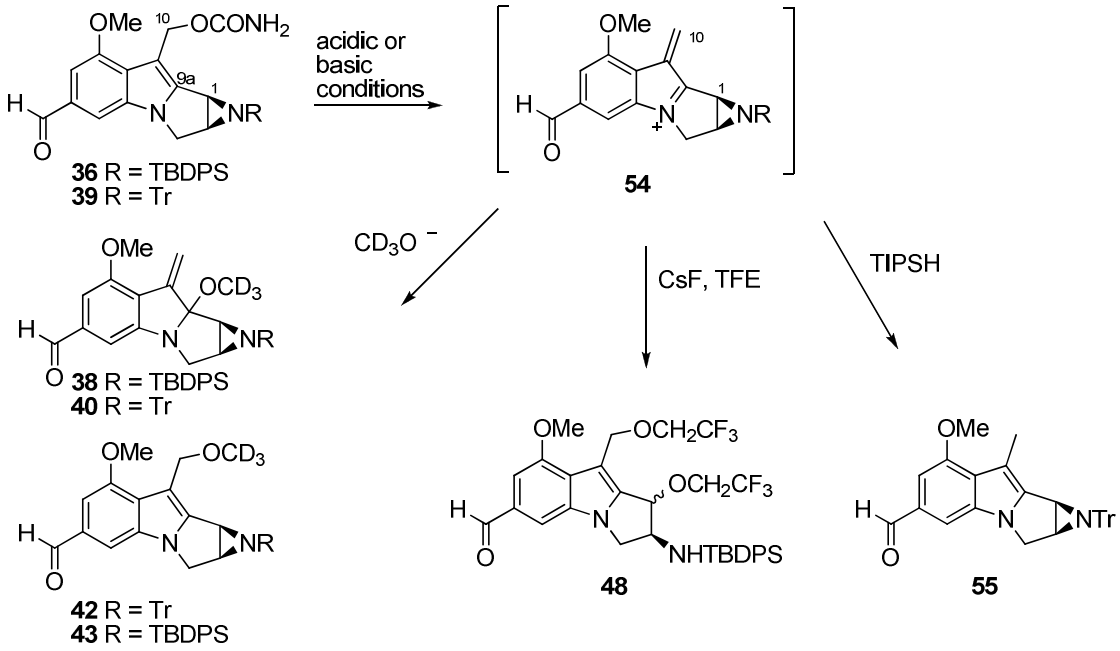

As shown above, the C(10) carbamate of **36** was much more susceptible to heterolysis than in the analogous aziridinomitosenes described by Kohn and Bobeck (Scheme 2-11).[41,29] Based on our observations, we believe that an S_N1 mechanism was responsible for cleavage of the C(10) carbamate under basic as well as acidic conditions. The electron rich indole should facilitate heterolysis at C(10) to form iminium ion **54**.[27,28b] The iminium ion can then be trapped by an available nucleophile, including the non-nucleophilic TFE, via an S_N1 mechanism. Trapping of **54** at C(9a) is also possible as shown by the formation of exocyclic alkenes **38** and **40**. Invoking the S_N1 formation of iminium ion **54**, which is disfavored in **49** due to the quinone, explains the differences in reactivity at C(10).

The proposed reductive activation of FK317 (**4**) invokes the formation of aziridinomitosene **7** as the active DNA cross-linking agent.[43] The tetracycle **7** has two sites that are active for DNA alkylation: the C(1) aziridine, and the C(10) carbamate. However, based on the observed reactivity of the carbamate at C(10) of **36**, the carbamate may have another role in

the activation pathway of the FR family. Therefore, it is apparent that DNA cross-linking by FK317 (and by analogy the FR family) is more complex than originally proposed.

In summary, the fully functionalized *N*-H aziridinomitosene of FK317 **4** remains an elusive target. The most direct route using deprotected **19** proved difficult due to insolubility and polarity; therefore, the synthesis continued with a silyl protected aziridinomitosene **29**. The bulky TBDPS protecting group of **29** allowed easier handling of the advanced tetracycles and enabled successful installation of the carbamate functionality; however, selective removal of the TBDPS could not be accomplished as **36** failed to react or decomposed under multiple reaction conditions. Although **7** was not obtained, the synthetic studies provide insight into the role of aziridinomitosene **7** as the proposed active DNA alkylating agent derived from FK317.

Experimental

General Methods. Solvents and reagents were purified as follows: diethyl ether and tetrahydrofuran (THF) were distilled from sodium/benzophenone or purified using an Anhydrous Engineering solvent purification system using columns packed with A-2 Alumina; dichloromethane (CH_2Cl_2) was distilled from P_2O_5 or purified using an Anydrous Engineering solvent purification system using columns packed with A-2 Alumina; CH_3CN was stirred over molecular sieves for 24 h, then distilled from P_2O_5; benzene, toluene, triethylamine, *i*-$PrEt_2N$, TMEDA, and DMPU were distilled from CaH_2; methanol was distilled over activated magnesium turnings, the purified reagents and solvents were used immediately or stored under nitrogen. Alkyl and aryllithiums were titrated using the procedure of Watson[44] before use. Unless otherwise noted, all chemicals were used as obtained from commercial sources and all reactions were performed under nitrogen atmosphere in glassware dried in an oven (140 °C) or flame dried and cooled under a stream of nitrogen. All reactions were stirred magnetically unless otherwise noted and liquid reagents were dispensed with all PP/PE plastic syringes or Hamilton Gastight microsyringes. Preparatory layer chromatography was performed using Whatman Partisil® K6F silica gel 60 Å 200 µm or 1000 µm plates. Flash chromatography was performed with 230-400 mesh silica gel 60.

(2*R*,3*R*)-3-iodomethyl-2-tributylstannyl-*N*-triphenylmethylaziridine (12)

To a solution of PPh_3 (0.56 mmol, 147 mg) in 2 mL toluene at 0 C was added diisopropylazodicarboxylate neat (0.56 mmol, 0.12 mL) via syringe, and the reaction mixture turned yellow. After 5 min of stirring, aziridinol **11** as a solution in toluene (0.37 mmol, 1.7 mL) was added to the PPh_3/DIAD mixture dropwise via cannula, and the mixture was stirred 5 min. Neat iodomethane (0.52 mmol, 0.03 mL) was added to the reaction mixture via syringe, and the mixture turned cloudy white. The reaction vessel was pulled out of the cooling bath, warmed to

rt, fitted with a reflux condenser and heated to 70 C. After 6 h, the reaction mixture was cooled to rt, and the solvent was removed under reduced pressure. The cloudy residue was purified immediately by flash column chromatography on silica gel (2 x 15 cm, 15:1 hexanes/ethyl acetate with 2% Et3N, Rf = 0.82). Fractions 7-11 provided 257 mg (97 %) of a clear colorless oil. Molecular ion (M – C4H9) calculated for C34H46INSn = 658.0993, found (EI) *m/z* = 658.1004, error = 2 ppm; 500 MHz ^{1}H NMR (CDCl3, ppm) δ 7.47 (6H, m) 7.27-7.24 (6H, m) 7.21-7.20 (3H, m) 3.57 (1H, dd, *J* = 10.0, 5.0 Hz) 3.00 (1H, dd, *J* = 9.5, 8 Hz) 1.62 (1H, ddd, *J* = 8.0, 6.8, 5.0 Hz) 1.5-1.4 (6H, m) 1.32 -1.24 (6H, m) 1.08-0.94 (7H, m) 0.86 (9H, t, *J* = 7.3 Hz); 100 MHz ^{13}C NMR (CDCl3, ppm) δ 144.1, 129.5, 127.3, 126.6, **76.0**, 39.0, 29.8, 29.2, 27.3, 13.6, 10.8, 10.4.

(3-methoxyphenyl)(1*H*-pyrrol-1-yl)methanol (23)

To a solution of pyrrole (1.84 mmol, 0.13 mL) in 1.5 mL THF at -78 °C was added *n*-BuLi in hexanes (1.52 M, 1.84 mmol, 1.21 mL) dropwise via syringe.[22] After 15 min at -78 °C, aldehyde **22** as a solution in THF (0.37 mmol, 0.5 mL) was added dropwise via cannula. The solution was stirred for 1 h at -78 °C, and then quenched with $(CF_3)_2CHOH$ (1.8 mmol, 0.19 mL). The mixture was stirred at -78 °C for 10 min, then warmed to rt and poured into H_2O. The mixture was extracted 3 x with Et_2O, the organic phase was washed 1 x with brine, and then dried over $MgSO_4$. Removal of the solvent under rotary evaporation provided a yellow oil. Purification by preparatory plate TLC on silica gel 60 Å (20 cm x 20 cm x 1000 µm) with 3:1 hexane/ethyl acetate, Rf = 0.29, provided 53 mg (71%) of pyrrole **23**. Molecular ion (M + H) calcd for $C_{12}H_{13}NO_2$ = 203.0946, found (electrospray) *m/z* = 203.0952, error = 3 ppm; IR (neat, cm^{-1}) 3431, OH; 400 MHz ^{1}H NMR ($CDCl_3$, ppm) δ 7.28 (1H, t, *J* = 10 Hz) 6.94-6.86 (3H, m) 6.82 (2H, t, *J* = 2.8 Hz) 6.52 (1H, d, *J* = 4.5 Hz) 6.21 (2H, t, *J* = 2.8 Hz) 3.79 (3H, s) 2.89 (1H, dd, *J* = 4.5, 1Hz); 100 MHz ^{13}C NMR ($CDCl_3$, ppm) 159.7, 141.0, 129.6, 119.1, 118.2, 114.2, 111.5, 109.2, 82.4, 55.2.

1-((*tert*-butyldimethylsilyloxy)(3-methoxyphenyl)methyl)-1*H*-pyrrole (**24**)

To a solution of **23** (25 mg, 0.12 mmol) in 1.2 mL CH_2Cl_2 at 0 °C was added imidazole (0.18 mmol, 12mg).[21] Neat TBSCl (23 mg, 0.15 mmol) was added in one portion, and the mixture turned cloudy white. The mixture was stirred and warmed to rt over 20 h, and then 1 mL of sat. $NaHCO_3$ was added. The mixture was extracted 3 x with CH_2Cl_2, washed 1 x with brine, and dried over Na_2SO_4. Rotary evaporation of the organic solvent provided a mixture of **23** and **24**. Purification by preparatory plate TLC on silica gel 60 Å (20 cm x 20 cm x 1000 µm) with 9:1 hexanes/ethyl acetate, Rf = 0.42, provided 22 mg (58%) of **24** as a yellow oil. Molecular ion (M + Na) calcd for $C_{18}H_{27}NO_2Si$ = 340.1709; found (electrospray) *m/z* = 340.1722, error = 4 ppm; 400 MHz ^{1}H NMR ($CDCl_3$, ppm) δ 7.23 (1H, t, *J* = 7.2 Hz) 6.95 (1H, br s) 6.88-6.80 (2H, m) 6.75 (2H, t, *J* = 2.1 Hz) 6.43 (1H, s) 6.14 (2H, t, *J* = 2.1 Hz) 3.78 (3H, s) 0.92 (9H, s) 0.12 (3H, s) -0.08 (3H, s); 100 MHz ^{13}C NMR ($CDCl_3$, ppm) δ 159.6, 143.2, 129.4, 119.0, 118.1, 113.6, 111.3, 108.5, 82.8, 55.2, 25.7, 18.1, -5.42, -5.45.

1-((3-methoxyphenyl)(triisopropylsilyloxy)methyl)-1*H*-pyrrole(25)

To a solution of pyrrole (1.05 mmol, 0.07 mL) in 4 mL THF at -78 °C, was added *n*-BuLi as a solution in hexanes (1.55 M, 0.65 mL, 1.0 mmol) dropwise via syringe. After stirring the solution at -78 °C for 15 min, aldehyde **21** (0.50 mmol, 0.06 mL) as a solution in 1.2 mL THF was added slowly to the cloudy solution via cannula. Upon addition the solution cleared. The solution was stirred for 30 min, and then triisopropylsilyl triflate (TIPSOTf) (1.0 mmol, 0.27 mL) was added slowly. After 30 min of stirring, the solution was diluted with 2 mL cold Et_2O, a scoopful of celite was added, and then the mixture was warmed to rt. Upon warming the colorless solution became pale yellow. The organic phase was decanted away from the solid material and removed under rotary evaporation to provide a yellow oil. The residue was purified by flash column chromatography on silica gel (3 x 15 cm, 15:1 hexanes/ethyl acetate, Rf = 0.36).

Fractions 10-16 provided 200 mg of **25** contaminated with an unknown impurity. Further purification using analytical preparatory plate TLC (200 x 200 x 200, 15:1 hexanes/ethyl acetate) provided 90 mg (50%) of clean **25.** Molecular ion calcd for (M + Na) $C_{21}H_{33}NO_2Si$: 382.2178; found (electrospray) *m/z* = 382.2168; error = 3 ppm; 500 MHz ^{1}H NMR ($CDCl_3$, ppm) δ 7.22 (1H, t, *J* = 8 Hz) 7.01 (1H, br s) 6.9 (1H, d, 10 Hz) 6.83-6.79 (3H, m) 6.49 (1H, s) 6.11 (2H, t, *J* = 2.2 Hz) 3.78 (3H, s) 1.20-1.10 (3H, m) 1.04 (9H, d, *J* = 7.5 Hz) 0.99 (9H, d, *J* = 7.5 Hz); 125 MHz ^{13}C NMR ($CDCl_3$, ppm) δ 159.8, 143.8, 129.5, 118.8, 118.1, 113.8, 111.2, 108.6, 83.2, 55.4, 18.1, 17.9, 12.5.

1-((3-methoxyphenyl)(triethylsilyloxy)methyl)-1*H*-pyrrole (**26**)

To a solution of pyrrole (7.1 mmol, 0.50 mL) in 7 mL THF at -78 °C was added a solution of *n*-BuLi in hexanes (1.44M, 6.5 mmol, 4.5 mL). An aliquot of C_4H_4NLi (0.62 M, 1.0 mmol, 1.67 mL) was added to a solution of aldehyde **21** in 5 mL THF at -78 °C. After stirring for 15 min, triethylsilyl triflate (0.23 mL, 1.0 mmol) was added dropwise via syringe. The yellow mixture was stirred at -78 °C for 30 min, then diluted with cold Et_2O. Celite was added and the organic phase was decanted off the inorganic solids, and the solvent was removed under an N_2 stream. The crude residue was purified by flash chromatography on silica gel (2 x 15 cm, 15:1 hexanes/ether with 2 % Et_3N in the eluent, Rf = 0.60) to provide 106 mg of (67%) of the pyrrole carbinol **26** as a yellow oil. Molecular ion (M + Na) calcd for $C_{18}H_{27}NO_2Si$ = 340.1709; found (electrospray) *m/z* = 340.1704, error = 1 ppm. 500 MHz ^{1}H NMR ($CDCl_3$, ppm) δ 7.23 (1H, t, *J* = 7.7 Hz) 6.95 (1H, br s) 6.88-6.80 (2H, m) 6.76 (2H, t, *J* = 2 Hz) 6.43 (1H, s) 6.14 (2H, t, *J* = 2Hz) 3.78 (3H, s) 0.91 (9H, t, *J* = 8.0 Hz) 0.60 (6H, q, *J* = 8.0 Hz); 100 ^{13}C NMR ($CDCl_3$, ppm) δ 159.6, 143.2, 129.3, 119.0, 118.1, 113.6, 111.4, 108.5, 82.6, 55.2, 6.6, 4.5.

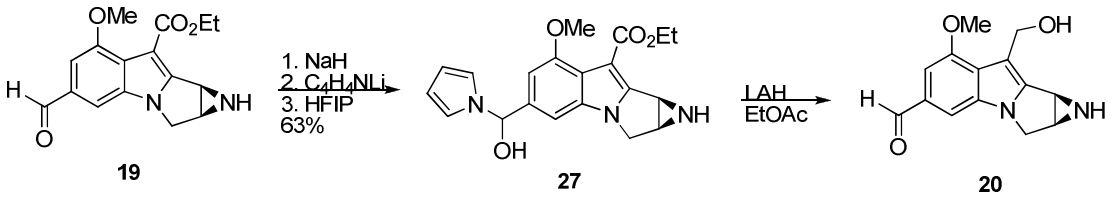

Attempted preparation of tetracyclic alcohol 20:

To a solution of **19**[13] (0.008 mmol, 2.5 mg) in 1 mL THF at -78 °C was added NaH as a solution in THF (0.25 M, 0.009 mmol, 0.04 mL) dropwise via syringe. Meanwhile, to a solution of pyrrole (0.06 mL, 0.040 mmol) in 0.20 mL THF at -78 °C was added *n*-BuLi as a solution in hexanes (0.43 M, 0.040 mmol, 0.09 mL) dropwise via syringe. The solution of C_4H_4NLi was stirred at -78 °C for 15 min, then transferred via cannula to the solution of **19** and NaH. Upon addition, the solution turned orange, and then the color faded to yellow. The mixture was stirred at -78 °C for 30 min, and then quenched with $(CF_3)_2CHOH$ (80 µL, 0.76 mmol). The crude mixture was warmed to rt, poured into H_2O, and extracted 3 x with EtOAc. The combined organic phases were washed with brine, and dried over $MgSO_4$. Rotary evaporation of the solvent produced a yellow residue as a mixture of **27** and **19**. The yellow residue was dissolved in EtOAc, washed with H_2O, dried over $MgSO_4$, and concentrated to provide a white film consisting of a mixture of diastereomers and nitrogen invertomers of **27**. Partial spectroscopic data for **27** in the presence of Et_3NHX: 400 MHz ^1H NMR ($CDCl_3$, ppm) ABq with broad doublets at 4.22-4.06 (2H) 4.03 (0.10H, unidentified s) 3.92-3.84 (3.7H, two s in a 1.0 to 0.9 ratio) 3.73(unidentified s) 3.58-3.48 (1H, br s) 3.49 (0.14H, unidentified s). The crude residue was used without purification.

To a solution of **27** and **19** from above (4.8 mg) in 0.5 mL Et_2O and 0.20 mL THF at 0 °C was added LAH as a solution in THF (0.5 M, 0.13 mL, 0.065 mmol) dropwise via syringe. The resulting cloudy green mixture was stirred at 0 °C overnight (temperature maintained in a cryocool). The mixture was quenched with ethyl acetate, and allowed to stir for another 40 min. Filtration through celite with methanol followed by solvent removal produced a yellow/orange

film. Analysis of the film by ^{1}H NMR showed an aldehyde peak at δ = 9.89 (CD_3OD); also, an alcohol was observed using IR spectroscopy: IR (neat, cm^{-1}) 3450, OH.

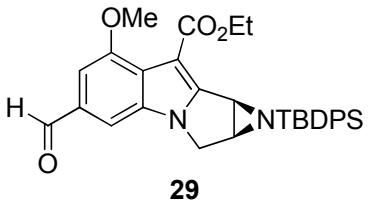

29

Preparation of *N*-TBDPS tetracyclic enoate (29)

To a solution of **19** in 1.9 mL CH_2Cl_2 was added *i*-Pr_2EtN (0.02 mL, 0.14 mmol). The solution was cooled to -78 °C and TBDPSOTF[26] as a solution in CH_2Cl_2 (0.62 M, 0.16 mL, 0.096 mmol) was added dropwise via syringe (1 drop/5 sec). After 30 min at -78 °C, the mixture was poured into pH 9.6 carbonate buffer. The mixture was extracted 3 x with CH_2Cl_2 (10 mL), and the combined organic phases were washed with brine and dried over Na_2SO_4. Removal of the solvent under rotary evaporation provided a yellow oil. The yellow oil was purified by flash chromatography on silica gel (2 x 15 cm, 2:1 hexanes/EtOAc with 2% Et_3N). Fractions 22-39 provided 37 mg of (72%) **29** as a pale yellow oil. Analytical TLC on silica gel 60 Å with 1:1 hexanes/EtOAc, Rf = 0.58. Molecular ion (M + Na) calculated for C32H34N2O4Si: 561.2186; found (electrospray) *m*/*z* = 561.2179, error = 1 ppm; IR (neat, cm^{-1}) 1721, 1690 C=O; 400 MHz ^{1}H NMR ($CDCl_3$, ppm) δ 9.98 (1H, s) 7.64-7.58 (4H, m) 7.48-7.32 (7H, m) 7.18 (1H, s) 4.29 (1H, dq, *J* = 12.0, 7.2 Hz) 4.27 (1H, d, *J* = 11.6) 4.08 (1H, m) 4.07 (1H, dd, *J* = 11.6, 3.6) 4.06 (3H, s) 3.62 (1H, d, *J* = 3.6 Hz) 3.84 (1H, dd, 3.6, 3.6 Hz) 1.15 (9H, s) 1.07 (3H, t, *J* = 7.2 Hz) 100 MHz NMR ^{13}C ($CDCl_3$, ppm) δ 191.8, 163.4, 154.7, 153.2, 135.85, 135.78, 134.7, 132.7, 131.9, 130.9, 129.8, 127.9, 127.7, 123.7, 107.6, 103.0, 101.3, 60.0, 56.0, 48.1, 40.6, 35.5, 27.6, 19.3, 14.0.

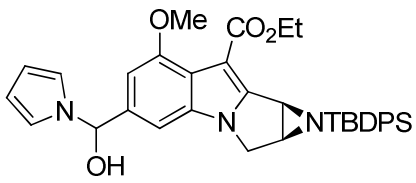

30

Preparation of tetracyclic pyrrole carbinol (30)

To a solution of pyrrole (0.10 mL, 1.44 mmol) in 3 mL THF at -78 °C was added *n*-BuLi as a solution in hexanes (0.92 mL, 1.40 M, 1.3 mmol) via syringe. The resulting C_4H_4NLi was stirred at -78 °C for 15 min. To a solution of aldehyde **29** (0.067 mmol, 36 mg) in 1.10 mL THF at -78 °C was added C4H4NLi (1.3 M, 0.13 mmol) as a solution in 0.39 mL THF/hexanes. The resulting solution was stirred at -78 °C for 15 min, and then $(CF_3)_2CHOH$ as a solution in Et_2O (0.10 mL, 1.9 M, 0.19 mmol) was added. The solution was diluted with 2 mL cold Et_2O, and a tipful of celite was added. The organic phase was decanted from the insoluble material, and the solvent was removed under N_2. The residue was immediately purified by preparative TLC on silica gel 60 Å (20 cm x 20 cm x 1000 μm) pre-treated with Et_3N vapors for ≥ 30 min, providing 33 mg of a 1:1 diastereomeric mixture of product as a residue; 2:1 hexanes/EtOAc, Rf = 0.28. IR (neat, cm^{-1}) 3411, OH; 1696, C=O; 400 MHz ^1H NMR ($CDCl_3$, ppm, 15% aldehyde **29** present, 42% Et_3N) δ 7.64-7.58 (9H, m) 7.48-7.32 (14H, m) 6.88-6.82 (6H, m) 6.68-6.62 (4H, m) 6.21 (3.5H, t, *J* = 2.5 Hz) 4.31-4.22 (2.75H, m) 4.17 (2H, d, *J* = 11.2 Hz) 4.10-4.02 (3.3H, m) 3.96-3.92 (8H, m) 3.57 (2H, d, *J* = 3.6 Hz) 3.31 (2H, dd, *J* = 3.6 Hz, 3.2 Hz) 1.14 (18H, m) 1.04 (6H, m).

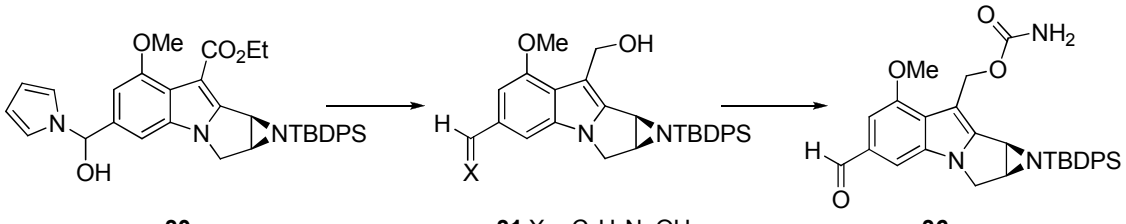

Preparation of tetracyclic carbamate aldehyde (36)

To a solution of pyrrole carbinol **30** (33.6 mg, 0.055 mmol) in 1 mL Et_2O at 0 °C was added LAH in a solution of THF (0.28 mL, 1.0 M, 0.28 mmol, 5 mol equiv) dropwise via syringe. The cloudy non-homogenous mixture was stirred vigorously at 0 °C. After 45 min, 0.5 mL EtOAc was added slowly at 0 °C, and the mixture was allowed to warm to rt and stirred for an addition hour. The crude mixture was then filtered through celite with CH_3CN (3 x 10 mL), and the combined organic washes were concentrated under reduced pressure to provide 17.4 mg of a 4:1 mixture of alcohols **31** and **32** as a clear bright green oil. Selected data for **31**: 400 MHz ^{1}H NMR ($CDCl_3$, ppm) δ 4.93 (1H, **A**BX dd, *J* = 12.4, 5.3 Hz) 4.73 (1H, A**B**X dd, *J* = 12.4, 8.2 Hz) 3.28 (1H, dd, *J* = 3.4, 3.4 Hz) 3.22 (1H, d, *J* = 4.0 Hz) 2.99 (1H, AB**X** dd, *J* = 8.2, 5.3 Hz). Selected data for **32**: IR (neat, cm^{-1}) 3539 OH, 1681 C=O; 400 MHz ^{1}H NMR ($CDCl_3$, ppm) δ 9.95 (1H, s) 7.62-7.58 (4H, m) 7.48-7.36 (6H, m) 7.32 (1H, s) 7.08 (1H, s) 4.95 (1H, **A**BX dd, *J* = 12.8, 5.6 Hz) 4.76 (1H, A**B**X dd, *J* = 12.8, 8.0 Hz) 4.26 (1H, d, *J* = 11.2 Hz) 4.06 (3H, s) 4.03 (1H, A**B**X dd, *J* = 11.2, 3.2 Hz) 3.6 (1H, AB**X** dd, *J* = 3.6, 3.2 Hz) 3.29 (1H, d, *J* = 3.6 Hz) 2.88 (1H, AB**X** dd, *J* = 8.0, 5.6 Hz) 1.15 (9H, s).

The mixture of alcohols **31** and **32** (17.4 mg, 0.035 mmol) in 1 mL CH_2Cl_2 was cooled to -78 °C. The solution was charged with Et_3N (0.72 M, 0.04 mmol) in 0.06 mL of CH_2Cl_2 and Fmoc-NCO? (0.46 M, 0.07 mmol) in 0.15 mL of CH_2Cl_2 was added via syringe. After 20 min of stirring at -78 °C, the yellow green solution was warmed to rt and stirred for 1 h (the mixture turned dark yellow upon warming). The CH_2Cl_2 was removed under N_2, and the crude residue

was dissolved in 1 mL THF and cooled to 0 °C. Next, TBAF on Al_2O_3? (314 mg, 0.18 mmol) was added in one portion and the mixture was stirred and warmed to rt in the cooling bath. After 2 h, the crude reaction mixture was filtered through celite with EtOAc and the solvent was removed under reduced pressure to provide 22 mg of residue. The residue was purified by preparative TLC on silica gel 60 Å (20 cm x 20 cm x 250 µm) pre-treated with Et_3N vapors for ≥ 30 min, providing **36** as a white amorphous powder; 1:1 hexanes/EtOAc; Rf = 0.28. Molecular ion calculated for $C_{30}H_{31}N_2O_2Si$: 479.2155; found (electrospray) *m/z* = 479.2168, error = 3 ppm; IR (neat, cm^{-1}) 3473, 3348, $CONH_2$; 400 MHz ^1H NMR ($CDCl_3$, ppm) δ 9.94 (1H, s) 7.63-7.61 (4H, m) 7.43-7.38 (6H, m) 7.31 (1H, s) 7.05 (1H, s) 5.47 (2H, AB q, *J* = 12.2 Hz) 4.41(1H, br s) 4.23 (1H, d, *J* = 11.2 Hz) 4.02 (1H, ABX dd, *J* = 11.2, 3.2 Hz) 3.97 (3H, s) 3.41 (1H, d, 4.0 Hz) 3.36 (1H, ABX dd, *J* = 4.0, 3.2 Hz) 1.15 (9H, s); 100 MHz ^{13}C NMR ($CDCl_3$, ppm) δ 192.0, 156.9, 154.6, 146.5, 135.9, 135.8, 132.1, 132.0, 130.0, 127.9, 127.8, 125.1, 104.5, 98.2, 59.6, 55.5, 47.5, 41.4, 33.2, 27.5, 19.3.

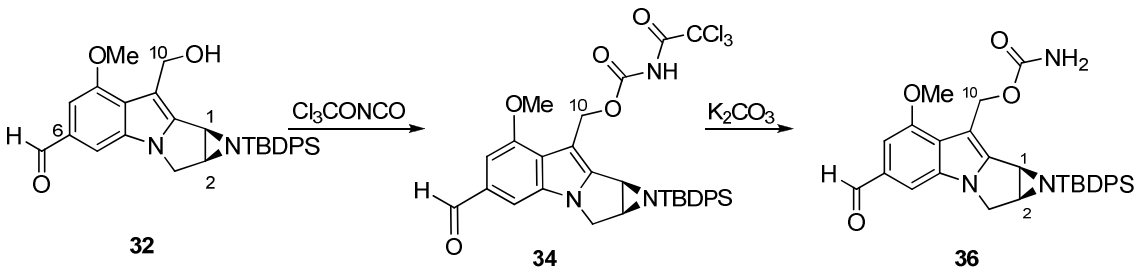

32 **34** **36**

Attempted preparation of tetracycle 34 and 36

To a solution of **32** (0.0046 mmol, 2.28 mg) in 0.30 mL CH_2Cl_2 at -78 °C was added trichloroacetyl isocyanate as a solution in CH_2Cl_2 (0.28 M, 0.0051 mmol, 18 µL) via microsyringe. The dark yellow solution was stirred at -78 °C for 1 h, and then pulled out of the cooling bath and allowed to warm to rt. After 1 h, pH 9.6 carbonate buffer was added and the mixture was stirred for 5 min, extracted 3 x with CH_2Cl_2, washed 1 x with brine, and dried over pulverized Na_2SO_4. Solvent removal provided a yellow film. Analysis of the residue by ^1H NMR spectroscopy ($CDCl_3$, ppm) showed a complex mixture; however, AB doublets at δ = 5.66

(J = 12.0 Hz) and 5.56 (J = 11.5 Hz) were observed. The crude residue was dissolved in 0.30 mL MeOH and 0.30 mL K_2CO_3 (5% w/v) in MeOH[29] and stirred vigorously for 2.5 h. The mixture was extracted with ethyl acetate and solvent removal under reduced pressure provided an orange film. Analysis of the residue by ^{1}H NMR spectroscopy showed loss of the AB doublets and a complex mixture of compounds.

^{1}H NMR scale reaction of tetracycle 29 with D_2O in CD_2Cl_2 (19)

A residue of **29** (2.3 mg) was dissolved in CD_2Cl_2 saturated with D_2O, and the sample was monitored by ^{1}H NMR spectroscopy. After 3 h of no reaction, the NMR tube containing the sample was gently heated with an oil bath to 35 °C; no deprotected **19** was observed after 2 h of heating.

^{1}H NMR scale reaction of tetracycle 29 with 2,2,2-trifluoroethyl alcohol in $CDCl_3$ (19)

A residue of **29** (2.3 mg) was dissolved in $CDCl_3$ with an excess of TFE, and the sample was monitored by ^{1}H NMR spectroscopy. After 3 h of no reaction, the NMR tube containing the sample was gently heated with an oil bath to 35 °C; no deprotected **19** was observed after 20 h.

^{1}H NMR scale reaction of tetracycle 29 with deuterated methanol (19)

A residue of **29** (2.3 mg) was dissolved in CD_3OD and monitored by ^{1}H NMR spectroscopy. New peaks were apparent between δ = 4.4 and 3.4 ppm after 1.5 h, and the intensities had continued to increase at 3 and 5 h. Also, two signals appeared upfield: a triplet at δ = 1.43 ppm corresponding to the CH_3 of the ethyl enoate, and a singlet at δ = 1.04 ppm corresponding to a new TBDPS species. After 20 h, no starting material was apparent by ^{1}H NMR. Selected data for **19**: Molecular ion (M + Na) calcd for $C_{16}H_{16}N_2O_4$ = 323.1, found (electrospray, nomial mass) *m/z* = 323.1; 400 MHz ^{1}H NMR (CD_3OD, ppm) δ 9.94 (1H, s) 7.72-7.66 (4H, m) 7.56 (1H, s)

7.48-7.38 (6H, m) 7.21 (1H, s) 4.37 (2H, q, *J* =7.2 Hz) 4.28 (1H, br s) 4.04-3.96 (4H, m) 3.75 (1H, br s) 1.43 (3H, t, *J* =7.2).

^{1}H NMR scale reaction of tetracycle 36 with deuterated methanol

A residue of **36** was dissolved in $CDOD_3$ and monitored by ^{1}H NMR spectroscopy over a 4 h period. After 15 min, the aziridine C(1) and C(2) protons at δ = 3.53 and 3.49 ppm, respectively as well as the C(10) methylene protons at δ = 5.41 and 5.34 ppm began to decrease in intensity. The singlet at 1.09 ppm corresponding to the *tert*-butyl of the TBPDS group was less intense, while a singlet at 1.01 ppm began to appear. At 45 min, the intensity of the C(1), C(2) and C(10) peaks had further decreased, and no new aziridine methine peaks were visible. By 2 h, the C(1) and C(2) peaks were no longer visible, and after 4 h, the singlet at 1.09 ppm had disappeared. While monitoring the sample, no peaks corresponding to **7** were observed; however, the presence of a *tert*-butyl signal at 1.01 ppm implies deprotection. After 2 days, the sample showed ring opened products which were not isolated.

^{1}H NMR scale reaction of tetracycle 29 with deuterated methoxide (19)

A residue of TBDPS aziridinomitosene **29** was dissolved in a solution of Cs_2CO_3 (5 mg) in 0.5 mL CD_3OD.[45] The sample was monitored by ^{1}H NMR spectroscopy over 5 h. No change was observed after 5 min, but after 15 min, a triplet, corresponding to the enoate of **19**, at δ = 1.43 ppm and a singlet, corresponding to a new TBDPS species, at δ = 1.01 ppm had appeared. After 1 and 4 h, the signal intensity of both the triplet and singlet had increased. At 5 h, the relative amount of **19** was determined by integration of the unobscured triplet at 1.43 ppm, and was determined to be 12 %.

^{1}H NMR scale reaction of tetracycle 36 with deuterated methoxide (38 and 43)

A residue of tetracycle **36** was dissolved in a mixture of Cs_2CO_3 (5 mg) in 0.5 mL CD_3OD and the sample was monitored by ^{1}H NMR spectroscopy every 15 min for 10 h. After 1 h, new signals corresponding to the C(1) and C(2) methine protons began appearing around δ = 3.5 and 3.4 ppm as well as two new ABX methylene protons appearing near δ = 4.7 and 4.9 ppm. Two methine protons upfield near 2.6 and 2.4 ppm also began appearing after 1 h. The intensity of these signals continued to increase during the 10 h period. At 17 h, all four methine signals were still present; however, after 6 d, the methine protons near δ = 3.5 and 3.4 ppm had disappeared, but the signals near δ = 2.6 and 2.4 ppm were still present. The sample was purified by analytical preparatory TLC on silica gel 60 Å (20 cm x 20 cm x 250 μm) pre-treated with Et_3N fumes (≥ 30 min) to provide a yellow residue. Selected data for **38**: Molecular ion (M + H) calcd for $C_{31}H_{31}D_3N_2O_3Si$ = 514.3, found (electrospray, nomial mass) *m/z* = 514.3; 500 MHz ^{1}H NMR ($CDCl_3$, ppm) δ 9.92 (1H, s) 7.45-7.30 (m) 6.89 (1H, s) 6.78 (1H, s) 6.29 (1H, s) 5.55 (1H, s) 4.01 (3H, s) 3.55 (1H, d, *J* = 12.0 Hz) 3.34 (1H, d, *J* = 12.0, 1.4 Hz) 2.66 (1H, d, *J* = 3.1 Hz) 2.43 (1H, dd, *J* = 3.1, 1.4 Hz) 0.84 (9H, s); Selected data for **43**: 500 MHz ^{1}H NMR ($CDOD_3$, ppm) δ 4.86 (1H, d, *J* = 11.0 Hz) 4.72 (1H, d, *J* = 11.0 Hz) 3.50 (1H, m) 3.40 (1H, d, *J* = 3.5 Hz).

^{1}H NMR scale reaction of tetracycle 39 with deuterated methoxide (40 and 42)

To a sample CD_3OD (0.50 mL) was added Cs_2CO_3 (10 mg, 0.03 mmol). Then the solvent was decanted away from any insoluble material, and then added to a residue of **36**. The sample stood at rt and was monitored by ^{1}H NMR spectroscopy. After 1.5 h, the ratio of compounds **39**:**40**:**42** was 75:11:14 (% determined by integration) as observed by ^{1}H NMR spectroscopy. After 26 h, the ratio of **39**:**40**:**42** observed by ^{1}H NMR spectroscopy was 12:42:44. After 67 h, the solvent was removed under N_2 flow and the residue was purified by analytical preparatory plate TLC on silica gel 60 Å (20 cm x 20 cm x 250 μm) pre-treated with Et_3N fumes (≥ 30 min) with 2:1 pentane/ethyl acetate providing **40** and **42** as yellow oils (yield not determined). Selected data for

40: Molecular ion (M +Na) calcd for $C_{34}H_{27}D_3N_2O_3$ = 540.2342, found (electrospray with formic acid) *m/z* = 540.2360, error = 3 ppm; 500 MHz ($CDCl_3$, ppm) δ 9.97 (1H, s) 7.26-7.20 (6H, m) 7.18-7.12 (9H, m) 6.96 (1H, d, *J* = 0.5 Hz) 6.93 (1H, s) 6.30 (1H, s) 5.47 (1H, s) 3.80 (1H, d, *J* = 12.5) 3.40 (1H, dd, *J* = 12.5, 1.5 Hz) 2.28 (1H, d, *J* = 4.5 Hz) 2.13 (1H, dd, *J* = 4.5, 1.5) 125 MHz ^{13}C ($CDCl_3$, ppm) δ 192.1, 157.1, 156.8, 144, 1, 140.2, 138.8, 129.3, 127.4, 126.6, 120.9, 114.4, 106.1, 104.0, 103.9, 73.8, 55.6, 51.5, 45.3, 37.0. Selected data for **42**: Molecular ion (M +Na) calcd for $C_{34}H_{27}D_3N_2O_3$ = 540.2342, found (electrospray with formic acid) *m/z* = 540.2341, error = 0.2 ppm; 500 MHz ^1H NMR ($CDCl_3$, ppm) δ 9.97 (1H, s) 7.49 (6H, d, *J* = 7.5 Hz) 7.38 (3H, d, *J* = 14.0 Hz) 7.30 (6H, t, *J* = 7.5 Hz) 7.25 (1H, m) 7.07 (1H, s) 4.90 (1H, d, *J* = 11.5 Hz) 4.73 (1H, d, *J* = 11.5 Hz) 4.44 (1H, d, *J* = 11.0 Hz) 4.10 (1H, dd, *J* = 11.0, 3.5 Hz) 3.04 (1H, d, *J* = 5.0 Hz) 3.01 (1H, dd, 5.0, 3.5 Hz); 125 MHz ^{13}C NMR ($CDCl_3$, ppm) δ 192.1, 154.8, 145.3, 144.1, 133.8, 131.8, 129.3, 128.3, 127.8, 127.1, 125.7, 109.0, 107.1, 98.1, 74.5, 66.2, 55.5, 47.4, 42.5, 35.1.

2-benzyl-1-(*tert*-butyldiphenylsilyl)-3-phenylaziridine (**45**)

To a solution of aziridine[??] (469 mg, 2.24 mmol) in 20 mL CH_2Cl_2 at -78 °C was added *i*-Pr_2NEt (0.58 mL, 3.36 mmol). One equiv of *tert*-butyldiphenylsilyl triflate (0.92 mL, 2.24 mmol) was added dropwise via syringe, and the solution was stirred at -78 °C. After 2.5 h, 0.5 equiv TBDPSOTf was added, and the reaction continued. After reaction completion according to TLC analysis, the mixture was poured into pH 7 buffer and extracted 3 x with CH_2Cl_2. The organic phase was washed with brine, and dried over Na_2SO_4. Removal of the solvent by rotary evaporation provided a cloudy white oil. Purification by flash chromatography on silica gel (3.5 x 15 cm, with 100 % hexanes and 2 % Et_3N) provided 777 mg (78 %) of **45**. Molecular ion (M + H) calcd for $C_{31}H_{33}NSi$ = 447.2382; found (electron impact) *m/z* = 447.2375, error = 2 ppm; 400 MHz ($CDCl_3$, ppm) δ 7.73-7.67 (2H, m) 7.62-7.56 (2H, m) 7.50-7.24 (11H, m) 7.12- 7.10 (3H, m) 6.74-6.67 (2H, m) 3.00 (1H, d, *J* = 4.8 Hz) 2.9 (1H, dd, *J* = 14.3, 3.5 Hz) 2.46 (1H, dd, *J* =

14.3, 8.8 Hz) 2.13 (1H, ddd, *J* = 8.8, 4.8, 3.5 Hz) 1.15 (9H, s); 100 MHz ^{13}C NMR ($CDCl_3$, ppm) δ 139.2, 128.3, 136.2, 133.4, 132.3, 129.49, 129.46, 128.8, 127.8, 127.53, 127.48, 126.7, 125.9, 40.8, 39.8, 34.5, 27.6, 19.2; an unknown signal at 29.3 ppm was also detected.

Deprotection of 45 with TBAF (Table 2-4, entry 1)

To a solution of aziridine **45** (0.24 mmol, 107.7 mg) in 2.4 mL DMF at rt was added TBAF as a solution in THF (1.0 M, 0.24 mL). After 3 h of stirring at rt, saturated $NaHCO_3$ (1.0 mL) was added. The mixture was extracted 3 x with Et_2O, the combined organics were washed 1 x with brine, and then dried over $MgSO_4$. Removal of the solvent by rotary evaporation provided an oil. Purification of the crude residue by flash chromatography on silica gel (2 x 15 cm silica gel, 1:1 hexanes/Et_2O, Rf = 0.18) provided 28.2 mg (56%) of aziridine **46**.[36]

NMR scale deprotection of 45 with TBAT (Table 2-4, entry 2)

Aziridine **45** was dissolved in approximately 1 mL DMF-d7, and a spatula tipfull of TBAT was added to the solution. Only **45** and TBAT were observed by ^{1}H NMR spectroscopy at 5 h and 3 d.

NMR scale deprotection of 45 with TBAT and TFE (Table 2-4, entry 3)

To a sample of **45** (0.58 mmol, 25.9 mg) in 1 mL DMF-d7 was added TFE (0.58 mmol, 4.2 µL) and TBAT (0.58 mmol, 32 mg). The sample was monitored by ^{1}H NMR spectroscopy. At 1 h, peaks corresponding to **46** had appeared; at 2 h, 27% (calculated by integration of the ^{1}H NMR signals) of **46** was present. After 24 h, 75% of **46** was present. Selected data for **46**: 400 MHz ^{1}H NMR (DMF-d7, ppm) δ 7.46 (2H, d, *J* = 7.2 Hz) 7.36 (2H, t, *J* = 7.4 Hz) 7.30-7.22 (3H, m) 7.20-7.08 (3H, m) 3.34(1H, dd, *J* = 9.0, 6.2 Hz) 2.55 (1H, dddd, *J* = 9.0, 7.2, 6.4, 6.4 Hz) 2.44 (1H, dd, *J* = 14.4, 6.4 Hz) 2.35 (1H, dd, *J* = 14.4, 6.4 Hz) 2.21 (1H, br dd, *J* = 7.2, 6.2 Hz).

NMR scale deprotection of 45 with CsF and TFE (Table 2-4, entry 4)

An oven dried NMR tube was charged with CsF (0.10 mmol, 15 mg) and capped with a rubber septum under an inert atmosphere. A solution of aziridine **45** in DMF-d7 (0.06 mmol, 27.5 mg, 0.5 mL) was then added to the NMR tube through the septum via syringe. Neat TFE (0.06 mmol, 4.3 µL) was then added to the NMR tube. The NMR tube was shaken for 30 sec and then the insoluble material was allowed to settle. The sample was monitored by ^{1}H NMR without spinning. After 10 min, **46** began to appear, and after 2 h, 48% of **46** was present. At 20 h, 93% of **46** was observed.

Deprotection of 45 with CsF and TFE in CH_3CN (Table 2-4, entry 5)

To a non-homogenous solution of **45** (0.26 mmol, 114.1 mg) in 1.8 mL CH_3CN as added CsF (0.30 mmol, 47 mg) as a solution in CH_3CN (0.8 mL) and TFE (0.10 mL, 1.39 mmol). The resulting white non-homogenous mixture was stirred vigorously. The solution cleared after 3 d of stirring, and a saturated solution of $NaHCO_3$ was added. The mixture was extracted 3 x with Et_2O, the combined organics were washed with brine, and dried over $MgSO_4$. Removal of the solvent under rotary evaporation provided a clear yellow oil. The residue was purified by preparatory plate TLC on silica gel 60 Å (20 cm x 20 cm x 1000 µm) pre-treated with Et_3N fumes ($\geq$ 30 min) with 9:1 hexane/ethyl acetate. Elution of the bands with ethyl acetate provided $TBDPSOCH_2CF_3$ (yield not determined), 13 mg (11%) of **45** and 22 mg (41%) of **46**. Selected data for $TBDPSOCH_2CF_3$:

Deprotection of 45 with CsF in TFE (Table 2-4, entry 6):

To a solution of aziridine **45** (0.33 mmol, 147 mg) in 1.3 mL TFE was added CsF was a solution in TFE (0.17 M, 2.0 mL, 0.33 mmol). Aziridine **45** was insoluble in TFE, so the reaction vessel was placed in a sonicator to break up the insoluble material. Then the non-homogenous solution was stirred vigorously at rt. After 2 d of stirring, 2 mL of satd $NaHCO_3$ was added, and the

mixture was extracted 3 x with Et_2O, washed 1 x with brine, and dried over $MgSO_4$. Solvent removal under rotary evaporation provided an oily residue. The crude residue was purified by flash chromatography with silica gel (2 x 15 cm, 3:1 hexanes/ethyl aceate, with 2% Et_3N in the eluent). Fractions 25-32 provided 42 mg (61%) of **46**.

NMR scale deprotection of 45 with TFE (Table 2-4, entry 7):

To a solution of **45** (0.049 mmol, 21.8 mg) in DMF-d7 was added neat TFE (0.049 mmol, 3.5 µL). The resulting sample was monitored by ^{1}H NMR. After 2 d, only 14% of **46** was observed by ^{1}H NMR.

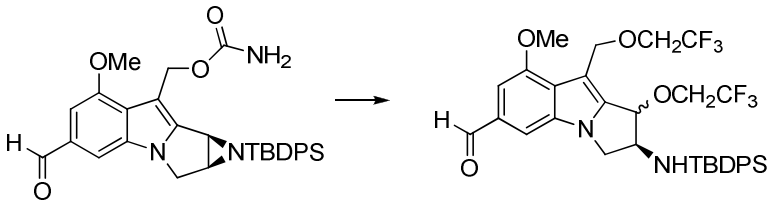

36 **47**

Attempted deprotection of 36 with CsF in TFE (47)

To a cloudy solution of **36** (0.0019 mmol, 1 mg) in 0.05 mL THF was added TFE (5.6 mmol, 0.40 mL). The solution cleared and turned bright yellow. A solution of CsF in TFE (0.11 M, 0.0022 mmol, 20 µL) was added to the reaction vessel via microsyringe. After no apparent reaction by TLC, another equiv of CsF was added at 2 and 5 h, and 2 equiv of CsF was added at 6.5 h for a total of 5 equiv of CsF. After 24 h of total reaction time, the solvent was removed under a flow of N_2 to provide an orange solid. The crude residue was purified by preparatory plate TLC on silica gel 60 Å (20 cm x 20 cm x 250 µm) pre-treated with Et_3N fumes ($\geq$ 30 min) with 100% ethyl acetate to provide a residue containing two compounds in approximately a 1:1 ratio (by integration of crude residue). Selected data for major diastereomer **47a**: Molecular ion (M + Na) calculated for $C_{34}H_{36}F_6N_2O_4Si$ = 701.2, found (electrospray, nomial mass) *m/z* = 701.3;

500 MHz partial ^{1}H NMR ($CDCl_3$, ppm) δ9.91 (1H, s) 7.70 (2H, dd, *J* = 8.1, 1.4 Hz) 7.65 (2H, dd, *J* = 8.1, 1.4 Hz) 7.46-7.37 (7H, m) 7.08 (1H, s) 5.09 (1H, d, *J* = 11.8 Hz) 4.99 (1H, d, *J* = 11.8 Hz) 4.74 (1H, s) 4.34 (1H, dd, *J* = 10.5, 5.5 Hz) 4.06-4.00 (1H, m) 4.00 (3H, s) 3.93 (2H, q, $J^{H,F}$= 8.8 Hz) 3.89 (1H, dd, *J* = 10.5, 2.0 Hz) 3.56-3.44 (2H, dq, *J* = 12.3 Hz, $J^{H,F}$ = 8.6) 1.01 (9H, s); 376 MHz ^{19}F ($CDCl_3$, ppm) δ -74.0 (t, $J^{F,H}$ = 8.8 Hz) -74.4 (t, $J^{F,H}$ = 8.6 Hz). Selected data for minor diastereomer **47b**: Molecular ion (M + Na) calculated for $C_{34}H_{36}F_6N_2O_4Si$ = 701.2, found (electrospray, nomial mass) *m/z* = 701.3; 500 MHz partial ^{1}H NMR ($CDCl_3$, ppm) δ 9.94 (1H, s) 5.11 (1H, d, *J* = 12.0 Hz) 4.85 (1H, d, *J* = 12.0 Hz) 4.56 (1H, d, *J* = 4.5 Hz) 4.09 (1H, m) 3.98-3.88 (4H, m) 3.84 (1H, m); 376 ^{19}F NMR (C_6D_6, ppm) δ -73.7 (dd, *J* = 9.0, 8.6 Hz) -73.9 (dd, *J* = 9.7, 8.3 Hz).

Chapter 2 Bibliography

1. Kiyoto, S.; Shibata, T.; Yamashita, M.; Komori, T.; Okuhara, M.; Terano, H.; Kohsaka, M.; Aoki, H.; Imanaka, H. A New Antitumor antibiotic, FR-900482 II. Production, Isolation, Characteriazation and Biological Activity. *J. Antibiot.* **1987**, 594.

2. Terano, H.; Takasa, S.; Hosada, J.; Kohsaka, M. A new antitumor antibiotic, FR66979. *J. Antibiot.*1989, 42, 145.

3. (a) Shimomura, K.; Manda, T.; Mukumoto, S.; Masuda, K.; Nakamura, T.; Mizota, T.; Matsumoto, S.; Nishigaki, F.; Oku, T.; Mori, J.; Shibayama, F. Antitumor activity of hematotoxicity of a new, substituted dihydro-benzoxazine, FK973, in mice. *Cancer Res.* 1988, *48*, 1166. (b) Masuda, K.; Nakamura, T.; Mizota, T.; Mori, J.; Shimomura, K. Interstrand DNA-DNA and DNA-protein cross-links by a new antitumor antibiotic, FK973, in L1210 cells. *Cancer Res.* **1988**, *48*, 5172.

4. (a)Naoe, Y.; Inami, M.; Kawamura, I.; Nishigaki, F.; Tsujimoto, S.; Matsumoto, S.; Manda, T.; Shimomura, K. Cytotoxic Mechanisms of FK317, a New Class of Bioreductive Agent with Antitumor Activity. *Jpn. J. Cancer Res.* 1998, *89*, 666. (b)Naoe, Y.; Inami, M.; Matsumoto, S.; Nishigaki, f.; Tsujimoto, S.; Kawamura, I.; Miyayasu, K.; Manda, T.; Shimomura, K. FK317: a novel substituted dihydrobenzoxazine with potent antitumor activity which does not induce vascular leak syndrome. *Cancer Chemother. Pharmacol.* **1998**, *42*, 31.

5. Rajski, S. R.; Williams, R. M. DNA Cross-linking Agents as Antitumor Drugs. *Chem Rev.* **1998**, *98*, 2723.

6. (a)Masuda, K.; Nakamura, T.; Shimomura, K. A New Antitumor antibiotic, FR-900482 V. Interstrand DNA-DNA cross-links in L1210 cells. *J. Antibiot.* **1988**, 1497. (b)Huang, H.; Rajski, S. R.; Williams, R. M.; Hopkins, P. B. FR66979 requires reductive activation to cross-link DNA efficiently. *Tetrahedron Lett.* **1994**, *35*, 9669. (c)Williams, R. M.; Rajski, S. R.; Rollins, S. B. FR900482, a close cousin of mitomycin C that exploits mitosene-based DNA cross-linking. *Chemistry & Biology* **1997**, *4*, 127. (d)Paz, M. M.; Hopkins, P.B. DNA-DNA interstrand Cross-linking by FR66979 and FR900482: Requirement of Metal Ions During Reductive Activation. *Tetrahedron Lett.* **1997**, *38*, 343.

7. (a) Shimomura, K.; Hirai, O.; Mizota, T.; Matsumoto, S.; Mori, J.; Shibayama, F.; Kikuchi, H. A New Antitumor antibiotic, FR-900482 III. Antitumor Activity in Transplantable Experimental Tumors. *J. Antibiot.* **1987**, 600. (b)Hirai, O.; Shimomura, K.; Mizota, T.; Matsumoto, S.; Mori, J.; Kikuchi, H. A New Antitumor antibiotic, FR-900482 IV. Hematological Toxicity in Mice. *J. Antibiot.* **1987**, 607.

8. Naoe, Y.; Inami, M.; Matsumoto, S.; Takagaki, S.; Fujiwara, T.; Yamazaki, S.; Kawamura, I.; Nishigaki, F.; Tsujimoto, S.; Manda, T.; Shimomura, K. FK317, a novel substituted diydrobenzoxazine, exhibits potent activity against human tumor xenografts in nude mice. *Jpn. J. Cancer Res.* **1998**, *89*, 1306.

9. Fukuyama, T.; Goto, S. Synthetic approaches toward FR900482. I. Stereoselective synthesis of a pentacyclic model compound. *Tetrahedron Lett.* 1989, *30*, 6491.

10. Woo, J.; Sigurdsson, S. T.; Hopkins, P. B. DNA interstrand cross-linking by reductively activated FR900482 and FR66979. *J. Am. Chem. Soc.* **1993**, *115*, 1199.

11.Vedejs, E.; Little, J. Aziridinomitosenes by anionic cyclization: Deuterium as a removable blocking group. *J. Am. Chem. Soc.* **2002,** *124*, 478.

12. Vedejs, E.; Little, J. D.; Seaney, L. M. Synthesis of the Aziridinomitosene skeleton by intramolecular Michael Addition: α-lithioaziridines and nonaromatic substrates. *J. Org. Chem.* **2004**, *69*, 1788.

13. Kim, M.; Vedejs, E. A synthetic approach towards the proposed tetracyclic aziridinomitosene derived from FK317. *J. Org. Chem.* **2004**, *69*, 7262.

14. Naoe, Y.; Inami, M.; Matsumoto, S.; Nishigaki, F.; Tsujimoto, S.; Kawamura, I.; Miyayasu, K.; Manda, T.; Shimomura, K. FK317: a novel substituted dihydrobenzoxazine with potent antitumor activity which does not induce vascular leak syndrome. *Cancer Chemother. Pharmacol.* **1998**, *42*, 31.

15. Kim, M.; Vedejs, E. A reinvestigation of 4-hydroxyindole-6-carboxylate synthesis from pyrrole-2-carboxyaldehyde: A facile synthesis of indoles and indolizines. *J. Org. Chem.* **2004**, *69*, 6945.

16. Vedejs, E.; Naidu, B. N.; Klapars, A.; Warner, D. L.; Li, V.; Na, Y.; Kohn, H. Synthetic enantiopure aziridinomitosenes: Preparation, reactivity, and DNA alkylation studies. *J. Am. Chem. Soc.* **2003**, *125*, 15796.

17. Robins, D. J.; Sakdarat, S. Synthesis of the pyrrolizidine base, (±)-supinidine. *J. Chem. Soc. Perkin 1*. **1979**¸ 1734.

18. Vedejs, E.; Klapars, A.; Warner, D. L.; Weiss, A. H. Reductive deprotection of N-tritylaziridines. *J. Org. Chem.* **2001**, *66*, 7542.

19. Han, I.; Kohn, H. 7-Aminoaziridinomitosenes: synthesis, structure, and chemistry. *J. Org. Chem.* **1991**, *56*, 4648.

20. Little, J. D. "Synthetic studies toward aziridinomitosenes and their derivatives." Ph.D., University of Wisconsin-Madison, Madison, Wisconsin, 2001.

21. Evans, D. A.; Borg, G.; Scheidt, K. A. Remarkably stable tetrahedral intermediates: Carbinols from nucleophilic additions to N-acylpyrroles. *Angew. Chem. Int. Ed.* **2002**, *41*, 3188.

22. Dixon, D. J.; Scott, M. S.; Luckhurst, C. A. A new chemoselective base-mediate protection/deprotection method for aldehydes. *Synlett* **2003**, 2317.

23. Bégué, J-P.; Bonnet-Delpon, D.; Crousse, B. Fluorinated alcohols: A new medium for selective and clean reaction. *Synlett* **2004**, 18.

24. Paquette, L. Lithium Aluminum Hydride. *Encyclopedia of Reagents for Organic Synthesis*. John Wiley & Sons: New York, 1995; Vol 5, pp 3009-3014.

25. Warner, D.L.; Hibberd, A. M.; Kalman, M.; Klapars, A.; Vedejs, E. *N*-silyl protecting groups for labile aziridines: Applications toward the synthesis of *N*-H aziridinomitosenes. *J. Org. Chem.* **2007**, *72*, 8519.

26. (a)Bassindale, A. R.; Stout, T. The synthesis of functionalized silyltriflates. *J. Organomet. Chem.* **1984**, *271*, 1. (b)Vloon, W. J.; Van den Bos, J. C.; Koomen, G. J.; Pandit, U. K. An alternative synthesis of (+)-sesbanimide A. *Recl. Trav. Chim. Pays-Bas* **1991**, *110*, 414.

27. Zein, N.; Kohn, H. The electrophilic and nucleophilic character of the carbon-10 methylene group in mitosenes revealed. *J. Am. Chem. Soc.* **1986**, *108***,** 296.

28. (a)Iyer, V. N.; Szybalski, W. Mitomycins and Porfiromycin: Chemical mechanism of activation and cross-linking of DNA. *Science* **1964**, *145*, 55. (b)Moore, H. W. Bioactivation as a model for drug design bioreductive alkylation. *Science* **1977**, *197*, 527.

29. Bobeck, D.R.; Warner, D. L.; Vedejs, E. Internal azomethine ylide cycloaddition methodology for access to the substituted pattern of Aziridinomitosene A. *J. Org. Chem.* **2007**, *72*, 8506.

30. Kočovský, P. Carbamates: A method of synthesis and some synthetic applications. *Tetrahedron Lett.* **1986**, *45*, 5521.

31. Vedejs, E.; Klapars, A.; Naidu, B. N.; Piotrowski, D. W.; Tucci, F. C. Enantiocontrolled synthesis of (1*S*, 2*S*)-6-desmethyl-(methylaziridino)mitosene. *J. Am. Chem. Soc.* **2000**, *122*, 5401.

32. Ueki, M.; Amemiya, M. Removal of 9-fluorenylmethyloxycarbonyl (Fmoc) group with tetrabutylammonium fluoride. *Tetrahedron Lett.* **1987**, *28*, 6617.

33. Ando, T.; Yamawaki, J.; Kawate, T.; Sumi, S.; Hanafusa, T. Fluoride salts on alumina as reagents for alkylation of phenols and alcohols. *Bull. Chem. Soc. Jpn.* **1982**, *55*, 2504.

34. Scheidt, K. A.; Chen, H.; Follows, B. C.; Chemler, S. R.; Coffey, S.; Roush, W. R. Tris(dimethylamino)sulfonium difluorotrimethylilicate, a mild reagent for the removal of silicon protecting groups. *J. Org. Chem.* **1998**, *63*, 6436.

35.(a)Urakawa, C.; Tsuchiya, H.; Nakano, K. New mitomycin, 10-decarbamoyl-oxy-9-dehydromitomycin B from *Streptomcyes caespitosus*. *J. Antibiot.* **1981**, 243. (b)Urakawa, C.; Tsuchiya, H.; Nakano, K. Preparation and biological activities of 10-decarbamoyloxy-9-dehydromitomycin B and its analogs. *J. Antibiot.* **1981**, 1152. (c)Kono, M.; Kasai, M.; Shirahata, K. Improved synthesis of mitomycin G. *Synth. Commun.* **1989**, *19*, 2041. (d)Benbow, J. W.; McClure, K. F.; Danishefsky, S. J. Intramolecular cycloaddition reactions of dienyl nitroso compounds: Application to the synthesis of mitomycin K. *J. Am. Chem. Soc.* **1993**, *115*, 12305.

36. Kitahonoki, K.; Kotera, K.; Matsukawa, Y.; Miyazaki, S.; Okada, T.; Takahashi, H.; Takano, Y. Formation of aziridines by lithium aluminum hydride reduction of ketoximes. *Tetrahedron Lett.* **1965**, 1059.

37. Cox, D. P.; Terpinski, J.; Lawrynowicz, W. Anhydrous" tetrabutylammonium fluoride: a mild but highly efficient source of nucleophilic fluoride ion. *J. Org. Chem.* **1984**, *49*, 3216.

38. Pilcher, A. S.; Ammon, H. L.; DeShong, P. Utilization of tetrabutylammonium triphenylsilyldifluoride as a fluoride source for nucleophilic fluorination. *J. Am. Chem. Soc.* **1995**, *117*, 5166.

39. (a)Taylor, W. G.; Remers, W. Structure and stereochemistry of some 1,2-disubstituted mitosenes from solvolysis of mitomycin C and mitomycin A. *J. Med. Chem.* **1975**, *18*, 307. (b)Chiu, I.-C.; Kohn, H. Synthesis and reactivity of trans-6-azabicyclo[3.1.0]hexan-2-ol derivatives and indanol[1,2-b]aziridine. Structural analogs of mitomycin C. *J. Org. Chem.* **1983**, *48*, 2857. (c)Nguy, N. M.; Chiu, L.-C.; Kohn. H. Synthesis and reactivity of 6- and 7-methoxyindano[1,2-b]aziridines. *J. Org. Chem.* **1987**, *52*, 1649.

40. Tomasz, M.; Chawla, A. K.; Lipmin, R. Mechanism of monofunctional and bifunctional alkylation of DNA by mitomcyin C. *Biochemistry* **1988**, *27*, 3182.

41. Tomasz, M.; Lipman, R. Reductive Metabolism and alkylating activity of mitomycin C induced by rat liver microsomes. *Biochemistry*, **1981**, *20*, 5056.

42. Li, V-S.; Choi, D.; Tang, M-S.; Kohn, H. Concerning *in vitro* mitomycin-DNA alkylation. *J. Am. Chem. Soc.* **1996**, *118*, 3765.

43. Williams, R. M.; Ducept, P. Interstrand cross-linking of DNA by FK317 and its deacetylated metabolites FR70496 and FR157471. *Biochemistry* **2003**, *42*, 14696.

44. Watson, S. c.; Eastham, J. F. Colored Indicators for Simple Direct Titration of Magnesium and Lithium reagents. *J. Organometallic Chem.* **1967**, *9*, 165.

45. Beckers, J. L.; Ackermans, M. T.; Boček, P. “Capillary Zone Electrophoresis in Methanol: Migration Behavior and Background Electrolytes.” *Electrophoresis* **2003**, *24*, 1544.

Chapter 3.

Synthesis of a 9-Oxo-pyrrolo[1,2-a]indole Related to FR900482

Brief Overview of Mitomycin C and FR900482

Over the last half century much interest has been dedicated to the DNA alkylating pro-drug mitomycin C (Scheme 3-1, **1**).[1-5] Mitomycin C is an effective anticancer agent selective for solid tumors and hypoxic cells due to its unusual mechanism of action.[6,7] An in depth discussion of the mechanism was provided in Chapter 1, but a brief overview is presented below. Enzymatic or chemical reductive activation of the quinone core to a leucoaziridinomitosene (**3a**) *in vivo* or *in vitro* is required for its activity. The leucoaziridinomitosene is responsible for cross-linking double stranded DNA, and the presence of the cross-link results in a catastrophic cellular event where the DNA can no longer undergo strand separation and replication.[3,4] The bioreductive activation events of **1** also lead to radical species such as hydroxyl radical and hydrogen peroxide, which cause cellular damage leading to severe side effects, thereby limiting the therapeutic dose range of **1**.[8,9] Even with its high cytotoxicity, **1** is marketed as Mutamycin® by Bristol-Meyers-Squibb, and it remains in use as a chemotherapeutic agent for the treatment of breast, head and neck, and non-small cell lung cancer.[10,11]

Scheme 3-1. Biosynthetic intermediates leading to **1** and **2**.

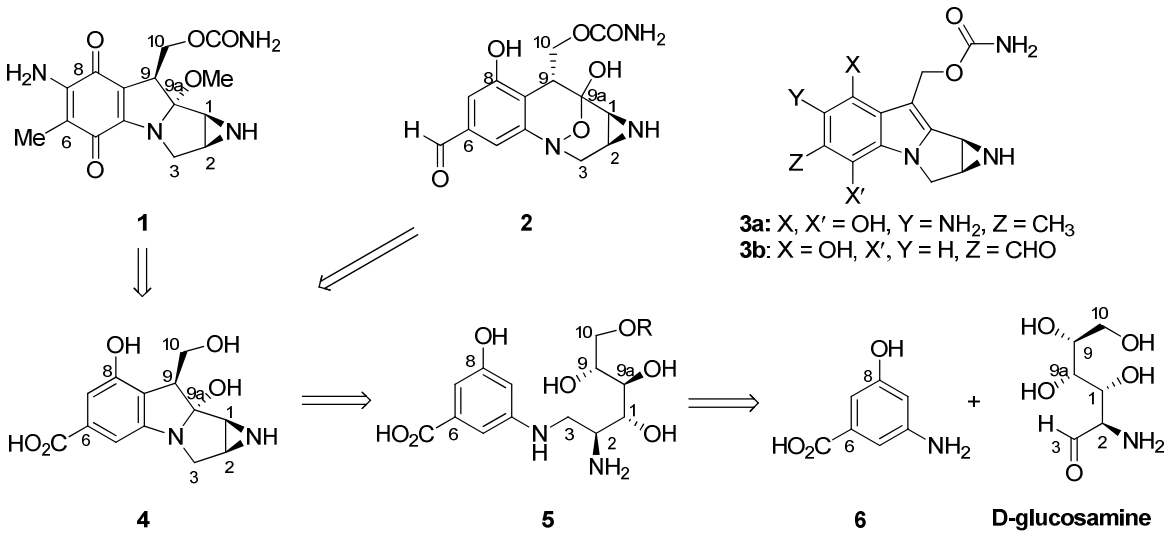

There have been many endeavors to design analogs of **1** with improved activity and reduced cytotoxicity. Thousands of analogs have been obtained either by way of synthesis or by doping the fermentation broths of the mitomcyin C producing organism with biosynthetic synthons.[2,12] In the late 1980s, scientists at the Fujisawa Pharmaceutical Company discovered a new class of compounds with the isolation of FR900482 (**2**), which was envisioned to be a viable alternative to **1**.[13] The FR class of compounds consist of a unique dihydrobenzoxazine core with a hydroxylamine hemi-aminal (Scheme 3-1). Importantly, this class of compounds also cross-links DNA upon reductive activation through aziridinomitosene **3b** (discussion in Chapter 1).[1,2] Unlike **1**, the reduction of **2** does not involve the formation of superoxide or the subsequent hydroxyl radicals and hydrogen peroxide; therefore, the FR class does not have the cytotoxicity problems associated with **1**. However, due to the occurrence of vascular leak syndrome as a severe side effect during clinical trials, the FR compounds did not live up to their early therapeutic potential.[14]

The relationship between Mitomycin C and FR900482

As alluded to in the previous section, the development of new compounds for the selective destruction of cancerous cells instead of healthy cells remains a goal of anticancer

research efforts. Scientists have recognized the high complexity of the mechanisms of action of these remarkable natural products, and that "elucidating cellular events that mediate cytotoxicity" may lead to the development of improved drug.[2] Also important to this research is the understanding of the biological origins and drug producing organisms that are involved in the biosynthesis of **1** and **2**. Therefore, to take full advantage of the therapeutic potential of the mitomycin and FR classes of compounds, a better comprehension of the biosynthetic pathways leading to each natural product is required.

Mitomycin C was isolated from multiple *Streptomyces* organisms including *S. lavendulae* NRRL 2564,[15] while FR900482 was isolated in 1987 from the fermentation broth of *S. sandaensis* No. 6879.[16] The building blocks of these anticancer antibiotics were determined through radioactive labeling studies. It was found that an intact D-glucosamine unit makes up carbons 1-3, 9-10, and the aziridine nitrogen (Scheme 3-1).[17,18] Also, uptake of L-[NH_2CO-^{13}C,^{15}N] citrulline in the biosynthesis of **1** was responsible for C(10) carbamate formation.[19,20] The most likely candidates for the origin of the remaining amino-methylbenzoquinone carbons were glucose or shikimic acid, derived from the Shikimate pathway of amino acid synthesis; however, neither of these labeled precursors were incorporated into **1**.[17,21] Finally, Anderson and coworkers identified the progenitor of the benzoquinone as the unusual amino acid 3-amino-5-hydroxy-benzoic acid (AHBA) **6**.[22] Amino acid **6** is biosynthetically derived via the recently discovered ammoniated shikimate pathway.[23] Scientists at the Fujisawa Pharmaceutical Co. found that [7-^{14}C] **6** was incorporated into **2** when *S. sandaensis* No. 6897 was inoculated with the labeled amino acid. Furthermore, D-[1-^{13}C]glucosamine was incorporated into **2** when it was added to fermentation broths.[24] These findings suggest that both **1** and **2** are derived from the same building blocks originating from two different organisms.

A possible explanation for similarities of **1** and **2**, i.e. incorporation of the same building blocks and the presence of the aziridine and carbamate in both, is that mitomycin C and FR900482 are derived from a common biosynthetic intermediate. It is proposed that a coupling

event between AHBA **6** and D-glucosamine could lead to functionalized amine **5**, with the intact D-glucosamine unit.[25] Subsequent oxidation and cyclization could produce mitosane **4**, which has the requisite carbons for formation of either **1** or **2** (Scheme 3-1). Evidence to support the proposal of a common biosynthetic intermediate in two different organisms has been obtained by the Sherman group.

Sherman and coworkers have identified the gene clusters of *S. lavendulea* and *S. sandaensis* responsible for the biosynthesis of **1** and **2**. Identification of the gene cluster of *S. lavendulea* was accomplished by gene disruption studies, and by monitoring the expression of **1** from mutant strains of *S. lavendulae*.[26] Preliminary assignment of enzyme function was possible based on these studies. Two enzymes, MitE, an acyl AMP ligase, and MitB, a glycosyl transferase, have been implicated in the condensation of the building blocks **6** and D-glucosamine thereby leading to amine **5** (Scheme 3-1).[25] Recent mapping of the gene cluster responsible for the synthesis of **2** showed that it possesses high identity and similarity to that of **1**.[27] Consequently, the function of enzymes in the *S. sandaensis* gene cluster can be assigned by analogy to the *S. lavendulae* gene cluster.

As implied above, the presence of the aziridine and carbamate in **1** and **2** implicates the divergence of the biosynthetic pathways at a relatively late stage, i.e. after installation of these functional groups. Subsequent tailoring steps such as amination, methylation, and oxidation to the quinone of **1** would occur after the point of divergence. Contributing to the hypothesis that the pathways diverge at a late stage is the presence of a cytochrome P450 hydroxylase in the gene cluster of *S. sandaensis* that is not present in *S. lavendulae*. Sherman *et. al.* propose that the hydroxylase could be responsible for the oxidation of the mitosane core of **4** to the hydroxylamine hemi-aminal of **2**.[27] Although structural features of **1** and **2** imply a certain order of events, the exact sequence of transformations in the biosynthetic pathways has not been determined.

In order for **4** to lead to **2**, oxidation of the mitosane core must occur. Dmitrienko confirmed that oxidation of the mitosane pyrrolo[1,2-a]indole core present in **1** to the dihydrobenzoxazine hydroxylamine hemi-aminal core of **2** is chemically possible.[28] The oxidation of 9a-hydroxy-2,3,9,9a-tetrahydropyrrolo[1,2-a] indole **7** with Davis' reagent resulted in ring expansion into the hydroxylamine hemi-aminal core **12** of the FR compounds (Scheme 3-2). Oxidation of the hemi-aminal **8** to N-oxide **9** followed by ring opening affords benzazocinone **11**, and subsequent condensation of the N-oxide onto the ketone then provides the bicycle **12**. An alternative mechanism for formation of **12** is oxidation of the ring opened tautomer **10** to hydroxylamine **11**. The successful oxidation of a mitosene as well as a mitosane into a dihydrobenzoxazine further supports the hypothesis that structurally different **1** and **2** are derived from a common biosynthetic intermediate.

Scheme 3-2. Conversion of pyrrolo[1,2-a]indole **8** to dihydrobenzoxazine **12**.

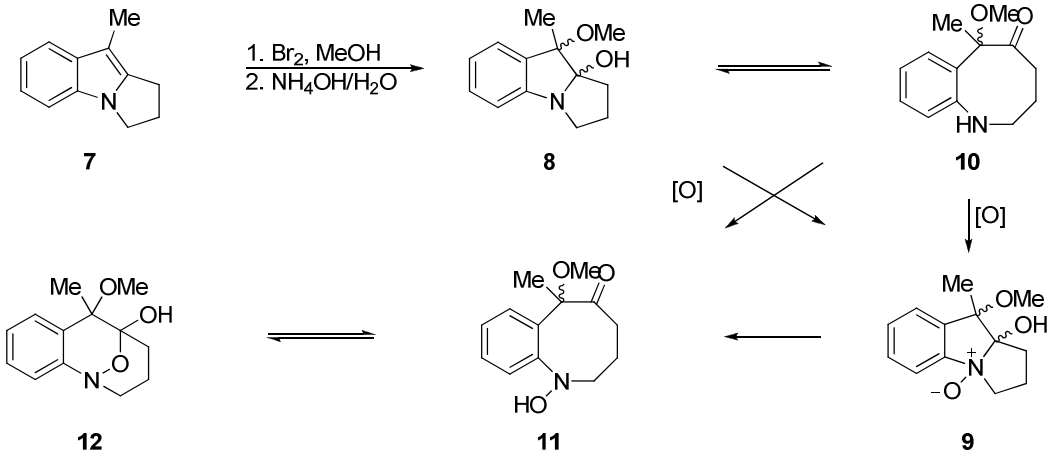

In an effort to investigate the point of divergence in the parallel pathways, and also to confirm the proposed enzymatic function, we have targeted the potential biosynthetic probes aziridinomitosane **13a** or **13b** for total synthesis (Scheme 3-3). In collaborative experiments, Sherman and coworkers will load thioesters **13a,b** onto an acyl carrier protein and subject it to purified enzymes obtained by over-expression of the genes from the biosynthetic pathways. High priority in testing will be given to the gene responsible for C(10) carbamoylation (mmcS);[27b]

presumably carbamate installation occurs before the point of divergence since the functionality is present in both **1** and **2**. The oxidases mmcN, and mmcT, as well as the unique oxidase from the FR900482 gene cluster will also be tested with **13a,b**. These enzymes are proposed to be responsible for oxidation of C(5) and C(7) in the biosynthesis of **1**, and therefore, substrate recognition by these enzymes should occur after the point of divergence of the two pathways. Furthermore, other enzymes potentially responsible for methylation of C(9a) and deoxygenation of C(6) will also be evaluated. Most notable in the biosyntheses is the difference in the stereochemistry at C(9) between **1** and **2**. Studies with the stereoisomer **13a,b** could elucidate where in the biosyntheses the stereochemistry difference arises. All of the above studies should facilitate a better understanding of the timing of events leading to the mitomycins and FR compounds, and ultimately lead to the exploitation of the biosynthesis for the construction of novel mitomycins. The key structural features of **13a**,**b** are the acid labile aziridine, hemi-aminal, and C(10) hydroxymethyl moieties. Thioesters **13a,b** are planned to arise from the α-hydroxy ketone mitosane **14a** or the allylic alcohol **14b** via late stage conversion of the ketone or the exocyclic methylene group to the hydroxymethyl group corresponding to the C(10) position of **1** and **2**. Below we describe the successful synthesis of a fully functionalized analog of α-hydroxy ketone **14a** en route to the desired pyrrolo[1,2-a] indole thioesters **13a,b**.

Scheme 3-3. Retrosynthesis of targeted probes **13a,b**.

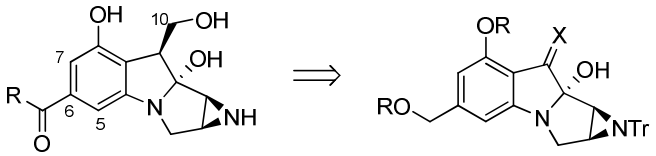

13a R = S-NAC
13b R = S-CoA

14a X = O
14b X = CH_2

Racemic syntheses of the pyrrolo[1,2-a] indole core

The mitosane core of the α-hydroxy ketone **13a** has been previously obtained by others in the context of the total synthesis of mitomcyin K, FR900482 and derivatives. In an endeavor to

quickly synthesize the mitomycin core, Danishefsky showed that under photolytic conditions, aryl nitro dienes are suitable substrates for [4 + 2] cycloaddition to form a pyrrolo-fused oxazine system (Scheme 3-A).[29] The photolysis of nitroaryl diene **1A**, which was expected to provide the fused oxazine **2A** based on an unfunctionalized model, gave almost exclusively the hemi-aminal **3A**. Trace amounts of **2A** were isolated, and conversion of **2A** into **3A** supported the intermediacy of **2a** in the formation of **3A**. The hemi-aminal could then be oxidized to the imide **4A** in moderate yield. Stereospecific installation of the aziridine precursor to the correct face of the substrate was accomplished using (phenylthio)methyl azide. Subsequent reduction of the imide and dehydroxylation via Barton deoxygenation of a thionothiaimidazolide provided tetracycle **6A**. Finally, photolytic cleavage of the triazoline followed by thioether reduction provided the aziridine **7A**. The α-methoxy ketone was then converted in three steps to (±)-mitomycin K. Although this route highlights an expedient synthesis of the mitosane core via the [4 + 2] cycloaddition of the arylnitroso diene, 7 steps are required to access the aziridinomitosane **7A** from hemi-aminal **3A**.

Scheme 3-A. Danishefsky's synthesis of (±)-mitomycin K.

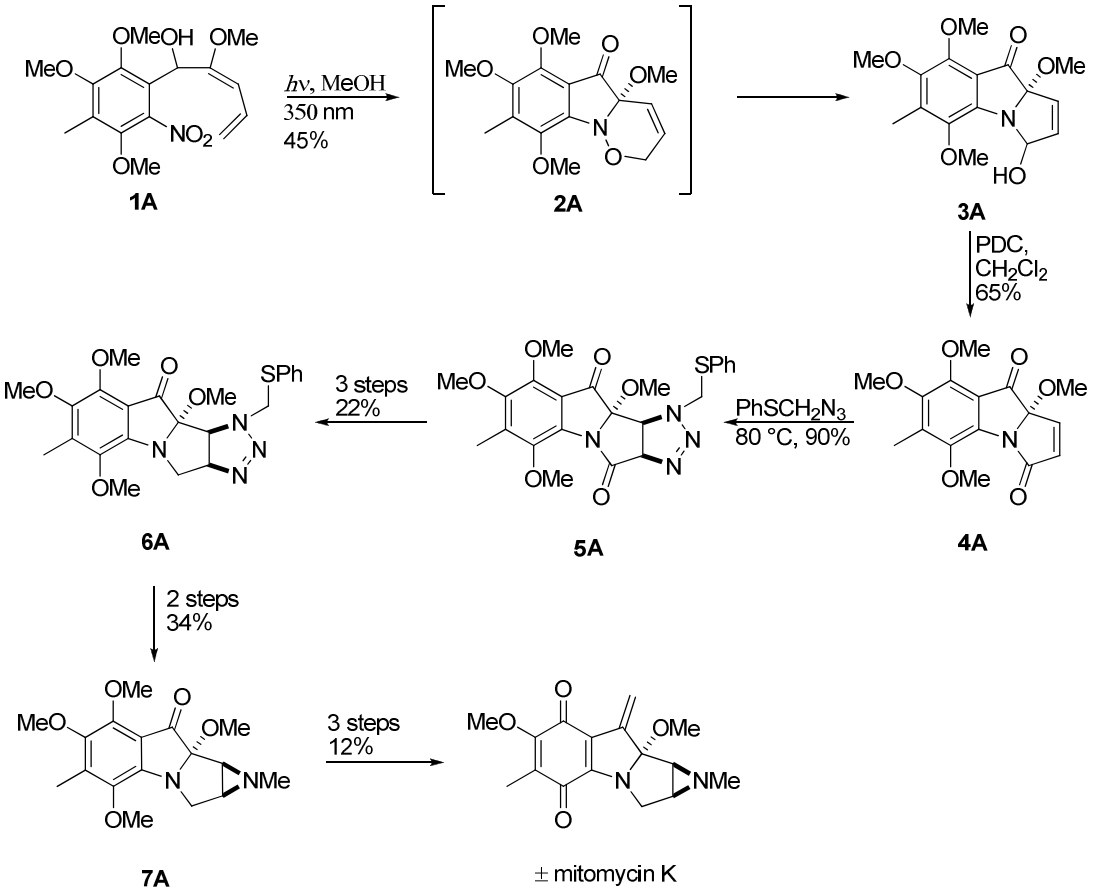

In another strategy, Ban and Shibasaki used a trannsannular cyclization approach to the hemi-aminal of a decarbamoyloxymitomycin derivative (Scheme 3-B).[30] Benzazocine **1B** was converted into allylic alcohol **2B** in 6 steps with good selectivity for the *cis* isomer. Unfortunately, direct installation of the aziridine from **2B** using epoxidation and subsequent ring opening was unsuccessful. Therefore, alcohol **2B** was converted into allylic carbamate **3B**, and the olefin was iodinated providing **4B** in good yield. Cleavage of the carbamate with K_2CO_3 and MeOH and subsequent intramolecular displacement of the iodide by the released nitrogen formed the aziridine ring on the correct face of the system. The alcohol was then oxidized with PCC to the benzazocinone **5B**. After unsuccessful attempts to effect the transannular cyclization with methyl trifluoromethanesulfonate (MeOTf), it was found that TMSOTf and TBSOTf induced the desired ring forming event with good stereoselectivity for the *trans* silyl ether aminal (**6B**).

Although the TMS derivative was unstable to purification, the TBS derivative **6B** could be isolated in high yield. The presence of the benzyl protecting groups was necessary for the "criss-cross" cyclization to occur as the TBS protected hydroquinone did not undergo cyclization. Global deprotection and oxidation of **6B** afforded the quinone **7B** in three steps. Overall, the Shibisaki synthesis of the mitosane from precursor **1B** required 11 steps including 3 for aziridine installation.

Scheme 3-B. Shibisaki's synthesis of the decarbamoyloxymitomycin **7B**.

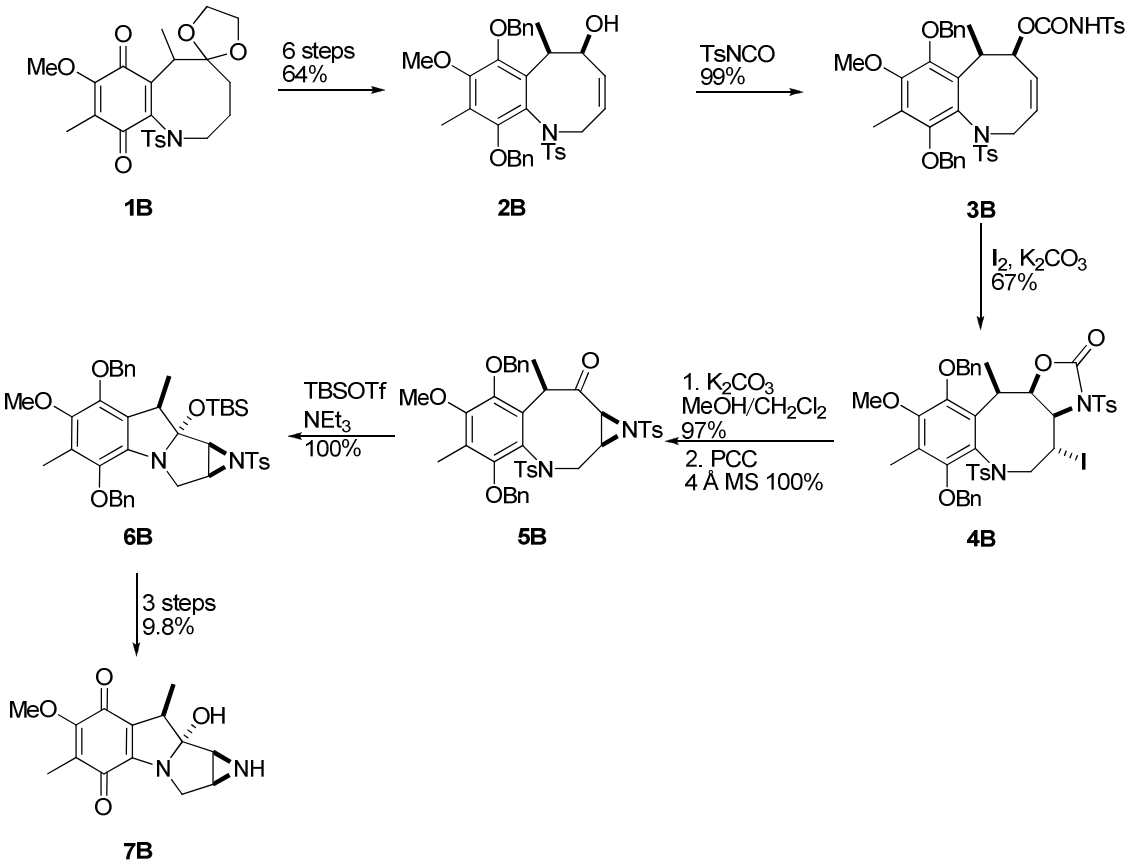

A third approach that has been used extensively to obtain the hemi-aminal core is the oxidation of a mitosene or pyrrolo[1,2-a] indole core. Dmitrienko showed that the pyrrolo[1,2-a] indole core can be oxidized using molecular bromine in methanol followed by basic workup to provide 2-hydroxy-3-methoxy-indolines.[28] Using a similar approach, Jimenez reported the oxidation of a mitosene with Davis' reagent (Scheme 3-C).[31] Jimenez synthesized the azido-

mesylate **2C** in 3 steps from 2-formylindole **1C**. Oxidation of the C(9)-C(9a) bond (mitomycin numbering) using Davis' reagent provided **4C** as a mixture of diastereomers most likely in equilibrium with the ring opened form **3C**. Each isomer could be isolated by chromatography; however, both reached an equilibrium mixture of 7:2 after 72h in $CDCl_3$. The less stable isomer was protected as a TBS ether providing **5C** as a 1:2 mixture of diastereomers. The 1:2 diastereomeric ratio of **5C** was retained upon conversion to **6C** by reduction of the azide and internal mesylate displacement. The more stable isomer of **4C** was reduced and cyclized with PPh_3 and NEt_3 to aziridine **7C**. Treatment with acetic anhydride then gave the diacetate hemi-aminal derivative **8C**.

Scheme 3-C. Jimenez's synthesis of the mitosane **6C** and **8C**.

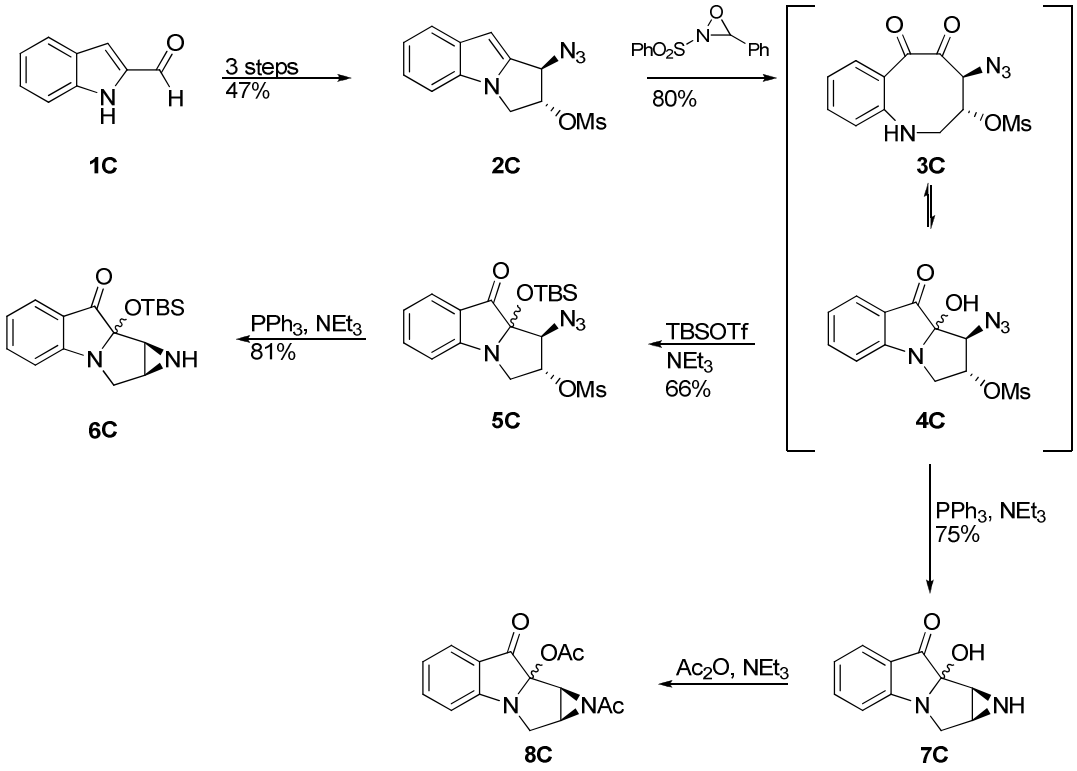

The same oxidation strategy was used in Jimenez's total synthesis of (±)-mitomycin K (Scheme 3-D).[32] Unfortunately, initial attempts to effect the oxidation of functionalized indole **1D** using Davis' reagent were unsuccessful. The desired transformation did not occur with hydrogen peroxide, *t*-butyl hydroperoxide in methanol, or *m*-CPBA. Successful oxidation was

achieved with (hexamethylphosphoramido)oxodiperoxomolybdenum (VI) (MoO_5•HMPA) providing a mixture of diastereomers **2D** and **3D** in good yield. Equilibration of these stereoisomers was possible with dilute HCl in MeOH over three days. Sequential aziridination of the desired diastereomer **2D** with PPh_3, installation of a methyl group on the aziridine nitrogen, and conversion of the ketone to an exocyclic olefin using Danishesky's protocol provided (±)-mitomycin K **6D**. The ultimate conversion of **2D** to **6D** confirmed the *trans* stereochemistry of the C(9a) methoxy and aziridine functional groups in **4D**. This efficient synthesis of mitosane **4D** required 2 steps from mitosene **1D**.

Scheme 3-D. Jimenez's racemic synthesis of (±)-mitomycin K.

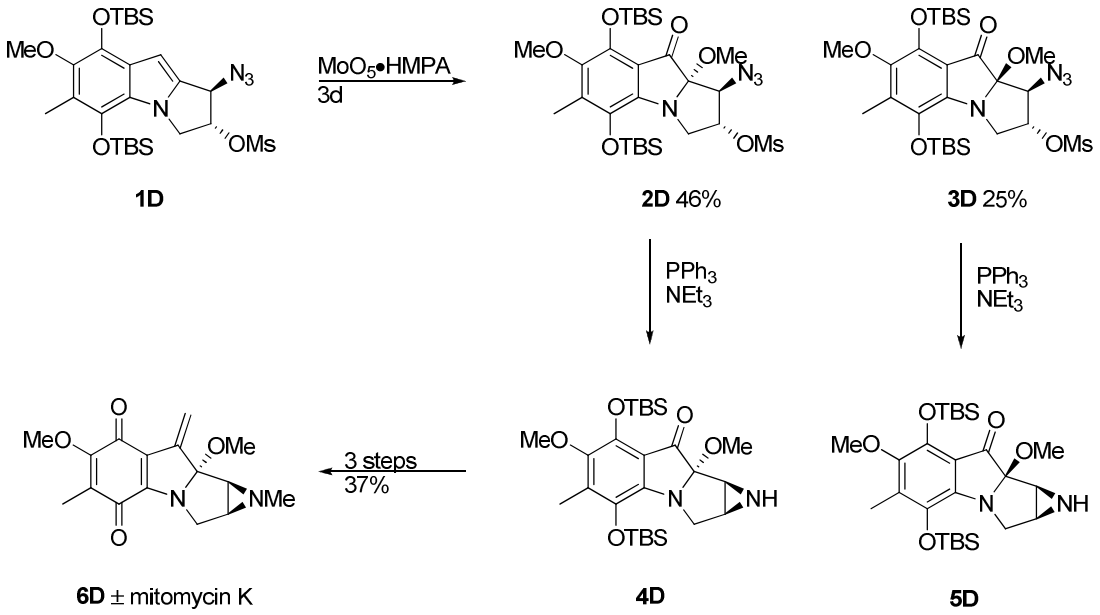

Asymmetric syntheses of the pyrrolo[1, 2-a]indole core

Miller's asymmetric approach to the mitosane core used a transannular cyclization strategy.[33] Starting from the commercially available isatin **1E**, the racemic N-Boc protected benzazocine **2E** was obtained in good yield over nine steps (Scheme 3-E). After screening 152 peptide catalysts, the peptidic catalyst **3E** was found to give good kinetic resolution of the racemic mixture with s = 27 to provide the alcohol **(–)-2E** with the desired stereochemistry in good yield (~40%, theoretical 47%) and good enantioselectivity (90% ee, 99% ee after single

recrystallization). Substrate directed epoxidation of the olefin using dimethyldioxirane, followed by Swern oxidation provided ketone **4E** in good yield. Subsequent cyclization using Ban's Lewis acid catalyzed conditions on **4E** provided the desired tetracycle; however, due to difficulties encountered in removing the ketal, a one step cyclization and deprotection procedure was sought. Thus, it was found that treating **4E** with trace amounts of HNO_3 in MeOH at 135 °C provided the deprotected α-methoxy ketone **5E** with the *anti* configuration between the methoxy and epoxide functionalities. Lewis-acid catalyzed ring opening of the epoxide followed by epimerization of the C(9a) stereocenter under acidic conditions provided **6E** as a mixture of stereoisomers. Mesylation of the azido-alcohol, reduction of the azide, and subsequent displacement of the mesylate provided the hemi-aminal **7E** in 42% yield in two steps. Only the *trans*-isomer was recovered; however, explanations for the absence of the other diastereomer were not presented.

Scheme 3-E. Miller's asymmetric synthesis of mitosane **7E**.

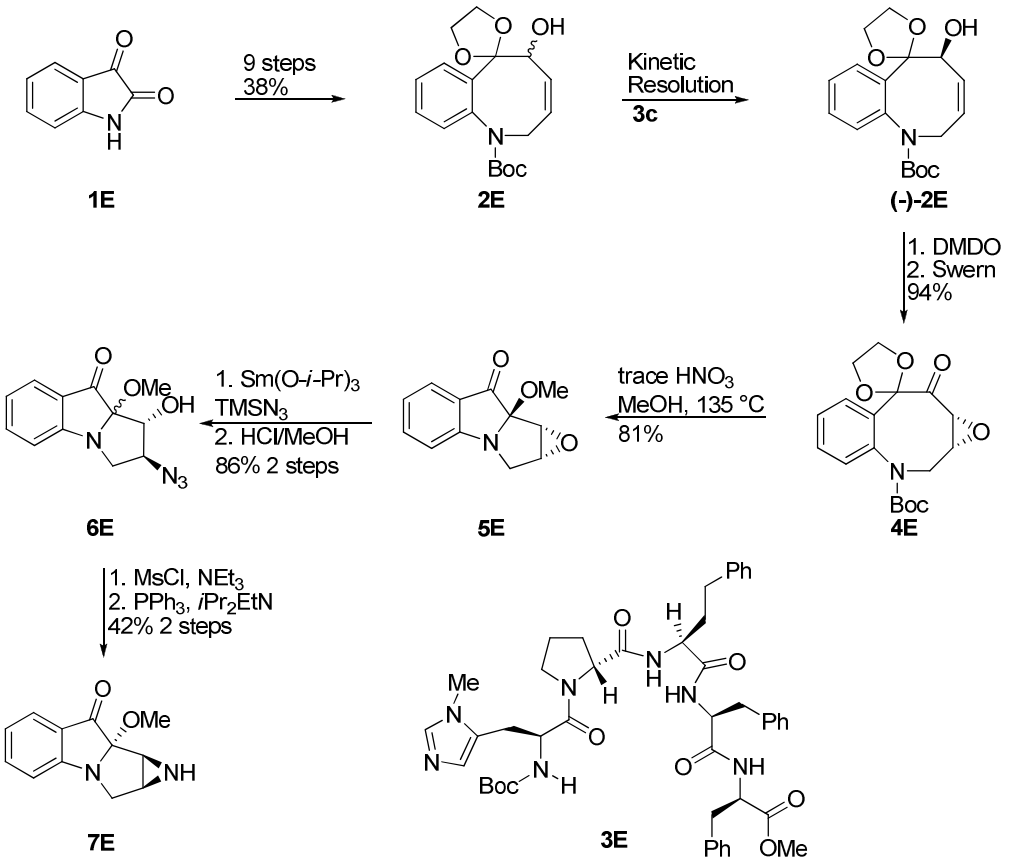

The mitosane hemi-aminals also have been targeted as key intermediates in the synthesis of the dihydrobenzoxazine core of the natural product FR900482 by Ziegler and coworkers.[34] Oxidation of the pyrrolo nitrogen of tetracycle **1F**, obtained by a radical cyclization of a chiral aziridinyl radical onto an appended indole, provided N-oxide **2F** (Scheme 3-F). Further rearrangement of **2F** under Polonovski conditions provided the desired hemi-aminals **3F**-**8F** as mixtures of regioisomers (Scheme 3-F). When R_1 was an acetyl group or benzyl carbonate good regioselectivity favoring tetracycles **5F** and **7F** was obtained. Ziegler and coworkers hypothesized that the acetate or carbonate, which are *cis* to the C(9a) proton could act as an internal base to facilitate regioselective formation of the iminium ion in the Polonovski reaction. Further oxidation of **5F** with *m*-CPBA forms the hydroxylamine hemi-aminal core, most likely through generation of an *N*-oxide followed by ring expansion.

Scheme 3-F. Ziegler's asymmetric synthesis of dihydrobenzoxazine **9F**.

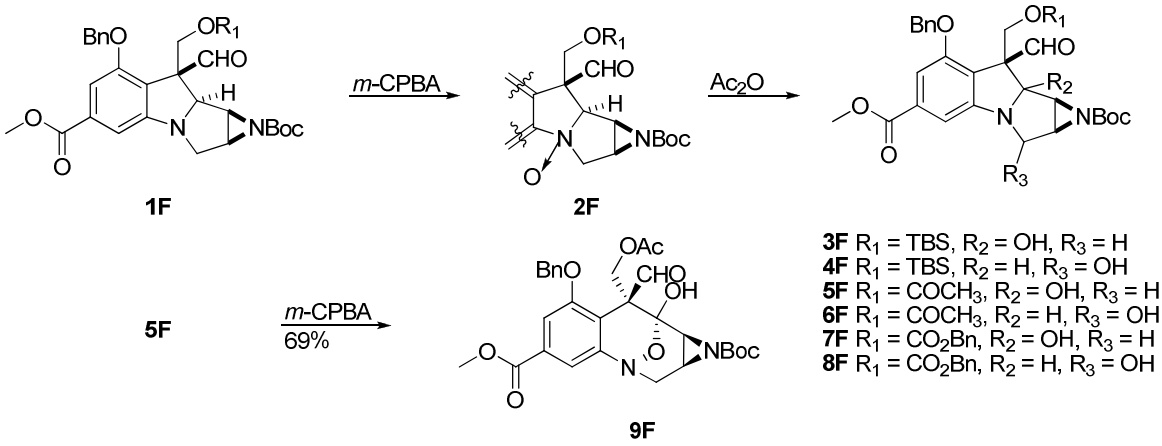

Trost and coworkers used a similar strategy to that of Ziegler to accomplish the asymmetric synthesis of *epi*-FR900482.[35] Using reductive amination, the functionalized *o*-iodo-aniline **1G** was coupled with the non-racemic aziridinol **2G** (Scheme 3-G). Further transformations, including a Heck arylation to form the tetracycle, resulted in the exocyclic olefin **3G** in good yield over 4 steps. Stereoselective (2.4:1 d.r.) dihydroxylation of the olefin with osmium tetraoxide and carbonate formation using triphosgene provided mitosene derivative **4G**. Oxidation of the mitosene under Polonovski conditions, *m*-CPBA and then Ac_2O, provided

aminal **5G** in moderate yield, apparently due to heteroatom directing effects. The dihydroxylamine hemi-aminal core of FR900482 was then accessed by oxidation of **5G** to **6G** with *m*-CPBA. Overall, the mitosane **5G** was obtained in 6 steps after the coupling of **1G** with chiral aziridinal **2G**. Finally, carbonate **6G** was converted to *epi*-(+) FR900482 in good yield over six steps.

Scheme 3-G. Trost's asymmetric synthesis of *epi*- (+)-FR900482.

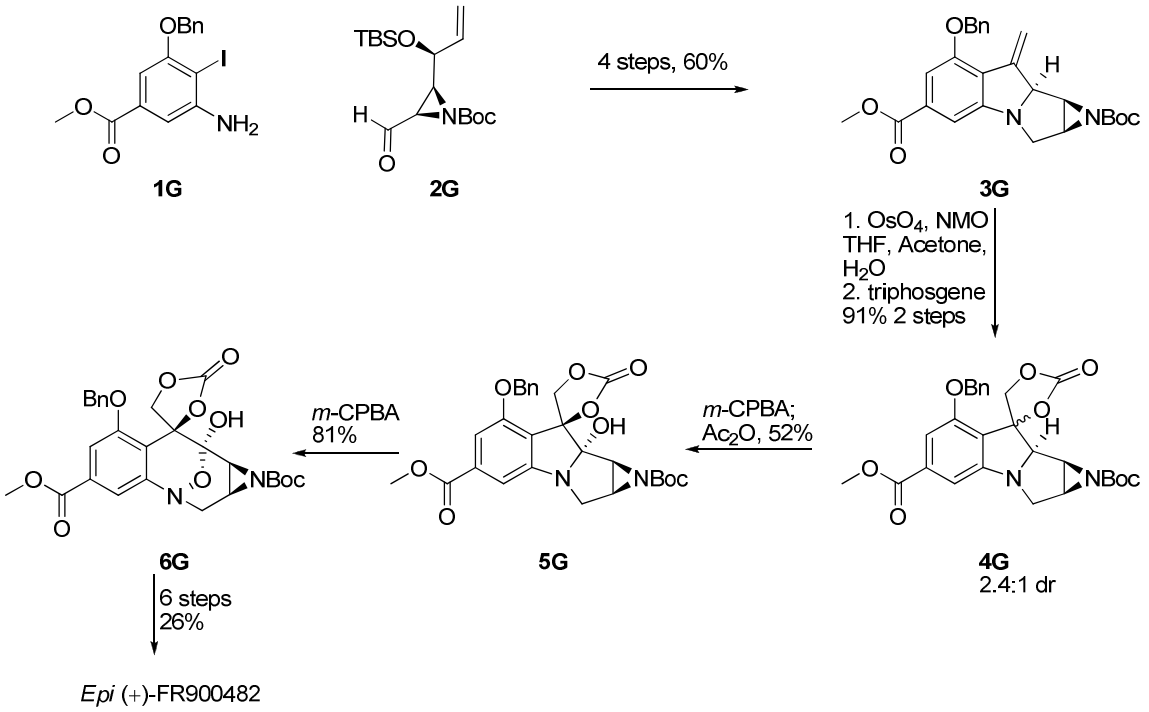

The successful syntheses of the mitosane hemi-aminals described above show three strategies to access the tetracycle from a variety of precursors: an intramolecular cycloaddition, transannular cyclization, and Polonovski oxidation. Furthermore, the hemi-aminals with an adjacent (C9) fully substituted sp^3 or sp^2 carbon can be subsequently transformed into intermediates leading to the mitomycins or the FR compounds. These examples support the validity of our strategy for the formation of thioesters **13a,b** from mitosanes **14a** or **14b**. Compound **14a** is structurally similar to the known hemi-aminals discussed above and should be amenable to further functionalization.

Multiple strategies for the asymmetric construction of **14a,b** have been considered (Scheme 3-4). However, the most direct route involves construction of **14a,b** from aziridinopyrrolidinone **15**. The formation of the C(9)-C(9a) bond of **14a,b** was envisioned to arise from stereoselective 1,2-addition of a vinyl lithium or an acyl anion equivalent into the appended lactam. Pyrrolidinone **15** was planned to be derived from 6-aryl-3,6-diazabicyclo[3.1.0]hexane **16**, furthermore known as an aziridinopyrrolidinone. We envisioned three different approaches to the key aziridinopyrrolidinone **16**. Route A, an intramolecular 1,2-addition of a lithioaziridine, derived from tin-lithium exchange of **17** into the carbamate to form the lactam. Route B involves dianion formation through stepwise deprotonation and tin-lithium exchange of aniline **18** followed by trapping with a phosgene equivalent to install the requisite carbonyl. Finally, the third approach, route C, involves transition metal catalyzed coupling of preformed aziridinolactam **19** with pre-functionalized aryl halide **20**. Each approach involves extensive use of the chiral aziridine for the key bond forming events.

Scheme 3-4. Retrosynthetic analysis of **14a,b**.

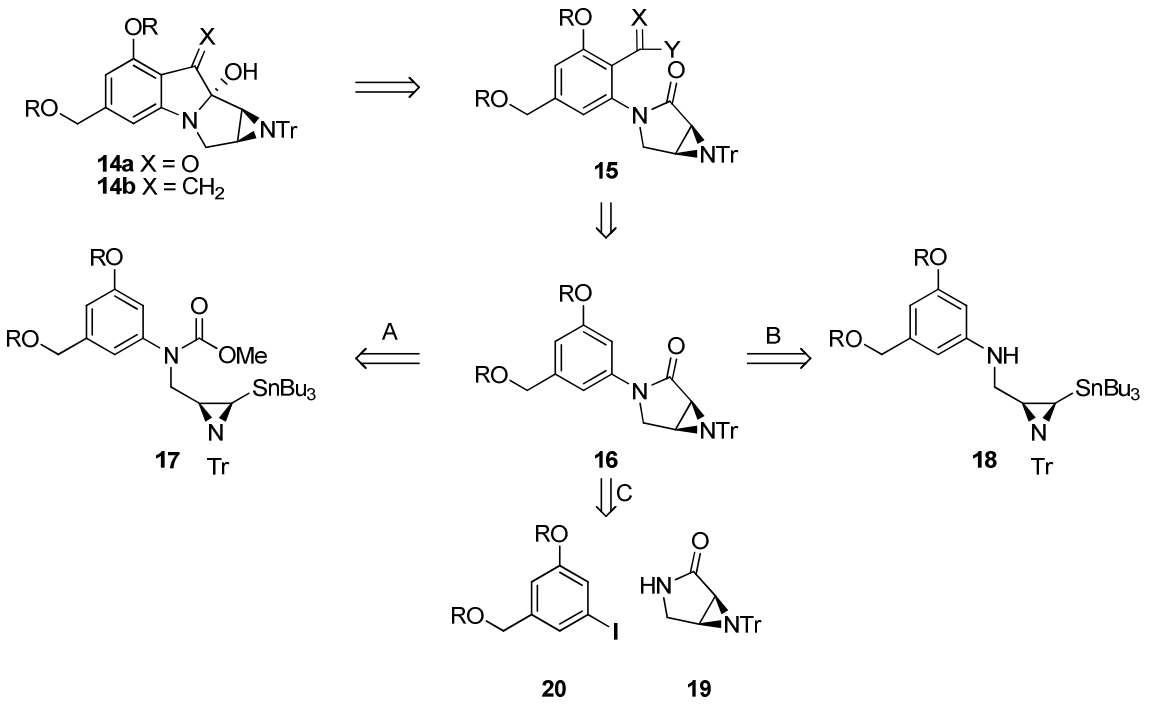

As implied by the strategies for the synthesis of **14a,b**, our group is interested in the efficient asymmetric construction of the aziridinomitosane by early installation of the aziridine moiety. Although the acid labile aziridine often limits the chemistry available for certain transformations, the ability to install the stereocenters of the aziridine from the rich chiral pool removes the difficulties in enantioselectively installing the stereocenters at a late stage. Furthermore, much effort has been spent developing new reactions and methodology that are amenable to the presence of the acid sensitive moiety. Therefore, while the primary goal is the total synthesis of **14a,b** and eventually **13a,b** for biosynthetic studies, a secondary goal is the extension of synthetic transformations that can be performed on the acid sensitive aziridine.

Part 1: Enantioselective synthesis of 3,6-diazabicyclo[3.1.0]hexanes

Route A: Tin-lithium exchange and intramolecular 1,2-addition

The strategy for intramolecular 1,2-addition of a lithioaziridine into an appended carbamate was based on the well known Parham cyclization. The Parham cyclization involves aryl metallation, usually by lithium/halogen exchange, followed by trapping an internal electrophile to form a ring. This route has been used extensively to form benzofused lactams and natural products with the isoindolinone lactam core.[36-40] Our approach differs from the conventional Parham cyclization in that the nucleophile is not at an sp^2 carbon, anion formation would occur by tin-lithium exchange, and the immediate product would not be a benzofused lactam.[41] Nevertheless, the development of route A began by determination of a suitable substrate for tin-lithium exchange.

The synthesis of the first generation tin-lithium precursor began with the commercially available methyl 3,5-dinitrobenzoate **21** (Scheme 3-5). Following the method of Herlt,[42] one nitro group was displaced by LiOMe to provide **22**. The ester was saponified with LiOH to provide the acid in good yield, which was then transesterified with Boc_2O and DMAP to give the *t*-butyl ester **23** in good yield over the two steps. Reduction of the nitro group with Pd/C and H_2 followed by treatment with Boc_2O provided the aniline-derived carbamate **24**. The carbamate

was then alkylated with the iodide **26** to provide the tin-lithium exchange precursor **25** in poor yield. The alkylation of **24** required high temperatures, long reaction times, and an excess of nucleophile to proceed, and it was found that the Boc group was partially cleaved from **24** (14% based on **24**) under the reaction conditions. Although the reaction was inefficient, a sufficient quantity of **25** was obtained to attempt the tin-lithium exchange.

Scheme 3-5. Synthesis of **25** and attempted tin-lithium exchange.

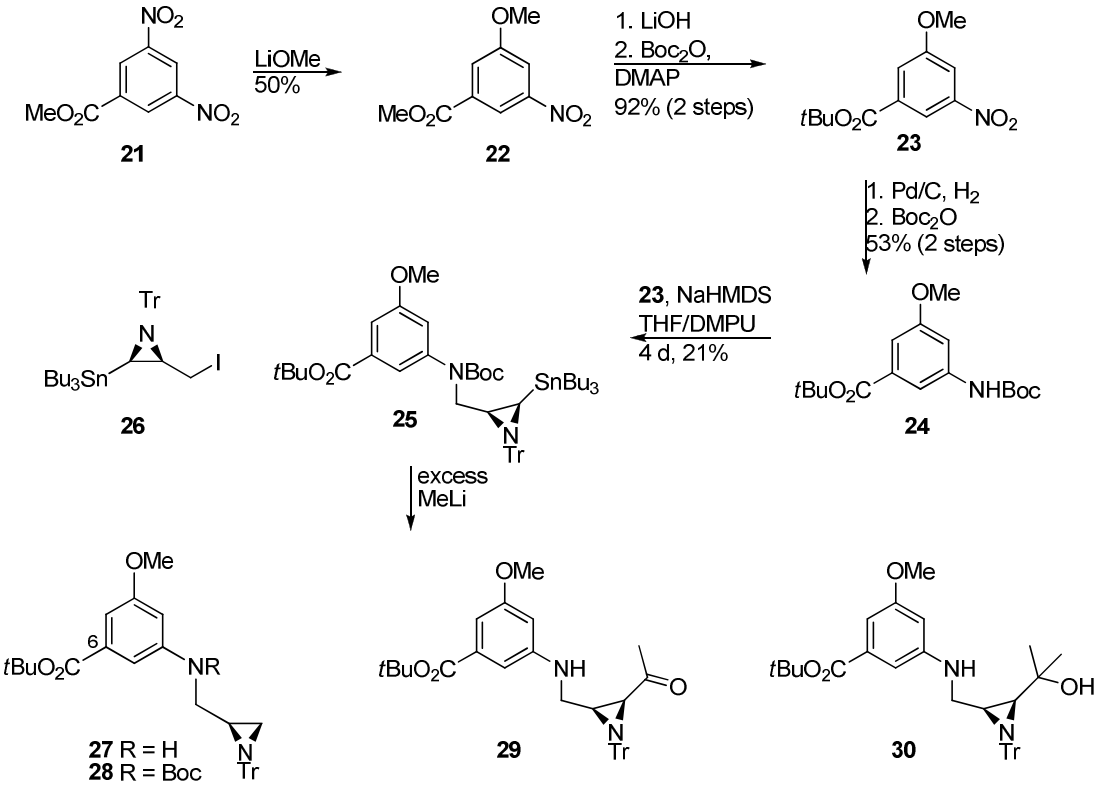

The key step in this strategy was the selective generation of the lithioaziridine via tin-lithium exchange, followed by intramolecular 1,2-addition into the carbamate. Using previously optimized conditions for tin-lithium exchange, carbamate **25** was treated with excess MeLi at -78 °C in THF. However, assay of the crude reaction mixture by ^{1}H NMR spectroscopy showed a complex mixture of products. Purification of the mixture did not provide clean material, but analysis of each band by ESMS showed ions tentatively assigned to compounds **27** – **30** (Scheme 3-5). Although the desired lactam formation had not taken place, complete tin-lithium exchange

had occurred based on the disappearance of the tributylstannane substituent by ^{1}H NMR spectroscopy. The presence of destannylated Boc-protected aniline **28**, suggested that 1,2-addition of the appended lithioaziridine might have been hindered by the bulky *t*-butyl carbamate. Also, the presence of **27** and **28** suggested that there was an acidic proton present that was capable of quenching the lithioaziridine. Although the source of the proton was not confirmed, the *t*-butyl benzoate at C(6) (aziridinomitosene numbering) would lower the pKa of one of the aryl protons, which could then be removed by an available organolithium species. The other products were tentatively assigned as ketone **29** and tertiary alcohol **30** based on analysis by ESMS and by ^{1}H NMR spectroscopy. The ABX dd pattern of the CH_2 methylene protons of **25** had changed, and the signals were shifted upfield from δ = 3.99 and 3.70 ppm to δ = 3.44 and 3.38 ppm, suggesting that the CH_2 was no longer next to the electron withdrawing carbamate, but instead next to an amine.

Based on the multiple byproducts and side reactions during the tin-lithium exchange, a second generation tin-lithium exchange precursor with a smaller aniline protecting group and a non-activating substituent at C(6) was targeted. Therefore, methylbenzoate **22** was reduced with DIBAL-H to provide benzyl alcohol **31**, which was then protected as allyl ether **32** in good yield (Scheme 3-6). Due to the incompatibility of the allyl group with palladium catalyzed hydrogenation, the remaining nitro group was reduced instead with Zn in AcOH to provide amine **33** in good yield. The amine was then protected as the sterically less hindered methyl carbamate **34**. Alkylation of **34** with known mesylate **35** proved more efficient than with the Boc derivative **25**, but the product **36** was still isolated in poor to moderate yield. Tin-lithium exchange on **36** with 2 equiv of MeLi in THF at -78 °C resulted in another complex mixture of products including ketone **38** (Table 3-1, entry 1). When 2 equiv of MeLi was used at -78 °C in Et_2O, starting material and ketone **38** were obtained (Table 3-1, entry 2). However, when only 1.3 equiv of MeLi was used at -78 or -90 °C in Et_2O, no tin-lithium exchange product was observed (Table 3-1, entries 3 and 4). These results suggest that tin-lithium exchange and ketone formation is slow

in Et_2O; therefore, **36** was treated with 4 equiv of MeLi at -90 °C for 1 h. Mostly starting material was recovered, but trace amounts of desired aziridinopyrrolidinone **37** and ketone **38** were also observed (Table 3-1, entry 5). Although the desired lactam had finally been observed, the presence of the ketone showed that the competitive side reaction was still problematic even at -90 °C in Et_2O.

Scheme 3-6. Synthesis of **36** and tin-lithium exchange.

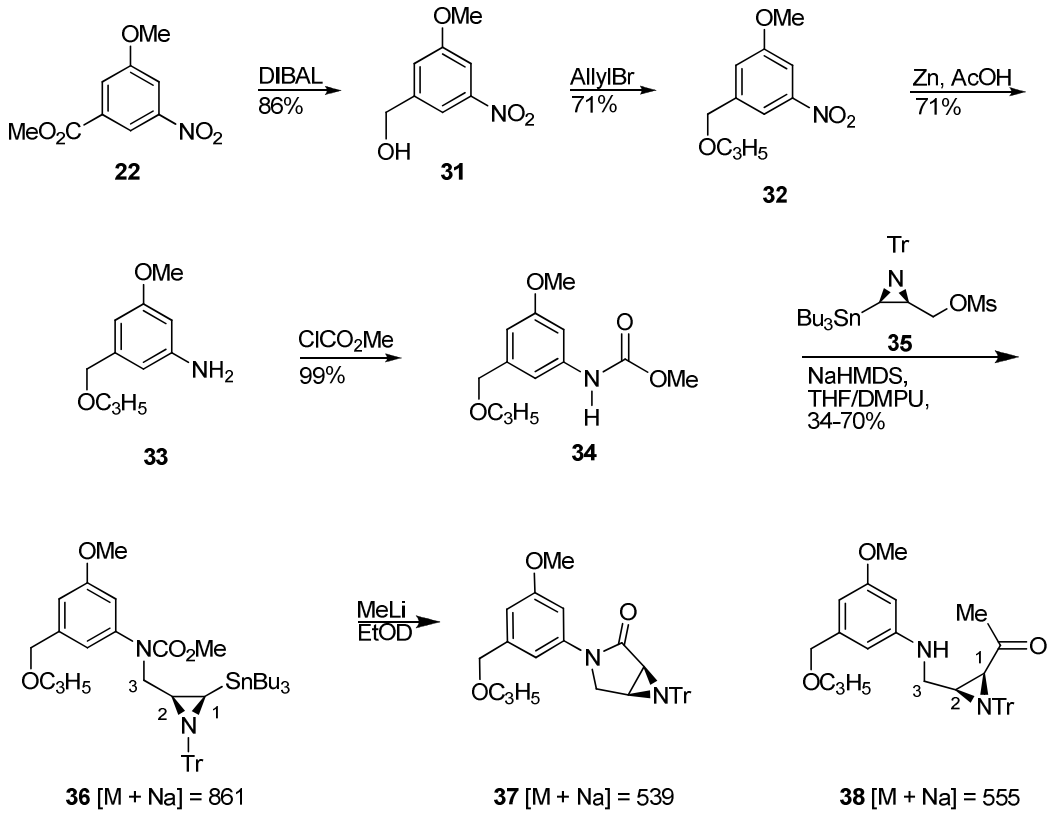

Table 3-1. Tin-lithium exchange on **36**

Entry	MeLi (equiv)	Solvent	T °C	Time	Ion by ESMS
1	2	THF	-78	1 h	555
2	2	Et_2O	-78	30 min	555, 861
3	1.3	Et_2O	-90	30 min	838, 861
4	1.3	Et_2O	-78	30 min	838, 861
5	4	Et_2O	-90	1 h	861, 539, 555

As described above, the major byproduct in the tin-lithium exchange of **36** was assigned as ketone **38**. Electrospray mass spectrometry of the byproduct showed an ion corresponding to

38 (M + Na, *m/z* = 555) implicating loss of the tributylstannane and methyl carbamate as well as incorporation of a methyl group under the reaction conditions. Furthermore, the ^{1}H NMR spectrum contained the distinctive signals for the aziridine methine protons of C(1) and C(2) shifted downfield at δ = 2.14 (d) and 1.98 ppm (dd), while the C(3) methylene protons, consisting of a more complex coupling pattern, had shifted upfield to δ = 3.44 and 3.39 ppm. The increased shielding and change in coupling pattern suggested that the C(3) methylene protons were coupling to an N-H as well as to the C(2) methine proton.

Based on the studies of Orita et.al. on the Parham cyclization,[40] the formation of the ketone **38** was not completely unexpected. During the attempted synthesis of 8-oxoberbines**,** they found that alkyllithiums, including MeLi, *n*-BuLi, *s*-BuLi, and *t*-BuLi, induce Parham cyclization of 3′,4′- or 4′,5′-dialkoxy-1-(2′-bromobenzyl)-2-ethoxycarbonyl-1,2,3,4-tetrahydroisoquinolines, and that any excess alkyllithium adds into the desired product in a 1,2 or 1,4 addition fashion. They concluded that subsequent addition of alkyllithium into the amide carbonyl of the 8-oxoberbine generated *in situ* is faster than the cyclization.[40] Therefore, formation of the ketone **38** can be attributed to an acyl transfer type mechanism where initial addition of the lithioaziridine forms the tetrahedral intermediate **39** (Scheme 3-7)**.** Decomposition of **39** should form lactam **37**.[43] Available MeLi can then attack the lactam **37** to form tetrahedral intermediate **40**, followed by displacement of aniline to form the methyl ketone **38**.[44] Acyl transfer in this system is competitive with tin-lithium exchange according to the evidence that mixtures of starting material **36** and ketone **38** are obtained with excess MeLi. Overall, the inability to obtain good conversion to the desired lactam, to induce tin-lithium exchange with 1 equiv of base, and to suppress formation of ketone **38** prompted us to investigate route B for formation of **37**.

Scheme 3-7. Formation of ketone **38**.

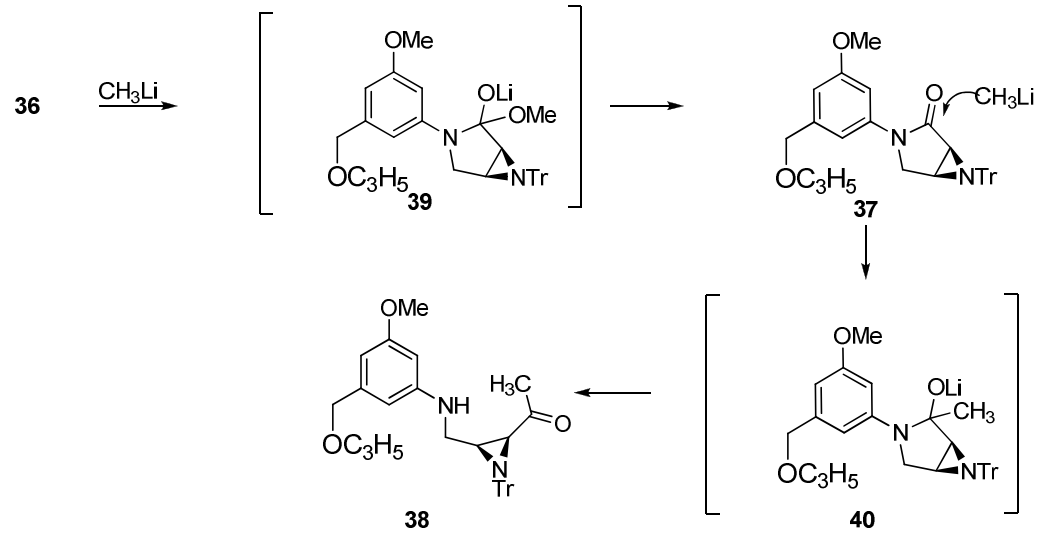

Route B: Dianion formation and trapping studies

Our second approach to aniline derived aziridinopyrrolidinone **16** involved generation of a dianion that could be trapped with a phosgene equivalent. It was envisioned that the dianion generated from stepwise deprotonation and tin-lithium exchange of an aniline derived aziridine would be capable of trapping an electrophile at the more basic carbanion. In fact, Goswami had shown that homoenolate dianions can be generated from secondary amides via deprotonation and tin-lithium exchange, and efficiently trapped at the carbanion with 1 equiv of various electrophiles.[45] However, if an appropriate phosgene equivalent was chosen as the electrophile, the deprotonated heteroatom could then also attack the electrophile in an intramolecular fashion; thereby forming a ring. This approach has been used to form benzo-fused lactones and lactams such as phthalides[46] and oxindoles[47] by dianion trapping with carbon dioxide; however, no prior examples of the formation of 3,6-diazabicyclo[3.1.0]hexanes could be found using this anionic cyclization strategy.

The dianion approach began by targeting the aniline derivative **44** for use as a model substrate (Scheme 3-8). The *N*-Boc aniline **42** was treated with aziridine **35** under the standard alkylation conditions to provide **43** in poor yield. Removal of the Boc protecting group under

commonly used acidic conditions was not viable due to the presence of the acid labile aziridine, and attempted hydrolysis of the Boc group under basic conditions was not successful. Therefore, carbamate **43** was heated to 185 °C without solvent to provide **44** in good yield.[48] Careful temperature control was required as overheating resulted in significant decomposition and reduced yield, but sufficient dianion precursor **44** became available to support studies on dianion formation.

Scheme 3-8. Dianion formation on model **44**.

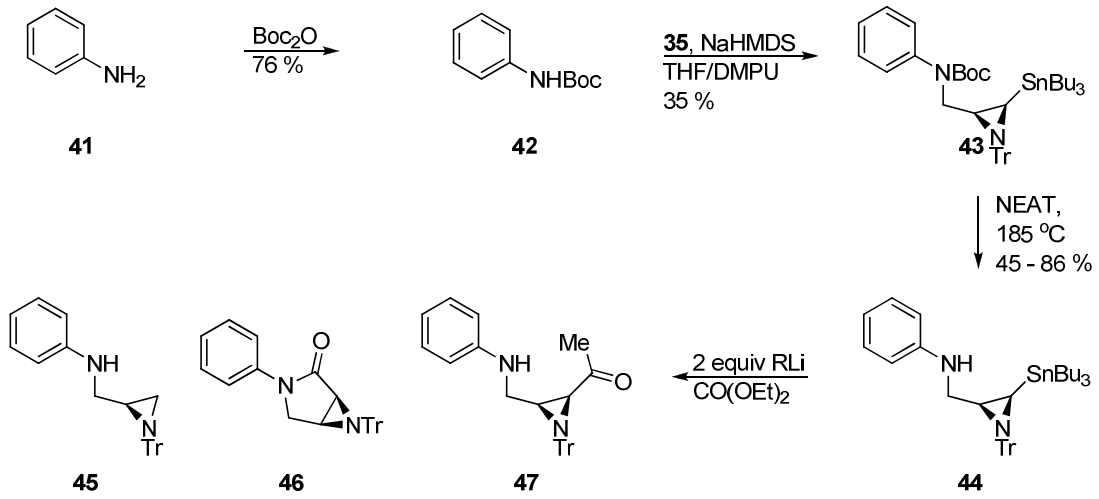

41 **42** **43** **45** **46** **47** **44**

It was expected that dianion formation would require an excess of base: one equivalent for deprotonation of the heteroatom, and one equivalent or more for tin-lithium exchange.[45] Therefore, **44** was treated with 2 equiv of MeLi (Table 3-2, entry 1) at -78 °C, and the anion was then quenched with 1.5 equiv of diethylcarbonate ($CO(OEt)_2$). This reaction gave mixtures of starting material **44**, destannylated aziridine **45,** and desired pyrrolidinone **46**. Treatment of **44** with excess MeLi, in order to facilitate complete tin-lithium exchange, resulted in a higher yield of **45** and small quantities of ketone **47** observed by ^{1}H NMR spectroscopy (Table 3-2, entry 2). The generation of destannylated aziridine **45** suggested that the lithioaziridine was being quenched before addition of the electrophile. If this was correct, the most likely proton source was unreacted starting material **44** present in the reaction mixture due to inefficient stirring.[45] In

order to inhibit the formation of **45**, deprotonation of the aniline had to be completed before any tin-lithium exchange occurred.

Studies by Goswami[45] and Kessler[49] on dianion formation via amide deprotonation and tin-lithium exchange demonstrated the necessity for completely deprotonating the heteroatom before promoting tin-lithium exchange. Goswami found that treating an amide with 1 equiv of *n*-BuLi, allowing the reaction to stir for 8 min and then adding a second equivalent of *n*-BuLi, allowed efficient trapping of the carbanion and reduced the formation of destannylated starting material.[45] Kessler ensured complete deprotonation of a glucosamine derivative before tin-lithium exchange by using 1 equiv of MeLi•LiBr before adding 1.3 equiv of *n*-BuLi.[49] Therefore, the dianion precursor **44** was treated with 1 equiv of *n*-BuLi and allowed to stir for 15 min at -60 °C. Then, 1 equiv of MeLi was added to promote tin-lithium exchange, and the reaction was quenched after 5 min with $CO(OEt)_2$ (Table 3-2, entry 3). The destannylated **45** was isolated in 48% yield along with a mixture of lactam **46** and ketone **47**. The recovery of substantial quantities of **45** was surprising, but when the reaction was repeated and allowed to warm to rt over 1 h, the desired lactam **46** was isolated in 46% yield along with trace amounts of **45** and **47** (Table 3-2, entry 4). Therefore, warming the reaction to rt after addition of $CO(OEt)_2$, is essential for efficient cyclization.

Table 3-2. Dianion formation on model carbamate **44**

					Results			
Entry	RLi (equiv)	T °C	$CO(OEt)_2$	Time	**44**	**45**	**46**	**47**
1	MeLi(2)	-78 to rt	1.5	5 min	n.d.	n.d.	n.d.	--
2	MeLi (4)	-78	4	5 min	4 %	39 %	12.5 %[a]	5 %[a]
3	*n*-BuLi (1) MeLi (1)	-78	10	5 min	n.d.	48%	10 %[a]	5 %[a]
4	*n*-BuLi (1) MeLi (1)	-78 to rt	10	1 h	--	n.d.	46 %	n.d.

[a] % based on integration of mixtures by ^{1}H NMR. n.d. not determined. -- not observed by ^{1}H NMR spectroscopy.

After the successful generation and trapping of the dianion on an aniline-derived model substrate, it was time to investigate the methodology on the fully functionalized aniline system

(Scheme 3-9). The Boc-protected aniline **48** was synthesized in good yield from aniline **33**. Aniline **48** was then alkylated with mesylate **35** under the standard conditions to give ca. 50% yield of aziridine **49**. As in the model, the Boc protecting group was removed under thermal conditions to provide dianion precursor **50**. Dianion formation and trapping with the optimized conditions provided a mixture of products including desired **37** (17%), destannylated **51** (15%), and starting material **50** (21%), as well as over-addition byproducts. However, attempts to improve the yield of **37** were unsuccessful. The complexity of the substrate made it difficult to determine the source of the proton that was trapping the dianion; however, incomplete heteroatom deprotonation or activation of an aryl proton for metallation could have been the culprit. Although the desired aziridinopyrrolidinone **37** had been obtained, the application of the dianion formation on the highly functionalized precursor was too inefficient to be pursued further.

Scheme 3-9. Dianion formation on fully functionalized **50**.

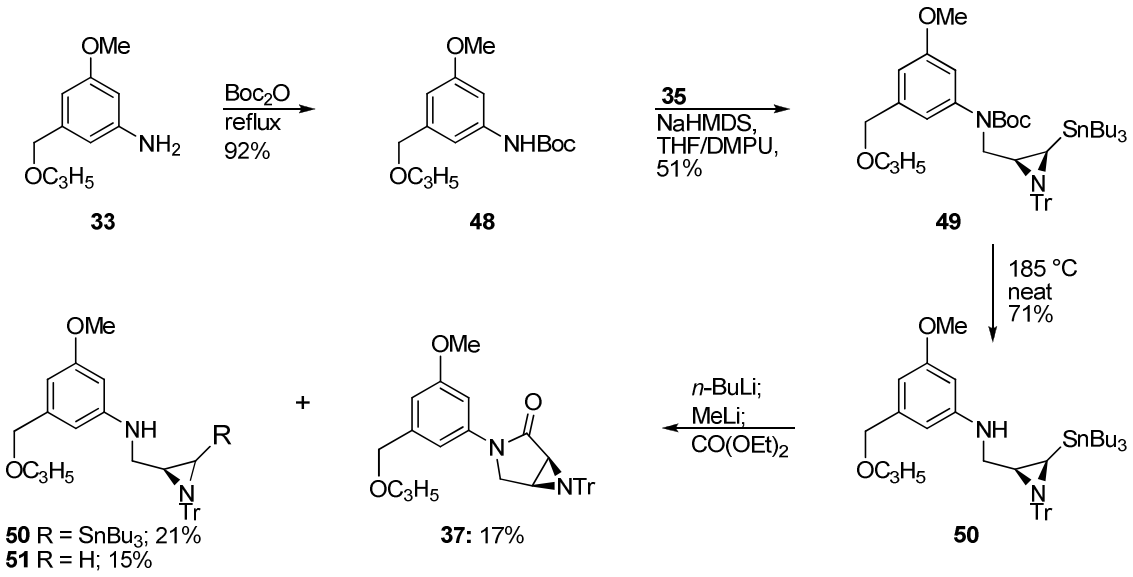

Route C: Transition metal-catalyzed coupling

The third approach envisioned towards analogs of **16** involved formation of the aryl-nitrogen bond via transition metal catalyzed coupling of a pre-functionalized aryl halide to an intact aziridinopyrrolidinone. Pyrrolidinones are known to be efficient coupling partners in Pd

and Cu catalyzed amination reactions,[50,51] and pre-functionalization of the aryl halide before installation of the acid labile aziridine would serve two purposes. First, the aryl halide would not be susceptible to acidic conditions, and therefore, a wide range of conditions could be used to install the functionality. Second, if the aryl subunit was functionalized before installation of the aziridine, fewer steps would be required to complete the synthesis of **13a** after introduction of the acid labile functionality. The key issues that needed to be addressed for this strategy were the synthesis of the aziridinolactam **19**, the functionalization of the aryl halide, and the optimization of the coupling reaction.

Although aziridinopyrrolidinones with the desired substitution pattern are known to some extent,[52] literature precedents to form the 3,6-diazabicyclo[3.1.0]hexane fused ring system were not conducive to our synthesis. Therefore, a new method for enantioselective formation of the 3,6-diazabicyclo[3.1.0]hexane ring system was required. Fortunately, dianion formation from a stannylaziridine and trapping with a phosgene equivalent provided the 3,6-diazabicyclo[3.1.0]hexane **46** in moderate yield (Scheme 3-8). If the phenyl substituent on the nitrogen was replaced with a labile nitrogen protecting group, then removal of the protecting group after cyclization would afford aziridinolactam **19**. Goswami showed that amides are suitable substrates for dianion formation; therefore, a carbamate that would undergo dianion formation was targeted.[45]

For the synthesis of **19**, the known mesylate **35** was treated with sodium azide to displace the mesylate leaving group and provide the azido aziridine **52** in excellent yield (Scheme 3-10). The high yield of the displacement is most likely due to the small size of the nucleophile. Importantly, a large excess of the nucleophile was no longer needed for efficient displacement of the mesylate to occur. Reduction of the azide with $LiAlH_4$ provided the amine **53**, which was unstable over time and to purification; therefore, it was used immediately without purification to form the carbamate **54**. Based on Goswami's example,[45] **54** would be suitable for dianion formation by deprotonation of the carbamate nitrogen followed by tin-lithium exchange.

Furthermore, once trapping of dianion **55** had occurred to form imide **59**, the imide could be cleaved to form the deprotected pyrrolidinone **19**.

Initial experiments focused on a two step procedure to form the ring system. The dianion was generated with 1 equiv of *n*-BuLi and 1 equiv of MeLi under the standard conditions, and then the lithioaziridine was trapped with excess Mander's reagent[53] to provide the imide aziridine **56**. Subsequent imide cleavage and ring formation with DMAP or DABCO was unsuccessful; however, K_2CO_3 in MeOH or NaOMe generated **19** in trace amounts. The main product from imide cleavage was the ester **57**. Fortunately, treatment of ester **57** with NaHMDS in THF provided 37% of the desired aziridinopyrrolidinone **19**. Although the lactam could be generated in two steps, the yield was rather poor. Therefore, it became necessary to re-evaluate the one step ring forming procedure.

Scheme 3-10. Dianion formation and trapping to form aziridinolactam **19**.

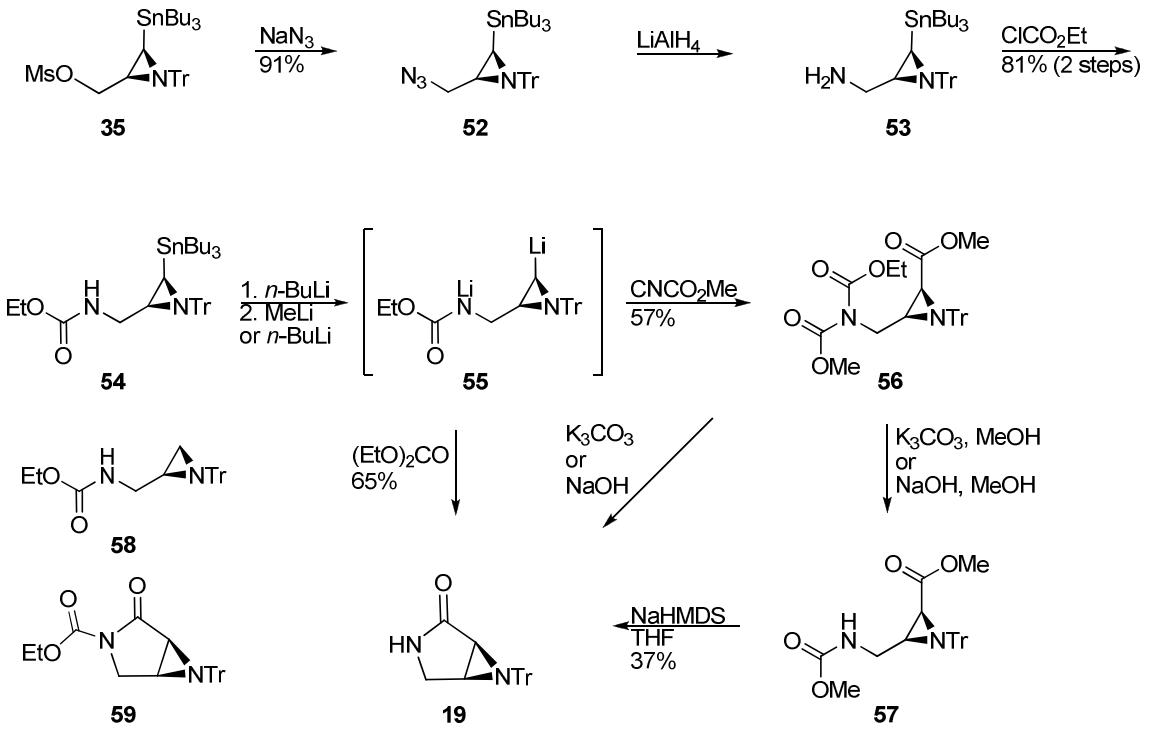

It was determined during evaluation of the two step procedure that the dianion could be trapped at both anionic sites by a good electrophile such as Mander's reagent. However, trapping

both nucleophilic sites with excess electrophile, i.e. formation of **56**, was undesired. Therefore, $CO(OEt)_2$, which afforded the desired lactam **46** in the dianion model system, was re-evaluated (Scheme 3-8).[54] During initial attempts at cyclization, we found it necessary to allow the reaction to slowly warm to rt after quenching the dianion **55** with $CO(OEt)_2$ because immediately stopping the reaction after addition of the electrophile led to poor yields of the cyclized product (Table 3-2, entry 3). In the event, quenching the dianion **55** with excess $CO(OEt)_2$ and warming the reaction over 4 h provided the desired pyrrolidinone **19** in moderate yield (50%) along with destannylated aziridine **58** and trace amounts of over-addition byproducts. The cyclized *N*-carboethoxy lactam **59** was never isolated or detected by ^{1}H NMR spectroscopy. The reaction appeared to be dependent on temperature and the rate of stirring. Therefore, the temperature was monitored internally and kept below -70 °C during deprotonation and tin-lithium exchange. Also, efficient stirring was necessary for good conversion as the major byproduct in this transformation was the protiodestannylated product **58** resulting from protonation of the lithioaziridine by unreacted **54**. The identity of **58** was confirmed by the loss of the tributyl stannane and by the presence of three aziridine peaks at δ = 1.73, 1.46, and 1.08 ppm in the ^{1}H NMR spectrum. Further optimization studies showed that *n*-BuLi was effective for tin-lithium exchange, and that MeLi was not necessary. Therefore, optimized conditions for cyclization of **54** to pyrrolidinone **19** involved initial deprotonation with 1 equiv of *n*-BuLi at -78 °C, ten minutes of stirring, followed by treatment with another equiv of *n*-BuLi, and then trapping the red dianion with $CO(OEt)_2$ while slowly warming to rt. Over-addition byproducts were sometimes seen by ^{1}H NMR spectroscopy in trace amounts. However, with tight temperature control and mechanical stirring the deprotected 3,6-diazabicyclo[3.1.0]hexane **19** could be generated in 65% yield on gram scale.

The second issue that needed to be addressed in this route was the coupling of pyrrolidinone **19** with an aryl halide. Using Buchwald's conditions for the Cu catalyzed coupling of amides to aryl iodides in a model study,[51] **19** was treated with 12 mol % CuI, 1 equiv *N*,*N*′-dimethylethylenediamine **60a** (Figure 3.1), K_3PO_4, and iodobenzene in toluene at 100 °C to

provide the coupled product **46** in good yield (Eq 1, Table 3-3, entry 1). Analysis of the crude reaction mixture by ^{1}H NMR spectroscopy showed recovered **19** as well as the product **46**. Fortunately, the valuable lactam **19** could be re-isolated from the reaction mixture. Aziridinopyrrolidinone **46** had been previously synthesized during the investigation of a dianion route, and as expected the ^{1}H NMR spectrum of the new material matched that of the prior sample. This was the first time that a model of the desired *N*-aryl aziridinopyrrolidinone **16** had been isolated in acceptable yield.

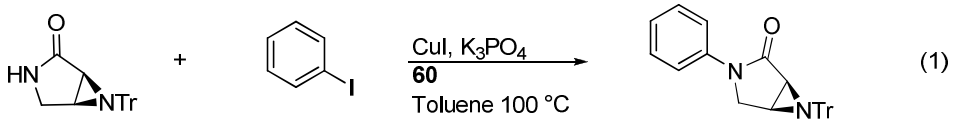

19 **46**

Since the coupling reaction had worked very well on the simple aryl iodide, we expanded the substrate scope to include aryl halides that were functionalized at the ortho position. It was hoped that *ortho* functionality installed before the coupling step would permit the final C-C bond forming event leading to the tetracycle. Various aryl iodides were synthesized from known *o*-iodobenzaldehyde **62** (Scheme 3-11). Homologation of aldehyde **62** with the Ohira-Bestmann[55] reagent provided the iodo-alkyne **63**, which was then protected as the TMS acetylene **64**[56] in good yield over the two steps. Furthermore, the aldehyde **62** could be converted into dithiane **65** by treatment with propanedithiol.[57] Finally, treatment of aldehyde **62** with catalytic ZnI_2 and TBSCN provided the TBS protected cyanohydrin **66** in good yield.[58] These ortho-functionalized aryl iodides were then subjected to copper catalyzed coupling conditions.

Scheme 3-11. Synthesis of *ortho*-functionalized aryl iodides.

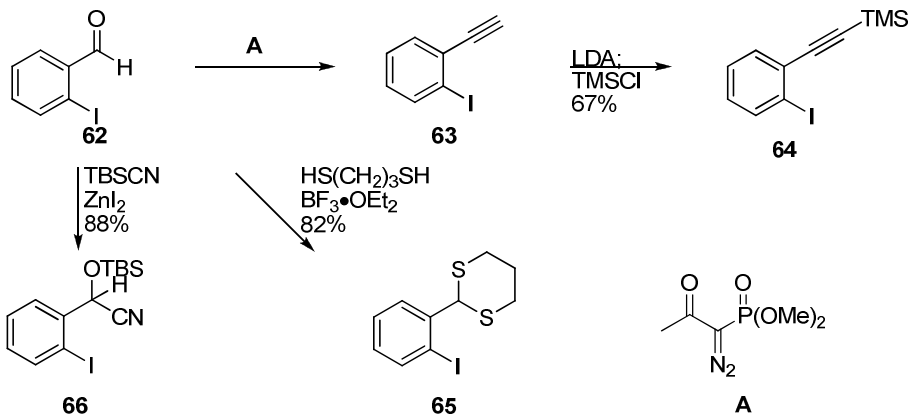

Table 3-3. Copper catalyzed coupling of aryl iodides with **19**[a]

Entry	Substrate	CuI	Time	Product	Yield
1		0.1	4 h	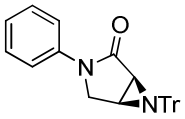 **46**	63%
2	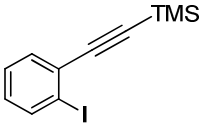 **64**	0.3	20 h	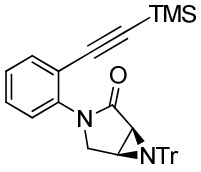 **67**	48%
3[b]		0.3	41 h		22%
4	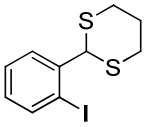 **65**	0.3	20 h	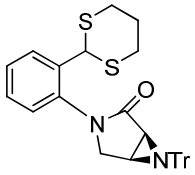 **68**	67%
5	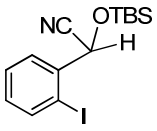 **66**	1.0	20 h	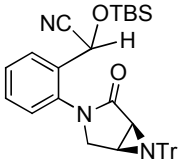 **69**	61%
6[c]	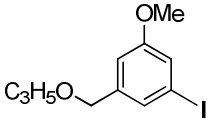 **70**	0.1	38 h	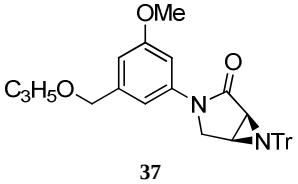 **37**	33%
7		0.3	48 h		73%

[a] Toluene used as solvent unless otherwise noted. [b] 1,4-dioxane used as solvent. [c] Ligand **60** used.

60 ± **61**

Figure 3-1. Diamine ligands used in Cu catalyzed coupling.

Due to the incomplete conversion to the coupled product **46** under the copper catalyzed conditions, we chose to optimize the reaction parameters during studies on the substrate scope. The TMS-acetylene iodide **64** was treated with 30 mol % CuI, 60 mol % *N,N′*-dimethylcyclohexanediame, K_3PO_4, and heated in toluene at 100 °C. The coupled acetylene **67** was isolated in 48% yield (74% b.r.s.m.) (Table 3-3, entry 2). Switching to 1,4-dioxane produced **67** in only 22% yield after 41 h (Table 3-3, entry 3). This experiment showed that toluene was the more efficient solvent, and therefore, it was used in further reactions. Coupling of the aryl dithiane **65** and **19** with 30 mol% catalyst in toluene provided dithiane **68** in 67% yield (Table 3-3, entry 4). Although good yields were obtained, the reaction still did not go to full conversion. Therefore, TBS cyanohydrin **66** was treated with a stochiometric amount of CuI, and coupled product **69** was isolated in good yield (Table 3-1, entry 5). However, the reaction was not complete after 20 h of stirring and heating. The copper-catalyzed coupling is known to be sensitive to the presence of O_2,[51] and even though every precaution was taken to eliminate exposure to air, traces of O_2 could be hindering the reaction by oxidizing the catalyst. Although complete conversion was not achieved with the simpler substrates that had been used to explore the coupling chemistry, attention was turned to the coupling of a highly functionalized aryl iodide.

In principle, coupling of a 1,3,5-trisubstituted aryl subunit with **19** would install all the requisite functionality for the fully functionalized system. Therefore, the aniline derivative **33** was converted to aryl iodide **70** under Sandmeyer conditions (Eq 2). The reaction was very poor yielding (8%), but enough material was obtained in order to attempt the key coupling reaction. When **70** was treated with diamine ligand **60** and only 10 mol % of CuI, the lactam **37** was

isolated in 33% yield after 38 h (Table 3-1, entry 6). However, the more reactive cyclohexanediamine ligand **61** in the presence of 30 mol % CuI provided **37** in 73% yield after 2 days (Table 3-1, entry 7). The reactions still did not reach full conversion, but the successful coupling of a highly substituted aryl iodide to the valuable aziridinopyrrolidinone **19** emphasized the potential of the coupling reaction of route C, and the viability of coupling the two pieces in order to efficiently reach the key intermediate **16**. Now that an efficient route to analogs of **16** had been developed, synthetic studies toward mitosane **14a**,**b** could continue with investigation of the key tetracycle bond-forming event.

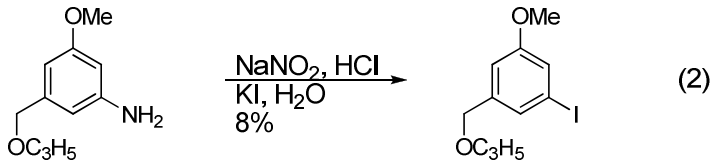

33 **70** (2)

Part 2: Enantioselective synthesis of a 9-oxo-pyrrolo[1,2-a]indole

Tetracycle Formation

Successful formation of the *N*-aryl aziridinopyrrolidinones **37**, **46** and **67**-**69** was the first major accomplishment in the synthesis of the biosynthetic probes **13a** and **13b**. The next key stage in the synthetic endeavor was installation of the final carbons required for tetracycle formation and the final C-C bond forming event. Many different routes to the tetracycle could be envisioned from the substrates obtained in the copper catalyzed amidation reactions. For example, the 1,3,5-functionalized arene **37** would require a subsequent functionalization at carbon **a** (Eq 3). Directed *ortho*-metallation using the methoxy substituent and lactam as directing groups should provide regioselective metallation at the common carbon.[59] Trapping of the aryllithium with an appropriate electrophile and further transformation could provide vinyl halide **71**. Finally, lithium-halogen exchange and 1,2-addition into the appended lactam would form the desired tetracycle **72**. Unfortunately, the susceptibility of the lactam of **37** to nucleophilic

addition by alkyllithiums was a concern because this route would require extensive use of strong base and/or alkyllithiums. Furthermore, the poor availability of the aryl halide **70**, as well as the number of steps and control of regioselectivity required to prepare an intermediate such as **71**, made this route less desirable. Therefore, strategies from the already synthesized *o*-functionalized lactams **67** – **69** were considered.

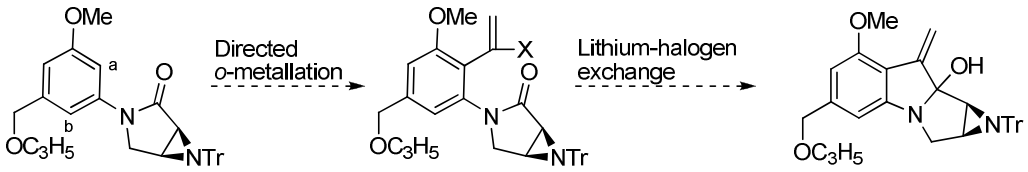

(3)

37 **71** **72**

Fortunately, a unique bond-forming event could be envisioned from TMS-acetylene substrate **67** that might solve the anticipated problems. Cha[60] and Sato[61] have shown that modified Kulinkovich reactions are suitable for affecting intramolecular nucleophilic acyl substitution reactions (INAS) of alkenes and alkynes. Sato invoked the formation of the nucleophilic titanacyclopropene **74** when ester **73** was treated with chlorotitaniumtriisopropoxide ($ClTi(Oi\text{-}Pr)_3$). The titanacycle reacts with the appended carbonyl to form the titanaoxacycle **75** (Scheme 3-12), which after hydrolysis affords the cyclized product **76**. Importantly, Sato found that the TMS group is essential for the reaction to occur. Meanwhile, Cha formed the mitosane core using a similar approach (Scheme 3-13). Treatment of the alkene **77** with cyclohexylmagnesium chloride formed the titanacyclopropane, which interacts with the appended imide to form titanaoxacyclopentane **78**. Trapping of the titanacycle with O_2,[60b] installed the requisite hydroxymethyl functionality of the mitomycins. We envisioned a similar approach to the mitosane core, where the cyclization of the TMS-acetylene via a titanocyclopropene would give an external olefin that could be stereoselectively oxidized to provide the desired hydroxymethyl group with the correct stereochemistry.

Scheme 3-12. INAS reaction of TMS-acetylenes

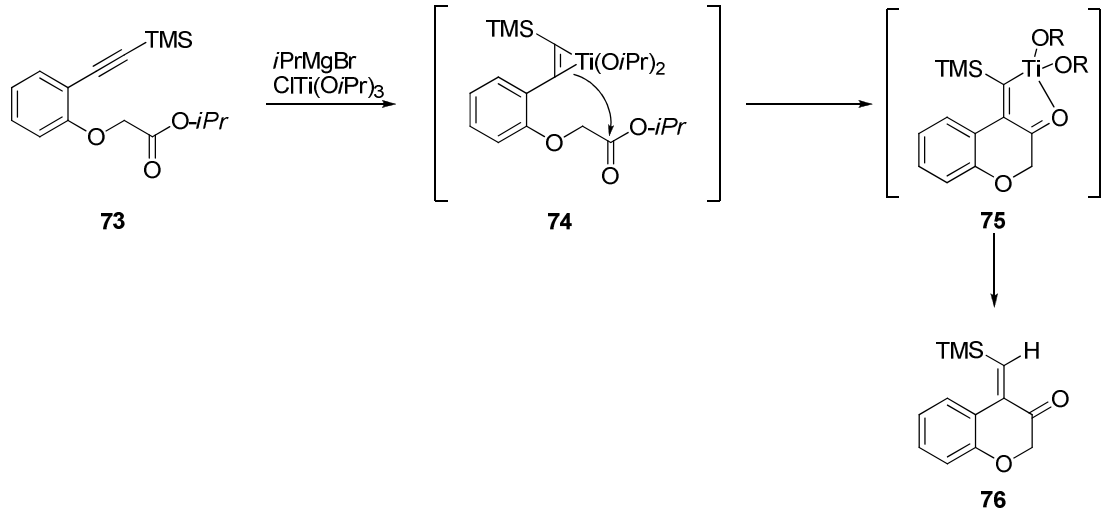

Scheme 3-13. Modified Kulinkovich reaction to form the mitosane core

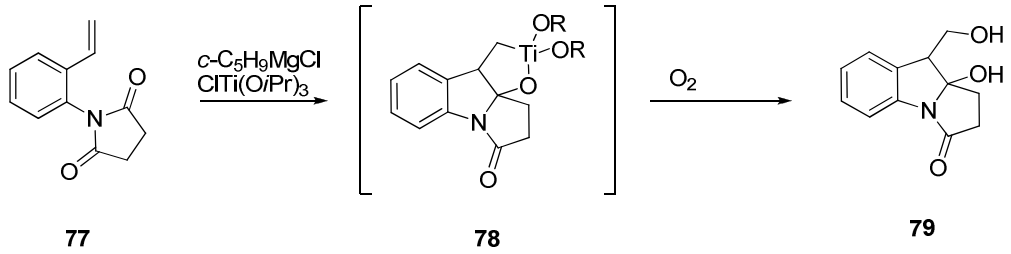

Following the Cha and Sato analogies, a mixture of TMS-acetylene **67** and chlorotitaniumtriisopropoxide was treated with isopropyl magnesium chloride (Scheme 3-14). However, the crude reaction mixture consisted of 21% unreacted starting material and a new product assigned as TMS alkene **80** after isolation (31%). The ^{1}H NMR spectrum of **80** showed a new doublet downfield at δ = 6.03 ppm with a *J* value of 15.0 Hz. Using two-dimenionsal COSY NMR spectroscopy, the alkenyl proton at δ = 6.03 ppm was observed to couple with another alkenyl proton at δ = 7.53 ppm. The large coupling constant was consistent with a *cis* olefin as reported by Soderquist.[62] The strongly deshielded alkenyl proton can be explained by proximity to the amide and phenyl groups. The formation of **80** showed that the titanium had bonded with the alkyne, but the desired bond forming event at the amide carbonyl had not occurred.

Using Cha's conditions with cyclopentyl magnesium chloride, which promotes facile ligand exchange between a titanacyclopropane and the alkyne substrate, provided a complex mixture of products upon deuterium quench and workup. Visible by ^{1}H NMR spectroscopy were two aziridine peaks upfield at δ = 2.32 (d, *J* = 4.5 Hz) and 2.17 (dd, *J* = 4.5, 2 Hz) ppm, which suggested the presence of a hemi-aminal containing an exocyclic olefin (Chapter 2, Table 2.3). Consequently, the product of the reaction was tentatively assigned as **81**. However, the material decomposed as it was concentrated (indicated by a color change from bright yellow/green to dark orange) and purification by silica gel chromatography provided many bands consisting of complex materials. One component of the purified mixture was assigned as mitosene **82** based on a pair of aziridine protons at δ = 3.00 (d, *J* = 5.0 Hz) and 2.94 (dd, *J* = 4.8, 3.8 Hz) ppm observed in the ^{1}H NMR spectrum (Chapter 2, Table 2.3). Attempts to improve the reaction or to derivatize the major product by oxidation of the mixture with OsO_4 and NMO resulted in complex mixtures. Although the observation of **81** and **82** by ^{1}H NMR spectroscopy of the crude reaction mixture showed that the C–C bond forming event was occurring, the inability to isolate the tetracycle or to oxidize it to an isolable derivative showed that this strategy was futile. However, other strategies to form the final tetracyclic bond could be pursued using dithiane **68** and silylated cyanohydrin **69**.

Scheme 3-14. INAS reaction of TMS-acetylene **67**

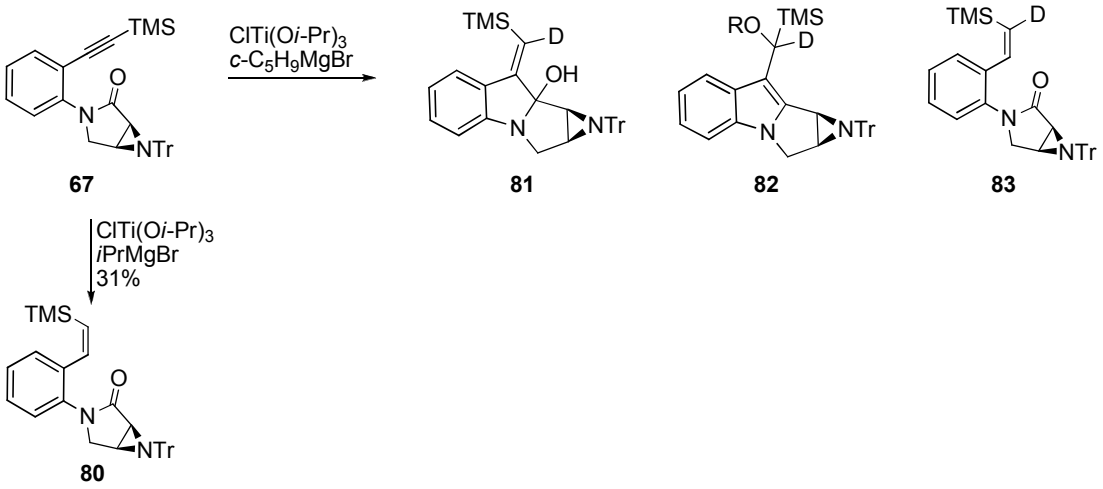

We envisioned using dithiane **68** and cyanohydrin **69** as acyl anion equivalents to form the final C(9)-C(9a) (mitosene numbering) bond of the tetracycle. It is known that anions generated by deprotonation of dithianes[63] and cyanohydrins[64] are nucleophiles that can add to carbonyls. Therefore, various bases were screened in the attempt to deprotonate dithiane **68** for intramolecular 1,2-addition. Treatment of dithiane **68** with *n*-BuLi resulted in addition of the *n*-BuLi into the lactam in accordance with our previous studies with lactams of the 3,6-diazabicyclo[3.1.0] hexane ring system. Lithium diisopropyl amide (LDA) gave a complex mixture of products when used to deprotonate **68**. Although starting material had been consumed, the main component could not be identified. By ^{1}H NMR spectroscopy the major product appeared to be a dimer of the dithiane, which could have formed by an intermolecular process. Finally, treatment of **68** with potassium hexamethyldisilylazide (KHMDS) and quenching the reaction with deuterated methanol resulted in recovered starting material with no deuterium incorporation (Eq 4). Since the dithiane was not deprotonated by KHMDS and gave undesired side reactions with LDA and *n*-BuLi, further anionic cyclization attempts focused on the cyanohydrin **69**.

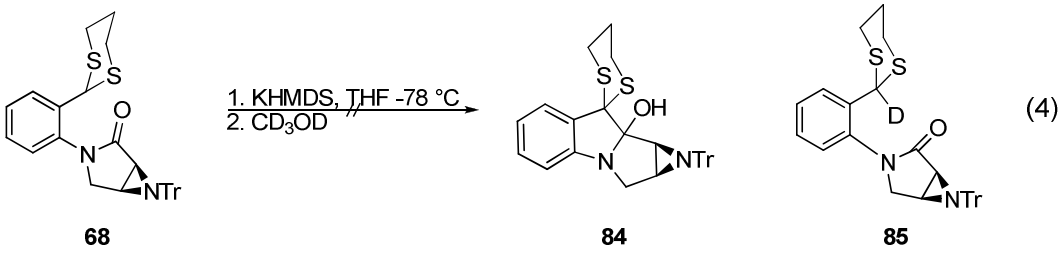

68 **84** **85** (4)

Successful tetracycle formation was accomplished by addition of the cyanohydrin anion of **69** to the appended lactam. After screening base, solvent, and temperature the optimal conditions for 1,2-addition were found to be slow addition of **69** as a non-homogenous solution in Et_2O to 1.3 equiv of LiHMDS at -78 °C in Et_2O, stirring for 30 min at -78 °C, followed by warming the reaction to 0 °C, and stirring for 10 min. Analysis of the crude reaction mixture by ^{1}H NMR spectroscopy showed tetracycle **88** as a 2:1 mixture of diastereomers (Scheme 3-15). It

was found that the major diastereomer was stable to purification and could be isolated, but the minor diastereomer decomposed on silica gel, NEt_3 deactivated silica gel, and basic alumina. While screening bases for this transformation, it was found that KHMDS was ineffective for addition. On the other hand, excess lithium diisopropylamide (LDA) effected the desired tetracycle formation, but the crude material was contaminated by complex side-products.

Scheme 3-15. Protected cyanohydrin addition into lactam **69**

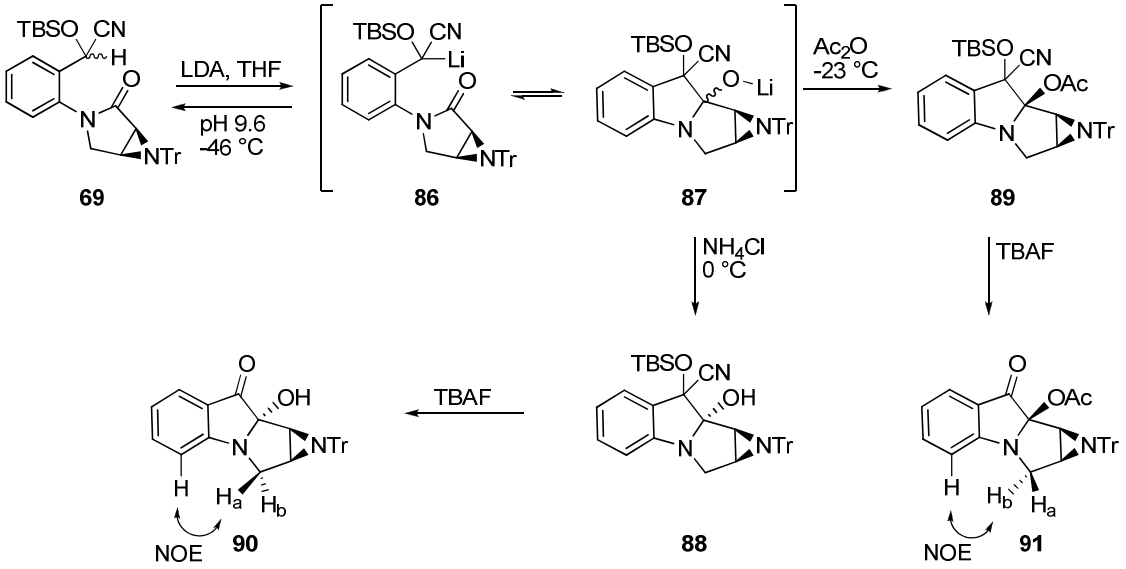

It became apparent that allowing the temperature to increase during the reaction was crucial for successful ring formation. With LDA as the base, allowing the temperature to reach 0 °C was essential for formation of the stable isomer, while trapping the tetrahedral intermediate at -12 °C with Ac_2O gave primarily the acetate derivative of the unstable isomer **89**. Furthermore, when a mixture of cyanohydrin diastereomers was treated with LDA and the reaction was quenched at -46 °C, only one diastereomer of cyanohydrin **69** was isolated. This suggests that deprotonation occurs at -78 °C, but that warming is essential for carbanion addition to the lactam. When the LiHMDS reaction was stopped at -12 to 0 °C, the more stable diastereomer was the major diastereomer formed; however, if the reaction was stirred at 0 °C for extensive periods of time (>30 min), more starting material was observed after quenching the reaction. Although the origins of product ratio discrepancies when using LDA versus LiHMDS are unclear, all of these

observations suggest that the addition product **87** is in equilibrium with carbanion **86**. Furthermore, stopping the reaction soon after reaching 0 °C was necessary for good conversion to the more stable tetracycle.

The major diastereomer of **88** and the acetate derivative **89** could be converted to the ketones **90** and **91** via removal of the silylated cyanohydrin with TBAF. Due to the locked ring system and the reduced flexibility with the sp^2 C(9) carbon, it was possible to perform 2D NOESY NMR experiments. The 2D NOESY NMR spectrum of the stable diastereomer showed an NOE correlation between H_a and an aryl proton on the benzene ring. This type of through space interaction would only be possible if the tertiary alcohol was on the opposite face of a *cis*-fused tetracycle relative to the aziridine. On the other hand, the acetate derivative **89** showed a NOE correlation between H_b and the analogous aryl proton, which is only possible if the acetoxy group is on the same face as the aziridine. The assigned stereochemistry was confirmed when the X-ray crystal structure of **90** was obtained (Fig 2). As expected, the alcohol and aziridine are on opposite faces of the tetracycle, and the desired diastereomer **88** is the more stable thermodynamic product of the cyclization. The stereochemistry at C(9a) obtained in the cyclization step matches the stereochemistry at C(9a) of mitomycin C, and is the stereochemistry required for the synthesis of the biosynthetic probes **13a,b**.

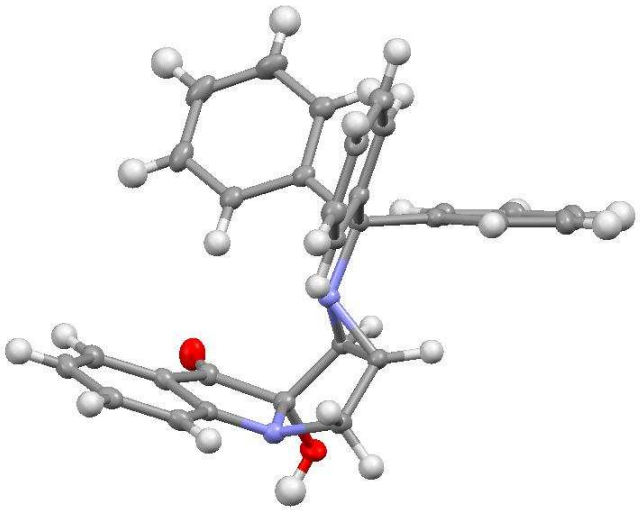

Figure 3-2. X-ray crystal structure of tetracycle **90**.

At this stage, we had successfully synthesized analogs of the advanced intermediate **14a** and the precursor **16** in the planned synthesis of **13a,b**. However, before applying the new methodology to the fully functionalized system, it seemed prudent to study addition of various masked methyl alcohols into the ketone to confirm that the C(10) carbon can be installed on 9-oxo-pyrrolo[1,2-a]indole substrates. Danishefsky showed that reductive ring opening of exocyclic epoxides derived from dihydrobenzoxazine derivatives provides the hydroxymethyl moiety of FR900482.[65] Therefore, various sulfur ylides were screened for epoxide (**92**) formation from the ketone **90**, but they were unreactive with the substrate. To avoid possible interference by the tertiary alcohol, the hydroxyl group was protected as silyl ether **93** (Scheme 3-16). When ketone **93** was treated with excess trimethylsilylmethyl lithium using Danishefsky's procedure, tertiary alcohol **94** was produced in 67% yield. Furthermore, transformation of the tertiary alcohol into the C(10) hydroxymethyl group of **95** can be envisioned using Danishefsky's precedent.[29] Therefore, an efficient synthesis of the model **90** was accomplished using the copper-catalyzed coupling of two pre-functionalized subunits, followed by a stereoselective

cyclization event. As shown below, the model ketone **93** was susceptible to nucleophilic addition, thereby facilitating installation of the C(10) hydroxymethyl moiety. Finally, with a clear strategy for preparing the 9-oxo-pyrrolo[1,2-a]indole, all that had been learned on accessing the α-hydroxy ketone **90** could now be applied to the synthesis of fully functionalized **14a**.

Scheme 3-16. Installation of the C(10) carbon.

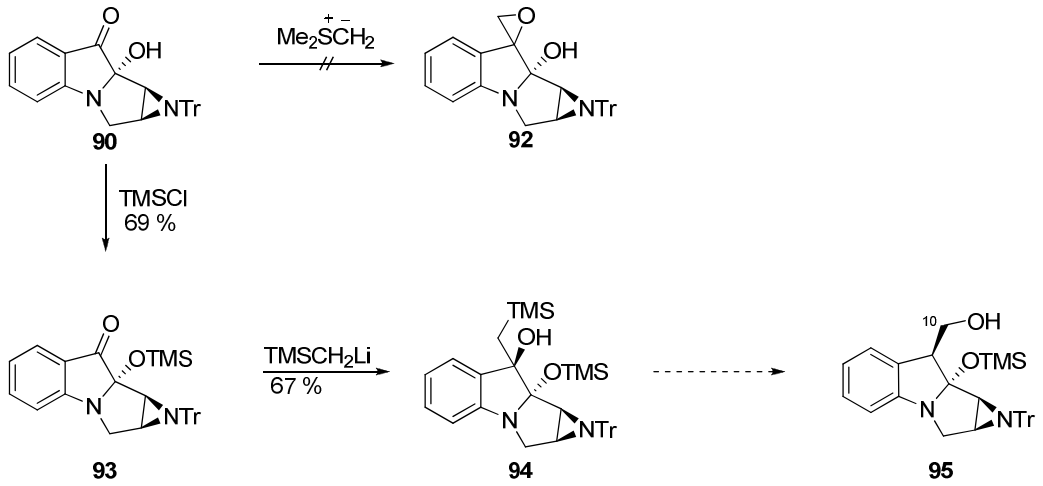

Synthesis of the fully functionalized 9-oxo-pyrrolo[1,2-a]indole 96

Investigations leading to model **90** revealed that the most efficient way to access the key aziridinopyrrolidinones **67-69** is coupling a pre-functionalized aryl subunit with the preformed aziridinopyrrolidinone **19**. Based on the chemistry utilized during these studies, the retrosynthetic analysis of **13a,b** was revised (Scheme 3-17). Late stage deprotection and C(10) installation can be envisioned from α-hydroxy ketone **96**. The tetracycle would be derived from the aldehyde **97** via an acyl anion equivalent addition into the appended lactam. Using the catalyzed amidation reaction, 3,6-diazabicylo[3.1.0]hexane **97** would be accessed from pyrrolidinone **19** and the fully protected and functionalized aryl triflate **98**. We decided to target the aryl triflate instead of the aryl iodide because of the high availability of phenols and the well precedented conversion of phenols into triflates. The conversion of phenols to iodides is less precedented,[66] and the conversion of an aryl amine into an iodide using the Sandmeyer reaction proved to be difficult on

a functionalized substrate (Eq 2). Aryl triflate **98** was envisoned to arise from known dibenzyl aldehyde **99**, which was available from 4-bromo-3,5-dihydroxy benzoic acid **100**.[67]

Scheme 3-17. Retrosynthetic analysis of thioesters **13a,b**.

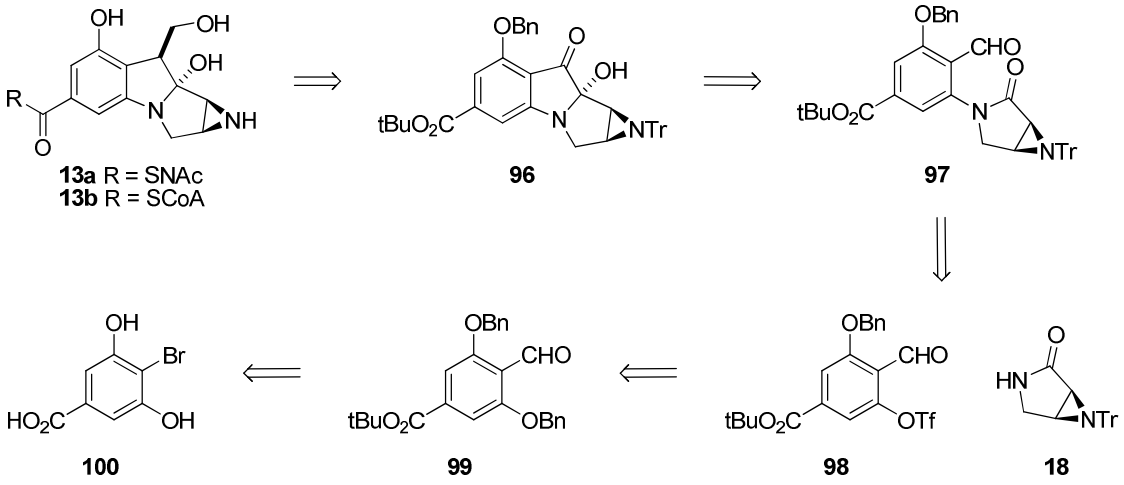

Following the procedure of Lampe,[67] acid **100** was converted to aldehyde **99** in 4 steps with an overall yield of 33% (Scheme 3-18). At this stage, desymmetrization of the molecule was required in order to obtain the desired phenol. Therefore, using a procedure reported by Stoddart[68] and Hendrickson[69] for monodebenzylation, **99** was treated with NaOMe in MeOH and 1,4-dioxane with 10% of Pd/C under an H_2 atmosphere to cleave only one benzyl group. As reported, it was important to monitor the uptake of H_2 because full debenzylation of the substrate was possible. However, when approximately 1 mol equiv of H_2 was consumed, the monodebenzylated phenol **101** could be isolated in moderate yield (53%) as pale yellow crystals. Treating phenol **101** with Tf_2O and K_3PO_4 in toluene and water provided the triflate **98** in good yield (80%).[70]

Scheme 3-18. Synthesis of aryl-triflate **98**.

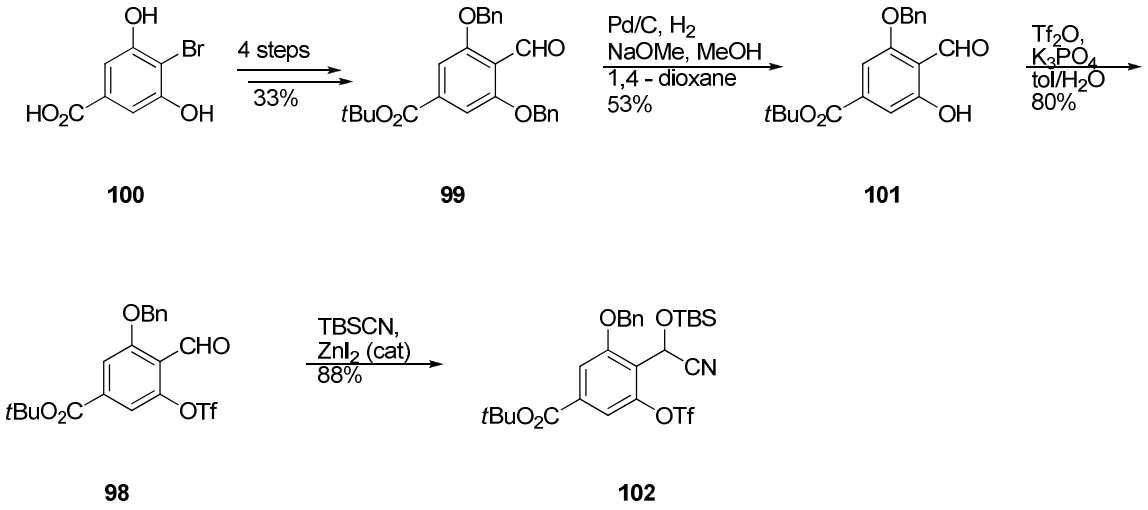

At this stage, it was necessary to consider which coupling partner would be successful in the transition metal-catalyzed amidation reaction. Although aryl triflates are known to undergo Pd-catalyzed[71] amidation reactions and intramolecular copper-catalyzed amidations,[72] they have not been reported to participate in copper-catalyzed *intermolecular* amidation reactions. Consequently, the ability of the triflate to undergo the previously optimized copper catalyzed coupling was suspect, and the conditions used to produce models **64-66** would need to be optimized for the triflate. Furthermore, the presence of the aldehyde would complicate the transformation because it would activate the triflate for oxidative addition, but it could also be susceptible to nucleophilic attack under the reaction conditions. In order to circumvent the expected sensitivity of the aldehyde, **98** was converted into cyanohydrin **102** using ZnI_2-catalyzed cyanosilylation conditions (88%).[58] Attempts to prepare the aryl iodide as the optimal coupling partner by nucleophilic displacement of the activated triflate with LiI were unsuccessful, so attention focused on the triflate.

Scheme 3-19. Palladium catalyzed coupling of **98** and **19**.

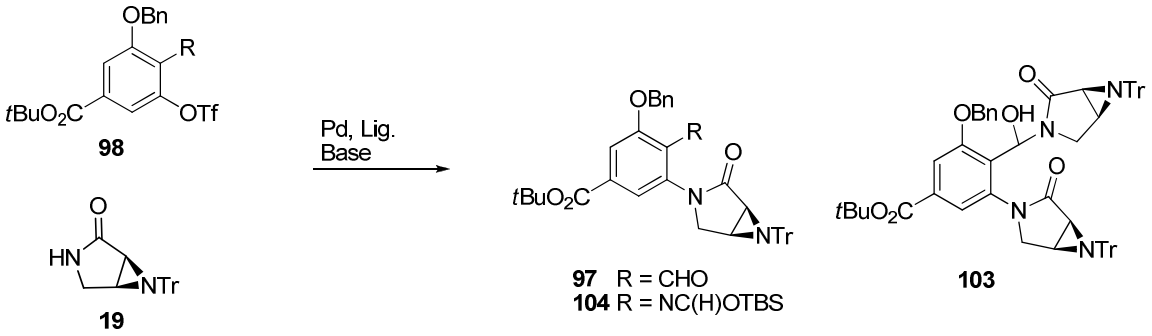

Table 3-4. Transition metal-catalyzed coupling of aryl triflate with **19**[a]

Entry	R	Pd	Ligand	Base	Temp (°C)	**97**	**103**
1	CHO	$Pd_2(dba)_3$ (2 mol%)	Xantphos (6 mol%)	Cs_2CO_3 (1.4)	80	23%	35%
2	CHO	$Pd_2(dba)_3$ (2 mol%)	Xantphos (6 mol%)	Cs_2CO_3 (1.4)	rt	--	nd[b]
3	CHO	$Pd(OAc)_2$ (1 mol%)	Xantphos (1.5 mol%)	Cs_2CO_3 (1.4)	80	9%	18%
4[c]	CHO	CuI (100 mol%)	**60b**	K_3PO_4 (1.4)	80	--	--
5	CHO	$Pd_2(dba)_3$ (2 mol%)	Xantphos (6 mol%)	K_3PO_4 (1.4)	80	64%	9 %
6	NCCHOTBS	$Pd_2(dba)_3$ (2 mol%)	Xantphos (6 mol%)	Cs_2CO_3 (1.4)	80	--	--
7[c]	NCCHOTBS	CuI (100 mol%)	**60b**	K_3PO_4 (1.4)	110	--	--

[a]Reaction run in 1,4-dioxane. [b]Major product by ^{1}H NMR spectroscopy. [c]Reaction run in toluene. **60b** = *N*,*N*′-dimethylcyclohexanediamine. nd = not determined. -- = not observed by ^{1}H NMR spectroscopy

Literature precedent demonstrates that palladium will catalyze aryl amidation reactions between amides and triflates.[50] Following procedures developed by Buchwald and coworkers, the triflate **98** was treated with 1.2 equiv of lactam **19** in the presence of 2 mol% $Pd_2(dba)_3$, xantphos, and Cs_2CO_3 (Scheme 3-18). Heating at 80 °C provided 23% yield of the desired adduct **97** after 1 h (Table 3-4, entry 1). Under these conditions, a significant amount of triflate had been converted into the phenol **101**, most likely by nucleophilic attack at the activated sulfur atom.[73] Also, a large amount of byproduct, assigned as **103** based on ESMS ([M + H] *m/z* = 991), was isolated in 35% yield. The byproduct had incorporated two equivalents of lactam, as evidenced

by two CH_2 ABX methylene pairs in the ^{1}H NMR spectrum, as well as one equiv of triflate. Structural assignment of **103** was facilitated by the presence of an exchangeable proton at δ = 8.66 ppm, and the heteronuclei coupling of the carbinolamide carbon at δ = 58.8 ppm to a proton at δ = 7.17 ppm. Assuming that nucleophilic addition into the aldehyde was a result of increased reactivity of the substrate at high temperatures, the reaction was run at rt; however, only **103**, **101**, and **19** were detected by ^{1}H NMR spectroscopy (Table 3-4, entry 2). Attempts to improve the reaction by switching the palladium source to $Pd(OAc)_2$ did not increase conversion to **97** (entry 3).[50] As expected, changing to copper-catalysis conditions did not give any product, most likely due to iminium ion formation between the diamine ligand and the aldehyde **98** (Table 3-4, entry 4). Based on the coupling results and the unavoidable formation of the byproduct **103**, even at rt, it was hypothesized that the byproduct formation was base catalyzed and that changing the base may be helpful. Therefore, K_3PO_4, which was successful in the copper-catalyzed coupling of aryl iodides (Table 3-3), was tested.[74] In the event, coupled product **97** was isolated in 64% yield, along with only 9% of **103** (Table 3-4, entry 5). Survival of the triflate was also improved under these conditions as evidenced by the increased yield, and the decreased amount of **101** observed by ^{1}H NMR spectroscopy of the crude reaction mixture.

Even though successful coupling had been accomplished with the aldehyde **98**, coupling of the cyanohydrin **102** would reduce the number of steps required after installation of the sensitive aziridine. Therefore, **102** was treated with $Pd_2(dba)_3$, xantphos, and Cs_2CO_3; however, decomposition products and **19** were the only compounds visible by ^{1}H NMR spectroscopy (Table 3-4, entry 6). The copper-catalyzed conditions gave only phenol **101** and lactam **19** (Table 3-4, entry 7). The lack of reactivity of the cyanohydrin **102** was not surprising because the electron withdrawing aldehyde should increase the reactivity of the conjugated triflate. Furthermore, the reaction might also be impeded by the sterically bulky silylated cyanohydrin.

The ability to access the functionalized aziridinopyrrolidinone **97** allowed the synthesis of the mitosane **96** to continue. Attempts to install the silylated cyanohydrin on **97** with catalytic

ZnI_2 and TBSCN resulted in significant decomposition of the substrate due to the Lewis acidic character of the catalyst (Scheme 3-20). However, the transformation of **97** to **104** could be effected using Greenlee's method (catalytic KCN, 18-crown-6 ether, and TBSCN),[75] affording **104** in approximately a 1:1 mixture of diastereomers at C(9a) in excellent yield (97%) (Scheme 3-19). The diastereomers could be separated by silica gel chromatography, but based on model **69**, separation was not necessary for the acyl anion addition. Therefore, the mixture of diastereomers was treated with 3 equiv of LiHMDS in Et_2O to afford a mixture of tetracycle **107** (54%) and recovered **104** (both diastereomers, 28%). Fortunately, only one diastereomer of **107** was apparent by ^1H NMR spectroscopy. The ^1H and ^{13}C NMR spectra of **107** correlated very well with the NMR spectra of the model tetracycles.

In comparison to model system **69**, cyclization of **104** to **107** was much more problematic. Following the optimized procedure developed in the model system resulted in poor conversion to **107** and recovery of both diastereomers of **104**. In order to achieve good conversion to the tetracycle, several changes in the procedure were necessary. First, before addition of base, the substrate was dissolved in toluene and the solvent was removed under N_2 flow to remove any residual water. The possibility of toluene acting as a cosolvent was discounted by poor conversion to **107** when toluene was added to a solution of **104** in Et_2O (tol:Et_2O, 1:2). Second, after stirring anion **105** at -78 °C, the cloudy solution was warmed slowly to 0 °C. During warming, lightening of the color near -15 °C was usually indicative of tetracycle formation. Finally, it was necessary to stir the solution for longer periods of time at 0 °C (~ 40 min) because quenching the reaction after only a few minutes at 0 °C gave poor conversion to **107**.

Determination of the C(9a) stereochemistry of **107** using two-dimensional NOESY NMR spectroscopy studies was inconclusive, so the silylated cyanohydrin was cleaved to produce the α-hydroxy ketone **96** in good conversion. The ^{13}C NMR spectra of **96** showed the characteristic hemi-aminal carbon signal at δ = 97.5 ppm which is consistent with previously synthesized α-

hydroxy ketone mitosanes.[31,33] One - dimensional NOE difference ^{1}H NMR spectroscopy studies confirmed that the alcohol was *trans* to the aziridine (Scheme 3-20). Irradiation of H_a showed a 16% enhancement of an aryl proton (H_c) and 3.4% enhancement of the C(2) aziridine proton H_d. Irradiation of H_b did not show any enhancement in the aryl region, but did show a 4% enhancement of H_d. In the model **90**, the NOE correlation between H_a and the aryl proton was only possible in the *trans* form as confirmed by the X-ray crystal structure, while the *cis* form showed a correlation between H_b and the aryl proton. Since the expected no through space interaction between H_b and H_c of **108** was not observed, the diastereomer obtained in the cyclization does not have the tertiary alcohol and aziridine on the same face. Accordingly, the desired diastereomer of **96** had been accessed with excellent diastereoselectivity during the addition step.

Scheme 3-20. Cyclization of **104**

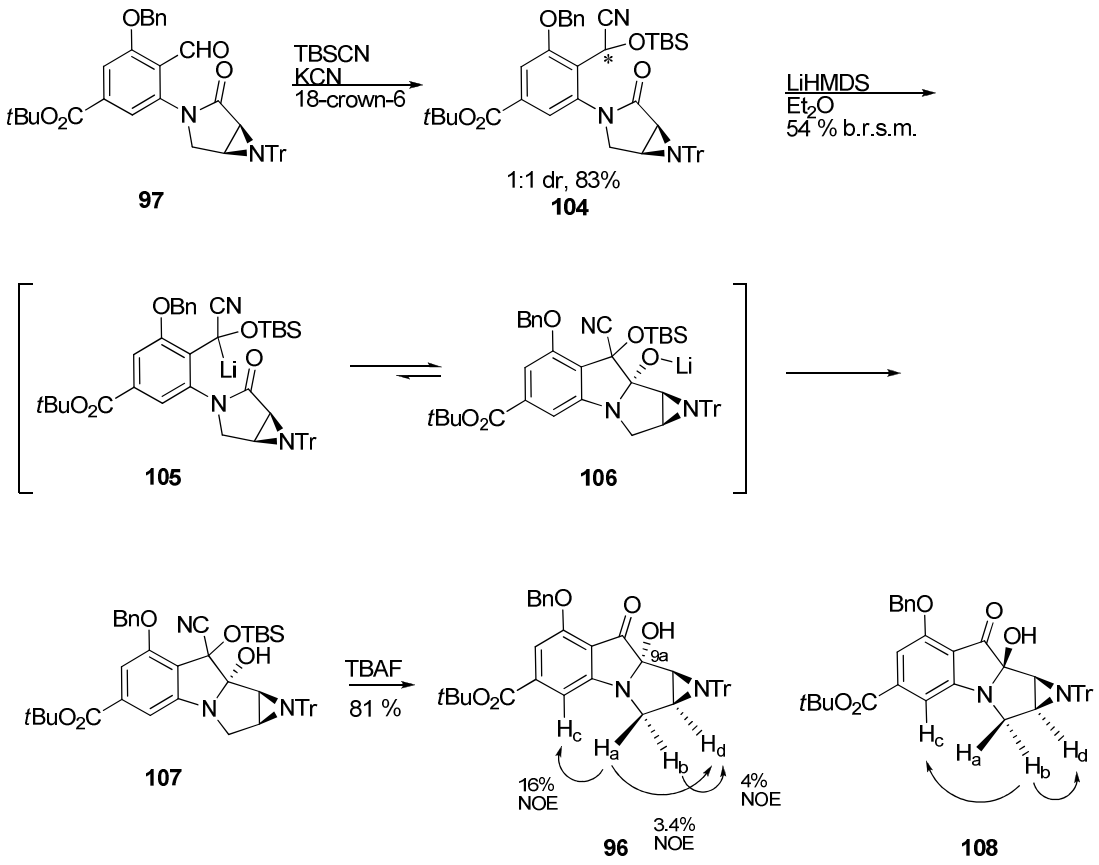

The results of the cyclization on the fully functionalized system are different than what was observed in the model study of silyl cycanohydrin **69**. As mentioned above, the cyclization of **104** required longer reaction time at higher temperatures in contrast to the model system. A decrease in reactivity of the anion of **104** due to the presence of the *para* electron withdrawing ester would account for the need of higher temperatures for cyclization. However, the electron donating *ortho* benzyloxy group, not present in **69**, would destabilize the anion **105** so that the equilibrium at 0 °C would favor the cyclized product **106**. Formation of larger quantities of cyclized product **107** than starting material **104** suggests that the equilibrium for the cyclization lies to the right at 0 °C (Scheme 3-20). Also, assuming that the diastereomers of **106** equilibrate via anion **105**, observation of only one diastereomer supports the conclusion that the equilibrium between **105** and **106** lies to the right. Furthermore, in contrast to the model, these results suggest that the *trans* diastereomer **107** is both the kinetic and thermodynamic product of the cyclization event of anion **105** at 0 °C.

Conclusions

After considerable effort, an appropriately functionalized analog of the mitosane **14a** has finally been obtained. The plan to construct the C(9)-C(9a) bond by anion addition to the appended lactam proved successful on both a model and a fully functionalized system using a deprotonated silyl cyanohydrin. However, construction of the tetracycle precursor took much effort and a critical evaluation of three distinct strategies. Fortunately, the powerful transition metal-catalyzed coupling of the key aziridinopyrrolidinone **19** with a pre-functionalized aryl halide or triflate allowed successful construction of the pivotal *N*-aziridinopyrrolidinone intermediate. Following this breakthough, the synthetic obstacles leading to the key tetracycle could ultimately be overcome, and the α-hydroxy ketone **96** could be synthesized stereoselectively in 9 steps (longest linear sequence) from the known mesylate **35**. Another notable observation made during the synthesis of these densely functionalized pyrrolo[1,2-a]indole derivatives was the difference in stability compared to the aziridinomitosene derivatives

of FK317. Mitosanes **88-93**, **107**, and **96** survived silica gel chromatography and storage in frozen benzene in contrast to their mitosene counterparts. The stability can be attributed to the absence of the indole functionality which activates the aziridine for facile ring opening.

It is worth noting that new chemistry involving the valuable chiral aziridine was developed during the synthetic endeavor towards **96**. Specific highlights include the formation of the azirdinolactam **19** using an unprecedented dianion trapping event. These intriguing conversions eventually enabled coupling of the sterically hindered chiral lactam aziridine **19** with a fully functionalized aryl triflate, resulting in a convergent and efficient synthesis of the tetracycle **96**. The stereochemistry of the fused ring system of **104** facilitates diastereoselective construction of the desired stereoisomer of the tetracycle during cyclization of a protected cyanohydrin anion. Particularly gratifying was the discovery that the stereoisomer needed for the synthetic probes **13a,b** corresponds to the more stable isomer formed from cyclization of the lithiated cyanohydrin ether. Studies toward completion of the target biosynthetic probes **13a** and **13b** can now proceed with a focus on installation of C(10) on **96**, global deprotection, and modifications of the probe as required for recognition by enzymes of the biosynthetic pathways of Mitomycin C and FR900482.

Experimental

General Methods. Solvents and reagents were purified as follows: diethyl ether and tetrahydrofuran (THF) were distilled from sodium/benzophenone or purified using an Anhydrous Engineering solvent purification system using columns packed with A-2 Alumina; dichloromethane (CH_2Cl_2) was distilled from P_2O_5 or purified using an Anydrous Engineering solvent purification system using columns packed with A-2 Alumina; CH_3CN was stirred over molecular sieves for 24 h, then distilled from P_2O_5; benzene, toluene, triethylamine, *i*-$PrEt_2N$, TMEDA, and DMPU were distilled from CaH_2; methanol was distilled over activated magnesium turnings, the purified reagents and solvents were used immediately or stored under nitrogen. Alkyl and aryllithiums were titrated using the procedure of Watson[76] before use. Unless otherwise noted, all chemicals were used as obtained from commercial sources and all reactions were performed under nitrogen atmosphere in glassware dried in an oven (140 °C) or flame dried and cooled under a stream of nitrogen. All reactions were stirred magnetically unless otherwise noted and liquid reagents were dispensed with all PP/PE plastic syringes or Hamilton Gastight microsyringes. Preparatory layer chromatography was performed using Whatman Partisil® K6F silica gel 60 Å 200 µm or 1000 µm plates. Flash chromatography was performed with 230-400 mesh silica gel 60.

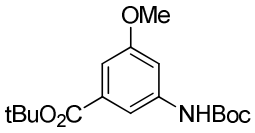

***tert*-Butyl 3-*(tert*-butoxycarbonylamino)-5-methoxybenzoate (24).** To a solution of *tert*-butyl 3-amino-5-methoxy benzoate[77] (0.93 mmol, 208 mg) in 9.3 mL THF was added Boc_2O (2.3 mmol, 502 mg) in one portion. The reaction flask was fitted with a reflux condenser and heated to 60 °C in an oil bath. After 2 d of stirring, the reaction was cooled to rt. The solution was partitioned between saturated aqueous $NaHCO_3$ and Et_2O and extracted 3 x with Et_2O, washed

with H_2O, and with brine. The organic phase was dried over $MgSO_4$ and concentrated to a white solid. The solid was crystallized from warm ethyl acetate and hexanes to produce 158 mg (53%) of **22** as white crystals, mp 149 °C; molecular ion calculated for $C_{17}H_{25}NNaO_5$ [M + Na] = 346.1630, found (electrospray) 346.1626, error = 1 ppm; IR (neat, cm^{-1}) 3337, 1707, 1697; 400 MHz ^1H NMR ($CDCl_3$, ppm) δ 7.44 (1H, br s) 7.32-7.28 (1H, m) 7.22- 7.18 (1H, m) 3.84 (3H, s) 1.58 (9H, s) 1.52 (9H, s); 100 MHz ^{13}C NMR ($CDCl_3$, ppm) δ 165.3, 160.2, 152.5, 129.5, 133.6, 111.7, 109.4, 108.4, 81.2, 80.8, 55.6, 28.3, 28.2.

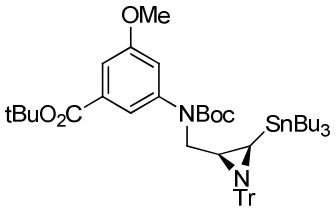

N-Boc aniline aziridine (25). To a solution of **24** (1.42, mmol, 460 mg) in 20 mL THF and 10 mL DMPU at -78 °C was added NaHMDS as a solution in THF (0.71 mL, 2.0 M, 1.42 mmol). The mixture was stirred at -78 °C for 5 min, then iodide **26** (0.47 mmol, 338 mg) in 3 mL THF was added via syringe, and the reaction turned light yellow. The solution was removed from the cooling bath and concentrated by half with a stream of N_2 while warming to rt. The flask was then fitted with a reflux condenser and heated to 60 °C. After 4 d, the reaction mixture was cooled to rt and acidified with pH 3 phosphate buffer. The mixture was extracted 3 x with Et_2O, washed with brine, and dried over $MgSO_4$. Removal of the solvent under rotary evaporation provided a cloudy yellow oil. The crude residue was purified by flash column chromatography (4 x 15 cm silica gel with 9:1 hexanes: ethyl acetate, Rf = 0.31) to provide 116 mg (21%) of **25** as a light yellow oil. Molecular ion calculated for [M + Na] $C_{51}H_{70}N_2NaO_5Sn$ = 933.4204, found (electrospray) 933.4238, error = 3 ppm; IR (neat, cm^{-1}) 1702; 400 MHz ^1H NMR ($CDCl_3$, ppm) δ 7.40-7.32 (7H, m), 7.19-7.10 (10 H, m) 6.49 (1H, t, *J* = 2.2 Hz) 4.00 (1H, dd, *J* = 14.0, 8.0 Hz) 3.70 (1H, dd, *J* = 14.0, 2.8 Hz) 1.55 (9H, s) 1.50-1.39 (15H, m) 1.32-1.19 (8H, m) 1.20-0.89 (7H,

m) 0.86 (9H, t, *J* = 7.2 Hz); 100 MHz ^{13}C NMR ($CDCl_3$, ppm) δ 165.1, 159.3, 154.1, 144.3, 142.6, 133.2, 129.5, 127.1, 126.4, 119.7, 117.7, 81.1, 80.6, 75.5, 55.5, 34.6, 29.3, 29.2, 28.5, 28.1, 27.3, 24.2, 13.7, 10.0.

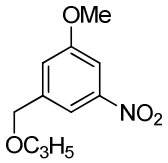

(3-Methoxy-5-nitrophenyl)allylmethylether (32). To a solution of starting alcohol **31**[78] (2.95 mmol, 541 mg) in 30 mL toluene was added Bu_4NI (0.15 mmol, 57 mg) and NaOH (5.9 mmol, 236 mg). Neat allylbromide (5.9 mmol, 0.51 mL) was added dropwise via syringe. The reaction vessel was fitted with a reflux condenser and heated to 90 °C. After 5 h, the non-homogenous orange mixture was cooled to rt and filtered through celite with Et_2O. The solvent was then removed under rotary evaporation. The crude reaction mixture was purified by flash column chromatography (3 x 16 cm silica gel, 9:1 hexanes: ethyl actate, Rf = 0.34). Fractions 14 – 20 provided 506 mg (77%) of product **32** as a clear colorless oil. Molecular ion calculated for $C_{11}H_{13}NO_2$, = 223.0845, found (EI) *m/z* = 223.0846, error = 0.4 ppm; 500 MHz ^{1}H NMR ($CDCl_3$, ppm) δ 7.81 (1H, d, *J* = 0.5 Hz) 7.64 (1H, t, *J* = 2.3 Hz) 7.24 (1H, d, *J* = 0.5 Hz) 6.0 – 5.9 (1H, m) 5.34 (1H, ddd, *J* = 17.1, 3.5, 1.3 Hz) 5.25 (1H, ddd, *J* = 10.4, 2.8, 1.3 Hz) 4.56 (2H, s) 4.08 (2H, ddd, *J* = 5.5, 1.5, 1.5 Hz) 3.89 (3H, s); 100 MHz ^{13}C NMR ($CDCl_3$, ppm) δ 164.2, 149.3, 141.6, 134.1, 119.7, 117.7, 114.6, 107.4, 71.7, 70.8, 55.9.

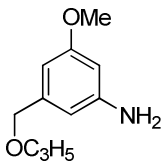

3-(Allyloxymethyl)-5-methoxyaniline (33). To a solution of nitro **32** (1.47 mmol, 328 mg) in 6 mL HOAc was added 1 equiv of Zn dust (8.82 mmol, 589 mg) every 10 min for 1 h. The non-

homogenous reaction was stirred vigorously for 2 h after which a saturated aqueous solution of $NaHCO_3$ was added to neutralize the solution. The mixture was poured into ethyl acetate and the aqueous phase was extracted 3 x with ethyl acetate. The organic phase was then washed 3 x with H_2O, with saturated $NaHCO_3$, with H_2O, and then with brine. Drying of the organic phase over Na_2SO_4 and rotary evaporation provided a cloudy orange oil. The crude reaction mixture was purified by flash column chromatography (3 x 16 cm silica gel with 1:1 hexanes: ethyl acetate, Rf = 0.13). Fractions 13-16 provided a clear yellow oil **33**. Molecular ion calculated for (M + H) $C_{11}H_{15}NO_2$ = 194.1181, found (electrospray) 194.1176, error = 2.6 ppm; IR (neat, cm^{-1}) 3457, 3359, 1597; 500 MHz ^{1}H NMR ($CDCl_3$, ppm) δ 6.31 (2H, dd, *J* = 7.5, 2.0 Hz) 6.16 (1H, t, *J* = 2.0 Hz) 6.0-5.9 (1H, m) 5.31 (1H, ddd, *J* = 17.4, 3.5, 1.5 Hz) 5.20 (1H, ddd, *J* = 10.4, 3.0, 1.5 Hz) 4.41 (2H, s) 4.01 (2H, ddd, *J* = 5.5, 1.5, 1.5 Hz) 3.76 (3H, s) 3.66 (1H, br s); 125 Hz ^{13}C NMR ($CDCl_3$, ppm) δ 160.9, 147.8, 140.8, 134.8, 117.1, 107.1, 100.3, 72.1, 71.1, 55.2.

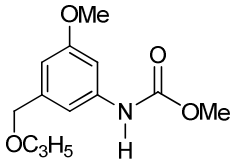

Methyl 3-(allyloxymethyl)-5-methoxyphenylcarbamate (34). To a solution of amine **33** (0.34 mmol, 66 mg) in 2.2 mL ethyl acetate (HPLC grade) and 1.1 mL H_2O was added solid $NaHCO_3$. The non-homogenous mixture was stirred vigorously and methyl chloroformate (0.37 mmol, 0.03 mL) was added via syringe. After 1.5 h, the solution was extracted 3 x with ethyl acetate, washed with brine, and dried over $MgSO_4$. Removal of the solvent under rotary evaporation provided 86 mg (100%) of pure **34** as a clear yellow oil. 3:1 hexanes: ethyl acetate (Rf = 0.29); Molecular ion [M + Na] calculated for $C_{13}H_{17}NO_4Na$ = 274.1055; found (electrospray) = 274.1053, error = 1 ppm; IR (neat, cm^{-1}) 3322, 1736, 1713, 1609; 500 MHz ^{1}H NMR ($CDCl_3$, ppm) δ 7.06 (1H, br s) 6.85 (1H, br s) 6.63 (1H, br t, *J* = 4.0 Hz) 6.59 (1H, br s) 5.95 (1H, m) 5.31 (1H, ddd, *J* = 17.3, 3.5, 1.5 Hz) 5.21 (1H, ddd, *J* = 10.3, 2.8, 1.5 Hz) 4.46 (2H, s) 4.02 (2H, ddd, *J* = 5.5, 1.5, 1.5 Hz)

3.81 (3H, s) 3.77 (3H, s); 100 MHz ^{13}C NMR ($CDCl_3$, ppm) δ 160.4, 153.9, 140.6, 139.0, 134.6, 117.2, 109.9, 108.2, 103.6, 71.8, 71.2, 55.3, 52.3.

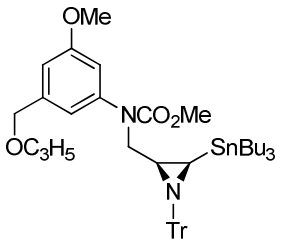

Methyl 3-(allyloxylmethyl)-5-methoxyphenyl((3-tributylstannyl)-1-tritylaziridin-2-yl) methyl) carbamate (36). To a solution of carbamate **34** (0.29 mmol, 73 mg) in 0.64 mL THF and 0.32 mL DMPU at -78 °C was added NaHMDS as a solution in THF (0.29 mL, 1.0 M, 0.29 mmol) and the reaction turned olive green. After 5 min, aziridine **35**[79] as a solution in THF (0.20 mL, 0.48 M, 0.95 mmol) was added via cannula. The reaction mixture was removed from the cooling bath and concentrated by half under N_2 while warming to rt. The reaction flask was then fitted with a reflux condenser and heated to 60 °C. After 2 d of heating, the reaction was cooled to rt, and 0.5 mL pH 3 phosphate buffer was added. The mixture was then poured into H_2O, extracted 3 x with Et_2O, washed with brine, and dried over $MgSO_4$. Rotary evaporation provided a cloudy orange oil. The crude reaction mixture was purified by flash column chromatography (2.5 x 15.2 cm silica gel with 5:1 hexanes: ethyl acetate with 2% NEt_3, Rf = 0.34). Fractions 19-40 provided 56 mg (70%) of **36**. Molecular ion calculated for [M + Na] $C_{47}H_{62}N_2NaO_4Sn$ = 861.3629, found (electrospray) *m/z* = 861.3655, error = 3 ppm; IR (neat, cm^{-1}) 1709; 500 MHz ^{1}H NMR ($CDCl_3$, ppm) δ 7.45 – 7.37 (6H, m) 7.20-7.12 (9H, m) 6.76 (1H, br s) 6.20 (1H, br s) 6.13 (1H, br s) 5.96- 5.86 (1H, m) 5.27 (1H, ddd, *J* = 17.3, 3, 1.5 Hz) 5.19 (1H, ddd, *J* = 10.4, 3.0, 1.0 Hz) 4.33 (2H, ABq, *J* = 12.3 Hz) 4.13(1H, m) 4.00-3.92 (2H, m) 3.77-3.58 (4H, s overlapping m) 1.56 -1.40 (6H, m) 1.34 – 1.20 (7H, m) 1.10 – 0.92 (6H, m) 0.87 (9H, t, *J* = 7.3 Hz) 0.75 (1H, d, *J* = 7.5 Hz); 100 MHz ^{13}C NMR ($CDCl_3$, ppm) δ 159.9, 155.7, 144.3, 141.7, 140.2, 134.7, 129.6,

127.1, 126.4, 118.5, 117.1, 112.1, 111.0, 75.6, 71.6, 71.1, 55.4, 53.2, 52.9, 29.2, 27.3, 24.4, 13.7, 10.0.

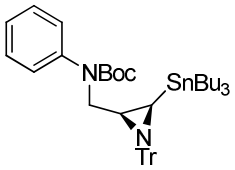

***tert*-Butyl phenyl((3-tributylstannyl)-1-tritylaziridin-2-yl)methyl)carbamate (43)**. To a solution of carbamate **42**[80] (1.26, 243 mg) in 2.8 mL THF and 1.4 mL DMPU at 78 °C was added NaHMDS as a solution in THF (1.4 mL, 0.97 M, 1.38 mmol). After 5 min of stirring, aziridine **35**[79] as a solution in THF (0.42 mL, 1.0 M, 0.42 mmol) was added via syringe. The reaction flask was removed from the cooling bath, warmed to rt, and concentrated by half under a stream of N_2. After concentration, the flask was fitted with a reflux condenser and heated to 60 °C. After 3 d, the reaction was cooled to rt and acidified with pH 3 phosphate buffer. The mixture was poured into H_2O, extracted 3 x with ethyl acetate, washed with brine, and dried over $MgSO_4$. Removal of the solvent under rotary evaporation provided a thick yellow oil. Purification by flash column chromatography (3 x 15 cm silica gel, 9:1 hexanes: ethyl acetate with 2% NEt_3, Rf = 0.42) provided 117 mg (36%) of **43** as an oil. Molecular ion calculated for (M + H) $C_{45}H_{60}N_2O_2Sn$ = 781.3755, found (electrospray) 781.3763, error = 1 ppm; IR (neat, cm^{-1}) 1698; 400 MHz ^1H NMR ($CDCl_3$, ppm) 7.35-7.32 (6H, m) 7.19-7.09 (12H, m) 6.78-6.73 (2H, m) 4.00 (1H, dd, *J* = 14.0, 8.0 Hz) 3.70 (1H, dd, *J* = 14.0, 2.8 Hz) 1.52-1.40 (7H, m) 1.32-1.22 (6H, m) 1.40-0.88 (6H, m) 0.88 (9H, t, *J* = 7.2 Hz) 0.79 (1H, d, *J* = 7.2H); 100 MHz ^{13}C ($CDCl_3$, ppm) δ 154.3, 144.3, 141.4, 129.6, 127.4, 127.1, 126.8, 126.3, 125.4, 80.2, 75.5, 52.5, 34.2, 29.2, 28.5, 27.3, 24.4, 13.7, 9.9.

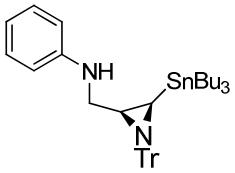

***N*-((3-tributylstannyl)-1-tritylaziridin-2-yl)methyl)aniline 44**. Carbamate **43** was heated neat with stirring to 180 °C in a sand bath. The sand bath temperature was maintained near 180 °C, but peaked at 190 °C. After 25 min of heating and stirring, the brown residue was cooled to rt. Purification by preparatory plate TLC on silica gel 60 Å (20 cm x 20 cm x 1000 µm) pretreated with NEt_3 fumes in 9 x 1 hexanes: ethyl acetate (Rf = 0.60) provided 46 mg (71%) of **44**. Molecular ion calculated for [M + Na] $C_{40}H_{52}N_2Sn$ = 681.3231, found (electrospray) 681.3248, error = 2.5 ppm; IR (neat, cm^{-1}) 3381; 500 MHz ^{1}H NMR ($CDCl_3$, ppm) δ 7.50-7.42 (5H, m) 7.28-7.10 (12H, m) 6.73 (1H, m) 6.50 (2H, dd, *J* = 8.5, 1.0) 3.91 (1H, dd, *J* = 5.5, 5.7 Hz) 3.29 (1H, ddd, *J* = 11.5, 5.5, 4.0 Hz) 3.15 (1H, ddd, *J* = 11.5, 5.7, 5.4) 1.57 (1H, ddd, *J* = 6.5, 5.4, 4.0) 1.50-1.32 (6H, m) 1.30-1.21 (6H, m) 1.10-0.88 (7H, m) 0.84 (9H, *J* = 7.3 Hz); 100 MHz ^{13}C NMR ($CDCl_3$, ppm) δ 148.2, 144.4, 129.6, 129.1, 128.3, 127.4, 126.6, 117.5, 113.2, 75.6, 46.9, 34.9, 29.2, 27.4, 24.7, 13.7, 10.2. Signal at 126.3 ppm due to trace contamination of sample with aziridine **43**.

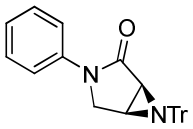

(*1S,5S*)3-phenyl-6-trityl-3,6-diazabicyclo[3.1.0]hexan-2-one (46). To a solution of **44** (0.026 mmol, 18 mg) in 0.52 mL THF at -78 °C was added *n*-BuLi as a solution in hexanes (19 µL, 1.56 M, 0.29 mmol). The reaction turned light orange and then faded to pale yellow. After 10 min of stirring in the cold bath, MeLi as a solution in Et_2O (32 µL, 0.794 M, 0.26 mmol) was added via microsyringe. The solution became light pink. The solution was warmed in a dry ice chloroform bath for 8 min, and the color faded to yellow within 5 min. Then the solution was cooled to -78

°C and diethylcarbonate (0.26 mmol, 0.03 mL) was added via syringe. The reaction flask was removed from the cooling bath and warmed to rt. After 1 h, the mixture was acidified with 0.6 mL saturated aqueous NH_4Cl and poured into H_2O. Extraction of the mixture 3 x with Et_2O, washing with brine, drying over $MgSO_4$, and removal of the solvent provided a yellow oily solid. Purification by preparatory plate TLC on silica gel 60 Å (20 cm x 20 cm x 1000 µm, 3:1 hexanes: ethyl acetate) provided 5 mg (46%) of **46**. Molecular ion calculated for [M + Na] C29H24N2NaO = 439.1786, found (electrospray) 439.1765, error = 5 ppm; IR (neat, cm^{-1}) 1702; 400 MHz ^1H NMR ($CDCl_3$, ppm) δ 7.7-7.66 (2H, m) 7.54-7.48 (6H, m) 7.42-7.37 (2H, m) 7.34-7.22 (9H, m) 7.20-7.14 (1H, m) 4.11 (1H, dd, *J* = 10.5, 1.0 Hz) 3.86 (1H, dd, *J* = 10.5, 4.0 Hz) 2.55 (1H, dd, *J* = 4.8, 4.0 Hz) 2.51 (1H, dd, *J* = 4.8, 0.8 Hz); 100 MHz ^{13}C NMR ($CDCl_3$, ppm) δ 171.3, 143.8, 139.5, 129.1, 128.9, 127.9, 127.2, 124.6, 119.8, 73.8, 50.6, 39.7, 31.8.

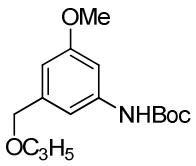

***tert*-Butyl 3-allyloxymethyl-5-methoxyphenylcarbamate (48).** To a solution of amine **33** (0.70 mmol, 135 mg) in 7 mL THF was added Boc_2O (1.75 mmol, 394 mg) in one portion. The reaction vessel was fitted with a reflux condenser and heated to 60 °C. After 18 h, the solution was cooled to rt and poured into H_2O. The mixture was washed 3 x with Et_2O, washed with brine, and dried over $MgSO_4$. Rotary evaporation provided a pale yellow oil. Purification of the crude reaction mixture by flash column chromatography (2 x 15 cm silica gel, 3:1 hexanes: ethyl acetate, Rf = 0.33) provided 163 mg (80%) of product **48** in fractions 9-13. Molecular ion calculated for [M + Na] $C_{16}H_{23}NNaNO_4$ = 316.1525, found (electrospray) *m/z* = 316.1512, error = 4 ppm; IR (neat, cm^{-1}) 3322, 1726, 1702, 1604; 500 MHz ^1H NMR ($CDCl_3$, ppm) δ 7.00 (1H, br s) 6.86 (1H, br s) 6.60 (1H, br s) 6.50 (1H, br s) 6.0 – 5.9 (1H, m) 5.30 (1H, ddd, *J* = 17.4, 3, 1.3 Hz) 5.20 (1H, ddd, *J* = 9.8, 2.7, 1.3 Hz) 4.45 (2H, s) 4.01 (2H, ddd, *J* = 6.0, 1.2, 1.0 Hz) 3.79

(3H, s) 1.51 (9H, s); 100 MHz ^{13}C NMR ($CDCl_3$, ppm) δ 160.3, 152.5, 140.4, 129.5, 134.6, 117.1, 109.8, 107.8, 103.3, 80.5, 71.8, 71.1, 55.3, 28.3.

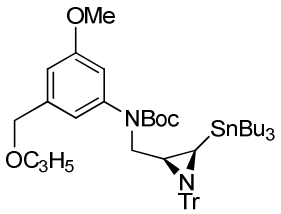

***tert*-Butyl 3-(allyloxymethyl)-5-methoxyphenyl((3-tributylstannyl)-1-tritylaziridin-2-yl) methyl)carbamate (49)**. To a solution of aniline **46** (0.78 mmol, 229 mg) in 1.7 mL THF and 0.87 mL DMPU at -78 °C was added sodium hexamethyldisilylazide as a solution in THF (0.88 mL, 0.89 mmol) via syringe. The solution turned dark yellow. After 5 min of stirring, aziridine **35**[79] (0.26 mmol, 185 mg) was added as a solution in 0.60 mL THF dropwise via cannula, and the yellow solution turned green. The reaction vessel was removed from the cooling bath and warmed to rt while concentrating by half under a stream of N_2. After reaching rt, the reaction vessel was fitted with a reflux condenser and heated to 60 °C. Over the heating period, 1 mL of THF was added to maintain solvent volume. After 4 d of heating, the reaction was cooled to rt and acidified with pH 3 phosphate buffer. The mixture was partitioned between H_2O and ethyl acetate, and extracted 3 x with ethyl acetate. The combined organic phases were washed with brine, dried over Na_2SO_4, and concentrated under reduced pressure to an orange/brown oil. Purification of the crude residue by flash column chromatography (3 x 15 cm silica gel with 9:1 hexanes: ethyl acetate with 2% NEt_3, Rf = 0.37) provided 150 mg of **49**. Molecular ion calculated for [M + N] $C_{50}H_{68}N_2NaO_4Sn$ = 903.4099, found (electrospray) 903.4119, error = 2 ppm; IR (neat, cm^{-1}) 1695, 1594; 500 MHz ^{1}H NMR ($CDCl_3$, ppm) δ 7.37-7.36 (5H, d, *J* = 7.0 Hz) 7.18-7.12 (9H, m) 6.72 (1H, s) 6.29 (1H, s) 6.26 (1H, s) 5.96-5.86 (1H, m) 5.25 (1H, ddd, *J* = 17.3, 3, 1.5 Hz) 5.17 (1H, ddd, *J* = 10.4, 3, 1.0) 4.32 (2H, ABq, *J* = 12.5 Hz) 3.99 (1H, dd, *J* = 14.3, 8.0 Hz) 3.97-3.89 (2H, m) 3.67 (1H, dd, *J* = 14.3, 2.5 Hz) 3.62 (3H, s) 1.52-1.38 (15H, m)

1.32-1.22 (9H, m) 1.06-0.90 (6H, m) 0.86 (9H, t, *J* = 7.3 Hz) 0.79 (1H, d, *J* = 7.0 Hz); 125 MHz ^{13}C NMR ($CDCl_3$, ppm) δ 159.7, 154.2, 144.4, 142.4, 139.8, 134.7, 129.6, 127.1, 126.4, 118.2, 117.0, 111.8, 110.5, 75.5, 71.6, 71.0, 55.3, 52.6, 34.1, 29.7, 29.3, 29.2, 28.6, 27.6, 27.4, 24.2, 13.7, 10.0, minor unknown impurity peaks at 80.3 and 1.0.

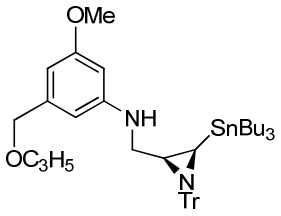

3-(Allyloxymethyl)-5-methoxy-*N*-((3-(tributylstannyl)-1-tritylaziridin-2-yl)methylaniline (50). Aniline **49** (0.14 mmol) was heated neat in a sand bath to ~ 190 °C under a flow of N_2. After 30 min, the brown residue was cooled to rt. Purification of the residue by preparatory plate TLC (200 x 200 x 1000, 9:1 hexanes: ethyl acetate, Rf = 0.29) provided 75 mg (69%) of **50**. Molecular ion calculated for [M + Na] $C_{45}H_{50}N_2NaO_2Sn$ = 803.3574, found (electrospray) 803.3610, error = 4.5 ppm; IR (neat, cm^{-1}) 3374; 400 MHz ^{1}H NMR ($CDCl_3$, ppm) δ 7.49-7.43 (6H, m) 7.30-7.18 (9H, m) 6.29 (1H, d, *J* = 1.2 Hz) 6.11 (1H, s,) 6.00-5.90 (2H, m) 5.30 (1H, ddd, *J* = 21.5, 4.5, 2.0 Hz) 5.20 (1H, ddd, *J* = 13, 3.3, 1.5 Hz) 4.41 (2H, s) 4.02-3.99 (2H, m) 3.94 (1H, dd, *J* = 4.8, 4.8 Hz) 3.76 (3H, s) 3.27 (1H, ddd, *J* = 11.6, 4.8, 4.0 Hz) 3.15 (1H, ddd, *J* = 11.6, 5.6, 4.8 Hz) 1.59-1.20 (13H, m) 1.12-0.80 (16H, m); 100 MHz ^{13}C NMR ($CDCl_3$, ppm) δ 160.9, 149.5, 144.4, 140.5, 134.9, 129.6, 127.4, 126.7, 117.0, 105.6, 102.1, 98.3, 75.6, 72.3, 71.0, 55.1, 46.8, 34.9, 29.2, 27.4, 24.7, 13.7, 10.2.

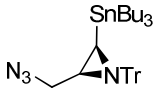

52

(*2S,3S*)-2-(Azidomethyl)-3-(tributylstannyl)-1-tritylaziridine (52). To a solution of mesylate **35**[79] (0.72 mmol, 493 mg) in 7.2 mL DMF was added NaN_3 (2.16 mmol, 140.4 mg). The reaction flask was fitted with a reflux condenser and the non-homogenous solution was heated to 60 °C. After 25 h, the temperature was increased to 85 °C. After 2 d total reaction time, the reaction was cooled to rt and poured into H_2O. The mixture was extracted 3 x with Et_2O, washed with brine, and dried over $MgSO_4$. Rotary evaporation provided a yellow oil. The crude reaction mixture was purified by flash column chromatography (3.5 x 15.24 cm, 15:1 hexanes: ethyl acetate with 2% NEt_3, Rf = 0.66 in 3:1 hexanes: ethyl acetate) and provided 408 mg (90%) of **52**. Molecular ion calculated for [M + Na] $C_{34}H_{46}N_4NaSn$ = 631.2823, found (electrospray) *m/z* = 631.2834, error = 2 ppm; IR (neat, cm^{-1}) 2095; 400 MHz ^{1}H NMR ($CDCl_3$, ppm) δ 7.48-7.46 (6H, m) 7.29-7.17 (9H, m) 3.51 (1H, dd, *J* = 15.9, 6.9 Hz) 3.37 (1H, dd, *J* = 15.9, 6.9) 1.50-1.36 (7H, m) 1.32-1.22 (6H, m) 1.02-0.90 (7H, m) 0.86 (9H, t, *J* = 9 Hz); 100 MHz ^{13}C NMR ($CDCl_3$, ppm) δ 144.2, 129.5, 127.3, 126.6, 75.5, 55.0, 34.6, 29.1, 27.4, 25.1, 13.7, 10.1.

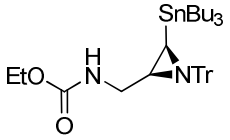

ethyl ((*2S,3S*)-3-(tributylstannyl)-1-tritylaziridin-2-yl)methylcarbamate (54). To a mixture of $LiAlH_4$ (11.2 mmol, 449 mg) in 24 mL Et_2O at 0 °C was added aziridine **51** as a solution in 29 mL Et_2O (5.3 mmol, 3.34 mg) dropwise via cannula. The reaction was stirred and warmed to rt in the cooling bath. After 2.5 h, the reaction vessel was cooled in an ice water bath, and the mixture was slowly quenched by sequential addition of 0.45 mL H_2O, 0.45 mL 15% NaOH, 1.35 mL H_2O. After stirring the mixture vigorously, the white precipitate was filtered through celite

with Et_2O. Solvent removal under reduced pressure provided **53** as a colorless oil. Due to significant loss of material during chromatrography, the material was taken into the next transformation without purification. A small sample of the material was purified by flash column chromatography (2 x 15 cm silica gel with 3:1 hexanes:ethyl acetate, 2% NEt_3, Rf = 0.67) to provide clean **53**. Molecular ion calculate for [M + Na] $C_{34}H_{48}N_2NaSn$ = 605.2918, found (electrospray) 605.2921, error = 0.5 ppm; IR (neat, cm^{-1}) 3390; 500 MHz ^{1}H NMR ($CDCl_3$, ppm) δ 7.50-7.48 (6H, m) 7.30-7.22 (6H, m) 7.22-7.16 (3H, m) 2.82 (2H, m) 1.52-1.38 (6H, m) 1.34-1.22 (10H, m) 1.02-0.82 (16H, m) unidentified peaks at ; 125 MHz ^{13}C NMR ($CDCl_3$, ppm) δ 144.6, 129.6, 127.3, 126.5, 75.4, 46.0, 38.7, 29.2, 27.4, 24.7, 13.7, 10.3.

To a solution of amine **53** (5.3 mmol) and 1.10 mL NEt_3 in 50 mL CH_2Cl_2 at 0 °C was added ethyl chloroformate (6.4 mmol, 0.64 mL) via syringe. The reaction flask was removed from of the cooling bath and warmed to rt. After 2.5 h, the reaction was cooled in a 0 °C ice bath, and saturated aqueous $NaHCO_3$ was added. The mixture was poured into H_2O and extracted 3 x with CH_2Cl_2, washed with brine, and dried over Na_2SO_4. Rotary evaporation provided a cloudy colorless oil. Purification of the crude reaction mixture by flash column chromatography (7 x 15 cm silica gel with 9:1 hexanes: ethyl acetate, Rf = 0.35) provided 2.41 g (92% over two steps) of **54**. Molecular ion calculated for [M + Na] $C_{37}H_{52}N_2NaO_2Sn$ = 699.2948, found (electrospray) *m/z* = 699.2976, error = 4 ppm; IR (neat, cm^{-1}) 3419, 1721; 400 MHz ^{1}H NMR ($CDCl_3$, ppm) δ 7.46-7.44 (6H, m) 7.28-7.24 (6H, m) 7.22-7.18 (3H, m) 4.72 (1H, br s) 4.14-4.02 (2H, m) 3.34 (1H, d, *J* = 2.5 Hz) 1.52-1.36 (7H, m) 1.31-1.18 (8H, m) 1.02-0.9 (6H, m) 0.86 (9H, t, *J* = 7.3 Hz); 100 MHz ^{13}C NMR ($CDCl_3$, ppm) δ 156.4, 144.3, 129.5, 127.4, 126.7, 75.5, 60.8, 44.5, 35.0, 29.2, 27.4, 24.6, 14.6, 13.7, 10.0; sample contaminated with benzene (128.3).

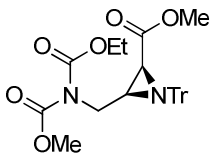

Imide 56. An oven dried flask cooled under N_2 flow was charged with a solution of amide **54** in toluene. The toluene was removed under a flow of N_2, and the reaction vessel was fitted with a thermocouple. To a solution of amide **54** (0.20 mmol, 134.4 mg) in 4 mL THF at -77 °C (internal) was added *n*-BuLi as a solution in hexanes (0.63 M, 0.35 mL, 0.22 mmol) dropwise via syringe (temperature < -75 °C). The reaction color turned bright yellow over ten minutes. A solution of MeLi in diethyl ether (0.83 M, 0.24 mL, 0.20 mmol) was added dropwise via syringe (temperature > -75 °C), and the yellow color darkened. The solution was warmed to -67 °C and stirred for 10 min, then cooled to -77 °C. To the solution was added Mander's reagent (1.0 mmol, 0.08 mL) dropwise via syringe, and the temperature spiked to -70 °C. After stirring the reaction in the cold bath for 1 h, the solution was quenched at low temperature with MeOH. After warming to rt, the mixture was poured into H_2O and extracted 3 x with Et_2O. The combined organic phases were washed with brine and dried over $MgSO_4$. Removal of the solvent under reduced pressure provided a cloudy yellow oil. Purification of the residue by preparatory plate TLC (200 x 200 x 10000, with 1:1 hexanes: ethyl acetate, Rf = 0.66) provided 57 mg (57%) of imide **56**. Molecular ion calculated for [M + Na] $C_{29}H_{30}N_2NaO_6$ = 525.2002, found (electrospray) 525.2014, error = 2.3ppm; IR (neat, cm^{-1}) 1794, 1748; 400 MHz ^{1}H NMR ($CDCl_3$, ppm) 7.52-7.47 (6H, m) 7.20-7.19 (9H, m) 4.27 (1H, dd, *J* = 14.7, 2.4) 4.17-4.09 (2H, m) 3.97 (1H, dd, *J* = 14.7, 7.8 Hz) 3.80 (3H, s) 3.76 (unidentified peak, 0.4H) 3.69 (3H, s) 1.94 (1H, d, *J* = 6.0 Hz) 1.78 (1H, ddd, *J* = 7.8, 6.0, 2.4 Hz) 1.52 (3H, t, *J* = 7.2 Hz); 100 MHz ^{13}C NMR ($CDCl_3$, ppm) δ 170.1, 153.9, 153.1, 143.4, 129.3, 127.7, 127.0, 75.1, 63.1, 53.7, 52.0, 44.1, 38.8, 36.0, 14.0.

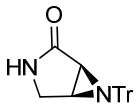

(*1S,5S*)-6-Trityl-3,6-diazabicyclo[3.1.0]hexan-2-one (19). An oven dried 3-neck flask was fitted with a mechanical stirrer and thermocouple. The flask was cooled under N_2, then charged with **54** (3.6 mmol, 2.4 g) and 70 mL THF, and the solution was cooled to -76.8 °C. To the solution was added n-BuLi as a solution in hexanes (1.46 M, 3.65 mmol, 2.5 mL) dropwise via syringe maintaining the internal temperature below -75.5 °C. The dark yellow solution stirred for 20 min, then a second equivalent of n-BuLi in hexanes (1.46 M, 3.80 mmol, 2.6 mL) was added slowly to maintain the internal temperature below -75 °C. The yellow color darkened to red upon addition. The temperature of the red dianion was maintained at -76 °C for 30 min, and then neat $CO(OEt)_2$ (10.8 mmol, 1.3 mL) was added dropwise via syringe. Slow addition of the electrophile was essential to maintain the temperature below -75 °C. After the first few drops the red color began to fade to yellow. The reaction vessel was pulled to the top of the cooling bath and slowly warmed to 19 °C over 4.5 h. The solution was poured into H_2O and extracted 3 x with Et_20, the combined organics were washed with brine, and then dried over $MgSO_4$. Removal of the solvent under rotary evaporation provided a white amorphous solid consisting of **19**, and protiodestannylated material. The highly insoluble material was loaded onto a silica gel plug (5.5 x 5 cm silica gel) eluted with 500 mL 2:1 hexanes: ethyl acetate, and then the solid at the top of the plug was dissolved with $CHCl_3$ and eluted with 500 mL 100% ethyl acetate to provide 804 mg (65%) of **19** (1:2 hexanes: ethyl acetate, Rf = 0.30); mp = decomposition 262 °C; Molecular ion calculated for [M + Na] $C_{23}H_{20}N_2NaO$ = 363.1473, found (electrospray) 363.1483, error = 2.8 ppm; IR (neat, cm^{-1}) 3225, 1701; 500 MHz ^1H NMR ($CDCl_3$, ppm) δ 7.50-7.46 (5H, m) 7.32-7.22 (10H, m) 5.21 (1H, br s) 3.72 (1H, d, *J* = 10.5 Hz) 3.38 (1H, dd, *J* = 10.5, 4.0 Hz) 2.52 (1H, ddd, *J* = 4.5, 4.0, 1.5) 2.25 (1H, ddd, *J* = 4.5, 1.5, 1.0 Hz); 125 MHz ^{13}C NMR ($CDCl_3$, ppm) δ 175.5, 144.0, 129.2, 127.8, 127.1, 73.8, 44.7, 37.5, 34.2.

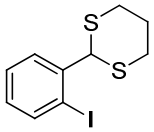

2-(2-Iodophenyl)-3,6-dithiane (65). To a solution of 2-iodobenzaldehyde (commercially available) **61** (1.23 mmol, 286 mg) in 12 mL CH_2Cl_2 was added 1,3-propanedithiol (1.19 mmol, 0.12 mL). Neat BF_3•Et_2O (0.23 mmol, 0.03 mL) was added via syringe, and the reaction turned cloudy. The reaction solution was stirred at rt for 18 h, then aqueous saturated $NaHCO_3$ was added. The mixture was extracted 3 x with CH_2Cl_2, the combined organic phase was washed with brine, and then dried over Na_2SO_4. Removal of the solvent under rotary evaporation provided an off-white solid consisting of 326 mg (82%) of **65 (**9:1 hexanes: ethyl acetate, Rf = 0.38) and 22 mg of **61** Molecular ion calculated for $C_{10}H_{11}IS_2$ = 321.9347, found (EI) 321.9352, error = 1.6 ppm; 500 MHz ^{1}H NMR ($CDCl_3$, ppm) δ 7.82 (1H, dd, *J* = 8.0, 1.5 Hz) 7.65 (1H, dd, *J* = 7.8, 1.7 Hz) 7.36 (1H, td, *J* = 14.0, 3.7 Hz) 6.98 (1H, td, *J* = 13.5, 3.9 Hz) 5.42 (1H, s) 3.14 (2H, m) 2.95 (1H, m) 2.92 (1H, m) 2.23-2.15 (1H, m) 2.00-1.88 (1H, m); 125 MHz ^{13}C NMR ($CDCl_3$, ppm) δ 141.5, 139.6, 130.0, 129.1, 129.0, 99.5, 56.7, 32.4, 25.1.

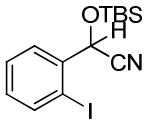

2-(*tert*-Butyldimethylsilyloxy)-2-(2-iodopheny)acetonitrile (66). To a solution of 2-iodobenzaldehyde (commercially available) (3.1 mmol, 708 mg) and ZnI_2 (0.09 mmol, 29 mg) in 31 mL CH_2Cl_2 at rt was added tetrabutylammonium cyanide (3.7 mmol, 522 mg) in one portion. After 5.5 h, the reaction mixture was filtered through celite with CH_2Cl_2, and the solvent was removed under rotary evaporation to provide a dark yellow oil. The crude residue was purified by flash column chromatography (4 x 15 cm silica gel with 15:1 hexanes: ethyl acetate, Rf = 0.44 9:1 hexanes: ethyl acetate) to provide 1.03 g (89%) of cyanohydrin **66**. Molecular ion calculated for [M + Na + MeOH] $C_{15}H_{24}INNaO_2Si$ = 428.0519, found (electrospray) 428.0520, error = 0.2

ppm; IR 1934; 400 MHz ^{1}H NMR ($CDCl_3$, ppm) δ 7.85 (1H, dd, *J* = 7.6, 1.2 Hz) 7.69 (1H, dd, *J* = 7.6, 1.6 Hz) 7.45 (1H, td, *J* = 14.0, 3.8 Hz) 7.10 (1H, td, *J* = 13.6, 3.8 Hz) 5.64 (1H, s) 0.94 (9H, s) 0.26 (3H, s) 0.17 (3H, s); 100 MHz ^{13}C NMR ($CDCl_3$, ppm) δ 139.6, 138.7, 131.0, 129.0, 128.2, 118.4, 96.2, 68.5, 25.6, 18.2, -5.1.

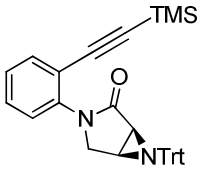

(*1S,5S*)-3-(2-(Trimethylsilylethynyl)phenyl)-6-trityl-3,6-diazabicyclo[3.1.0]hexan-2-one (67). To a mixture of pyrrolidinone **19** (0.14 mmol, 48 mg), K_3PO_4 (0.29 mmol, 62 mg), and CuI (0.03 mmol, 5 mg) in 1.2 mL toluene under an atmosphere of N_2 was added *N*,*N*′-dimethylcyclohexane diamine (0.06 mmol, 10 μL) via microsyringe following the procedure of Klapars.[81] The iodide **64** (0.09 mmol, 26 mg) as a solution in 0.6 mL toluene was added to the mixture via cannula. The mixture was then heated to 100 °C. After 26 h, the gray mixture was cooled to rt, filtered through silica gel with ethyl acetate and the solution was concentrated to a dark tan oil. Purification of the crude residue by preparatory plate chromatography (200 x 200 x 1000, 3:1 hexane: ethyl acetate, Rf = 0.41) provided 22 mg (48%) of **67** as a clear colorless oil. Molecular ion calculated for [M + Na] $C_{34}H_{32}N_2NaOSi$ = 535.2182, found (electrospray) 535.2194; IR (neat, cm^{-1}) 2242, 2149, 1705; 400 MHz ^{1}H NMR ($CDCl_3$, ppm) δ 7.56-7.51 (7H, m) 7.44-7.40 (2H, m) 7.34-7.22 (10H, m) 4.22 (1H, dd, *J* = 10.8 4.0) 3.91 (1H, d, *J* = 10.8) 2.55 (1H, dd, *J* = 4.8, 4.0) 2.47 (1H, d, *J* = 4.8 Hz) 0.134 (9H, s); 100 MHz ^{13}C NMR ($CDCl_3$, ppm) 172.1, 143.0, 140.2, 134.1, 129.6, 129.2, 127.9, 127.8, 127.3, 127.1, 121.1, 101.9, 100.1, 73.8, 51.9, 38.6, 32.8, -0.18.

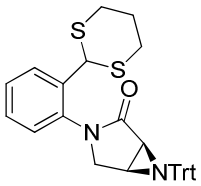

(*1S,5S*)-3-(2-Dithianylphenyl)-6-trityl-3,6-diazabicyclo[3.1.0]hexan-2-one (68). To a mixture of iodide **65** (0.23 mmol, 74 mL), lactam **19** (0.27 mmol, 88 mg), K_3PO_4 (0.46 mmol, 98 mg), and CuI (0.07 mmol, 13 mg) in 2.3 mL degassed toluene under an N_2 atmosphere was added *N*,*N*′-dimethylcyclohexane diamine (0.14 mmol, 23 µL) via microsyringe. The mixture was heated to 110 °C. After 20 h, the grey mixture was cooled to rt, filtered through silica gel with ethyl acetate, and concentrated. The residue was purified by flash column chromatography (2 x 15 cm silica gel with 2:1 hexanes:ethyl acetate) to provide 75 mg (61%) of dithiane **68** contaminated with 3.6 mg of aldehyde corresponding to acid catalyzed hydrolysis of the dithiane. Pure samples of **68** can be obtained by purification on NEt_3 deactivated silica gel (2:1 hexanes: ethyl acetate, 2% NEt_3, Rf = 0.19). Molecular ion calculated for [M+Na] $C_{33}H_{30}N_2NaS_2$ = 557.1697, found (electrospray) 557.1705, error = 1.4 ppm; IR (neat, cm^{-1}) 3056, 1704; 500 MHz ^{1}H NMR ($CDCl_3$, 45 °C, ppm) δ 7.80 (1H, dd, *J* = 7.5, 1.5 Hz) 7.58 (6H, m) 7.40-7.30 (8H, m) 7.28-7.22 (4H, m) 7.15 (1H, d, *J* = 8.0) 5.70 (1H, br s) 4.14 (1H, d, *J* = 11.0 Hz) 3.74 (1H, dd, *J* = 11.0, 4.5 Hz) 3.04-2.93 (2H, m) 2.83 (1H, m) 2.72 (1H, m) 2.61 (1H, dd, *J* = 4.5, 4.5 Hz) 2.53 (1H, d, *J* = 4.5 Hz) 1.98-1.82 (2H, m) NMR sample heated to resolve broad peaks; 100 MHz ^{13}C NMR ($CDCl_3$, 35 °C, ppm) δ 171.8, 144.1, 137.6, 135.4, 129.9, 129.4, 129.3, 129.2, 128.7, 127.9, 127.3, 73.8, 53.8, 45.4, 38.6, 32.9, 32.4, 32.0, 25.1.

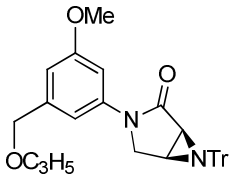

3,6-Diazabicyclo[3.1.0]hexan-2-one (37). To a mixture of pyrrolidinone **19** (0.038 mmol, 13.1 mg), K_3PO_4 (0.64 mmol, 13.6 mg), and CuI (0.01 mmol, 1.9 mg) in 0.60 mL toluene under an atmosphere of N_2 was added *N*, *N*′-dimethylcyclohexane diamine (0.02 mmol, 3 µL) via microsyringe according to the method of Klapars.[81] The iodide **70** was added as a solution in toluene (0.31 M, 0.32 mmol, 0.10 mL). The reaction mixture was heated to 100 °C, and the reaction turned a grayish/purple color. During the reaction course, lost solvent was replaced with 0.50 mL toluene, and after 48 h of heating and stirring, the reaction was cooled to rt and filtered through silica gel with ethyl acetate. The crude mixture was purified by preparatory plate TLC on silica gel 60 Å (20 cm x 20 cm x 1000 µm) with 1:1 hexanes: ethyl acetate (Rf = 0.61) to provide 12 mg (73%) of lactam **37**. Molecular ion calculated for [M + Na] $C_{34}H_{32}N_2NaO_3$ = 539.2311, found (electrospray) 539.2313, error = 0.4 ppm; IR (neat, cm^{-1}) 1705; 400 MHz ^{1}H NMR ($CDCl_3$, ppm) δ 7.50 (6H, d, *J* = 7.6 Hz) 7.34-7.22 (10H, m) 7.18 (1H, m) 6.74 (1H, m) 5.98 (1H, m) 5.33 (1H, ddd, *J* = 21.5, 4.0, 2.0 Hz) 5.23 (1H, ddd, *J* = 13.0, 3.5, 1.5 Hz) 4.53 (2H, s) 4.10 (1H, d, *J* = 10.8 Hz) 4.06 (2H, ddd, *J* = 7.1, 1.5, 1.5Hz) 3.85 (3H, s) 3.82 (1H, dd, *J* = 10.8, 4.0 Hz) 2.53 (1H, dd, *J* = 4.9, 3.6 Hz) 2.49 (1H, dd, *J* = 4.9, 0.8 Hz); 100 MHz ^{13}C NMR ($CDCl_3$, ppm) δ 171.3, 160.2, 143.8, 140.7, 140.4, 134.6, 129.1, 127.8, 127.1, 117.3, 110.8, 108.9, 105.2, 73.8, 72.0, 71.2, 55.4, 50.7, 39.9, 31.8.

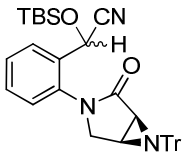

Protected cyanohydrin 69. To a mixture of pyrrolidinone **19** (0.29 mmol, 99 mg) K_3PO_4 (0.48 mmol, 102 mg), and CuI (0.24 mmol, 47 mg) in 0.80 mL toluene under an atmosphere of N_2 was

added *N, N′*-dimethylcyclohexane diamine (0.48 mmol, 78 µL) via microsyringe and the mixture became teal green. The iodide **66** (0.24 mmol, 90 mg) as a solution in 0.40 mL toluene, was added via cannula. The reaction mixture was heated to 110 °C and the color turned gray at ~80 °C. After 38.5 h, the reaction mixture was cooled to rt and filtered through silica gel with ethyl acetate. Solvent removal under rotary evaporation provided a brown oil. Purification by flash column chromatography (2 x 15 cm silica gel with 3 x 1 hexanes: ethyl acetate, Rf = 0.37, 0.27) provided 80 mg (57%) of a mixture of two diastereomers of product **69**. Molecular ion calculated for [M + Na] $C_{37}H_{39}N_3NaO_2Si$ = 608.2709, found (electrospray) 608.2722, error = 2 ppm; IR (neat, cm^{-1}) 1701; Diastereomer 1: 500 MHz ^{1}H NMR ($CDCl_3$, ppm) 7.74 (1H, d, *J* = 7.5 Hz) 7.58-7.42 (7H, m) 7.36-7.28 (6H, m) 7.28-7.73 (5H, m) 5.91 (1H, s) 4.08 (1H, d, *J* = 11.0 Hz) 3.95 (1H, ddd, *J* = 11.0, 4.0, 0.7 Hz) 2.63 (1H, dd, *J* = 5.5, 4.0 Hz) 2.51 (1H, d, *J* = 5.5 Hz) 0.99 (9H, s) 0.30 (3H, s) 0.22 (3H, s); 100 MHz ^{13}C NMR ($CDCl_3$, ppm) δ 171.8, 142.8, 135.4, 124.7, 129.8, 129.1, 128.6, 127.9, 127.2, 126.6, 119.4, 73.8, 60.2, 53.1, 38.3, 33.2, 25.6, 18.2, -5.3. Diastereomer 2: 500 MHz ^{1}H NMR ($CDCl_3$, ppm) δ 7.82-7.78 (1H, m) 7.64-7.50 (6H, m) 7.46-7.38 (2H, m) 7.34-7.28 (6H, m) 7.28-7.22 (1H, m) 7.18-7.12 (1H, m) 5.97 (1H, s) 4.19 (1H, d, *J* = 10.8 Hz) 3.79 (1H, dd, *J* = 11.2, 4.0 Hz) 100 MHz ^{13}C NMR ($CDCl_3$, ppm) 171.7, 143.8, 135.1, 134.7, 130.1, 129.2, 128.9, 127.9, 127.2, 127.0, 126.7, 119.6, 74.2, 59.7, 52.3, 38.4, 33.4, 25.6, 18.2, -5.18, -5.22.

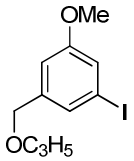

70

1-(allyloxymethyl)-3-iodo-5-methoxybenzene 70. To a solution of **33** (1.01 mmol, 196 mg) in 4.8 mL HCl at 4 °C was added $NaNO_2$ as a solution in H_2O (0.50 mL, 1.52 mmol, 84 mg) slowly via syringe. The pink solution turned dark brown. The diazonium salt was stirred at 0 °C for 45

min. Cold KI was added dropwise via syringe, the solution was diluted with 10 mL CH_2Cl_2, and warmed to rt. After 4 h, the mixture was poured into 15 % (w/v) NaOH, washed 3 x with H_2O and back extracted with CH_2Cl_2. The organic phase was then washed with aq. NaS_2O_3, and dried over Na_2SO_4. Removal of the solvent under rotary evaporation provided a brown oil. Purification of the residue by 2 preparatory TLC plates (200 x 200 x 1000, 50:9:1 Hex:CH_2Cl_2:MeOH) provided 23 mg (8%) of **70**. Molecular ion calculated for $C_{13}H_{11}IO_2$ = 303.9960, found (EI) 303.9948, error = 4 ppm; 400 MHz ^{1}H NMR ($CDCl_3$, ppm) δ 7.29-7.27 (2H, m) 7.16 (1H, dd, *J* = 2.0, 2.0 Hz) 6.86 (1H, m) 6.00-5.89 (1H, m) 5.31 (1H, ddd, *J* = 21.6, 4.3, 1.5 Hz) 5.22 (1H, ddd, *J* = 13.0, 3.5, 1.5 Hz) 4.34 (2H, s) 4.04-4.01 (2H, ddd, *J* = 7, 2, 1.8 Hz) 3.78 (3H, s); 100 MHz ^{13}C NMR ($CDCl_3$, ppm) δ 160.1, 141.7, 124.4, 128.8, 122.2, 117.4, 112.8, 94.2, 71.2, 70.9, 55.4.

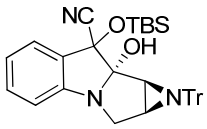

Mitosane model cyanohydrin OTBS ether 88. To a solution of LiHMDS (0.18 mmol, 31 mg) in 1 mL Et_2O at -78 °C (internal temperature) was added the cyanohydrin **69** (0.14 mmol, 80 mg) in 3.6 mL Et_2O in three portions over 20 min (max internal temp during addition was -64 °C). The cloudy mixture turned dark yellow in color after the addition was complete. The mixture was stirred at -76 °C for 10 min, warmed to -10 °C, and then placed in a 0 °C ice bath. The reaction was quenched after 10 min at 0 °C with 1.0 mL saturated NH_4Cl, and then stirred vigorously for 40 min. The mixture was partitioned between H_2O and Et_2O, and extracted 3 x with Et_2O. The combined organic phases were washed with brine, dried over $MgSO_4$, and concentrated to a light brown oil. The residue was purified by preparatory plate TLC (200 x 200 x 1000 µm silica gel, 3:1, hexanes: ethyl acetate) to provide 64 mg (80 %) of **88** as a mixture of diastereomers (0.82:0.11:0.07). The mixture of diastereomers was sufficiently pure to use in the

subsequent reaction. Selected data for the major 9a*(S)*-diastereomer: Molecular ion calculated for [M + Na] $C_{37}H_{39}N_3NaO_2Si$ = 608.3, found (electrospray, nominal) 608.2; IR (neat, cm^{-1}) 3501; 500 MHz ^1H NMR ($CDCl_3$, ppm) δ 7.60-7.52 (1H, d, *J* = 7.5 Hz) 6.99 (1H, t, *J* = 7.5 Hz) 6.81 (1.0H, d, *J* = 8.0 Hz) 4.16 (1H, s) 3.85 (1H, d, *J* = 12.8 Hz) 3.39 (1H, d, *J* = 12.8) 2.30 (2H, narrow m) 0.86 (9H, s) 0.34 (3H, s) -0.09 (3H, s); 100 MHz ^{13}C NMR ($CDCl_3$, ppm) δ 154.6, 144.1, 132.8, 129.2, 127.4, 126.5, 126.3, 126.0, 119.1, 117.4, 110.2, 103.7, 74.5, 73.4, 51.3, 43.0, 36.4, 25.5, 18.2,

-3.6, -3.8.

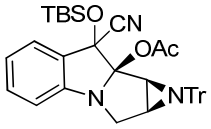

Mitosane model protected acetate 89. To a solution of diisopropylamine (0.17 mmol, 24µL) in 1 mL THF at 0 °C (internal) was added n-BuLi as a solution in hexanes (1.49 M, 0.11 mL, 0.16 mmol) via syringe. The solution was stirred at 1 °C for 15 min, and then cooled to -78 °C. The lactam **69** was added as a solution in THF (0.60 mL, 0.079 mmol) slowly via cannula (temperature spiked to -70 °C), and the solution became orange. After stirring for 20 min at -70 °C, the reaction was warmed to -24 °C, and maintained at the temperature with a dry ice bath. After two hours, acetic anhydride (0.17 mmol, 16µL) was added dropwise via syringe. The brown solution was warmed to 15 °C, and poured into Et_2O and H_2O. The mixture was extracted 3 x with Et_2O, washed with brine, and dried over $MgSO_4$. Removal of the solvent provided a brown oil consisting of a mixture of products. The fraction of interest was unstable over 20 min on silica gel, silica gel deactivated with NEt_3 fumes, and basic alumina. However, quick partial purification by two consecutive developments on a preparatory plate TLC (200 x 200, 5:1 hexanes: ethyl acetate, 2% NEt_3) was possible to provide a mixture enriched in **89**. Molecular ion calculated for [M + Na] $C_{39}H_{41}N_3NaO_3Si$ = 650.3, found (nominal) 650.2; partial spectroscopic

data for **89**: 500 MHz ^{1}H NMR ($CDCl_3$, ppm) δ 4.31 (1H, C(3)Ha, d, *J* = 9.5 Hz) 3.27 (1H, C(1), d, *J* = 3.0 Hz) 2.96 (1H, C(3)Hb, dd, *J* = 9.5, 3.5 Hz) 2.60 (1H, C(2), dd, *J* = 3.5, 3.0 Hz); 100 MHz ^{13}C NMR ($CDCl_3$, ppm) δ 109.1 [C(9a)], 55.4 [C(3)], 43.8 [C(1)], 41.1 [C(2)]; Carbon assignments are based on HSQC NMR spectroscopy.

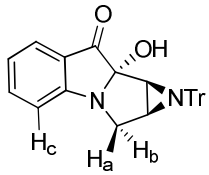

2-Hydroxy-9-trityl-6,9-diaza-4,5-benzotricyclo[6.1.0 ^{2,6}]nonan-3-one 90. To a solution of cyanohydrin **88** (0.034 mmol, 20 mg) in 0.70 mL THF at 0 °C was added 41 µL of tetrabutylammonium fluoride as a solution in THF (1.0 M) dropwise via microsyringe. Upon the first drop the solution color turned tan, which faded to yellow. The reaction solution was allowed to stir and warm to rt in the cooling bath. After 1 h, 45 min, the solution was diluted with Et_2O, and the mixture was extracted 3 x with Et_2O, and the combined organic phase was washed with brine, and then dried over $MgSO_4$. Removal of the solvent provided a bright yellow/green oil. Purification by analytical preparatory plate TLC on silica gel 60 Å (20 cm x 20 cm x 200 µm) with 1:1 hexanes: ethyl acetate (Rf = 0.47) provided 12 mg (80%) of **90**. The sample was crystallized from 0.30 mL of warm Et_2O with > 0.05 mL acetone. Molecular ion calculated for [M + Na] $C_{30}H_{24}N_2NaO_2$ = 467.1735, found (electrospray) 467.1738, error = 0.6 ppm; IR (neat, cm^{-1}) 3392, 1704, 1609; 500 MHz ^{1}H NMR ($CDCl_3$, ppm) δ 7.75 (1H, d, *J* = 7.5 Hz) 7.66 (1H, m) 7.21-7.12 (15H, m) 7.00 (2H, m) 3.81 **(**1H, d, *J* = 12.0 Hz) 3.57 (1H, dd, *J* = 12.0, 2.0 Hz) 2.75 (1H, s) 2.42 (1H, d, *J* = 4.5 Hz) 2.29 (1H, dd, *J* = 4.2, 1.7 Hz); 100 MHz ^{13}C NMR ($CDCl_3$, ppm) δ = 198.9, 163.9, 143.8, 138.6, 129.0, 127.5, 126.8, 124.7, 122.2, 120.9, 112.4, 97.0, 74.0, 51.4, 41.9, 40.4. The stereochemistry was assigned based on the correlation of H_a and H_c observed by two-dimensional NOESY NMR spectroscopy and confirmed by X-ray crystallography.

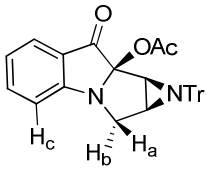

Mitosane model protected ketone 91. To a solution of **89** (0.02 mmol, 11 mg) in 0.20 mL THF at 0 °C was added TBAF as a solution in THF (1.0M, 0.027 mmol, 27 µL) via syringe. The solution was stirred and warmed to rt; after 45 min, the solution was diluted with Et_2O and poured into a saturated solution of $NaHCO_3$. The mixture was extracted 3 x with Et_2O, washed with brine, and dried over $MgSO_4$. Solvent removal provided a residue consisting of an unstable mixture of products including **91**. Separation (partial) by analytical preparatory plate TLC (200 x200, in 1:1 hexanes, ethyl acetate, Rf = 0.50) provided a yellow residue enriched in **91**. Partial spectroscopic data for **91**: 500 MHz ^{1}H NMR ($CDCl_3$, ppm) δ 4.19 (1H, C(3)Ha, dd, *J* = 12.0, 1.0 Hz) 3.52 (1H, C(3)Hb, dd, *J* = 12.0, 4.5Hz) 2.51 (1H, C(1), d, *J* = 5.5 Hz) 2.44 (1H, C(2) ddd, 5.5, 4.5, 1.0 Hz); 100 MHz ^{13}C NMR ($CDCl_3$, ppm) δ 169.5 (O_2CMe), 143.9 (C9a), 137.5, 123.7, 122.0, 114.9, 57.6 (C3), 44.6 (C1), 41.9 (C2). Proton and carbon assignments are based on COSY and HSQC NMR spectroscopy. The assigned stereochemistry is based on was assigned based on correlations between H_b and H_c by two - dimensional NOESY NMR spectroscopy.

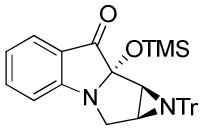

Mitosane model TMS protected α-hydroxy ketone 93. To a solution of **90** (0.20 mmol, 89 mg) and *N, N*-dimethylaminopyridine (0.60 mmol, 73 mg) in 2 mL CH_2Cl_2 at 0 °C was added NEt_3 (1.2 mmol, 1.7 mL). Trimethylchlorosilane (0.60 mmol, 0.08 mL) was added dropwise via syringe. After 1 h of warming and stirring, the solution was cooled in a 0 °C ice bath and diluted with CH_2Cl_2. The mixture was poured into saturated aqueous $NaHCO_3$ and extracted 3 x with

CH_2Cl_2, dried over Na_2SO_4, and the organic phase was concentrated to a tan oil. The crude residue was purified by flash column chromatography (1.5 x 15 cm, 3:1 hexanes: ethyl acetate, Rf = 0.53) to provide 71 mg (69%) of **93**. Molecular ion calculated for [M + Na] $C_{33}H_{32}N_2NaO_2Si$ = 539.3231, found (electrospray) 539.2142, error = 2 ppm; IR (neat, cm^{-1}) 1721, 1609; 400 MHz ^1H NMR ($CDCl_3$, ppm) δ 7.77 (1H, m) 7.64 (1H, m) 7.21-7.12 (15H, m) 7.20-6.94 (2H, m) 3.79 (1H, d, *J* = 12.0 Hz) 3.44 (1H, dd, *J* = 12.0, 2.0 Hz) 2.46 (1H, d, *J* = 4.0 Hz) 2.19 (1H, dd, *J* = 4.0, 2.0 Hz) 0.02 (8H, s); 100 MHz ^{13}C NMR ($CDCl_3$, ppm) 199.3, 163.3, 143.9, 138.0, 129.1, 127.5, 126.7, 124.4, 123.2, 120.7, 112.2, 98.1, 74.0, 51.3, 42.8, 40.4, 1.07.

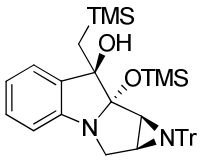

Tertiary trimethylsilylmethyl alcohol 94. To a solution of **93** (0.029 mmol, 15 mg) in 1.4 mL THF at -10 °C (internal) was added trimethylsilylmethyllithium as a solution in ether (0.48 M, 0.15 mmol, 0.31 mL) dropwise via syringe (temperature < -8 °C) following the procedure of Danishefsky.[29] The tan solution was quenched after 10 min with 1 mL saturated NH_4Cl. The mixture was extracted 3 x with ethyl acetate, washed with brine, and dried over Na_2SO_4. Solvent removal under rotary evaporation provided a brown oil consisting of 1 diastereomer of a new product. The residue was purified by preparatory plate TLC (200 x 200 x 200, 3:1 hexanes: ethyl acetate, Rf = 0.53) pretreated with NEt_3 fumes to provide 12 mg (67%) of **94**. Molecular ion calculated for [M + Na] $C_{37}H_{44}N_2NaO_2Si_2$ = 627.2839, found (electrospray) 627.2842, error = 0.5 ppm; IR (neat, cm^{-1}) 3545; 500 MHz ^1H NMR ($CDCl_3$, ppm) δ 7.30-7.24 (2H, m) 7.22-7.13 (15H, m) 6.87 (H, t, *J* = 7.0 Hz) 6.69 (1H, d, *J* = 8.0 Hz) 3.89 (1H, d, *J* = 12.4 Hz) 3.41 (1H, dd, *J* = 12.4, 1.2 Hz) 2.34 (1H, s) 2.13 (2H, narrow m) 1.31 (2H, s) -0.04 (3H, s) -0.14 (3H, s); 100 MHz ^{13}C NMR ($CDCl_3$, ppm) δ 151.9, 144.1, 135.3, 129.4, 129.0, 127.8, 126.8, 124.2, 118.7, 110.5, 108.9, 82.3, 74.4, 52.9, 45.1, 37.3, 28.2, 2.1, 0.4.

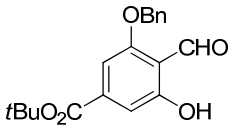

***tert*-Butyl (3-benzyloxy)-4-formyl-5-hydroxybenzoate (101)**. An oven dried 3-neck flask was equipped with a 2-way joint leading to a volumetric cylinder adapted to measure gas evolution. The flask was charged with aldehyde **99**[67] (4.1 mmol, 1.72 g), Pd/C (0.08 mmol, 85 mg), 32 mL MeOH, 8 mL 1,4-dioxane, and 1.3 mL NaOMe (4.9 M, 6.15 mmol). Hydrogen gas was bubbled through the reaction mixture and used to fill the volumetric cylinder by 42 mL. After 1.5 h, 35 mL of H_2 was added, and after another 30 min, 15 mL of H_2 was added. The reaction was monitored by TLC, and after consumption of 91 mL H_2 (measured using the volumetric cylinder) the reaction mixture was filtered though celite with Et_2O. The orange organic phase was acidified with 2.0 M HCl to produce a bright yellow solution. The yellow organic phase was washed 2 x with H_2O and with brine. It was then dried over $MgSO_4$, and the solvent was removed under reduced pressure to provide a pale yellow solid consisting of phenol **101**, diol, and **99**. The crude residue was recrystallized from warm $CHCl_3$ and small amounts of Et_2O to provide 651 mg (48%) of phenol **101**; mp = 162 °C; Molecular ion calculated for [M + Na] $C_{19}H_{20}NaO_5$ = 351.1208, found (electrospray) 351.1202, error = 1.7 ppm; IR (neat, cm^{-1}) 1715, 1656; 500 MHz ^{1}H NMR ($CDCl_3$, ppm) δ 11.86 (1H, s) 10.44 (1H, s) 7.44-7.36 (5H, m) 7.15 (1H, br s) 7.10 (1H, d, *J* = 1.5 Hz) 5.19 (2H, s) 1.59 (9H, s); 100 MHz ^{13}C NMR ($CDCl_3$, ppm) 194.5, 164.2, 163.2, 161.2, 140.5, 135.5, 128.8, 128.5, 127.6, 112.8, 111.5, 102.7, 82.3, 70.9, 28.0.

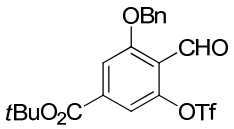

***tert*-Butyl (3-benzyloxy)-4-formyl-5-(trifluoromethylsulfonyloxy)benzoate (98).** To a solution of phenol **101** (1.16 mmol, 381 mg) in 12 mL toluene was added 9 mL of a 30% solution of

K_3PO_4 in H_2O (w/v). The biphasic mixture was stirred vigorously and cooled in a 0 °C ice bath. Neat trifluoromethanesulfonic anhydride (Tf_2O) (2.3 mmol, 0.39 mL) was added slowly via syringe. The cloudy reaction turned pale yellow and cleared while stirring. The reaction mixture was removed from the cooling bath and warmed to rt while stirring vigorously. After 1.5 h, the phases were separated and the organic phase was washed with brine, and then dried over Na_2SO_4. Removal of the solvent under rotary evaporation provided a yellow oil. The crude residue was purified by flash column chromatography (3.5 x 16 cm, 5:1 hexanes: ethyl acetate, Rf = 0.36) to provide 429 mg (80%) of triflate **98**. Molecular ion calculated for [M + Na] $C_{20}H_{19}F_3NaO_7S$ = 483.0701, found (electrospray) = 483.0714, error = 3 ppm; IR (neat, cm^{-1}) 1718, 1700, 1423; 500 MHz ^1H NMR ($CDCl_3$, ppm) 10.51 (1H, s) 7.75 (1H, s) 7.50-7.35 (6H, m) 5.27 (2H, s) 1.61 (9H, s); 100 MHz ^{13}C NMR ($CDCl_3$, ppm) δ 186.2, 162.8, 161.9, 147.9, 138.7, 134.9, 129.1, 129.0, 127.8, 120.7, 118.7 (q, *J* = 320 Hz),117.2, 115.8, 114.1, 83.4, 72.0, 28.1.

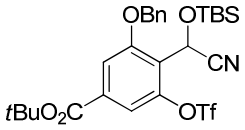

102

Triflate 102. To a solution of aldehyde **98** (0.27 mmol, 125 mg) in 2.7 mL CH_2Cl_2 was added ZnI_2 (0.008 mmol, 3 mg) and *tert*-butyldimethylsilyl cyanide (0.33 mmol, 47 mg). The mixture was stirred for 4 h at rt, then diluted with CH_2Cl_2 and filtered through celite. Solvent removal under N_2 flow provided an orange oil. The residue was purified by flash column chromatography (2.5 x 15 cm silica gel with 9:1 hexanes: ethyl acetate, Rf = 0.30) to provide 142 mg (88%) of **102** a clear colorless oil. Molecular ion calculated for [M + Na] $C_{27}H_{34}F_3NO_7SSi$ = 624.1675, found (electrospray) = 624.1672, error = 0.5 ppm; IR (neat, cm^{-1}) 1721, 1617, 1581; 500 MHz ^1H NMR ($CDCl_3$, ppm) 7.65 (1H, d, *J* = 1.3 Hz) 7.57 (1H, d, *J* = 1.3 Hz) 7.48-7.35 (5H, m) 6.04 (1H, s,) 5.22 (2H, s) 1.59 (9H, s) 0.84 (9H, s) 0.16 (3H, s) 0.07 (3H, s); 100 MHz ^{13}C NMR

($CDCl_3$, ppm) δ 163.0, 156.7, 148.0, 135.6, 134.9, 128.8, 128.7, 127.8, 122.2, 117.5, 115.0, 112.9, 82.8, 71.7, 54.6, 28.0, 25.4, 18.1, -5.4, -5.4; unidentified peaks at 120.0, 116.9, 25.7, and -3.0.

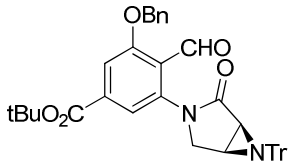

97

N-aryl-3,6-diazabicyclo[3.1.0]hexan-2-one 97. To a two-neck flask fitted with a three-way joint was added pyrrolidinone **19** (0.93 mmol, 340 mg) and K_3PO_4 (1.09 mmol, 229 mg). Under a glove box atmosphere was added $Pd_2(dba)_3$, (0.015 mmol, 14 mg) and xantphos ligand (0.046 mmol, 27 mg). The flask was fitted with a reflux condenser, and using the three way joint the system was evacuated and back filled 3 x with Ar. To the system was added 3 mL 1,4-dioxane, and triflate **98** (0.77 mmol, 356 mg) in 3 mL 1,4-dioxane. The orange/red reaction flask was heated to 80 °C and turned olive green near 60 °C. After 18 h of heating, the mixture was cooled to rt, filtered through silica gel with CH_2Cl_2, and concentrated under reduced pressure to an orange oil consisting of product **97** and phenol **101** (19%). The crude residue was purified by flash column chromatography (4 x 15 cm silica gel with 3:1 hexanes: ethyl acetate, Rf = 0.27) to provide 320 mg (64%) of **97** as an amorphous solid. Molecular ion calculated for $C_{42}H_{38}N_2NaO_5$ = 673.2678, found (electrospray) = 673.2699, error = 3 ppm; IR (neat, cm^{-1}) 1708; 500 MHz ^1H NMR ($CDCl_3$, ppm) δ 10.47 (1H, s) 7.64 (1H, d, *J* = 1.5 Hz) 7.57-7.50 (7H, m) 7.47-7.34 (6H, m) 7.31 (6H, t, *J* = 8.0 Hz) 7.27-7.22 (3H, m) 5.22 (2H, s) 4.07 (1H, d, *J* = 10.5) 3.85 (1H, dd, *J* = 10.5, 4.0 Hz) 2.59 (1H, dd, *J* = 4.5, 4.0 Hz) 2.44 (1H, d, *J* = 4.5 Hz) 1.61 (9H, s); 100 MHz ^{13}C NMR ($CDCl_3$, ppm) δ 189.4, 171.6, 163.9, 160.6, 143.9, 137.6, 127.2, 135.5, 129.2, 128.8, 128.5, 127.8, 127.5, 127.1, 125.8, 120.5, 112.8, 82.5, 73.9, 71.2, 52.7, 38.4, 33.1, 29.1.

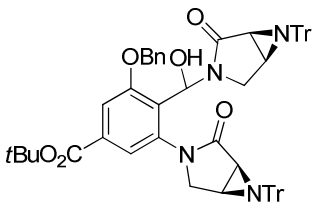

carbinolamide 103. An oven dried 2-neck flask was fitted with a 3-way joint, and charged with aziridinopyrrolidinone **19** (1.07 mmol, 365 mg), Cs_2CO_3 (1.25 mmol, 407 mg), $Pd(OAc)_2$ (0.009 mmol, 2 mg), and xantphos (0.013 mmol, 8 mg). The flask was fitted with a reflux condenser and the system was evacuated and backfilled 3 x with Ar using the three way joint. Under an Ar atmosphere, the triflate **98** was added as a solution in 1,4-dioxane (0.89 mL, 0.88 mmol, 405 mg) via syringe. The non-homogenous orange mixture was heated to 80 °C and stirred vigorously. After 3 h, the mixture was cooled to rt, diluted with CH_2Cl_2, filtered through silica gel, and concentrated under reduced pressure. The crude mixture consisted of lactam **19**, phenol **101**, **97**, and carbinolamide **103**. Purification of the crude residue by flash column chromatography (4 x 15 cm silica gel, 3:1 hexane: ethyl acetate) provided 159 mg (~18%) of **103** contaminated by small amounts of impurities. The material was then purified again by preparatory plate chromatography (200 x 200 x 1000, 1:1 hexanes: diethyl ether, Rf = 0.13, developed plate twice). Molecular ion calculated for [M + Na] $C_{65}H_{58}N_4NaO_6$ = 1013.4254, found (electrospray) 1013.4263, error = 1 ppm; IR (neat, cm^{-1}) 3240, 1711, 1677; 400 MHz ^{1}H NMR ($CDCl_3$, ppm) δ 8.66 (1H, s) 7.50-7.34 (14H, m) 7.26-7.15 (23H, m) 5.13 (2H, ABq, *J* = 12.2 Hz) 4.01 (1H, d, *J* = 10.8 Hz) 3.88 (1H, d, *J* = 11.2 Hz) 3.70 (1H, dd, *J* = 10.8, 3.6 Hz) 3.09 (1H, dd, *J* = 10.6, 3.0 Hz) 2.55 (1H, dd, *J* = 4.4, 3.6 Hz) 2.43 (1H, d, *J* = 4.4 Hz) 2.31 (2H, narrow m) 1.57 (9H, s); 100 MHz ^{13}C NMR ($CDCl_3$, ppm) δ 173.3, 172.6, 165.1, 156.8, 156.4, 143.7, 136.2, 134.0, 129.1, 128.5, 127.9, 127.9, 127.8, 127.3, 127.2, 127.1, 114.7, 114.2, 105.1, 81.4, 74.0, 73.8, 70.8, 58.8, 49.5, 48.7, 38.6, 38.0, 33.4, 33.0, 29.7 (grease), 28.1

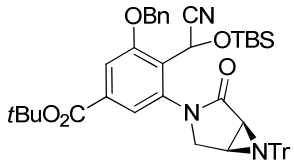

N-aryl-3,6-diazabicyclo[3.1.0]hexan-2-one cyanohydrin ether 104. To a solution of **97** (0.28 mmol, 182 mg) in 4 mL CH_2Cl_2 at 0 °C was added 18-crown-6 ether as a solution in CH_2Cl_2 (1.6 mL, 0.11 mmol, 29 mg) via cannula. To the clear solution was added tetrabutylammonium cyanide (0.42 mmol, 61 mg) and then potassium cyanide (0.05 mmol, 3.4 mg). The non-homogenous solution was stirred and warmed to rt in the cooling bath. After 2 h, the solvent was removed under rotary evaporation to provide a tan oil. The residue was purified by flash column chromatography (2 x 16 cm silica gel, 1:1 hexanes, ether, Rf = 0.56, 0.26) to give two diastereomers in a ratio of ca 1:1 (diastereomer 1:2). Molecular ion calculated for [M + Na] $C_{49}H_{53}N_3NaO_5Si$ = 812.3652, found (electrospray) 814.3672, error = 2.5 ppm; IR (neat, cm^{-1}) 1710; Diastereomer 1: 400 MHz ^{1}H NMR (55 °C, $CDCl_3$, ppm) δ 7.62 (1H, d, *J* = 1.2 Hz) 7.53-7.48 (9H, m) 7.40-7.20 (12H, m) 5.9 (1H, s) 5.23 (2H, ABq, *J* = 12.0 Hz) 4.01 (1H, d, *J* = 10.8 Hz) 3.80 (1H, br d, *J* = 8.0 Hz) 2.59 (1H, dd, *J* = 4.4, 4.2 Hz) 2.51 (1H, d, *J* = 4.4 Hz) 1.55 (9H, s) 0.78 (9H, s) 0.08 (3H, s) 0.00 (3H); 100 MHz ^{13}C NMR (55 °C, $CDCl_3$, ppm) δ 172.2, 164.0, 157.6, 143.8, 138.2, 135.8, 135.2, 129.2, 128.6, 128.2, 127.8, 127.6, 127.1, 122.0, 119.7, 113.1, 81.9, 74.1, 71.3, 56.6, 54.0, 38.3, 33.3, 28.1, 25.4, 18.0, -5.2, -5.3; Diastereomer 2: 500 MHz ^{1}H NMR (45 °C, $CDCl_3$, ppm) δ 7.61 (1H, s) 7.54-7.44 (9H, m) 7.41-7.22 (14H, m) 5.87 (1H, br s) 5.24 (1H, d, *J* = 11.5 Hz) 5.19 (1H, d, *J* = 11.5 Hz) 4.06 (1H, dd, *J* = 10.7, 3.7 Hz) 3.91 (1H, d, *J* = 10.7 Hz) 2.63 (1H, dd, *J* = 4.5, 3.7 Hz) 2.52 (1H, d, *J* = 4.5) 1.56 (9H, s) 0.78 (9H, s) 0.07 (3H, s) -0.03 (3H, s); 100 MHz ^{13}C NMR (45 °C, $CDCl_3$, ppm) δ 171.6, 164.2, 157.7, 144.0, 135.9, 135.3, 129.3, 128.7, 128.3, 127.95, 127.88, 127.7, 127.6, 127.3, 118.4, 113.0, 82.0, 74.1, 71.5, 56.5, 53.8, 38.4, 33.2, 28.2, 25.5, 18.0, -5.0, -5.2. ^{1}H NMR spectroscopy was conducted at temperatures between 45 – 55 °C in order to resolve the C(1), C(2), and C(3) proton signals. ^{13}C

NMR spectroscopy was conducted at temperatures between 45 – 55°C in order to resolve the C(3) carbon signal.

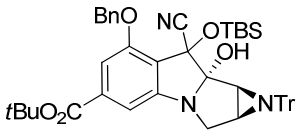

Protected mitosane cyanohydrin 107. A solution of **104** (0.33 mmol, 264 mg) in toluene was concentrated under a stream of N_2. To the resulting residue was added 5.5 mL Et_2O, and a white precipitate appeared. The mixture was stirred vigorously and cooled to -78 °C (internal). To the mixture was added LiHMDS as a solution in Et_2O (5 mL, 0.99 mmol, 171 mg) slowly to keep the temperature below -76 °C. The mixture immediately turned bright yellow upon addition of the base. The mixture was stirred at -78 °C for 30 min, and was then warmed to 0 °C slowly over 30 min. The reaction lightened to pale yellow near -17 °C. When the reaction temperature reached 0.5 °C, the vessel was placed in a 0 °C bath, and was allowed to stir. After 40 min of stirring, 2 mL saturated NH_4Cl was added, the reaction exothermed to 6 °C, then cooled to 3 °C. The mixture was extracted 3 x with ethyl acetate, washed with brine, and dried over $MgSO_4$, and concentrated under reduced pressure to give a yellow residue consisting of **107**, and the two diastereomers of **104** in a ratio of 2:1 (prod: starting material). The crude residue was purified by flash column chromatography (3 x 15 cm silica gel, 2:1 hexanes: ether, Rf = 0.41) to provide 153 mg (58%) of **107**. Molecular ion calculated for [M + Na] $C_{49}H_{53}N_3NaO_5Si$ = 814.3652, found (electrospray) 814.3672, error = 2.5 ppm; IR (neat, cm^{-1}) 3426, 1713, 1700, 1594; 500 MHz ^1H NMR ($CDCl_3$, ppm) δ 7.58-7.52 (8H, m) 7.84-7.36 (2H, m) 7.34-7.28 (7H, m) 7.26-7.22(4H, m) 7.10 (1H, d, *J* = 1.0 Hz) 5.22 (2H, ABq, *J* = 11.8 Hz) 4.19 (1H, d, *J* = 10.0 Hz) 3.39 (1H, s) 2.96 (1H, dd, *J* = 10.0, 3.5 Hz) 2.70 (1H, d, *J* = 4.5 Hz) 2.58 (1H, dd, *J* = 4.5, 3.5 Hz) 1.59 (9H, s) 0.41 (9H, s) 0.00 (3H, s) -0.40 (3H, s); 100 MHz ^{13}C NMR ($CDCl_3$, ppm) 164.9, 155.1, 153.7, 143.9,

136.9, 135.7, 129.4, 128.6, 128.2, 127.9, 127.9, 127.1, 122.9, 117.7, 109.8, 107.7, 104.3, 81.6, 76.4, 74.3, 70.5, 54.3, 42.5, 41.4, 28.1, 25.2, 17.9, -4.7, -4.8.

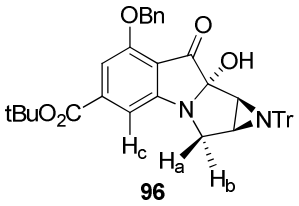

96

9-oxo-pyrrolo[1,2a[indole mitosane 96. To a solution of **107** (0.024 mmol, 19 mg) in 0.50 mL THF at 0 °C was added TBAF dropwise via syringe. Upon the first drop, the solution turned bright yellow. The reaction solution was allowed to stir and warm to rt in the cooling bath. After 2.5 h, the solution was cooled in a 0 °C bath and saturated aqueous $NaHCO_3$ was added. The mixture was extracted 3 x with CH_2Cl_2, and the combined organic phase was washed with brine and dried over $MgSO_4$. Removal of the solvent under rotary evaporation provided a fluorescent yellow/green residue. The crude residue was purified by analytical preparatory plate TLC on silica gel 60 Å (20 cm x 20 cm x 200 µm) with 3:1 hexanes: ethyl acetate (Rf = 0.25) to provide 12 mg (77%) of a bright yellow/green oil. Molecular ion calculated for [M + Na] $C_{42}H_{38}N_2NaO_5$ = 673.2678, found (electrospray) = 673.2688 , error = 1.5 ppm; IR (neat, cm^{-1}) 3421, 1705, 1615, 1584; 500 MHz ^1H NMR ($CDCl_3$, ppm) δ 7.61 (2H, d, *J* = 7.0) 7.45-7.40 (2H, m) 7.37-7.37 (1H, m) 7.21-7.10 (15H, m) 7.05 (1H, s) 5.35 (2H, ABq, *J* = 12.2 Hz) 3.84 (1H, d, *J* = 12.0 Hz) 3.52 (1H, dd, *J* = 12.0, 2.0 Hz) 2.98 (1H, s) 2.41 (1H, d, *J* = 4.5 Hz) 2.26 (1H, dd, *J* = 4.5, 2.0 Hz) 1.64 (9H, s); 100 MHz ^{13}C NMR ($CDCl_3$, ppm) δ 195.9, 164.9, 164.7, 157.3, 143.8, 142.3, 136.1, 129.1, 128.7, 128.0, 127.6, 126.9, 126.9, 113.4, 105.4, 104.6, 97.5, 82.2, 74.0, 70.4, 51.4, 41.8, 40.1, 28.2. The stereochemistry was assigned based on a 16% NOE enhancement between H_a and H_c (7.05 ppm) and by analogy to model **90**.

Chapter 3 Bibliography

1. Wolkenberg, S. E.; Boger, D. L. “Mechanisms of in Situ Activation for DNA-targeting Antitumor Agents.” *Chem. Rev.* **2001**, *102*, 2477.

2. Rajski, S. R.; Williams, R. M. “DNA Cross-linking Agents as Antitumor Drugs.” *Chem. Rev.* **1998**, *98*, 2723.

3. Tomasz, M.; Palom, Y. “The Mitomycin Bioreductive Antitumor Agents: Cross-linking and Alkylation of DNA as the Molecular basis of Their Activity.” *Pharmacol. Ther.* **1997**, *76*, 73-87.

4. Tomasz, M. “Mitomycin C: small, fast, and deadly (but very selective).” *Chemistry and Biology* **1995**, *2*, 575.

5. Kasai, M.; Kono, M. “Studies on the Chemistry of Mitomycins.” *Synlett* **1992**, 778.

6. Kennedy, K. A.; Teicher, B. A.; Rockwell, S.; Sartorelli, A. C. “The Hypoxic Tumor Cell: A Target for Selective Cancer Chemotherapy.” *Biochemical Pharmocology* **1980**, *29*, 1.

7. Kennedy, K. A.; Rockwell, S.; Sartorelli, A. C. “Preferential Activation of Mitomycin C to Cytotoxic Metabolites by Hypoxic Tumor Cells.” *Cancer Res.* **1980**, *40*, 2356.

8. Bachur, N. R.; Gordon, S. L.; Gee, M. V.; Kon, H. “NADPH cytochrome P-450 reductase activation of quinone anticancer agents to free radicals.” *Proc. Natl. Acad. Sci.* **1979**, *76*, 954.

9. Fridovich, I. “Superoxide Radical and Superoxide Dismutase.” *Acc. Chem. Res.* **1972**, *5*, 321.

10. Bradner, W. T. “Mitomycin C: A Clinical Update.” *Can. Treat. Rev.* **2001**, *27*, 35.

11. Crooke, S. T.; Bradner, W. T. “Mitomycin C: a review.” *Can. Treat. Rev.* **1976**, *3*, 121.

12. (a) Iyengar, B. S.; Remers, W. A.; Bradner, W. T. “Preparation and Antitumor Activity of 7-Substitution 1,2-Aziridinomitosenes.” *J. Med. Chem.* **1986**, *29*, 1864. (b)Arai, H.; Kanda, Y.; Ashizawa, T.; Morimoto, M.; Gomi, K.; Kono, M.; Kasai, M. “Synthesis and Antitumor Activity of Novel Mitomycin Derivatives Containing Functional Groups at the C-6 Methyl Position.” *J. Med. Chem.* **1994**, *37*, 1794.

13. (a) Iwami, M.; Kyoto, S.; Terano, H.; Kohsaka, M. Aoki, H.; Imanaka, H. “A New Tumor Antibiotic, FR900482. Taxonomic Studies on the producing strain. A New Species of Streptomyces.” *J. Antibiot*. **1987**, *40*, 589. (b) Kiyoto, S.; Shibata, T.; Yamashita, M.; Komori, T.; Okuhata, M.; Terano, H.; Kohsaka, M.; Aoki, H.; Imanka, H. “A New Antitumor Antibiotic, FR900482. Production, Isolation, Characterization, and Biological Activity.” *J. Antibiot.* **1987**, *40*, 594. (c) Shimomura, K.; Hirai, O.; Mizota, T.; Matsumoto, S.; Shibayama, F.; Kikuchi, H. A “New Antitumor Antibiotic, FR900482. Antitumor activity in transplantable experimental tumors.” *J. Antibiot.* **1987**, *40*, 600. (d) Hirai, O; Shimomura, K.; Mizota, T.; Matsumoto, S.; Mori, J.; Kikuchi, H. “A New Antitumor Antibiotic, FR900482. Hematological Toxicity in Mice.” *J. Antibiot.* **1987**, *40*, 607.

14. Pazdur, R.; Ho, D-H; Daugherty, K. ; Bradner, W. T.; Krakoff, I. H.; Raber, M. N. “Phase 1 trial of FK973: Description of a delayed vascular leak syndrome.” *Investigation New Drugs* **1991**, *9*¸377.

15. (a)Wakaki, S.; Marumo, H.; Tomioka, K.; Shimizu, G.; Kato, E.; Kamada, H.; Kudo, S.; Fujimoto." Isolation of New Fractions of Antitumor Mitomycins." *Antibiots. Chemoth.* **1958**, *8*, 228. (b) Hata, T.; Sano, Y.; Sugawara, R.; Matsumae, A.; Kanamori, K.; Shima, T.; Hoshi, T. "Mitomycin, A New Antibiotic from Strepotmyes. I." *J. Antibiot. Ser. A.* **1956**, *9*, 141.

16. Iwami, M.; Kiyoto, S.; Terano, H.; Kohsaka, M.; Aoki, H.; Imanaka, H. "A New Antitumor Antibiotic, FR900482. I. Taxonomic Studies on the Producing Strain: A New Species of the Genus *Streptomyces*." *J. Antibiot.* **1987**, *40*, 589.

17. Hornemann, U.; Cloyd, J. C. "Studies on the Biosynthesis of the Mitomycin Antibiotics by *Streptomyces verticillatus*." *Chem. Commun.* **1971**, 301.

18. Hornemann, U.; Aikman, M. J. "Mitomycin Biosynthesis by *Streptomyces verticillatus.* Incorporation of the Amin-group of D[^{15}N]Glucosamine into the Aziridine Ring of Mitomycin B." *J.C.S. Chem. Comm.* **1973**, 88.

19. Hornemann, U.; Kehrer, J. P.; Nunez, C. S.; Ranieri, R. L. "D-Glucosamine and L-Citrulline, Precursors in Mitomycin Biosynthesis by *Streptomyces verticallatus*." *J. Am. Chem. Soc.* **1974,** *96*, 320.

20. Hornemann, U.; Eggert, J. H. "Utilization of the Intact Carbamoyl Group of L-[NH_2CO-^{13}C,^{15}N] Citrulline in Mitomycin Biosynthesis by *Streptomyces verticillatus." J. Antibiot.* **1975**, *28*, 841.

21. Bezanson, G. S.; Vining, L. C. "Studies on the Biosynthesis of Mitomycin C by *Strepotmyces verticillatus*." *Can. J. Biochem.* **1971**, *49*, 911.

22. Anderson, M. G.; Kibby, J. J.; Rickars, R. W.; Rothschild, J. M. "Biosynthesis of the Mitomycin Antibiotics from 3-amin-5-hydroxybenzoic acid." *J.C.S. Chem. Comm.* **1980**, 1277.

23. (a) Kim, C-G.; Yu, T-W;, Fryhle, C.B.; Handa, S.; Floss, H.G. "3-Amino-5-hydroxybenzoic Acid Synthase, the Terminal Enzyme in the Formation of the Precursor of mC_7N Units in Rifamycin and Related Antibiotics." *J. Biol. Chem.* **1998**, *273*, 6030. (b) Yu, T-W.; Müller, R.; Müller, M.; Zhang, X.; Draeger, G.; Kim, C-G.; Leistner, E.; Floss, H. G. "Mutational Analysis and Reconstituted Expression of the Biosynthetic Genes Involved in the Formation of 3-Amino-5-hydroxybenzoic Acid, the Starter Unit of Rifamycin Biosynthesis in *Amycolatopsis mediterranei* S699." *J. Biol. Chem.* **2001**, *276*, 12546.

24. Fujita, T.; Takase, S.; Otsuka, T.; Terano, H.; Kohsaka, M. "Precursors in the Biosynthesis of FR900482, A Novel Antitumor Antibiotic Produced by *Streptomyces Sandaensis.*" **1988**, *41*, 392.

25. Chamberland, S.; Grüschow, S.; Sherman, D. H., Williams, R. M. "Synthesis of Potential Early-Stage Intermediates in the Biosynthesis of FR900482 and Mitomycin C." *Org. Lett.* **2009**, *11*, 791.

26. (a) Varoglu, M.; Mao, Y.; Sherman, D. H. "Mapping the Mitomycin Biosynthetic Pathway by Functional Analysis of the MitM Aziridine *N*-Methyltransferase." *J. Am. Chem. Soc.* **2001**, *123*, 6712. (b) Mao, Y.; Varoglu, M.; Sherman, D. H. "Molecular characterization and anaylsis of the biosynthetic gene cluster for the antitumor antibiotic mitomycin C from *Streptomyces lavendulae* NRRL 2564." *Chem. Biol.* **1999**, *6*, 251.

27. Mao, Y.; Sherman, D. H. *unpublished work.*

28. Dmitrienko, G. I.; Denhar, D.; Mithani, S.; Prasad, G. K. B.; Taylor, N. J. "A New Approach to the Bicyclic Hydroxylamine Hemiketal Ring System of Antitumor-Antibiotic FR900482 via Oxidative Ring Expansion of a Tetrahydropyrrolo[1,2-a]indole." *Tetrahedron Lett.* **1992**, *33*, 5705.

29. Benbow, J. W.; McClure, K. F.; Danishefsky, S. J. "Intramolecular Cycloaddition Reactions of Dienyl Nitroso Compounds: Application to the Synthesis of Mitomycin K." *J. Am. Chem. Soc.* **1993**, *115*, 12305.

30. (a) Ban, Y.; Nakajima, S.; Yoshida, K.; Mori, M. Shibasaki, M. "Synthetic approaches toward mitomycin: synthesis of the decarbamoyloxymitomycin derivative." *Heterocycles* **1994**, *39*, 657. (b) Nakajima, S.; Yoshida, K.; Mori, M.; Ban, Y. Shibasaki, M. "Synthetic approaches toward mitomycins: synthesis of the decarbamoyloxymitomycin derivative." *J.C.S.Chem. Commun.* **1990**, 468.

31. Wang, Z.; Jimenez, L. S. "Synthesis of the Tetracyclic Mitomycin Skeleton via a Dialkylvinylsulfonium Salt." *J. Am. Chem. Soc.* **1994**, *116*, 4977.

32. Wang, Z.; Jimenez, L. S. A Total Synthesis of (±)-Mitomycin K. Oxidation of the Mitosene C9-9a Double Bond by (Hexamethylphosphoramido)oxodiperoxomolybdenum (VI) (MoO_5•HMPA). *Tetrahedron Lett.* **1996**, *37*, 6049.

33. (a) Papaioannou, N.; Blank, J. T.; Miller, S. J. "Enantioselective Synthesis of an Aziridinomitosane and Selective Functionalizations of a key Intermediate." *J. Org. Chem.* **2003**, *68*, 2728. (b) Papioannou, N.; Evans, C. A.; Blank, J. T.; Miller, S. J. "Enantioselective Synthesis of a Mitosane Core Assisted by Diversity-Based Catalyst Discovery." *Org. Lett.* **2001**, *3*, 2879.

34. Ziegler, F. E.; Belema, M. "Chiral Aziridinyl Radicals: An Application to the Synthesis of the Core Nucleus of FR900482." *J. Org. Chem.* **1997**, *62*, 1083.

35. Trost, B. M.; O'Boyle, B. M. "Synthesis of 7-*Epi* (+)-FR900482: An Epimer of Comparable Anti-Cancer Activity." *Org. Lett.* **2008**, *10*, 1369.

36. (a) Arrasate, S.; Lete, E.; Sotomayor, N. "Metalation and α-amidoalkylation reactions in the stereocontrolled synthesis of fused isoquinoline systems." In *New Methods for the Asymmetric Synthesis of Nitrogen Heterocycles*; Vicario, J. L.; Badia, D.; Carrillo, L., Eds; Research Signpost: Trivadrum, India, 2005, pp 223. (b) Sotomayor, N.; Lete, E. "Aryl and heteroaryllithium compounds by metal-halogen exchange. Synthesis of carbocyclic and heterocyclic systems." *Current Organic Chemistry* **2003**, *7*, 275.

37. Moreau, A.; Lorion, M.; Couture, A.; Deniau, E.; Grandclaudon, P. "A New Total Synthesis of Porritoxin." *J. Org. Chem.* **2006**, *71*, 3303.

38. Moreau, A.; Couture, A.; Deniau, E.; Grandclaudon, P.; Lebrun, S. "First Total Synthesis of cichorine and zinnimidine." *Org. Biomol. Chem.* **2005**, *3*, 2305.

39. de la Fuente, M. C.; Domínguez, D. "Synthesis of chromeno[4,3,2-*cd*]isoindolin-2-ones and chromeno[4,3,2-*de*]isoquinolin-3-ones. Electrophilic versus anionic cyclization of carbamates." *Tetrahedron* **2004**, *60*, 10019.

40. Orito, K.; Miyazawa, M.; Kanbayashi, R.; Tatsuzawa, T.; Tokuda, M.; Suginome, H. "Benzolactams. 4. Reactions of 3′,4′- or 4′,5′-Dialkoxy-Substituted 1-(2′-Bromobenzyl)-2-ethoxycarbonyl-1,2,3,4-tetrahydroisoquinolines with Alkyllithium. 1,2 and 1,4 Additions of Alkyllithium to Benzolactams." *J. Org. Chem.* **2000**, *65*, 7495.

41. Beddoes, R. L.; Davies, M. P. H.; Thomas, E. J. "Synthesis of the Tricyclic Nucleus of the Alkaloid Stemofoline: X-Ray Crystal Structure of (4RS,5RS,7SR,10RS)-10-Butyl-5-hydroxy-1-azatricyclo[5.3.0.$0^{4,10}$]decan-2-one." *J. Chem. So. Chem. Commun.* **1992**, 538.

42. Herlt, A. J.; Kibby, J. J.; Rickards, R. W. "Synthesis of Unlabelled and Carboxyl-Labelled 3-Amino-5-hydroxybenzoic Acid." *Aust. J. Chem.* **1991**, *34*, 1319.

43. Fernández-Megia, E.; Iglesias-Pintos, J. M.; Sardina, F. J. "Enantiomerically Pure Highly Functionalized α-Amino Ketones from the Reaction of Chiral Cyclic *N*-(9-Phenylfluoren-9-yl) α-Amido Esters with Organolithium Reagents." *J. Org. Chem.* **1997**, *62*, 4770.

44. Pattenden, L. C.; Adams, H.; Smith, S. A.; Harrity, J. P. A. "Development of a [3+3] Approach to Tetrahydropyridines and its Application in Indolizidine Alkaloid Synthesis." *Tetrahedron* **2008**, *64*, 2951.

45. Goswami, R.; Corcoran, D. E. "Homoenolate Dianions of Secondary Amides Via Tin/Lithium Exchange." *Tetrahedron Lett.* **1982**, *23*, 1463.

46. (a) Trost, B. M.; Rivers, G. T.; Gold, J. M. "Regiocontrolled Synthesis of Hydroxyphthalides. Synthesis of (±)-Isoochracinic Acid and a Zealeranone Intermediate." *J. Org. Chem.* **1980**, *45*, 1835. (b) Uemura, M.; Tokuyama, S.; Sakan, T. "Selective Nuclear Lithiation of Aromatic Compounds: Facile Synthesis of Methoxyphthalide Derivatives by Carboxylation of the Lithio-Compounds." *Chem. Lett.* **1975**, 1195.

47. (a) Rewcastle, G. W.; Denny, W. A. "Lithiation Routes to Oxindoles and 2-Indolinethiones: Precursors to 2,2′-Dithiobisindoles with Tyrosine Kinase Inhibitory Properties." *Heterocycles* **1994**, *37*, 701. (b) Katritsky, A. R.; Fan, W-Q.; Akutagawa, K.; Wang, J. "Carbon Dioxide: A Reagent for the Simultaneous Protection of Nucleophilic Centers and the Activation of Alternative Locations to Electrophilic Attack. 16.[1] A Novel Synthetic Method for the Side-chain Functionalization of *N*-Methyl-o-Toluidine and For the Preparation of 2-Substituted *N*-Methylindoles." *Heterocycles* **1990**, *30*, 407.

48. Rawal, V. H.; Jones, R. J.; Cava, M. P. "Photocyclization Strategy for the Synthesis of Antitumor Agent CC-1065: Synthesis of Dideoxy PDE-I and PDE-II. Synthesis of Thiophene and Furan Analogs of Dideoxy PDE-I and PDE-II." *J. Org. Chem.* **1987**, *52*, 19.

49. Hoffman, M.; Kessler, H. "Competition of Deprotonation and Tin-Lithium Exchange in the Generation of a Glycosyl Dianion." *Tetrahedron Lett.* **1997**, *38*, 1903.

50. Yin, J.; Buchwald, S. L. "Pd-Catalyzed Intermolecular Amidation of Aryl Halides: The Discovery that Xantphos Can Be Trans-chelating in a Palladium Complex." *J. Am. Chem. Soc.* **2002**, *124*, 6043.

51. Klapars, A.; Huang, X.; Buchwald, S. L. “A General and Efficient Copper Catalyst for the Amidation of Aryl Halides.” *J. Am. Chem. Soc*. **2002**, *124*, 7421.

52. Kametani, T.; Kigawa, Y.; Ihara, M. “Studies on the Synthesis of Heterocyclic Compounds. Synthesis of 3-benzyl-6-methyl-2-oxo-3,6-diazabicyclo[3.1.0]hexane as a Synthetic Intermediate of Mitomycins.” *Tetrahedron* **1979**, *35*, 313.

53. Mander, L. N.; Shing, T. K. M.; Yeung, Y. Y. “Methyl Cyanoformat.” In *e-EROS Encyclopedia of Reagents of Organic Synthesis* [Online]. John Wiley & Sons, Ltd.: 2006. DOI: 10.1002/047084289X.rm168.pub2.

54. Lamblin, M.; Couture, A.; Deniau, E.; Grandclaudon, P. “Alternative and Complementary Approaches to the Asymmetric Synthesis of C3 Substituted NH Free or *N*-substituted isoindolin-1-ones.” *Tetrahedron: Asymmetry* **2008**, *19*, 111.

55. Ohira, S. “Methanolysis of Dimethyl(1-Diazo-2-oxopropyl)Phosphonate: Generation of Dimethyl(Diazomethyl)Phosphonate and Reaction with Carbonyl Compounds.” *Synth. Commun.* **1989**, *19*, 561.

56. (a) Bondarenko, L.; Hentschel, S.; Greiving, H.; Grunenberg, J.; Hopf, H.; Dix, I.; Jones, P. G.; Ernst, L. “Intramolecular Reactions in Pseudo-Geminally Substituted [2.2]paracyclophanes.” *Chem.-Eur. J.* **2007**, *13*, 3950. (b) Karpov, G. V.; Popik, V. V. “Triggering the Bergman Cyclization by Photochemical Ring Contraction. Facile Cycloaromatization of Benzannulated Cyclodeca-3,7-diene-1,5-diynes.” *J. Am. Chem. Soc.* **2007**, *129*, 3792.

57. Tsantrizos, Y. S.;Yang, X.; McClory, A. “Studies on the Biosynthesis of the Fungal Metabolite Oudenone. 2. Synthesis and Enzymatic Cyclization of an α-Diketone, Open-chain Precursor into Oudenone in Cultures of *Oudemansiella radicata*.” *J. Org. Chem.* **1999**, *64*, 6609.

58. Golinshi, M.; Brock, C. P.; Watt, D. S. “Addition of *tert*-Butyldimethyl- or *tert*-butyldiphenysilyl Cyanide to Hindered Ketones.” *J. Org. Chem.* **1993**, *58*, 159.

59. Snieckus, V. “Directed ortho-Metalation. Tertiary Amide and *O*-Carbamate Directors in Synthetic Strategies for Polysubstituted Aromatics.” *Chem. Rev.* **1990**, *90*, 879.

60. (a) Lee, J.; Du Ha, J.; Cha, J. K. “New Synthetic Method for Functionalized Pyrrolizidine, Indolizidine, and Mitomycin Alkaloids.” *J. Am. Chem. Soc.* **1997**, *119*, 8127. (b) Lee, J.; Cha, J. K. “Facile Preparation of Cyclopropylamines from Carboxamides.” *J. Org. Chem.***1997**, *62*, 1584.

61. Okamoto, S.; Kasatkin, A.; Zubaidha, P. K.; Sato, F. “Intramolecular Nucleophilic Acyl Substitution Reactions Mediated by $XTi(O\text{-}i\text{-}Pr)_3$ (X = Cl, O-*i*-Pr)/2*i*-PrMgBr Reagent. Efficient Synthesis of Functionalized Organotitanium Compounds from Unsaturated Compounds.” *J. Am. Chem. Soc*. **1996**, *118*, 2208.

62. Soderquist, J. A.; Santiago, B. “Alkynylsilanes to *cis*-Vinylsilanes via Hydroboration.” *Tetrahedron Lett.* **1990**, *31*, 5113.

63. For recent examples: (a) Deguest, G.; Bischoff, L.; Fruit, C.; Marsais, F. “Anionic, in Situ Generation of Formaldehyde: A Very Useful and Versatile Tool in Synthesis.” *Org. Lett.* **2007**, *9*,

1165. (b) Wilson, R. A.; Chan, L.; Wood, R.; Brown, R. C. D. “Synthesis and Derivatisation of a Novel Spiro[1-benzofuran-2,4′-piperidin]-3-one scaffold.” *Org. Biomol. Chem.* **2005**, *3*, 3228.

64. (a) Kraus, G. A.; Wan, Z. “Synthesis of Angularly-Fused Aromatic Antibiotics. Preparation of the ABC Ring System of Aquayamycin.” *Tetrahedron Lett.* **1997**, 6509. (b) Hong, F-T.; Paquette, L. A. “Efficient Stereocontrolled Synthesis of the ABC Subunit of Dumsin.” *Tetrahedron Lett.* **1994**, *35*, 1994.

65. Schkeryantz, J. M.; Danishefsky, S. J. “Total Synthesis of (±)-FR900482.” *J. Am. Chem. Soc.* **1995**, *117*, 4722.

66. (a) Wang, Z.; Ning, S.; Cusick, J. R.; Williams, L. J. “Designed rearrangement of a spriodiepoxide.” *Synlett* **2008**, 213. (b) Thompson, A. L. S.; Kabalka, G. W.; Akula, M. R.; Huffman, J. W. “The conversion of phenols to the corresponding aryl halids under mild conditions.” *Synthesis* **2005**, 547.

67. Lampe, J. W.; Hughes, P. F.; Biggers, C. K.; Smith, S. H.; Hu, H. “Total Synthesis of (-)- and (+)-Balanol.” *J. Org. Chem.* **1996**, *61*, 4572.

68. Curtis, W. D.; Stoddart, F. “1,6,13,18,25,30-Hexaoxa[6.6.6](1,3,5)cyclophane. Attempted Synthesis of a [4] Cryptand.” *J. C. S. Perkin I* **1977**, 220.

69. Hendrickson, J. B.; Ramsay, M. V. J.; Kelly, T. R. “New Synthesis of Depsidones. Diploicin and gangaleoidin.” *J. Am. Chem. Soc.* **1972**, *94*, 6834.

70. Frantz, D. E.; Weaver, D. G.; Carey, J. P.; Kress, M. H.; Dolling, U. H. “Practical Synthesis of Aryl Triflates under Aqueous Conditions.” *Org. Lett.* **2006**, *8*, 2627.

71. Ritter, K. “Synthetic Transformations of Vinyl and Aryl Triflates.” *Synthesis* **1993**, 735.

72. Pineschi, M.; Bertolini, F.; Crotti, P.; Macchia, F. “Facile Regio- and Stereoselective Carbon-Carbon Coupling of Phenol Derivatives with Aryl Aziridines.” *Org. Lett.* **2006**, *8*, 2627.

73. Wolfe, J. P.; Buchwald, S. L. “Palladium-Catalyzed Amination of Aryl Triflates.” *J. Org. Chem.* **1997**, *62*, 1264.

74. (a) Anderson, K. W.; Mendez-Perez, M.; Priego, J.; Buchwald, S. L. “Palladium-Catalyzed Amination of Aryl Nonaflates.” *J. Org. Chem.* **2003**, *68*, 9563. (b) Old, D. W.; Harris, M. C.; Buchwald, S. L. “Efficient Palladium-Catalyzed *N*-Arylation of Indoles.” *Org. Lett.* **2000**, *2*, 1403. (c) Wolfe, J. P.; Tomori, H.; Sadighi, J. P.; Yin, J.; Buchwald, S. L. “Simple, Efficient Catalyst System for the Palladium-Catalyzed Amination of Aryl Chlorides, Bromides, and Triflates.” *J. Org. Chem.* **2000**, *65*, 1158.

75. Greenlee, W.J.; Hangauer, D.G. “Addition of Trimethylsilyl cyanide to α-substituted ketones: Catalyst Efficiency.” *Tetrahedron Lett.* **1983,** *24*, 4559.

76. Watson, S. c.; Eastham, J. F. Colored Indicators for Simple Direct Titration of Magnesium and Lithium reagents. *J. Organometallic Chem.* **1967**, *9*, 165.

77. Nakahira, H.; Kimura, H.; Kobayashi, T.; Hochigai, H. “Preparation of Imidazopyridinone Derivatives as DPP-IV Inhibitors for the Treatment of Diabetes.” PCT. Int. Appl. WO 2005051949 A1 20050609, 2005.

78. Ple, P.; Juang, F. H. “Preparation of Quinazoline Derivatives for use in Cell Proliferative Disorders or Disease assocd. with Angiogenesis and/or Vascular Permability.” PCT. Int. Appl. WO 2006040526 A1 20060420, 2006.

79.Vedjes, E.; Little, J. D.; Seaney, L. M. “Synthesis of the Aziridinomitosene Skeleton by Intramolecular Michael Addition: α-Lithioaziridines and Nonaromatic Substrates.” *J. Org. Chem.* **2004**, *69*, 1788.

80. Moraczewski, A. L.; Banaszynski, L. A.; From, A. M.; White, C. E.; Smith, B. D. “Using Hydrogen Bonding to Control Carbamate C-N Rotamer Equilibria.” *J. Org. Chem.* **1998**, *63*, 7258.

81. Kehoe, J. M.; Kiley, J. H.; English, J. J.; Johnson, C. A.; Peterson, R. C.; Haley, M. M. “Carbon Networks Based on Dihydrobenzoannulenes. 3. Synthesis of Graphyne Substructures.” *Org. Lett.* **2000**, *2*, 969.

Appendix A

X-ray Crystal Structure of **90**

Asymmetric Unit

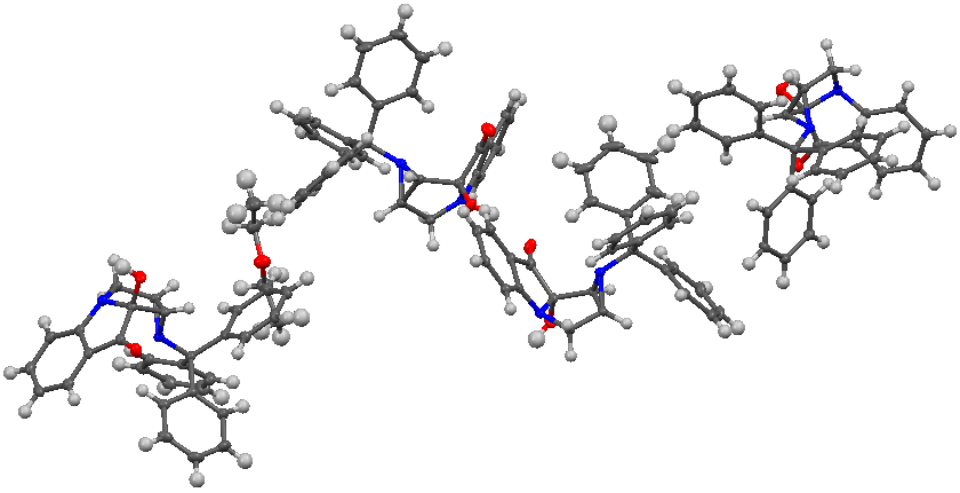

One crystallographically independent molecule of the asymmetric unit

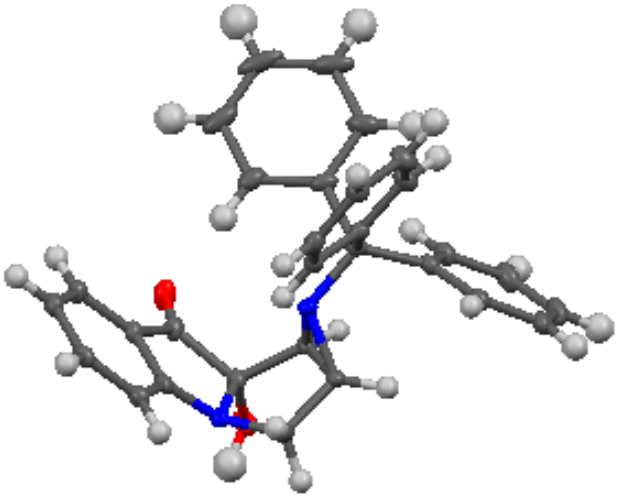

Structure Determination.

Yellow needles of **sd40** were grown from a diethyl ether solution at 25 deg. C. A crystal of dimensions 0.34 x 0.19 x 0.13 mm was mounted on a Bruker SMART APEX CCD-based X-ray diffractometer equipped with a low temperature device and fine focus Mo-target X-ray tube (λ = 0.71073 A) operated at 1500 W power (50 kV, 30 mA). The X-ray intensities were measured at 85(1) K; the detector was placed at a distance 5.055 cm from the crystal. A total of 3182 frames were collected with a scan width of 0.5° in ω and 0.45° in phi with an exposure time of 15 s/frame. The integration of the data yielded a total of 132594 reflections to a maximum 2θ value of 56.70° of which 12817 were independent and 11858 were greater than $2\sigma(I)$. The final cell constants (Table 1) were based on the xyz centroids of 9977 reflections above $10\sigma(I)$. Analysis of the data showed negligible decay during data collection; the data were processed with SADABS and corrected for absorption. The structure was solved and refined with the Bruker SHELXTL (version 2008/3) software package, using the space group P2(1) with Z = 2 for the formula $4(C_{30}H_{24}N_2O_2)\cdot C_4H_{10}O$. There are 4 crystallographically independent molecules in the asymmetric unit. All of the molecules have the same 'S' chirality based on assignment to a known center. During refinement, Friedel pairs were merged for this light-atom structure. All non-hydrogen atoms were refined anisotropically with the hydrogen atoms placed in idealized positions except for those involved in hydrogen bonding which were allowed to refine isotropically. Full matrix least-squares refinement based on F^2 converged at R1 = 0.0368 and wR2 = 0.0913 [based on I > 2sigma(I)], R1 = 0.0410 and wR2 = 0.0943 for all data. Additional details are presented in Table 1 and are given as Supporting Information in a CIF file.

Sheldrick, G.M. SHELXTL, v. 2008/3; Bruker Analytical X-ray, Madison, WI, 2008.

Sheldrick, G.M. SADABS, v. 2008/1. Program for Empirical Absorption Correction of Area Detector Data, University of Gottingen: Gottingen, Germany, 2008.

Saint Plus, v. 7.53a, Bruker Analytical X-ray, Madison, WI, 2008.

Table 1. Crystal data and structure refinement for sd40.

Identification code	sd40
Empirical formula	C124 H106 N8 O9
Formula weight	1852.17
Temperature	85(2) K
Wavelength	0.71073 A
Crystal system, space group	Monoclinic, P2(1)
Unit cell dimensions	a = 20.3120(9) A alpha = 90°. b = 9.5308(4)A beta =107.355(1)°. c = 26.2849(12) A gamma = 90 °.
Volume	4856.8(4) A^3
Z, Calculated density	2, 1.267 Mg/m^3
Absorption coefficient	0.080 mm^-1
F(000)	1956
Crystal size	0.34 x 0.19 x 0.13 mm
Theta range for data collection	1.05 to 28.35 deg.
Limiting indices	-27<=h<=27, -12<=k<=12, -35<=l<=35
Reflections collected / unique	132594 / 12817 [R(int) = 0.0514]
Completeness to theta = 28.35	99.7 %
Absorption correction	Semi-empirical from equivalents
Max. and min. transmission	0.9897 and 0.9733
Refinement method	Full-matrix least-squares on F^2
Data / restraints / parameters	12817 / 1 / 1288
Goodness-of-fit on F^2	1.030
Final R indices [I>2sigma(I)]	R1 = 0.0368, wR2 = 0.0913
R indices (all data)	R1 = 0.0410, wR2 = 0.0943

Absolute structure parameter	0(10)
Largest diff. peak and hole	0.527 and -0.320 e.A^-3

Table 2. Atomic coordinates (x 10^4) and equivalent isotropic displacement parameters (A^2 x 10^3) for sd40. U(eq) is defined as one third of the trace of the orthogonalized Uij tensor.

	x	y	z	U(eq)
O(1)	2113(1)	6300(2)	9357(1)	24(1)
O(2)	1781(1)	9235(2)	9106(1)	23(1)
O(3)	2452(1)	1337(2)	-248(1)	25(1)
O(4)	2830(1)	4254(2)	30(1)	24(1)
O(5)	2554(1)	4075(2)	5555(1)	26(1)
O(6)	2573(1)	1086(2)	5745(1)	25(1)
O(7)	2587(1)	8810(2)	5128(1)	27(1)
O(8)	2656(1)	5916(2)	4794(1)	23(1)
O(9)	6112(1)	4971(2)	2827(1)	34(1)
N(1)	1088(1)	8933(2)	9699(1)	17(1)
N(2)	157(1)	7390(2)	8959(1)	15(1)
N(3)	3836(1)	3623(2)	-226(1)	18(1)
N(4)	4316(1)	2088(2)	684(1)	16(1)
N(5)	1375(1)	1238(2)	5233(1)	17(1)
N(6)	1064(1)	2598(2)	6046(1)	15(1)
N(7)	3877(1)	6370(2)	5076(1)	18(1)
N(8)	3743(1)	7965(2)	4199(1)	16(1)
C(1)	1738(1)	6979(2)	9550(1)	17(1)
C(2)	1358(1)	8325(2)	9286(1)	17(1)
C(3)	419(1)	9628(2)	9450(1)	18(1)
C(4)	150(1)	8927(2)	8911(1)	18(1)
C(5)	719(1)	8081(2)	8815(1)	17(1)
C(6)	-345(1)	6518(2)	8550(1)	15(1)
C(7)	-973(1)	6264(2)	8752(1)	16(1)
C(8)	-1001(1)	6778(2)	9242(1)	18(1)
C(9)	-1562(1)	6465(2)	9424(1)	20(1)
C(10)	-2091(1)	5620(2)	9127(1)	21(1)
C(11)	-2070(1)	5113(2)	8635(1)	21(1)
C(12)	-1520(1)	5444(2)	8449(1)	19(1)
C(13)	2(1)	5078(2)	8548(1)	16(1)
C(14)	516(1)	4624(2)	8999(1)	19(1)
C(15)	832(1)	3318(2)	9010(1)	23(1)
C(16)	623(1)	2429(2)	8574(1)	24(1)
C(17)	95(1)	2854(2)	8129(1)	23(1)
C(18)	-211(1)	4164(2)	8114(1)	19(1)
C(19)	-563(1)	7229(2)	8002(1)	17(1)
C(20)	-1119(1)	8166(2)	7868(1)	19(1)
C(21)	-1280(1)	8932(2)	7397(1)	25(1)
C(22)	-900(1)	8755(3)	7041(1)	28(1)
C(23)	-350(1)	7826(3)	7166(1)	26(1)
C(24)	-177(1)	7084(2)	7645(1)	21(1)
C(25)	1140(1)	7916(2)	10090(1)	16(1)
C(26)	1551(1)	6771(2)	10042(1)	17(1)
C(27)	1679(1)	5664(2)	10406(1)	21(1)
C(28)	1386(1)	5722(2)	10820(1)	22(1)
C(29)	976(1)	6869(2)	10867(1)	21(1)

C(30)	846(1)	7970(2)	10508(1)	19(1)
C(31)	2973(1)	1895(2)	-297(1)	18(1)
C(32)	3304(1)	3205(2)	20(1)	18(1)
C(33)	4441(1)	4213(2)	184(1)	22(1)
C(34)	4386(1)	3619(2)	706(1)	20(1)
C(35)	3696(1)	2946(2)	601(1)	18(1)
C(36)	4561(1)	1256(2)	1188(1)	16(1)
C(37)	4370(1)	1948(2)	1656(1)	18(1)
C(38)	4800(1)	2939(2)	1987(1)	20(1)
C(39)	4597(1)	3616(2)	2385(1)	25(1)
C(40)	3958(1)	3338(2)	2452(1)	27(1)
C(41)	3519(1)	2382(2)	2119(1)	24(1)
C(42)	3726(1)	1690(2)	1728(1)	21(1)
C(43)	5348(1)	1091(2)	1312(1)	18(1)
C(44)	5692(1)	1459(2)	946(1)	22(1)
C(45)	6406(1)	1267(2)	1067(1)	26(1)
C(46)	6778(1)	691(3)	1547(1)	31(1)
C(47)	6441(1)	305(3)	1912(1)	34(1)
C(48)	5735(1)	510(2)	1798(1)	25(1)
C(49)	4228(1)	-210(2)	1059(1)	18(1)
C(50)	3928(1)	-640(2)	538(1)	21(1)
C(51)	3624(1)	-1963(2)	421(1)	27(1)
C(52)	3630(1)	-2887(2)	828(1)	31(1)
C(53)	3946(1)	-2489(2)	1350(1)	32(1)
C(54)	4237(1)	-1164(2)	1466(1)	25(1)
C(55)	3905(1)	2556(2)	-568(1)	18(1)
C(56)	3389(1)	1528(2)	-641(1)	17(1)
C(57)	3347(1)	386(2)	-984(1)	21(1)
C(58)	3832(1)	286(2)	-1256(1)	23(1)
C(59)	4345(1)	1314(2)	-1183(1)	24(1)
C(60)	4396(1)	2447(2)	-841(1)	22(1)
C(61)	2053(1)	3313(2)	5377(1)	19(1)
C(62)	1968(1)	1890(2)	5628(1)	18(1)
C(63)	956(1)	429(2)	5503(1)	20(1)
C(64)	1136(1)	1058(2)	6056(1)	18(1)
C(65)	1751(1)	1978(2)	6135(1)	16(1)
C(66)	901(1)	3313(2)	6500(1)	16(1)
C(67)	110(1)	3517(2)	6330(1)	17(1)
C(68)	-303(1)	3233(2)	5814(1)	18(1)
C(69)	-1008(1)	3527(2)	5662(1)	20(1)
C(70)	-1306(1)	4134(2)	6018(1)	21(1)
C(71)	-896(1)	4425(2)	6536(1)	25(1)
C(72)	-198(1)	4102(2)	6691(1)	23(1)
C(73)	1207(1)	4805(2)	6543(1)	20(1)
C(74)	1330(1)	5429(2)	6102(1)	25(1)
C(75)	1575(1)	6801(2)	6129(1)	36(1)
C(76)	1684(1)	7571(3)	6590(1)	45(1)
C(77)	1557(1)	6969(3)	7032(1)	41(1)
C(78)	1323(1)	5593(3)	7012(1)	29(1)
C(79)	1165(1)	2472(2)	7019(1)	18(1)
C(80)	763(1)	1407(2)	7142(1)	20(1)
C(81)	1031(1)	519(2)	7575(1)	24(1)
C(82)	1705(1)	684(3)	7899(1)	29(1)
C(83)	2109(1)	1739(3)	7786(1)	28(1)
C(84)	1845(1)	2624(2)	7350(1)	22(1)
C(85)	1055(1)	2261(2)	4864(1)	17(1)
C(86)	1443(1)	3493(2)	4915(1)	18(1)
C(87)	1208(1)	4641(2)	4579(1)	20(1)
C(88)	570(1)	4536(2)	4196(1)	20(1)
C(89)	186(1)	3290(2)	4144(1)	20(1)
C(90)	418(1)	2142(2)	4471(1)	19(1)
C(91)	3128(1)	8199(2)	5166(1)	18(1)
C(92)	3174(1)	6903(2)	4826(1)	18(1)

C(93)	4151(1)	5733(2)	4668(1)	20(1)
C(94)	3739(1)	6427(2)	4151(1)	18(1)
C(95)	3147(1)	7187(2)	4250(1)	17(1)
C(96)	3666(1)	8863(2)	3718(1)	16(1)
C(97)	4399(1)	9121(2)	3681(1)	17(1)
C(98)	4984(1)	8587(2)	4053(1)	19(1)
C(99)	5643(1)	8878(2)	4016(1)	23(1)
C(100)	5723(1)	9727(2)	3610(1)	23(1)
C(101)	5142(1)	10265(2)	3237(1)	24(1)
C(102)	4488(1)	9959(2)	3268(1)	21(1)
C(103)	3204(1)	8183(2)	3202(1)	18(1)
C(104)	2483(1)	8289(2)	3068(1)	21(1)
C(105)	2060(1)	7617(2)	2619(1)	25(1)
C(106)	2345(1)	6835(3)	2295(1)	29(1)
C(107)	3058(1)	6698(2)	2427(1)	27(1)
C(108)	3482(1)	7368(2)	2877(1)	22(1)
C(109)	3374(1)	10277(2)	3836(1)	18(1)
C(110)	3051(1)	11212(2)	3426(1)	24(1)
C(111)	2807(1)	12501(2)	3541(1)	31(1)
C(112)	2870(1)	12881(2)	4061(1)	31(1)
C(113)	3197(1)	11980(2)	4469(1)	28(1)
C(114)	3452(1)	10693(2)	4359(1)	21(1)
C(115)	4246(1)	7388(2)	5422(1)	17(1)
C(116)	3821(1)	8467(2)	5512(1)	18(1)
C(117)	4088(1)	9554(2)	5872(1)	21(1)
C(118)	4786(1)	9557(2)	6135(1)	22(1)
C(119)	5208(1)	8483(2)	6042(1)	21(1)
C(120)	4953(1)	7397(2)	5687(1)	21(1)
C(121)	6719(1)	4151(3)	3023(1)	32(1)
C(122)	6506(1)	2674(3)	3100(1)	34(1)
C(123)	6256(1)	6407(3)	2802(1)	38(1)
C(124)	5581(2)	7184(3)	2615(1)	42(1)

Table 3. Bond lengths [A] and angles [deg] for sd40.

O(1)-C(1)	1.219(2)
O(2)-C(2)	1.398(2)
O(3)-C(31)	1.225(2)
O(4)-C(32)	1.395(2)
O(5)-C(61)	1.224(2)
O(6)-C(62)	1.403(2)
O(7)-C(91)	1.223(2)
O(8)-C(92)	1.396(2)
O(9)-C(123)	1.405(3)
O(9)-C(121)	1.420(3)
N(1)-C(25)	1.395(2)
N(1)-C(2)	1.472(2)
N(1)-C(3)	1.476(2)
N(2)-C(5)	1.462(2)
N(2)-C(4)	1.470(2)
N(2)-C(6)	1.494(2)
N(3)-C(55)	1.393(3)
N(3)-C(32)	1.469(2)
N(3)-C(33)	1.482(2)
N(4)-C(35)	1.462(2)
N(4)-C(34)	1.466(2)
N(4)-C(36)	1.496(2)
N(5)-C(85)	1.392(2)
N(5)-C(62)	1.472(2)
N(5)-C(63)	1.476(2)

N(6)-C(65)	1.468(2)
N(6)-C(64)	1.474(2)
N(6)-C(66)	1.494(2)
N(7)-C(115)	1.388(2)
N(7)-C(92)	1.473(2)
N(7)-C(93)	1.477(2)
N(8)-C(95)	1.459(2)
N(8)-C(94)	1.472(2)
N(8)-C(96)	1.497(2)
C(1)-C(26)	1.466(2)
C(1)-C(2)	1.549(3)
C(2)-C(5)	1.522(2)
C(3)-C(4)	1.514(3)
C(4)-C(5)	1.491(3)
C(6)-C(19)	1.533(2)
C(6)-C(7)	1.540(2)
C(6)-C(13)	1.544(3)
C(7)-C(8)	1.396(3)
C(7)-C(12)	1.397(3)
C(8)-C(9)	1.392(3)
C(9)-C(10)	1.383(3)
C(10)-C(11)	1.392(3)
C(11)-C(12)	1.385(3)
C(13)-C(14)	1.396(3)
C(13)-C(18)	1.396(3)
C(14)-C(15)	1.397(3)
C(15)-C(16)	1.388(3)
C(16)-C(17)	1.390(3)
C(17)-C(18)	1.390(3)
C(19)-C(24)	1.398(3)
C(19)-C(20)	1.400(3)
C(20)-C(21)	1.389(3)
C(21)-C(22)	1.389(3)
C(22)-C(23)	1.386(3)
C(23)-C(24)	1.395(3)
C(25)-C(30)	1.398(3)
C(25)-C(26)	1.404(3)
C(26)-C(27)	1.396(3)
C(27)-C(28)	1.388(3)
C(28)-C(29)	1.402(3)
C(29)-C(30)	1.383(3)
C(31)-C(56)	1.451(3)
C(31)-C(32)	1.540(3)
C(32)-C(35)	1.516(3)
C(33)-C(34)	1.518(3)
C(34)-C(35)	1.491(3)
C(36)-C(37)	1.541(3)
C(36)-C(43)	1.541(3)
C(36)-C(49)	1.545(3)
C(37)-C(42)	1.400(3)
C(37)-C(38)	1.400(3)
C(38)-C(39)	1.392(3)
C(39)-C(40)	1.385(3)
C(40)-C(41)	1.388(3)
C(41)-C(42)	1.387(3)
C(43)-C(44)	1.393(3)
C(43)-C(48)	1.399(3)
C(44)-C(45)	1.400(3)
C(45)-C(46)	1.377(3)
C(46)-C(47)	1.385(3)
C(47)-C(48)	1.389(3)
C(49)-C(50)	1.386(3)
C(49)-C(54)	1.401(3)

C(50)-C(51)	1.397(3)
C(51)-C(52)	1.383(3)
C(52)-C(53)	1.383(3)
C(53)-C(54)	1.389(3)
C(55)-C(60)	1.395(3)
C(55)-C(56)	1.405(3)
C(56)-C(57)	1.400(3)
C(57)-C(58)	1.381(3)
C(58)-C(59)	1.401(3)
C(59)-C(60)	1.390(3)
C(61)-C(86)	1.463(3)
C(61)-C(62)	1.541(3)
C(62)-C(65)	1.524(2)
C(63)-C(64)	1.513(3)
C(64)-C(65)	1.489(3)
C(66)-C(79)	1.535(3)
C(66)-C(73)	1.542(3)
C(66)-C(67)	1.545(2)
C(67)-C(68)	1.392(3)
C(67)-C(72)	1.401(3)
C(68)-C(69)	1.395(3)
C(69)-C(70)	1.384(3)
C(70)-C(71)	1.394(3)
C(71)-C(72)	1.387(3)
C(73)-C(74)	1.391(3)
C(73)-C(78)	1.401(3)
C(74)-C(75)	1.393(3)
C(75)-C(76)	1.377(4)
C(76)-C(77)	1.388(4)
C(77)-C(78)	1.390(3)
C(79)-C(80)	1.400(3)
C(79)-C(84)	1.404(3)
C(80)-C(81)	1.392(3)
C(81)-C(82)	1.390(3)
C(82)-C(83)	1.385(3)
C(83)-C(84)	1.395(3)
C(85)-C(86)	1.398(3)
C(85)-C(90)	1.400(3)
C(86)-C(87)	1.398(3)
C(87)-C(88)	1.387(3)
C(88)-C(89)	1.405(3)
C(89)-C(90)	1.384(3)
C(91)-C(116)	1.453(3)
C(91)-C(92)	1.543(3)
C(92)-C(95)	1.524(3)
C(93)-C(94)	1.519(3)
C(94)-C(95)	1.491(3)
C(96)-C(97)	1.539(3)
C(96)-C(109)	1.541(3)
C(96)-C(103)	1.542(3)
C(97)-C(98)	1.391(3)
C(97)-C(102)	1.402(3)
C(98)-C(99)	1.399(3)
C(99)-C(100)	1.387(3)
C(100)-C(101)	1.388(3)
C(101)-C(102)	1.386(3)
C(103)-C(108)	1.393(3)
C(103)-C(104)	1.403(3)
C(104)-C(105)	1.391(3)
C(105)-C(106)	1.383(3)
C(106)-C(107)	1.391(3)
C(107)-C(108)	1.393(3)
C(109)-C(114)	1.393(3)

C(109)-C(110)	1.401(3)
C(110)-C(111)	1.391(3)
C(111)-C(112)	1.384(3)
C(112)-C(113)	1.380(3)
C(113)-C(114)	1.396(3)
C(115)-C(120)	1.396(3)
C(115)-C(116)	1.405(3)
C(116)-C(117)	1.399(3)
C(117)-C(118)	1.379(3)
C(118)-C(119)	1.401(3)
C(119)-C(120)	1.387(3)
C(121)-C(122)	1.503(4)
C(123)-C(124)	1.507(4)

C(123)-O(9)-C(121)	112.55(19)
C(25)-N(1)-C(2)	107.89(15)
C(25)-N(1)-C(3)	119.75(15)
C(2)-N(1)-C(3)	110.30(14)
C(5)-N(2)-C(4)	61.15(13)
C(5)-N(2)-C(6)	118.86(14)
C(4)-N(2)-C(6)	120.38(15)
C(55)-N(3)-C(32)	108.33(15)
C(55)-N(3)-C(33)	121.69(16)
C(32)-N(3)-C(33)	110.05(15)
C(35)-N(4)-C(34)	61.23(13)
C(35)-N(4)-C(36)	118.27(14)
C(34)-N(4)-C(36)	119.44(15)
C(85)-N(5)-C(62)	108.03(15)
C(85)-N(5)-C(63)	118.99(15)
C(62)-N(5)-C(63)	110.46(14)
C(65)-N(6)-C(64)	60.79(13)
C(65)-N(6)-C(66)	118.88(14)
C(64)-N(6)-C(66)	119.01(15)
C(115)-N(7)-C(92)	108.21(15)
C(115)-N(7)-C(93)	121.16(16)
C(92)-N(7)-C(93)	110.11(14)
C(95)-N(8)-C(94)	61.17(12)
C(95)-N(8)-C(96)	119.19(14)
C(94)-N(8)-C(96)	119.98(15)
O(1)-C(1)-C(26)	130.71(18)
O(1)-C(1)-C(2)	123.00(17)
C(26)-C(1)-C(2)	106.28(15)
O(2)-C(2)-N(1)	114.07(16)
O(2)-C(2)-C(5)	106.22(15)
N(1)-C(2)-C(5)	104.09(15)
O(2)-C(2)-C(1)	112.99(15)
N(1)-C(2)-C(1)	104.06(14)
C(5)-C(2)-C(1)	115.29(16)
N(1)-C(3)-C(4)	104.15(15)
N(2)-C(4)-C(5)	59.15(12)
N(2)-C(4)-C(3)	111.58(16)
C(5)-C(4)-C(3)	108.31(15)
N(2)-C(5)-C(4)	59.70(12)
N(2)-C(5)-C(2)	113.67(15)
C(4)-C(5)-C(2)	107.25(15)
N(2)-C(6)-C(19)	111.97(15)
N(2)-C(6)-C(7)	107.24(14)
C(19)-C(6)-C(7)	110.92(15)
N(2)-C(6)-C(13)	106.46(14)
C(19)-C(6)-C(13)	113.19(15)
C(7)-C(6)-C(13)	106.69(15)
C(8)-C(7)-C(12)	118.58(17)
C(8)-C(7)-C(6)	122.00(16)

C(12)-C(7)-C(6)	119.36(16)
C(9)-C(8)-C(7)	120.27(18)
C(10)-C(9)-C(8)	120.62(18)
C(9)-C(10)-C(11)	119.51(18)
C(12)-C(11)-C(10)	120.03(18)
C(11)-C(12)-C(7)	120.95(17)
C(14)-C(13)-C(18)	118.11(18)
C(14)-C(13)-C(6)	119.95(17)
C(18)-C(13)-C(6)	121.84(16)
C(13)-C(14)-C(15)	121.13(19)
C(16)-C(15)-C(14)	120.07(19)
C(15)-C(16)-C(17)	119.16(19)
C(18)-C(17)-C(16)	120.71(19)
C(17)-C(18)-C(13)	120.76(18)
C(24)-C(19)-C(20)	117.78(17)
C(24)-C(19)-C(6)	121.62(17)
C(20)-C(19)-C(6)	120.26(16)
C(21)-C(20)-C(19)	121.19(18)
C(22)-C(21)-C(20)	120.4(2)
C(23)-C(22)-C(21)	119.25(19)
C(22)-C(23)-C(24)	120.4(2)
C(23)-C(24)-C(19)	120.95(19)
N(1)-C(25)-C(30)	126.71(18)
N(1)-C(25)-C(26)	112.88(16)
C(30)-C(25)-C(26)	120.39(18)
C(27)-C(26)-C(25)	121.27(17)
C(27)-C(26)-C(1)	131.54(18)
C(25)-C(26)-C(1)	107.05(16)
C(28)-C(27)-C(26)	118.14(19)
C(27)-C(28)-C(29)	120.37(19)
C(30)-C(29)-C(28)	121.95(18)
C(29)-C(30)-C(25)	117.89(18)
O(3)-C(31)-C(56)	129.95(18)
O(3)-C(31)-C(32)	123.12(17)
C(56)-C(31)-C(32)	106.93(16)
O(4)-C(32)-N(3)	114.63(16)
O(4)-C(32)-C(35)	104.76(15)
N(3)-C(32)-C(35)	104.69(15)
O(4)-C(32)-C(31)	113.50(15)
N(3)-C(32)-C(31)	103.99(15)
C(35)-C(32)-C(31)	115.24(16)
N(3)-C(33)-C(34)	104.24(15)
N(4)-C(34)-C(35)	59.26(12)
N(4)-C(34)-C(33)	111.68(17)
C(35)-C(34)-C(33)	108.20(16)
N(4)-C(35)-C(34)	59.50(12)
N(4)-C(35)-C(32)	114.31(15)
C(34)-C(35)-C(32)	107.31(16)
N(4)-C(36)-C(37)	112.48(15)
N(4)-C(36)-C(43)	106.88(14)
C(37)-C(36)-C(43)	111.50(15)
N(4)-C(36)-C(49)	106.05(14)
C(37)-C(36)-C(49)	111.43(15)
C(43)-C(36)-C(49)	108.20(15)
C(42)-C(37)-C(38)	117.94(17)
C(42)-C(37)-C(36)	119.98(17)
C(38)-C(37)-C(36)	121.83(17)
C(39)-C(38)-C(37)	120.75(19)
C(40)-C(39)-C(38)	120.3(2)
C(39)-C(40)-C(41)	119.66(19)
C(42)-C(41)-C(40)	120.03(19)
C(41)-C(42)-C(37)	121.26(19)
C(44)-C(43)-C(48)	117.92(18)

C(44)-C(43)-C(36)	122.18(17)
C(48)-C(43)-C(36)	119.86(17)
C(43)-C(44)-C(45)	120.71(19)
C(46)-C(45)-C(44)	120.5(2)
C(45)-C(46)-C(47)	119.4(2)
C(46)-C(47)-C(48)	120.4(2)
C(47)-C(48)-C(43)	121.1(2)
C(50)-C(49)-C(54)	117.75(19)
C(50)-C(49)-C(36)	121.32(17)
C(54)-C(49)-C(36)	120.91(17)
C(49)-C(50)-C(51)	121.3(2)
C(52)-C(51)-C(50)	120.3(2)
C(53)-C(52)-C(51)	119.2(2)
C(52)-C(53)-C(54)	120.5(2)
C(53)-C(54)-C(49)	121.0(2)
N(3)-C(55)-C(60)	127.63(18)
N(3)-C(55)-C(56)	112.49(16)
C(60)-C(55)-C(56)	119.85(18)
C(57)-C(56)-C(55)	121.89(17)
C(57)-C(56)-C(31)	130.87(18)
C(55)-C(56)-C(31)	107.22(17)
C(58)-C(57)-C(56)	118.17(19)
C(57)-C(58)-C(59)	119.77(19)
C(60)-C(59)-C(58)	122.75(18)
C(59)-C(60)-C(55)	117.57(19)
O(5)-C(61)-C(86)	130.48(19)
O(5)-C(61)-C(62)	123.04(17)
C(86)-C(61)-C(62)	106.48(16)
O(6)-C(62)-N(5)	113.81(16)
O(6)-C(62)-C(65)	107.57(15)
N(5)-C(62)-C(65)	104.49(15)
O(6)-C(62)-C(61)	111.79(15)
N(5)-C(62)-C(61)	104.00(14)
C(65)-C(62)-C(61)	115.10(16)
N(5)-C(63)-C(64)	104.19(15)
N(6)-C(64)-C(65)	59.40(12)
N(6)-C(64)-C(63)	112.57(16)
C(65)-C(64)-C(63)	108.64(15)
N(6)-C(65)-C(64)	59.81(11)
N(6)-C(65)-C(62)	113.08(15)
C(64)-C(65)-C(62)	107.13(15)
N(6)-C(66)-C(79)	111.71(15)
N(6)-C(66)-C(73)	107.44(15)
C(79)-C(66)-C(73)	112.88(15)
N(6)-C(66)-C(67)	106.57(14)
C(79)-C(66)-C(67)	112.31(15)
C(73)-C(66)-C(67)	105.48(15)
C(68)-C(67)-C(72)	118.42(17)
C(68)-C(67)-C(66)	122.03(16)
C(72)-C(67)-C(66)	119.38(16)
C(67)-C(68)-C(69)	120.64(17)
C(70)-C(69)-C(68)	120.56(18)
C(69)-C(70)-C(71)	119.24(18)
C(72)-C(71)-C(70)	120.26(18)
C(71)-C(72)-C(67)	120.85(18)
C(74)-C(73)-C(78)	118.6(2)
C(74)-C(73)-C(66)	120.03(18)
C(78)-C(73)-C(66)	121.21(19)
C(73)-C(74)-C(75)	120.6(2)
C(76)-C(75)-C(74)	120.4(3)
C(75)-C(76)-C(77)	119.7(2)
C(76)-C(77)-C(78)	120.3(2)
C(77)-C(78)-C(73)	120.4(3)

C(80)-C(79)-C(84)	117.79(18)
C(80)-C(79)-C(66)	120.73(16)
C(84)-C(79)-C(66)	120.99(17)
C(81)-C(80)-C(79)	121.09(18)
C(82)-C(81)-C(80)	120.4(2)
C(83)-C(82)-C(81)	119.2(2)
C(82)-C(83)-C(84)	120.6(2)
C(83)-C(84)-C(79)	120.8(2)
N(5)-C(85)-C(86)	112.87(16)
N(5)-C(85)-C(90)	126.47(18)
C(86)-C(85)-C(90)	120.65(18)
C(87)-C(86)-C(85)	121.33(17)
C(87)-C(86)-C(61)	131.42(19)
C(85)-C(86)-C(61)	107.13(17)
C(88)-C(87)-C(86)	118.16(19)
C(87)-C(88)-C(89)	120.13(18)
C(90)-C(89)-C(88)	122.20(18)
C(89)-C(90)-C(85)	117.52(18)
O(7)-C(91)-C(116)	130.37(19)
O(7)-C(91)-C(92)	122.87(17)
C(116)-C(91)-C(92)	106.76(16)
O(8)-C(92)-N(7)	114.07(16)
O(8)-C(92)-C(95)	104.94(15)
N(7)-C(92)-C(95)	104.27(14)
O(8)-C(92)-C(91)	113.56(15)
N(7)-C(92)-C(91)	103.69(15)
C(95)-C(92)-C(91)	116.24(16)
N(7)-C(93)-C(94)	104.11(15)
N(8)-C(94)-C(95)	58.99(12)
N(8)-C(94)-C(93)	111.67(16)
C(95)-C(94)-C(93)	108.26(15)
N(8)-C(95)-C(94)	59.84(12)
N(8)-C(95)-C(92)	113.33(15)
C(94)-C(95)-C(92)	107.17(15)
N(8)-C(96)-C(97)	106.57(14)
N(8)-C(96)-C(109)	106.14(14)
C(97)-C(96)-C(109)	108.10(15)
N(8)-C(96)-C(103)	112.64(15)
C(97)-C(96)-C(103)	111.06(15)
C(109)-C(96)-C(103)	112.01(15)
C(98)-C(97)-C(102)	118.22(17)
C(98)-C(97)-C(96)	122.47(17)
C(102)-C(97)-C(96)	119.28(17)
C(97)-C(98)-C(99)	120.85(18)
C(100)-C(99)-C(98)	120.22(19)
C(99)-C(100)-C(101)	119.34(18)
C(102)-C(101)-C(100)	120.48(19)
C(101)-C(102)-C(97)	120.87(18)
C(108)-C(103)-C(104)	118.00(18)
C(108)-C(103)-C(96)	121.40(17)
C(104)-C(103)-C(96)	120.46(17)
C(105)-C(104)-C(103)	120.97(19)
C(106)-C(105)-C(104)	120.25(19)
C(105)-C(106)-C(107)	119.57(19)
C(106)-C(107)-C(108)	120.2(2)
C(103)-C(108)-C(107)	121.02(19)
C(114)-C(109)-C(110)	117.84(18)
C(114)-C(109)-C(96)	120.70(17)
C(110)-C(109)-C(96)	121.41(17)
C(111)-C(110)-C(109)	120.7(2)
C(112)-C(111)-C(110)	120.7(2)
C(113)-C(112)-C(111)	119.1(2)
C(112)-C(113)-C(114)	120.5(2)

C(109)-C(114)-C(113)	121.0(2)
N(7)-C(115)-C(120)	127.19(18)
N(7)-C(115)-C(116)	112.55(16)
C(120)-C(115)-C(116)	120.21(18)
C(117)-C(116)-C(115)	121.49(17)
C(117)-C(116)-C(91)	131.33(18)
C(115)-C(116)-C(91)	107.17(17)
C(118)-C(117)-C(116)	118.16(19)
C(117)-C(118)-C(119)	120.17(19)
C(120)-C(119)-C(118)	122.46(18)
C(119)-C(120)-C(115)	117.50(18)
O(9)-C(121)-C(122)	108.13(19)
O(9)-C(123)-C(124)	108.2(2)

Symmetry transformations used to generate equivalent atoms:

Table 4. Anisotropic displacement parameters (A^2 x 10^3) for sd40. The anisotropic displacement factor exponent takes the form: -2 pi^2 [h^2 a*^2 U11 + ... + 2 h k a* b* U12]

	U11	U22	U33	U23	U13	U12
O(1)	21(1)	31(1)	21(1)	3(1)	9(1)	6(1)
O(2)	23(1)	26(1)	18(1)	0(1)	7(1)	-10(1)
O(3)	20(1)	32(1)	24(1)	-4(1)	9(1)	-6(1)
O(4)	26(1)	25(1)	22(1)	3(1)	6(1)	11(1)
O(5)	17(1)	35(1)	24(1)	6(1)	3(1)	-6(1)
O(6)	21(1)	32(1)	21(1)	-2(1)	4(1)	12(1)
O(7)	16(1)	33(1)	30(1)	-6(1)	5(1)	4(1)
O(8)	21(1)	25(1)	22(1)	3(1)	6(1)	-7(1)
O(9)	28(1)	29(1)	43(1)	0(1)	6(1)	-1(1)
N(1)	19(1)	17(1)	15(1)	-1(1)	4(1)	-1(1)
N(2)	15(1)	14(1)	16(1)	-1(1)	4(1)	-1(1)
N(3)	18(1)	18(1)	19(1)	2(1)	5(1)	-2(1)
N(4)	16(1)	15(1)	16(1)	1(1)	3(1)	-1(1)
N(5)	19(1)	17(1)	15(1)	0(1)	5(1)	2(1)
N(6)	16(1)	14(1)	16(1)	-1(1)	5(1)	1(1)
N(7)	18(1)	17(1)	19(1)	1(1)	6(1)	2(1)
N(8)	16(1)	15(1)	18(1)	1(1)	6(1)	1(1)
C(1)	13(1)	22(1)	16(1)	1(1)	3(1)	-2(1)
C(2)	16(1)	19(1)	17(1)	-1(1)	5(1)	-1(1)
C(3)	21(1)	15(1)	19(1)	-2(1)	4(1)	2(1)
C(4)	20(1)	15(1)	17(1)	0(1)	3(1)	-1(1)
C(5)	17(1)	18(1)	15(1)	1(1)	4(1)	-2(1)
C(6)	17(1)	15(1)	14(1)	-1(1)	4(1)	0(1)
C(7)	14(1)	15(1)	17(1)	2(1)	5(1)	2(1)
C(8)	20(1)	15(1)	19(1)	0(1)	6(1)	1(1)
C(9)	21(1)	24(1)	16(1)	1(1)	7(1)	2(1)
C(10)	17(1)	24(1)	24(1)	3(1)	8(1)	2(1)
C(11)	16(1)	21(1)	25(1)	-2(1)	5(1)	0(1)
C(12)	19(1)	19(1)	18(1)	-2(1)	6(1)	1(1)
C(13)	16(1)	16(1)	18(1)	0(1)	8(1)	-1(1)
C(14)	21(1)	17(1)	20(1)	2(1)	8(1)	0(1)
C(15)	24(1)	21(1)	23(1)	5(1)	7(1)	4(1)
C(16)	30(1)	18(1)	27(1)	2(1)	14(1)	4(1)
C(17)	28(1)	21(1)	24(1)	-6(1)	13(1)	-2(1)
C(18)	20(1)	20(1)	18(1)	-2(1)	8(1)	-1(1)
C(19)	18(1)	16(1)	15(1)	0(1)	3(1)	-3(1)

C(20)	20(1)	19(1)	16(1)	-1(1)	3(1)	-1(1)
C(21)	23(1)	23(1)	22(1)	3(1)	-2(1)	-1(1)
C(22)	32(1)	32(1)	18(1)	7(1)	2(1)	-5(1)
C(23)	28(1)	33(1)	19(1)	2(1)	8(1)	-6(1)
C(24)	21(1)	23(1)	18(1)	-1(1)	5(1)	-2(1)
C(25)	15(1)	18(1)	15(1)	-2(1)	1(1)	-4(1)
C(26)	15(1)	22(1)	14(1)	0(1)	4(1)	-1(1)
C(27)	19(1)	23(1)	19(1)	2(1)	4(1)	2(1)
C(28)	24(1)	24(1)	16(1)	3(1)	4(1)	-2(1)
C(29)	21(1)	25(1)	18(1)	-3(1)	7(1)	-6(1)
C(30)	20(1)	20(1)	19(1)	-5(1)	6(1)	-3(1)
C(31)	16(1)	21(1)	16(1)	0(1)	3(1)	2(1)
C(32)	18(1)	18(1)	19(1)	2(1)	5(1)	3(1)
C(33)	23(1)	19(1)	22(1)	2(1)	3(1)	-5(1)
C(34)	21(1)	15(1)	20(1)	0(1)	3(1)	-2(1)
C(35)	19(1)	17(1)	17(1)	-1(1)	4(1)	2(1)
C(36)	15(1)	16(1)	15(1)	0(1)	3(1)	0(1)
C(37)	19(1)	17(1)	16(1)	1(1)	4(1)	3(1)
C(38)	20(1)	20(1)	18(1)	1(1)	3(1)	1(1)
C(39)	28(1)	24(1)	20(1)	-5(1)	1(1)	3(1)
C(40)	32(1)	30(1)	18(1)	-2(1)	7(1)	8(1)
C(41)	22(1)	32(1)	20(1)	3(1)	8(1)	5(1)
C(42)	20(1)	23(1)	19(1)	0(1)	4(1)	-1(1)
C(43)	16(1)	17(1)	20(1)	-3(1)	3(1)	0(1)
C(44)	19(1)	21(1)	25(1)	-2(1)	6(1)	-1(1)
C(45)	22(1)	26(1)	34(1)	-6(1)	13(1)	-3(1)
C(46)	18(1)	37(1)	38(1)	-7(1)	5(1)	7(1)
C(47)	25(1)	42(1)	30(1)	1(1)	1(1)	11(1)
C(48)	23(1)	28(1)	25(1)	4(1)	7(1)	6(1)
C(49)	16(1)	16(1)	23(1)	-2(1)	7(1)	-1(1)
C(50)	19(1)	19(1)	23(1)	-3(1)	5(1)	1(1)
C(51)	23(1)	23(1)	33(1)	-9(1)	5(1)	-1(1)
C(52)	29(1)	19(1)	48(1)	-6(1)	15(1)	-5(1)
C(53)	42(1)	20(1)	40(1)	4(1)	21(1)	-3(1)
C(54)	32(1)	20(1)	25(1)	1(1)	12(1)	-2(1)
C(55)	18(1)	19(1)	16(1)	4(1)	3(1)	2(1)
C(56)	16(1)	20(1)	15(1)	3(1)	3(1)	2(1)
C(57)	18(1)	23(1)	19(1)	2(1)	3(1)	1(1)
C(58)	27(1)	24(1)	20(1)	0(1)	7(1)	6(1)
C(59)	22(1)	30(1)	24(1)	7(1)	12(1)	7(1)
C(60)	18(1)	24(1)	23(1)	6(1)	7(1)	-1(1)
C(61)	16(1)	24(1)	19(1)	3(1)	7(1)	2(1)
C(62)	16(1)	21(1)	16(1)	1(1)	4(1)	4(1)
C(63)	26(1)	15(1)	19(1)	-1(1)	9(1)	-1(1)
C(64)	23(1)	14(1)	18(1)	-1(1)	8(1)	2(1)
C(65)	16(1)	17(1)	16(1)	2(1)	5(1)	4(1)
C(66)	15(1)	14(1)	18(1)	-2(1)	4(1)	1(1)
C(67)	16(1)	15(1)	19(1)	0(1)	5(1)	0(1)
C(68)	20(1)	16(1)	18(1)	1(1)	6(1)	1(1)
C(69)	20(1)	19(1)	18(1)	2(1)	3(1)	-2(1)
C(70)	15(1)	24(1)	24(1)	1(1)	4(1)	-1(1)
C(71)	21(1)	32(1)	25(1)	-6(1)	10(1)	2(1)
C(72)	19(1)	30(1)	18(1)	-6(1)	5(1)	-1(1)
C(73)	14(1)	14(1)	30(1)	-4(1)	3(1)	0(1)
C(74)	19(1)	18(1)	39(1)	4(1)	7(1)	2(1)
C(75)	20(1)	19(1)	64(2)	12(1)	6(1)	1(1)
C(76)	20(1)	15(1)	87(2)	-1(1)	-2(1)	0(1)
C(77)	24(1)	24(1)	62(2)	-19(1)	-5(1)	3(1)
C(78)	20(1)	25(1)	38(1)	-12(1)	2(1)	1(1)
C(79)	18(1)	21(1)	14(1)	-2(1)	5(1)	3(1)
C(80)	20(1)	24(1)	16(1)	-2(1)	6(1)	2(1)
C(81)	33(1)	24(1)	20(1)	2(1)	13(1)	4(1)
C(82)	31(1)	37(1)	19(1)	7(1)	8(1)	12(1)

C(83)	23(1)	42(1)	17(1)	0(1)	3(1)	7(1)
C(84)	20(1)	28(1)	18(1)	-1(1)	6(1)	2(1)
C(85)	18(1)	19(1)	15(1)	0(1)	8(1)	4(1)
C(86)	15(1)	22(1)	16(1)	2(1)	6(1)	1(1)
C(87)	21(1)	21(1)	21(1)	3(1)	9(1)	-1(1)
C(88)	21(1)	22(1)	17(1)	4(1)	6(1)	4(1)
C(89)	17(1)	26(1)	16(1)	-2(1)	4(1)	4(1)
C(90)	19(1)	21(1)	18(1)	-2(1)	5(1)	0(1)
C(91)	17(1)	21(1)	18(1)	0(1)	6(1)	-1(1)
C(92)	16(1)	18(1)	20(1)	0(1)	5(1)	-2(1)
C(93)	23(1)	17(1)	21(1)	2(1)	8(1)	3(1)
C(94)	22(1)	14(1)	19(1)	0(1)	7(1)	0(1)
C(95)	17(1)	15(1)	17(1)	1(1)	4(1)	-1(1)
C(96)	16(1)	16(1)	16(1)	1(1)	3(1)	1(1)
C(97)	17(1)	15(1)	20(1)	-2(1)	6(1)	-1(1)
C(98)	20(1)	18(1)	20(1)	1(1)	6(1)	-1(1)
C(99)	17(1)	23(1)	26(1)	-2(1)	4(1)	1(1)
C(100)	20(1)	23(1)	28(1)	-5(1)	11(1)	-5(1)
C(101)	26(1)	23(1)	25(1)	0(1)	12(1)	-3(1)
C(102)	22(1)	19(1)	21(1)	2(1)	6(1)	0(1)
C(103)	21(1)	16(1)	16(1)	1(1)	4(1)	-2(1)
C(104)	22(1)	19(1)	20(1)	1(1)	3(1)	0(1)
C(105)	21(1)	26(1)	24(1)	3(1)	-2(1)	-2(1)
C(106)	35(1)	27(1)	19(1)	0(1)	-1(1)	-8(1)
C(107)	37(1)	25(1)	20(1)	-2(1)	10(1)	-4(1)
C(108)	23(1)	22(1)	20(1)	1(1)	7(1)	-1(1)
C(109)	13(1)	15(1)	24(1)	0(1)	4(1)	-1(1)
C(110)	22(1)	21(1)	26(1)	1(1)	4(1)	1(1)
C(111)	26(1)	19(1)	43(1)	5(1)	2(1)	6(1)
C(112)	24(1)	18(1)	51(1)	-8(1)	10(1)	0(1)
C(113)	26(1)	23(1)	36(1)	-11(1)	13(1)	-4(1)
C(114)	20(1)	18(1)	26(1)	-2(1)	8(1)	-2(1)
C(115)	19(1)	18(1)	14(1)	3(1)	6(1)	0(1)
C(116)	15(1)	23(1)	16(1)	2(1)	5(1)	0(1)
C(117)	22(1)	23(1)	19(1)	0(1)	8(1)	1(1)
C(118)	23(1)	26(1)	18(1)	-1(1)	6(1)	-5(1)
C(119)	15(1)	27(1)	21(1)	6(1)	4(1)	-2(1)
C(120)	18(1)	23(1)	20(1)	6(1)	5(1)	3(1)
C(121)	24(1)	33(1)	38(1)	-1(1)	6(1)	0(1)
C(122)	26(1)	30(1)	40(1)	-4(1)	4(1)	2(1)
C(123)	40(1)	36(1)	40(1)	6(1)	15(1)	-2(1)
C(124)	54(2)	35(1)	34(1)	3(1)	9(1)	10(1)

Table 5. Hydrogen coordinates (x 10^4) and isotropic displacement parameters (A^2 x 10^3) for sd40.

	x	y	z	U(eq)
H(2)	1991(15)	9750(40)	9350(12)	39(8)
H(4)	2654(15)	4680(40)	-267(12)	43(8)
H(6)	2544(16)	420(40)	5516(13)	48(9)
H(8)	2685(14)	5510(30)	5094(11)	35(7)
H(3A)	482	10648	9410	22
H(3B)	100	9483	9665	22
H(4A)	-196	9409	8609	21
H(5A)	760	7984	8447	20
H(8A)	-636	7343	9453	22
H(9A)	-1581	6836	9754	24

H(10A)	-2466	5388	9257	25
H(11A)	-2434	4539	8428	25
H(12A)	-1514	5109	8110	23
H(14A)	653	5213	9304	23
H(15A)	1190	3037	9318	27
H(16A)	838	1542	8578	28
H(17A)	-59	2241	7832	28
H(18A)	-568	4441	7806	23
H(20A)	-1391	8281	8103	23
H(21A)	-1652	9580	7318	30
H(22A)	-1016	9265	6716	34
H(23A)	-90	7694	6923	32
H(24A)	210	6472	7730	25
H(27A)	1959	4893	10372	25
H(28A)	1464	4981	11072	26
H(29A)	782	6890	11154	25
H(30A)	565	8739	10544	23
H(33A)	4423	5251	185	26
H(33B)	4877	3914	120	26
H(34A)	4607	4109	1051	24
H(35A)	3449	2975	878	21
H(38A)	5235	3153	1940	24
H(39A)	4898	4273	2612	30
H(40A)	3822	3799	2725	32
H(41A)	3077	2201	2158	29
H(42A)	3424	1029	1505	25
H(44A)	5441	1843	611	26
H(45A)	6635	1537	815	32
H(46A)	7262	560	1627	38
H(47A)	6694	-103	2242	41
H(48A)	5511	253	2054	30
H(50A)	3928	-23	254	25
H(51A)	3413	-2230	61	33
H(52A)	3420	-3784	750	38
H(53A)	3963	-3127	1632	38
H(54A)	4446	-902	1827	30
H(57A)	2996	-301	-1029	25
H(58A)	3817	-477	-1492	28
H(59A)	4671	1234	-1376	29
H(60A)	4753	3123	-793	26
H(63A)	1077	-580	5519	23
H(63B)	458	534	5315	23
H(64A)	1071	501	6360	21
H(65A)	2105	2045	6492	20
H(68A)	-104	2836	5563	21
H(69A)	-1286	3308	5311	23
H(70A)	-1784	4349	5912	26
H(71A)	-1095	4846	6783	30
H(72A)	74	4280	7048	27
H(74A)	1245	4916	5779	30
H(75A)	1667	7208	5827	43
H(76A)	1847	8509	6606	54
H(77A)	1631	7499	7351	49
H(78A)	1240	5186	7317	35
H(80A)	299	1288	6926	23
H(81A)	751	-206	7648	29
H(82A)	1887	81	8196	35
H(83A)	2569	1862	8008	33
H(84A)	2130	3338	7276	26
H(87A)	1477	5470	4612	24
H(88A)	392	5309	3968	24
H(89A)	-246	3233	3876	24
H(90A)	154	1303	4429	23

H(93A)	4079	4704	4651	24
H(93B)	4650	5930	4745	24
H(94A)	3691	5968	3799	22
H(95A)	2694	7246	3965	20
H(98A)	4935	8017	4336	23
H(99A)	6037	8493	4270	27
H(10F)	6170	9938	3588	28
H(10D)	5193	10848	2958	28
H(10B)	4095	10322	3007	25
H(10C)	2281	8829	3286	25
H(10G)	1573	7695	2536	30
H(10H)	2056	6395	1984	35
H(10I)	3256	6145	2210	33
H(10E)	3968	7268	2964	26
H(11E)	2997	10962	3066	29
H(11H)	2594	13127	3258	37
H(11I)	2691	13751	4136	37
H(11F)	3248	12237	4828	33
H(11G)	3683	10091	4644	26
H(11B)	3796	10271	5934	25
H(11D)	4981	10288	6379	27
H(11C)	5686	8500	6230	26
H(12B)	5248	6686	5626	25
H(12F)	7009	4537	3367	39
H(12G)	6990	4164	2766	39
H(12C)	6223	2677	3344	50
H(12D)	6918	2099	3250	50
H(12E)	6238	2285	2755	50
H(12H)	6527	6563	2550	45
H(12I)	6529	6751	3157	45
H(12J)	5304	6804	2272	63
H(12K)	5670	8183	2575	63
H(12L)	5329	7072	2878	63

Table 6. Hydrogen bonds for sd40 [A and deg.].

D-H...A	d(D-H)	d(H...A)	d(D...A)	<(DHA)
O(2)-H(2)...O(3)#1	0.82(3)	1.92(3)	2.716(2)	163(3)
O(4)-H(4)...O(1)#2	0.86(3)	1.98(3)	2.741(2)	147(3)
O(6)-H(6)...O(7)#3	0.86(4)	1.86(4)	2.714(2)	170(3)
O(8)-H(8)...O(5)	0.86(3)	1.90(3)	2.713(2)	157(3)

Symmetry transformations used to generate equivalent atoms:
#1 x,y+1,z+1 #2 x,y,z-1 #3 x,y-1,z

Appendix B

Selected NMR Spectra

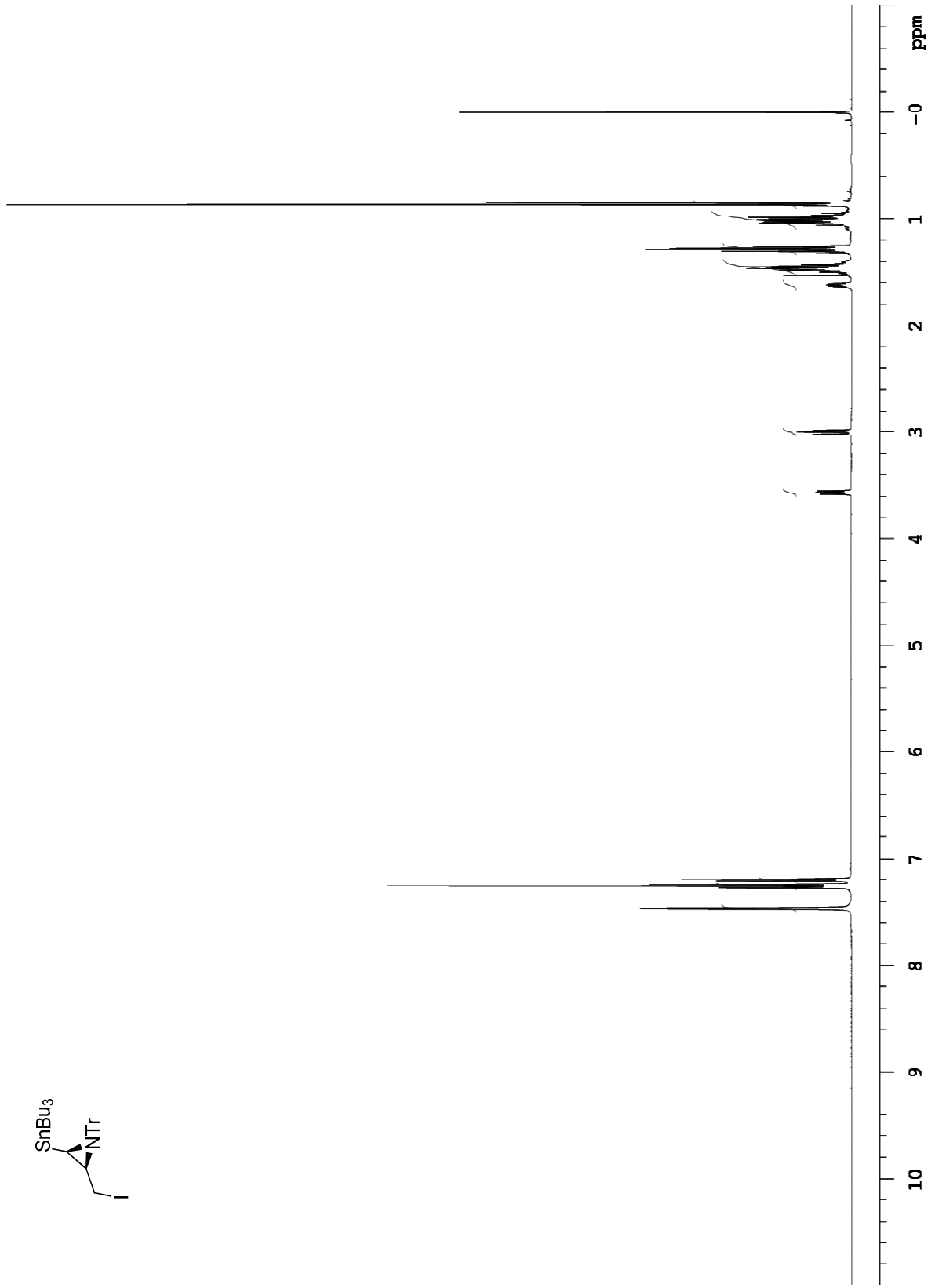
SnBu3
NTr
I
ppm
10
9
8
7
6
5
4
3
2
1
0

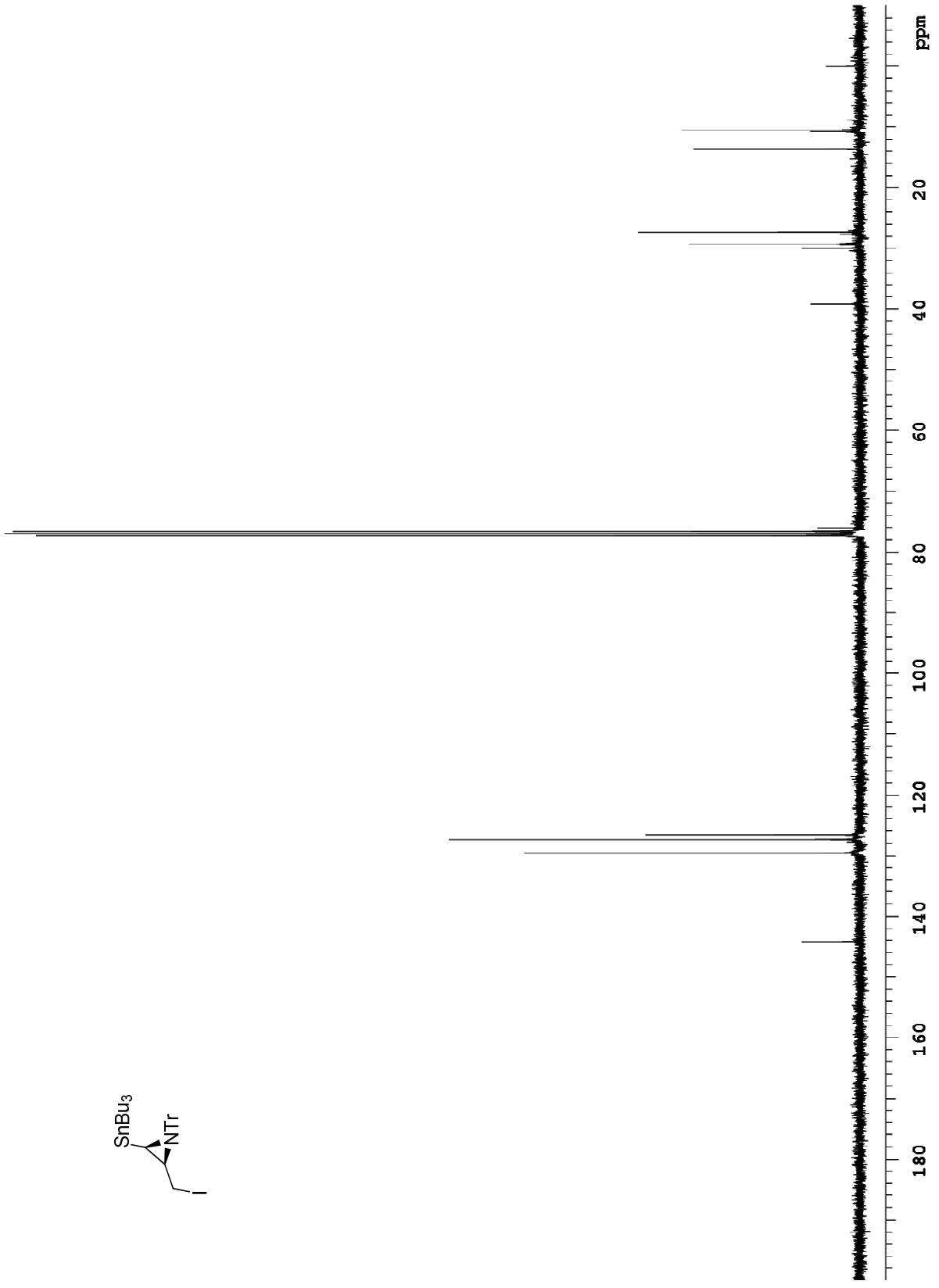
SnBu3
NTr
I
ppm
180
160
140
120
100
80
60
40
20

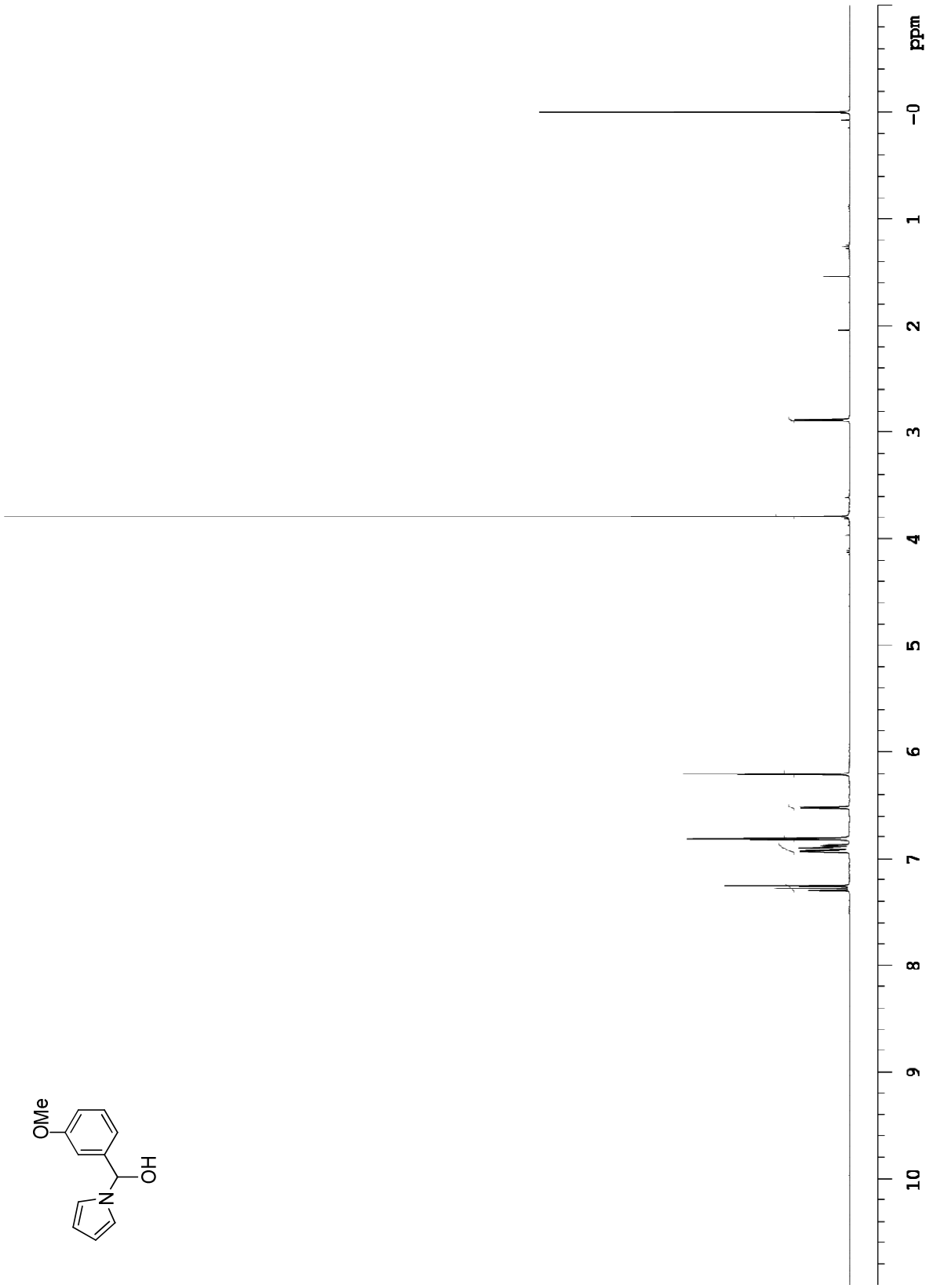
OMe
OH
N
ppm
10
9
8
7
6
5
4
3
2
1
0

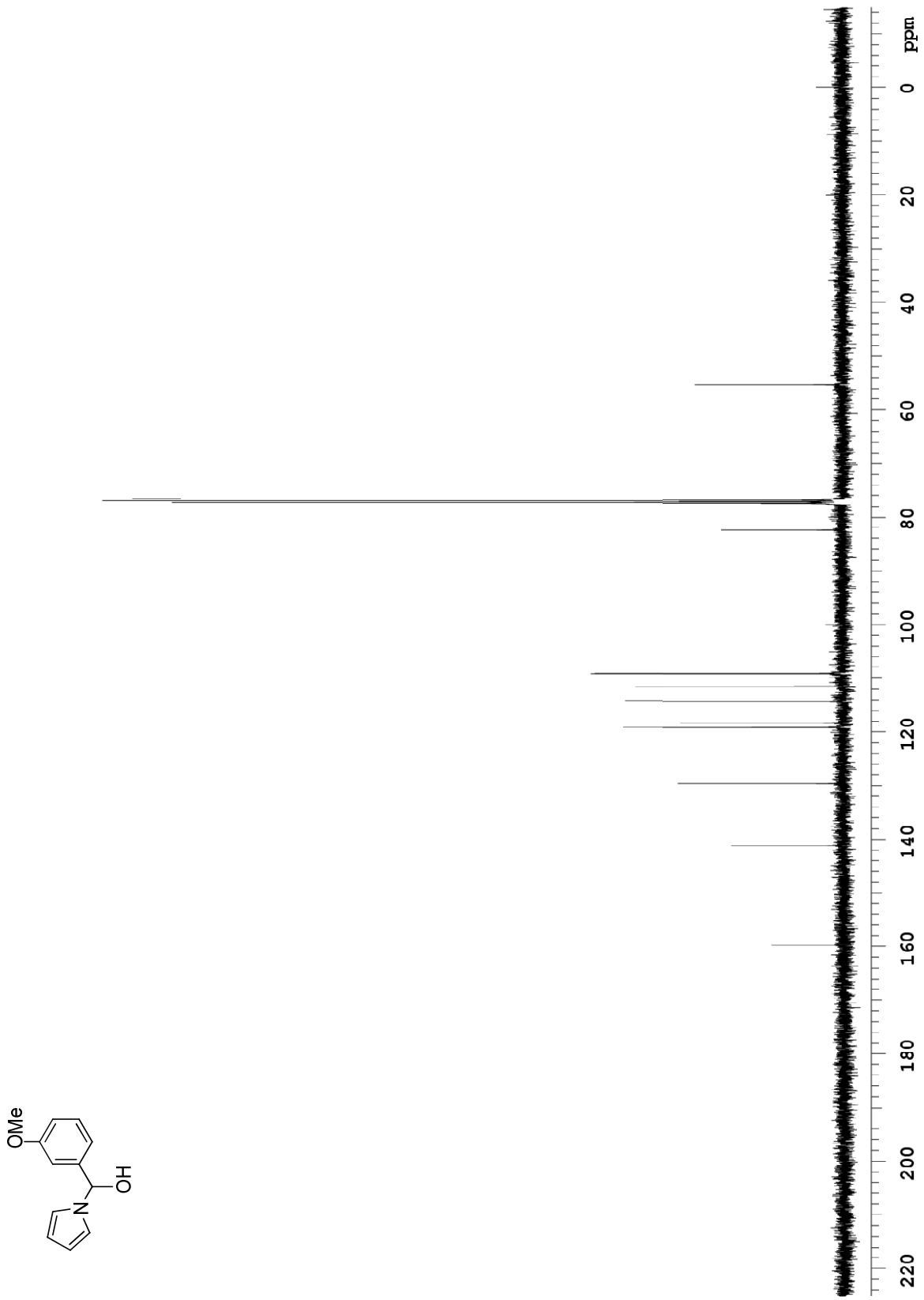
OMe
OH
N
ppm
0
20
40
60
80
100
120
140
160
180
200
220

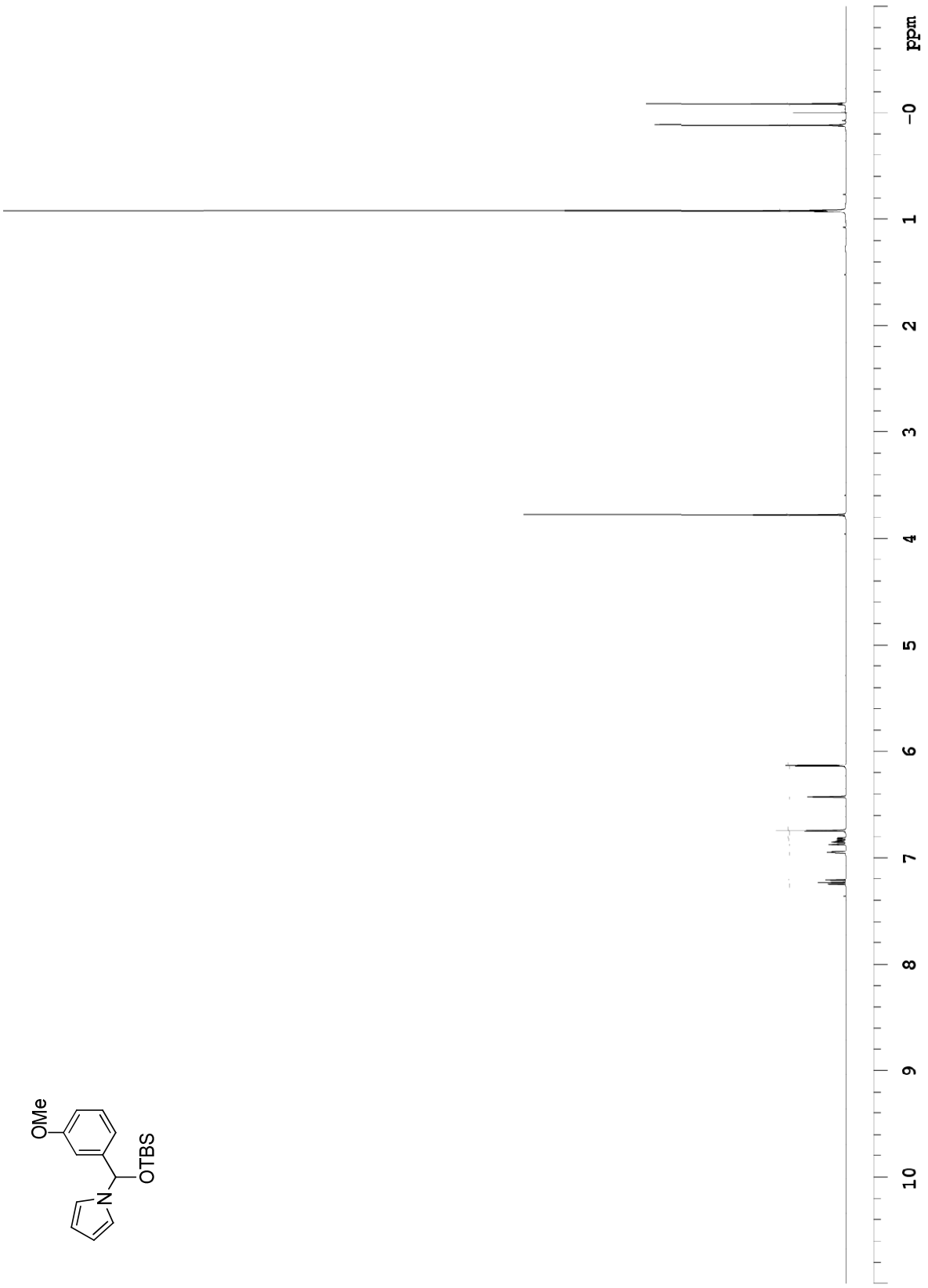
OMe
OTBS
N
ppm
10
9
8
7
6
5
4
3
2
1
0

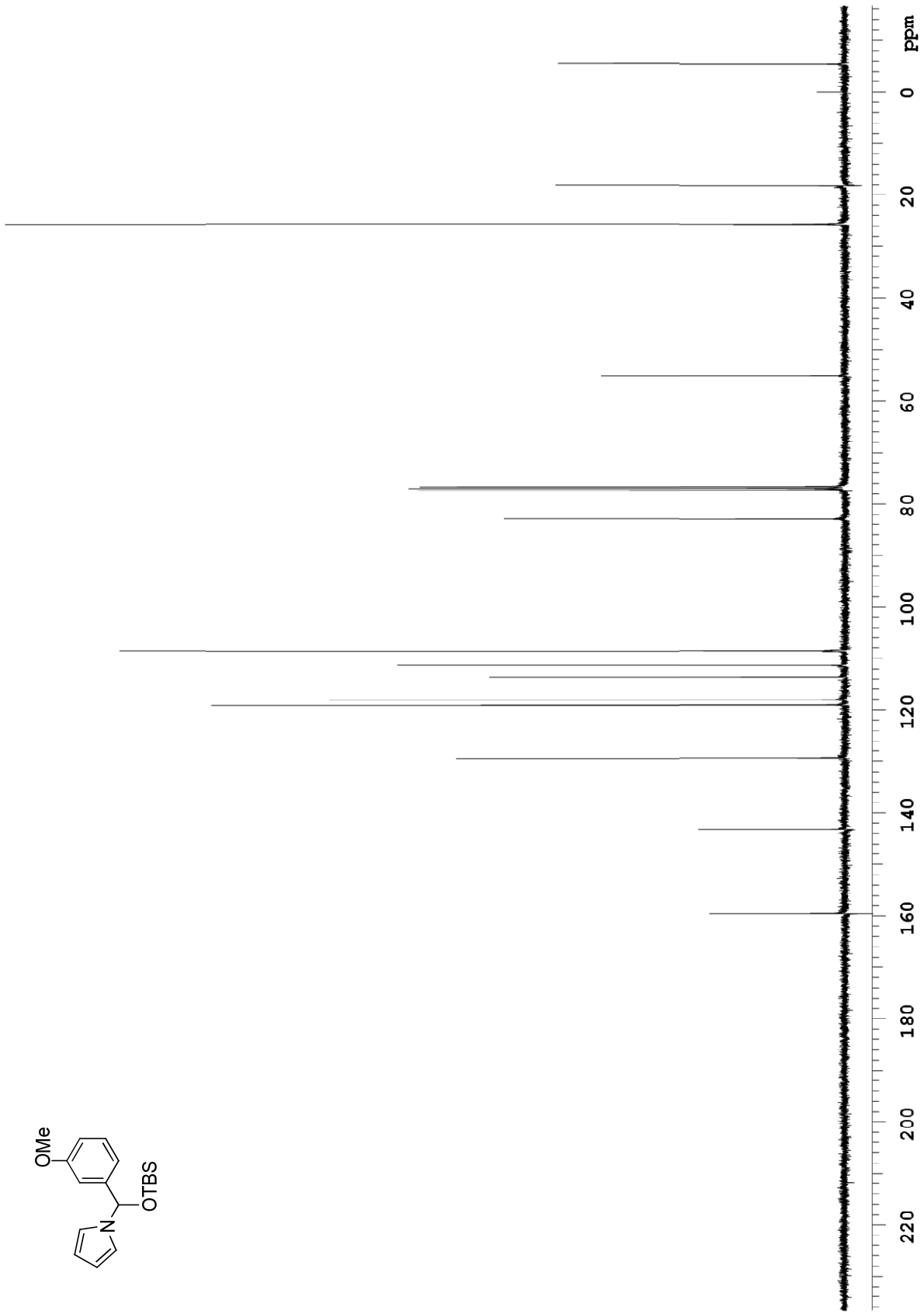
ppm
0
20
40
60
80
100
120
140
160
180
200
220
OMe
OTBS
N

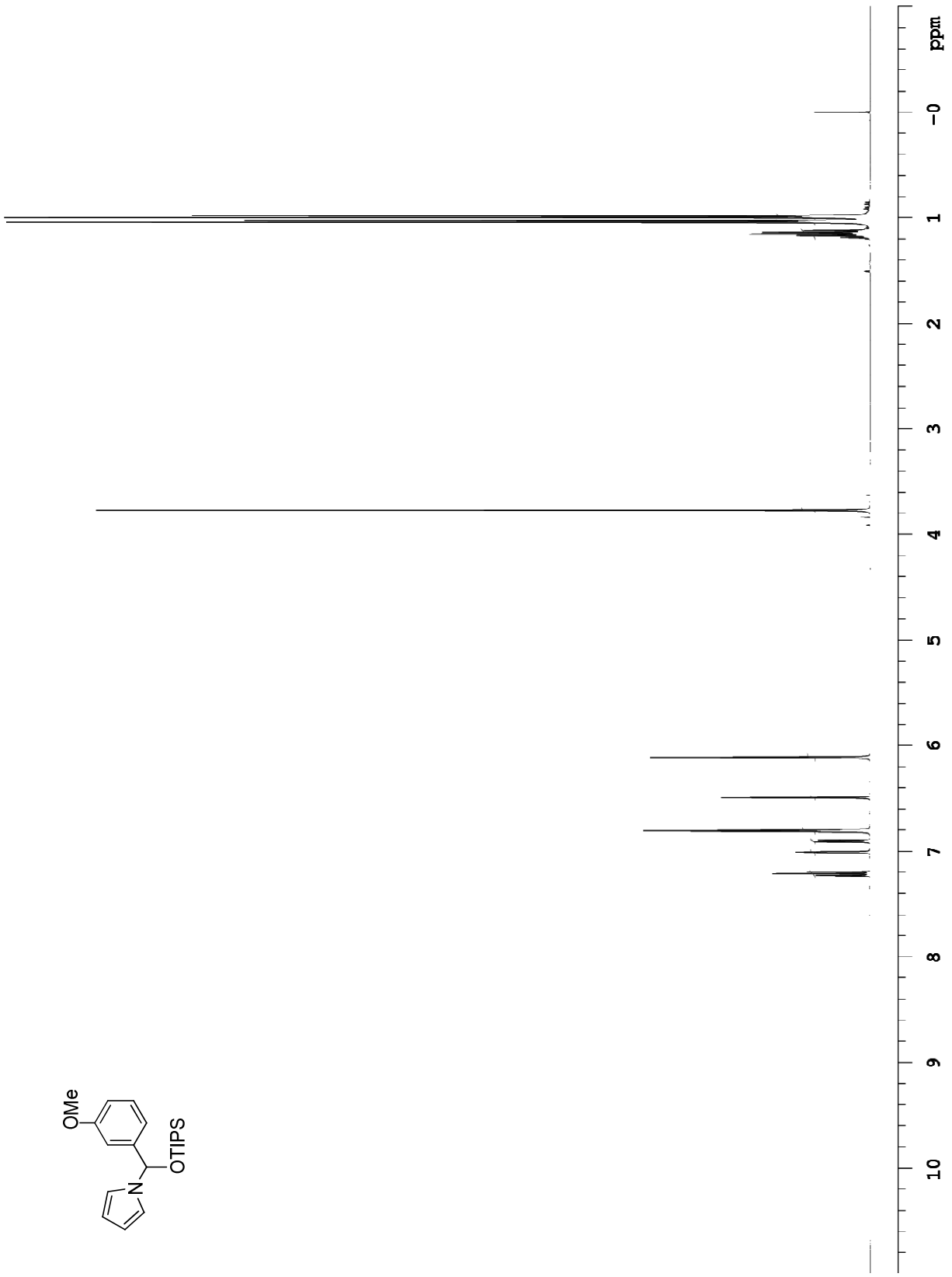
ppm
10
9
8
7
6
5
4
3
2
1
0
OMe
OTIPS
N

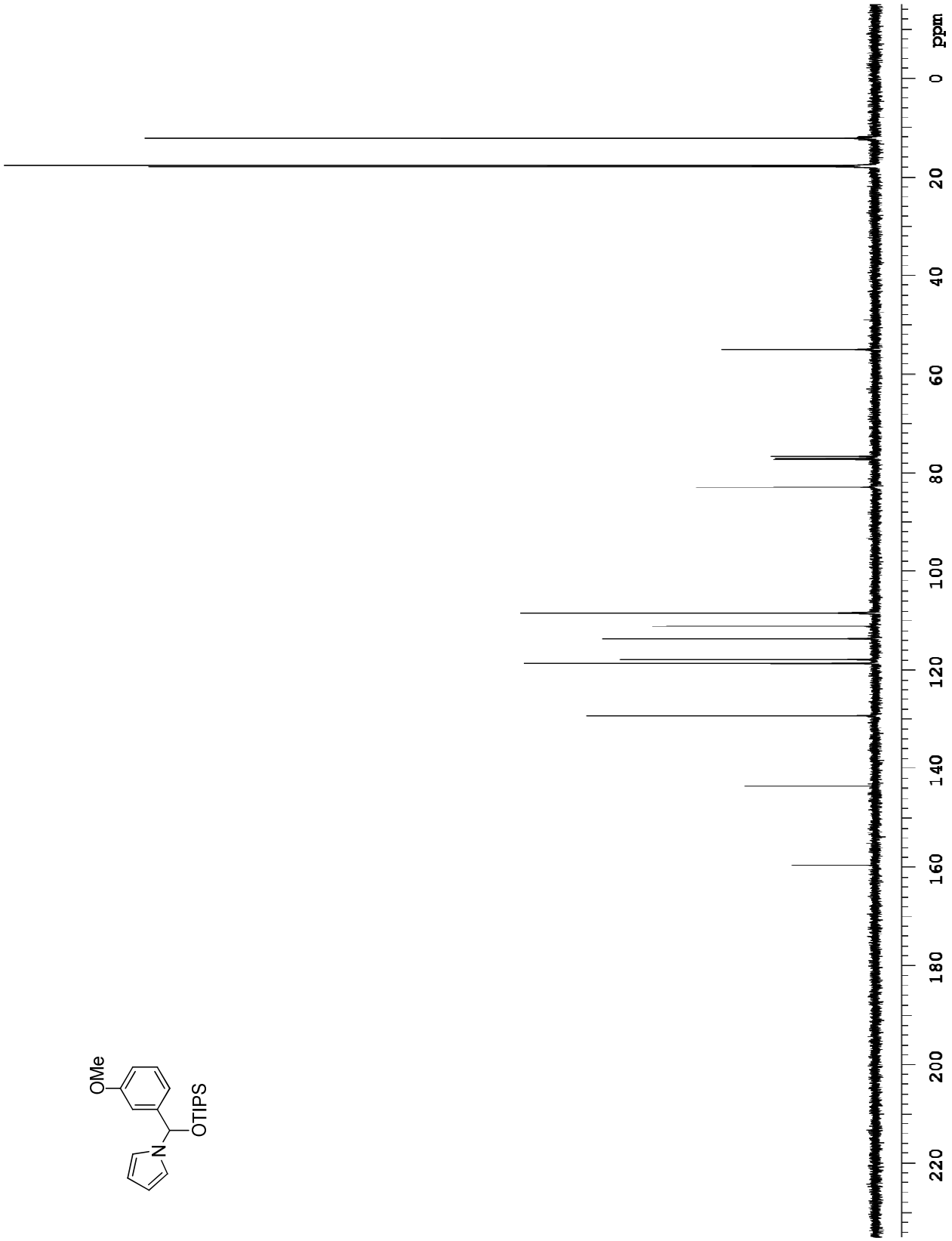
ppm
0
20
40
60
80
100
120
140
160
180
200
220
OMe
OTIPS
N

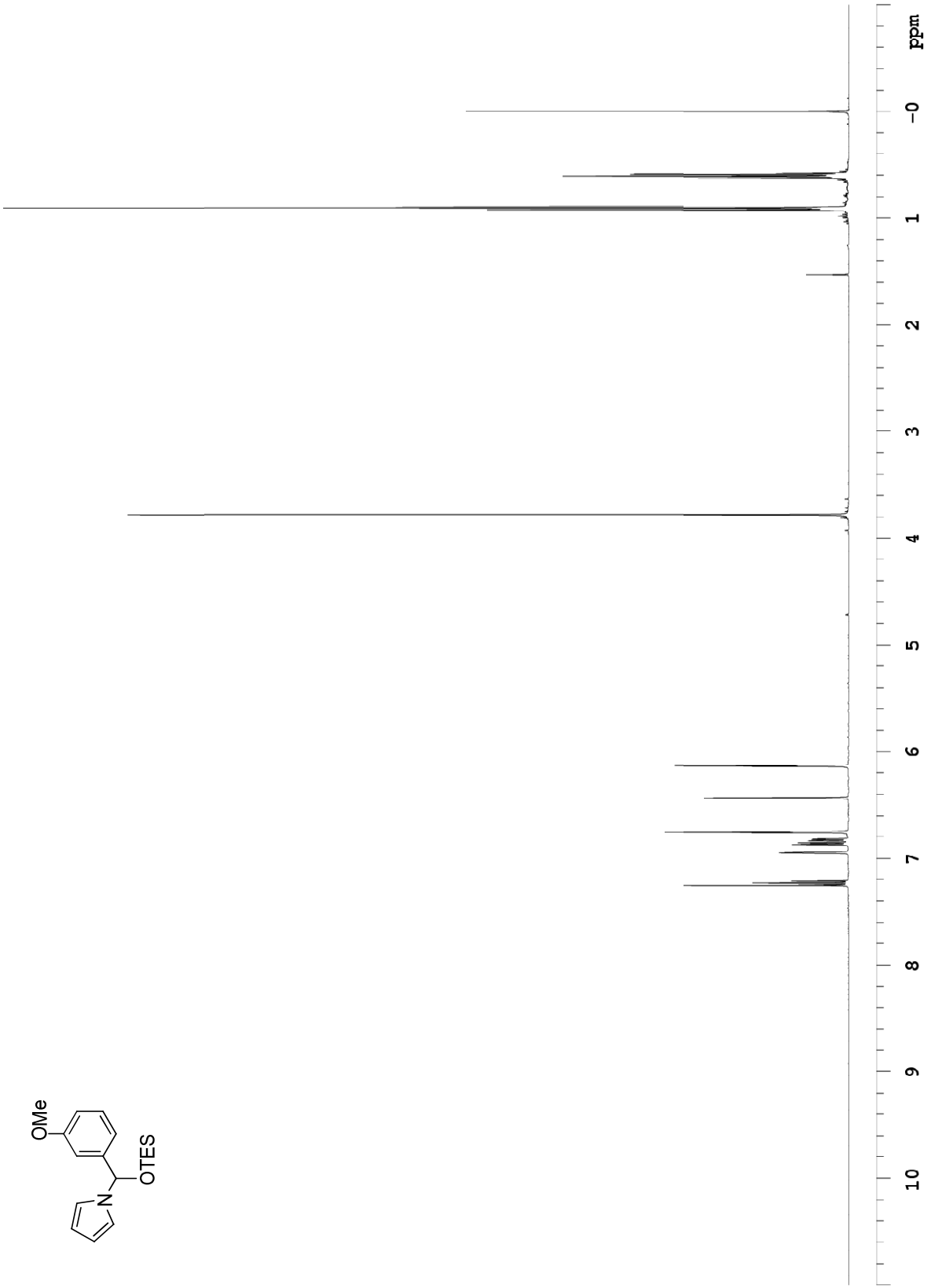
OMe
OTES
N
ppm
10
9
8
7
6
5
4
3
2
1
0

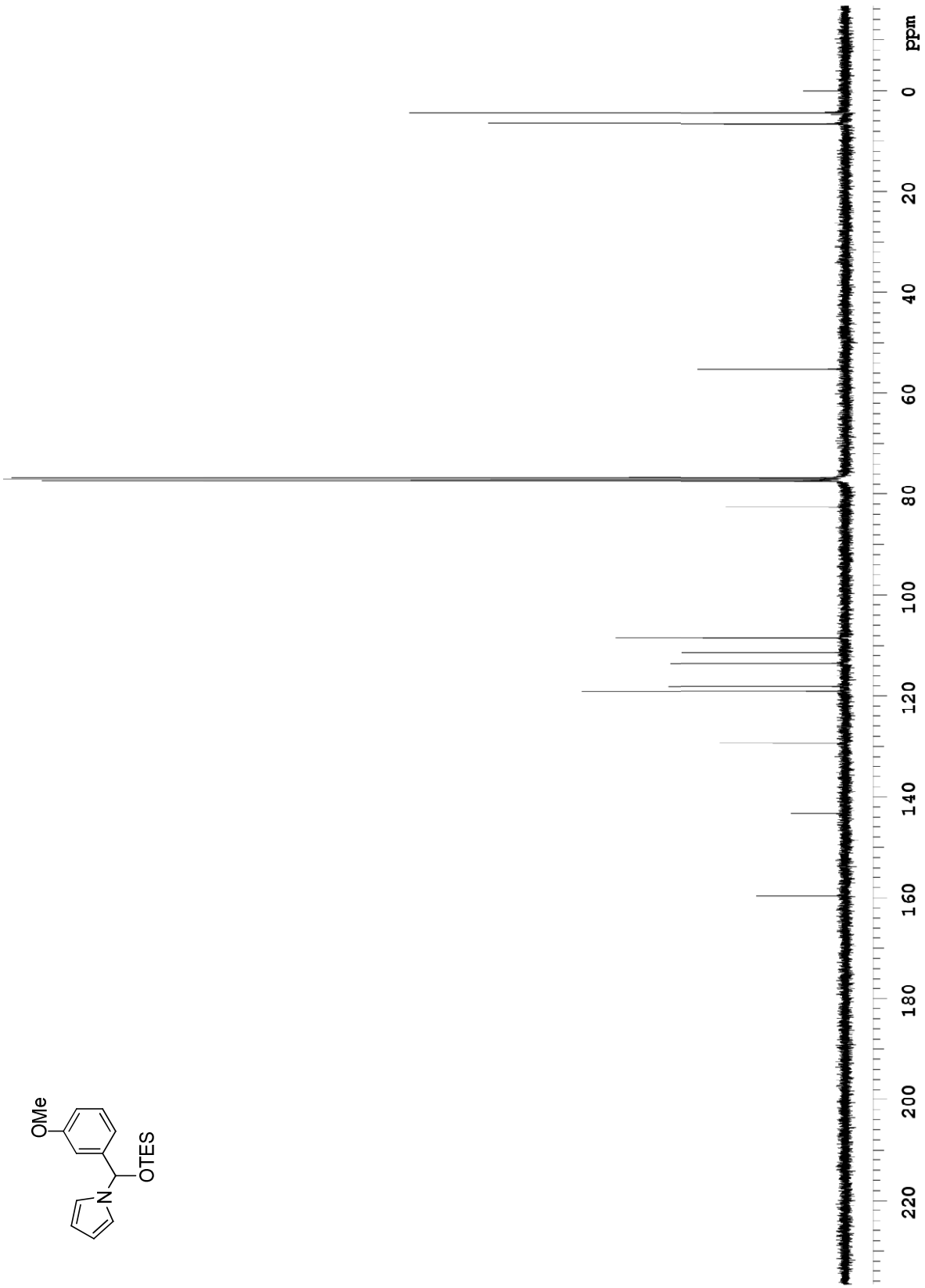
OMe
OTES
N
ppm
0
20
40
60
80
100
120
140
160
180
200
220

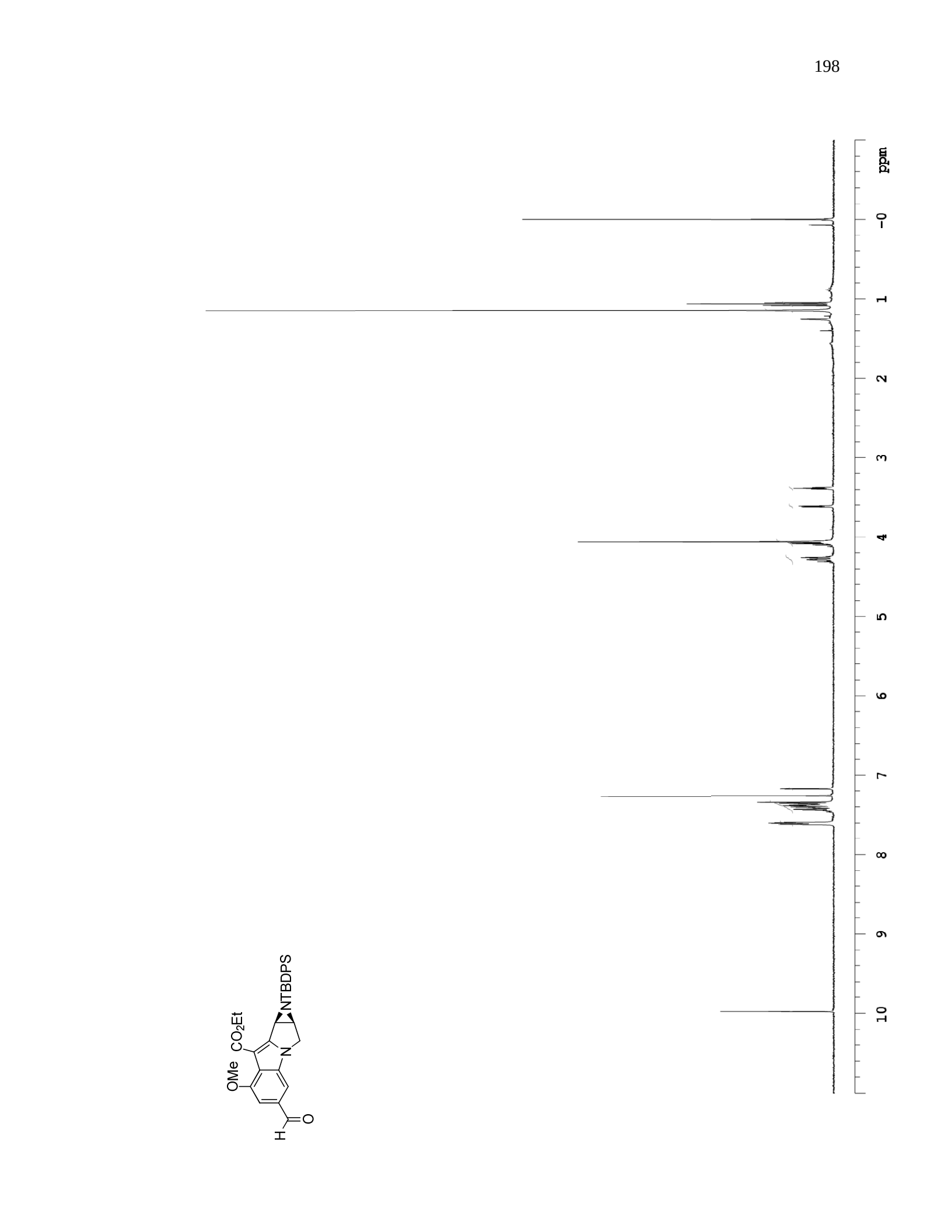
OMe
CO2Et
NTBDPS
N
O
H
ppm
10
9
8
7
6
5
4
3
2
1
0

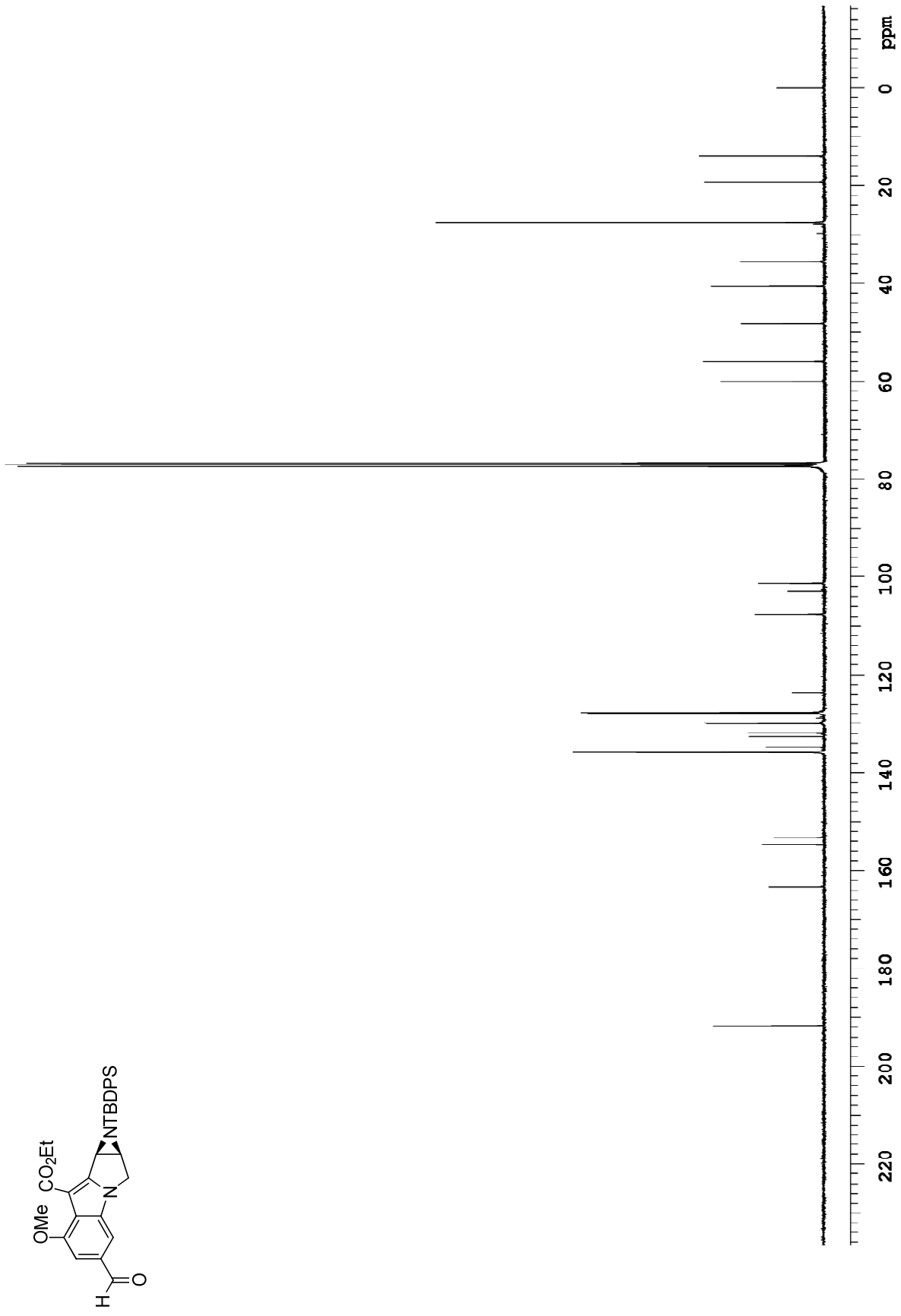
ppm
0
20
40
60
80
100
120
140
160
180
200
220
OMe
CO2Et
NTBDPS
N
O
H

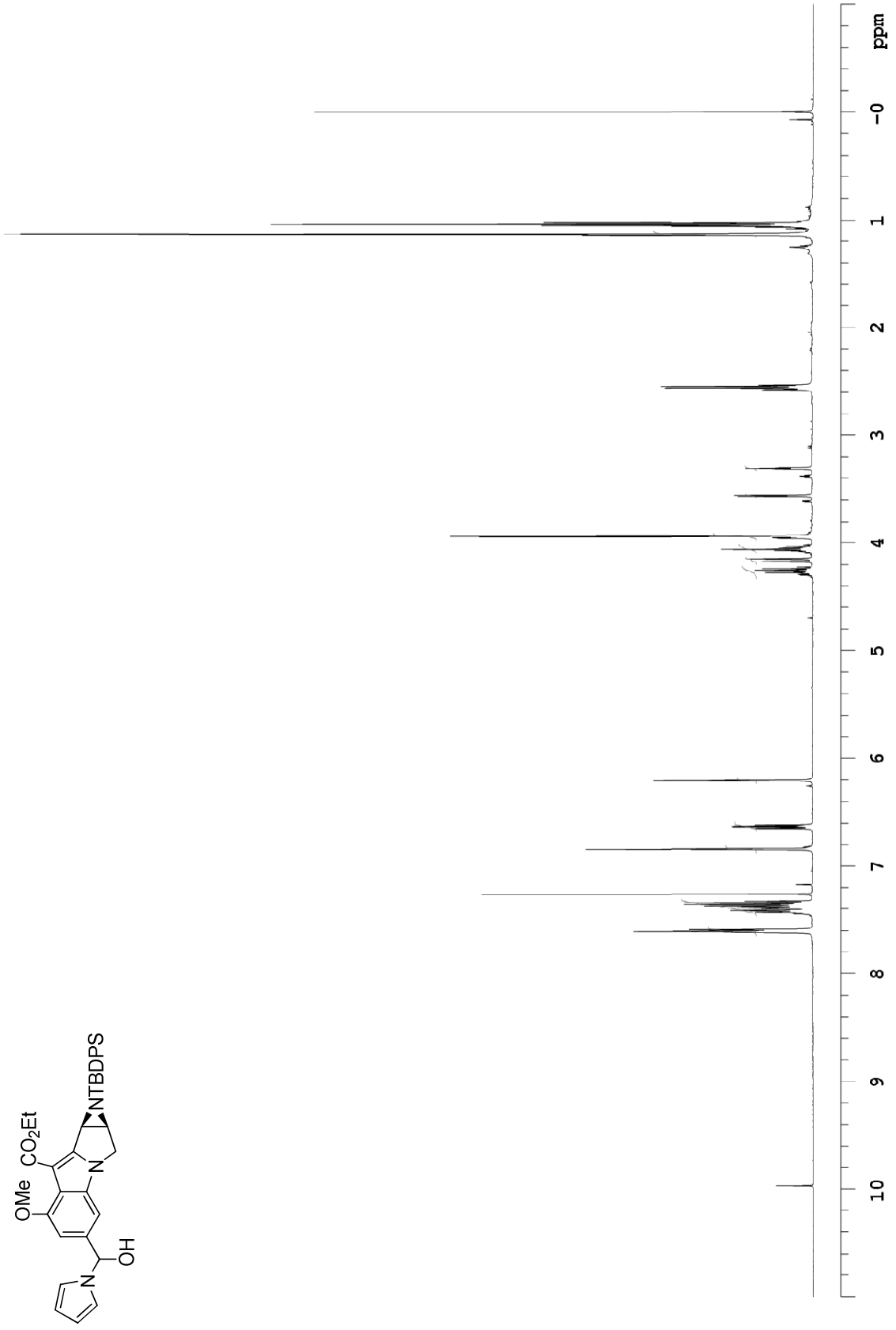
NTBDPS
CO2Et
OMe
OH
N
N
ppm
10
9
8
7
6
5
4
3
2
1
0

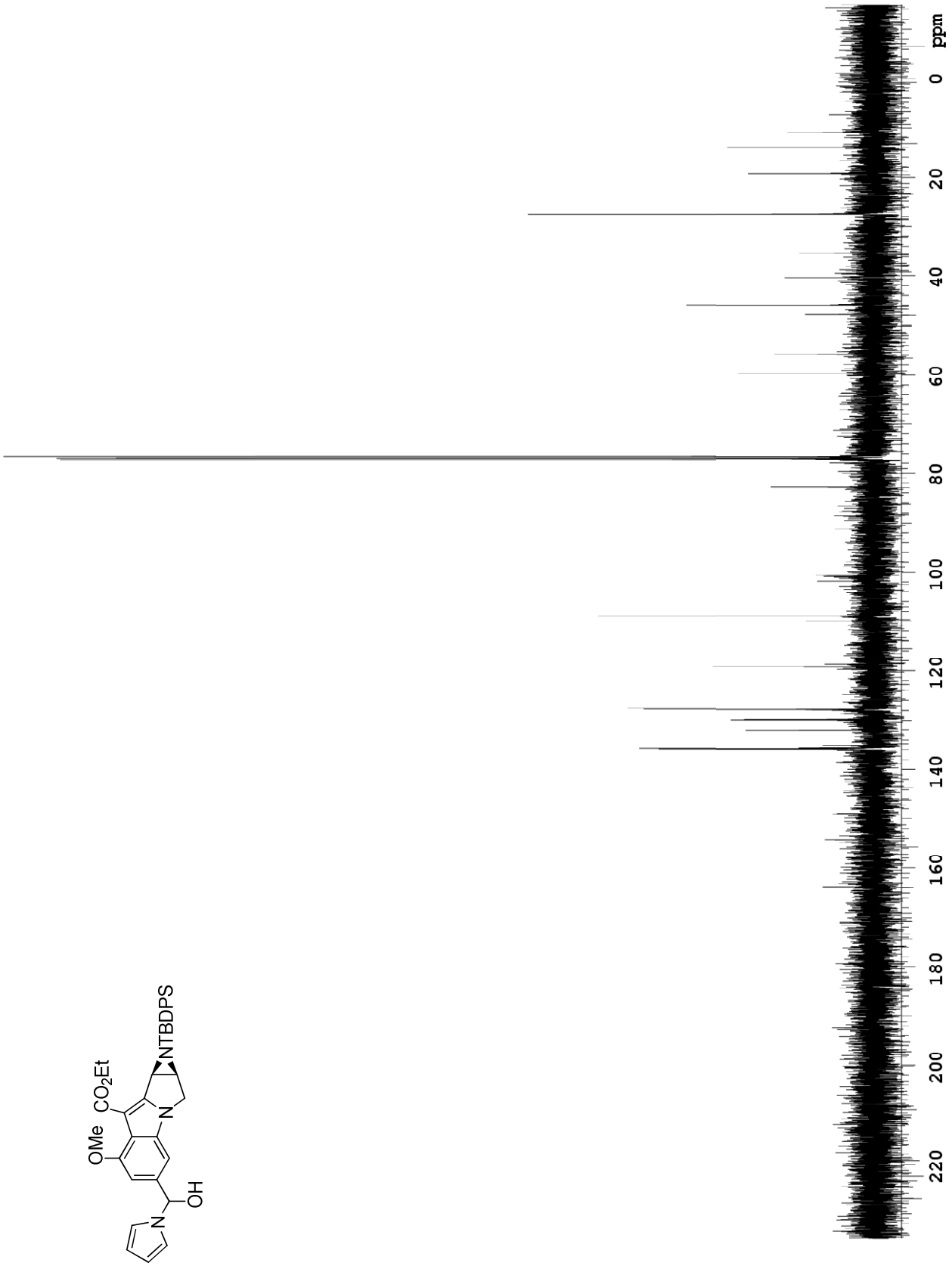
NTBDPS
CO2Et
OMe
OH
N
N
ppm
0
20
40
60
80
100
120
140
160
180
200
220

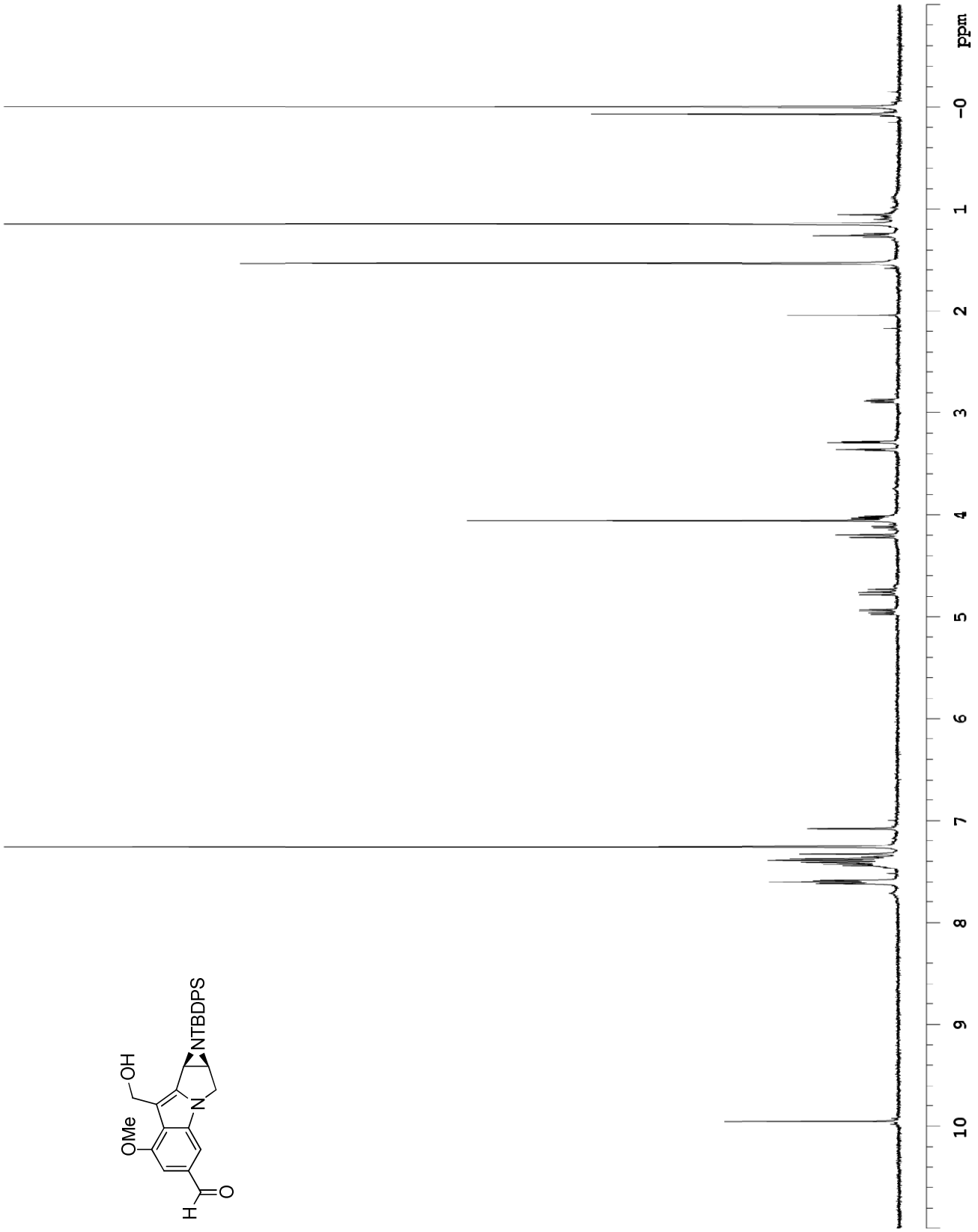
NTBDPS
OH
OMe
N
O
H
ppm
10
9
8
7
6
5
4
3
2
1
0

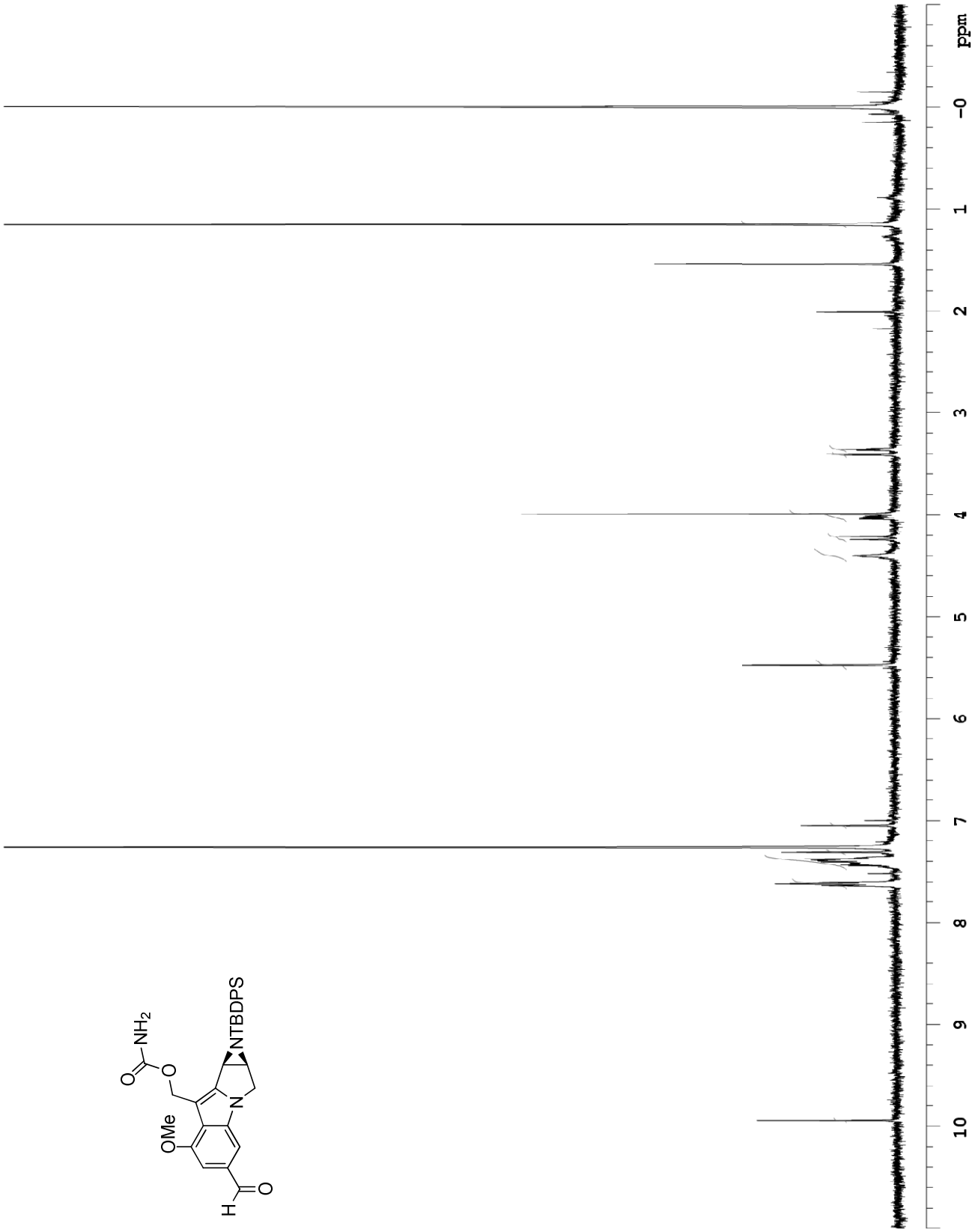
NTBDPS
OMe
O
NH2
O
H
O
N
ppm
10
9
8
7
6
5
4
3
2
1
0

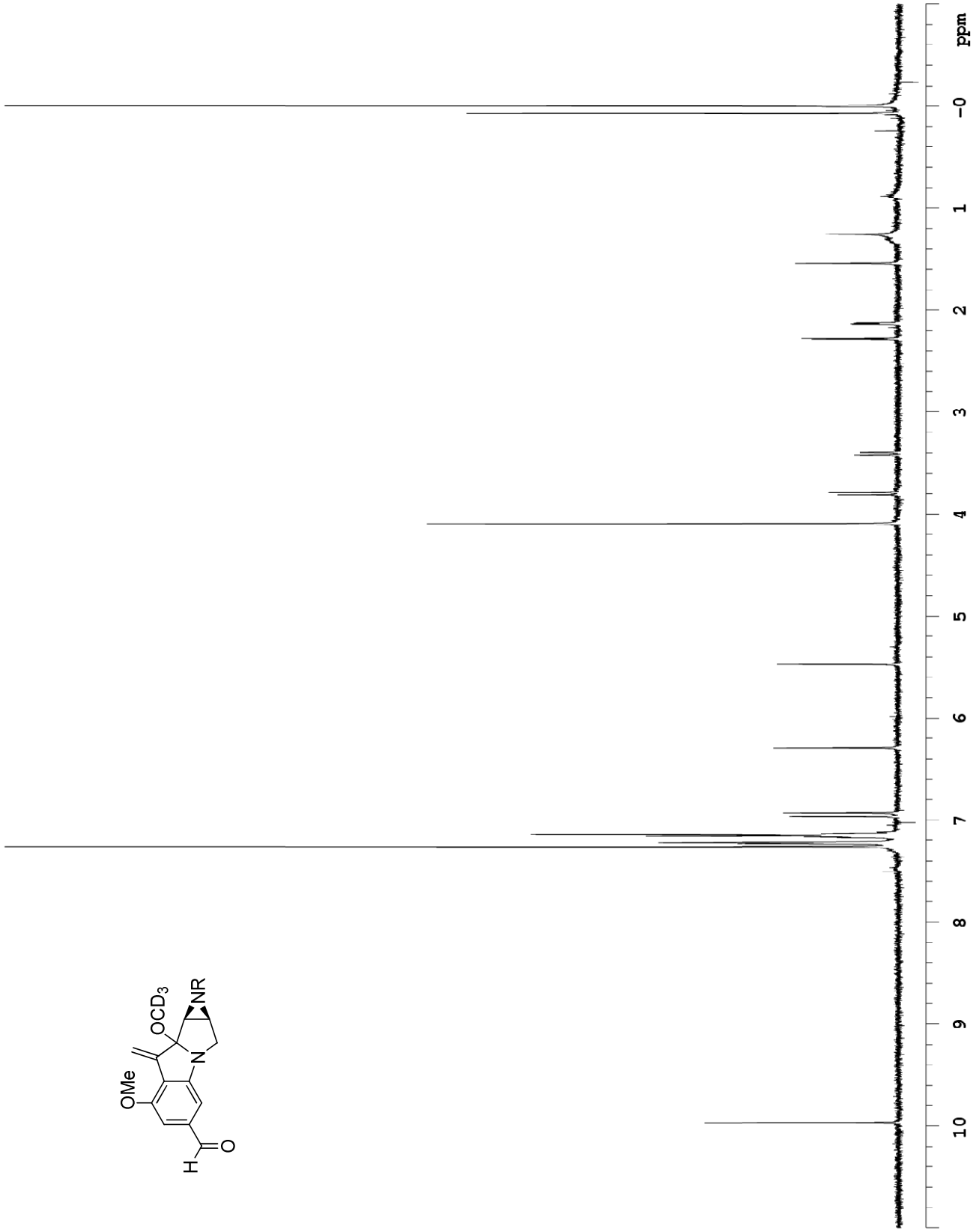
ppm
10
9
8
7
6
5
4
3
2
1
0
OMe
OCD3
NR
N
H
O

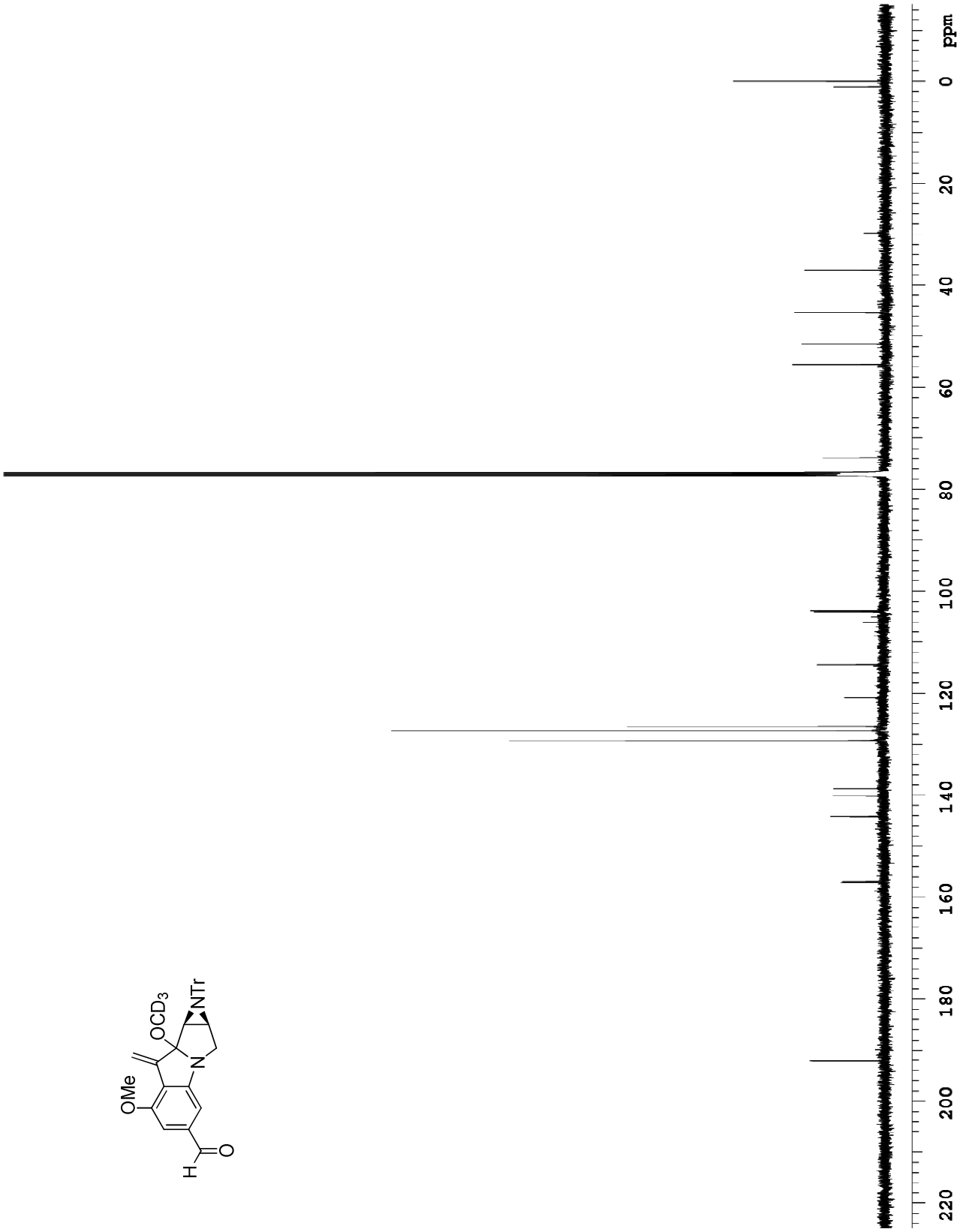
OMe
OCD3
NTr
N
O
H
ppm
0
20
40
60
80
100
120
140
160
180
200
220

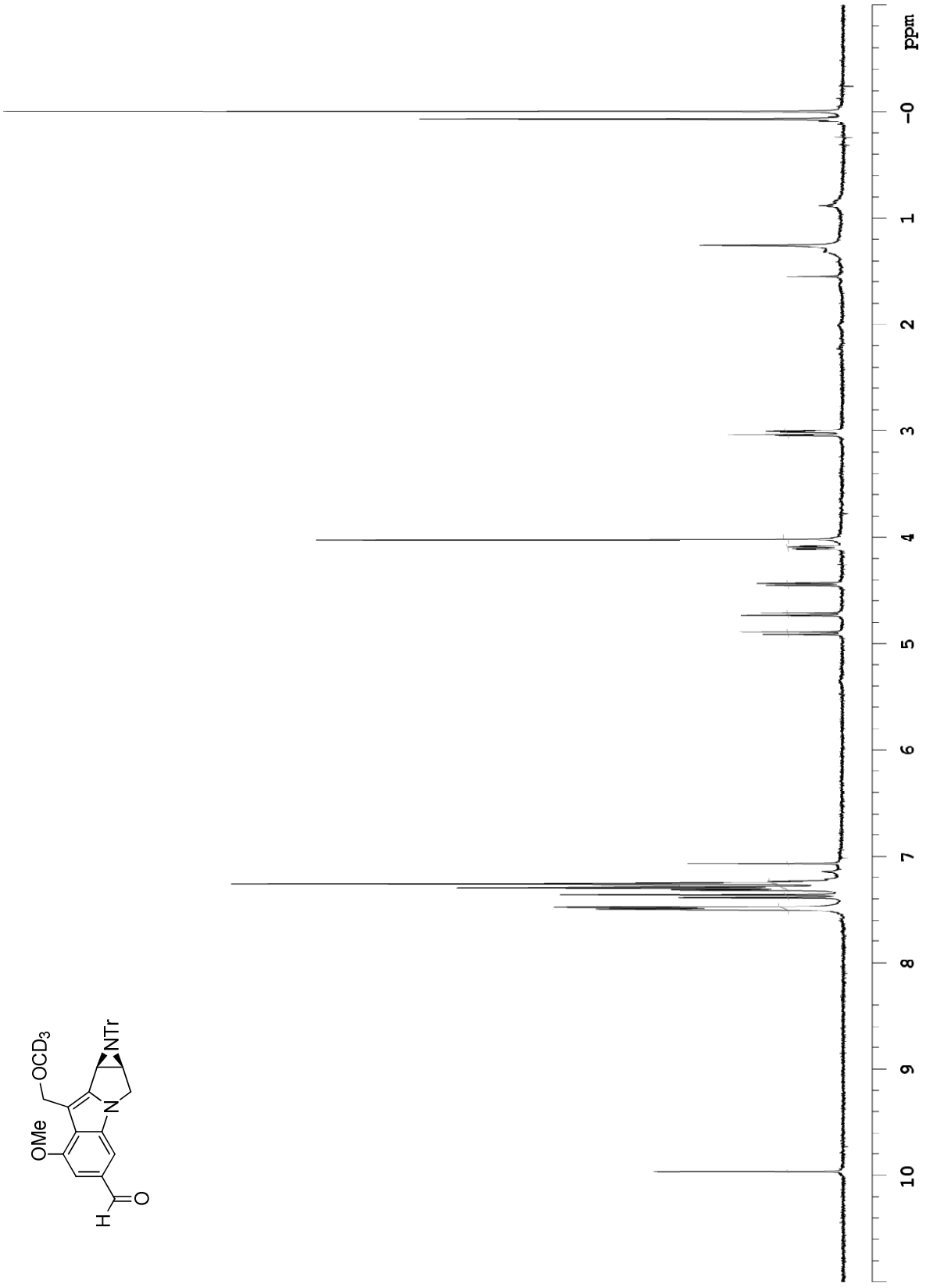
OCD3
NTr
N
OMe
O
H
ppm
10
9
8
7
6
5
4
3
2
1
0

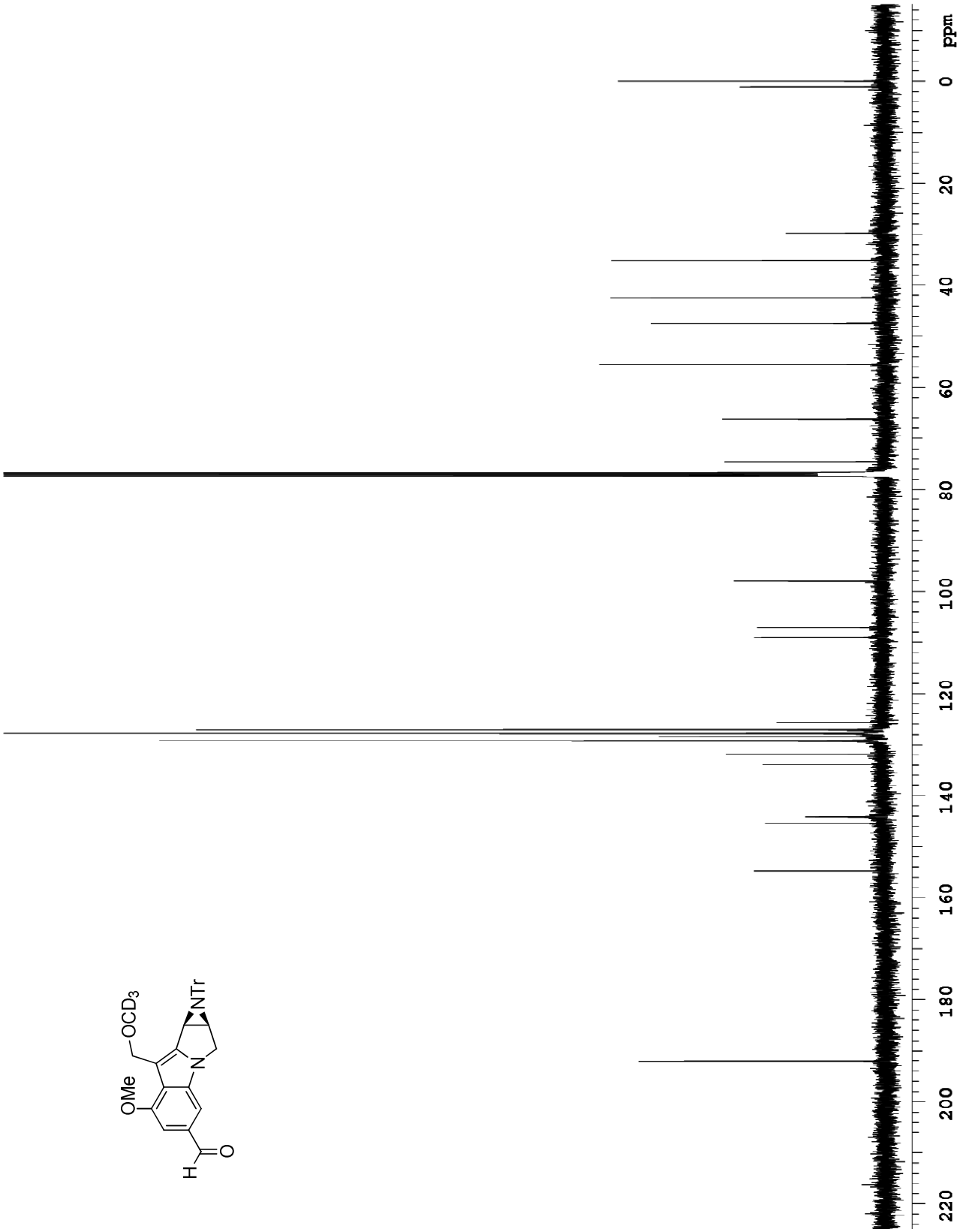
ppm
0
20
40
60
80
100
120
140
160
180
200
220
OCD3
NTr
N
OMe
H
O

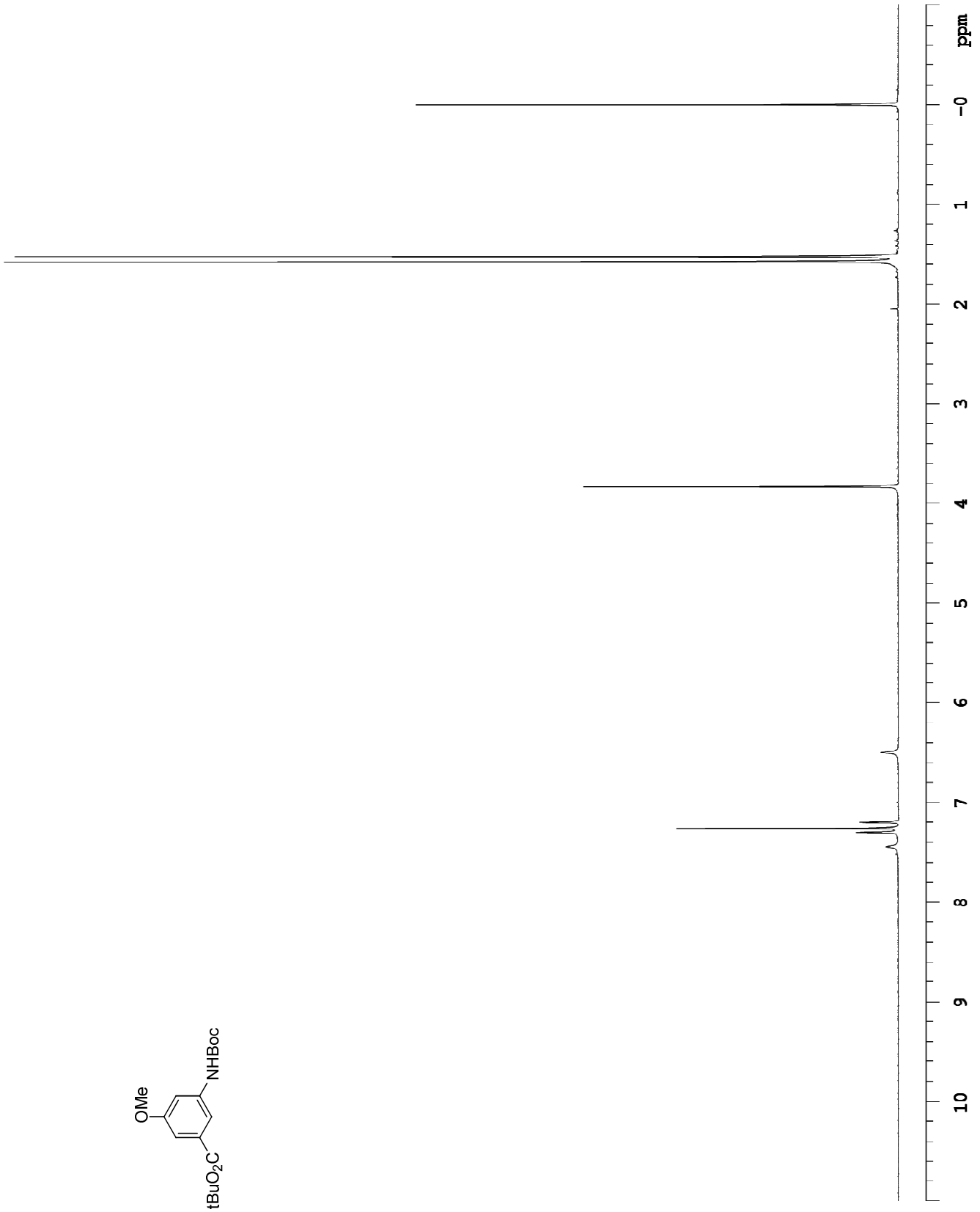
ppm
10
9
8
7
6
5
4
3
2
1
0
OMe
NHBoc
tBuO2C

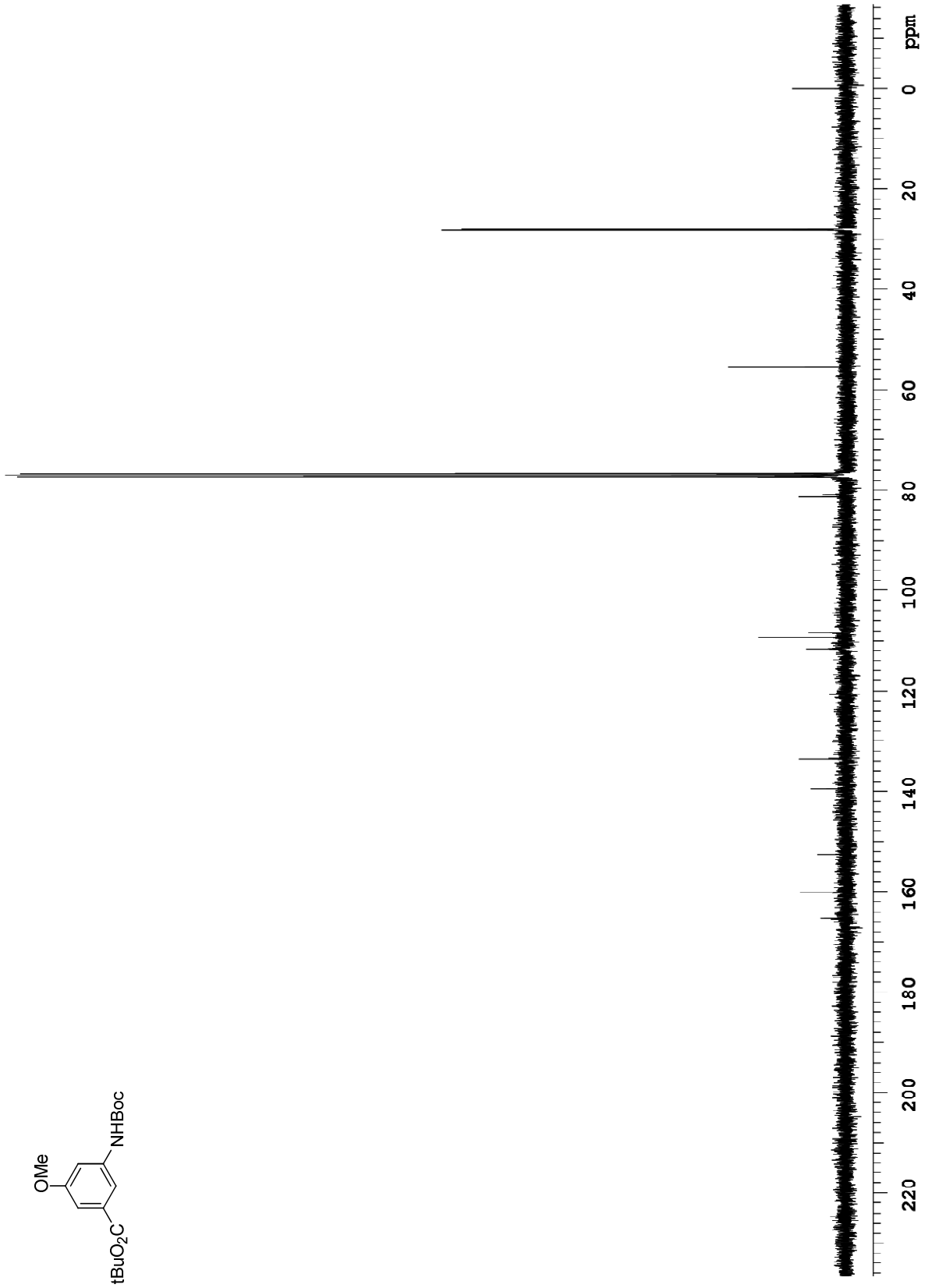
OMe
NHBoc
tBuO2C
ppm
0
20
40
60
80
100
120
140
160
180
200
220

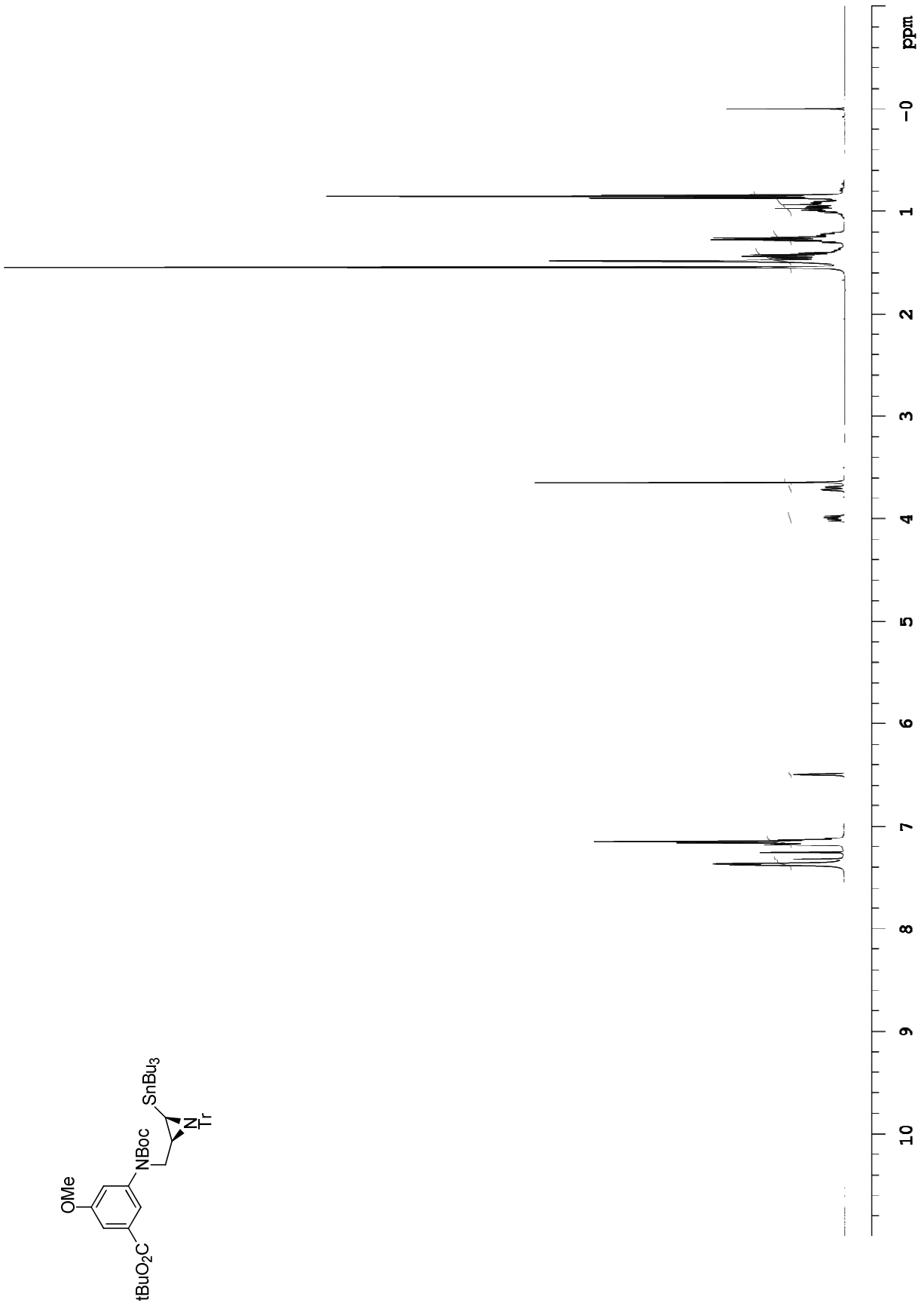
OMe
NBoc
SnBu3
N
Tr
tBuO2C
ppm
10
9
8
7
6
5
4
3
2
1
0

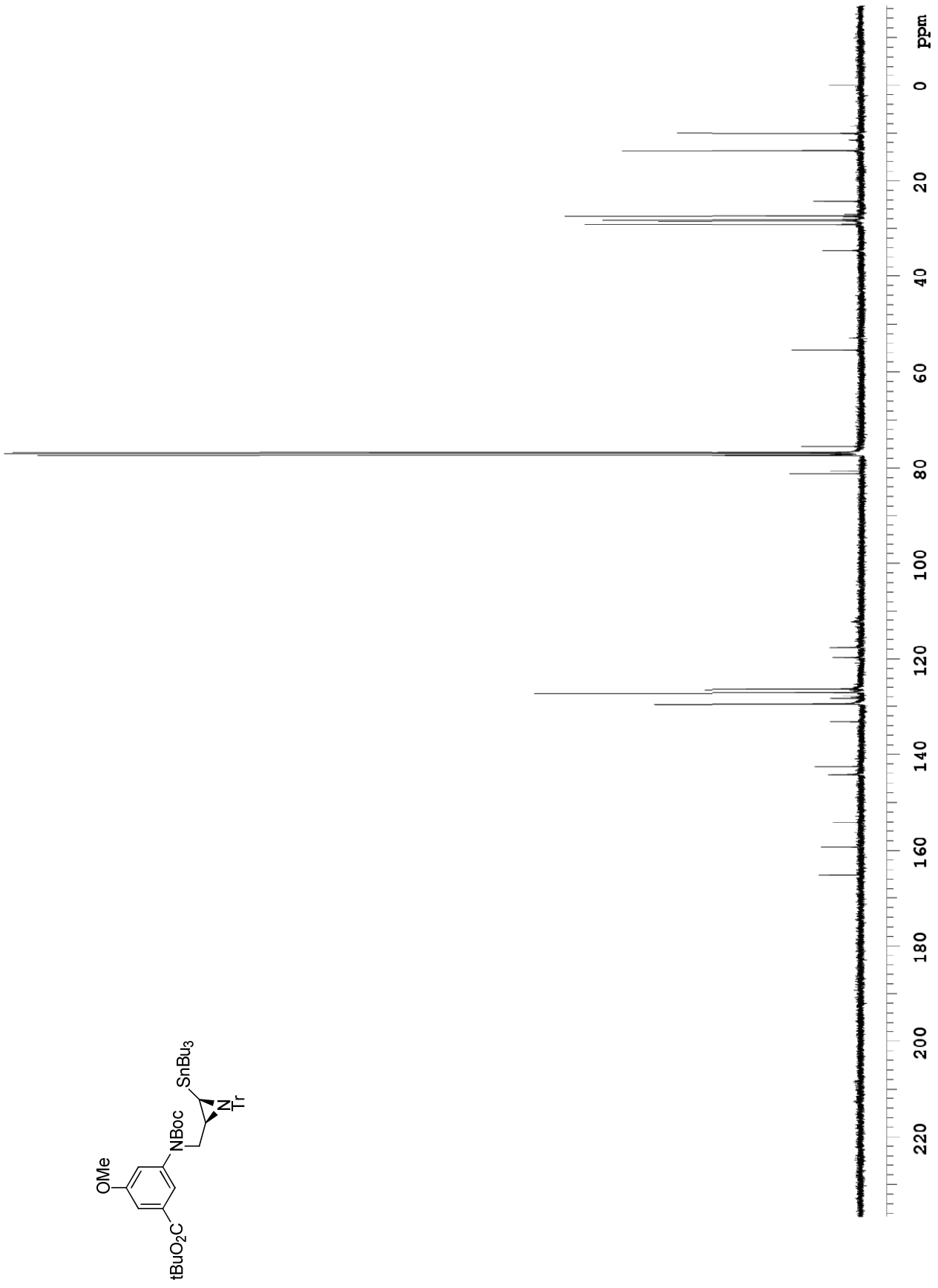
OMe
NBoc
SnBu3
N
Tr
tBuO2C
ppm
0
20
40
60
80
100
120
140
160
180
200
220

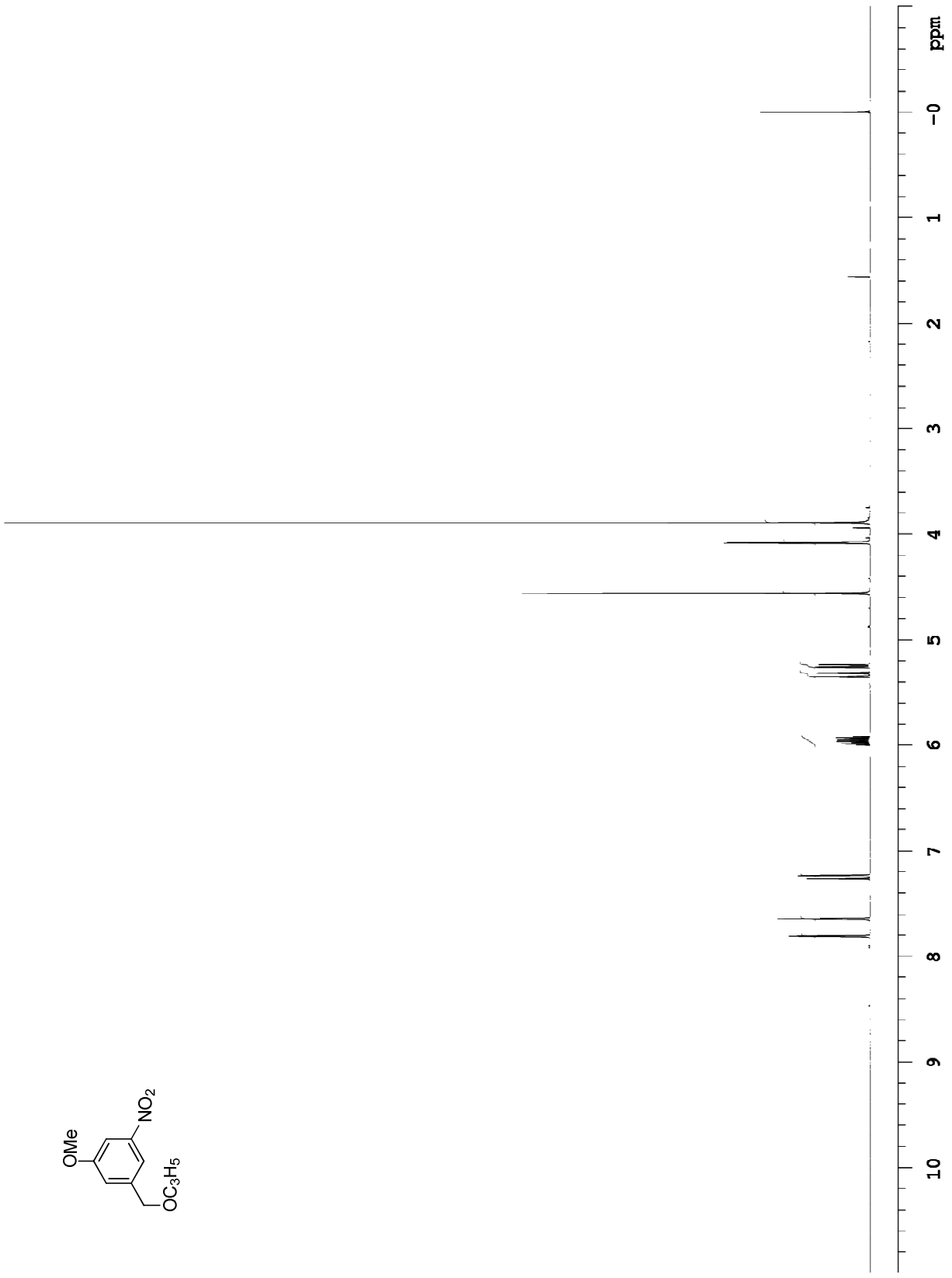
OMe
NO2
OC3H5
ppm
10
9
8
7
6
5
4
3
2
1
0

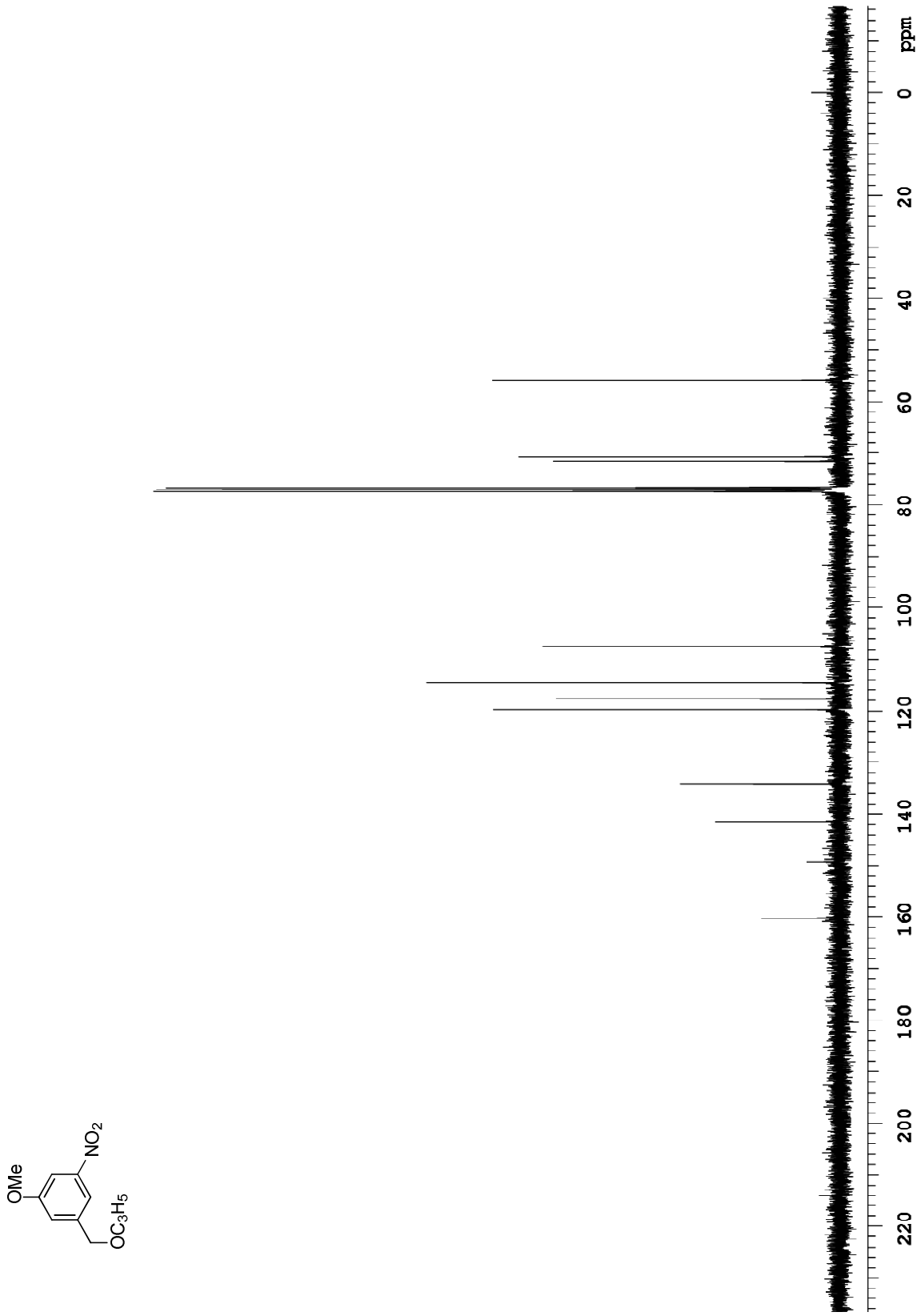
OMe
NO2
OC3H5
ppm
0
20
40
60
80
100
120
140
160
180
200
220

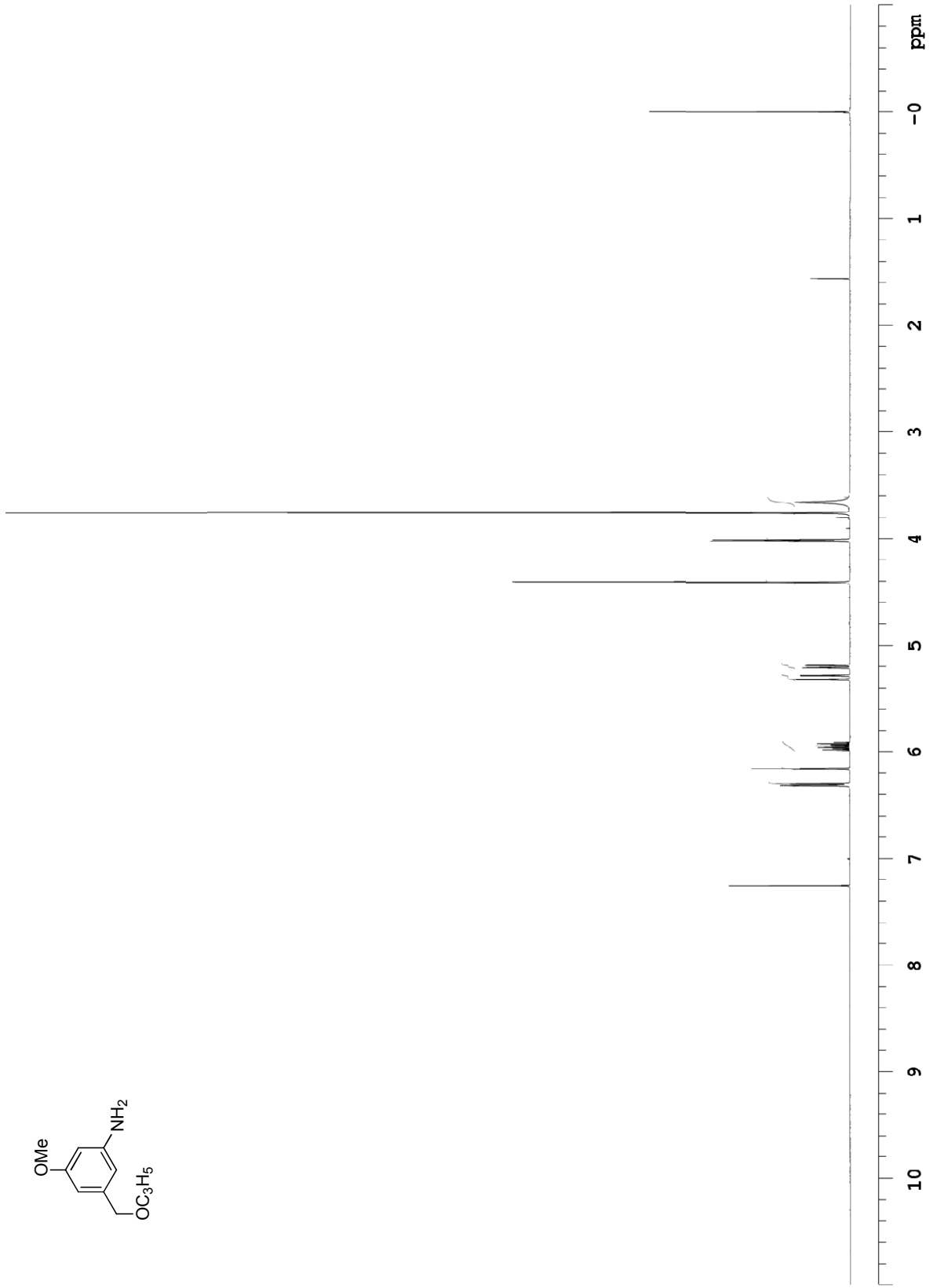
OMe
NH2
OC3H5
ppm
10
9
8
7
6
5
4
3
2
1
0

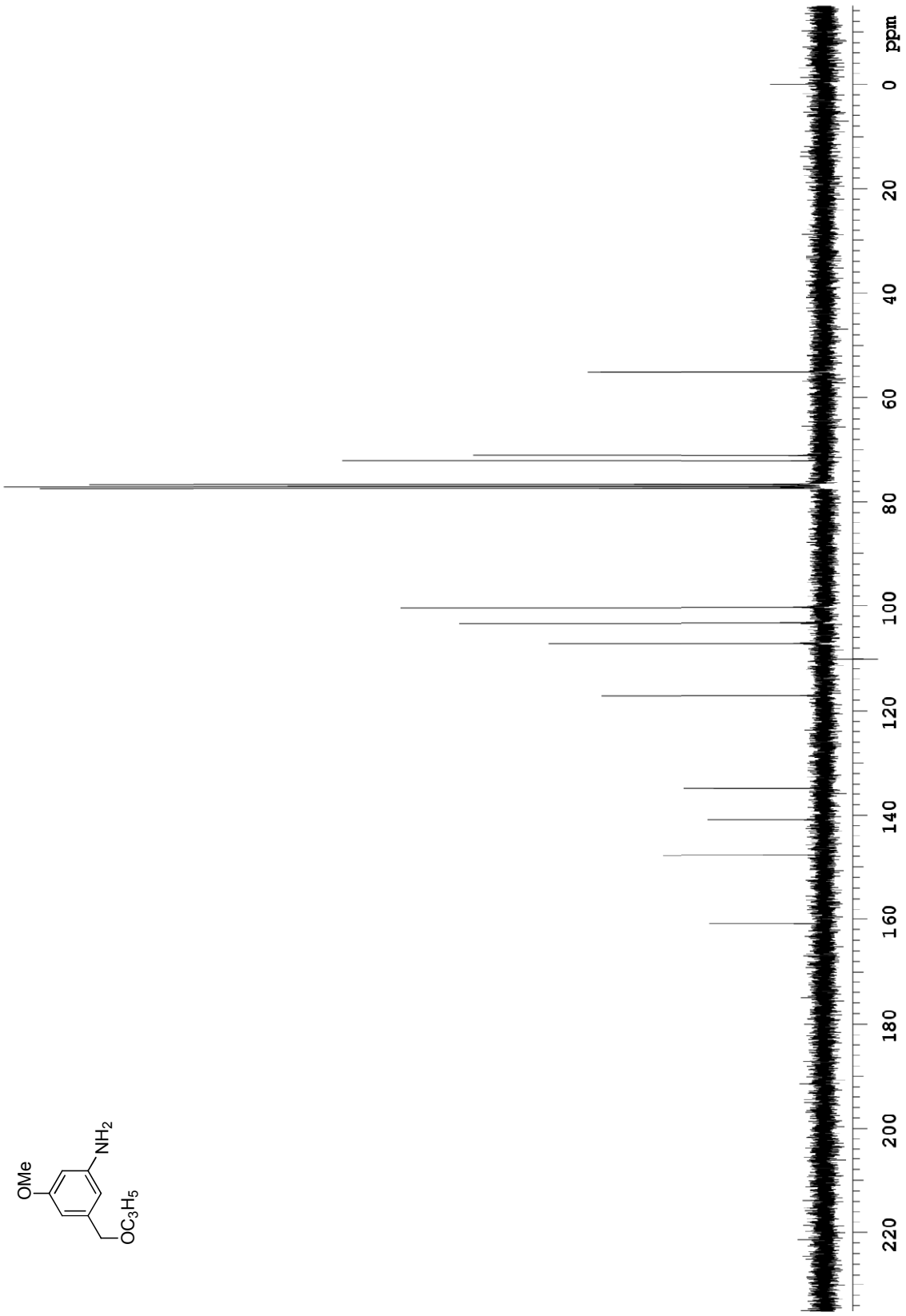
ppm
0
20
40
60
80
100
120
140
160
180
200
220
OMe
NH2
OC3H5

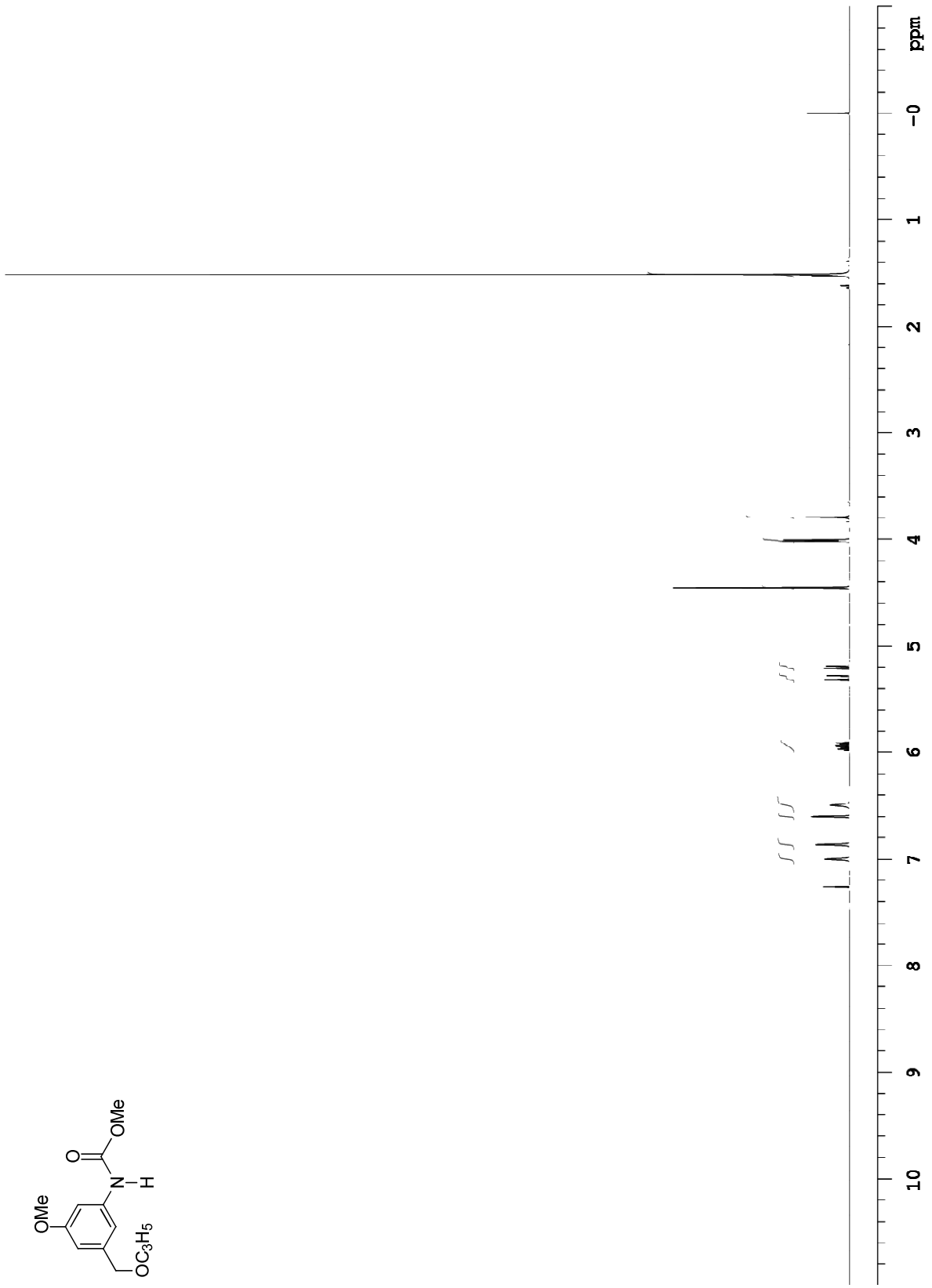
OMe
O
OMe
N
H
OMe
OC3H5
ppm
10
9
8
7
6
5
4
3
2
1
0

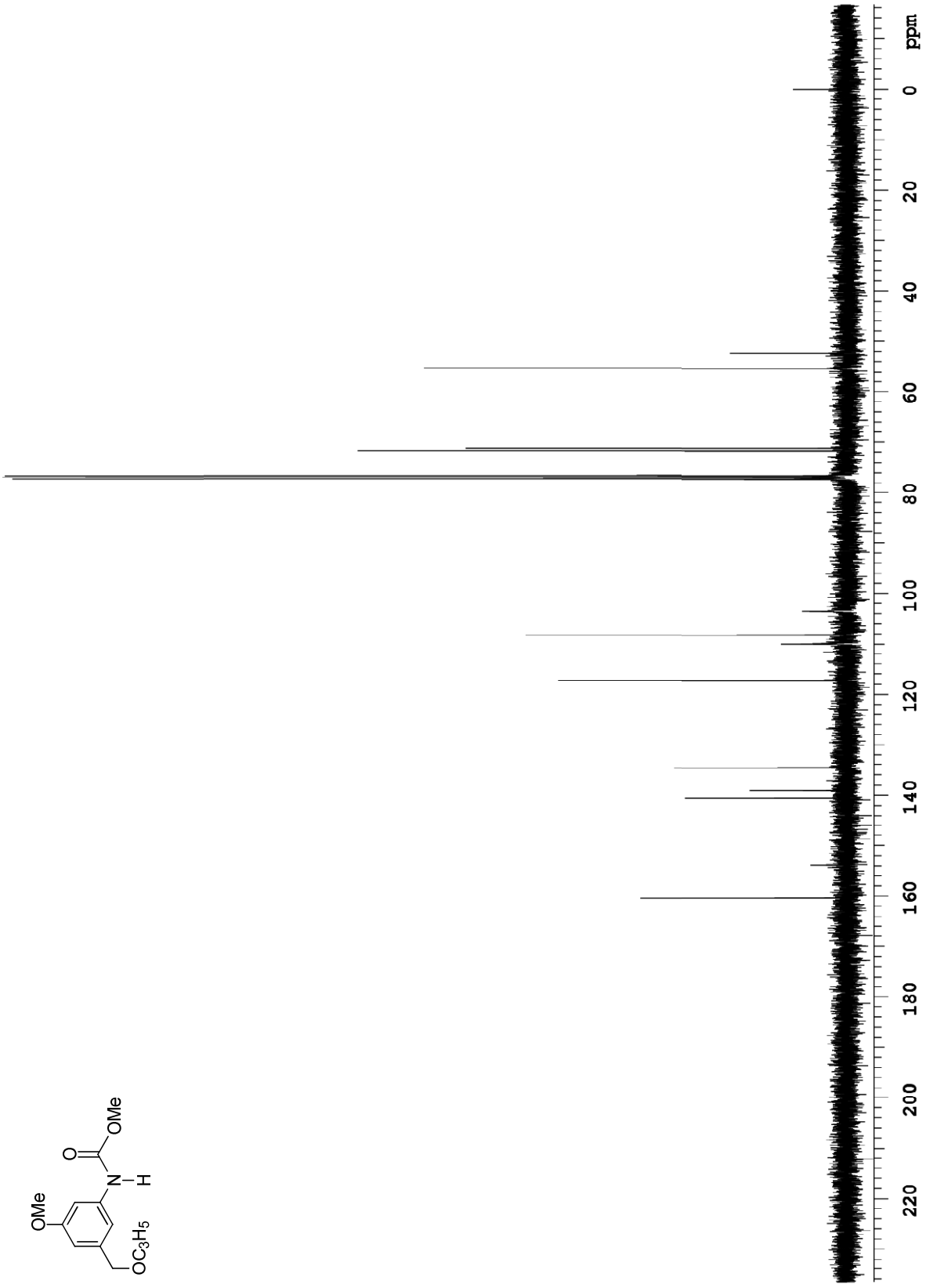
OMe
O
OMe
N
H
OMe
OC3H5
ppm
0
20
40
60
80
100
120
140
160
180
200
220

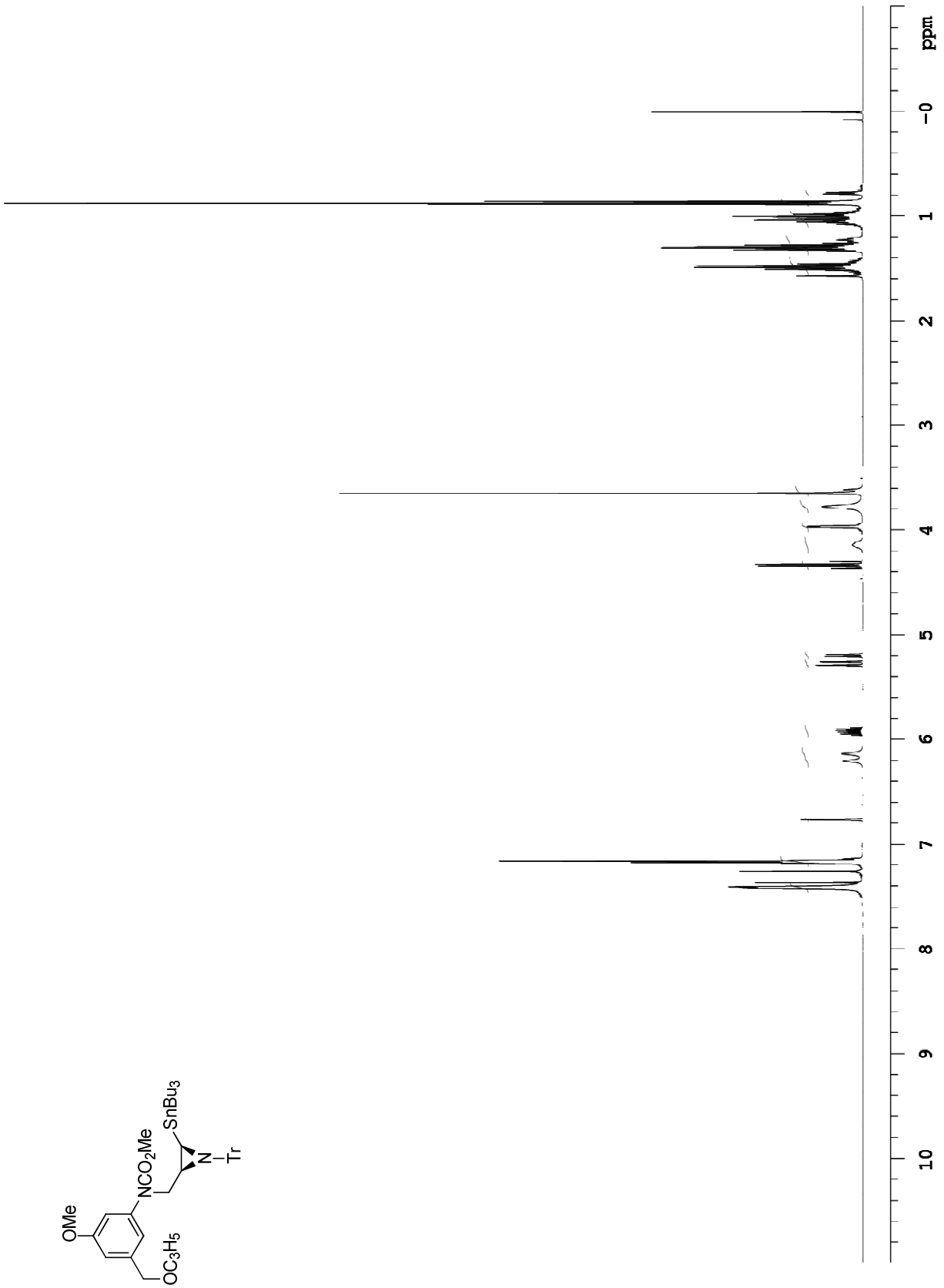
OMe
OC3H5
NCO2Me
SnBu3
N
Tr
ppm
10
9
8
7
6
5
4
3
2
1
0

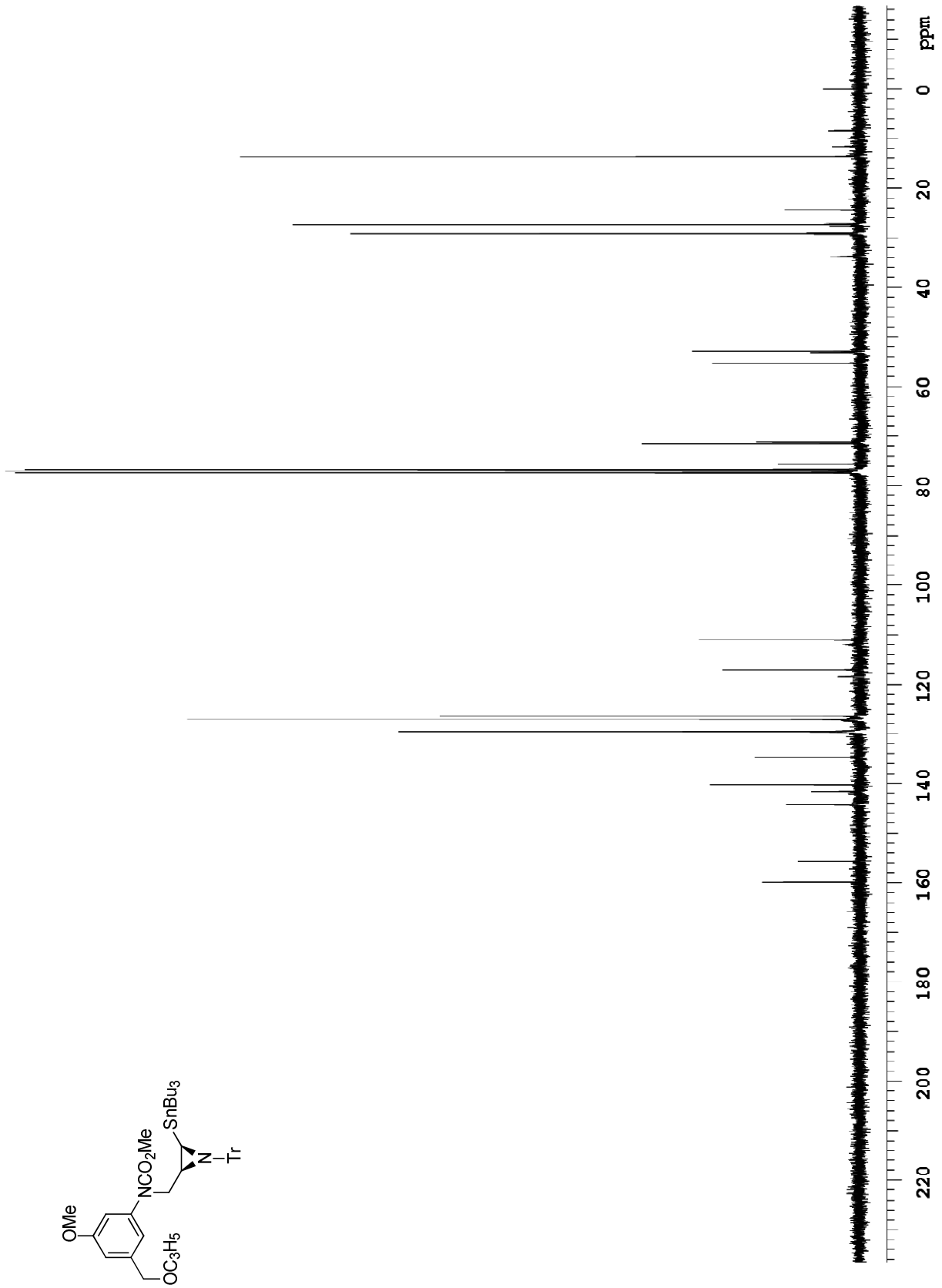
OMe
NCO2Me
SnBu3
N
Tr
OC3H5
ppm
0
20
40
60
80
100
120
140
160
180
200
220

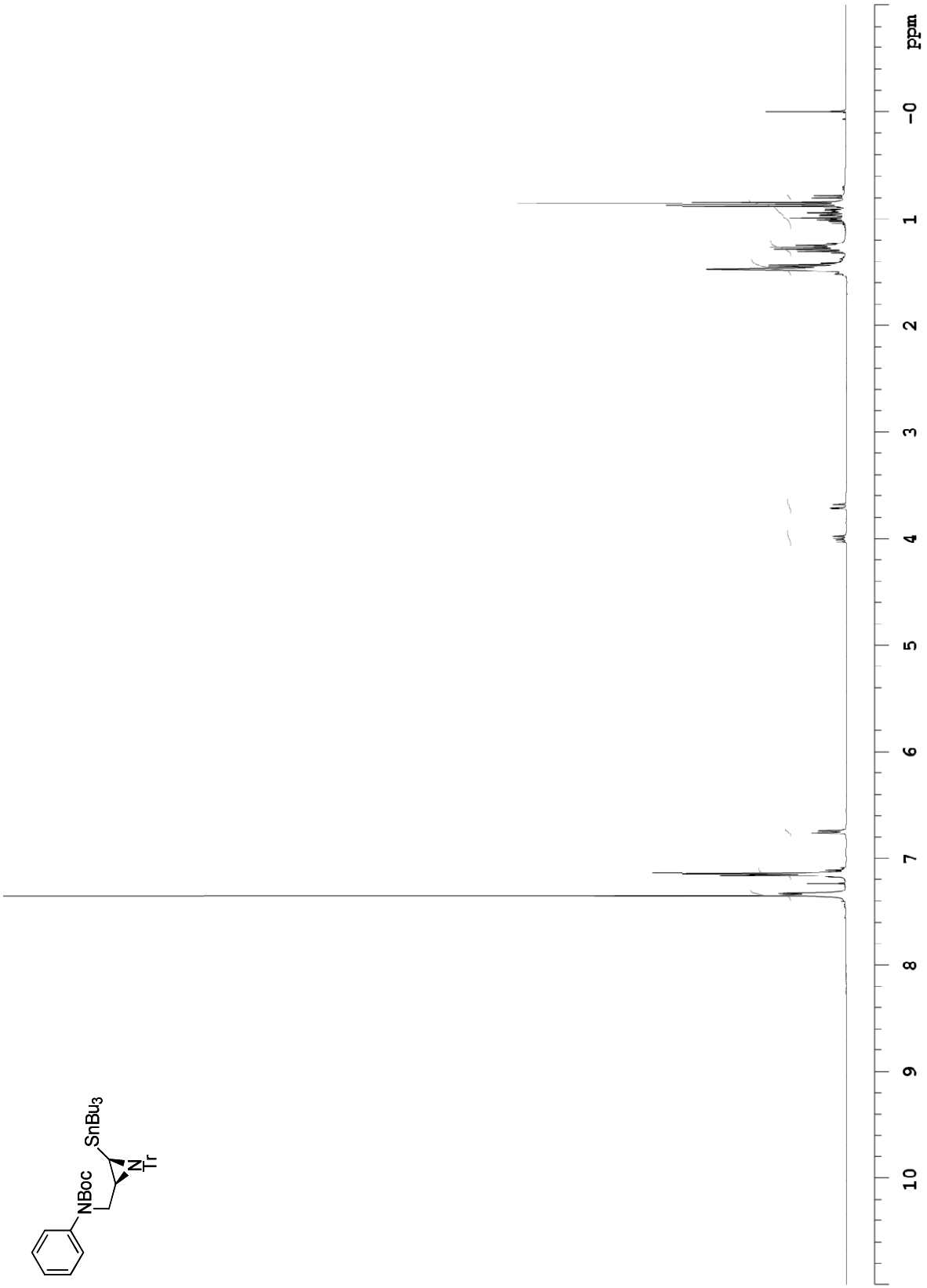
NBoc
SnBu3
N
Tr
ppm
10
9
8
7
6
5
4
3
2
1
0

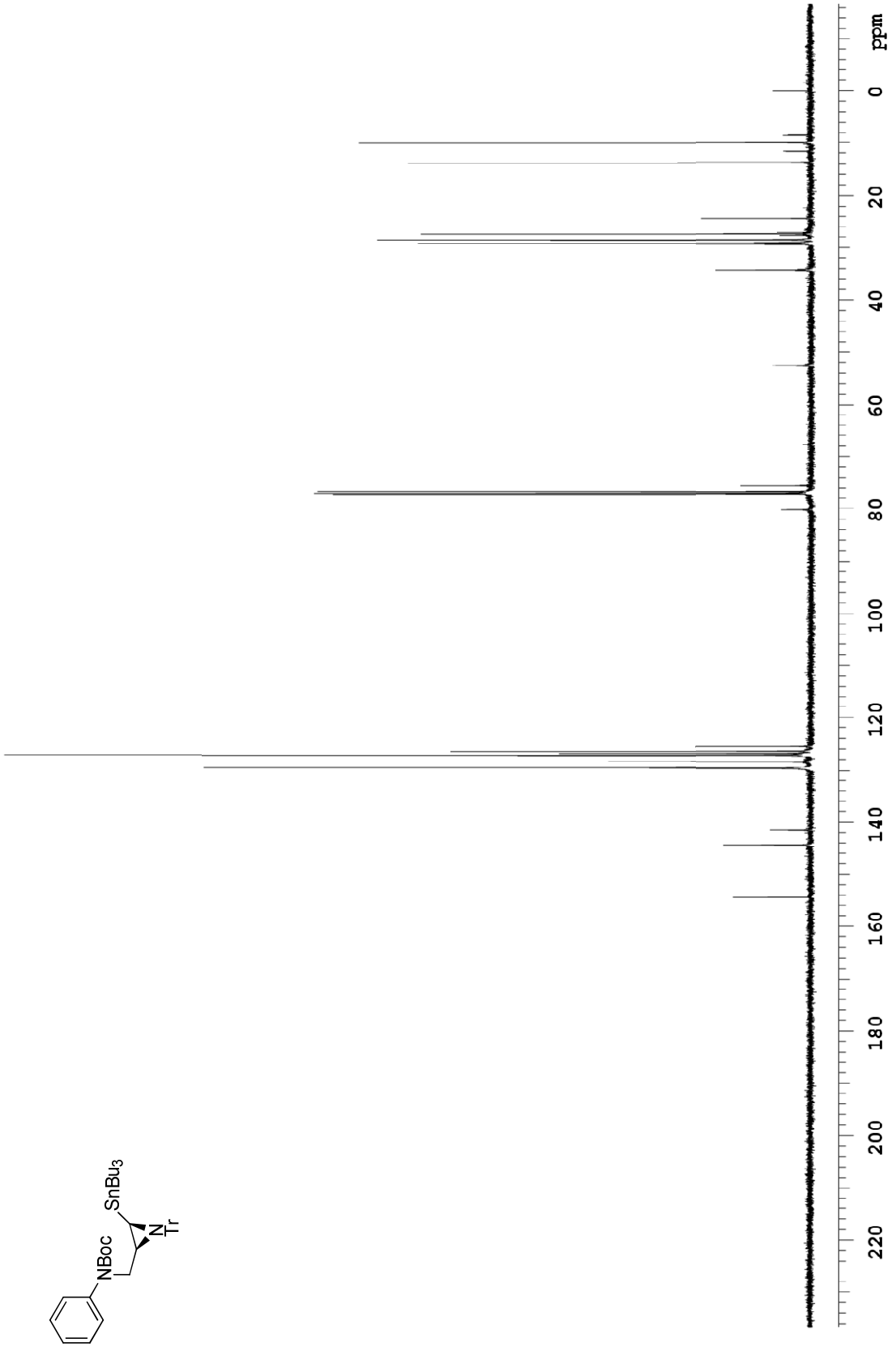
NBoc
SnBu3
N
Tr
ppm
0
20
40
60
80
100
120
140
160
180
200
220

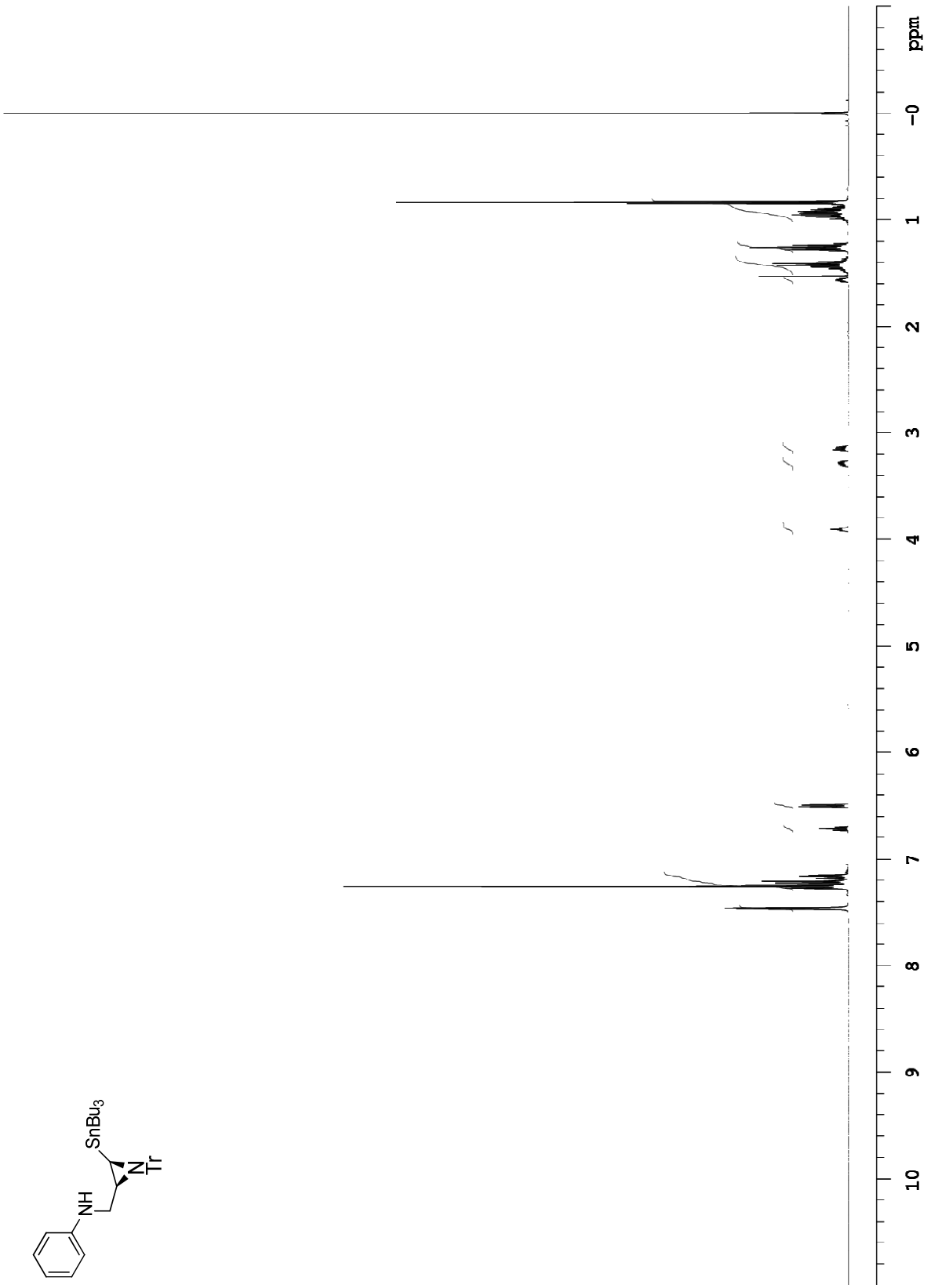
SnBu3
N
Tr
NH
ppm
10
9
8
7
6
5
4
3
2
1
0

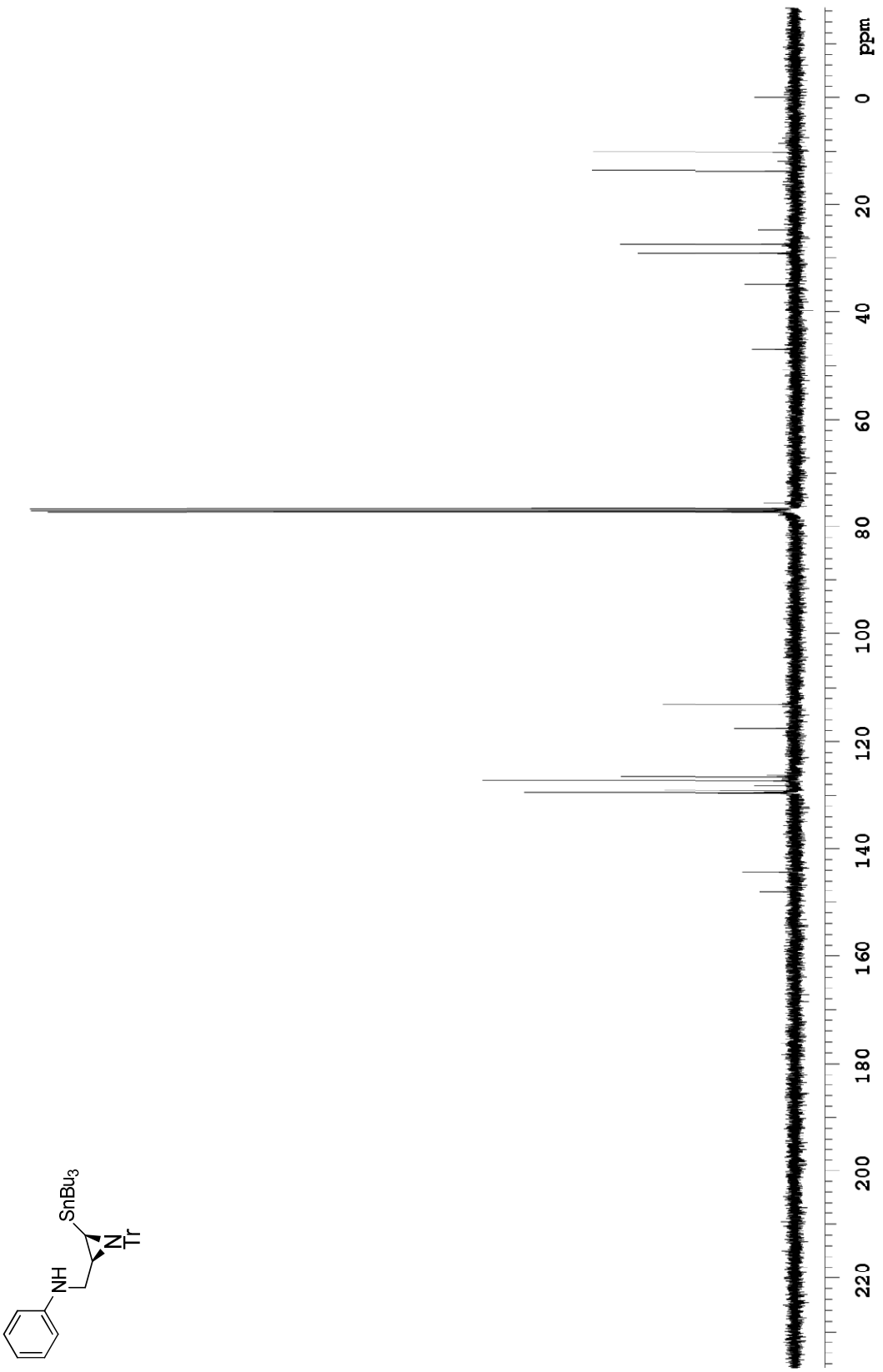
SnBu3
N
Tr
NH
ppm
0
20
40
60
80
100
120
140
160
180
200
220

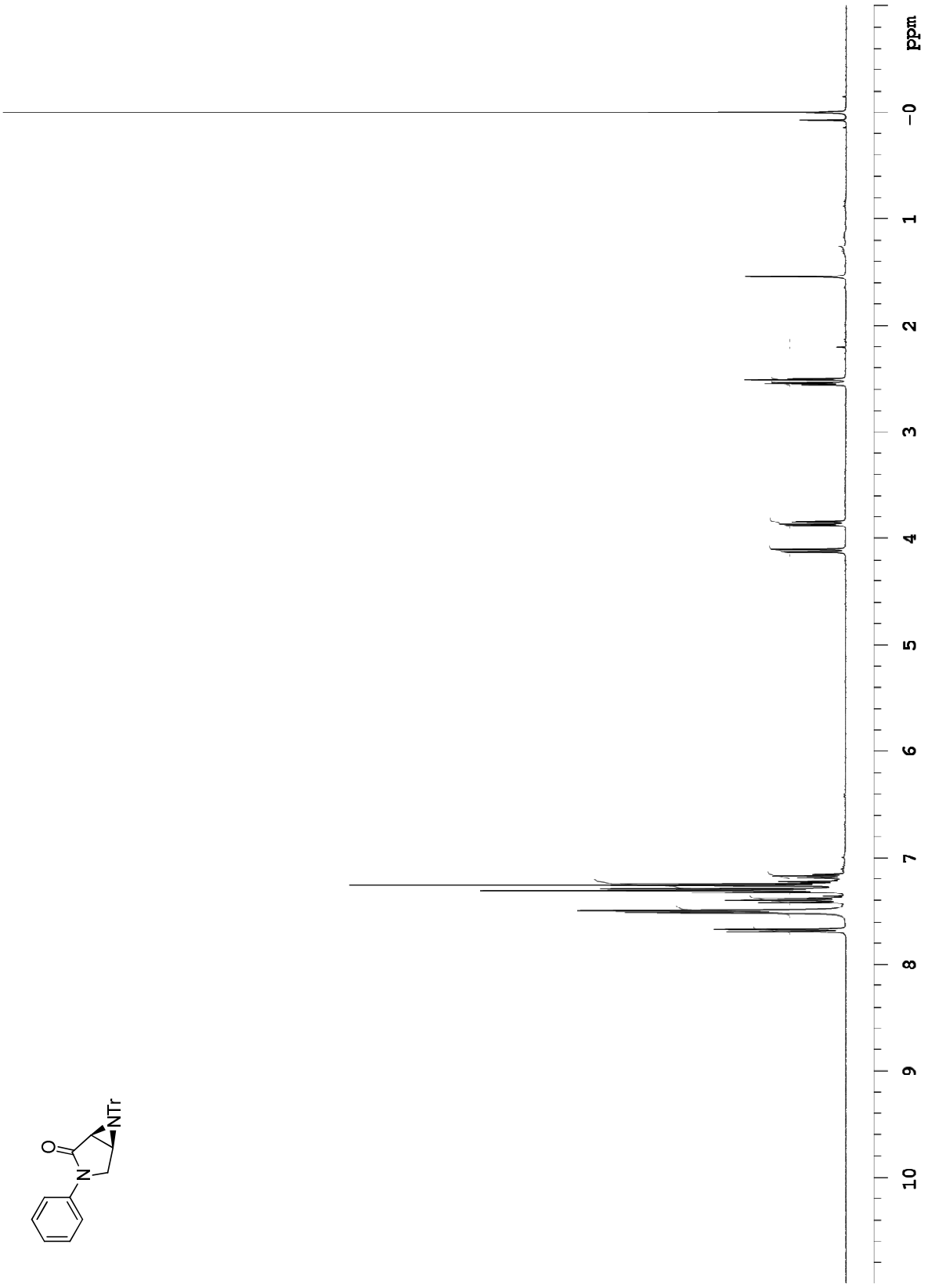
NTr
O
N
ppm
10
9
8
7
6
5
4
3
2
1
0

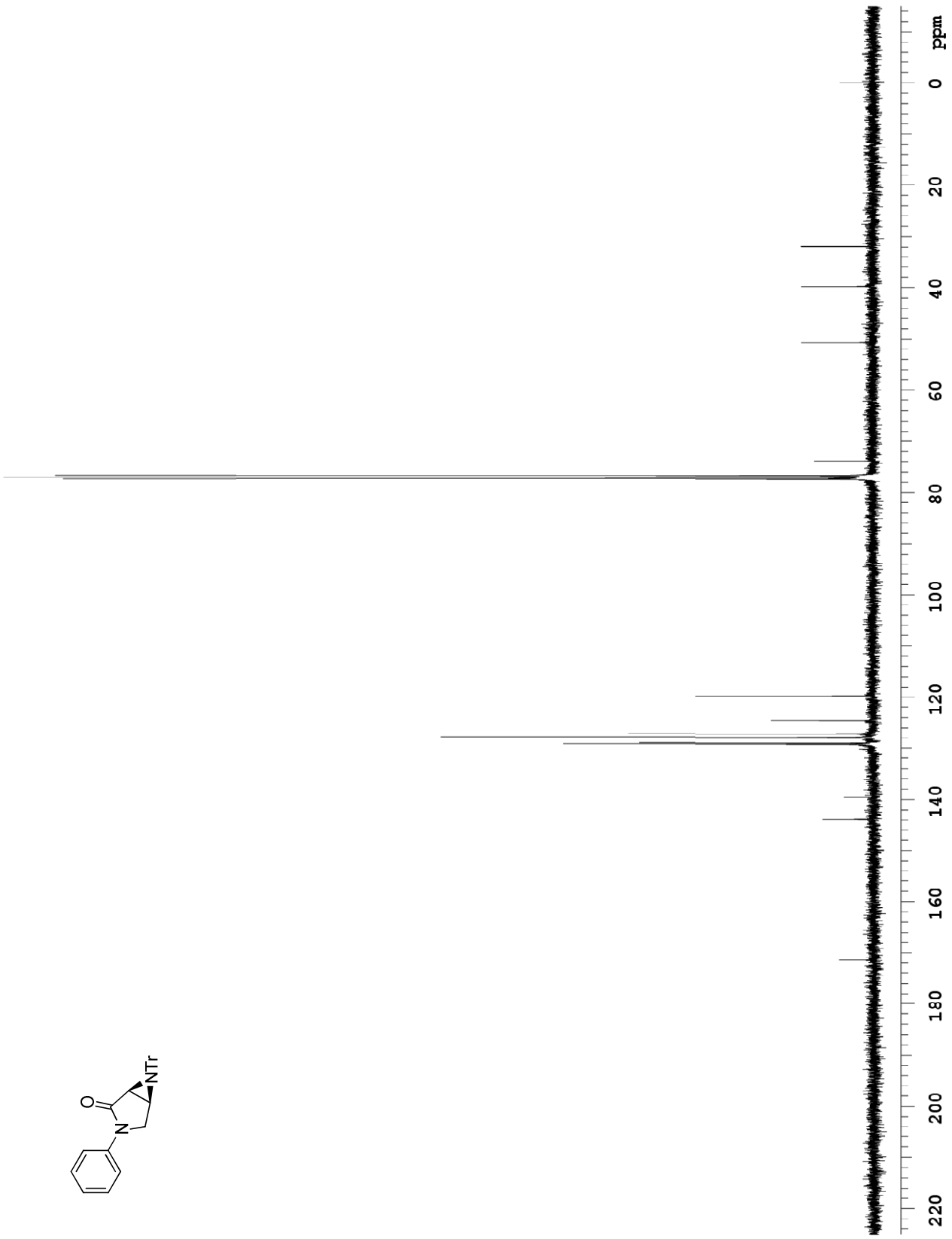
NTr
O
N
ppm
0
20
40
60
80
100
120
140
160
180
200
220

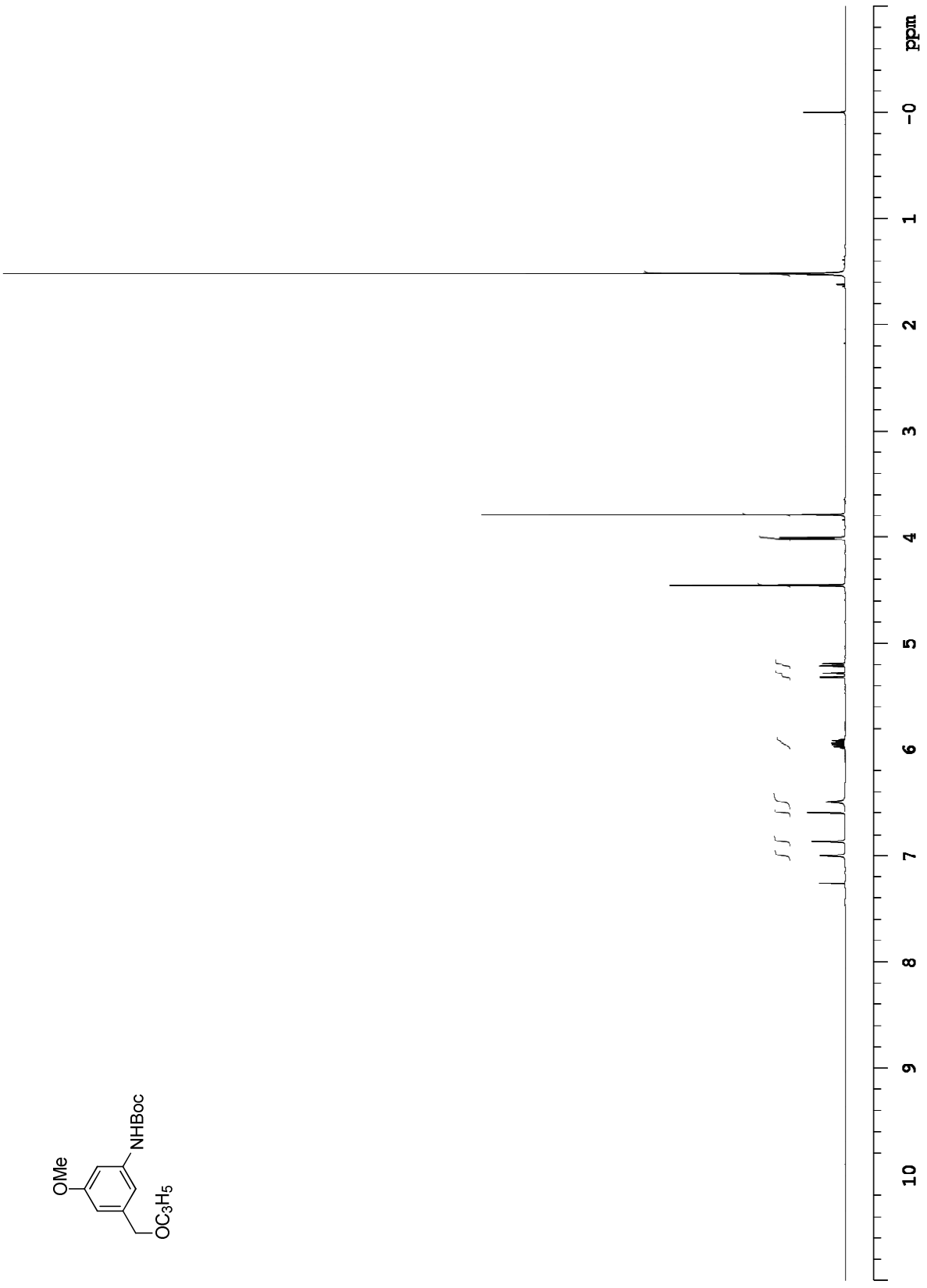
NHBoc
OMe
OC3H5
ppm
10
9
8
7
6
5
4
3
2
1
0

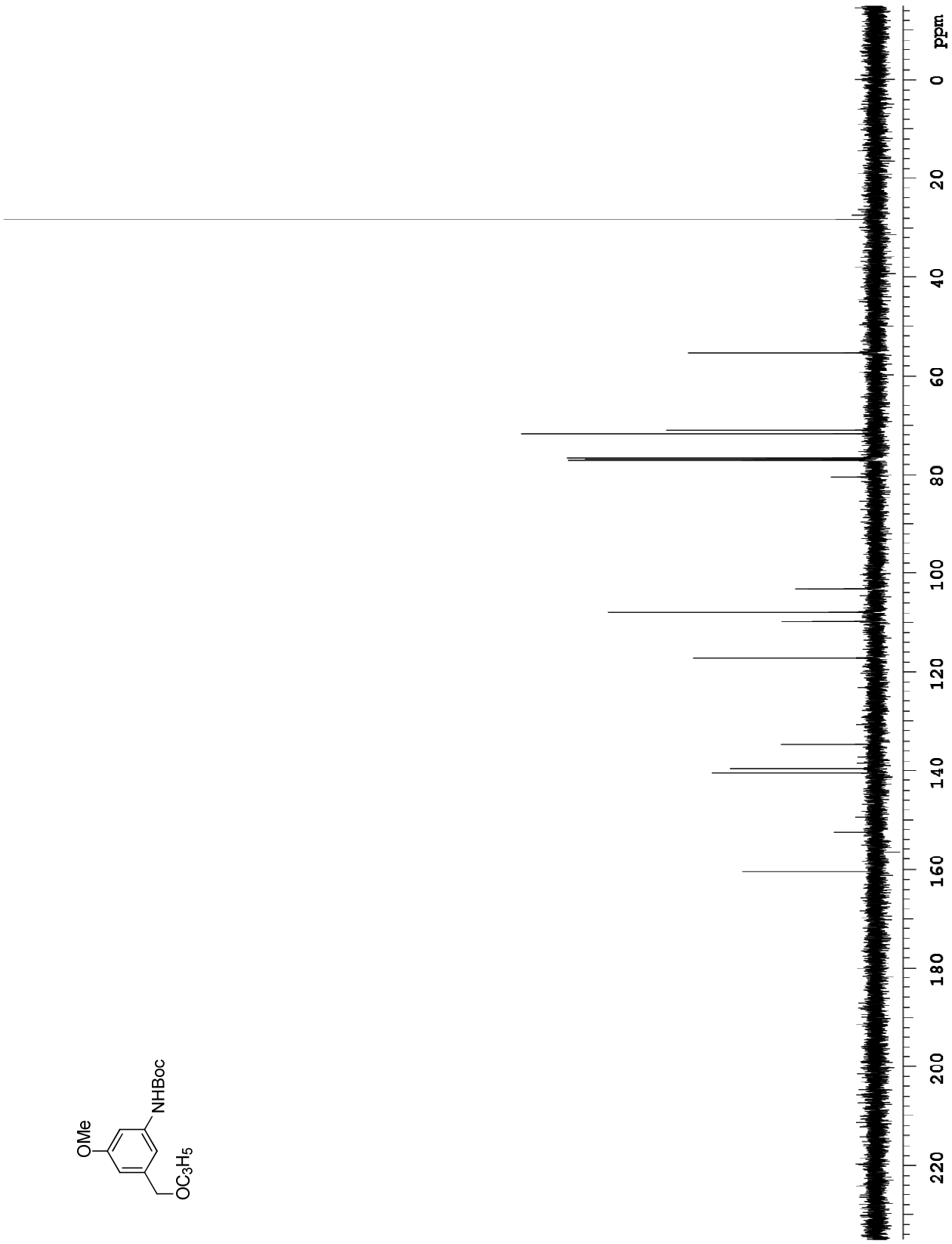
OMe
NHBoc
OC3H5
ppm
0
20
40
60
80
100
120
140
160
180
200
220

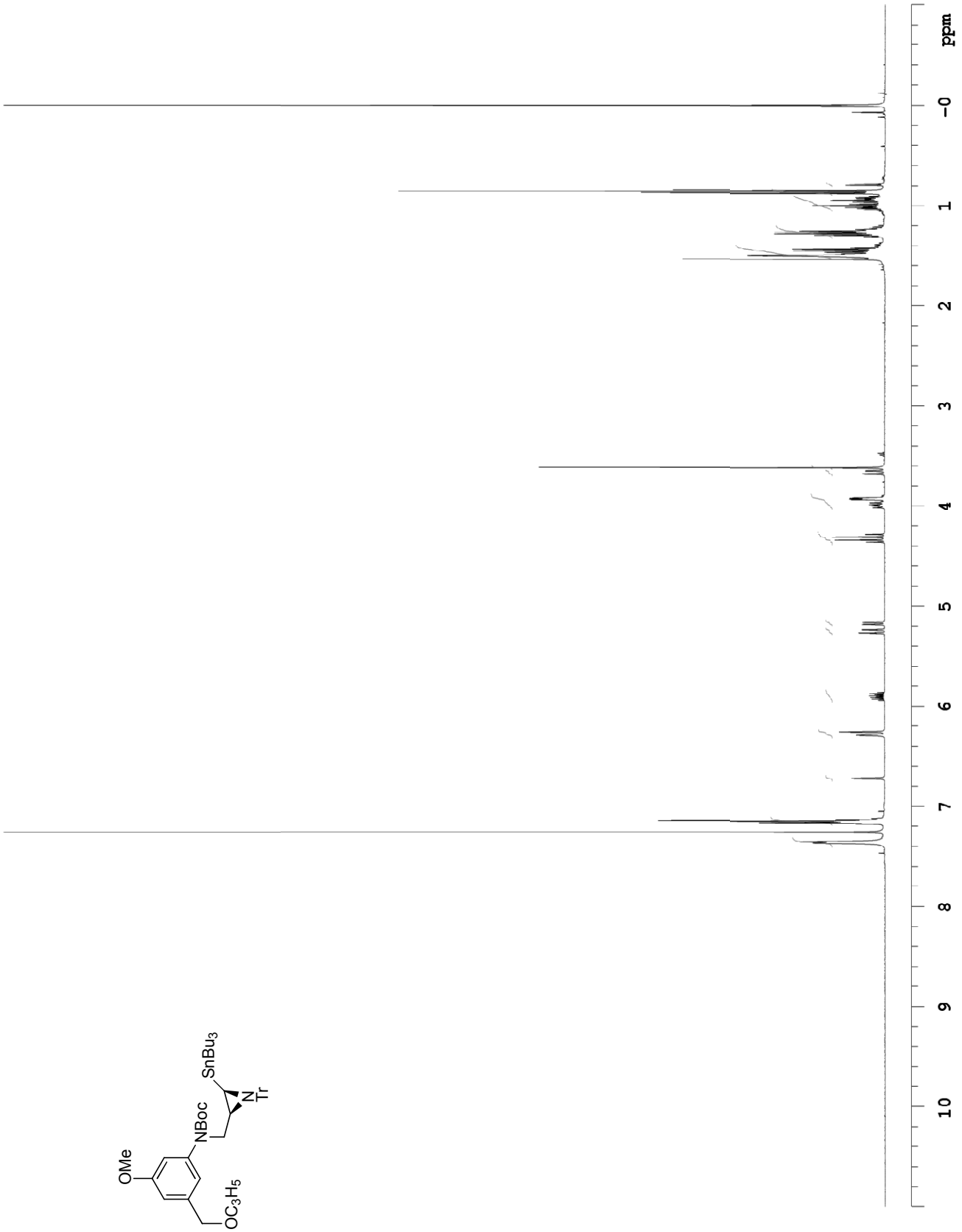
OMe
OC3H5
NBoc
SnBu3
N
Tr
ppm
10
9
8
7
6
5
4
3
2
1
0

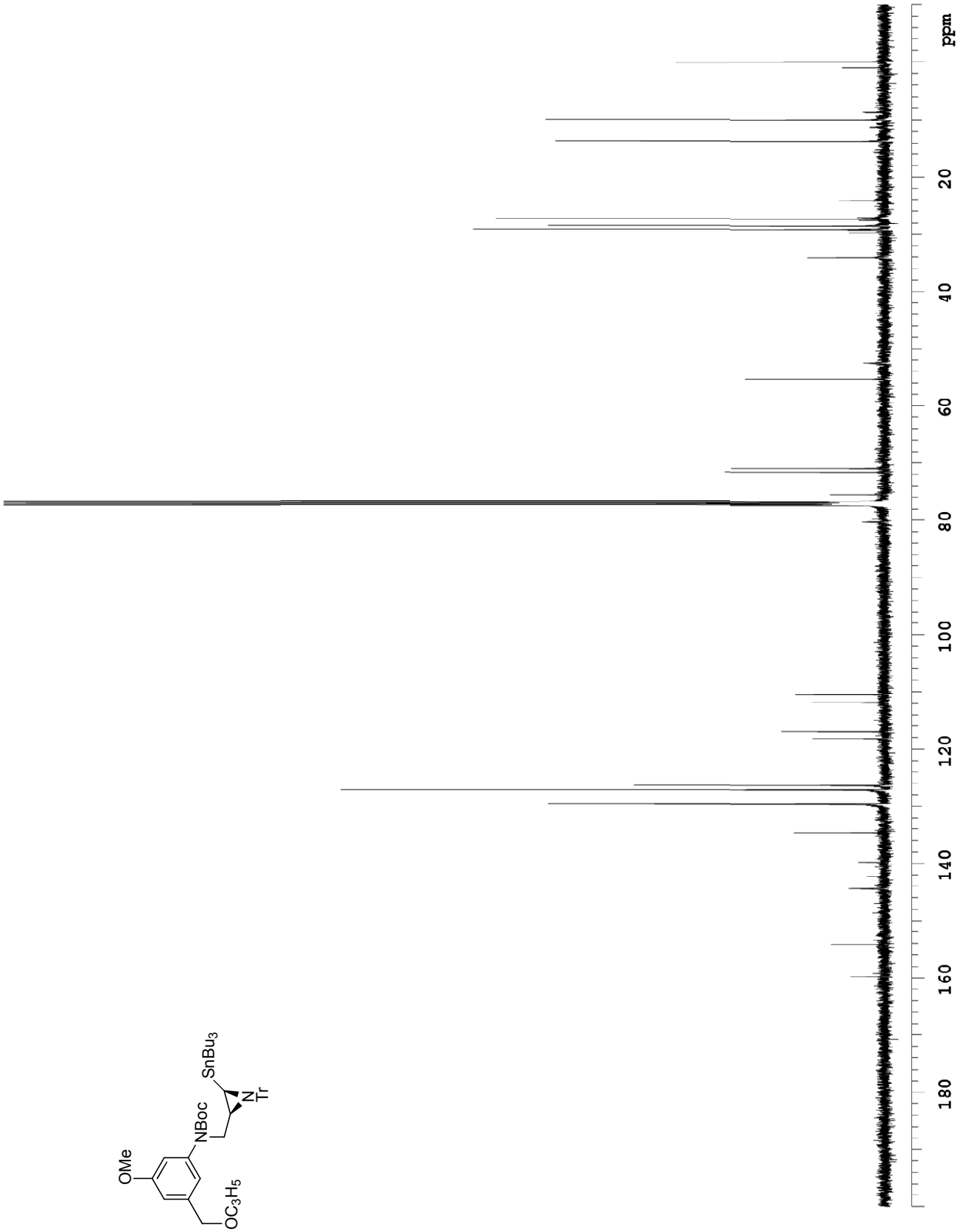
ppm
20
40
60
80
100
120
140
160
180
OMe
NBoc
SnBu3
N
Tr
OC3H5

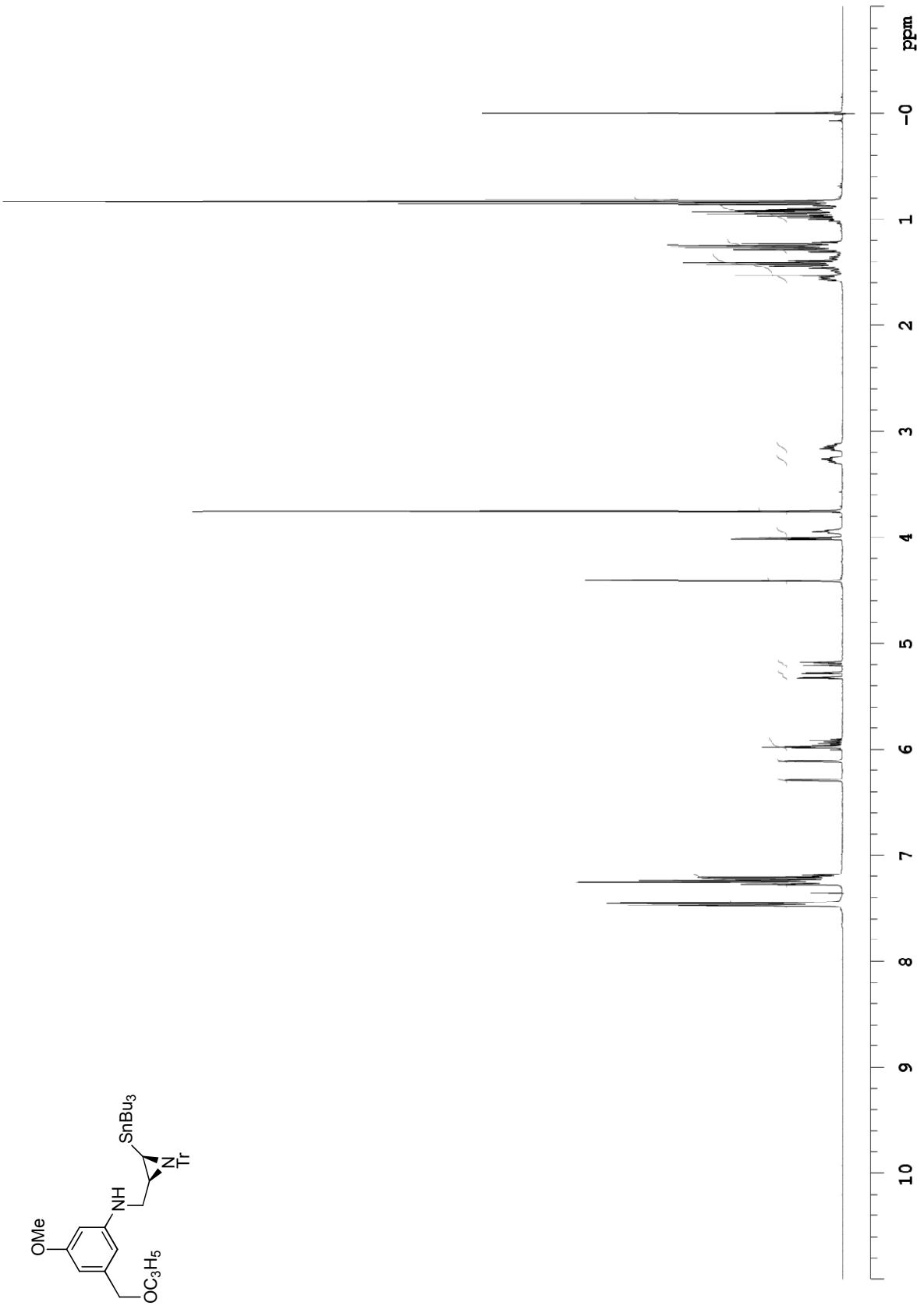
OMe
NH
SnBu3
N
Tr
OC3H5
ppm
10
9
8
7
6
5
4
3
2
1
0

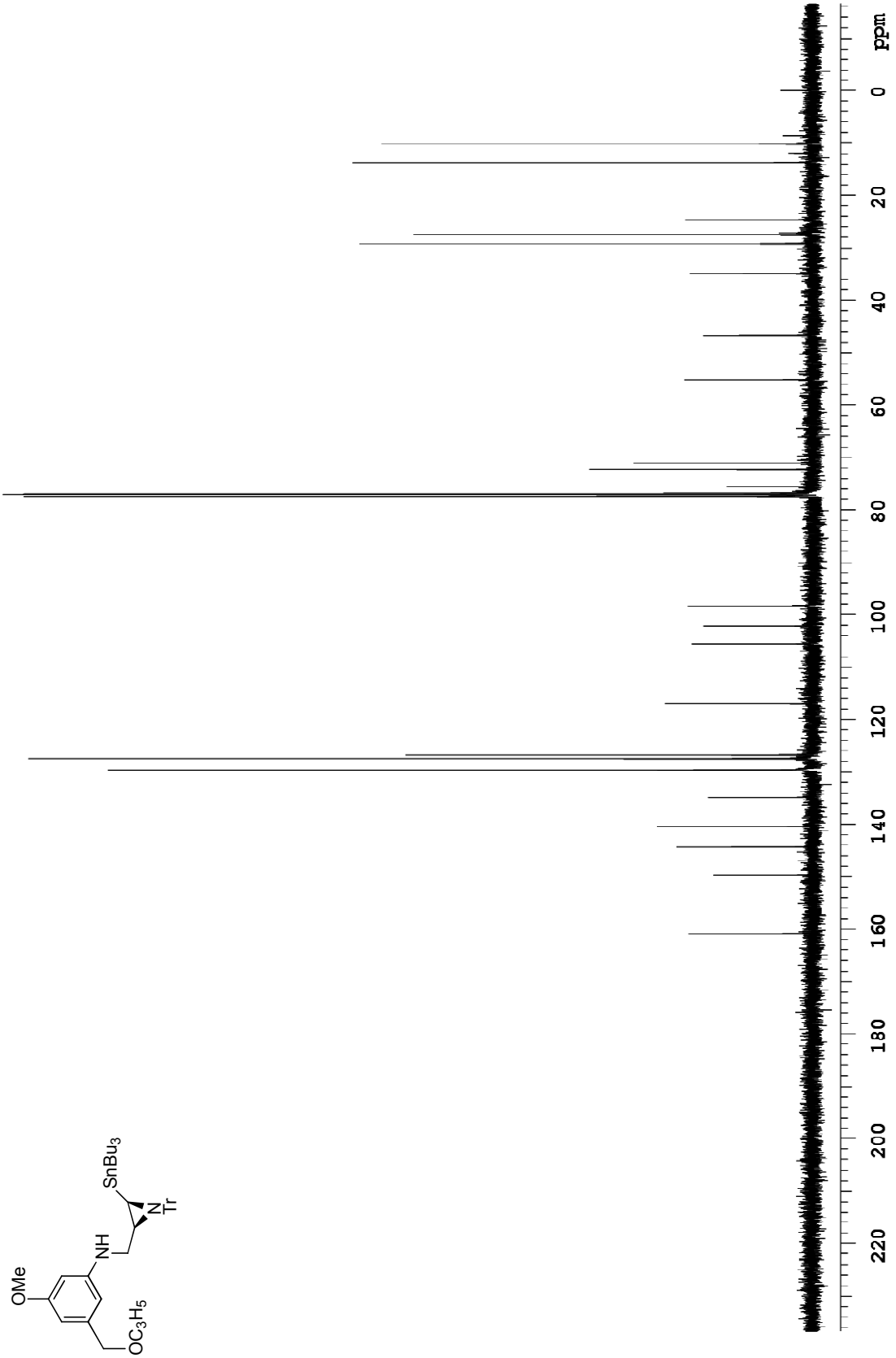
ppm
0
20
40
60
80
100
120
140
160
180
200
220
OMe
NH
SnBu3
N
Tr
OC3H5

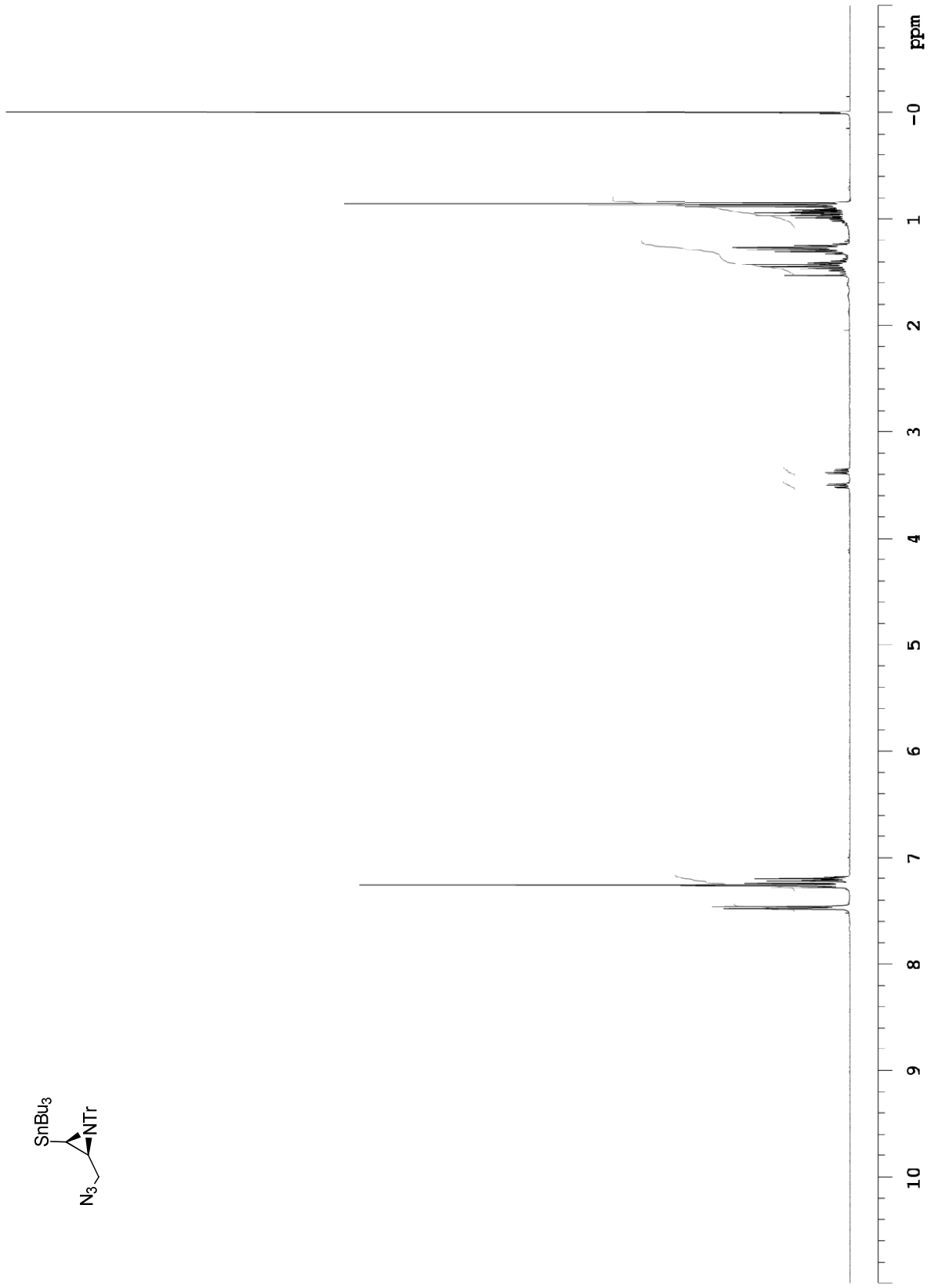
SnBu3
NTr
N3
ppm
10
9
8
7
6
5
4
3
2
1
0

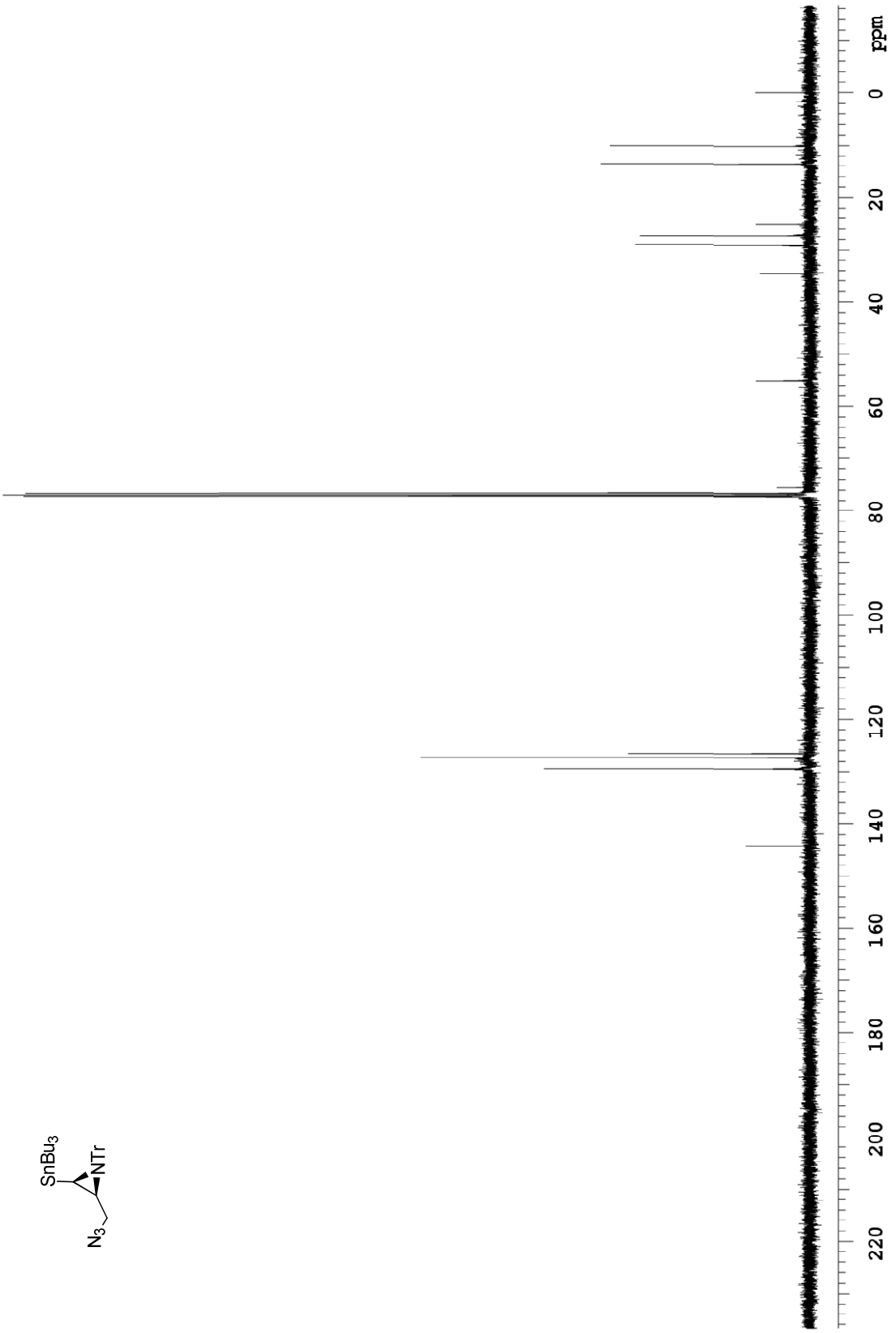
SnBu3
NTr
N3
ppm
0
20
40
60
80
100
120
140
160
180
200
220

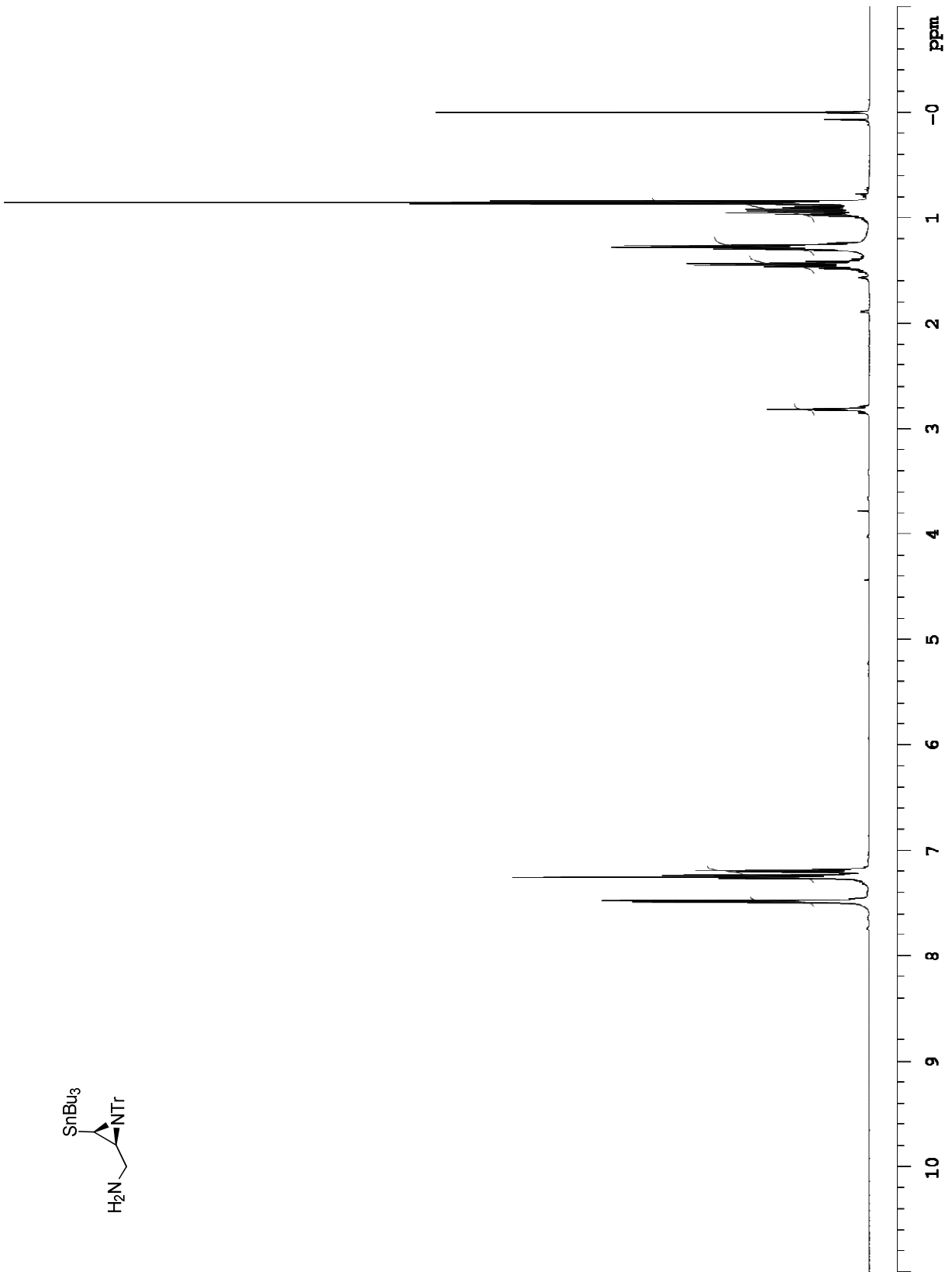
SnBu3
NTr
H2N
ppm
10
9
8
7
6
5
4
3
2
1
0

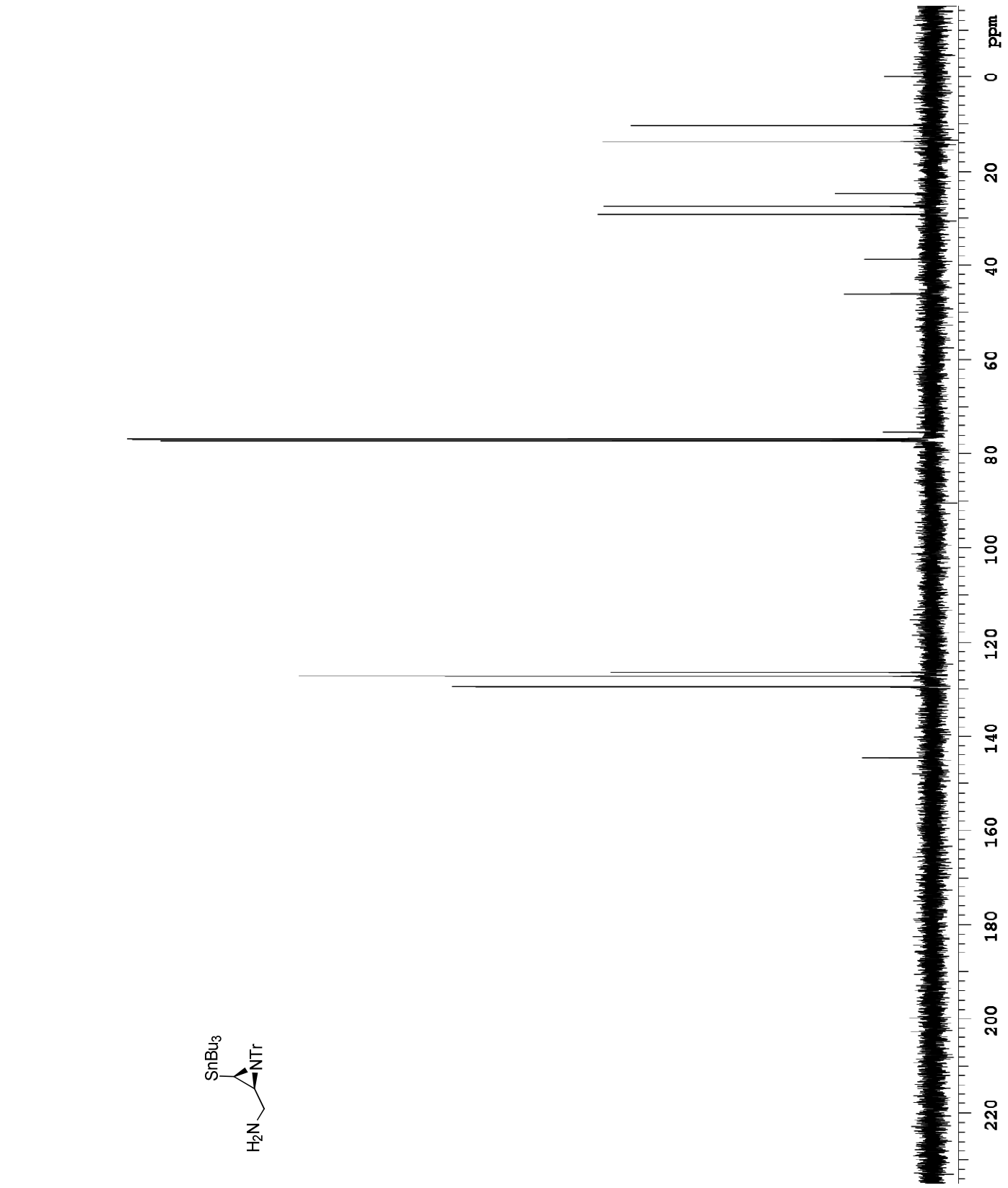
SnBu3
NTr
H2N
ppm
0
20
40
60
80
100
120
140
160
180
200
220

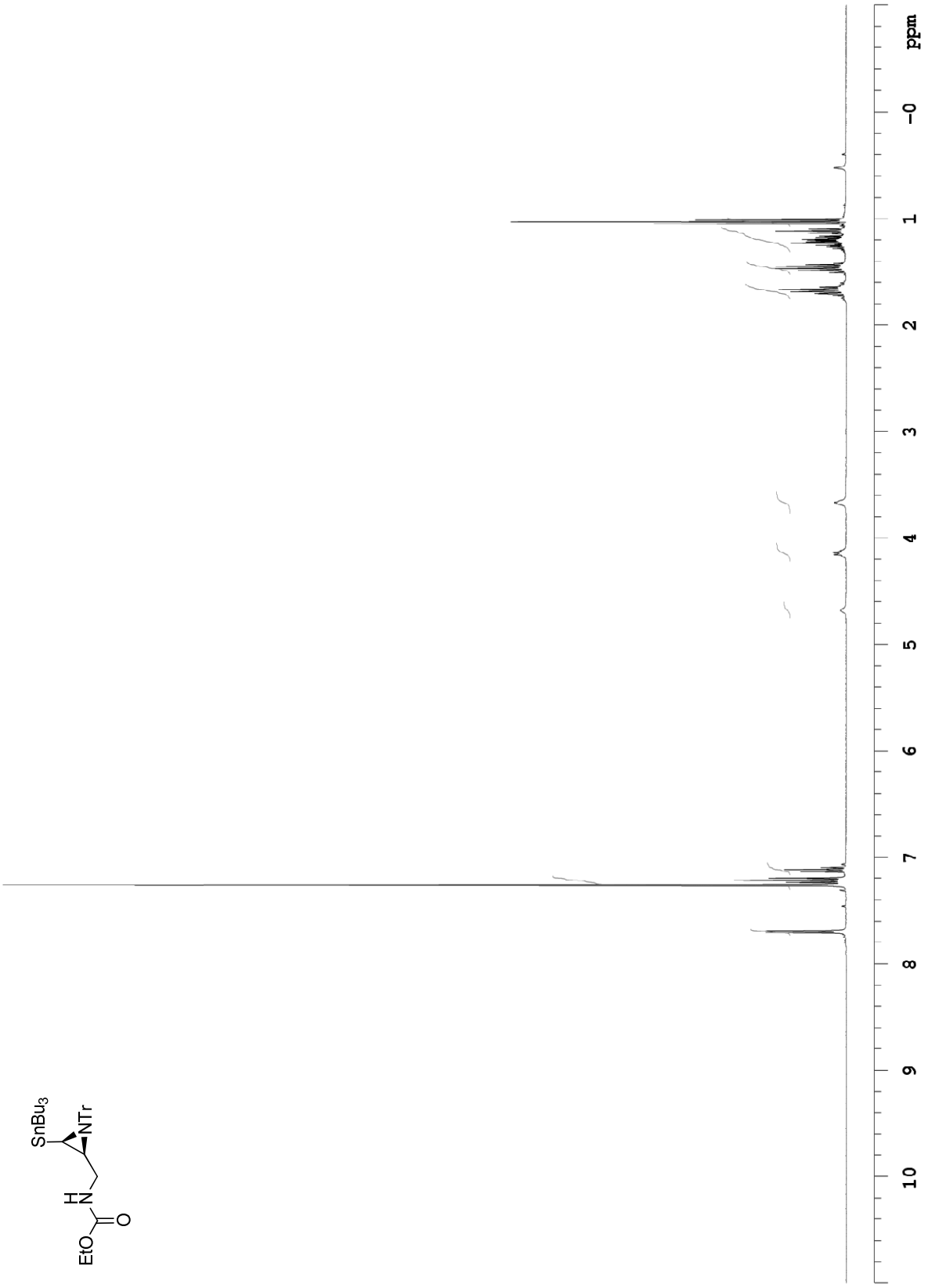
SnBu3
NTr
H
N
EtO
O
ppm
10
9
8
7
6
5
4
3
2
1
0

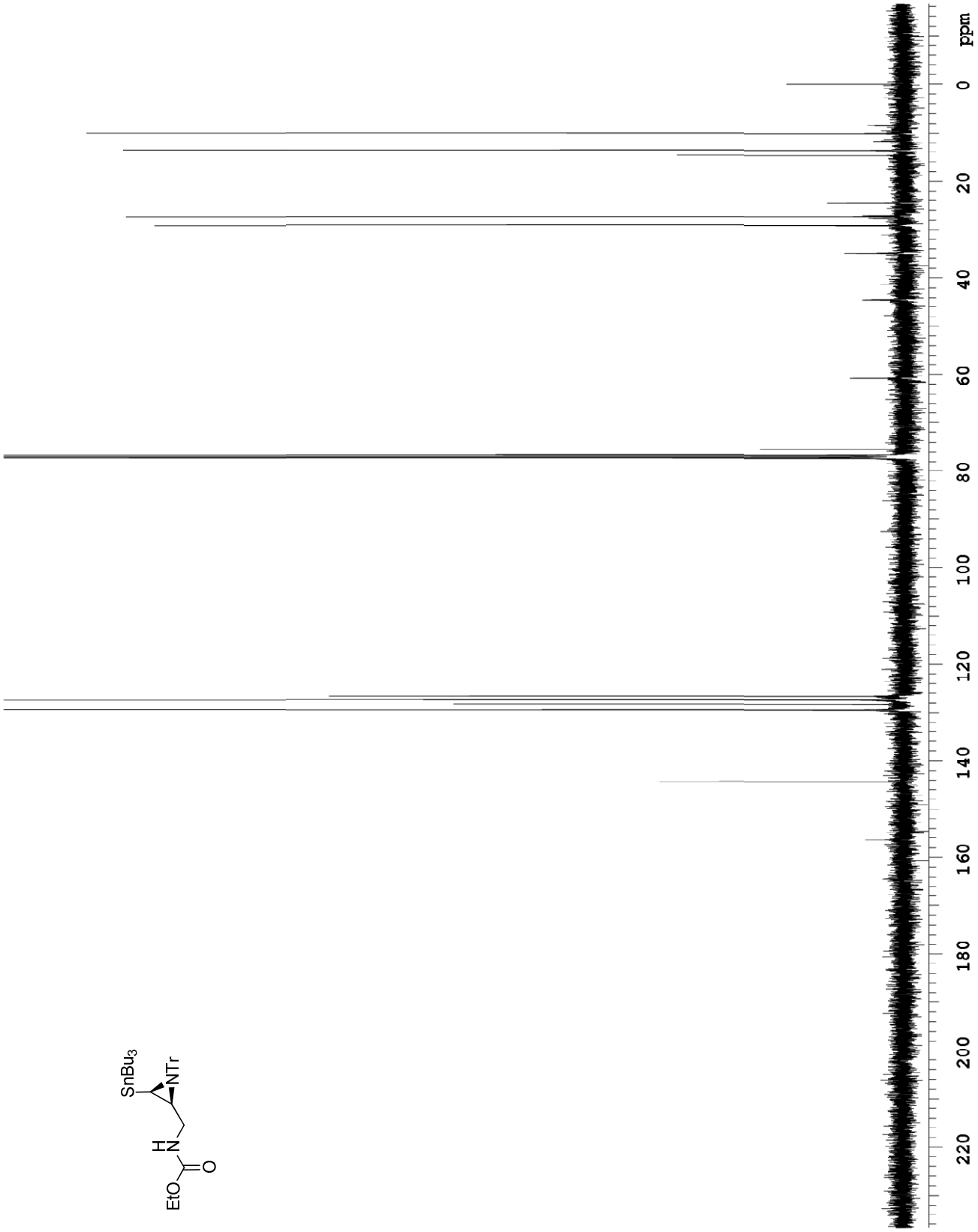
SnBu3
NTr
H
N
EtO
O
ppm
0
20
40
60
80
100
120
140
160
180
200
220

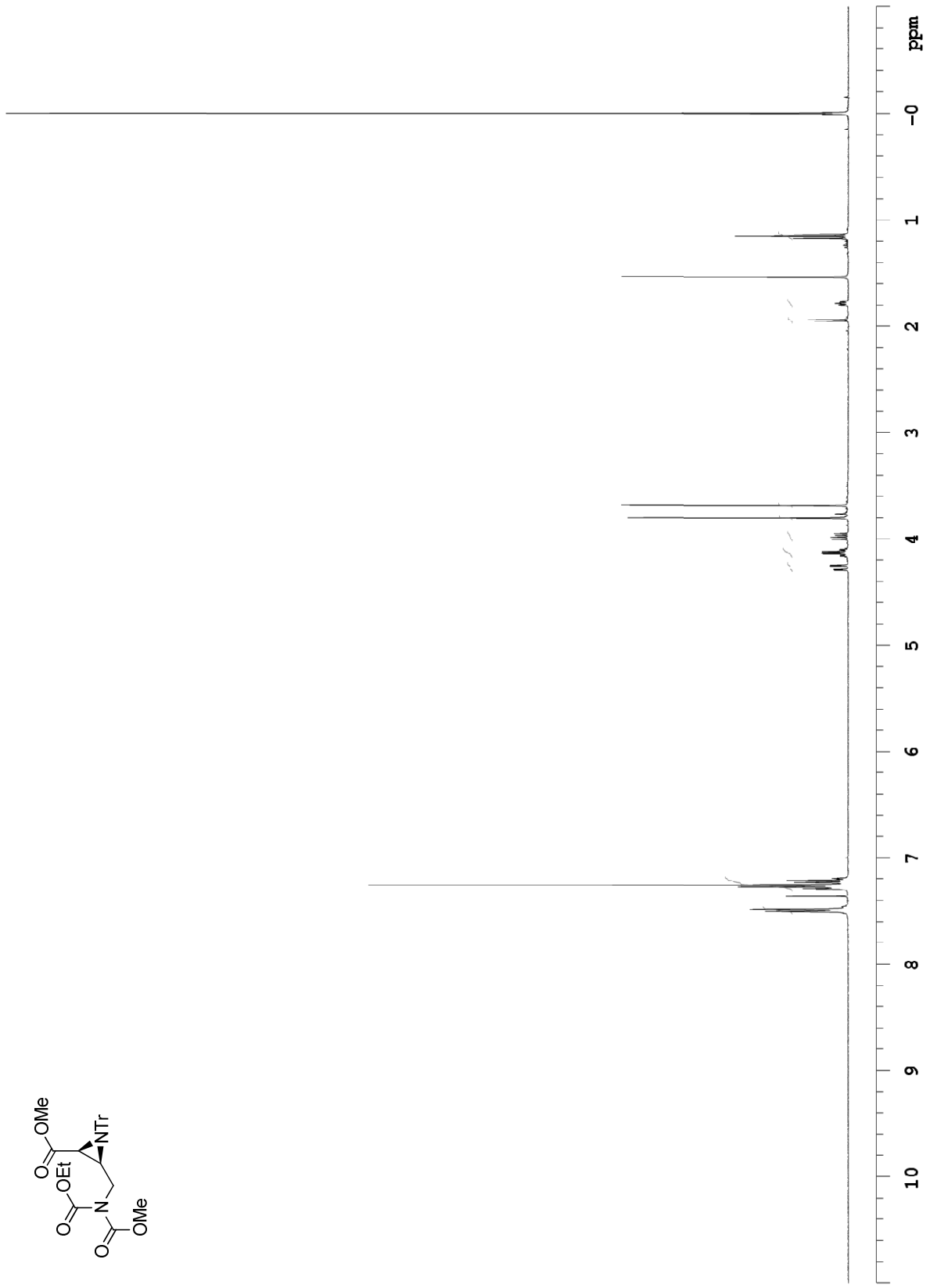
OMe
O
OEt
O
N
O
OMe
NTr
ppm
10
9
8
7
6
5
4
3
2
1
0

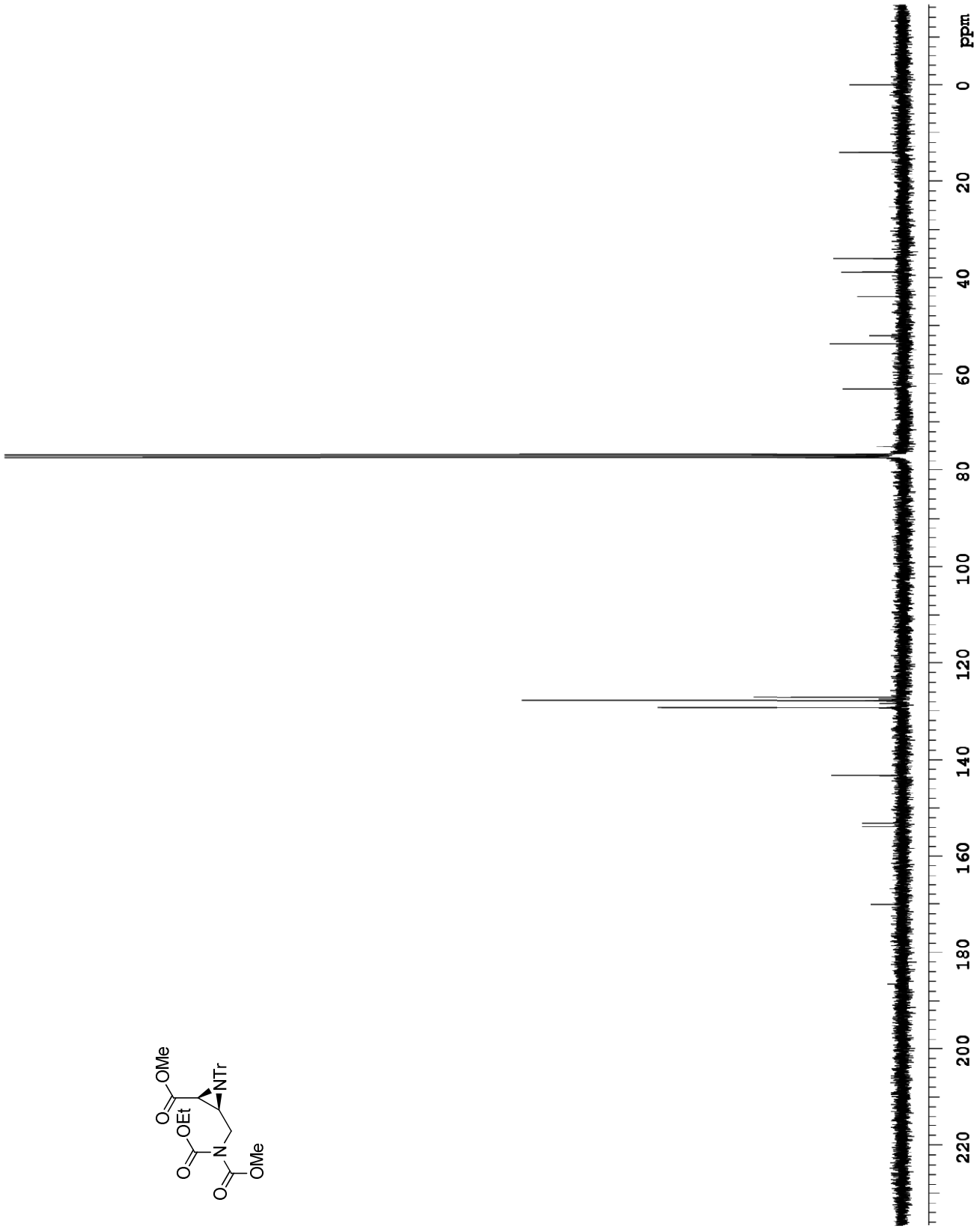
O
OMe
O
OEt
N
NTr
O
OMe
ppm
0
20
40
60
80
100
120
140
160
180
200
220

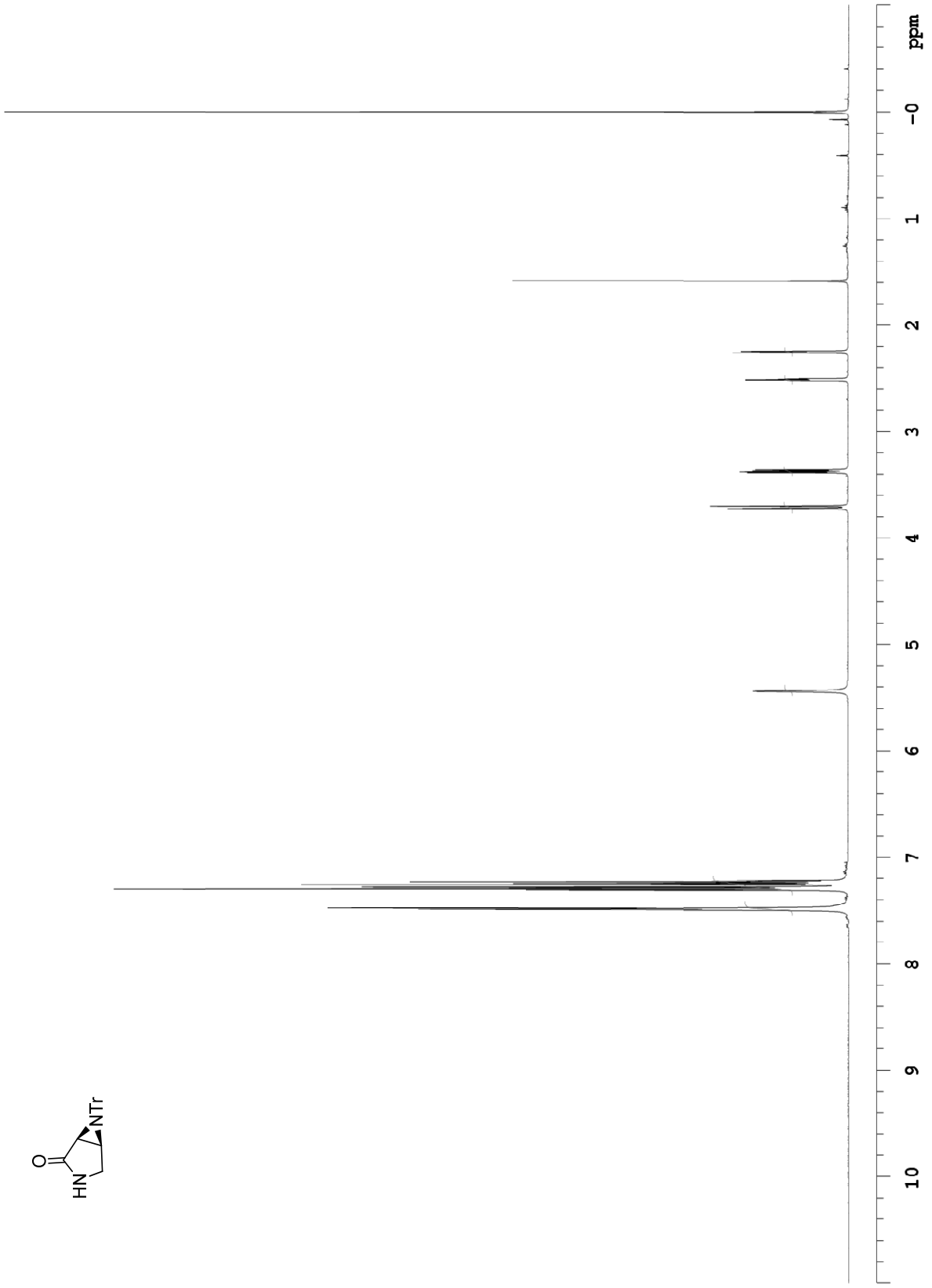
ppm
10
9
8
7
6
5
4
3
2
1
0
O
HN
NTr

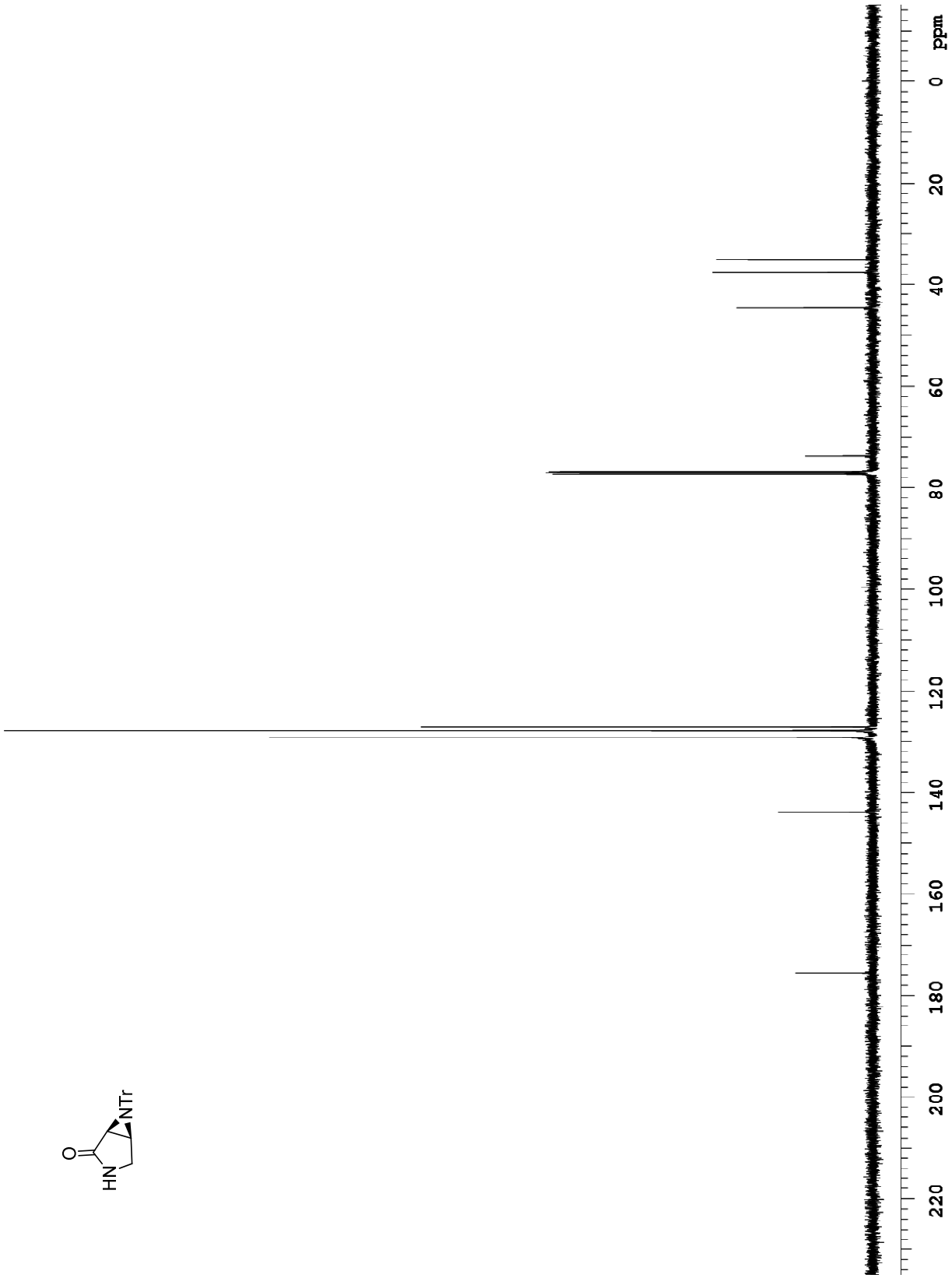
NTr
O
HN
ppm
0
20
40
60
80
100
120
140
160
180
200
220

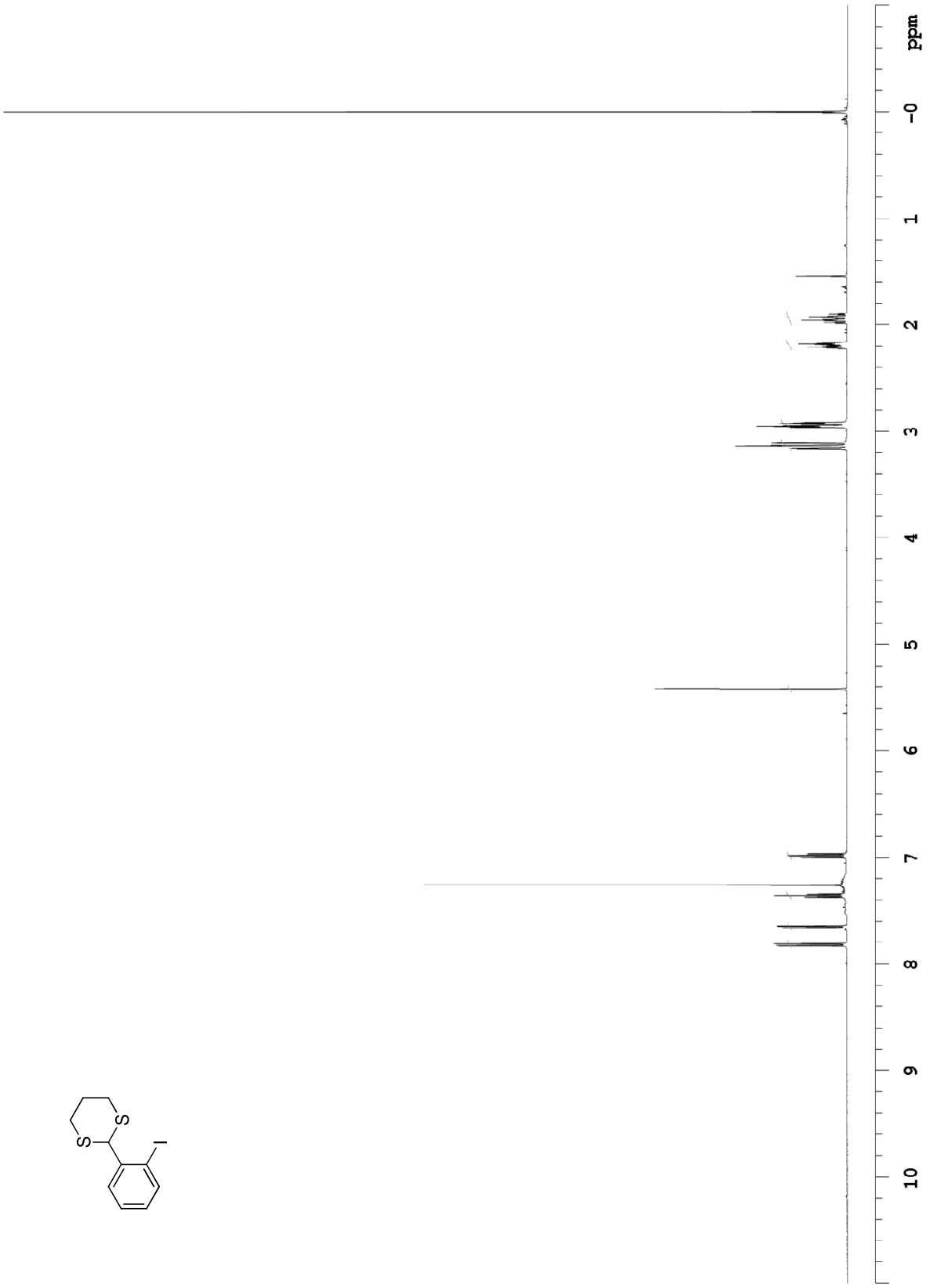
ppm
0
1
2
3
4
5
6
7
8
9
10
S
S
I

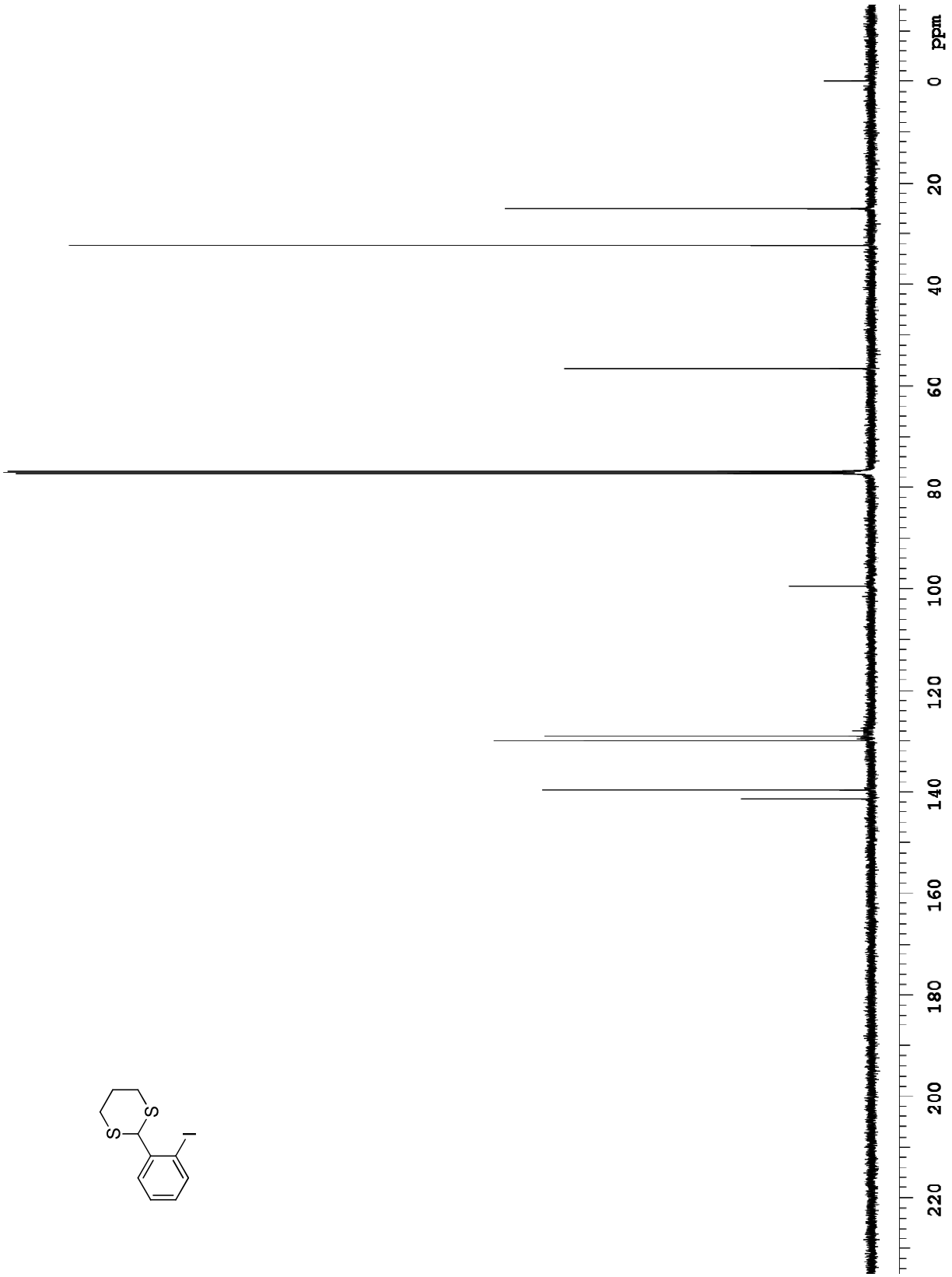
ppm
0
20
40
60
80
100
120
140
160
180
200
220
S
S
I

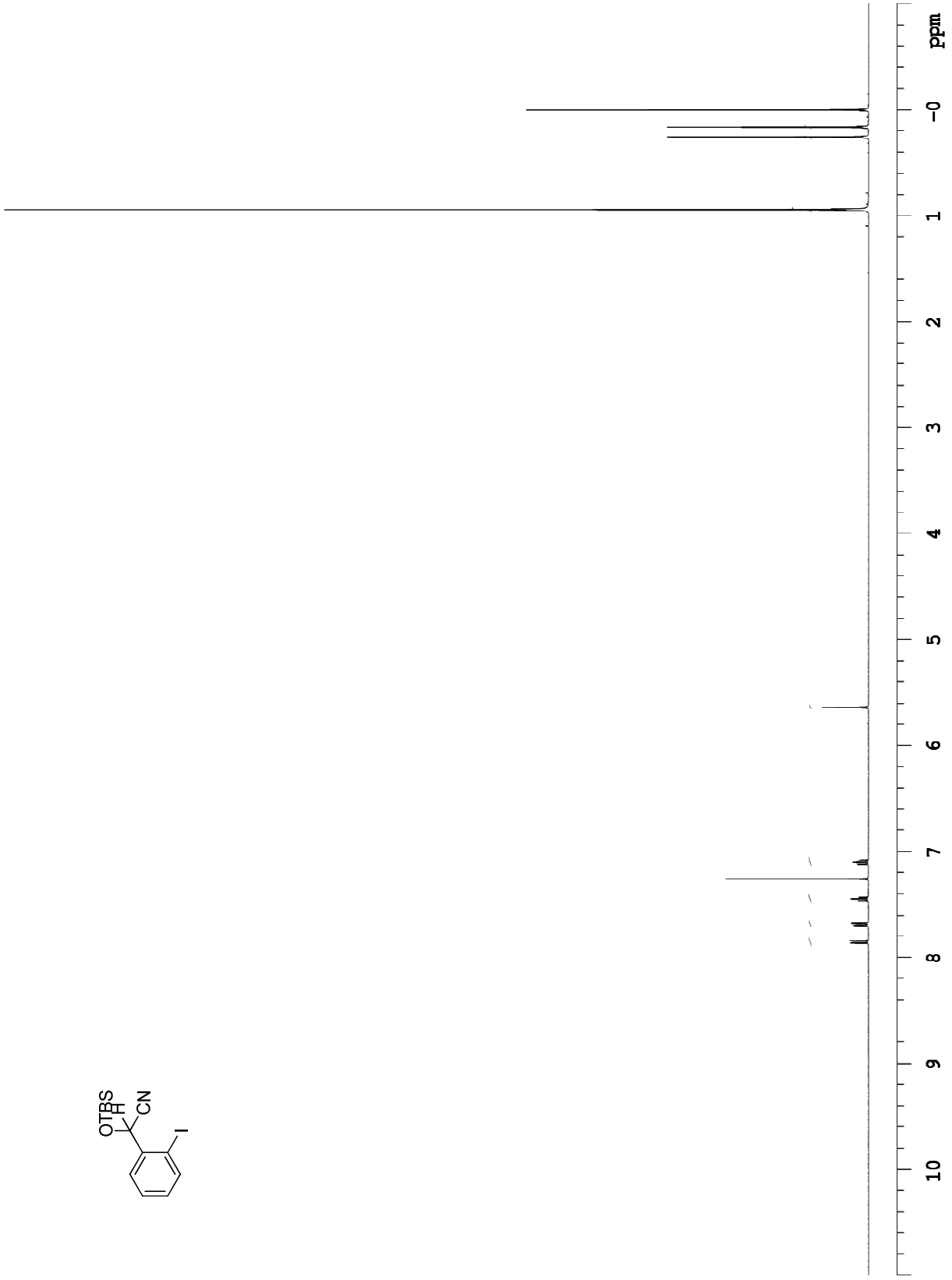
ppm
−0
1
2
3
4
5
6
7
8
9
10
OTBS
H
CN
I

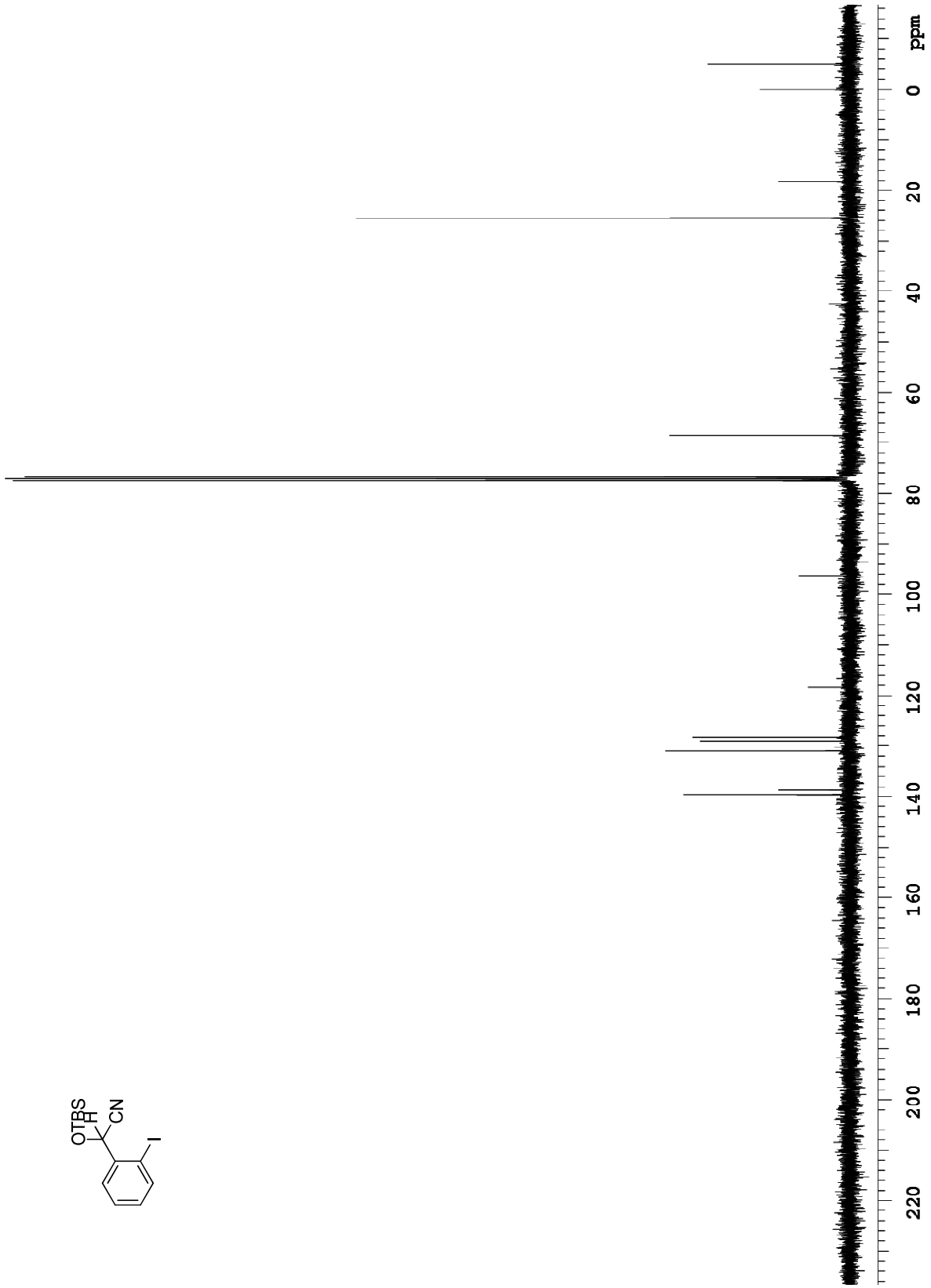
OTBS
H
CN
I
ppm
0
20
40
60
80
100
120
140
160
180
200
220

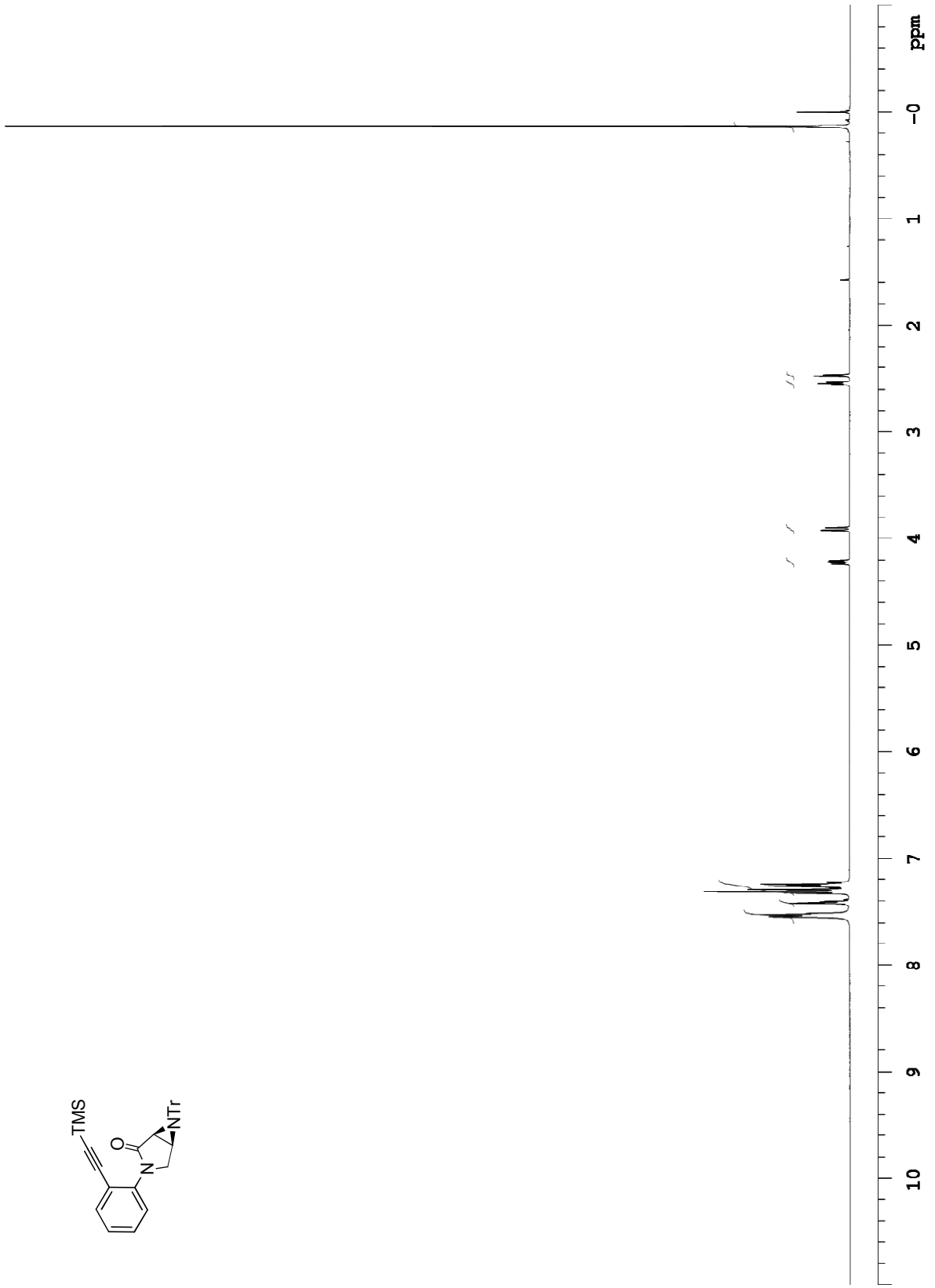
TMS
O
N
NTr
ppm
−0
1
2
3
4
5
6
7
8
9
10

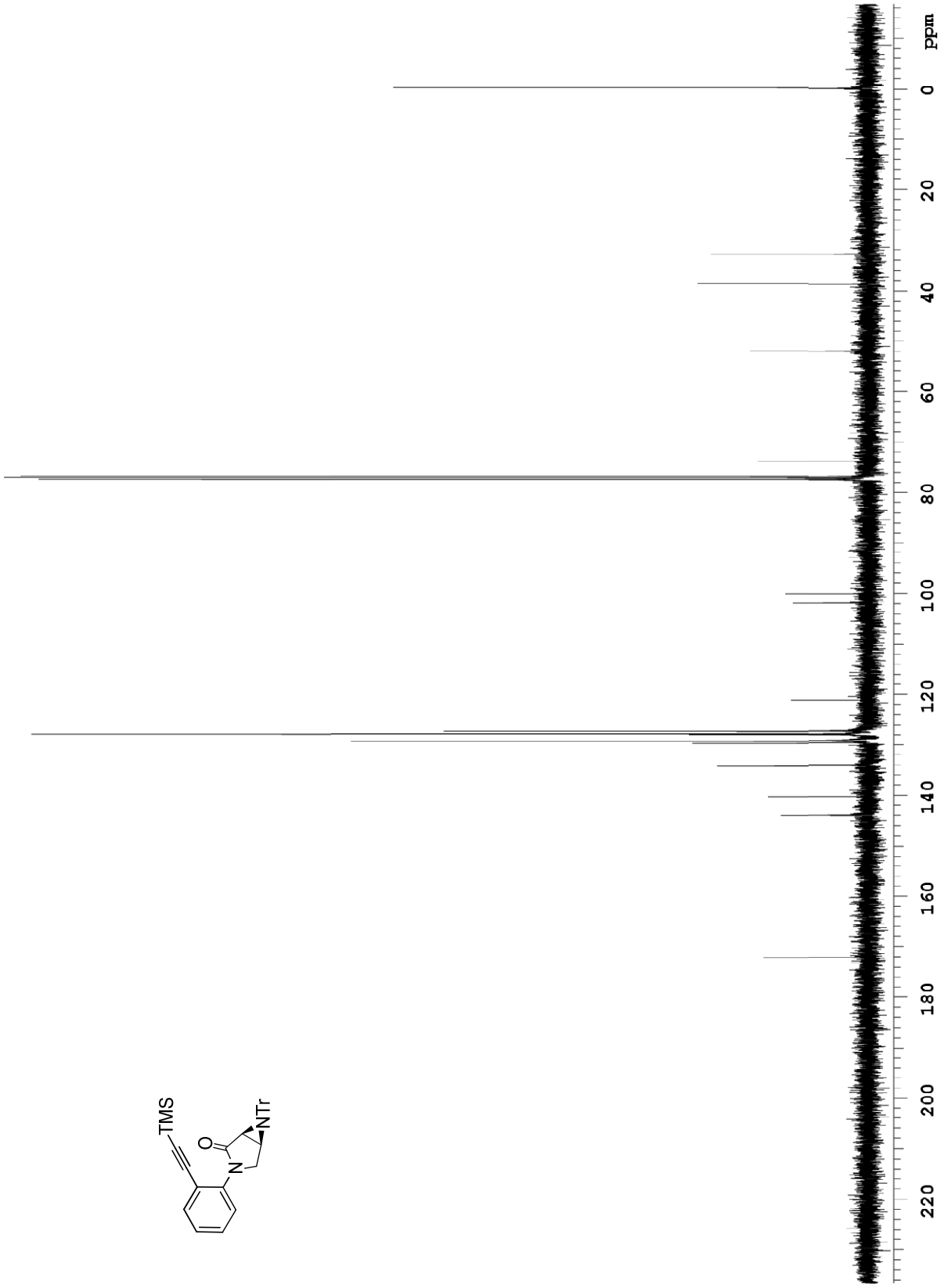
TMS
O
N
NTr
ppm
0
20
40
60
80
100
120
140
160
180
200
220

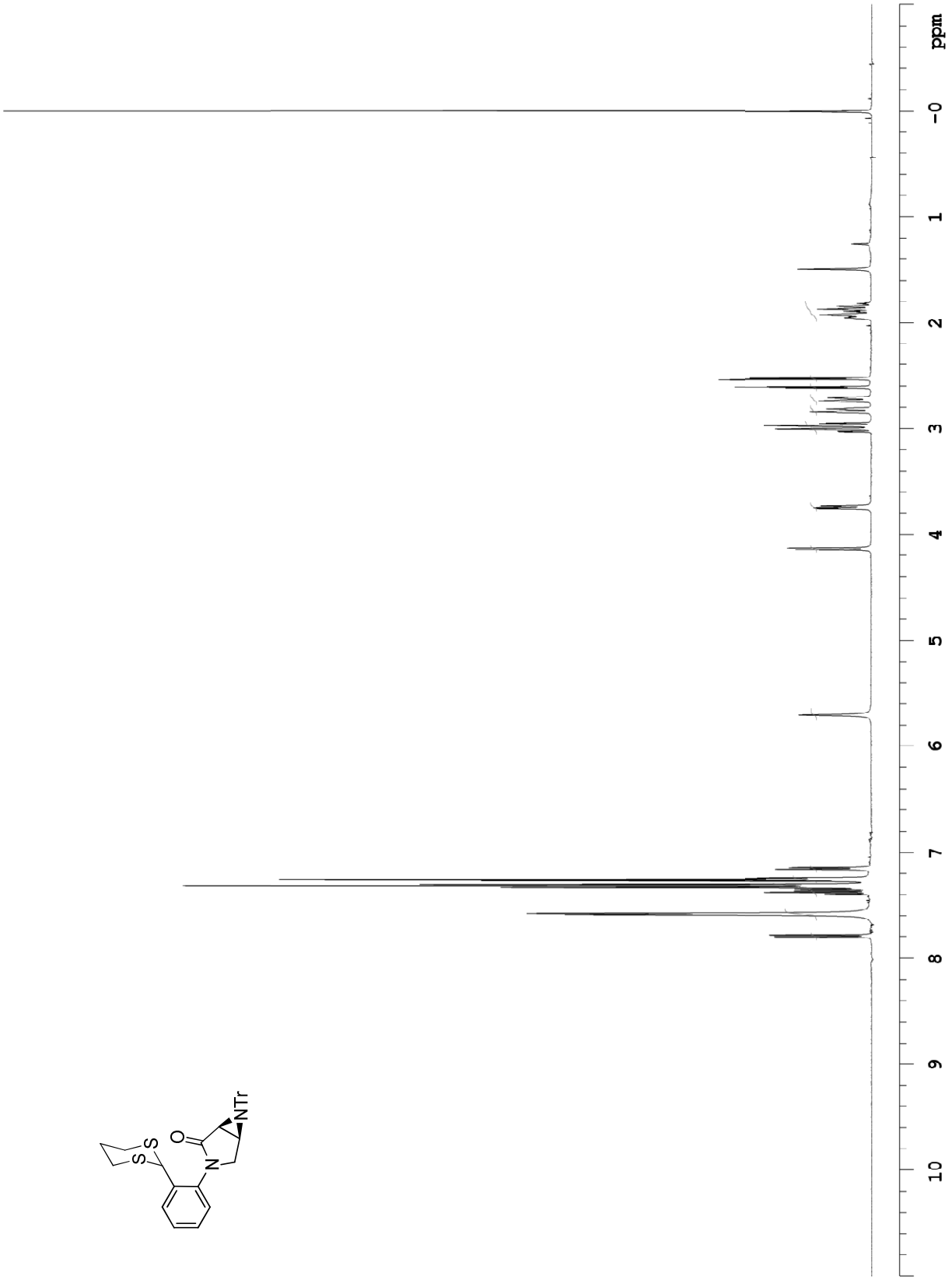
ppm
10
9
8
7
6
5
4
3
2
1
−0
S
S
O
N
NTr

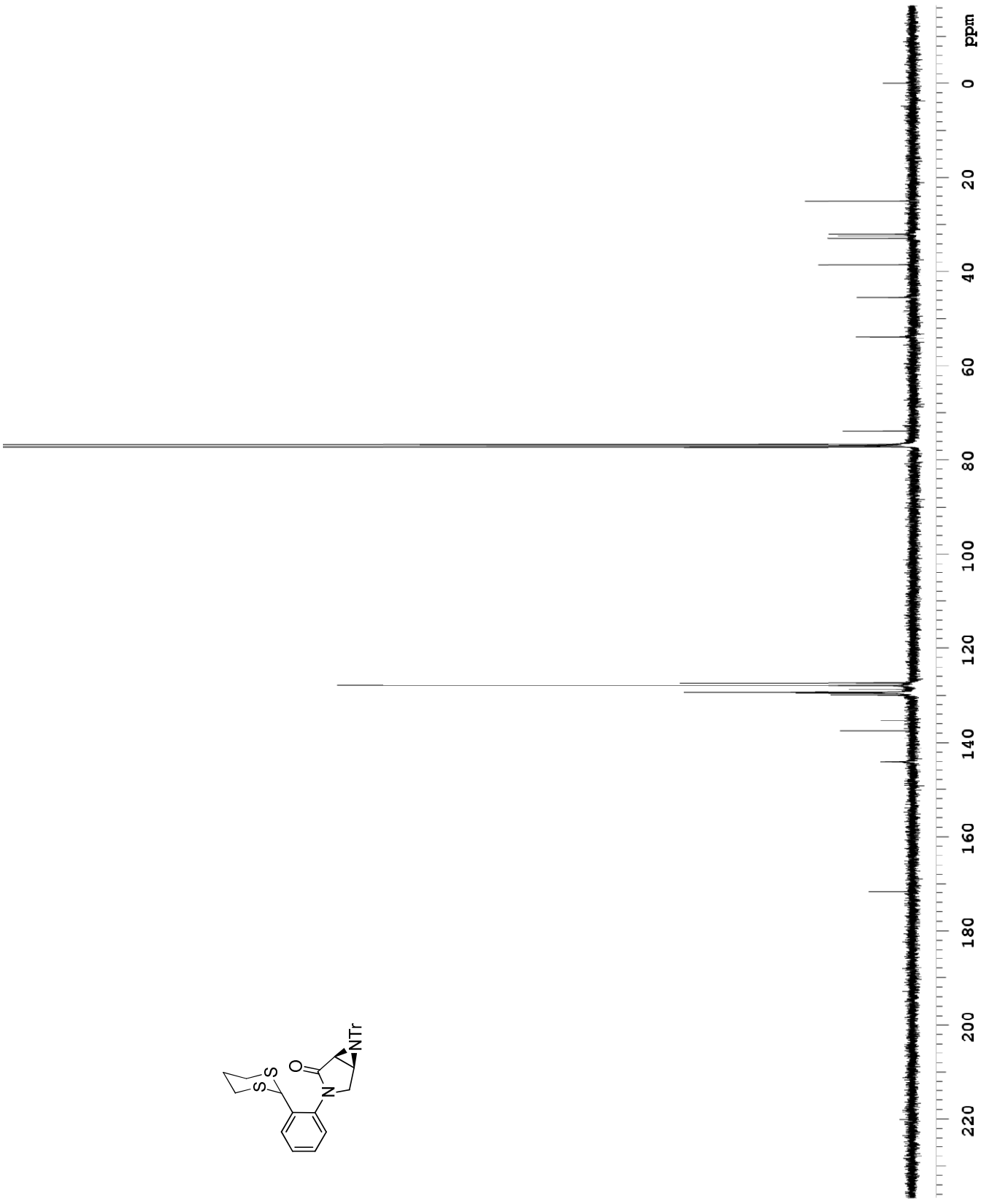
ppm
0
20
40
60
80
100
120
140
160
180
200
220
S
S
O
N
NTr

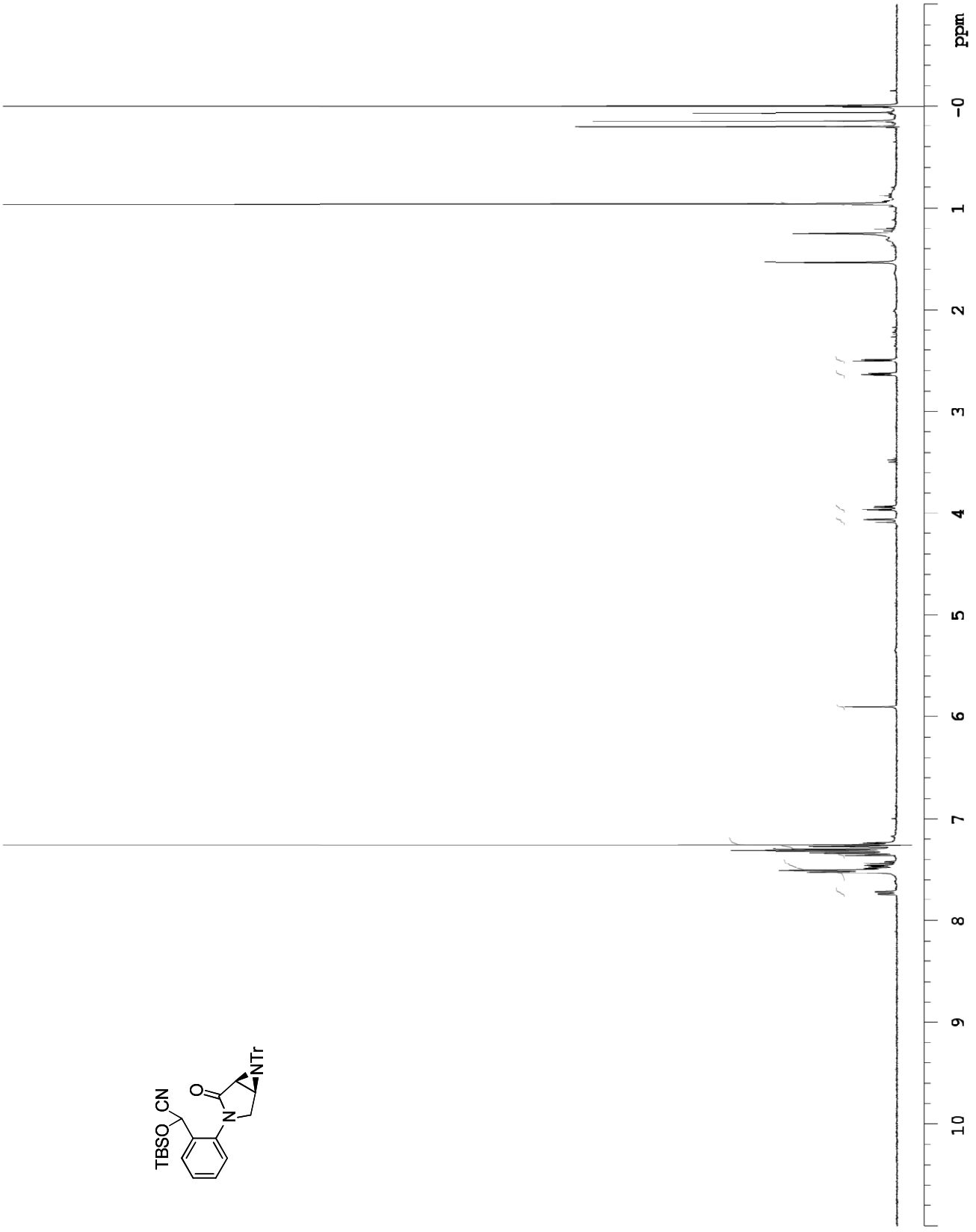
TBSO
CN
O
N
NTr
ppm
10
9
8
7
6
5
4
3
2
1
0

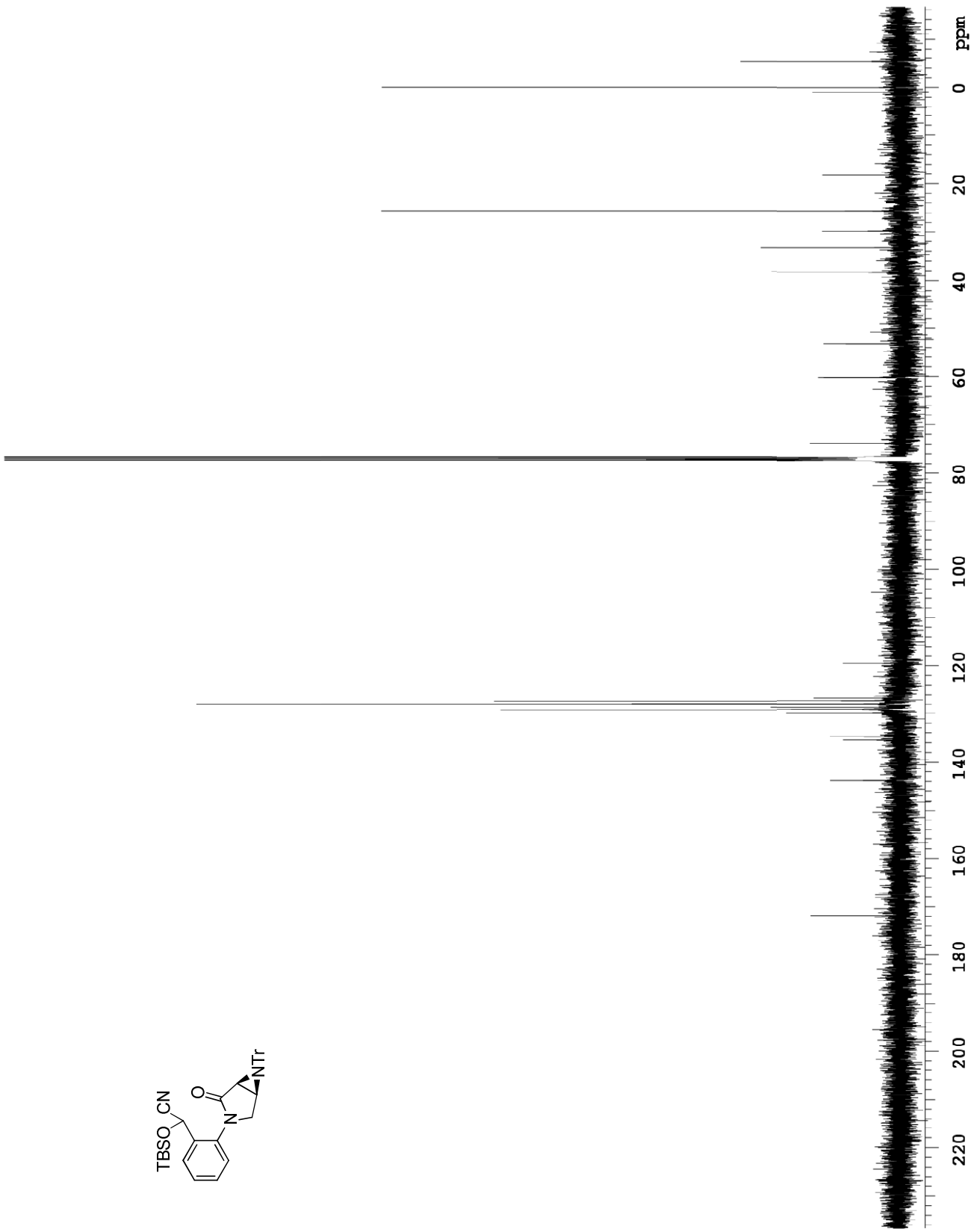
ppm
0
20
40
60
80
100
120
140
160
180
200
220
TBSO
CN
O
N
NTr

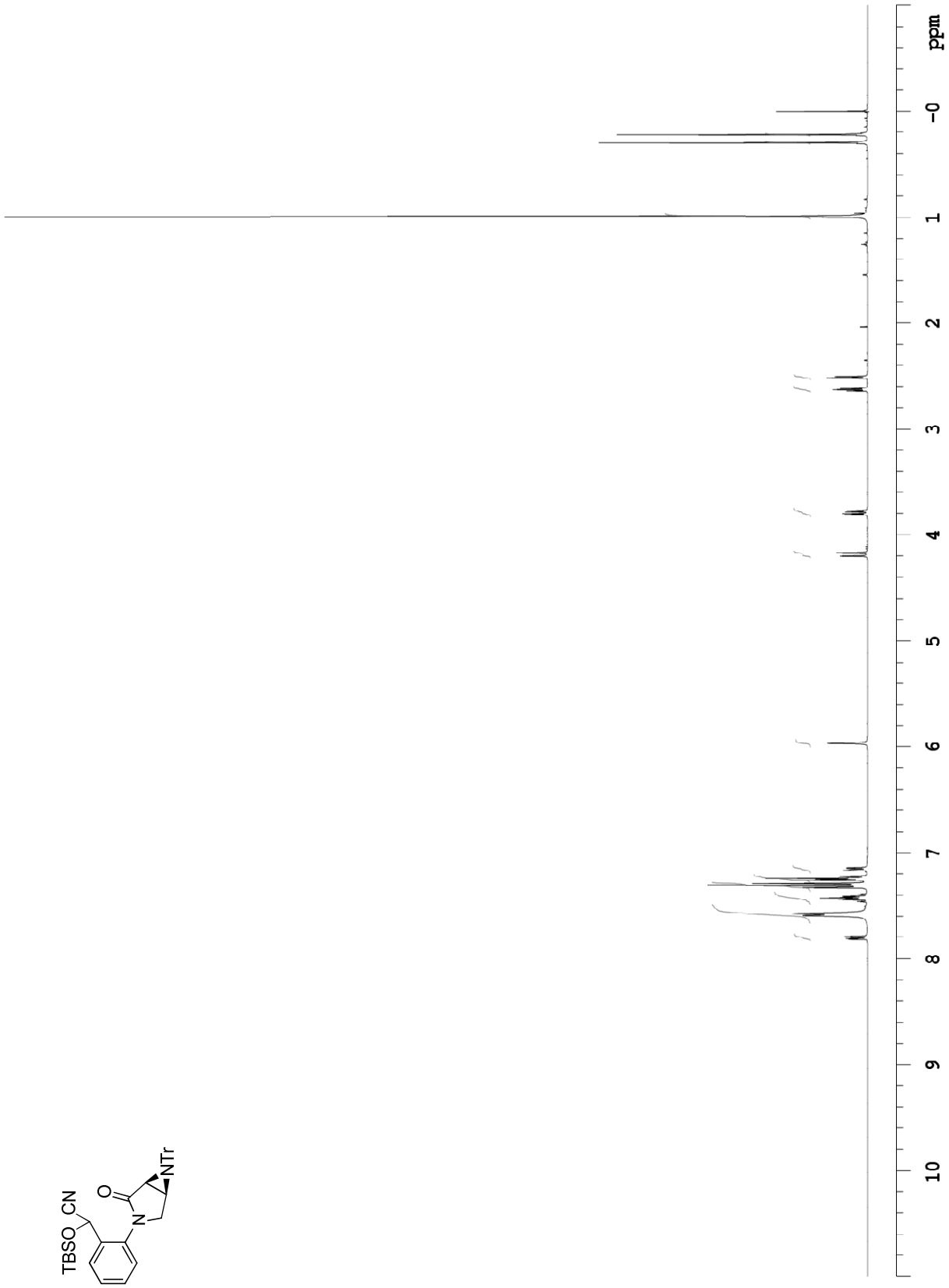
TBSO
CN
O
N
NTr
ppm
10
9
8
7
6
5
4
3
2
1
0

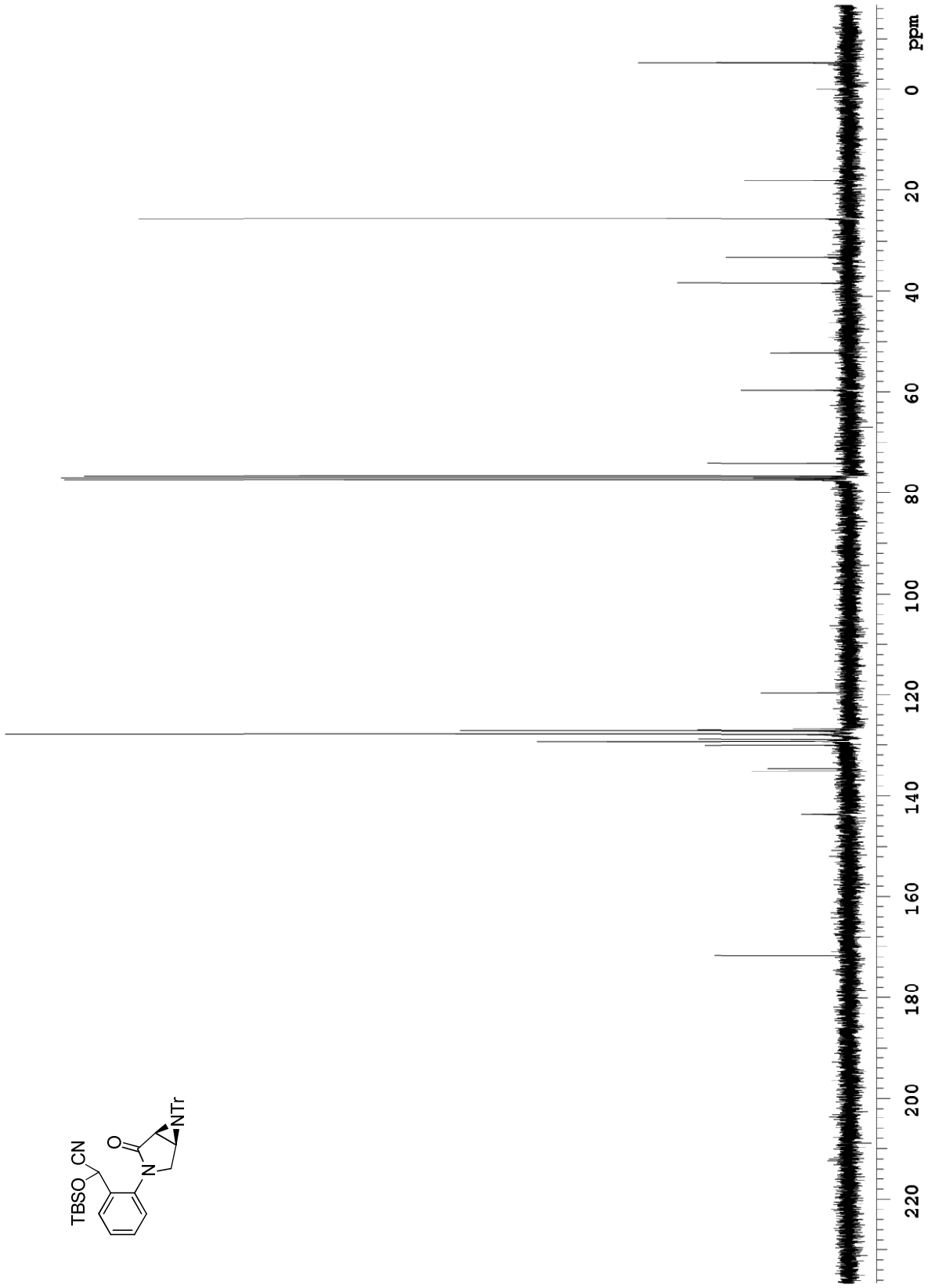
TBSO
CN
O
N
NTr
ppm
0
20
40
60
80
100
120
140
160
180
200
220

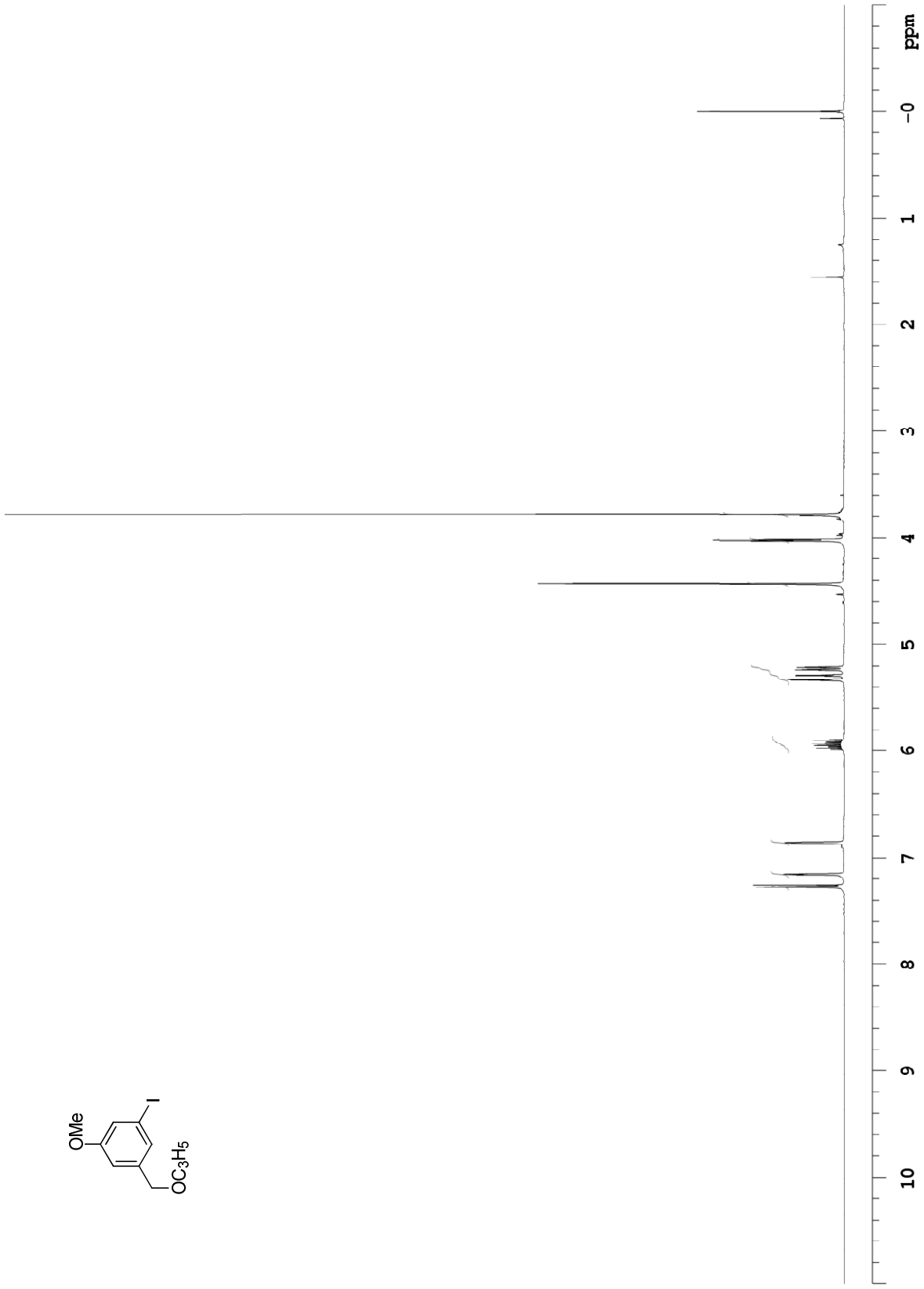
ppm
10
9
8
7
6
5
4
3
2
1
0
OMe
I
OC3H5

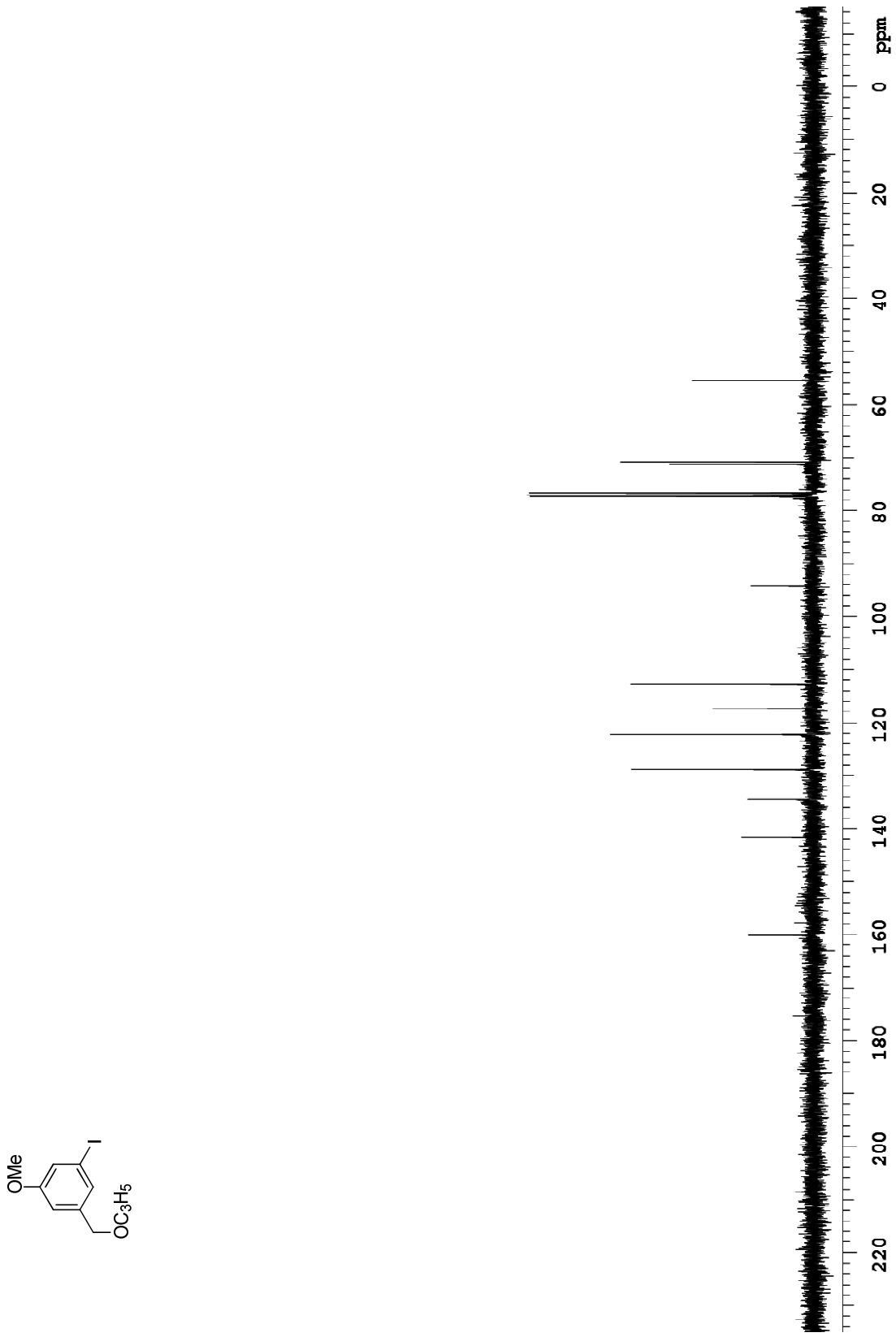
OMe
I
OC3H5
ppm
0
20
40
60
80
100
120
140
160
180
200
220

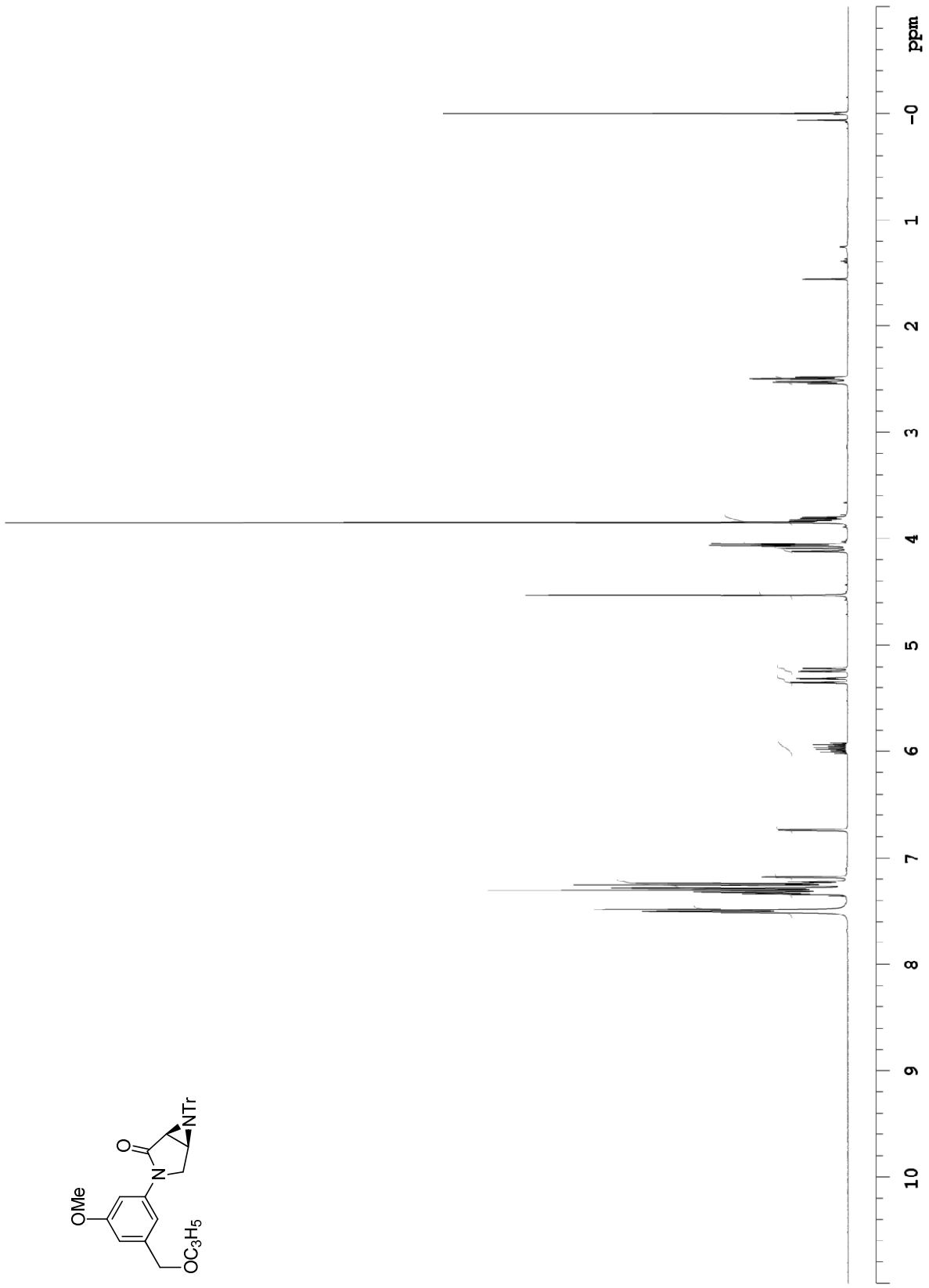
ppm
10
9
8
7
6
5
4
3
2
1
−0
OMe
O
N
NTr
OC3H5

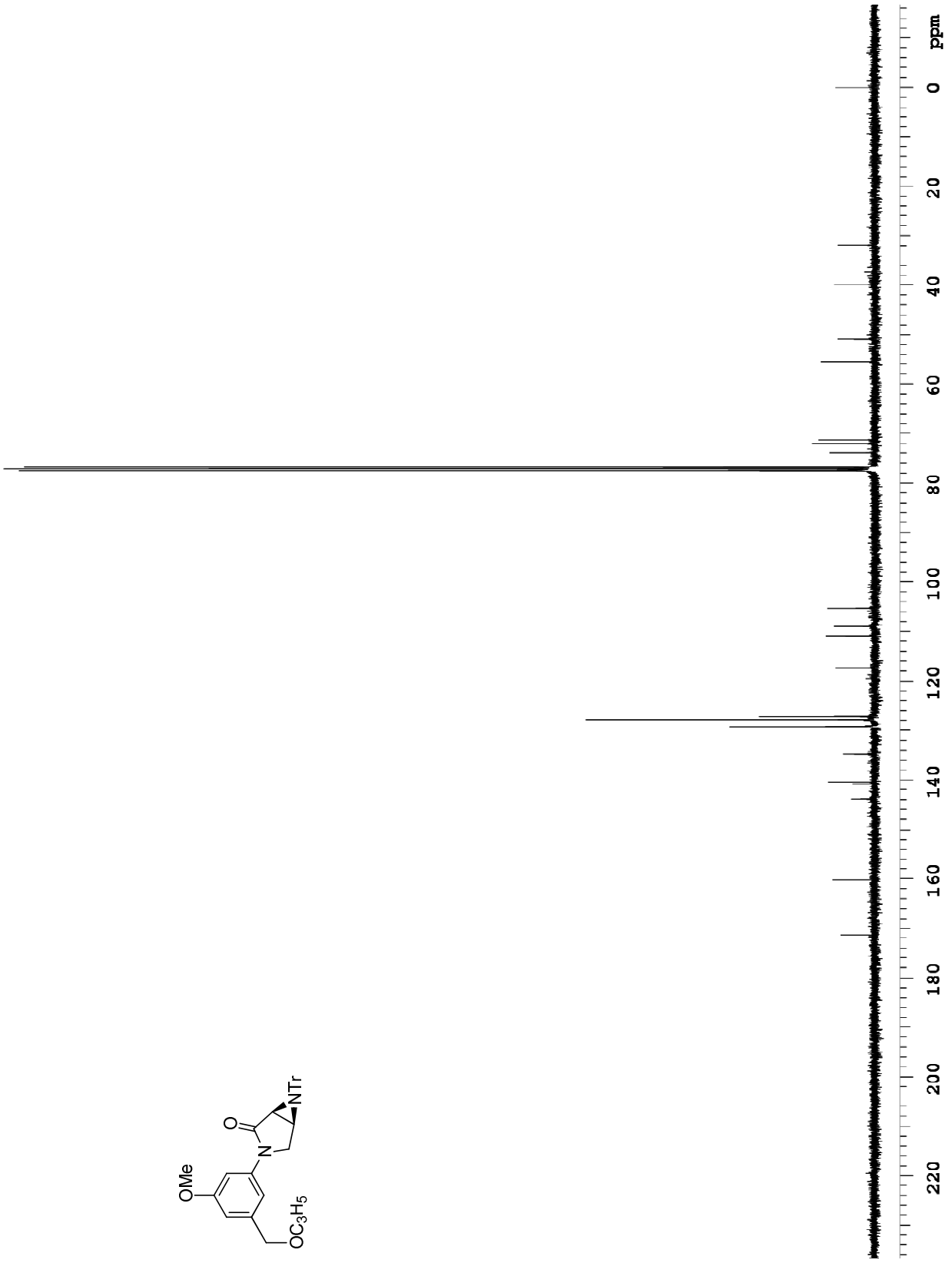
OMe
O
N
NTr
OC3H5
ppm
0
20
40
60
80
100
120
140
160
180
200
220

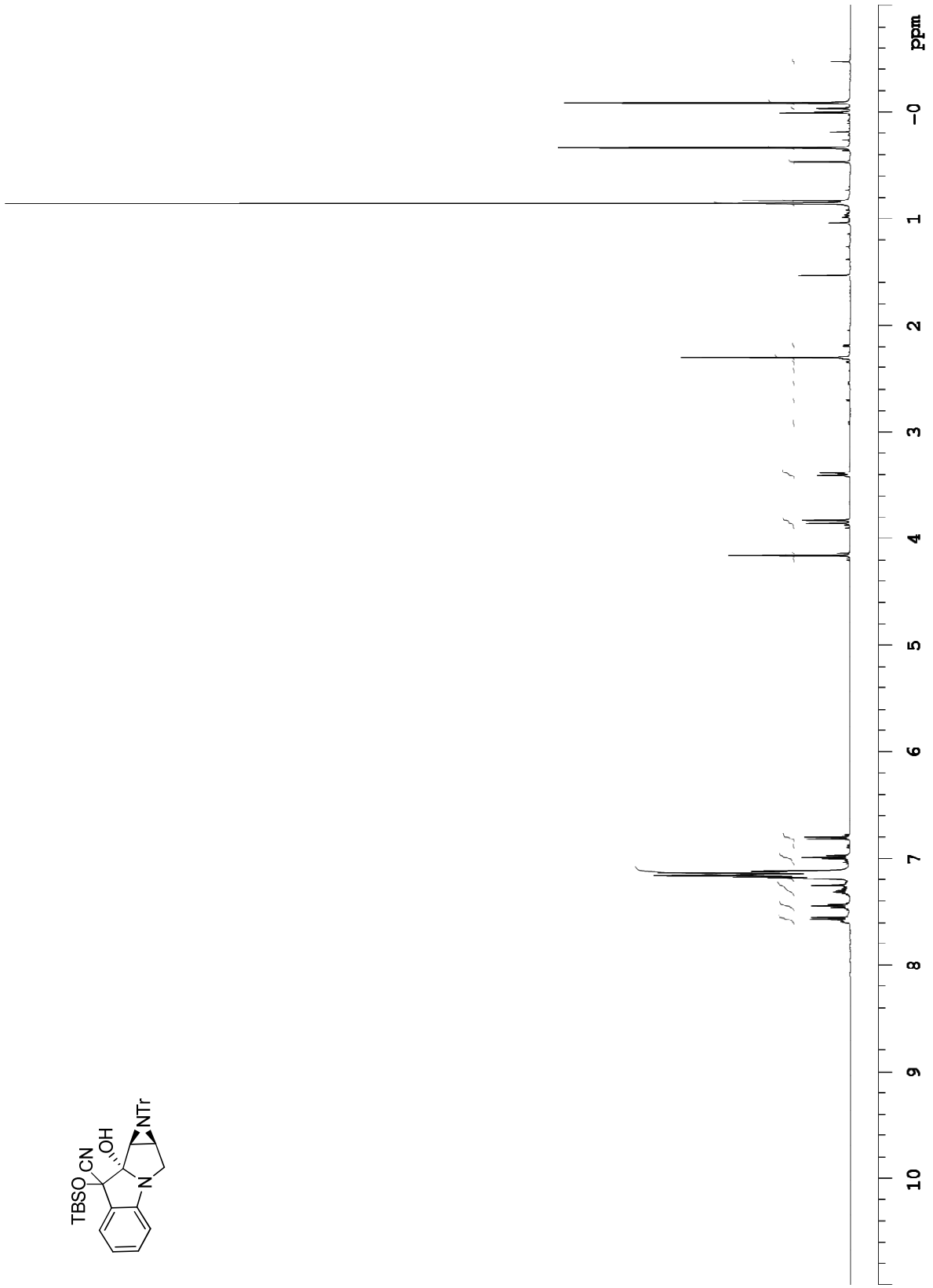
TBSO
CN
OH
NTr
N
ppm
10
9
8
7
6
5
4
3
2
1
0

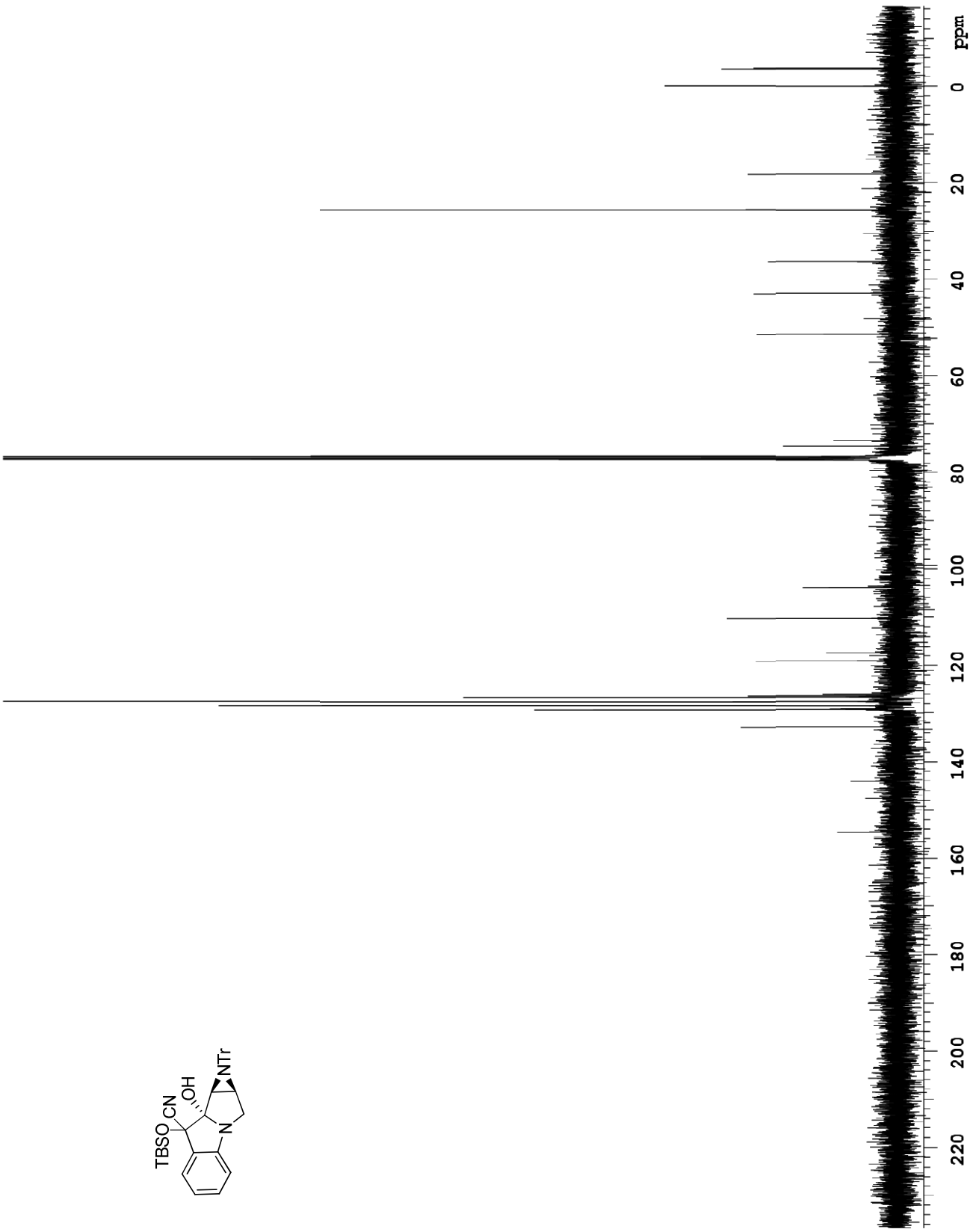
TBSO
CN
OH
NTr
N
ppm
0
20
40
60
80
100
120
140
160
180
200
220

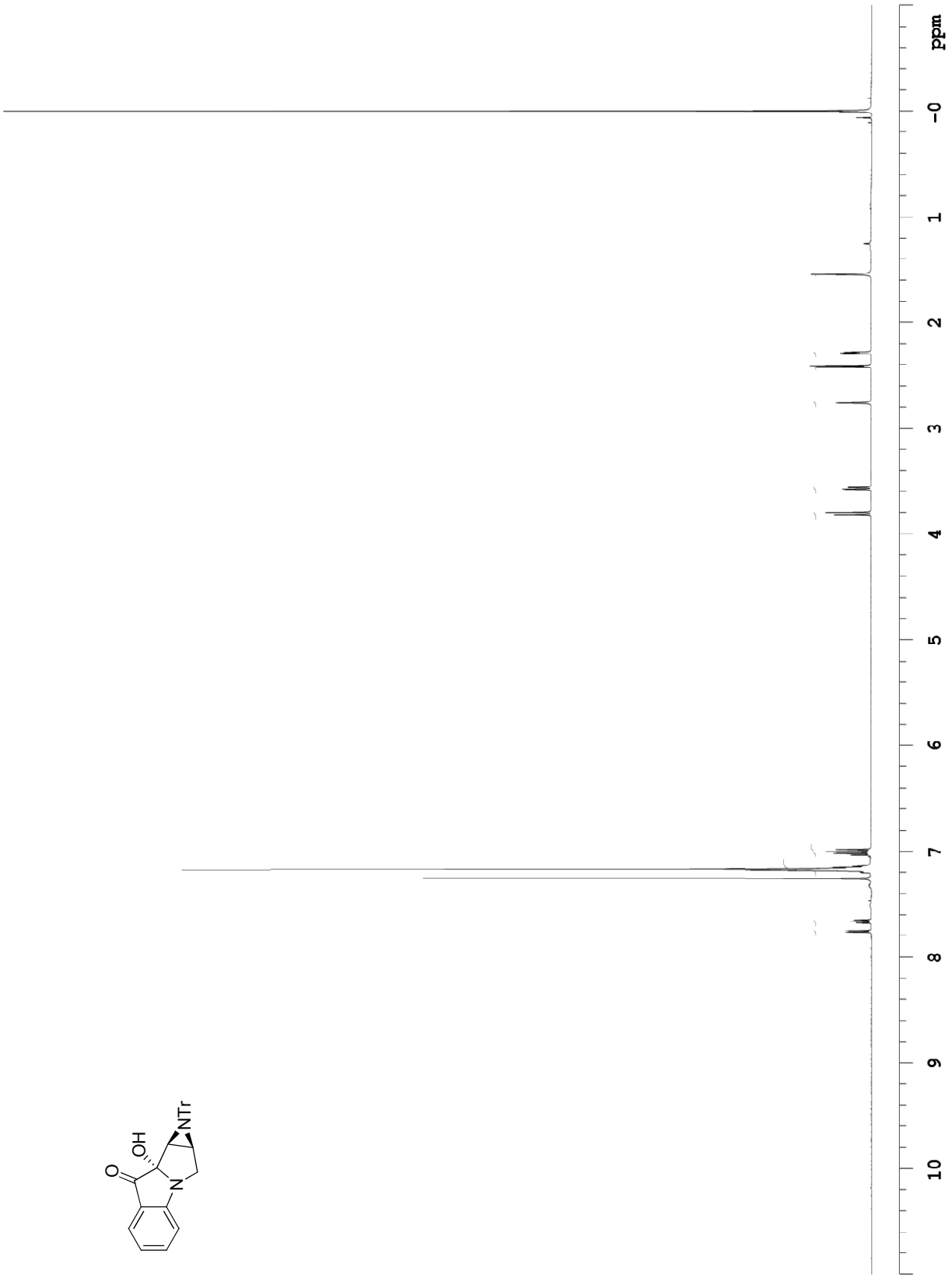
ppm
10
9
8
7
6
5
4
3
2
1
0
O
OH
N
NTr

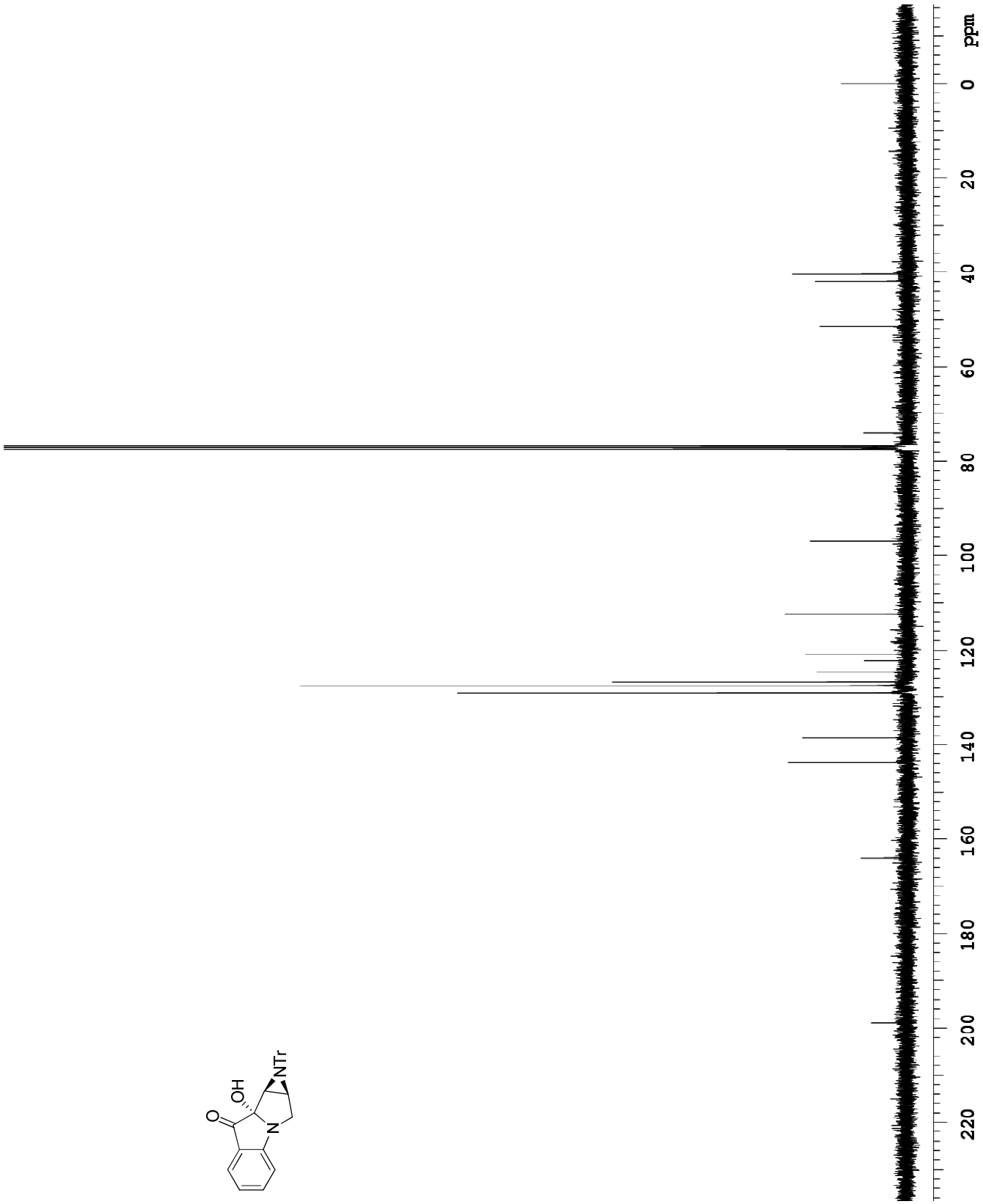
ppm
0
20
40
60
80
100
120
140
160
180
200
220
OH
NTr
O
N

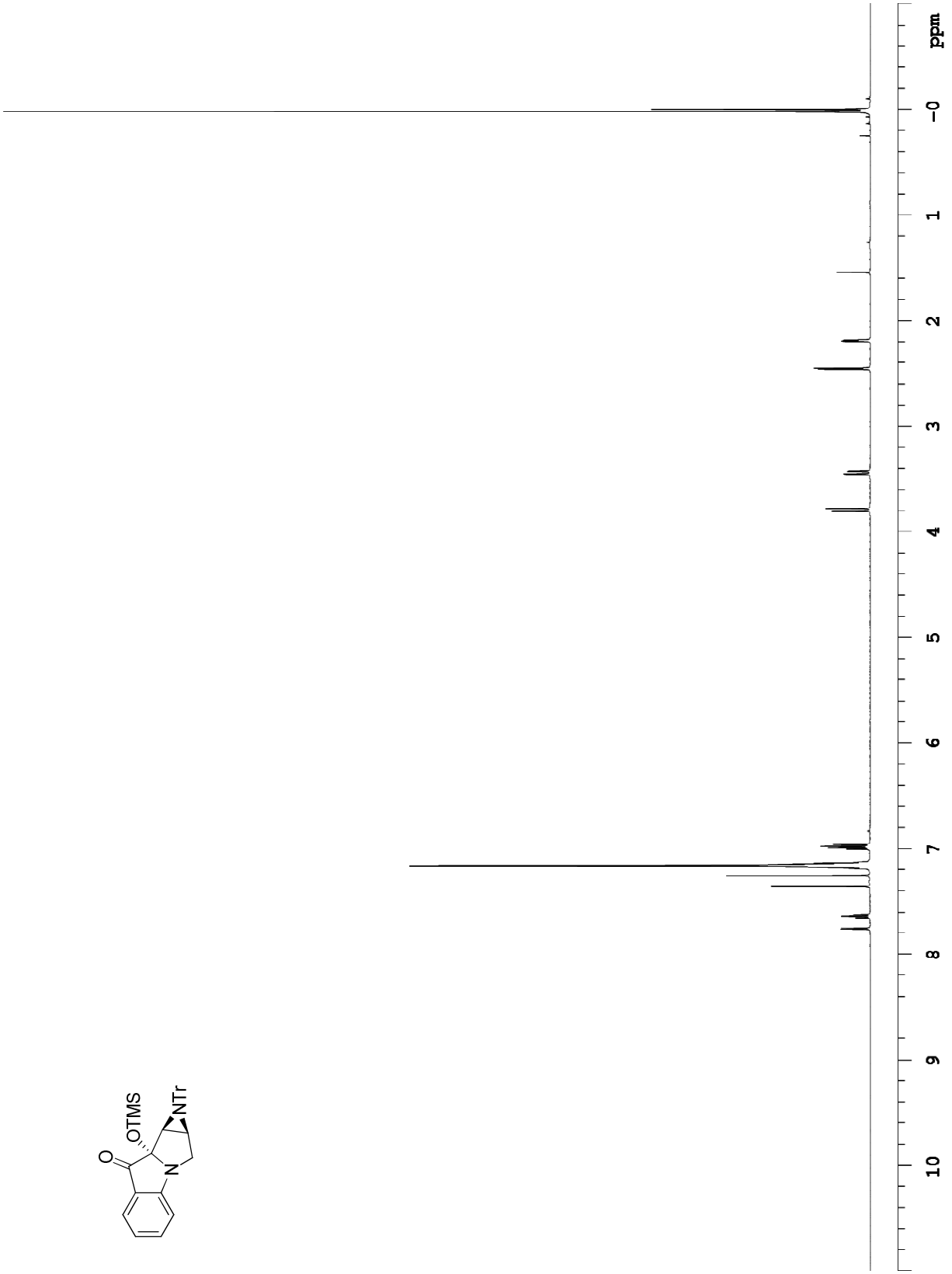
ppm
10
9
8
7
6
5
4
3
2
1
0
O
OTMS
NTr
N

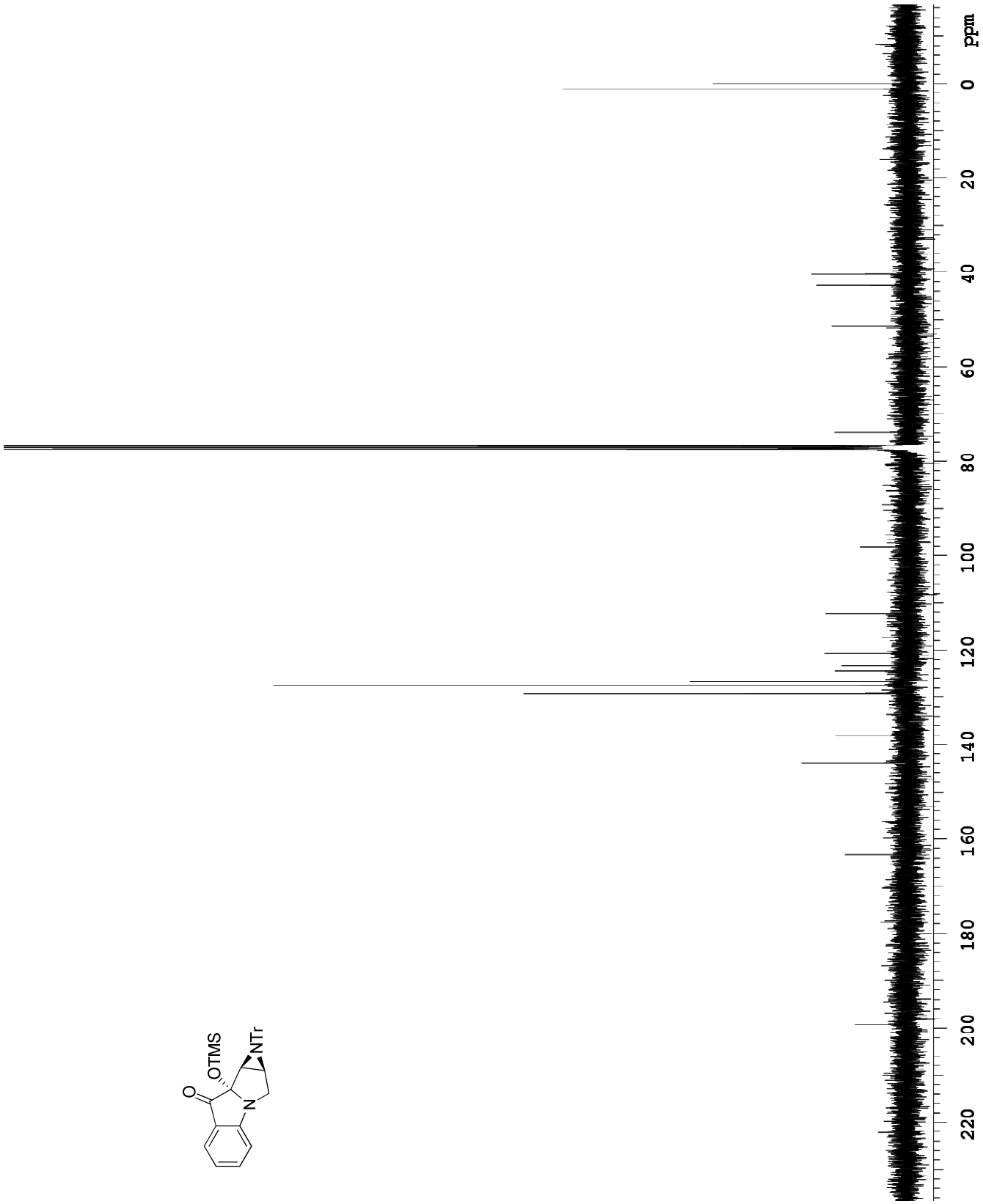
ppm
0
20
40
60
80
100
120
140
160
180
200
220
OTMS
NTr
O
N

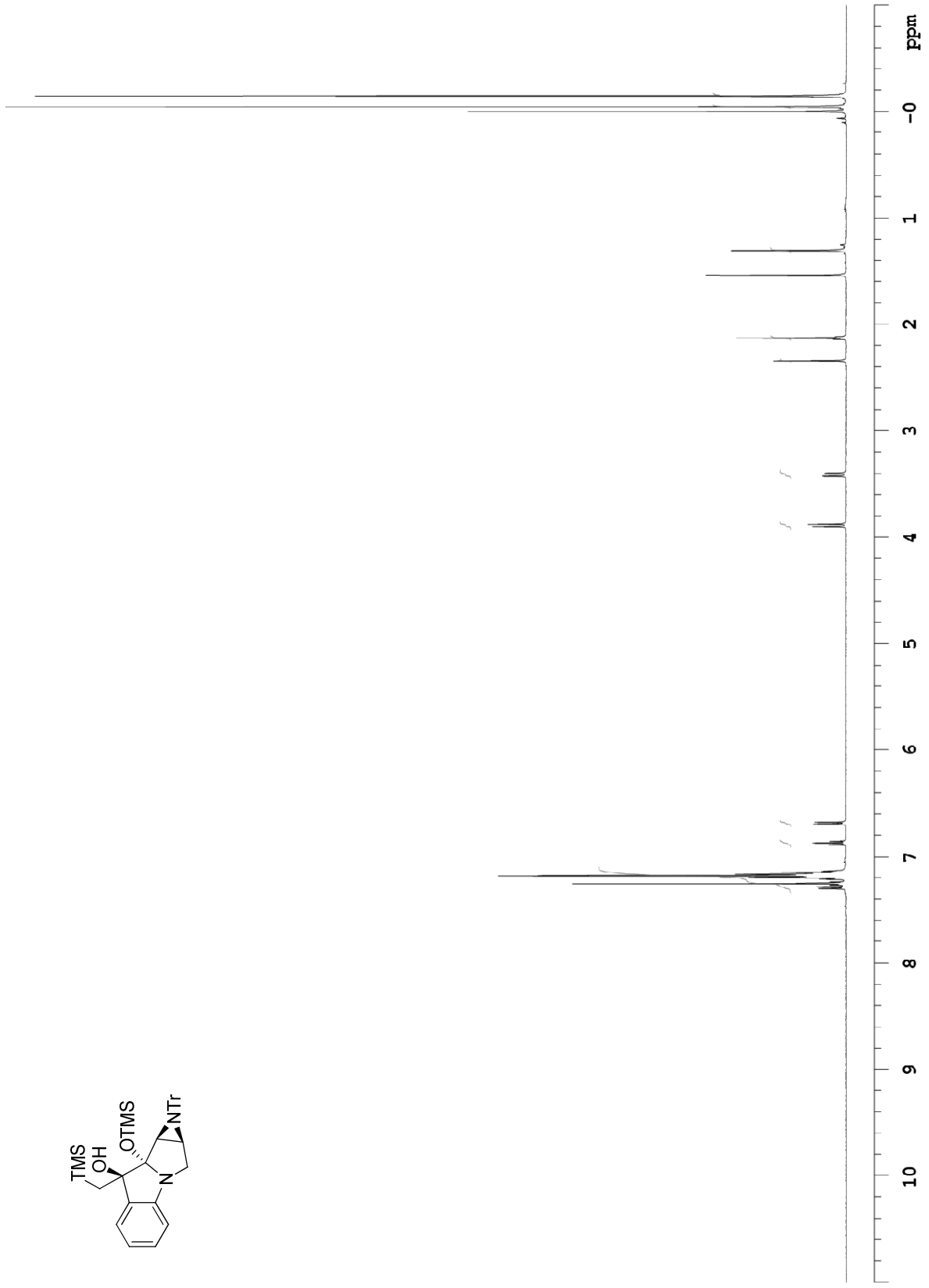
ppm
10
9
8
7
6
5
4
3
2
1
0
TMS
OH
OTMS
NTr
N

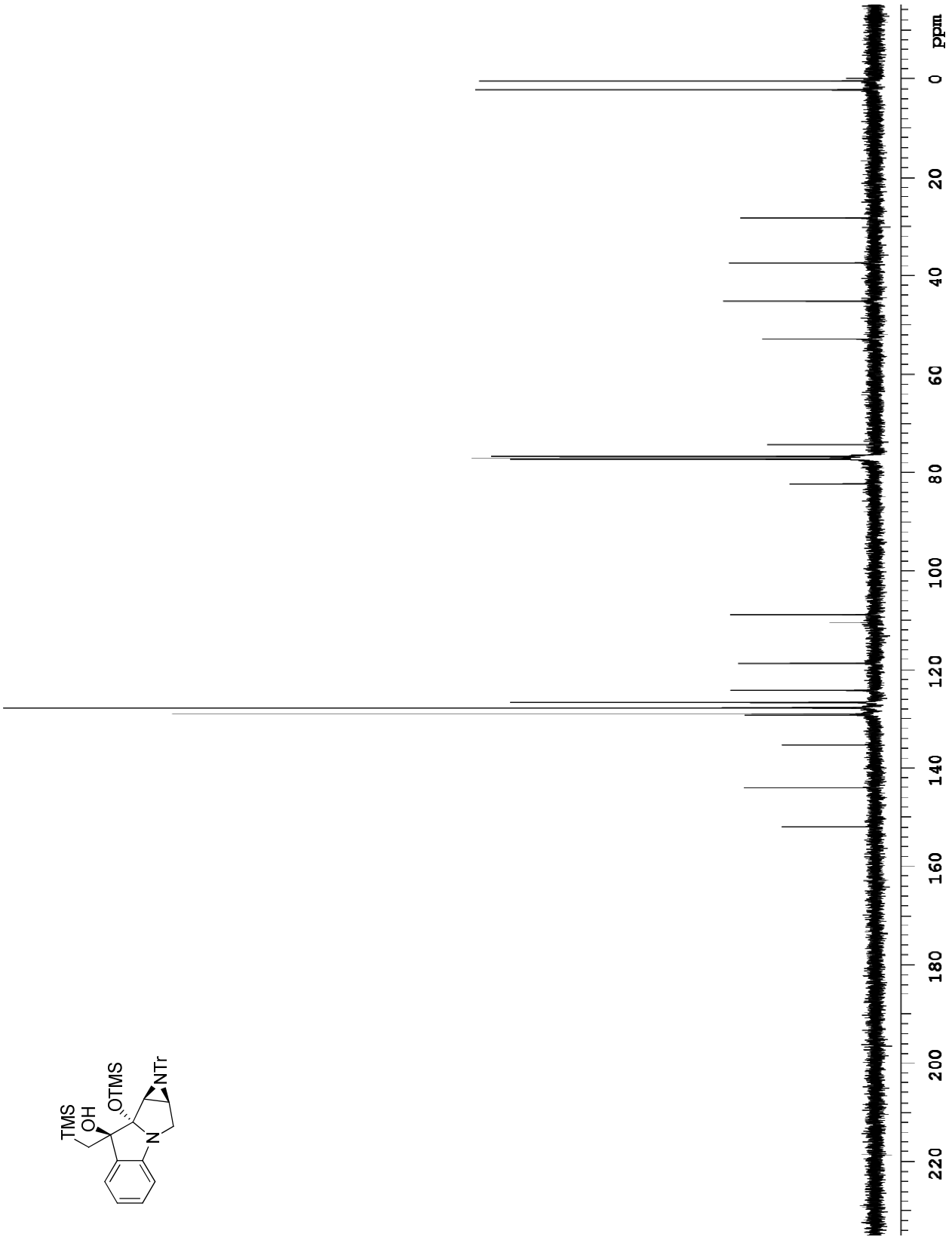
TMS
OH
OTMS
NTr
N
ppm
0
20
40
60
80
100
120
140
160
180
200
220

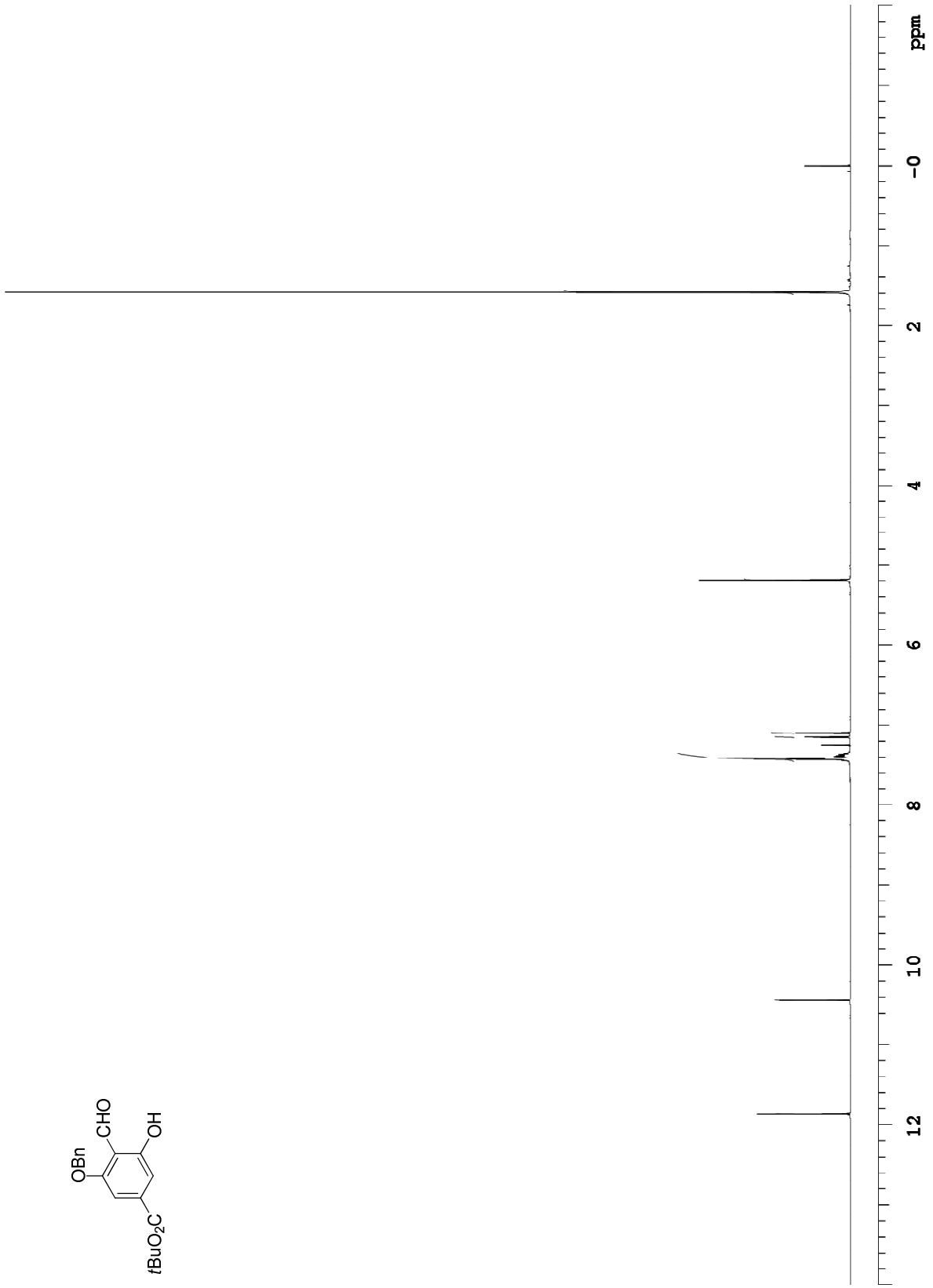
ppm
12
10
8
6
4
2
0
OBn
CHO
OH
tBuO2C

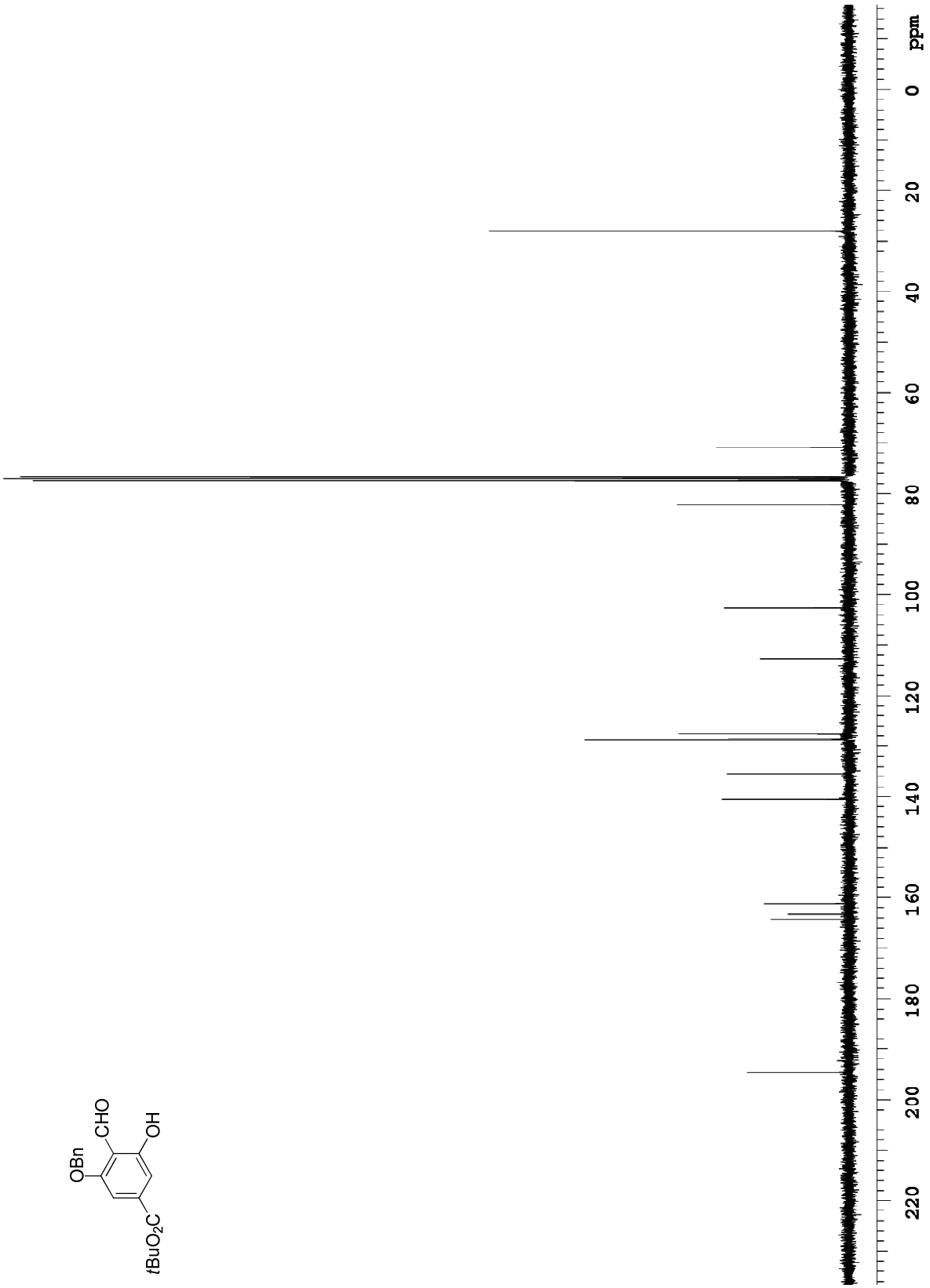
OBn
CHO
OH
tBuO2C
ppm
0
20
40
60
80
100
120
140
160
180
200
220

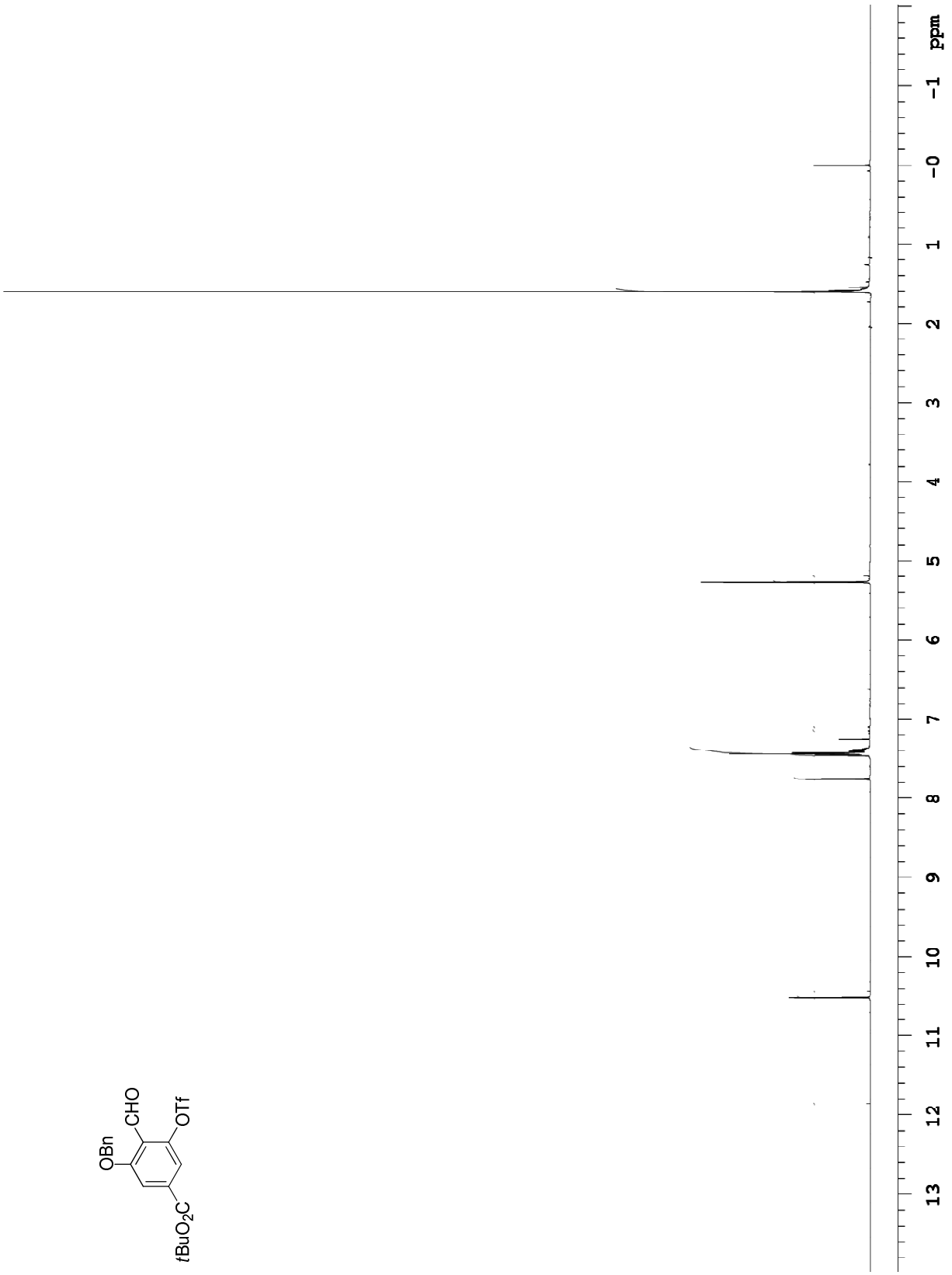
ppm
13
12
11
10
9
8
7
6
5
4
3
2
1
0
−1
OBn
CHO
OTf
tBuO2C

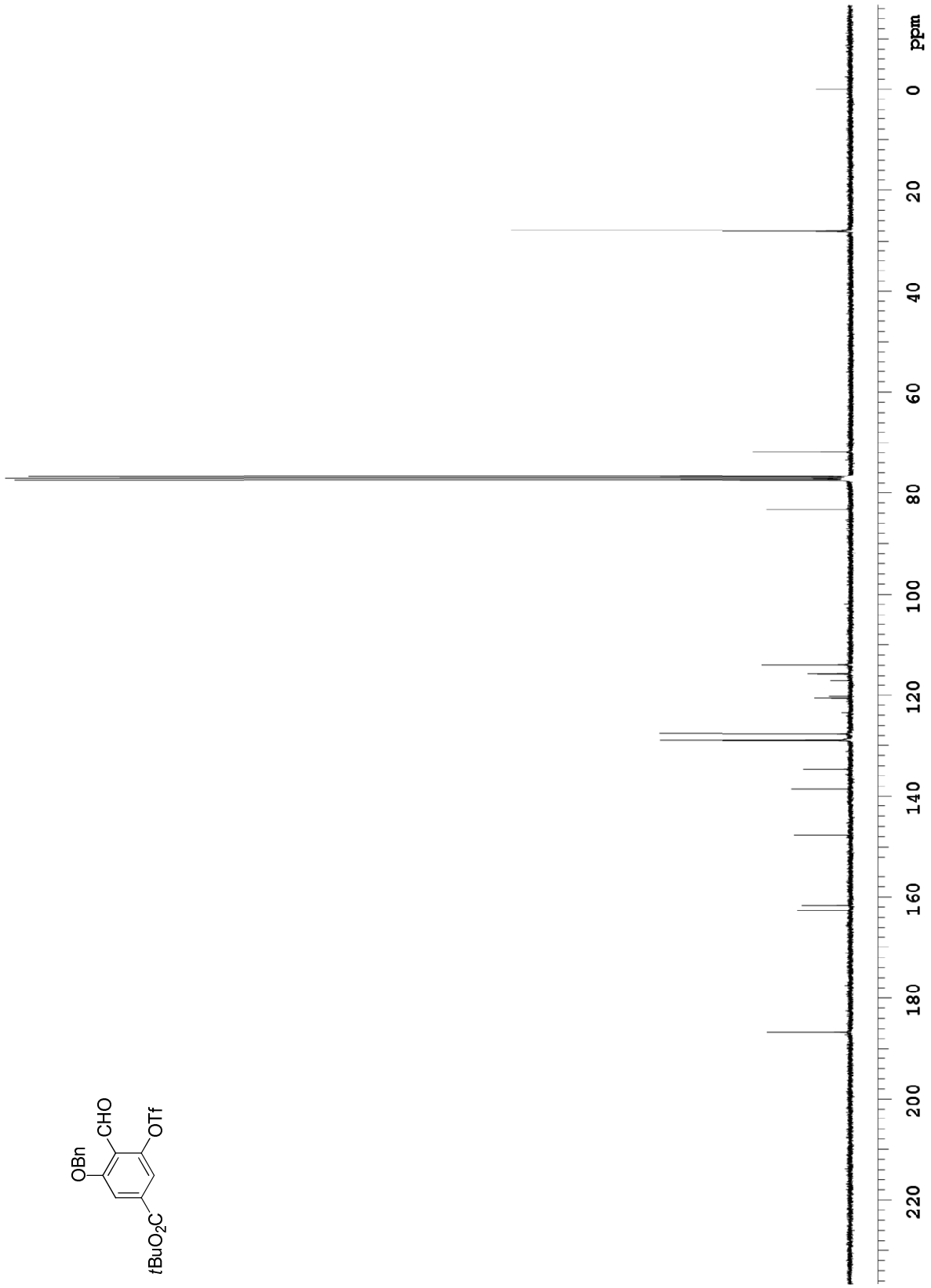
ppm
0
20
40
60
80
100
120
140
160
180
200
220
OBn
CHO
OTf
tBuO2C

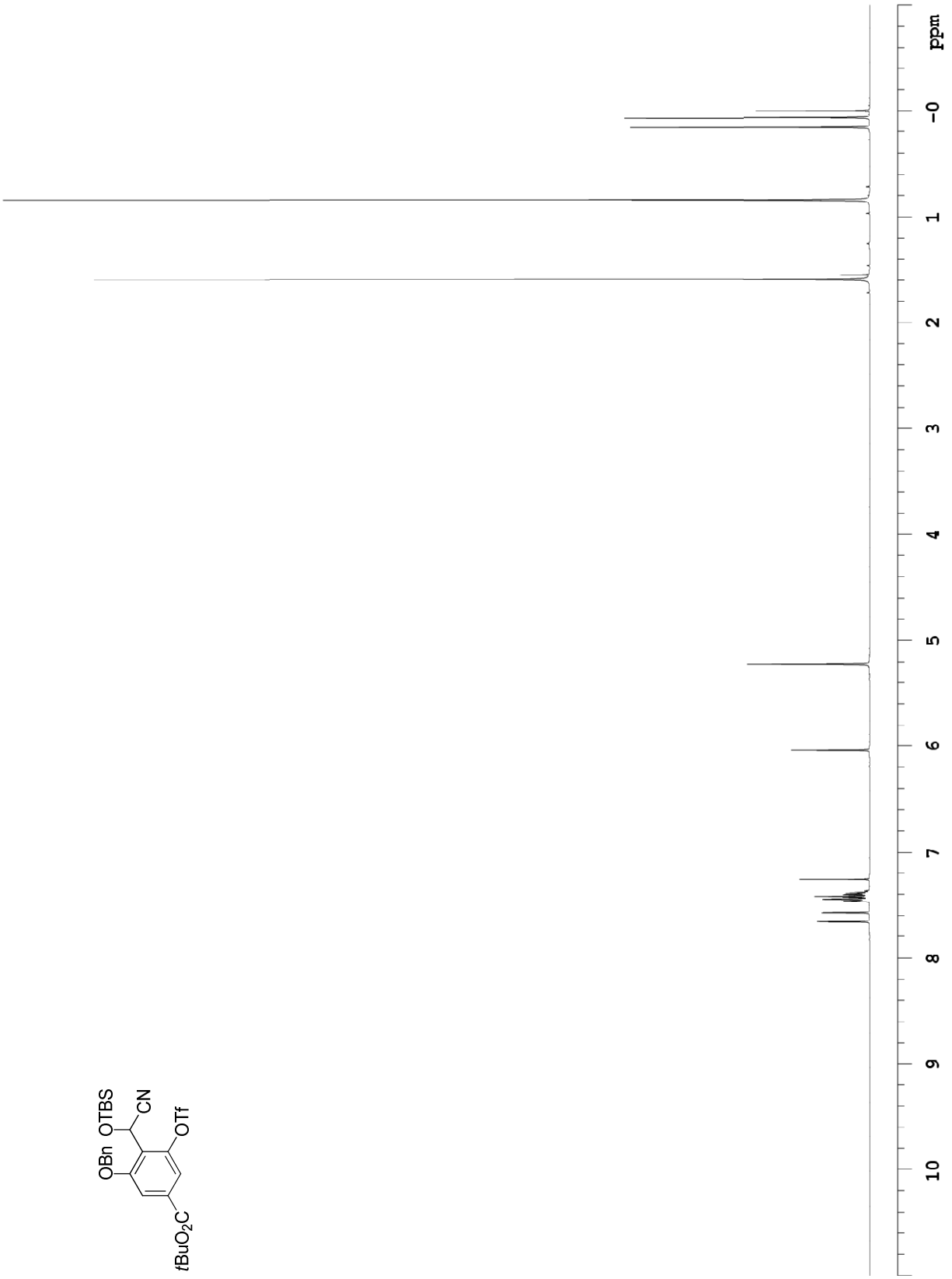
ppm
10
9
8
7
6
5
4
3
2
1
−0
OBn
OTBS
CN
OTf
tBuO2C

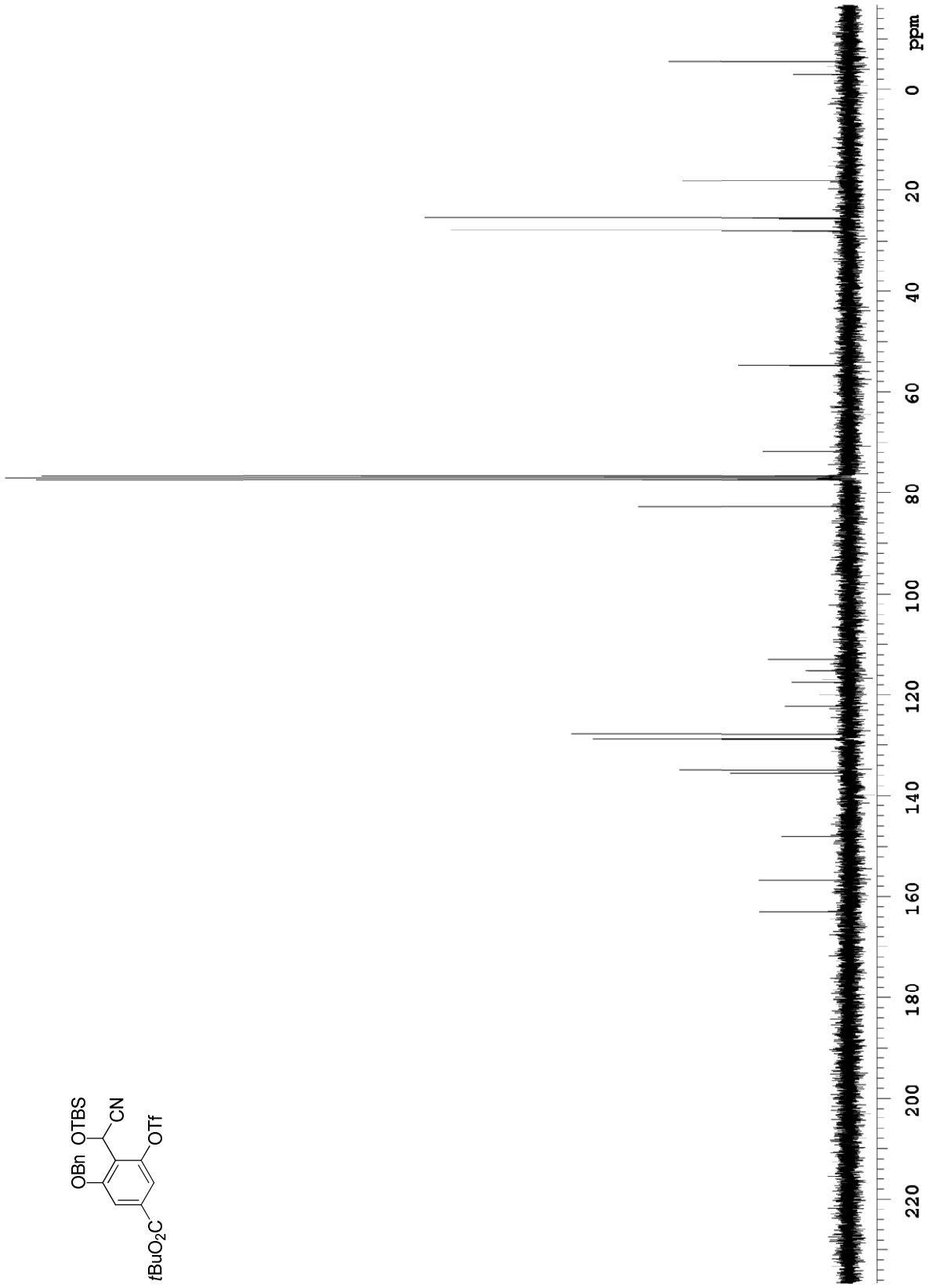
OBn
OTBS
CN
OTf
tBuO2C
ppm
0
20
40
60
80
100
120
140
160
180
200
220

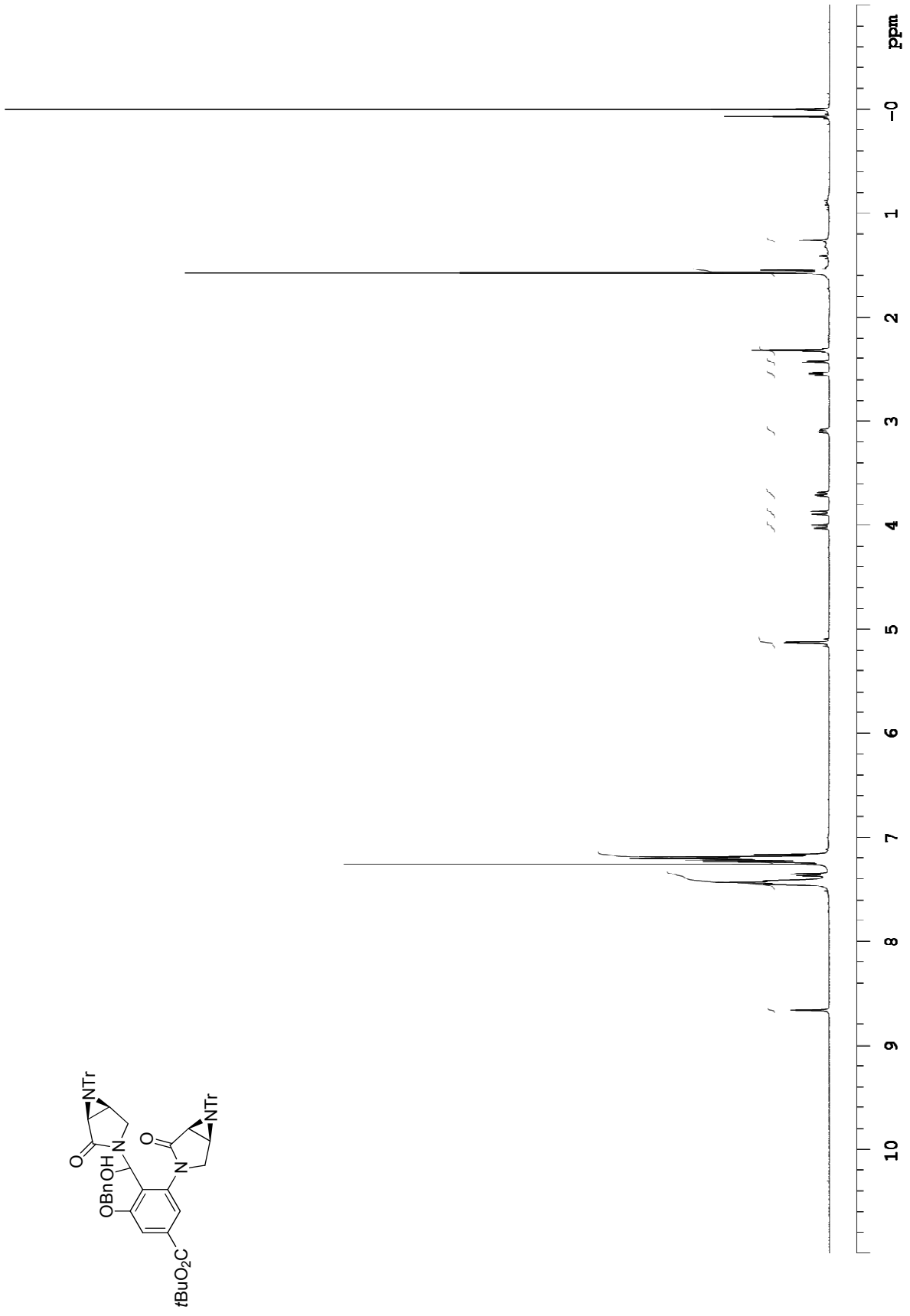
NTr
O
N
OBnOH
O
N
NTr
tBuO2C
ppm
10
9
8
7
6
5
4
3
2
1
0

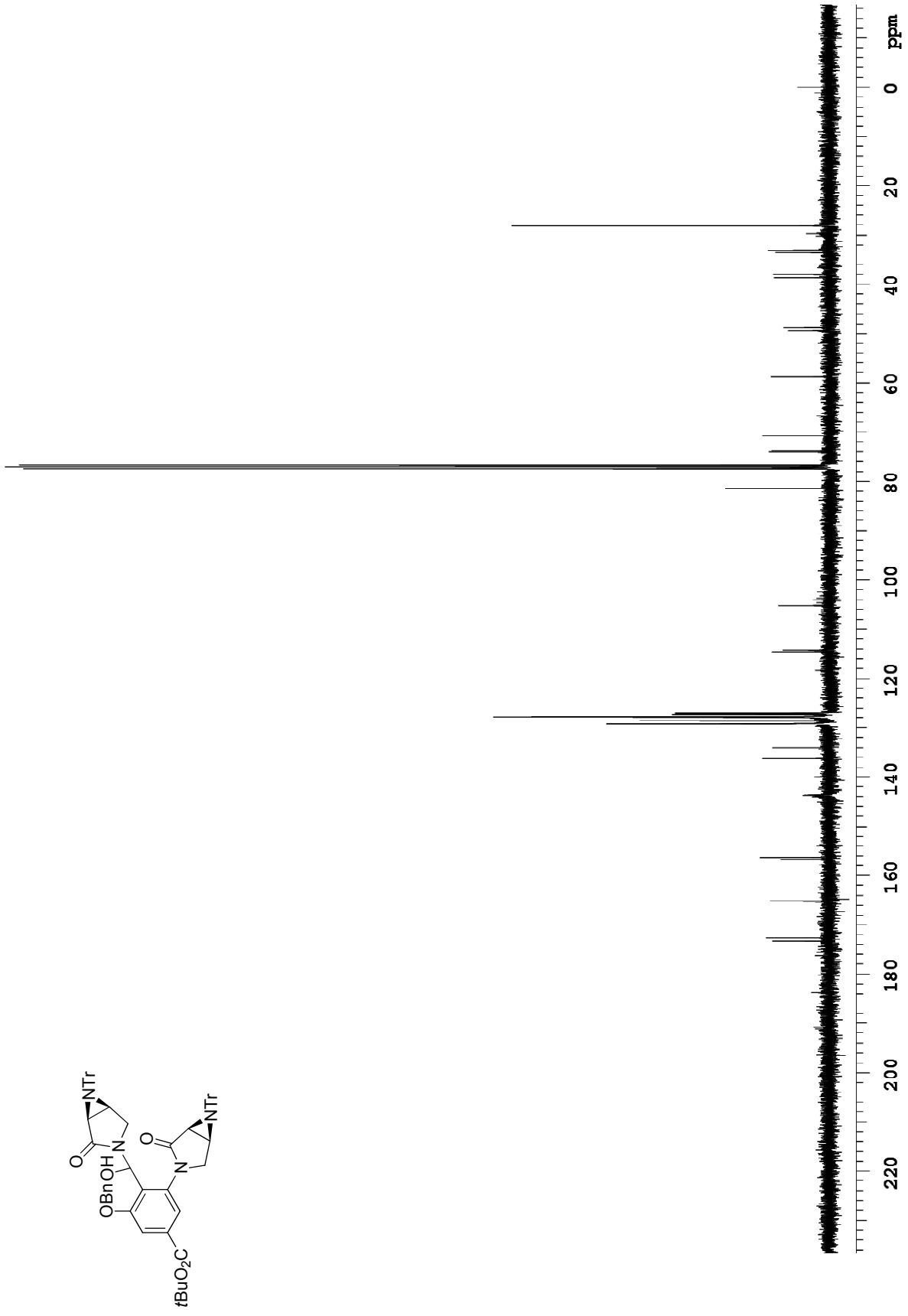
NTr
O
N
OBnOH
O
N
NTr
tBuO2C
ppm
0
20
40
60
80
100
120
140
160
180
200
220

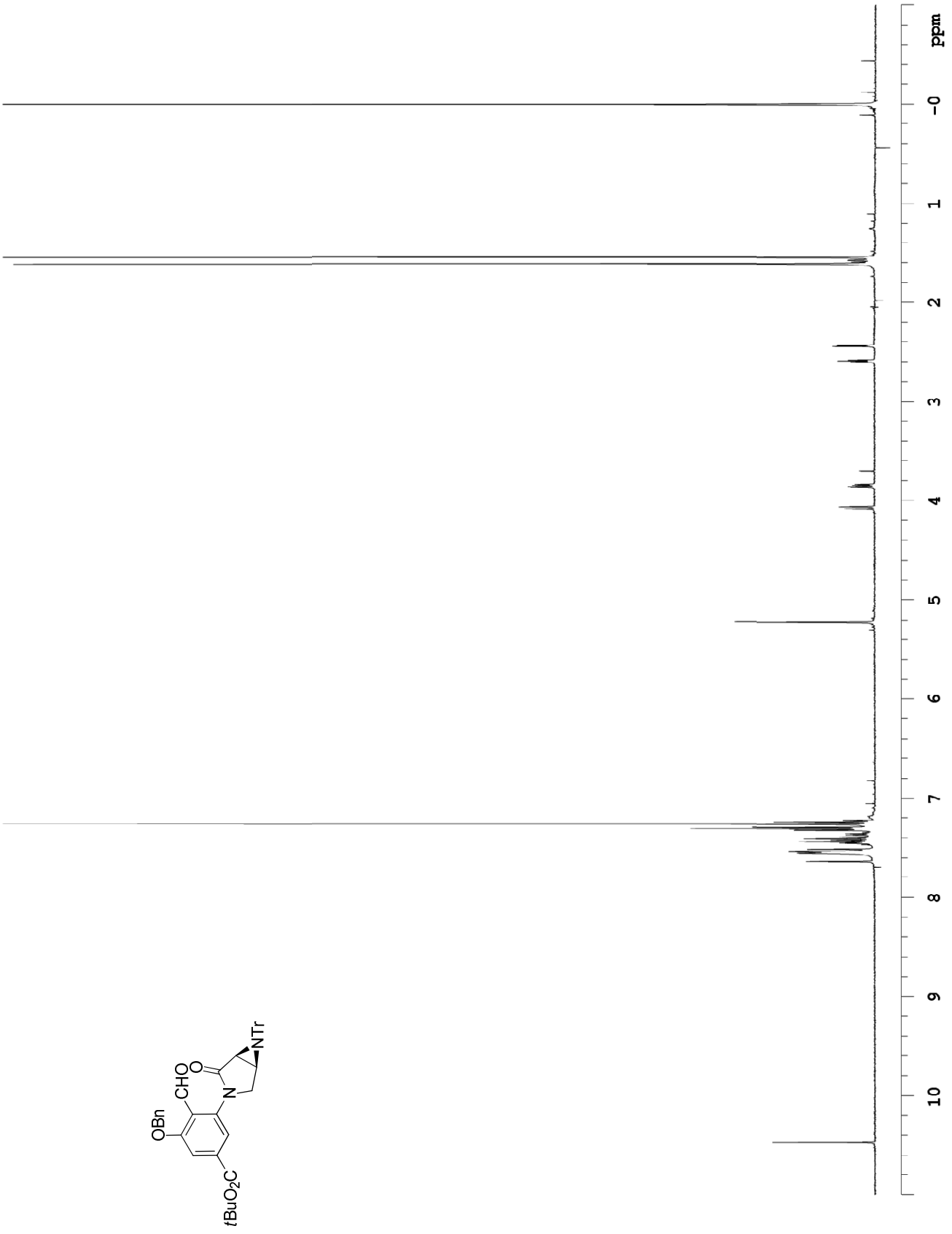
ppm
10
9
8
7
6
5
4
3
2
1
−0
NTr
CHO
O
N
OBn
tBuO2C

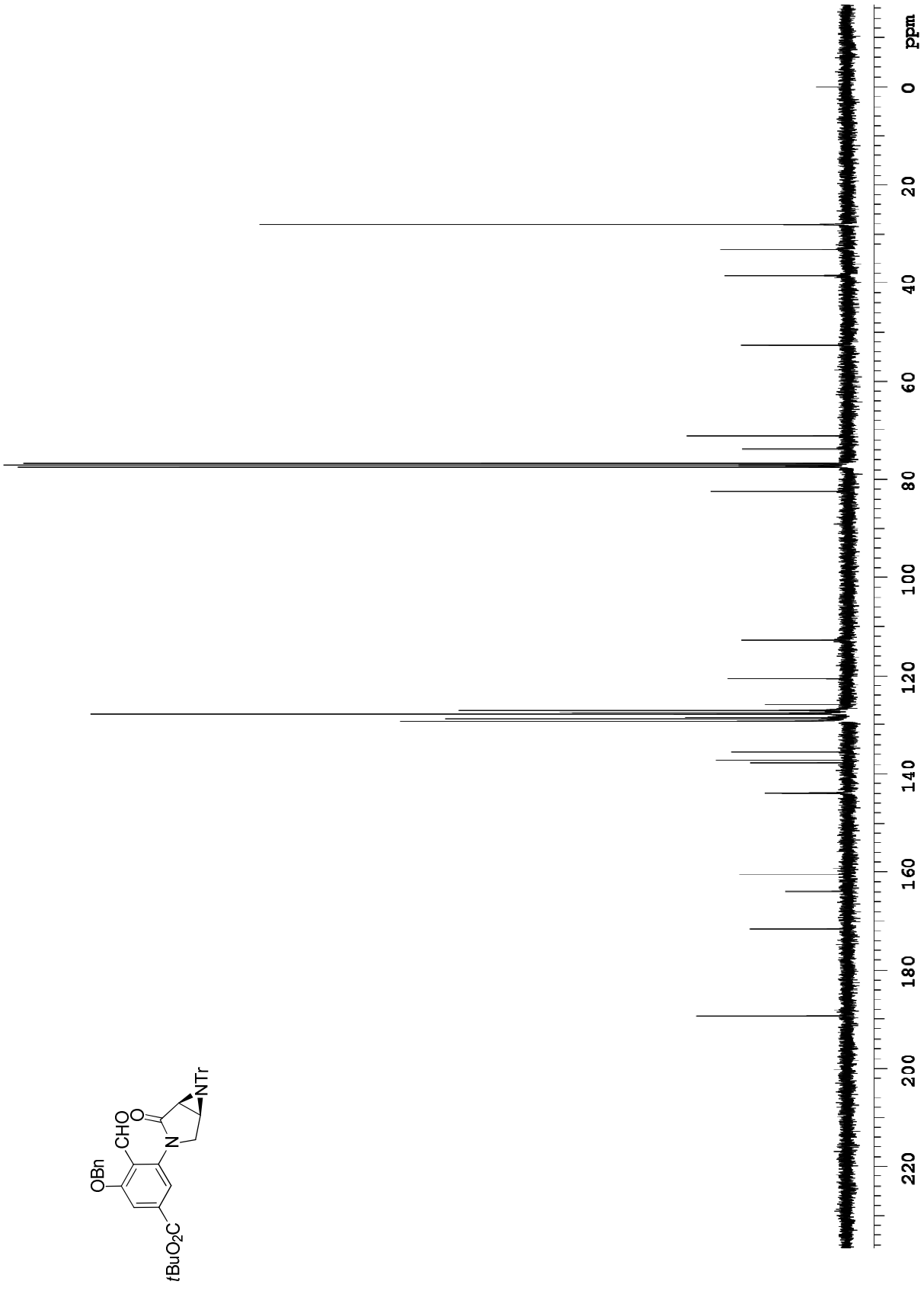
ppm
0
20
40
60
80
100
120
140
160
180
200
220
NTr
O
CHO
N
OBn
tBuO2C

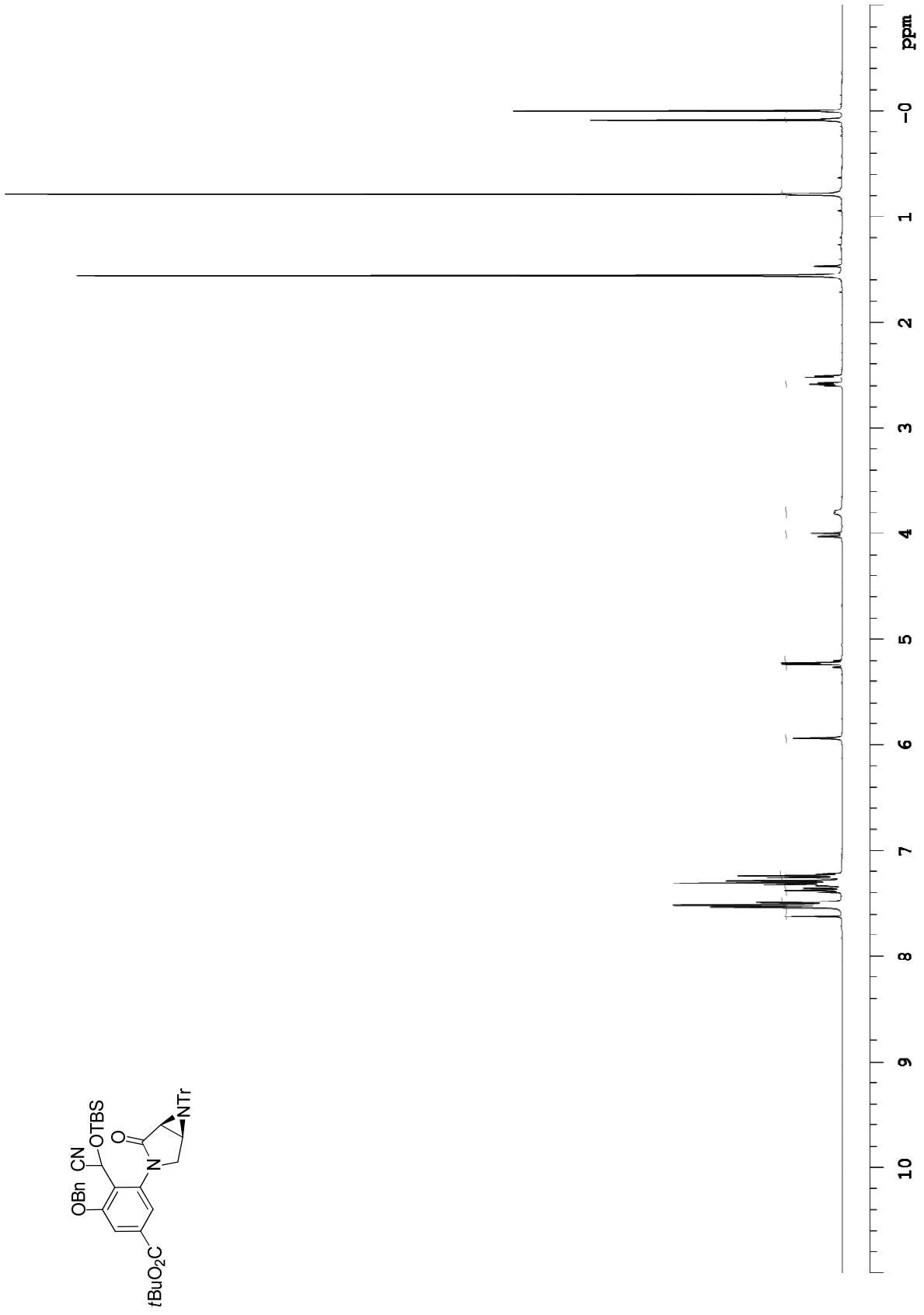
ppm
10
9
8
7
6
5
4
3
2
1
0
OBn
CN
OTBS
O
N
NTr
tBuO2C

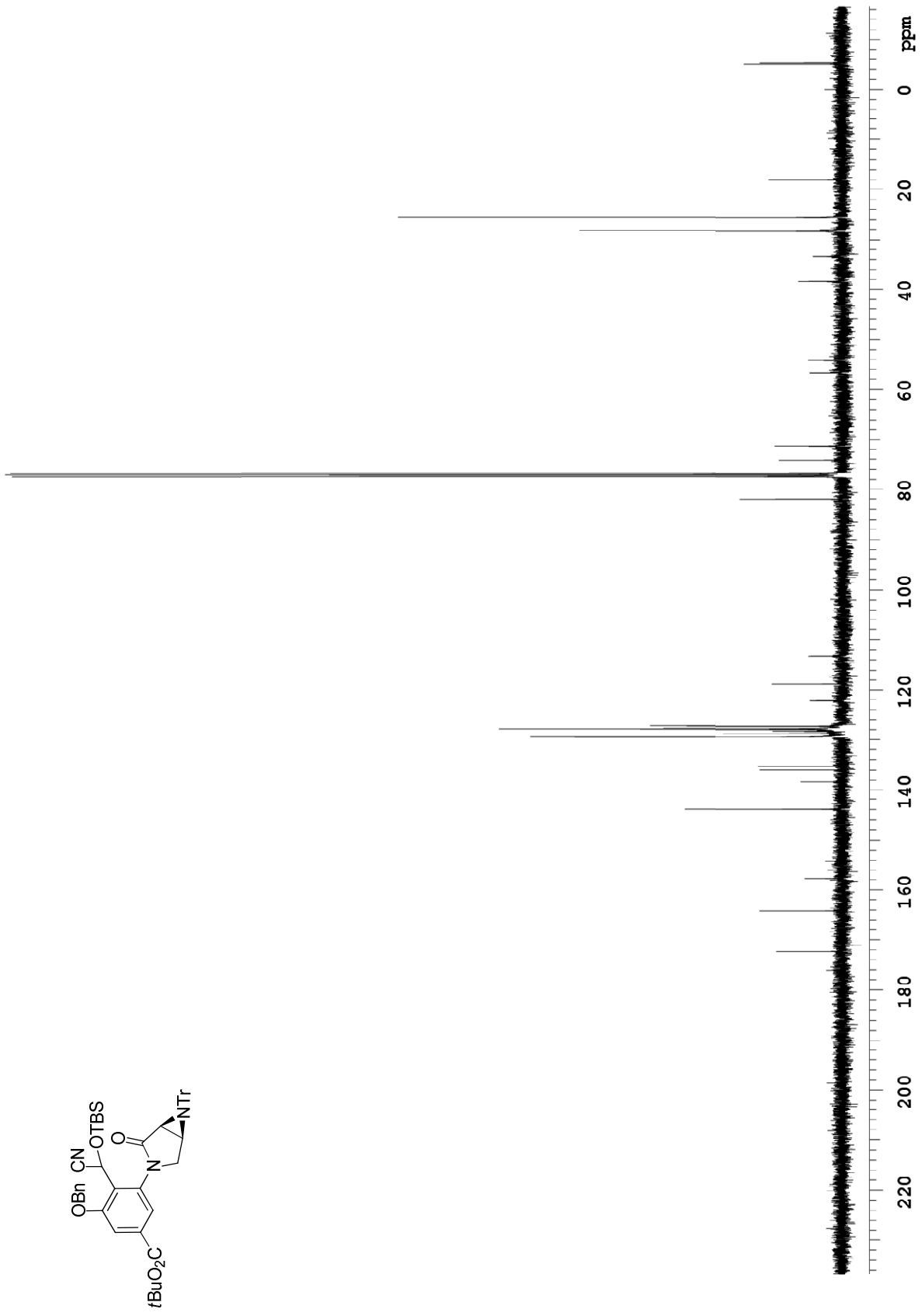
ppm
0
20
40
60
80
100
120
140
160
180
200
220
OBn
CN
OTBS
O
N
NTr
tBuO2C

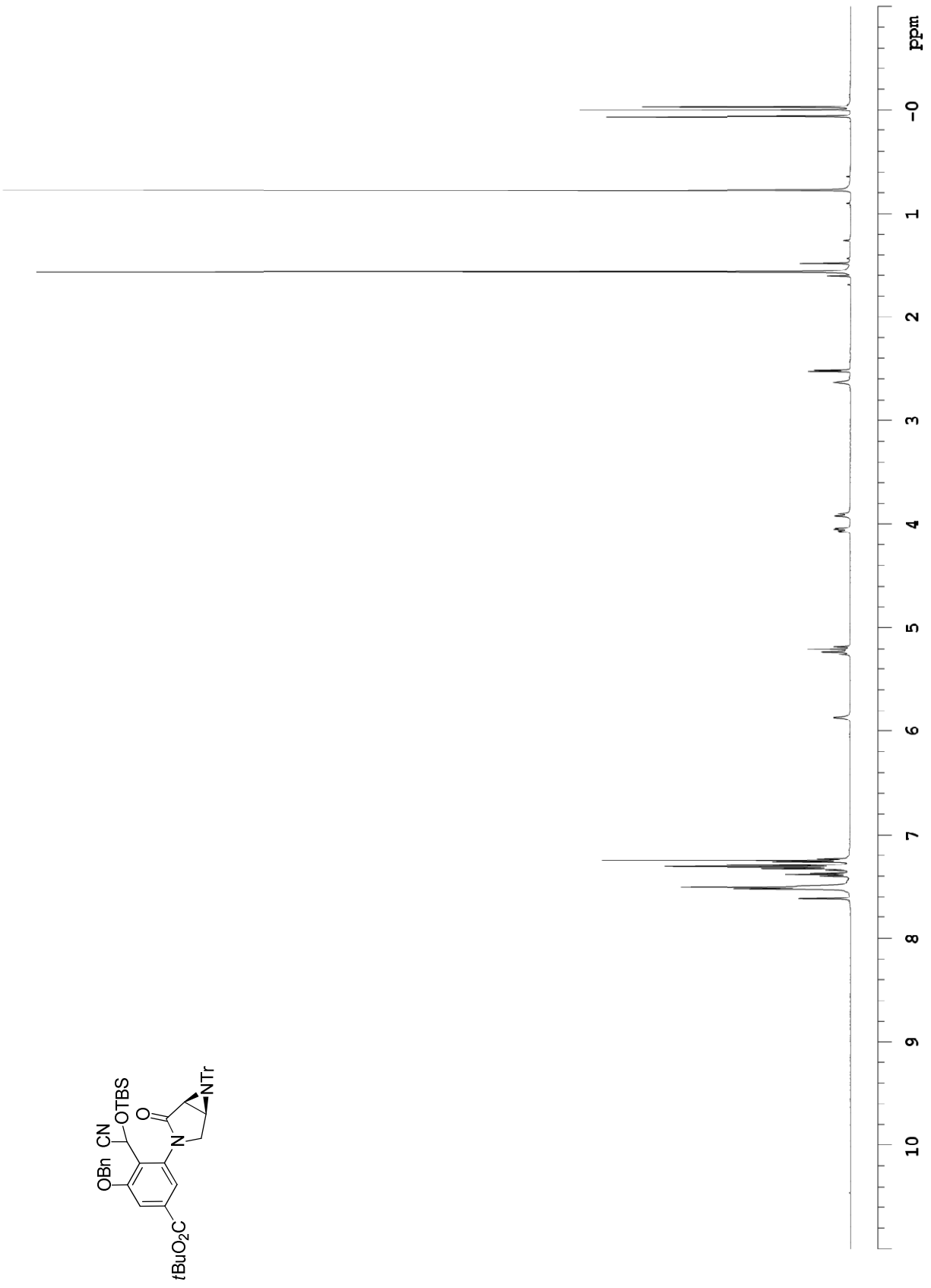
ppm
10
9
8
7
6
5
4
3
2
1
−0
OBn
CN
OTBS
O
N
NTr
tBuO2C

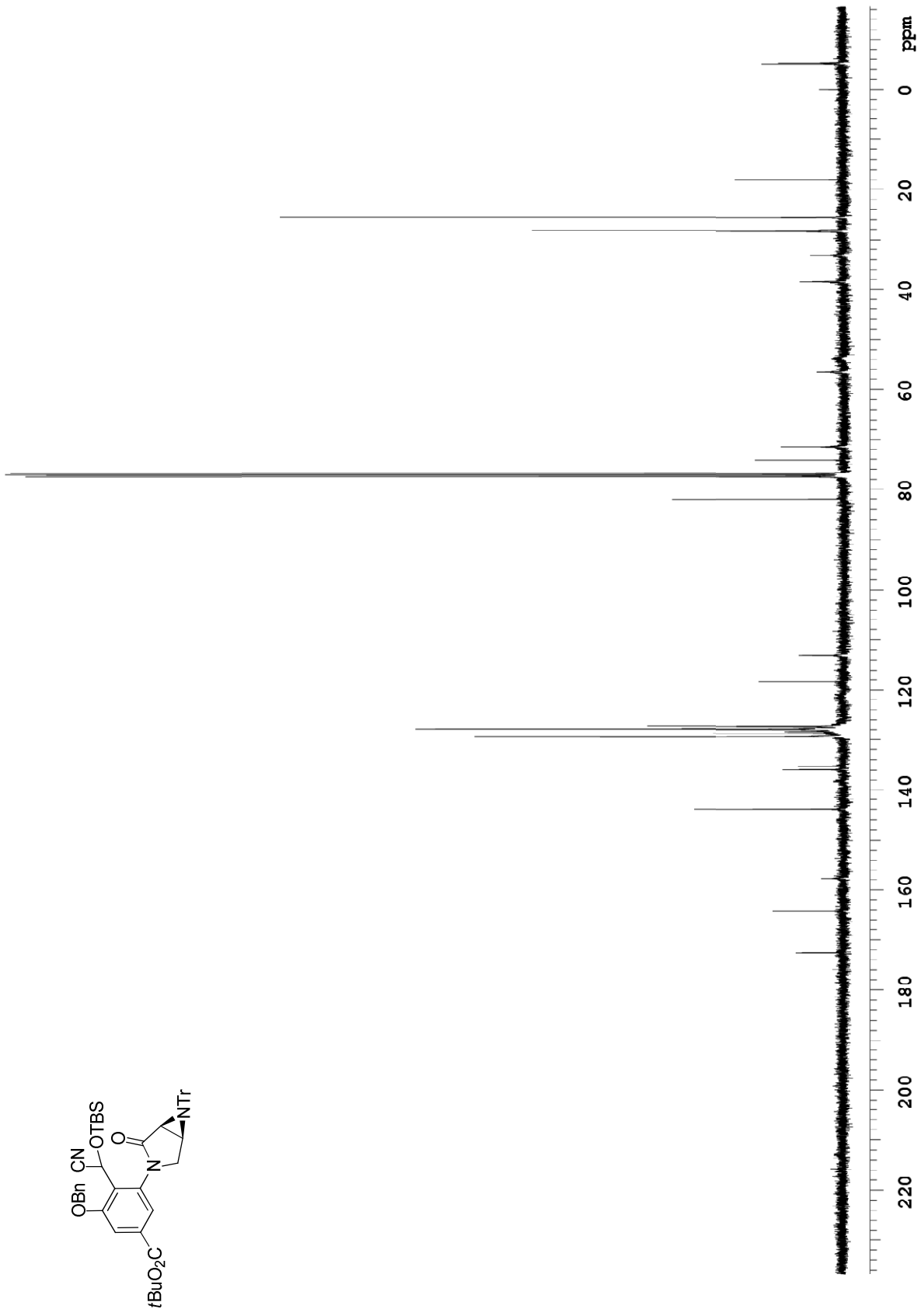
OBn
CN
OTBS
O
N
NTr
tBuO2C
ppm
0
20
40
60
80
100
120
140
160
180
200
220

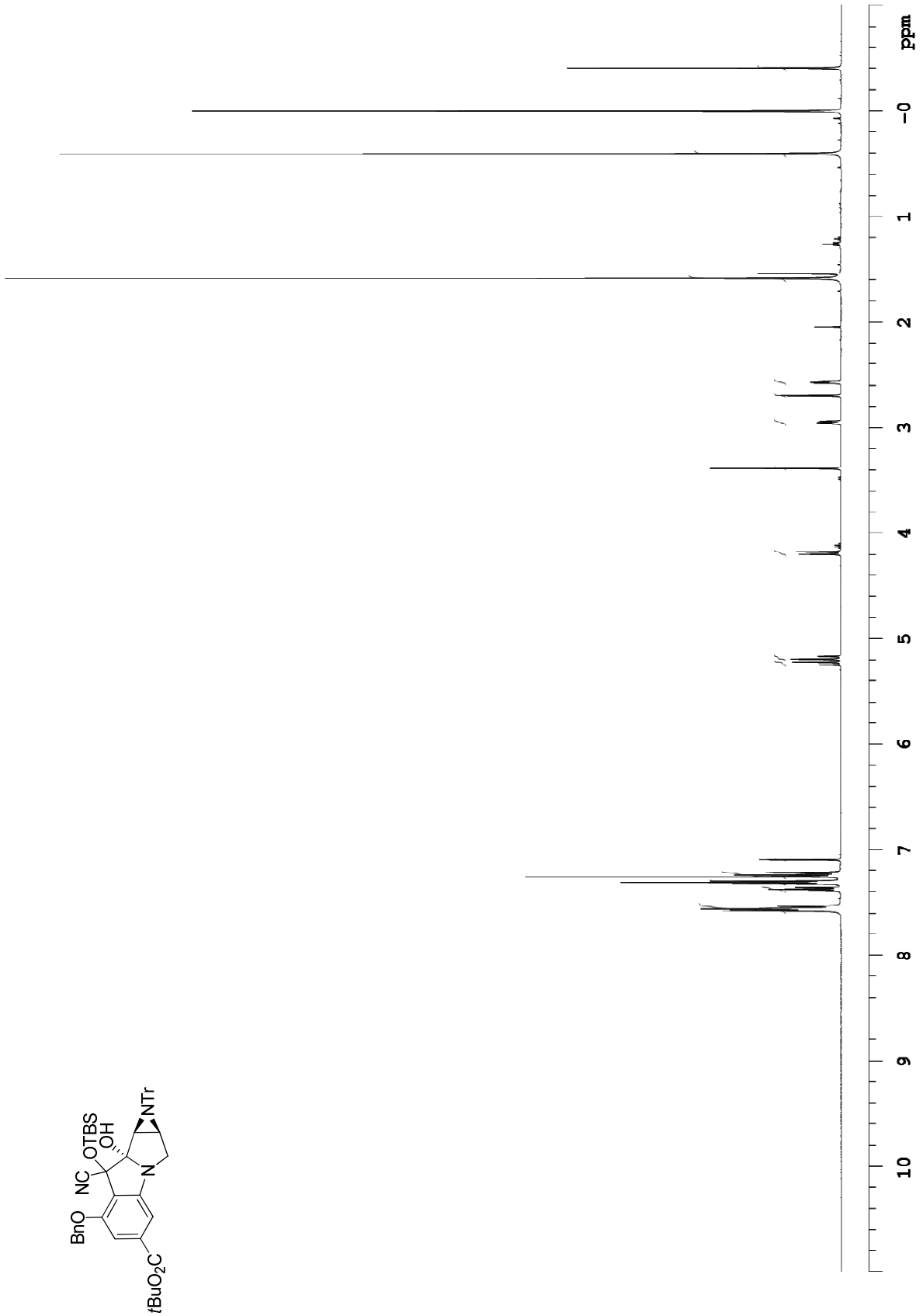
ppm
10
9
8
7
6
5
4
3
2
1
0
NTr
OTBS
OH
NC
N
BnO
tBuO2C

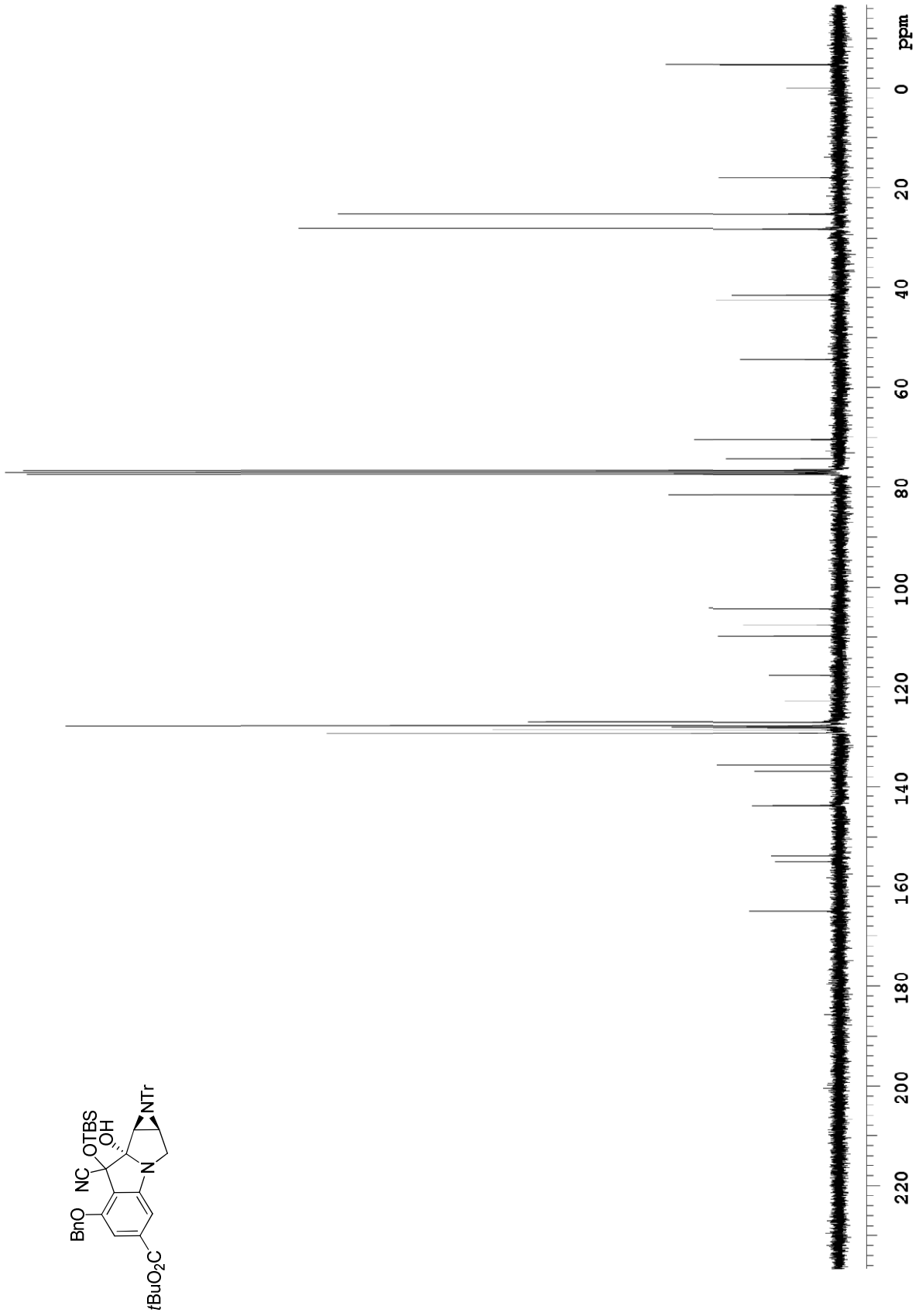
ppm
0
20
40
60
80
100
120
140
160
180
200
220
BnO
NC
OTBS
OH
NTr
N
tBuO2C

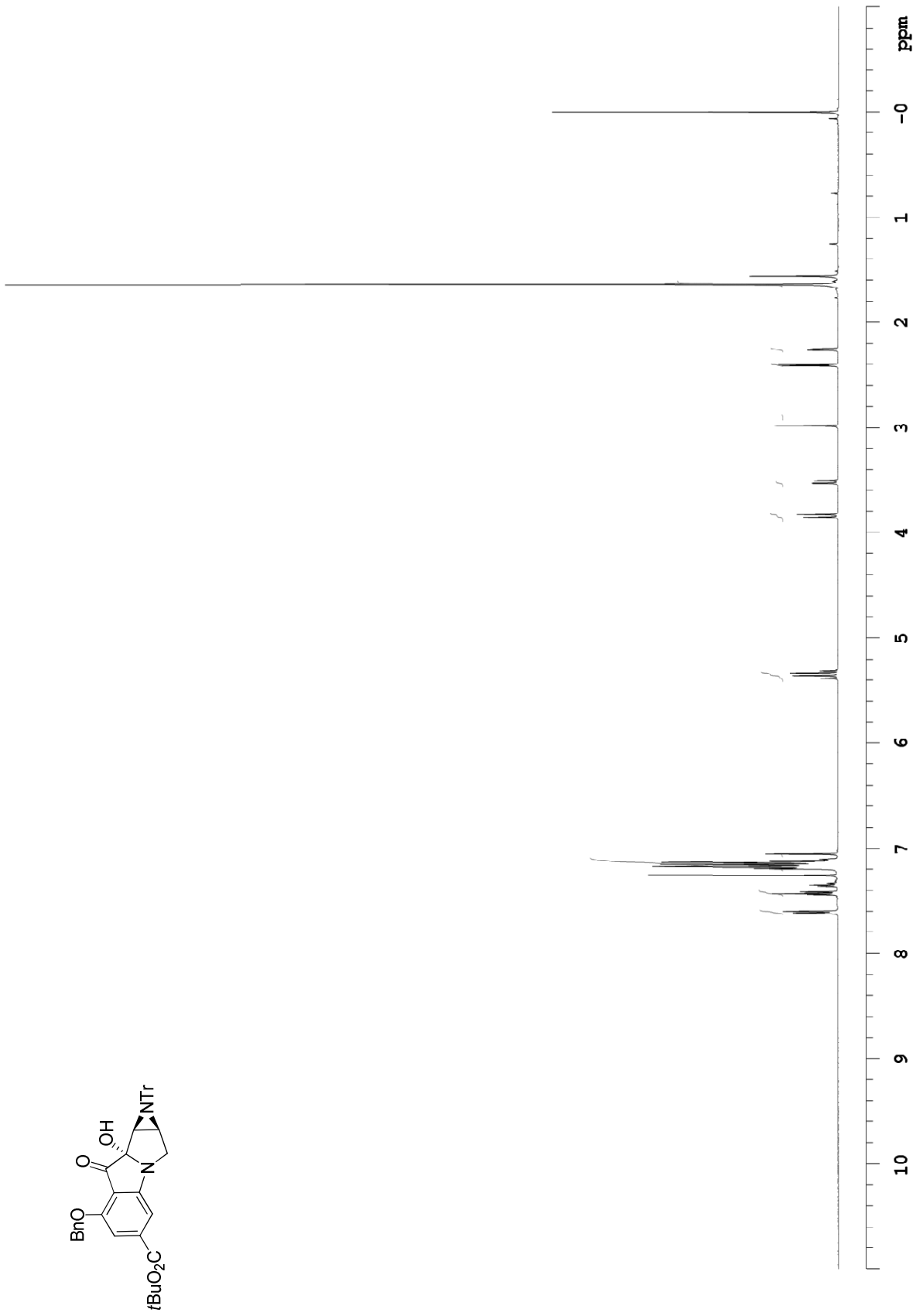
ppm
10
9
8
7
6
5
4
3
2
1
−0
OH
NTr
O
N
BnO
tBuO_2C

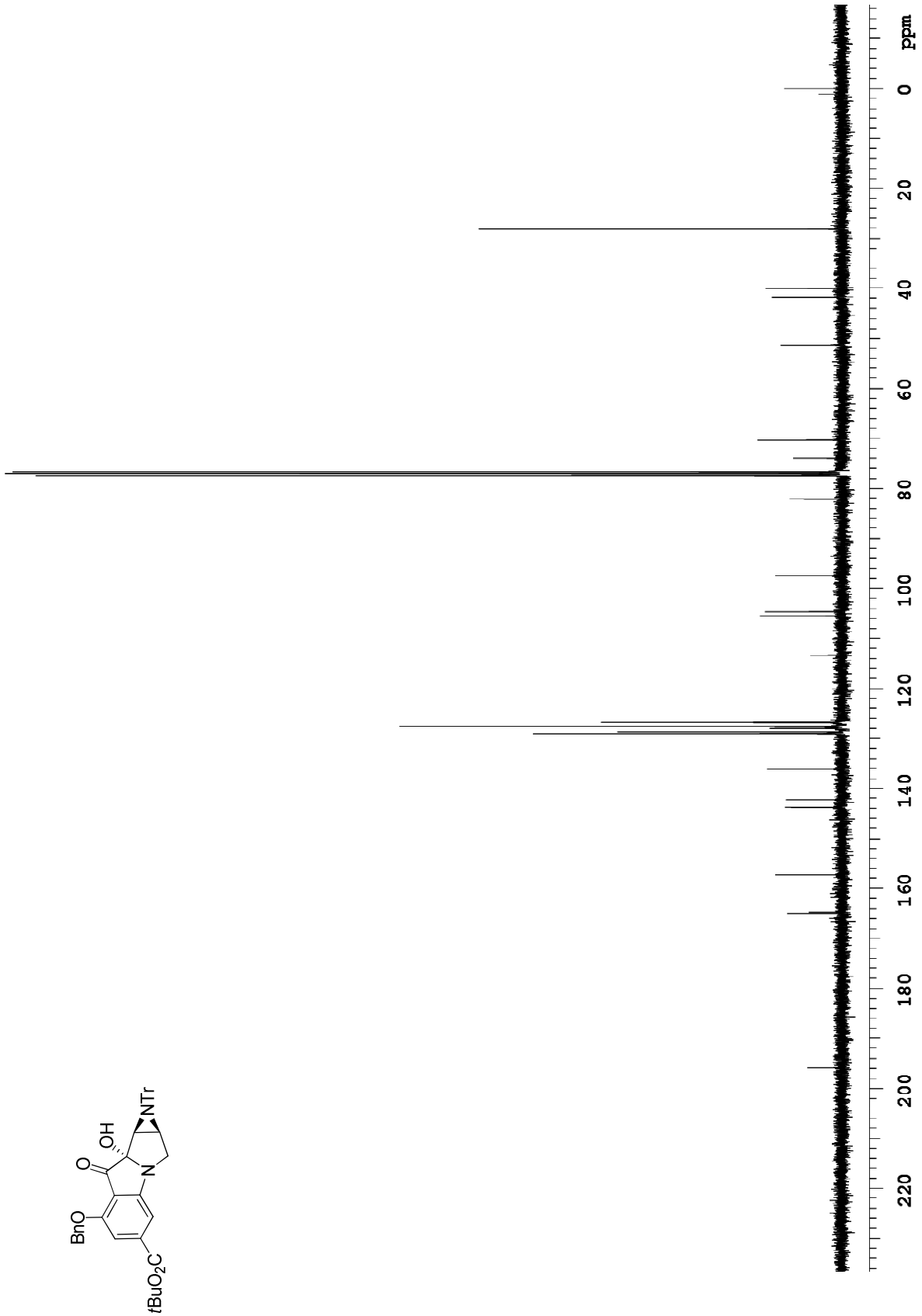
ppm
0
20
40
60
80
100
120
140
160
180
200
220
BnO
O
OH
N
NTr
tBuO2C